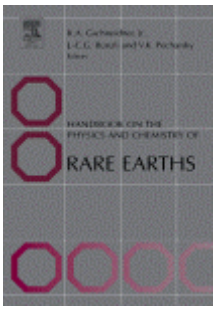

Handbook on the Physics and Chemistry of Rare Earths volume 9

Elsevier, 1987

Edited by: Karl A. Gschneidner, Jr. and LeRoy Eyring
ISBN: 978-0-444-87045-2

Handbook on the Physics and Chemistry of Rare Earths, edited by K.A. Gschneidner, Jr. and L. Eyring

PREFACE

Karl A. GSCHNEIDNER, Jr., and LeRoy EYRING

These elements perplex us in our rearches [sic], *baffle us in our speculations, and haunt us in our very dreams. They stretch like an unknown sea before us – mocking, mystifying, and murmuring strange revelations and possibilities.*

Sir William Crookes (February 16, 1887)

There are those who feel that the rare earth elements are destined to play an even greater role in our "high-tech" society in the future than they have in the past. This judgement is based upon the trend of increasing applications resulting from the electronic structures of these materials that lead to their unusual optical, magnetic, electrical and chemical properties so adaptable to the demands now being placed on materials. The "Handbook" seeks to provide topical reviews and compilations of critically reviewed data to aid in the design and fabrication of the required new materials. Four additional chapters in this tradition are the contents of this volume.

The development of lasers containing rare earth species sparked an interest in glasses containing these elements. Reisfeld and Jørgensen discuss excited-state phenomena in vitreous rare-earth-containing substances. The description of the chemistry and crystal chemistry of complex inorganic compounds of the rare earths is continued by Niinistö and Leskelä from the previous volume. Here they consider the phosphates, arsenates, selenates and selenites, oxohalogen compounds and vanadates. Encapsulation and transport of charged hydrophilic species from an aqueous medium into a hydrophobic phase are promoted by ionophores. The properties and applications of rare earth complexes with synthetic ionophores are described by Bünzli. Finally, Shen and Ouyang review their own work and that of others in the application of rare earth coordination catalysts in stereospecific polymerization. These Ziegler–Natta type catalysts provide tools for, among other things, the design of electrically conducting polymers.

CONTENTS

CONTENTS OF VOLUMES 1–8

VOLUME 1: METALS

VOLUME 2: ALLOYS AND INTERMETALLICS

VOLUME 3: NON-METALLIC COMPOUNDS – I

VOLUME 4: NON-METALLIC COMPOUNDS – II

VOLUME 5

VOLUME 6

VOLUME 7

VOLUME 8

Handbook on the Physics and Chemistry of Rare Earths, edited by K.A. Gschneidner, Jr. and L. Eyring

Chapter 58

EXCITED STATE PHENOMENA IN VITREOUS MATERIALS

Renata REISFELD
Department of Inorganic Chemistry, Hebrew University (Givat-Ram) 91904 Jerusalem, Israel

Christian K. JØRGENSEN
Department of Inorganic, Analytical and Applied Chemistry University of Geneva, CH 1211 Geneva 4, Switzerland

Contents

Symbols

A_{ij} = transition probability from state E_i to state E_j
a = dimensionless constant $1/(\alpha\hbar\omega)$ in eq. (21)
B = preexponential factor of rate of multiphonon deexcitation in eq. (18)
B^* = modified B in eq. (21)
B_{ji} = probability of absorption
c = velocity of light in vacuum
c_n = molar concentrations
E^0 = standard oxidation potential
E^1, E^3 = Racah parameters of interelectronic repulsion
ΔE = energy gap between two J-levels
e_i = number of degenerate states with identical energy
F^2, F^4, F^6 = Slater–Condon–Shortley parameters of interelectronic repulsion
h = Planck constant
$\hbar$ = $(h/2\pi)$
J = quantum number of angular momentum in (approximate or perfect) spherical symmetry
K = Kossel number of electrons
k = Boltzmann constant
m = rest mass of electron
N = coordination number
n = refractive index
q = number of electrons (in 4f shell)
P = oscillator strength
P_{ed} = oscillator strength of electric dipolar transition
P_{et} = oscillator strength of electron transfer band
P_{md} = oscillator strength of magnetic dipolar transition
R_0 = critical radius of energy transfer
S = quantum number of total spin
S_{ED} = electric dipolar line strength in eq. (8)
S_{MD} = magnetic dipolar line strength in eq. (8)
T = absolute temperature
U_t = Judd–Ofelt matrix element ($t = 2$, 4 or 6)
$U^{(t)}$ = Judd–Ofelt tensor
W_{NR} = rate of nonradiative relaxation
Z = atomic number

z = ionic charge; oxidation state
α = parameter of multi-phonon de-excitation in eq. (18)
β = amplification coefficient in eq. (10)
β, β_{ij} = branching ratio
Δ = sub-shell energy difference ($= 10\,Dq$) in octahedral d-shell
δ = one-sided half-width of absorption band; one-electron function (orbital) with the quantum number $\lambda = 2$ in linear symmetry
ε = molar extinction coefficient in eq. (2)
ζ_{4f}, ζ_{5f}, ζ_{5d} = Landé parameter of spin–orbit coupling
η = quantum yield
η_{tr} = efficiency of energy transfer eq. (35)
λ = wavelength
ν = frequency
π = (also) one-electron function (orbital) with the quantum number $\lambda = 1$ in linear symmetry
σ = wave number ($= \nu/c$); one-electron function (orbital) with the quantum number $\lambda = 0$ in linear symmetry
σ_p = stimulated emission cross section at peak
τ = lifetime
τ_{rad} = τ_R radiative (Einstein) lifetime
τ_{av} = average lifetime, eq. (36)
Ψ = many-electron wave function
Ω_t = Judd–Ofelt parameter ($t = 2$, 4 or 6) of transition probability
ω = in phonon energy $\hbar\omega$; quantum number of relativistic one-electron function in linear symmetry in eq. (39)

1. Introduction – the vitreous state

From a spectroscopic point of view, the trivalent rare earths R(III) fall in two main categories: (a) the closed-shell scandium(III), yttrium(III), lanthanum(III), and lutetium(III), having their first excited electronic states in the far ultraviolet (well above 6 eV or 48000 cm^{-1}); and (b) the twelve cases, starting with praseodymium(III) and ending with ytterbium(III), containing 2 to 13 electrons in a partly filled 4f shell, correspondingly.

Many of these systems have their first excited states at quite low energy, and the corresponding absorption bands occur in the far infrared, and were detected only recently. An exceptional case is represented by the half-filled $4f^7$ gadolinium(III), having the first excited state at 32100 cm^{-1} (4 eV), as was shown by Urbain in 1909. The fluorescence from this state is characterized by a narrow line in the ultraviolet. The narrow absorption bands attracted general attention, and were already considered by Bunsen and Kirchhoff (before 1864) as closely resembling the atomic spectral lines. The situation became muddled around 1908 by the detection of narrow emission lines of ruby, $Al_{2-x}Cr_xO_3$, and other systems containing $3d^3$ chromium(III) surrounded by an almost regular octahedron of six oxygen ligating atoms. Around 1955 (cf. Jørgensen, 1969, 1971) it was clarified

that this emission arises from the lowest doublet level to the quartet ground state of three electrons in three d-like, roughly nonbonding orbitals, whereas the broad absorption bands of Cr(III) and numerous other cases of partly filled d-shells involve the two strongly anti-bonding orbitals as well. The optical spectra in transition metal elements have only a remote similarity with the free-ion transitions, whereas in the lanthanides the narrow absorption bands are almost invariant, also with respect to the few known free-ion levels. As can be seen in fig. 1, the theory of atomic spectra allows identification of definite J-levels of $4f^q$ (Reisfeld and Jørgensen, 1977). The spectral assignments below 3 or 4 eV were almost completed by Carnall, Fields and Rajnak (Carnall et al., 1968). The minor shift of the center of each J-level, the *nephelauxetic effect*, was first observed by Hofmann and Kirmreuther in 1910. From a comparison of the reflection spectra of Er_2O_3 and other erbium(III) compounds, it was possible to derive important conclusions about chemical bonding, and particularly to define an upper limit for the (weak) anti-bonding character of 4f orbitals (Jørgensen, 1976, 1979), and the separations of the $(2J + 1)$ mutually orthogonal eigenstates belonging to a given J-level (typically below 400 cm^{-1} or 0.05 eV). Information about the holohedrized symmetry of the rare-earth site was obtained by Durville et al. (1983). Cerium(III) and the bivalent lanthanides show features which are intermediate between typical trivalent lanthanides and chromium(III). The broad-band luminescence in Ce(III) and Eu(II) has a much shorter lifetime (in the 10^{-7} s range) than the narrow-line luminescence to the excited low-lying J-levels of Eu(III), Gd(III) and Tb(III), with lifetimes above one millisecond.

The narrow absorption bands of solutions were used to monitor separation of colored lanthanides having adjacent atomic numbers, and were the major tool used by Auer von Welsbach when separating praseodymium and neodymium in 1885. The corresponding bands in glasses served as wavelength standards in spectrophotometers. The strongest visible band of Nd(III) absorbs selectively the two yellow sodium lines, circumventing interference in potassium and rubidium spectral lines in gas flames. Glass goggles containing neodymium thus assist glassblowers to see the red glow of glass objects under work.

The technological interest in glasses containing rare earths suddenly arose upon the development of solid-state *lasers*. Originally, crystals (Weber, 1979; Reisfeld and Jørgensen, 1977) such as doped perovskite $Nd_xY_{1-x}AlO_3$, doped garnet $Nd_xY_{3-x}Al_5O_{12}$, or stoichiometric pentaphosphate NdP_5O_{14}, were considered as the most important materials. However, it was soon realized (Reisfeld, 1976b) that glass lasers have enormous advantages over crystals, in that they are easily prepared in large rods by melting together the constituent components, easily shaped, and show less optical inhomogeneity, being isotropic by nature. Actually, the first terawatt * lasers in the SHIVA system (functioning 1978) at Livermore

* terawatt = 10^{12} W equivalent of 1000 joules released in a nanosecond pulse, corresponding to a packet of light with the length, 30 cm, divided by the refractive index n of the glass.

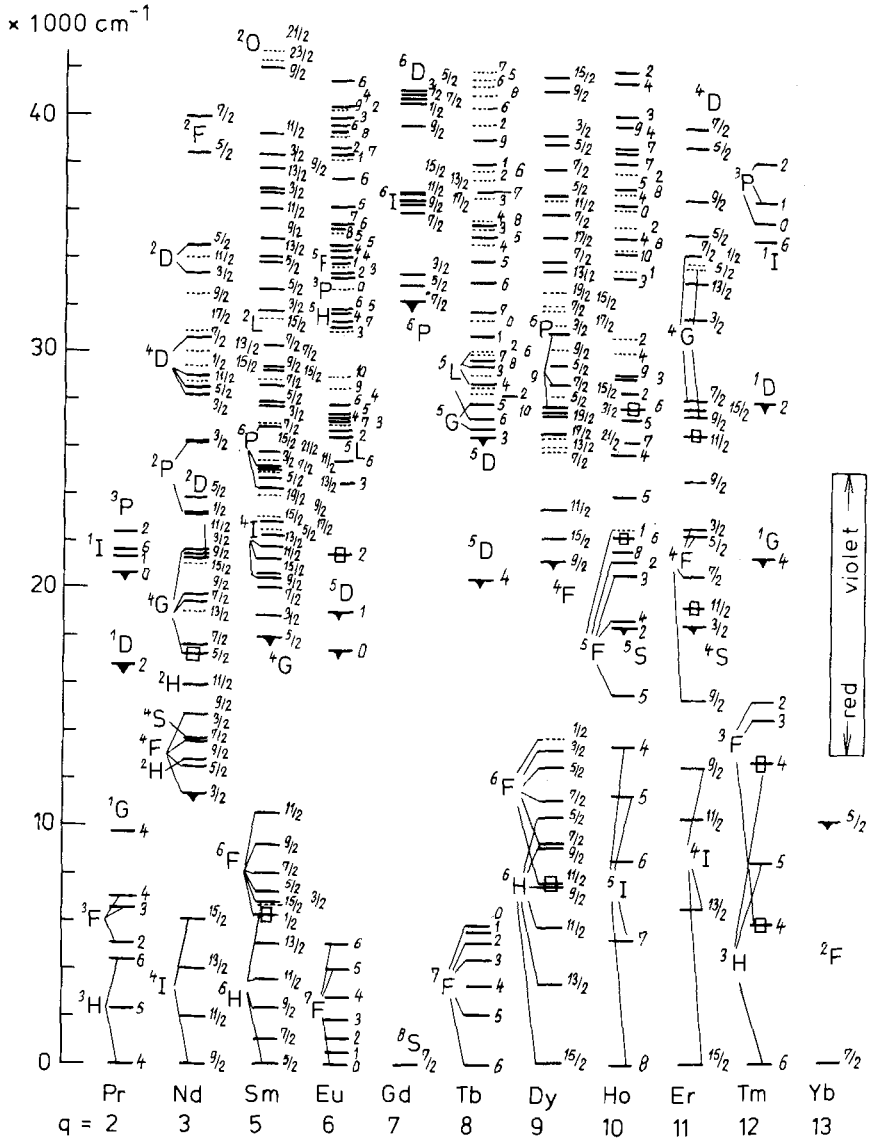

Fig. 1. Energy levels of trivalent lanthanides below 43000 cm^{-1} (5.3 eV) arranged according to the number q of 4f electrons. Excited levels known frequently to luminesce are indicated by a black triangle. The excited levels corresponding to hypersensitive transitions from the ground state are marked with a square. For each lanthanide, J is given to the right (in the notation of atomic spectroscopy, J is added to the Russell–Saunders terms as lower-right subscripts). When the quantum numbers S and L are reasonably well-defined, the terms are indicated to the left. It may be noted that the assignments $^3H_4$ and $^3F_4$ in thulium(III) previously were inverted; these two levels with $J \approx 4$ actually have above 60% of ^3H and ^3F character, respectively. Calculated J-levels are shown as dotted lines. They are taken from Carnall et al. (1968) who also contributed decisively to the identification of numerous observed levels, mainly by using the Judd–Ofelt parametrization of band intensities.

National Laboratory, for thermonuclear fusion in carefully prepared DT (deuterium–tritium) pellets, were huge neodymium glass lasers using the transition from the fourth excited J-level $^4F_{3/2}$ to the first excited J-level $^4I_{11/2}$. Since the latter level is 2000 cm^{-1} (about 10 kT at room temperature) above the ground state $^4I_{9/2}$, it is much easier to satisfy the primordial condition for lasers of *population inversion* (which means that the molar concentration of the emitting state is higher than that of the final state). In a Nd(III) *four-level laser*, the population of the terminal level is the fraction $\approx e^{-10} \approx 3 \times 10^{-5}$ of that of the ground state. In contradistinction, in a three-level laser (such as a ruby) at least 51% of the Cr(III) has to be pumped into the long-lived excited state in order to achieve population inversion, requiring a tremendous amount of energy. Though high-power d-group lasers (Hammerling et al., 1985) tend to have problems of self-absorption in the excited state, obscuring the laser emission, they are still the favored choice for tunable emission over a rather broad interval of photon energy, the selected laser transition going from the thermalized upper electronic state (of which the populated part stretches over a few times kT) to the broad continuum of the electronic ground state (not showing resolved vibronic structure in condensed matter, in contrast to most gaseous molecules). Hence, such a tunable laser is a four-level laser, because the luminescent transition terminates in a relatively high-lying part of the continuum following the electronic ground state, hardly showing any Boltzmann population. As discussed at the Conference on Lasers and Optoelectronics (organized by the Optical Society of America in Baltimore, May 1985, to commemorate the 25th anniversary of the ruby laser) a major candidate is crystalline alexandrite $Al_{2-x}Cr_xBeO_4$, to which we return at the end of this section. Nevertheless, the less tunable, but much more high-powered terawatt lasers are all neodymium(III) glass lasers, including the NOVETTE and NOVA systems functioning at Livermore National Laboratory since 1982 (Holzrichter, 1985; Holzrichter et al., 1985). Each of the ten lasers in NOVA is able to supply 10^5 J ns pulses at a power level of 10^{14} W.

It is not easy to give a sharp definition of a vitreous material. It is certainly amorphous in the sense of not being so crystalline as to give a Debye X-ray diffraction diagram of resolved lines. However, not all amorphous materials are vitreous, since it is felt to be necessary that vitreous materials exhibit translucency.

It is now generally recognized that any melt will freeze to a glass (noncrystalline solid) if cooled at a certain minimum rate. We therefore no longer ask *whether* a composition can be obtained as a glass, but just at *what critical cooling rate*. This concept is formalized as the *Kinetic Theory of Glass Formation* (Uhlmann and Kreidl, 1983). In an increasing number of cases the rate can be estimated from first principles, thus reinforcing the usefulness of the concept.

As to predicted or resulting glass forming *structures*, certain restricted but technologically important fields were successfully covered by certain recipes, like the Zachariasen–Warren rules. They retain some usefulness. But by and large

atomistic bases for glass formation and the resulting structures must now be considered as variable, as in the case of crystal structures. We find glasses with structures closely related to those of the corresponding crystals, as well as glasses quite different from their crystalline counterpart. We find glasses with considerable close-range order, or with complete randomness. We find covalent as well as ionic bonds. And in all these respects any intermediates.

Among the most recent texts considering glass are those by Mackenzie (1964), Wong and Angell (1976), McMillan (1979), Rawson (1980), Uhlmann and Kreidl (1980, 1983, 1984), Waseda (1980), Guntherrodt and Beck (1981), Feltz (1983), Kreidl (1984), McLellan and Shand (1984), and Vogel (1984).

Most people think of vitreous materials as exceedingly viscous liquids, but it is difficult to be perfectly certain that *all* glasses are undercooled in the sense that they would be thermodynamically stable by crystallizing in reasonably sized crystals. It is true that this is the fate of many glass samples, when kept in vacuo or in an unreactive atmosphere for weeks, years or centuries. Fortunately, thermodynamics always has a limited jurisdiction for all pragmatic purposes; in any given system, some reactions proceed to equilibrium and others (such as nuclear transmutation to iron) do not take place perceptibly.

The glasses made along the Mediterranean coast during the last three millennia are typically mixed oxides, with sodium, potassium, calcium, and lead silicates as the major components. In the last century, borates and phosphates have also gained much importance, in particular in laboratory glass, by creating mechanical strength compatible with a rather low temperature of softening ("melting"). It is a general rule of thumb among glassmakers that the more minor components are added, and the farther the glass is removed from a simple stoichiometric ratio, the less the final product runs the risk of slowly crystallizing ("devitrifying"). However, the dehydration by heating of $Na^+(HO)_2PO_2^-$ produces a glass 1Na:1P:3O with the same composition as cyclic metaphosphates $P_nO_{3n}^{-n}$ and almost the same composition as the chain polyphosphates obtained by intercalating PO_3 groups (such as CH_2 links in *n*-alkanes) in pyrophosphate, giving $O_3P(OPO_2)_{n-2}OPO_3^{-n-2}$. There is good reason to believe that the $NaPO_3$ glass contains nearly all its P(V) as localized tetrahedral groups (as in the polyphosphates) surrounded by four terminal or bridging oxygen atoms. Even chemical elements can be vitreous; high-purity selenium can be prepared as a translucent red glass, analogous to the metastable latex-like modification of sulfur obtained by rapid cooling of the red-brown melt with cold water.

The textbooks describe the industrially important types of glass as large network modifier cations Na(I), K(I), Ca(II), Pb(II), . . . , accommodated (with rather long M–O internuclear distances) within the cavities of the network former, the ramified polyanion formed by borate, silicate, phosphate, . . . , or by a mixture of such oxo-complexes of small atoms of nonmetallic elements. However, the real situation may be even more complicated, as exemplified by the fluoride glasses in section 6.1. The absorption spectra (Weyl, 1959; Landry et al., 1967) of

d-group ions clearly indicate octahedral coordination of green $Cr(III)O_6$ (comparable to crystalline corundum-type Cr_2O_3 and beryl-type emerald $Be_3Al_{2-x}Cr_xSi_6O_{18}$), pale green $Fe(II)O_6$, pink $Co(II)O_6$, and yellow to green $Ni(II)O_6$. This octahedral trend is likely to occur also for $Mg(II)O_6$. On the other hand, the large Ca(II), Th(IV), and all the rare earths, may accept various *coordination numbers* $N = 7, 8, 9, 10, \ldots$, and different (usually low) symmetries for the local site. It is worth noting that N in inorganic compounds (generally consisting of anion-bridged architectures as opposed to molecules, allowing N to be above the oxidation state) is essentially, but not entirely, determined by relative atomic size (Jørgensen and Reisfeld, 1982b; Jørgensen, 1983, 1984) and that the aqua ions, in hydrated crystals and in solution, fall into three main categories: strictly tetrahedral $N = 4$, such as $Be(OH_2)_4^{+2}$, the large group of octahedral $N = 6$, and then the high N independent of local symmetry. Among cations in aqueous solution, a fourth group of exceptionally large cations such as Rb^+, Cs^+ and Ba^{+2} may have the same relationship to the ambient solvent as $N(CH_3)_4^+$ and $Co(NH_3)_6^{+3}$. In a sense, such ions may start with the second hydration sphere surrounding $Cr(OH_2)_6^{+3}$.

The picture of high, varying N and widely differing local symmetry has been verified for fluorescent trivalent lanthanides by measurements of inhomogeneous linewidth. The technique FLN (fluorescence line-narrowing) has been used for excitation of the nondegenerate state $^5D_0$ of Eu(III), and for determining the various sites (Brecher and Riseberg, 1976; Durville et al., 1983), vide infra.

Our description so far has assumed a straightforward glass, without evidence of regular structure on a scale of 100 or 1000 Å. It is possible to perform experiments in the future (assisted by electron micrographs) of conceivable relations between FLN and inhomogeneities in the micrometer (10000 Å) range. However, we possess even today materials that are manifestly heterogeneous on such scales, but which still remain vitreous.

Among such materials are the consecutive intermediate states (gel glass → fully dehydrated glass) (Levy et al., 1984), where by heating to 110°C or 200°C the emission spectrum of incorporated Eu(III), obtained by hydrolysis of $Si(OCH_3)_4$ at room temperature (similar to aqua ions in D_2O), changes to stronger bonding to the silica gel and concomitant more detailed and intense bands; by heating of the sample to 600°C the spectrum becomes similar to that of Eu(III) in conventional silicate glass. It may be noted that the hypersensitive transition (cf. section 2.2) $^5D_0 \rightarrow {}^7F_2$ becomes much more intense in the heat-treated gel glass, similar to the saturated red cathodoluminescence $Eu_xY_{2-x}O_2S$, which is more suitable for color television than $Eu_xY_{1-x}VO_4$, which was used originally (Blasse, 1979). There is a large future open for preparation of gel glass below 100°C by hydration and dehydration of appropriate mixtures of alkoxides such as $B(OA)_3$, $Al(OA)_3$, $Si(OA)_4$, $Ti(OA)_4$, ... Among several advantages are that rare-earth complexes of organic ligands and fluorescent organic dye stuffs can be incorporated without excessive heating (Reisfeld et al., 1983b) and (partly because of absence of

collisions between excited states, quenching their luminescence in solvents of low viscosity) frequently with exceptionally high quantum yields.

The commercially available Vycor glass (Corning 7930) consists essentially of 96 wt% SiO_2 and $4B_2O_3$. The chemically reactive precursor of this glass has been leached by hot hydrochloric acid to remove large amounts of alkali borates, the product having pores with an average diameter of 40 Å and 28% void volume. This Vycor glass, when stored, is usually soaked with distilled water, which can be replaced by an aqueous salt solution after desiccation. The fluorescence spectra of seven lanthanides adsorbed in such porous glass (Mack et al., 1983) are much more intense than of aqua ions, and again with strong hypersensitive transitions. It may be noted that the quantum yield of the lowest $4d^6$ triplet state (just below the intense, inverted electron-transfer band, where a 4d-like electron jumps to the lowest-lying empty molecular orbital delocalized on the heterocyclic ligands) of the ruthenium(II) dipyridyl complex $Ru(dip)_3^{+2}$ is much higher in porous glass (Reisfeld et al., 1983b) than in low-viscosity solvents, and the same is true for several fluorescent organic ions and molecules (Wheeler and Thomas, 1982; Reisfeld et al., 1983b; Avnir et al., 1984). Such enhanced luminescence (and decreased photodegradation of the organic colorants) is of great interest for flat-plate solar concentrators using consecutive total reflections of the trapped light (Reisfeld and Jørgensen, 1982), and perhaps also for lasers, as discussed in section 3. It is important to note that in all cases gel glasses and porous glasses can be prepared with the dimensions of heterogeneous composition much smaller than the wavelength of visible light, thus avoiding light scattering.

Frequently, devitrification of a glass produces a fine dispersion of extremely small crystallites of a stoichiometric composition differing from the original glass. Thus, a few percent of rare earths form permanently limpid glasses with 60 to 70 wt.% WO_3 and the $Na_4P_2O_7$ forms the remaining 30 to 40%. However, in systems where more than 70% tungsten(VI) oxide occurs, microcrystallites of orthophosphates are precipitated. X-ray powder-diagrams show existence of $PrPO_4$ and $EuPO_4$ of the monoclinic monazite-type and $HoPO_4$ and $TmPO_4$ of the tetragonal xenotime- (zircon-) type (Reisfeld et al., 1975; Mack et al., 1981, 1985). It should be noted that powder-diagram lines of crystallites do not exclude the presence of larger amounts of a vitreous phase. The europium(III) fluorescence of such phospho-tungstate glasses has been selectively excited in the crystalline and vitreous components (Durville et al., 1983), and provides interesting information about the holohedrized symmetry and the differing behavior of the local site in the vitreous phase.

Molten glasses which have been heated under such circumstances that a major component of the cooled material is microcrystallites, are, when cooled, called *glass ceramics*. Such materials are well-known from opalescent kitchenware, and generally they show more mechanical strength against breaking and scratching than conventional glasses. For spectroscopists, it is interesting that translucent, and even limpid glass ceramics can be obtained, where all the microcrystallites are

considerably smaller than the wavelength of violet light. The preparation of such transparent glass ceramics may need somewhat special conditions. Thus chromium(III) in 0.2 molar concentration (1.2×10^{19} ions/cm^3) has been incorporated in glass ceramics prepared typically at 1570°C with titanium(IV) or zirconium(IV) oxide as the nucleating agent (Reisfeld et al., 1984a; Kisilev et al., 1984; Bouderbala et al., 1985; Reisfeld et al., 1986b). Cr(III) concentrates in the microcrystallites are shown from powder diagrams to be the cubic spinel-type $MgAl_{2-x}Cr_xO_4$ and $ZnAl_{2-x}Cr_xO_4$ (gahnite), or the less stoichiometric types, petalite and β-quartz; and the quantum yield of emission from both the lowest excited quartet and doublet state is exceptionally large. This may represent a useful alternative to crystalline alexandrite $Al_{2-x}Cr_xBeO_4$ as laser material, avoiding handling the highly toxic BeO dust during the preparation. Further work on europium(III) and other rare earths in glass ceramics is in progress in Haifa and Jerusalem.

2. Intensities of absorption and emission

The J-levels of trivalent lanthanides, containing a partly filled shell $4f^q$, have the paradoxical aspect of being treated as atomic spectra, while the corresponding gaseous ions, M^{+3}, are hardly known (Martin et al., 1978; Goldschmidt, 1978). Disregarding comments made by Ellis in 1936, to the effect that ^3P of $4f^2$ produces the three narrow bands of Pr(III) in the blue, the identification started (Gobrecht, 1937, 1938) around the single absorption band of ytterbium(III) at 10300 cm^{-1} due to a transition from $^2F_{7/2}$ to the only other J-level, $^2F_{5/2}$ of $4f^{13}$. This energy difference demonstrates spin–orbit coupling nearly as strong as in the 6p shell of the mercury atom, and was used by Gobrecht for his estimation of the total width $(2L+1)\zeta_{4f}$ of the lowest (S, L) term of other $4f^q$ in the asymptotic limit of Russell–Saunders coupling. It is interesting for our purposes that he used a vitreous material, the borax bead of molten $Na_2B_4O_7$ (introduced by Berzelius for blowpipe analysis of minerals) for the infrared spectra. This was done to avoid the O–H stretching frequency close to 3500 cm^{-1} and its numerous overtones (Jørgensen, 1985), looking like narrow, weak $4f^q$ bands. For the same reason, Carnall (1979) has used perchlorates in deuterium oxide since 1962 and has also studied spectra in a mixture of $LiNO_3$ and KNO_3 melting at 150°C. For reasons to become apparent below, the proton-free borax bead also showed several fluorescent lines, which were helpful in identifying low-lying J-levels. Narrow-line emission of Sm(III), Eu(III), and Tb(III) had been studied by Tomaschek and Deutschbein since 1932. For comparison it may be mentioned that the level of Yb^{+3} lies at 10214 cm^{-1} (Bryant, 1965). We know twelve among the 13 J-levels of Pr^{+3} (Sugar, 1965). The highest $^1S_0$ has remained controversial, though it is detected (Lee et al., 1984) close to 47000 cm^{-1} in Pr(III). Finally, the seven J-levels of ^7F in $[54]4f^8Tb^{+3}$ between 0 and 5654 cm^{-1} (Spector and Sugar, 1976)

are the only instances of J-levels of $[54]4f^q$ identified in *gaseous* M^{+3}. Many such J-levels, however, have been identified (Martin et al., 1978) in Pr^{+2}, Nd^{+2}, Sm^{+2}, Eu^{+2} (the first excited $^6P_{7/2}$ at 28200 cm^{-1}), Gd^{+2} (where the lowest $[54]4f^8$ level $^7F_6$ is situated 2381 cm^{-1} above the ground state $^9D_2$ belonging to $[54]4f^75d$), Tb^{+2}, Ho^{+2}, Er^{+2}, and Tm^{+2}. Such M^{+2} allow interesting comparisons with the (almost coinciding) J-levels of $[54]4f^q6s^2$ in the gaseous M atom. For $q = 2$ to 12, the parameters of interelectronic repulsion in the SCS (Slater–Condon–Shortley) treatment, as streamlined by Racah (1949) (cf. Goldschmidt, 1978) are even more prominent than the Landé parameter ζ_{4f} of spin–orbit coupling, known to increase smoothly from 644 cm^{-1} in Ce^{+3} to 2918 cm^{-1} in Yb^{+3}, and hence, the model for the numerous J-levels (119 for both $q = 6$, 7, and 8) is technically intermediate coupling, though the lowest (S, L) term is remarkably close to Russell–Saunders coupling. Since there are three independent parameters of interelectronic repulsion, the pioneer work on $4f^{12}$ thulium(III) (Bethe and Spedding, 1937) and on $4f^3$ neodymium(III) (Satten, 1953) uncritically adopted an assumption about quite small ratios F^6/F^2 (SCS) and E^1/E^3 (Racah), resulting in good agreement with the energy differences between terms with the same S_{max} as the ground term (these distances are always multiples of E^3), whereas terms with $S = (S_{max} - 1)$ were predicted far too low (Jørgensen, 1955). However, since the J-levels are quite crowded from $q = 4$ to 10, the complete calculations in intermediate coupling (Jørgensen, 1957b; Elliott et al., 1957) were not sufficiently convincing for assignments in cases where several J-levels were predicted within an interval of a few thousand cm^{-1}. The last identifications of J-levels exclusively based on predicted energies were probably $4f^{11}$ erbium(III) (Wybourne, 1961), and subsequent work was significantly assisted by the Judd–Ofelt theory for intensities discussed in section 2.1 (Carnall et al., 1968).

Whereas the position of J-levels of $4f^q$ in condensed matter is treated by the same techniques as monatomic entities, the probabilities of absorption and emission between J-levels are an entirely different problem. In gaseous M^{+3} nearly all observable transitions (Condon and Shortley, 1953) are *electric dipolar*, occurring between states of opposite (even and odd) parity (if the electron configuration is a satisfactory description, one electron changes its l value one unit up or down) and J obeys the selection rule $J \rightarrow (J + 1)$, J or $(J - 1)$, and at least one of the J values (original and final state) is positive. Hence, many atoms are left with metastable states (such as the first excited $J = 2$ state of neon, argon, krypton, and xenon, or the first odd $J = 0$ state of mercury) which cannot decay radiatively to the ground state, but can disappear only by further excitation (by absorbing another photon) or by collisions with other atoms or surfaces. A highly excited J-level of a monatomic entity typically cascades down through a series of intermediate states (each time of opposite parity), and may encounter difficulties in arriving all the way down to the ground state. For instance, as soon as a J-level of M^{+3} belongs, like all subsequent lower J-levels, to the configuration $[54]4f^q$, there is hardly any hope left for downward transitions if M^{+3} is sufficiently

isolated at low pressure in an electric discharge. Such levels (Martin et al., 1978) have mainly been determined from their transitions to and from $[54]4f^{q-1}5d$ of opposite parity.

The fundamental concept for transition probabilities in monatomic entities is the *oscillator strength* P (called f by many authors). Einstein pointed out in 1917 that if the interactions between an isolated atom and the photons in the electromagnetic field (providing an energy density per unit volume proportional to T^4 at a state of thermal equilibrium, and hence a specific heat of empty space proportional to T^3) did not modify the distribution of momentum mv, the probability A_{ij} going from the state E_i to one of the lower states E_j is a constant of nature times the cube of the frequency ν_{ij}^3 times the probability of absorption B_{ji}, going from E_j to E_i. In this thermodynamical argument, not involving the detailed electronic structure of the atom, *spontaneous emission* was predicted as an enhancement of emission in the case of increasing concentration of E_i if thermal equilibrium with E_j is not established (Reisfeld and Jørgensen, 1977).

When quantum mechanics developed after 1925, the oscillator strength was introduced for atoms $P = A_{ij}mc/8\pi^2\sigma^2e^2$ (with $\sigma = \nu/c$ the wave number) and for electric-dipole transitions, $P = (e_2/e_1)\,\langle|\bar{r}|^2/\text{bohr}^2\rangle$ ($h\nu/3$ rydberg) with the electric dipole moment $\bar{r}$ (the "transition moment") of $\Psi_1\,\Psi_2$ where e_1 states possess the same energy E_1 (the "degeneracy number") and e_2 mutually orthogonal states have E_2. Hence, the lifetime τ of the exponential decay of unperturbed atoms is, with $1\text{ eV} = 8065.48\text{ cm}^{-1}$:

$$\tau = (e_2/e_1)\,2.3 \times 10^{-8}\text{ s}/P(h\nu/\text{eV})^2\,. \tag{1}$$

The half-life $t_{1/2}$ (usually given for radioactive decay) is $\tau(\ln 2)$ with the result that $\tau = 1.4427\,t_{1/2}$ and the unit of time in eq. (1) is 1.6×10^{-8} s for the half-life. It is a quantum-mechanical sum rule that the absorption lines in a system with K electrons have the sum of all P values equal to K. This means that most of the oscillator strength for higher K originates in inner shells, which is of importance not only for X-ray absorption spectra, but also in determining electric polarizabilities (Salzmann and Jørgensen, 1968; Jørgensen, 1975) proportional to the summation over $P/(h\nu)^2$. In most cases, a major part of P is due to transitions to continuum states rather than to discrete levels. The P can be evaluated for the hydrogen atom (Condon and Shortley, 1953) and its value is 0.416 for the Lyman α line $1s \rightarrow 2p$, 0.079 for $1s \rightarrow 3p$ and only 0.07 for all the higher $1s \rightarrow np$. In comparison with hydrogen, the transitions in the sodium atom from [10]3s to [10]3p have $P = 0.32$ for $^2P_{1/2}$ and 0.65 for $^2P_{3/2}$ [approximately proportional to the number $e = (2J + 1)$ of states in the excited level], and atoms with two outer s electrons (except helium) can show P for $^1S_0 \rightarrow {}^1P_1$ of the order 1.5.

Even though Einstein's argument for a Maxwellian distribution of mv cannot be strictly applied in condensed matter, his relation between transition probabilities in emission and absorption still holds. Chemists usually introduce a molar

extinction coefficient ε via Beer's law

$$\log_{10}(I_0/I) = \varepsilon cl = [\varepsilon_1 c_1 + \varepsilon_2 c_2 + \cdots]l \tag{2}$$

for a single species in concentration C (moles/1000 cm^3) in a path l (cm) attenuating the intensity of monochromatic light from I_0 to I (the term between braces indicates the result of additive absorption of species simultaneously present), and the area as a function of wave number σ ($h\nu = hc\sigma$) gives

$$P = 4.32 \times 10^{-9} \int_{\text{band}} \varepsilon \, \mathrm{d}\nu = 9.20 \times 10^{-9} \varepsilon_{\max} \delta \, , \tag{3}$$

where the second expression is the result for a Gaussian error curve having the maximum $\varepsilon_{\max}$ at $\sigma_{\max}$ and the one-sided half-width δ, that is $\varepsilon = \varepsilon_{\max}/2$ for $(\sigma_{\max} + \delta)$ and for $(\sigma_{\max} - \delta)$.

In comparison with the yellow sodium lines, P for most inorganic compounds is rather modest (Jørgensen, 1963). The highest value for a band in the visible is 0.18 for PtI_6^{-2} and the electron transfer band of MnO_4^- in the green has only $P = 0.03$.

2.1. *Judd–Ofelt parameters*

The typical values of P between 10^{-7} and 10^{-5} clearly show that the absorption bands of trivalent lanthanides in solution, glasses, and crystals are strongly forbidden. On the other hand, most excited J-levels in the visible give absorption bands of comparable area, excepting the moderate to low intensity of spin-forbidden transitions (as known from atomic spectra), modifying the total spin-quantum numbers S in the Russell–Saunders approximation.

Broer, Gorter and Hoogschagen (Broer et al., 1945) analyzed this situation, based on a quite complete set of P values for aqua ions between 9000 and 30000 cm^{-1}, and concluded that the major mechanism for transitions is induced electric-dipole arising from a very weak mixing of the order of magnitude of the ground state $4f^q$ wave function (being odd for q odd, and even for q even) with functions of the opposite parity. Two kinds of external perturbations were suggested, deviations from a local center of inversion of the distribution of nuclei of neighbor atoms, and deviations on a short time scale (Jørgensen, 1971) due to vibrational motion of neighbor nuclei. The distinction between these two mechanisms may make sense in crystals, but is very moot in liquids. The two explanations have in common a rather tolerant selection rule, namely that J at most changes by 6 units (this is derived from the triangular conditions of Gaunt, 6 being twice the $l = 3$ for f electrons); and since at most twenty J-levels had been identified in the visible, it was not felt to provide a very informative restriction. Broer et al. (1945) argued that a few transitions might be *magnetic dipolar*, where the transition

probabilities can be evaluated (Condon and Shortley, 1953) without going beyond the monatomic picture. However, not only is it a selection rule for magnetic dipolar transitions that J changes by at most 1 unit, but nearly all the probability (for $q \neq 7$) is concentrated on the transition to the first excited level of the same term, normally situated in the far infrared. Carnall et al. (1968) have tabulated the corresponding oscillator strengths P_{md}, which are of the order of magnitude of 10^{-7}. Several spin-forbidden transitions in the visible and ultraviolet may show P_{md} slightly below 10^{-7}. A famous case is $^7F_0 \rightarrow {}^5D_1$ at 19000 cm^{-1} and $^7F_1 \rightarrow {}^5D_0$ at 16800 cm^{-1} of $4f^6$ europium(III), where both transitions are known, both in absorption and in emission, e.g. in fluoride glasses (Reisfeld et al., 1983c).

The arguments about low local symmetry allowing electric dipolar transitions to a small extent were rendered much more quantitative by two independent studies (Judd, 1962; Ofelt, 1962). In the Judd–Ofelt treatment, there are six kinds of parameters, falling in two quite distinct categories. Supposing the total wave function for a given initial J-level is known in intermediate coupling, $\langle f^q[\gamma SL]J|$, and for a given terminal J'-level (all primes referring to the terminal level), it is possible to evaluate nondiagonal elements between the unprimed and the primed wave functions of *three tensors*, $U^{(t)}$, with $t = 2$, 4, and 6. On the other hand, the neighbor material in condensed matter (or in a gaseous molecule) is characterized by three *material parameters* Ω_t. The radiative rates of emission are given in eq. (8) in section (2.5), where the strength of magnetic dipolar transitions, S_{md}, has been explicitly evaluated by Carnall (1979) in eqs. (24.11) to (24.14). As discussed by Peacock (1975) and Carnall (1979), previously there were used slightly different material parameters, for which the transcription to Ω_t is well-defined, but the latter parameters (usually given in the unit square picometer $1\ pm^2 = 10^{-20}\ cm^2$) have turned out to be more practical. The oscillator strength P for an absorption band, from which (the usually much smaller) P_{md} deriving from the probability as magnetic-dipole transition has been subtracted, is then

$$P - P_{md} = \frac{8\pi^2 m\nu}{27h(2J+1)} \frac{(n^2+2)^2}{n} [\Omega_2 U_2 + \Omega_4 U_4 + \Omega_6 U_6], \tag{4}$$

where m is the mass of the electron. For $n = 1.5$, eq. (4) has the numerical form (J being for the initial state before absorption)

$$P - P_{md} = 1.204 \times 10^{10} \frac{\sigma}{(2J+1)} 12.04[\Omega_2 U_2 + \Omega_4 U_4 + \Omega_6 U_6], \tag{5}$$

where the constant 12.04 is replaced by 18 for $n = 2$ and by 10.70 for $n = 1.333$ (water). Originally, both Judd and Ofelt, and several other pioneers, hoped to derive the material parameters Ω_t from wave functions of the lanthanide and of the neighbor (ligating) atoms, but it does not seem to have succeeded better than

within one order of magnitude. What is more deplorable is that comparative calculations on highly differing materials do not illustrate the trends such as the ratio (Ω_2/Ω_6) discussed below. It is worthwhile to note that Krupke (1966) concluded that the spectroscopically accessible configuration $4f^{q-1}5d$ (cf. Jørgensen, 1969) is not nearly as important for the size of Ω_t as $4f^{q-1}g$, where it is clear that the g-like radial function in condensed matter has a much smaller average radius than the almost hydrogenic 5g-radial functions (even in atoms with Z as high as radium).

For trivalent lanthanides with q from 2 (praseodymium) to 12 (thulium), eq. (5) is overdetermined, in so far as only three Ω_t have to be determined from typically 5 to 16 experimental P values. This gives rise to a statistical uncertainty for each Ω_t, which turns out to be 15 to 50%, indicating the varying degree of validity of the Judd–Ofelt treatment in differing cases. On the other hand, the matrix elements U_t do hardly vary at all when the same M(III) is incorporated in different materials. Since the nephelauxetic effect shifts the J-level energy differences mainly by a scaling factor 0.97 to 1.01, it is rare that the modified eigenvectors in intermediate coupling influence U_t by as much as 10 percent, which is negligible compared to the uncertainty of Ω_t inherent in eq. (5). It is true, of course, that the 4f group M(II), or 5f group M(III), or M(IV) would have entirely different U_t.

2.2. Ω_2 *as indicator of covalent bonding*

Around 1955 it was generally felt that a given $4f^q$ transition in a given trivalent lanthanide produces an absorption band of roughly the same area in different environments, and hence roughly the same oscillator strength P according to eq. (3). Then, Moeller and Ulrich (1956) reported that tris(acetylacetonates) of neodymium(III), holmium(III) and erbium(III) have one, two, and two absorption bands of unheard of intensity, respectively, more than 10 times higher than in the aqua ions, and considerably broader. At first, this unexpected phenomenon was compared with anomalous high band intensities in d-group complexes of phosphines and arsines (Jørgensen, 1969) and it might be explained by a few of the $4f^q$ transitions borrowing intensity from the exceedingly strong bands of the "conjugated" ligands in the near ultraviolet. Then Carnall (1979) found the same bands to be quite intense in molten nitrates, and it remained a general characteristic of such cases that the ligands had some "conjugated" features, like bidentate nitrate, carbonate, acetate, and other carboxylates and anions of biological and synthetic amino-acids (Bukietynska and Choppin 1970; Karraker, 1971; Henrie et al., 1976).

Jørgensen and Judd (1964) discussed this spectacular behavior, pointing out that the examples had in common an extremely high value of Ω_2 in eq. (5), and they proposed to call transitions with a large matrix element U_2 *hypersensitive*

pseudoquadrupolar. In monatomic entities (Condon and Shortley, 1953) a few electric-quadrupole transitions are known, such as [18]4s→[18]3d in potassium with $P \sim 10^{-6}$, but it would be difficult (Broer et al., 1945) to obtain P above 10^{-7} in lanthanides, which is entirely insufficient. This is the reason why these transitions are not considered genuine quadrupolar. However, the matrix elements U_2 are exactly those determining the quadrupole strength S_{eq} and the hypersensitive transitions in lanthanide(III) compounds are pseudoquadrupolar in the sense that they have the same absolute selection rules (J changing at most 2 units) and numerical relative size. In the asymptotic limit of Russell–Saunders coupling, by far the largest U_2 occurs (for transitions from the ground state S_0, L_0, J_0) to the level (S_0, $L_0 - 2$, $J_0 - 2$), such as $^4G_{5/2}$ in the yellow of Nd(III). In lanthanides, intermediate coupling is sufficiently pronounced that two levels of Ho(III) with $J = 6$ at 22100 and 27700 cm^{-1} have large U_2 (representing mixtures of $^5G_6$ with $^3H_6$) and two levels of Er(III) with $J = 11/2$ at 19200 and 26400 cm^{-1} ($^4G_{11/2}$ mixed with $^2H_{11/2}$ in the case of the lower level in the green; for eigen-vectors, see Wybourne, 1961).

The hypersensitive pseudoquadrupolar transitions represent by far the most extensive variation of $4f^q$ intensity, the most extreme case being NdI_3 vapor (Gruen and DeKock, 1966) where the transition to $^4G_{5/2}$ has $\varepsilon_{max} = 345$ and $P = 5.3 \times 10^{-4}$, 60 times as high as in the aqua ion. The first idea one gets is a decisive influence of strong covalent bonding related to the low electronegativity of the iodide ligands, and to the unusually short internuclear distance corresponding to the exceptionally low coordination number N. Jørgensen and Judd (1964) discussed several alternatives for explaining high Ω_2, the most plausible being the imperfection of describing the surrounding atoms by an invariant dielectric constant n, as inherent in the semiclassical correction factors containing n in equations (4) and (8). This explanation, based on an *inhomogeneous dielectric constant* (as conceivable already in a gaseous NdI_3 molecule), still seems to be the most attractive (Peacock, 1975; Judd, 1979) and, in his 1979 paper, Judd gave up especially the idea prevailing in the end of the sixties that the major condition for a large Ω_2 is a sufficiently low local symmetry for allowing one vector (or one p orbital, if one prefers) to have total symmetry. This condition had been related to the possibility of the "ligand field" (Jørgensen, 1971) containing a specific component enhancing pseudoquadrupolar transitions. The concept of the dynamic polarization of the ligand electronic structure by the quadrupole moment of the optical transition has been applied (Mason, 1979 and 1980) both to the 4f and the d-group compounds. This concept is closely related to that of the inhomogeneous dielectric constant (Judd, 1979).

Table 1 gives the three Ω_t values for a series of compounds of eight trivalent lanthanides. Rather than attempting to give a complete compilation of the rather unwieldy literature, we attempt to select the values with the lowest degree of uncertainty (inherent in the overdetermined equations, when more than three transitions are taken into account). Obviously, the emphasis is on vitreous

TABLE 1
Judd–Ofelt parameters (unit: 1 $pm^2 = 10^{-20}$ cm^2). *

Lanthanide, material	Ω_2	Ω_4	Ω_6	Reference **
$4f^2$ praseodymium(III)				
$Pr_xLa_{1-x}F_3$ crystal	0.12 ± 0.9	1.77 ± 0.8	4.78 ± 0.5	a
ZBLA fluoride glass	0.12 ± 0.2	3.7 ± 0.5	5.3 ± 0.4	b
Li_2O, B_2O_3 glass	0.8 ± 1.4	3.8 ± 0.6	3.6 ± 0.6	c
Na_2O, B_2O_3 glass	0.8 ± 1.5	4.1 ± 0.6	3.1 ± 0.7	c
K_2O, B_2O_3 glass	2.1 ± 0.9	2.9 ± 0.4	1.7 ± 0.4	c
Na_2O, TeO_2 glass	2.8 ± 1.9	6.5 ± 0.8	4.6 ± 0.8	c
ZnO, TeO_2 glass	2.6 ± 2.0	7.3 ± 0.8	5.4 ± 0.9	c
BaO, TeO_2 glass	4.9 ± 2.4	6.5 ± 1.1	5.4 ± 1.1	c
$4f^3$ neodymium(III)				
$Nd_xLa_{1-x}F_3$ crystal	0.35 ± 0.14	2.57 ± 0.36	2.50 ± 0.33	a
fluoroberyllate glass	0.23 ± 0.27	3.92 ± 0.40	4.60 ± 0.12	d
fluorophosphate glass	1.86 ± 0.28	4.13 ± 0.41	5.02 ± 0.18	d
$50ZrF_4:23BaF_2:25NaF:2NdF_3$	1.95 ± 0.26	3.65 ± 0.38	4.17 ± 0.17	e
Nd(III) aqua ion, solution	0.93 ± 0.3	5.00 ± 0.3	7.91 ± 0.4	f
$Nd_xY_{3-x}Al_5O_{12}$ crystal	0.2	2.7	5.0	g
$Nd_xY_{1-x}AlO_3$ crystal	1.24	4.68	5.85	h
$Nd_xGd_{2-x}(MoO_4)_3$ crystal	4.22	2.57	2.35	i
$Li_2O:2\ SiO_2$ glass	3.3	4.9	4.5	j
$Na_2O:2\ SiO_2$ glass	4.2	3.2	3.1	j
$K_2O:2\ SiO_2$ glass	5.0	2.4	2.0	j
$Na_2O:5\ SiO_2$ glass	4.1	2.9	2.6	j
$0.4\ Nd_2O_3:99.6\ SiO_2$ glass	6.1	4.5	4.3	j
$15\ Li_2O:20\ BaO:65\ SiO_2$ glass	2.8	4.0	3.9	j
$15\ Na_2O:20\ BaO:65\ SiO_2$ glass	3.6	3.4	3.5	j
$15\ K_2O:20\ MgO:65\ SiO_2$ glass	5.1	4.1	2.8	j
$15\ K_2O:20\ CaO:65\ SiO_2$ glass	4.6	3.6	2.9	j
$15\ K_2O:20\ SrO:65\ SiO_2$ glass	3.8	3.3	2.7	j
$15\ K_2O:20\ BaO:65\ SiO_2$ glass	3.7	2.8	2.3	j
$15\ K_2O:18\ BaO:66\ B_2O_3$ glass	3.9	3.9	4.3	j
$15\ K_2O:18\ BaO:66\ P_2O_5$ glass	2.7	5.4	5.4	j
$15\ K_2O:18\ BaO:66\ GeO_2$ glass	6.0	3.7	2.9	j
$20\ Na_2O:79\ TeO_2$ glass	4.06 ± 0.16	4.8 ± 0.2	4.6 ± 0.1	k
$Nd_xY_{2-x}O_3$ crystal	8.55 ± 0.4	5.25 ± 0.8	2.89 ± 0.6	a
$LiNO_3 + KNO_3$ melt	11.2 ± 0.3	2.6 ± 0.3	4.1 ± 0.4	l
$0.13\ Nd_2S_3:0.87\ La_2S_3:3\ Al_2S_3$ glass	9.45	4.84	6.54	m
$NdW_{10}O_{35}^{-7}$ in solution	0.8 ± 0.5	5.6 ± 0.6	7.0 ± 0.3	n
$Nd(dbm)_3$ in methanol	48	5.3	12.4	o
$Nd(dbm)_3, H_2O$ crystal	45	12	1.2	p
$NdBr_3$ vapor	180	9	9	q
$CsNdI_4$ vapor	130	–	–	r
NdI_3 vapor	275	9	9	q
$4f^5$ samarium(III)				
Sm(III) aqua ion, solution	0.9 ± 0.8	4.1 ± 0.3	2.7 ± 0.3	f

TABLE 1 (continued)

Lanthanide, material	Ω_2	Ω_4	Ω_6	Reference **
$4f^5$ samarium(III) (*cont'd*)				
borate glass	2.42	4.62	4.16	s
phosphate glass	4.31	4.28	5.78	s
germanate glass	3.97	3.33	2.85	s
tellurite glass	3.17	3.65	1.61	s
$LiNO_3 + KNO_3$ melt	8.1 ± 2	4.5 ± 0.5	3.7 ± 0.5	l
$4f^6$ europium(III)				
$Eu_xLa_{1-x}F_3$	1.19	1.16	0.39	t
zirconium fluoride glass	0.93	2.61	2.17	u
Eu(III) aqua ion, solution	1.46	6.66	5.40	f
phosphate glass	4.12	4.69	1.83	u
$Eu_xY_{1-x}AlO_3$ crystal	2.7	6.3	0.8	h
$Eu_xY_{2-x}O_3$ crystal	9.9	2.2	0.3	v
$4f^9$ dysprosium(III)				
$Dy_xLa_{1-x}F_3$ crystal	1.1	1.4	0.9	w
Dy(III) aqua ions, solution	1.5	3.44 ± 0.2	3.46 ± 0.3	f
Na_2O, P_2O_5 glass	1.46 ± 2.0	1.16 ± 0.2	1.97 ± 0.1	c
Na_2O, TeO_2 glass	3.7 ± 1.4	1.15 ± 0.2	2.22 ± 0.1	c
ZnO, TeO_2 glass	4.3 ± 1.4	1.32 ± 0.2	2.53 ± 0.1	c
BaO, TeO_2 glass	3.2 ± 0.9	1.35 ± 0.1	2.47 ± 0.1	c
$LiNO_3 + KNO_3$ melt	14.4 ± 0.3	1.4 ± 0.4	3.16 ± 0.2	l
$4f^{10}$ holmium(III)				
$Ho_xLa_{1-x}F_3$ crystal	1.16	1.38	0.88	h
ZBLA fluoride glass	2.28	2.08	1.73	x
ZBLA fluoride glass	2.43 ± 0.03	1.67 ± 0.09	1.84 ± 0.03	y
Ho(III) aqua ion, solution	0.36 ± 0.1	3.14 ± 0.2	3.07 ± 0.2	f
$Ho_xY_{1-x}AlO_3$ crystal	1.82	2.38	1.53	h
Li_2O, CaO, B_2O_3 glass	6.83 ± 0.3	3.15 ± 0.4	2.53 ± 0.3	z
phosphate glass	5.60 ± 0.3	2.72 ± 0.4	1.87 ± 0.3	z
tellurite glass	6.92 ± 0.2	2.81 ± 0.3	1.42 ± 0.2	z
$LiNO_3 + KNO_3$ melt	16.4 ± 0.2	3.6 ± 0.3	2.3 ± 0.2	l
$La_2S_3 : 3\ Al_2S_3$ glass	8.1	3.8	1.4	m
$HoW_{10}O_{35}^{-7}$ solution	3.5 ± 0.2	2.4 ± 0.3	2.6 ± 0.2	n
$4f^{11}$ erbium(III)				
$Er_xLa_{1-x}F_3$ crystal	1.07	0.28	0.63	aa
$46\ PbF_2 : 22\ ZnF_2 : 30\ GaF_3$ glass	1.54 ± 0.25	1.13 ± 0.4	1.19 ± 0.2	ab
ZBLA fluoride glass	2.54	1.39	0.96	ac
ZBLA fluoride glass	3.26	1.85	1.14	ab
Er(III) aqua ion, solution	1.59 ± 0.12	1.95 ± 0.2	1.90 ± 0.1	f
$ErCl_3, 6H_2O$ in CH_3OH	3.20 ± 0.22	3.25 ± 0.16	0.8 ± 0.3	ad
$ErCl_3, 6H_2O$ in C_2H_5OH	5.0 ± 0.2	2.5 ± 0.2	0.6 ± 0.3	ad
$ErCl_3, 6H_2O$ in $n\text{-}C_3H_7OH$	5.5 ± 0.2	2.5 ± 0.2	0.7 ± 0.3	ad
$Er_xY_{1-x}AlO_3$ crystal	1.06	2.63	0.78	h

TABLE 1 (continued)

Lanthanide, material	Ω_2	Ω_4	Ω_6	Reference **
$4f^{11}$ erbium(III) (*cont'd*)				
$Er_xY_{0.5-x}Zr_{0.5}O_{1.75}$ crystal	2.92 ± 0.2	0.78 ± 0.3	0.57 ± 0.2	ae
$Er_xY_{2-x}O_3$ crystal	4.6 ± 0.3	1.2 ± 0.2	0.48 ± 0.3	a
borate glass	11.3 ± 0.6	3.6 ± 1	2.2 ± 0.5	af
phosphate glass	9.9 ± 0.5	3.7 ± 0.8	1.9 ± 0.4	af
germanate glass	9.3 ± 0.4	1.5 ± 0.6	0.7 ± 0.3	af
tellurite glass	11.8 ± 0.3	2.0 ± 0.3	1.7 ± 0.2	af
$LiNO_3 + KNO_3$ melt	15.8 ± 1.2	2 ± 2	1.4 ± 0.9	l
$La_2S_3 : 3\,Al_2S_3$ glass	3.74	4.33	0.90	m
$ErW_{10}O_{35}^{-7}$ in solution	6.7 ± 0.7	2.3 ± 0.4	1.4 ± 0.2	n
$Er(dbm)_3, H_2O$ crystal	35	1.1	6.6	p
$Er(dpm)_3$ vapor	46	2.7	3.7	q
$ErCl_3(AlCl_3)_x$ vapor	25.8 ± 0.5	2.7 ± 0.9	2.0 ± 0.4	ag
$ErBr_3$ vapor	60	1.5	1.7	q
ErI_3 vapor	100	–	–	q
$4f^{12}$ thulium(III)				
Tm(III) aqua ion, solution	0.8 ± 0.6	2.1 ± 0.3	1.86 ± 0.2	f
fluorophosphate glass	4.12	1.47	0.72	ah
borate glass	6.0 ± 1.4	3.1 ± 0.6	1.8 ± 0.4	ai
phosphate glass	5.7 ± 0.8	3.0 ± 0.3	0.8 ± 0.2	ai
germanate glass	4.0 ± 0.9	1.6 ± 0.5	0.8 ± 0.4	ai
tellurite glass	5.5 ± 0.8	2.9 ± 0.4	1.6 ± 0.2	ai
$Tm_xY_{1-x}AlO_3$ crystal	0.67	2.30	0.74	h
$Tm_xY_{2-x}O_3$ crystal	4.07	1.46	0.61	a
$LiNO_3 + KNO_3$ melt	10.4 ± 2	2.8 ± 0.7	1.7 ± 0.4	l

* The bidentate ligands dbm^- and dpm^- are dibenzoylmethide (also named 1,3-diphenyl-1,3-propanedionate) and dipivaloylmethide, respectively. ZBLA is a fluoride glass of molar composition $57\,ZrF_4 : 34\,BaF_2 : 4\,AlF_3 : 5\,RF_3$ (in part LaF_3).

** References:

(a) Krupke (1966).
(b) Eyal et al. (1985).
(c) Hormadaly and Reisfeld (1979).
(d) Brecher et al. (1978).
(e) Lucas et al. (1978).
(f) Carnall (1979).
(g) Krupke (1971).
(h) Weber et al. (1973).
(i) Spector et al. (1977).
(j) Jacobs and Weber (1974).
(k) Weber et al. (1981).
(l) Carnall et al. (1978b).
(m) Reisfeld (1982).
(n) Peacock (1973).
(o) Mehta and Tandon (1970).
(p) Kirby and Palmer (1981).
(q) Gruen et al. (1967).
(r) Liu and Zollweg (1974).
(s) Boehm et al. (1979).
(t) Weber (1967b).
(u) Blanzat et al. (1980).
(v) Weber (1968).
(w) Xu et al. (1984).
(x) Tanimura et al. (1984).
(y) Reisfeld et al. (1985a).
(z) Reisfeld and Hormadaly (1976).
(aa) Weber (1967a).
(ab) Reisfeld et al. (1983a).
(ac) Shinn et al. (1983).
(ad) Keller et al. (1982).
(ae) Greenberg et al. (1982).
(af) Jørgensen and Reisfeld (1983b).
(ag) Carnall et al. (1978a).
(ah) Kermaoui et al. (1984).
(ai) Reisfeld (1975).

materials, where equation (5) offers the advantage that each of the three Ω_t is an average value for all kinds of sites, weighted by their concentration. However, some crystalline materials and complexes in solution are included for comparison. The observation by Øye and Gruen (1969) that the vapor pressure of $NdCl_3$ is enormously increased by the simultaneous presence of aluminum chloride, has been extended to terbium (Caird et al., 1981b) and to erbium (Carnall et al., 1978a), though the exact composition of the volatile adducts $RCl_3(AlCl_3)_x$ is not known. These ternary chloride vapors show that a huge Ω_2 can occur outside condensed matter, again suggesting a predominant influence of the closest neighbor atoms.

The complexes of bidentate β-diketonates, where the hypersensitive transitions were discovered (Moeller and Ulrich, 1956) have been further studied (Kirby and Palmer, 1981; Richardson, 1982a). The Judd–Ofelt parameters and the luminescence of Eu(III) and Tb(III) [replacing calcium(II) with comparable ionic radius] have been informative about many biological materials (Horrocks and Sudwick, 1981; Richardson, 1982b) and absorption spectra of neodymium(III) complexes of multidentate amino-acids (Bukietynska and Mondry, 1985).

Not only are the Ω_2 values above 10 pm^2 in many materials in table 1 (and the main feature in common for these cases is perhaps short internuclear distances R–X) but, to the contrary, in a few cases, Ω_2 is almost as small as its experimental uncertainty, such as in several aqua ions (Carnall, 1979), in the lead zinc gallium fluoride glasses (though it is twice as big for barium zirconium fluoride glass) and in $R_xLa_{1-x}F_3$ crystals. The experimental uncertainty [in the sense of equation (5) being overdetermined] is less serious for erbium (Jørgensen and Reisfeld, 1983b) where $\Omega_2 = 1.59 \pm 0.12\ pm^2$ but in a recent study (Carnall et al., 1984) of $5f^8$ berkelium(III) aqua ions, it was decided to fix $\Omega_2 = 0.1\ pm^2$, resulting in an uncertainty below 10% of $\Omega_4 = 18.8$ and $\Omega_6 = 18.3\ pm^2$. The same fixation for $5f^7$ curium(III) aqua ions results in $\Omega_4 = 17.9$ and $\Omega_6 = 38.6\ pm^2$. We discuss in the next section, §2.3, why the Judd–Ofelt treatment is less successful in the beginning of the f-groups, such as $4f^2$ praseodymium(III) and $5f^2$ uranium(IV); but it is beyond discussion (Jørgensen, 1957b) that the 5f-group aqua ions U(III), Np(III), Pu(III), and Am(III) show oscillator strengths some 30 times higher than the analogous Nd(III) to Eu(III). The fact that U(IV), Np(IV) and Pu(IV) aqua ions show lower P than M(III) may be related to the higher excitation energy $5f \rightarrow 6d$ in M(IV) (Jørgensen, 1957b, 1969). Nevertheless, a fixation of Ω_2 around a few pm^2 for 5f group aqua ions would seem less radical, though perhaps more arbitrary. It is true that $4f^3$ to $4f^{13}$ aqua ions might as well have $\Omega_2 = 1\ pm^2$ without impeding the precision of the predicted P to any significant extent. Comparison of the high electron transfer band wave numbers (and concomitant high optical electronegativity) of fluorides and aqua ions (Jørgensen, 1970; Reisfeld and Jørgensen, 1977) compared with mixed oxides in crystalline or vitreous state suggests a common trend of particularly weak covalent bonding providing low Ω_2 values.

2.3. Ω_4 and Ω_6 as indicators of viscosity

It was made clear very early (Jørgensen, 1957b, and 1963) that the variation of the oscillator strength, equation (3), of internal $4f^q$ transitions in lanthanides as a function of the surrounding ligands is quite different from the (frequently much more intense) absorption bands of 3d, 4d, and 5d group compounds in condensed matter, though both kinds of transitions are parity-forbidden, and could not occur as electric dipolar transitions in monatomic entities. Although the constitution of 4f group aqua ions in solution is still quite controversial (Jørgensen and Reisfeld, 1982b), it seems that the (perhaps overwhelming) majority of early lanthanides (with large ionic radii) in noncomplexing salt (perchlorate, chloride, bromide, . . .) solutions at moderate concentration (say, below 1 molar anion) occur as $R(OH_2)_9^{+3}$ with a trigonal symmetry close to the point group D_{3h}, quite similar to the crystal structures of bromates $[R(OH_2)_9](BrO_3)_3$ and ethylsulfates $[R(OH_2)_9](C_2H_5OSO_3)_3$ (Morrison and Leavitt, 1982), whereas a tendency toward $R(OH_2)_8^{+3}$ grows more pronounced after samarium (though each of the series of bromates and ethylsulfates are isotypic for yttrium and all the lanthanides). The latter species in solution may, like $Mo(CN)_8^{-4}$, be a tetragonal (Archimedean) anti-prism of point group D_{4d}, or have lower symmetry, or, as is entirely conceivable, be a mixture of several symmetries having the coordination number $N = 8$ in common. Anyhow, the various aqua ions with $N = 9$ and 8 do not have a high symmetry, like d-group $M(OH_2)_6^{+z}$ ($z = 2$ and 3) exemplifying (or at last being close to) O_h. This situation carries across to glasses, where the rare earths represent mixtures of $N = 9$, 8, and probably 7, with quite variable internuclear distances R–X, whereas many d-group ions, such as chromium(III) and nickel(II), remain close to octahedral $N = 6$ in oxide and fluoride glasses.

In d-group spectra, there is not a black-or-white distinction between the presence or absence of a center of inversion, but it still has to be admitted that $3d^7$ cobalt(II) exhibits a (exceptionally pronounced) difference between tetrahedral (point group T_d) CoX_4^{-2} (X = chloride, bromide, or iodide) having P up to 0.009 (Jørgensen, 1963; Mason, 1980) for the transition from the quartet ground state to the highest quartet term, and $Co(OH_2)_6^{+2}$ having P a hundred times smaller, but still five times larger than each of the five most intense quartet–quartet transitions in neodymium(III) aqua ions.

It took some time to recognize cases of unusually weak $4f^q$ transitions in lanthanides on a site with an inversion center in crystals. Thus, the reflection spectrum is conspicuously weak (Jørgensen et al., 1965a) of the pyrochlore $Er_2Ti_2O_7$, where $Er(III)O_8$ is a cube contracted along one of its body diagonals. and hence has the point group D_{3d} with a center of inversion; and the cubic C-type R_2O_3 has three quarters of the R nuclei on a low-symmetry site C_2 and one quarter on a site with center of inversion S_6 (frequently called C_{3i}). The absorption bands of the latter minority site are exceedingly weak, but the positions of the excited states can be detected, such as $^5D_0$ of Eu(III), by laser

excitation of fluorescence. If such excited states are slightly below the corresponding *J*-levels accessible by light absorption, they may become very efficient traps for energy, especially at certain intervals of low temperature, and their proportion of the luminescence yield may be much higher than expected from their concentration. It is well-known from studies of paramagnetic resonance of traces, say of gadolinium(III), incorporated in fluorite-type crystals (CaF_2, SrF_2, BaF_2, CdF_2, CeO_2 and ThO_2) that most of the R(III) sites show perceptibly low symmetry because of the charge compensation needed, such as an additional F^- on interstitial positions, $R(III)F_7O$ with one oxygen nucleus, etc., and only a smaller part remains cubic $R(III)F_8$ or $R(III)O_8$ with the charge-compensating substitution far away (Catlow et al., 1984). Thus, only 1 to 15% of erbium(III) in CaF_2 (dependent on concentration and heat treatment of the crystal) are on cubic sites, the rest are distributed on several other types (Moore and Wright, 1981). On the other hand, Er(III) in cadmium fluoride (charge-compensated by Li, Na, K, or Ag) is about half on cubic sites and the rest on a definite site with point-group C_{2v} (Ensign and Byer, 1972). $Eu_xTh_{1-x}O_{2-0.5x}$ shows several sites (Porter and Wright, 1982).

Whereas $N = 6$ is not too rare for rare earths, even approximations to octahedral symmetry (excepting scandium) are highly unusual. They must occur in the perovskites $LaErO_3$, $LaTmO_3$, and $LaYbO_3$, stable below about 650°C (Jørgensen and Rittershaus, 1967); but the most striking example is MX_6^{-3}, which can be studied both in acetonitrile solution (hexa-chlorides and -bromides, Ryan and Jørgensen, 1966; and hexa-iodides, Ryan, 1969) and in the cubic elpasolite type Cs_2NaRCl_6 where each Cartesian axis contains an alternating string of ClRClNaClRClNa$\cdots$ nuclei (for references, see Morrison and Leavitt, 1982). Like the octahedral $5f^2$ uranium(IV) complexes UX_6^{-2}, the bands are an order of magnitude weaker than in the aqua ions (excepting the hypersensitive pseudoquadrupolar transitions of comparable intensity) and finely structured. The electronic origin can sometimes (but not always) be seen as a sharp line, followed at slightly higher wave numbers by the three fundamental frequencies of MX_6 having odd parity. At room temperature, three "hot" bands are observed at lower wave numbers, at the same distances from the purely electronic transition, and due to the Boltzmann population of the three odd vibrations superposed on the electronic ground state. This unique behavior of the hexahalide complexes constitutes a textbook example of vibronic assistance of parity-forbidden transitions, and has also been observed in the "ruby lines" of the $5d^3$ systems ReX_6^{-2} and IrF_6. It may be added that a crystal structure of $M(OH_2)_6(ClO_4)_3$ (M = erbium, terbium, thallium, and even lanthanum) crystallized from strong perchloric acid (with very low water vapor pressure) contains octahedral aqua ions (Glaser and Johansson, 1981). There are no comments about very pale pink Er(III), and further spectroscopic investigation may be worthwhile, though the vibrational amplitudes obviously are larger for M–O distances than for the heavy halide ligands. The similarity of erbium and thallium(III) is known from other

situations; cubic C-type Er_2O_3 and Tl_2O_3 have almost the same unit cell parameter, whereas it is smaller for In_2O_3 than for Lu_2O_3.

For our purpose, the 10 times smaller Ω_4 and Ω_6 in octahedral hexahalide complexes, and comparable low values for lanthanides on crystalline sites with a center of inversion (we do not know any definite case with 100 times less intensity), are only an instructive curiosity, in so far as aqua ions and other complexes in solution, and nearly all glasses and crystals, show a moderate variation of both Ω_4 and Ω_6 between 1 and 5 pm^2 in contrast to Ω_2 varying from below 1 to 40 pm^2 in condensed matter (table 1) and even up to 275 pm^2 for NdI_3 vapor. Before 1983, it was the general opinion that the moderate variation of Ω_4 and Ω_6 was rather unpredictable, but a closer analysis of Er(III) (Jørgensen and Reisfeld, 1983b) suggested that these two parameters increase with increasing vibrational amplitudes of the R–X distances. Rigid crystals show low values, though the local symmetry is low like in LaF_3 or in statistically disordered fluorites such as $R_xTh_{1-x}O_{2-0.5x}$ or $R_xY_{0.5-x}Zr_{0.5}O_{1.75}$, which are known to contain a large percentage of the rare earth as $R(III)O_7$, lacking one oxygen nucleus relative to a cube. Hence, the small Ω_4 and Ω_6 may not be nearly as much a question of high local symmetry as of the extent of vibrational dispersion, and even MX_6^{-3} (and gaseous $ErBr_3$) may be determined by modest vibrational amplitude. The trend as a function of decreasing ridigity in table 1 is hexahalide complexes < crystalline mixed oxides < glasses < viscous solutions < aqua ions < halide vapors < complexes of large organic ligands, returning to the ideas of Broer et al. (1945). It is difficult to understand why Ω_4 and Ω_6 differ by less than 30% in the majority of cases, when compared to the much smaller Ω_2 values for several aqua ions and vitreous and crystalline fluorides. From the point of view of monoatomic entities, the matrix elements U_4 and U_6 of eq. (4) represent the probabilities of 2^t, that is 16- and 64-pole transitions. The order of magnitude of P for such transitions in one partly filled shell characterized by the average value $\langle r^t \rangle$ and occurring at a wavelength λ is $10^{-8(t-1)}$ in the visible region (Jørgensen and Reisfeld, 1983b), though they would be more perceptible for the X-ray region, since P is proportional to $\langle r^t \rangle^2/\lambda^{2t-1}$. However much oscillator strengths around 10^{-24} and 10^{-40} are ludicrously small, and however much pseudo-16- and pseudo-64-polar transitions have comparable intensity when both U_4 and U_6 are positive, it remains true that the material parameters Ω_4 and Ω_6 in condensed matter are (astronomically huge) constants multiplying the practically vanishing intensity of 16- and 64-pole transitions in the gaseous ion R^{+3}. This is not a tautological statement, since 5 to 16 observed P values usually can be inserted in eq. (5).

It is important to realize that the apparent 256-polar transitions for $t = 8$ and analogous higher, even, t values are not observed (which is astonishing in view of the great extent of configuration intermixing in many-electron atoms). Thus, absorption from the ground state $^6H_{15/2}$ of $4f^9$ dysprosium(III) to $^6F_{1/2}$ is excluded, though it is safely predicted to be close to 13700 cm^{-1} in an entirely free

window in the absorption spectrum. However, such a state can be the final state of luminescence from a higher level (here $^4F_{9/2}$). Absorption is equally forbidden to excited levels with $J = 1$ and 0 of Ho(III) and to $J = 1/2$ of Er(III). This selection rule is very efficient in $4f^6$ europium(III) where the Boltzmann population of $^7F_1$ (only some 300 to 400 cm^{-1} above the ground state $^7F_0$) allows at most transitions toward J-levels of 7, but not to 8 and higher values, of which six are predicted between 27000 and 40000 cm^{-1} (Carnall et al., 1968). The situation is even more extreme in $5f^6$ americium(III) (Pappalardo et al., 1969) where the ground state with $J = 0$ (squared amplitude 0.48 $^7F_0$ and some 40% quintet character) is not followed by $J = 1$ before 2720 cm^{-1}, and only transitions to $J = 2$, 4, or 6 have one nonvanishing U_t. The strongest transition of Am(III) in the visible is to $J = 6$ ($\varepsilon = 350$ and $P = 5 \times 10^{-4}$ of the aqua ion at 19800 cm^{-1}, varying between 19630 cm^{-1} in solid $AmCl_3$ and 19250 cm^{-1} in AmI_3 because of nephelauxetic effect) analogous to $^5L_6$ of Eu(III) at 25400 cm^{-1}.

There is one well-characterized exception from the selection rules (Broer et al., 1945) of the Judd–Ofelt treatment. Some, but not all, europium(III) compounds show a very narrow emission line from $^5D_0$ (somewhere between 17200 and 17300 cm^{-1}) to $^7F_0$ and even fewer compounds show detectable absorption in the opposite direction, as was used (Geier and Jørgensen, 1971) to distinguish the temperature-dependent concentrations in solution of two ethylenediaminetetraacetate complexes differing in constitution by one mole of coordinated water. The narrow-line absorption is useful for site-selective laser excitation of Eu(III) in vitreous and crystalline materials, and the subsequent emission to $^7F_1$ and $^7F_2$ for investigating the local holohedrized symmetry of the sites (Durville et al., 1983). The group-theoretical apology for the occurrence of this highly forbidden transition is the mixing of $^7F_0$ and/or $^5D_0$ by the nonspherical "ligand field" with sublevels of the same symmetry type originating in other levels with positive J (Porcher and Caro, 1980). This is a plausible explanation for a transition normally having P much smaller than 10^{-8} found in the complex of a multidentate amino-acid (Geier and Jørgensen, 1971) but Blasse and Bril (1967a) pointed out that certain mixed oxides emit $^5D_0 \rightarrow {}^7F_0$ with far higher yield than others, and that it does not seem entirely determined by low symmetry of the local site (though, of course, it is less well known than in a stoichiometric crystal) but rather a kind of polaizability (perhaps akin to the low point groups allowing totally symmetric vectors) different from the pseudoquadrupolar Ω_2 effects. It is characteristic for $^5D_0$ luminescence to $^7F_0$ and $^7F_1$ that no vibronic structure can normally be detected.

We have mentioned several times that the Judd–Ofelt treatment is not numerically perfect. This can be seen from the number of measured P values, usually being well above 3, overdetermining eq. (5) for the evaluation of the three Ω_t. Various explanations have been proposed. In the original theory (Judd, 1962; Ofelt, 1962) the total width of the excited configuration of opposite parity mixing (to a very small extent) with $4f^q$ has to be negligible compared with the distance

between the two configurations. This is also a fair approximation, but all kinds of extraneous parameters creep in from moderate deviations from this assumption. It must be recognized that (in close analogy to parametrization of the energy levels) there is an optimum number of free parameters (say a quarter, or at most one half, of the numbers in the data to be described) in such a case. Thus, two parameters Ω_2 and $\Omega_4 = \Omega_6$ would work nearly as well for many materials in table 1, and look more attractive than three, in spite of the implicit belief by Broer et al. (1945) that Ω_6 is much smaller than Ω_4.

One of the spectacular difficulties for the Judd–Ofelt treatment (Peacock, 1975; Reisfeld and Jørgensen, 1977) is praseodymium(III) aqua ions, having their last band before 46000 cm^{-1}, the transition at 22600 cm^{-1} to $^3P_2$ with $P = 15 \times 10^{-6}$ (which is a record, since all other visible bands of trivalent lanthanide aqua ions have P below 10^{-5}). Nevertheless, the $^3H_4 \rightarrow {}^3P_2$ transition has $U_6 = 0.136$ [smaller than $U_6 = 0.341$ for $^6H_{5/2} \rightarrow {}^6F_{7/2}$ of samarium(III) aqua ions at 9200 cm^{-1} with $P = 2 \times 10^{-6}$, or $U_6 = 0.715$ for $^6H_{15/2} \rightarrow {}^6F_{7/2}$ of dysprosium(III) aqua ions at 11100 cm^{-1} with $P = 2.7 \times 10^{-6}$] and this value is also out of proportion with $U_6 = 0.042$ for $^4I_{9/2} \rightarrow {}^4F_{9/2}$ of neodymium(III) aqua ions at 14800 cm^{-1}, having $P = 0.7 \times 10^{-6}$. It cannot save the situation that $^3H_4 \rightarrow {}^3P_2$ also has $U_4 = 0.036$. This quantity is 0.173 for $^3H_4 \rightarrow {}^3P_0$ and should provide all the observed intensity $P = 2.5 \times 10^{-6}$ of the latter transition. Accepting Ω_6 close to 33 pm^2 for Pr(III) aqua ions procures another difficulty, the two transitions from $^3H_4$ to $^3F_3$ ($U_6 = 0.698$) and $^3F_4$ ($U_6 = 0.485$) should then have a total P more than three times their observed sum 13×10^{-6}. There have been several reactions to this discrepancy; it may be argued that the Judd–Ofelt treatment is not meaningful for Pr(III), though it is quite successful for Nd(III) and most of the subsequent lanthanides; or that one has to exclude $^3P_2$ (as done in table 1) and only consider the other transitions. One might also have argued that the $^3P_2$ surplus intensity is due to configuration interaction (via nondiagonal elements of interelectronic repulsion) between $5d^2$ and $4f^2$ (perhaps also then explaining the relatively large bandwidth, as discussed in section 2.4). However, it is rather difficult to explain why $^3P_1$ and $^3P_0$ are so much weaker, intermixing of configurations as distant as $5d^2$ and $4f^2$ not being strongly dependent on J. It is true that $^3P_2$ is situated about halfway between the ground state $^3H_4$ and the first excited state of 4f5d of Pr(III) in condensed matter, but one has to admit (Jørgensen, 1969) that this is also true (typically 0.3 to 0.6 times the distance) for many excited J-levels of other lanthanides not showing strong deviations from the Judd–Ofelt treatments. Recently, this problem was taken up again (Eyal et al., 1985) for Pr(III) in a barium zirconium fluoride glass. It was argued (cf. Peacock, 1975) that if the perturbing odd configuration is relatively close to $4f^2$, eq. (5) is essentially supplemented by $\Omega_3 U_3 + \Omega_5 U_5$ (vanishing in the original Judd–Ofelt assumption). It is certainly not cheerful to introduce two new parameters, but the justification is the luminescence of $^3P_0$ going to $^3H_5$ in 11% of the cases (cf. the branching ratios in section 3.1) whereas all the U_t (for even t) vanish for this

transition. Though an alternative would be J-mixing by nonspherical symmetry, it was felt that the effect is so pronounced that it is easier to accept the relatively small values of Ω_3 and Ω_5 (about a quarter of Ω_4 and Ω_6, respectively), which in turn have relatively weak influence on all other detectable absorption and emission probabilities.

Praseodymium(III) is the first lanthanide that can be treated relatively meaningfully according to Judd and Ofelt. There are much more serious problems in the beginning of the 5f group. Auzel et al. (1982) have shown that three Ω_t are entirely inadequate for $5f^2$ uranium(IV), where the energy levels recently could be compared (Jørgensen, 1982) with gaseous ion U^{+4}. One of the surprises is that the level with $J = 4$ (squared amplitudes 0.478 $^1G_4$, 0.496 $^3F_4$, and 0.026 $^3H_4$) at 16656 cm^{-1} almost coincides with $J = 2$ (0.548 $^1D_2$, 0.334 $^3P_2$, and 0.118 $^3F_2$) at 16465 cm^{-1} [corresponding to the identification by Jørgensen (1959), for $\zeta_{5f} \approx$ 1600 cm^{-1}], showing that the two strongest absorption bands of U(IV) aqua ions in the visible ($P = 2.1 \times 10^{-4}$ centered at 15400 cm^{-1}; and $P = 1.6 \times 10^{-4}$ centered at 20500 cm^{-1} being mainly $^1I_6$) formally are spin-forbidden. The high P values compared to octahedral UX_6^{-2} show that the aqua ion distinctly lacks a center of inversion. Comparison with reflection spectra of ternary fluorides with differing N for U(IV) suggests $N = 9$ as for Nd(III) (Folcher et al., 1978). The pronounced intermediate coupling in the 5f group corresponds to the Landé parameter ζ_{5f}, being twice as large, but the SCS or Racah parameters of interelectronic repulsion are only 0.6 times those of the analogous 4f group species. Consequently, many small U_t matrix elements for almost spin-forbidden transitions in the 4f group are much larger in the 5f group, and the ground state does not have a very well-defined S. Carnall et al. (1984) argue that the Judd–Ofelt treatment with the appropriate U_t values becomes applicable to Am(III), Cm(III), Bk(III), and subsequent elements. On the other hand, "ligand field" mixing of J is not a general problem for 5f group M(III) with splittings of a given J-level only about twice the splitting in the corresponding lanthanide, but can certainly be in 5f group M(IV) and higher oxidation states, though the J-mixing seems to vary a lot with the ligands.

Inductive parametrization (rather than deductive evaluation from radial functions etc. from necessarily approximate wavefunctions) always stimulates an appetite for physical significance of the mechanism. This is a relatively minor problem for parameters of interelectronic repulsion, which are typically some $(z + 2)/(z + 3)$ times the Hartree–Fock integrals for gaseous 3d-group M^{+z} and some 0.7 times in the 4f group (Jørgensen, 1962a,b), suggesting some kind of dielectric effect. Among the Judd–Ofelt parameters, the origin of Ω_2 is most likely to be the inhomogeneous dielectric, not so much because of precise numerical calculations being possible but because the other suggestions all remain strongly insufficient (Judd, 1979). The comparable, and roughly standard-size Ω_4 and Ω_6 may seem somewhat enigmatic at the moment. It is worthwhile to compare with the d-group compounds. It is quite striking that the spin-allowed

broad absorption bands have oscillator strengths P_{dd} related to the P_{et} of the first strong *electron transfer band* (Jørgensen, 1963, 1970) via the expression for second-order perturbations

$$P_{dd} = P_{et}(h\nu_{dd}/h\nu_{et})H_{af}^2/(h\nu_{et} - h\nu_{dd})^2 , \tag{6}$$

which has been further studied by Fenske (1967). It is striking that the effective nondiagonal element H_{af} (usually between 1500 and 2500 cm^{-1}) is close to the double-sided half-width 2δ of eq. (3), suggesting a dependence on vibrational amplitude. The low intensities of d-group fluoride and aqua complexes are then related to the unusually high $h\nu_{et}$ (Jørgensen, 1970).

Yamada and Tsuchida (1953) introduced a *hyperchromic series* of intensities of cobalt(III) complexes, which is also valid for other octahedral, typical Werner complexes of chromium(III) and rhodium(III):

$$\begin{aligned} F^- < OH_2 < Cl^- < NH_3 < Br^- < SO_4^{-2} < NO_3^- < OH^- < C_2O_4^{-2} \\ < CO_3^{-2} < NO_2^- < SO_3^{-2} < CrO_4^{-2} < NCS^- < (C_2H_5O)_2PS_2^- . \end{aligned} \tag{7}$$

It may be added that solutions of Cr(III) and Ni(II) in strong solutions of sulfuric acid (mainly containing $HOSO_3^-$) have a hyperchromic position between F^- and OH_2 and that Claus E. Schäffer found a similar behavior in the heteropoly-anions $CrMo_6O_{21}^{-3}$ and $CoMo_6O_{21}^{-3}$, possibly representing cases of restricted vibrational amplitude.

When the d-group complexes are not octahedral, they seem to exploit autonomous sources of intensity, such as the tetrahedral CoX_4^{-2} discussed above, and many complexes of phosphorus- and arsenic-containing ligands (Jørgensen, 1969). These propensities are extreme in copper(II) complexes (Jørgensen, 1975) and even more so in palladium(II). (Rasmussen and Jørgensen, 1968; Jørgensen and Parthasarathy, 1978), including complexes of the neutral ligands OH_2 and NH_3. In one way, the lanthanide aqua ions show some of these tendencies too, compared with MX_6^{-3}.

The reason why the trivalent lanthanides do not present a hypsochromic series like eq. (7) is probably the same as why the nephelauxetic effect takes extreme proportions in R_2O_3 and several mixed oxides (Jørgensen et al., 1965a; Jørgensen and Rittershaus, 1967), is not nearly as pronounced in the pyrochlore $Er_2Ti_2O_7$ and is very weak in aqua ions and in complexes of bidentate nitrate $R(O_2NO)_5^{-2}$ and icosahedral $R(O_2NO)_6^{-3}$, i.e., the former cases have much shorter R–O distances. The contraction of M–O distances is much less going to Cr_2O_3 and NiO from the corresponding aqua ions, but they can be artificially prolongated in brick-red ilmenite-type $Ni_xCd_{1-x}TiO_3$ compared with yellow $NiTiO_3$ (Jørgensen, 1969).

Our colleague Minas D. Marcantonatos has pointed out that the electron transfer bands of lanthanide complexes in solution (Jørgensen, 1962c; Ryan and Jørgensen, 1966; Ryan, 1969) also show quite varying intensities (though much

weaker than in the d-group because of the much smaller extent of spatial coexistence of the filled orbitals of the ligands with the partly filled 4f shell), and that it is conceivable that a part of the Ω_t has an origin similar to eq. (6). On the one hand, this does not seem too likely in the case of $^7F_0 \rightarrow {}^5D_2$ absorption lines situated inside the broad electron transfer band of orange europium(III) bromide and dithiocarbamate complexes, but on the other hand it is difficult to evaluate P_{et} for electron transfer bands in solids. The general trend of decreasing Ω_t from Nd(III) to Tm(III) does not seem to have a singularity toward lower values (rather the opposite; Carnall, 1979) at Gd(III).

2.4. *Radiative and factual lifetimes*

The rationalization of absorption band intensities in lanthanide compounds (as developed since 1945) got in the Judd–Ofelt treatment a form in eq. (8) (see §2.5) directly involving the Einstein transition probabilities $A(J, J')$. In the case of resonant absorption and emission being the only process occurring (like sodium atoms in yellow light), eq. (1) gives a direct relation between the (radiative) lifetime τ and the oscillator strength P. As an important example of such a resonant situation can be mentioned $\tau = 10.9$ ms for the first excited state $^6P_{7/2}$ of gadolinium(III) aqua ions (Carnall, 1979) at 31200 cm^{-1}, of which three quarters of $P_{obs} = 7.3 \times 10^{-8}$ is due to P_{md} and less than 2×10^{-8} to P_{ed}, to be compared with a total $P_{obs} = 2.88 \times 10^{-6}$ for the six closely adjacent ^6I_J at 35800 to 36700 cm^{-1}.

The more general question is whether the sum of transition rates (in s^{-1}) $A_{i0} + A_{i1} + A_{i2} + \cdots + A_{i(i-1)}$ of a given excited level E_i to the ground state E_0 and to all the J-levels from E_i to $E_{(i-1)}$ situated between E_0 and E_i is well described (Weber, 1967a, 1968) by the Judd–Ofelt treatment, the U_t matrix elements being evaluated between differing excited levels (for a useful compilation, see Carnall et al., 1977) and assuming the parameters Ω_t to be the same as derived from absorption spectra (and also the rates of magnetic dipole transitions). Carnall (1979) gives τ (in ms) for the "classical" fluorescent J-levels of aqua ions, 6.3 for $^4G_{5/2}$ of Sm(III), 9.7 for $^5D_0$ of Eu(III), 9.0 for $^5D_4$ of Tb(III) and 1.85 for $^4F_{9/2}$ of Dy(III). These values are far in excess of the observed lifetimes, and most materials containing Sm(III) or Dy(III) do not fluoresce perceptibly. This is due to various mechanisms of nonradiative relaxation with rates much higher than A_{ij}, to be discussed at length in section 4. In the normal situation, the quantum yield of luminescence is $\eta = \tau_{obs}/\tau_{rad}$ and dependent on the material and on the distance between E_i and the closest lower $E_{(i-1)}$; this ratio can easily be 10^{-3} or 10^{-5} with no luminescence being detectable in practice. On the other hand, gadolinium(III) perchlorate, or chloride dissolved in deuterium oxide (Vuilleumier et al., 1982; Marcantonatos et al., 1982; Vuilleumier, 1984; Jørgensen, 1985), has τ_{obs} close to 10 ms for the ultraviolet emission, to be compared with 6 ms in light water. The only values in the interval 10 to 30 ms

observed in the d-groups belong to the lowest quartet excited state of $3d^5$ manganese(II) in crystalline chlorides and bromides (Oelkrug and Kempny, 1976), in phosphate (Reisfeld et al., 1984b) and related glasses, and in vitreous and crystalline Mn(II) fluorides, to be discussed in section 6.1.

References to early uses of Judd–Ofelt parameters to predict radiative lifetimes from a higher to a lower excited J-level in materials with established Ω_t values are summarized by Reisfeld (1975) and by Reisfeld and Jørgensen (1977). The main use of such results is to predict the branching ratio $\beta = A_{in}/\Sigma A_{ij}$ for the proportion of the quantum yield $\beta\eta$ going from E_i to E_n, as discussed in section 3.1 (selected examples are given in tables 3 and 4). Excepting pathological conditions, the branching ratio is independent of the nonradiative de-excitation, which is only manifest in the factor η. Observed and calculated β were compared for fluorite-type $Er_xY_{0.5-x}Zr_{0.5}O_{1.75}$ (Greenberg et al., 1982) and again compared with erbium(III) in fluoride glasses (Reisfeld et al., 1983a). The same problem was studied (Reisfeld et al., 1983c) for europium(III) in barium zirconium fluoride glass, exceptionally fluorescent also from $^5D_2$ and $^5D_3$. $4f^{10}$ holmium(III) in this glass shows luminescence from eight excited J-levels to the ground state $^5I_8$ and also, in many cases, to $^5I_7$ and $^5I_6$ (Tanimura et al., 1984; Reisfeld et al., 1985a; Jørgensen et al., 1986). The branching ratios from $4f^8$ terbium(III) $^5D_4$ to the seven ^7F_J levels are strongly influenced by the exceedingly high $\Omega_2 = 20\ pm^2$ in $TbCl_3(AlCl_3)_x$ vapor, where $\Omega_4 = 2.3$ and $\Omega_6 = 3.0\ pm^2$ (Caird et al., 1981a). On the other hand, the absorption from $^7F_6$ to $^5D_4$ has only $P = 8.4 \times 10^{-8}$, slightly higher than 5×10^{-8} for Tb(III) aqua ions.

It is expected that excited J-levels of lanthanides on sites with a center of inversion, to which the weak absorption has not been detected, may have quite long radiative lifetimes, and perhaps unusual branching ratios. At this point the hexa-halide complexes occupy a prominent position. At 300 K, the observed lifetimes τ are 22 ms for $^4I_{13/2}$, 6.5 ms for $^4I_{9/2}$, and 3.8 ms for $^4F_{9/2}$ in the cubic elpasolite-type $Cs_2NaErCl_6$ (Ryba-Romanowski et al., 1982). The two latter values are 21 and 8.5 ms at 77 K, and may be compared with the observed $\tau = 13$ ms for $^4I_{13/2}$ and 11 ms for $^4I_{11/2}$ in low-symmetry $Er_xLa_{1-x}F_3$ (Weber, 1967a), similar to the calculated τ_{rad}; and the more differing $\tau_{rad} = 21$ ms for $^4I_{9/2}$ and $\tau = 0.15$ ms; and 1.87 ms and 0.75 ms, respectively, for $^4F_{9/2}$ (showing lower yield η). Elpasolite-type $Cs_2NaNdCl_6$ shows observed $\tau = 1.23$ ms at 300 K and 5 ms at 77 K of $^4F_{3/2}$. There is not only an influence of the temperature (as in the erbium compound) but also of concentration quenching, since $Cs_2NaNd_{0.01}Y_{0.99}Cl_6$ shows $\tau = 4.1$ ms at 300 K and 11 ms at 77 K (Tofield and Weber, 1974). The situation is more complicated in $Cs_2NaTbCl_6$ and $Cs_2NaTb_{0.01}Y_{0.99}Cl_6$ (Thompson et al., 1977), where the luminescent transitions (from $^5D_4$ and $^5D_3$), changing J by one unit, are essentially magnetic dipolar and do not show extensive vibrational structure, whereas the other transitions are mainly vibronic (i.e., simultaneously changing the electronic and vibrational quantum numbers). The same behavior is observed (Serra and Thompson, 1976) in

$Cs_2NaY_{1-x}Eu_xCl_6$, where a unique case of coexcited vibrations accompanying $^5D_0 \rightarrow {}^7F_0$ luminescence, as well as $^5D_0 \rightarrow {}^7F_2$, are observed. It would seem that if τ_{rad} is above 50 ms for J-levels of R(III), the vibronic mechanism takes over and is still able to provide a minute transition probability.

With the exception of hexa-halide complexes, the general impression of 4f-group absorption and emission spectra is that of essentially pure electronic transitions (with weak to very weak mixing of parity) not accompanied by coexcited vibrations. The situation is exactly the opposite in the broad bands of 3d- and 4d-group compounds, which are technically blurred-out vibronic structures obeying the Franck–Condon principle (though it has not been established in a general sense that they are always due to totally symmetric stretching frequencies) and where the electronic origin may not be observable at much lower wave number than the perceptible beginning of the absorption band. However, there may be a little more coexcited vibronic quasi-continua (Jørgensen, 1985) in the background of 4f spectra than usually realized. It is very striking that some absorption bands, e.g., of Ho(III) and Er(III) aqua ions in solution, are much sharper, and some, such as $^3P_2$ of Pr(III) and nearly all bands of Tm(III), are relatively broader. In a d-group compound, such a difference between the "ruby lines" and usual, broad bands would be ascribed to Franck–Condon coexcitation, but such an explanation cannot be adapted here in its simplest form. However, Caro et al. (1985) pointed out that the sublevels of a definite J-level measured in the absorption spectrum of a solid compound at 4 K tend to become quite broad above the average energy of the J-level, compared to very sharp lines at lower wave numbers. Besides antiferromagnetic effects in nondiluted compounds, such a behavior can be ascribed to the dense distribution of vibronic levels mixing up with the higher sublevels. Furthermore, supernumerary sublevels may be due to vibronic near-resonances. Though such sublevels tend to equilibrate thermally within a given J-level, it does not seem likely that the broadening discussed by Caro et al. can be due to Heisenberg's uncertainty principle, which would bring the time scale of the phenomenon down in the 10^{-13} to 10^{-14} s range. This particular complication of exceedingly narrow, and less narrow, sublevels may play an important role in glasses (in particular in view of the low libration frequencies of order of $10\,cm^{-1}$) where the conditioned reflex otherwise is inhomogeneous broadening exclusively due to nonequivalent sites.

The excited J-levels of trivalent lanthanides escape lifetimes above 50 ms by exceptional vibronic couplings. They may be more frequent than suspected, because a quantum yield 5×10^{-4} still corresponds to an observed lifetime around 0.01 ms. Really long lifetimes are not conceivable without trapping of energy. Due to the exceedingly small ζ_{2p} in carbon and adjacent elements, the first excited triplet state of an organic molecule or ion may show a τ_{rad} of several seconds, especially if fully deuteriated. This phenomenon is often called "phosphorescence", in analogy to certain inorganic solids showing (frequently nonexponential) decay for hours or days. In the latter case, the rate of phosphorescence is

determined by the Arrhenius activation energy for a (non-Franck–Condon) process where energy (stored somewhere else in the solid) slowly diffuses to the emitting luminophore. There is no sharp conceptual limit between such a diffusion taking days or months, and the *thermoluminescence* where energy provided by the presence of radioactive isotopes, or by the cosmic radiation, is stored for centuries or millennia, and suddenly liberated by heating to an appropriate temperature. This phenomenon is of great interest for the study of ceramics and other archeological objects, and is also known from several minerals, such as many fluorite crystals emitting (one time) bright violet light by heating to a temperature well below red heat.

Quantum yields of luminescence (Reisfeld, 1972) were determined in standard references, varying the excitation wavelength for $^4G_{5/2}$ emission of samarium(III) and $^5D_0$ emission of europium(III) in phosphate glasses, and for $^6P_{7/2}$ emission of gadolinium(III) and $^5D_4$ emission of terbium(III) in borate glasses.

2.5. *Radiative transition probabilities and laser cross sections of rare earth ions in glasses*

For most practical purposes the oscillator strengths and the connected radiative transition probabilities obtained from the absorption spectra correspond to some average values due to the total number of sites. This is also true for the nonradiative transition probabilities, which are obtained from the measured average lifetimes and average quantum efficiencies of fluorescence.

The positions of the spectra of the rare earth ions which are due to intraconfigurational f–f transitions in amorphous materials are only slightly dependent on the host. However, a small shift of the free-ion levels to lower energies, the nephelauxetic effect, can be observed as a result of covalency between the rare earths and the matrix. This is especially evident in chalcogenide glasses (Reisfeld, 1982). The intensity of the transitions can to a good approximation be calculated by the Judd–Ofelt theory, in which the calculated matrix elements of the transitions are combined with the experimentally obtained intensity parameters (Reisfeld and Jørgensen, 1977). The radiative transition probabilities of the rare earths in glasses are composed mainly of the electric-dipole contribution and to a much lesser extent by the magnetic-dipole contribution (Reisfeld, 1976a).

The spontaneous emission rate is

$$A(aJ:bJ') = \frac{64\pi^4\nu^3}{3hc^3(2J+1)}\left[\frac{n(n^2+2)^2}{9}S_{\mathrm{ED}} + n^3 S_{\mathrm{MD}}\right], \tag{8.1}$$

$$S_{\mathrm{MD}}(aJ:bJ') = \frac{e^2h^2}{4m^2c^2}\,|\langle f^N[\gamma SL]J||\boldsymbol{L}+2\boldsymbol{S}||f^N[\gamma'S'L']J'\rangle|^2, \tag{8.2}$$

$$S_{\mathrm{ED}}(aJ:bJ') = e^2\sum_{t=2,4,6}\Omega_t|\langle f^N[\gamma SL]J||U^{(t)}||f^N[\gamma'S'L']J'\rangle|^2, \tag{8.3}$$

where n is the refractive index, J the initial level, J' the terminal level, ν the frequency of emitted light in s^{-1}, S_{ED} the forced electric-dipole strength and S_{MD} the magnetic line strength.

The matrix elements are calculated from the reduced matrix elements of Nielson and Koster (1964) and the 3j and 6j symbols (Rotenberg et al., 1959) as described by Wybourne (1975).

The Ω parameters have been calculated in crystal matrices and glasses from the absorption spectra and calculated matrix elements.

It was discussed previously (Reisfeld 1984b) that the matrix elements of the majority of rare earth ions are only insignificantly dependent on the environment in which they are situated. The main factor responsible for differences in intensity of the various transitions are the three intensity parameters.

This statement is relaxed to some extent when rare earth ions form a covalent bond with the host matrix. Covalent bonding may have the effect of lowering the electronic levels of the free ion due to the nephelauxetic effect, as first suggested by C.K. Jørgensen.

In crystals, and even more so in glasses, the rare earths are distributed over a large number of nonequivalent sites and the intensity parameters are the average values of Ω. We have discussed previously that Ω_2 is strongly enhanced by covalent bonding, which is equivalent to the dynamic polarization of the ligands by the quadrupole moment of the transitions. The covalency effect can be clearly seen from the fact that the Ω_2 parameters are the smallest in fluorides (both crystals and glasses), which are known to have the least covalent bonding with the rare earths. The Ω_2 parameters are much higher in oxide glasses than in fluoride glasses and are in general higher in glasses than in crystals. The reason for such behavior arises from a large number of different sites in oxide glasses and lower symmetry in which the rare earth ion is situated. In fluoride glasses the number of different sites is much smaller, as exemplified by the narrower absorption and emission spectra of, for example, Er(III) (Reisfeld et al., 1983a) and Ho(III) (Shinn et al., 1983; Reisfeld et al., 1985a) in these glasses as compared to oxide glasses.

When Ω_2 parameters are plotted versus atomic numbers of the rare-earth ions, a monotonous ascending function is obtained for each host. The lowest values are due to fluoride hosts and the highest to phosphate and tellurite. Ω_4 and Ω_6, when plotted in a similar way, exhibit a descending function of the atomic number, the absolute magnitude being smallest for fluoride and highest for phosphate and tellurite glasses.

The praseodymium (Eyal et al., 1985) exhibits an exceptional behavior towards the Judd–Ofelt theory. In this ion the proximity of 5d orbitals to 4f orbitals invalidates the assumption in the Judd–Ofelt theory that the energy difference between the 5d and 4f states is much larger than the energy differences within the 4f states. This is reflected in the hypersensitivity of the $^3H_4 \rightarrow {}^3P_2$ transition and in the large error in the Ω parameters when this transition is included in the

calculation. Since the Judd–Ofelt theory is not completely valid for Pr(III), the odd matrix elements U_3 and U_5 cannot be neglected when the contribution to the transition is significant. This is especially the case for the transitions $^3P_0 \rightarrow {}^3H_5$ and $^3P_0 \rightarrow {}^3F_3$, in which the even matrix elements vanish. In this specific case the product $\Omega_5 U_5$ for the transition $^3P_0 \rightarrow {}^3H_5$ as calculated from the branching ratios is 0.21 pm^2 (the square picometer 10^{-20} cm^2 is a convenient unit for Ω_t values), one third of the product $\Omega_4 U_4$ for the strong emission $^3P_0 \rightarrow {}^3H_4$. Another odd t product for the transition $^3P_0 \rightarrow {}^3F_3$ observed in the system studied by Szymanski (1984) is estimated by us to be $\Omega_3 U_3 = 0.02$ pm^2. These values indicate that the corresponding Ω_5 and Ω_3 should be of the same order of magnitude as the even Ω_2, Ω_4, and Ω_6 (Eyal et al., 1985).

The enhancement of Eu(III) luminescence in glasses can be also achieved by embedding small silver particles (Malta et al., 1985) in the glass. The question whether the enhancement is due to interaction of the silver plasmons with the medium, or due to radiative trapping of Eu(III) luminescence is still disputable.

2.6. *Hole burning*

The radiative transition probabilities for each site of the rare earth in glass are different; the measured absorption and emission bands correspond to the average value. By using a narrow laser beam whose width $\Delta\nu_i$ is smaller than the homogeneous, $\Delta\nu_h$, and inhomogeneous, $\Delta\nu_{ih}$, linewidth, it is possible to excite ions which are resonant with the laser beam within the homogeneous line and to bring it to saturation. Thus, with narrow-band excitation very narrow and photochemically stable holes can be "burned" into the absorption bands of the rare earth in glass.

Spectral hole burning has been observed, for example, by Nikitin et al. (1978), in Nd(III) laser glass in the emission band, due to the $^4F_{3/2} \rightarrow {}^4I_{11/2}$ transition at temperature as high as 300 K (Friedrich and Haarer, 1984).

Recently, Pedrini et al. (1985) studied the photoionization of excited states of lanthanides in crystals, and the effects of hole burning in fluorite-type $Sm_xCa_{1-x}F_2$. Most of the recent extensive work on hole burning is done on crystals at liquid helium temperature. A quite innovating study (Winnacker et al., 1985a,b) involves $4f^6$ samarium(II) in the tetragonal crystal $Ba_{1-x}Sm_xFCl$, allowing a two-step photoionization where the excited J-levels $^5D_0$ and $^5D_1$ (corresponding to narrow absorption bands at 687.9 and 629.7 nm, respectively) are photoionized by another photon, losing an electron to Sm(III) present. At 2 K, the states (with a lifetime of about a millisecond) acquire holes with a width of only 25 MHz for $x = 10^{-4}$ and of some 1 GHz for $x = 0.005$. Since the inhomogeneous broadening of 16 GHz (0.5 cm^{-1}) allows burning of 200 distinct holes, such a system may be revolutionary for frequency-domain optical data storage. Macfarlane et al. (1985) have also used the 25 MHz holes to measure small linear Stark and nonlinear Zeeman coefficients of the $^7F_0$–$^5D_0$ transitions. Contrary to many

other materials, the holes persist even after heating to 300 K for a few days. Since glasses can show effects of hole burning (and have intrinsically more inhomogeneity to start with), memory devices may be feasible with differing time scales of persistence, even at room temperature.

3. Luminescence

3.1. *Branching ratios*

The rare-earth ions with electron configuration $4f^q$ show a very characteristic spectroscopy due to the fact that the 4f shell is well shielded from the surroundings. This is also more or less true for the transthorium ions ($5f^q$). These electronic configurations yield optical properties which cannot be observed for other metal ions. These, in turn, lead to many important applications, for lasers, cathode-ray tubes, luminescent lamps and X-ray imaging.

If we consider the optical spectrum of a rare-earth ion, either in absorption or in emission, we are immediately struck by a large number of sharp lines. Their position seems to be independent of the surroundings. Their intensity ratios vary strongly, indicating certain selection rules, which are reflected by the branching ratio defined as the ratio of a specific radiative transition from a given level divided by the sum of all the radiative transitions from this level. The branching ratio is defined as $\beta_{ij} = A_{ij}/\Sigma A_{ik}$ (the ratio between the transition probability A_{ij} and the sum over all the probabilities A_{ik} of transitions to lower states, including A_{ij}).

When two emitting levels are close enough (the separation being about $200\,\mathrm{cm}^{-1}$ or less) a thermalization takes place and the branching ratio has the following form

$$\beta_{ij} = \frac{\Sigma_i\, g_i \exp(-\Delta E_i/kT) A_{ij}}{\Sigma_i \Sigma_j\, g_i \exp(-\Delta E_i/kT) A_{ij}} \,. \tag{9}$$

3.2. *Glass lasers and rare-earth-based luminescent solar concentrators*

Research on neodymium lasers increased rapidly in the 1970's because of the requirement of large neodymium glass lasers for fusion research. Laser-driven fusion is one approach to a long-term solution of the world's energy supply problems as it is based on the inexhaustible fuel deuterium, which is obtained from water. The unique capability of lasers to produce a very high instantaneous power density over a very small area introduces the possibility of driving thermonuclear fuel to extremely high temperatures and densities at which fusion is expected to occur (Weber, 1976; Reisfeld and Jørgensen, 1977; Brown, 1981).

The demonstration of the scientific feasibility of the initiation of a fusion burn

with the energy produced from the pellet exceeding the absorbed beam energy can be attempted with laser energies of the order of 0.33 to 0.5 MJ and lifetimes of a few nanoseconds. Such a laser, the NOVA neodymium glass laser, is now operating in the Lawrence Livermore National Laboratory.

Neodymium-doped yttrium aluminum garnet lasers have found extensive applications as range finders and have also become standard laboratory equipment for research in photochemistry and related fields.

High-efficiency laser emission has also been observed from yttrium lithium fluoride doped with Er(III) (Chicklis et al., 1972), Tm(III) (Jenssen et al., 1975), Ho(III) (Karayanis et al., 1976; Barnes et al., 1979), and Nd(III) (Knights et al., 1982).

All glass lasers developed to date have used a rare earth as the active ion and optical pumping for excitation (Stokowski, 1982). Of these, flash-lamp-pumped neodymium glass lasers are the most frequently used and the most widely investigated. The spectroscopic data needed for estimation of the laser characteristics are usually obtained from small samples (Reisfeld and Jørgensen, 1977). The data include absorption, emission, nonradiative relaxation, energy transfer probabilities and laser cross sections. Laser operation predictions can be made from such data without actually demonstrating laser action.

Stimulated emission cross sections of neodymium vary with glass composition. We have previously shown that the amount of covalency between the glass-forming medium and the neodymium ion increases significantly with the emission cross section (Reisfeld, 1982). This fact is demonstrated by the very high cross section of Nd(III) in chalcogenide glasses. The decision about the type of glass laser to be used for a specific application depends on the emission wavelength, pulse duration, signal output and optical configuration requirements.

Additional work is still needed to establish the relative merits of various glasses for lasers. This work includes investigation of spectral inhomogeneities and their effects on large-signal energy extraction, laser-induced damage threshold as a function of wavelength and pulse duration for a wider range of glass compositions (Weber, 1982).

3.2.1. *Luminescent solar concentrators*

The world's conventional energy supplies, which are based mainly on readily available fossil fuel sources, are diminishing rapidly. The main approach to the energy crisis – nuclear fusion – is raising a great deal of hope but its practicability has still to be demonstrated. There is no doubt that solar energy, which is clear and nonhazardous, could contribute considerably to a solution of the energy problem if appropriate methods were developed to collect, concentrate, store and convert solar radiation, which is diffuse and intrinsically intermittent (Reisfeld and Jørgensen, 1982). Owing to the original efforts of the National Aeronautics and Space Administration to supply electric current from silicon photovoltaic (PV) cells to space vehicles, such devices are now available at a cost of about $8

per watt of power. At present, large-scale solar cell arrays are operating in inaccessible locations distant from conventional electricity plants. Previous price estimates (predicting a decrease in cost to $1 to $2 per watt in 1984), which were obtained by making comparisons with the aluminum or electronic computer industries, were slightly optimistic, as the difficulties of preparing inexpensive silicon with a high photoelectric yield cannot easily be removed by increased production. One way of lowering the price of PV electricity is to concentrate the solar radiation, particularly the part that is most efficient in PV energy conversion. It is hoped that this can be achieved with luminescent solar concentrators (LSC) (Reisfeld and Jørgensen, 1982).

The operation of an LSC is based on the absorption of solar radiation in a collector containing a fluorescent species in which the emission bands have little or no overlap with the absorption bands. The fluorescence emission is trapped by total internal reflection and concentrated at the edges of the collector, which is usually a thin plate (Reisfeld and Jørgensen, 1982). LSCs have the following advantages over conventional solar concentrators: (a) they collect both direct and diffuse light; (b) there is good heat dissipation of nonutilized energy by the large area of the collector plate in contact with air, so that essentially "cold light" reaches the PV cells; (c) tracking the sun is unnecessary; and (d) the luminescent species can be chosen to allow matching of the concentrated light to the maximum sensitivity of the PV cell.

3.2.2. *Requirements for glass lasers and luminescent solar concentrators: similarities and differences*

The requirements for a glass laser are (cf. fig. 2)
(a) high absorption of the exciting light,
(b) population inversion of the emitting level,
(c) high quantum efficiency of light emission,
(d) high cross section of stimulated laser emission,
(e) nonradiative quick relaxation of the lower laser level.

The requirements of LSCs are
(a) large absorption in a broad spectral range,
(b) high population of the emitting level,
(c) high quantum efficiency of light emission,
(d) high intensity of emitted light,
(e) Stokes shift between the emitted and absorbed light.

As can be seen, the requirements for both devices are quite similar; however, they are more stringent for lasers than for LSCs. An additional need is that the materials will be stable towards corrosion by light, heat, and humidity.

3.2.3. *Basic parameters of a laser*

The basic parameters of the solid-state laser operation are the following:

(a) The threshold of laser action is defined as the minimum input power or energy needed to start the laser action.

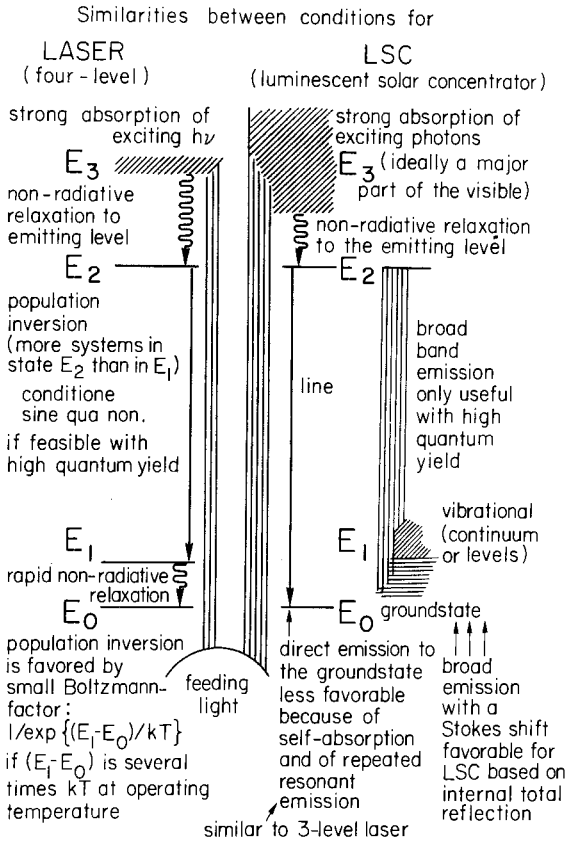

Fig. 2. Comparison between (desirable or indispensable) conditions for four-level lasers and luminescent solar concentrators (LSC).

(b) The output power of the laser, P_{out}, for a given peak power pumping [for a pulsed laser, P_{out} is given in joules per pulse, for a continuous operation (CW) in watts].

(c) The spectral distribution of the emitted radiation is defined by a central wavelength λ_0 or frequency ν_0 and linewidth $d\lambda$ (or $d\nu$) of the emission.

(d) The spatial distribution of energy in the laser beam, both in position and in direction (the latter is usually specified by a mean angular divergence).

The R laser consists of a resonant cavity, containing the amplifying medium, the excited rare-earth ions incorporated in crystals, glasses, or liquids. The laser medium (tube or rod) is placed between two parallel mirrors, having reflection coefficients R_1 and R_2. The mirrors may be placed separately or evaporated directly on the ends of the rod.

Oscillations may be sustained in the laser if the amplification of the radiation through the active material is sufficient to compensate for the fraction of energy lost due to all causes. In other words, in order for a fluorescent material to exhibit laser operation, the round-trip optical gain resulting from the optical pumping,

must exceed round-trip losses within the cavity. In each passage through the laser the intensity of the radiation is increased by a factor $e^{\beta L}$ by virtue of the amplification in the material, where L is the length between the mirrors and β the amplification coefficient, expressed as

$$\beta(\nu) = k(\nu_0)\,\Delta N\,, \tag{10}$$

where $k(\nu_0)$ is the absorption coefficient at maximum wave number ν, and ΔN is the population inversion.

The threshold of laser oscillation is attained when the peak value β of the amplification curve satisfies the equation

$$\beta L > \gamma\,, \tag{11}$$

where γ is the loss factor after single passage. Equation (11) is the simplest formulation of the threshold condition.

Thus, a laser of a given length and mirror reflectivity will operate only if the population inversion is large enough to ensure the amplification per unit length satisfying the equation

$$\beta = \Delta N\, k(\nu)_0 \geqslant \frac{\gamma}{L}\,. \tag{12}$$

This equation combines the requirements for the qualities of the resonator design (L and γ) and the amplifying medium which is related to the population inversion ΔN and the radiative transition probabilities reflected in the absorption coefficient $k(\nu)_0$.

We shall summarize briefly the parameters for the laser design, which are extensively discussed elsewhere (Lengyel, 1971). The laser medium spontaneously emits light into an extremely large number of oscillator modes. The usual optical resonators (Yariv, 1975) provide appreciable feedback for only a limited number of modes, which are the resonator modes (Kogelnik, 1966). From this concentration of radiation in the small number of modes arises the coherence of laser light.

An important parameter of a resonator mode is its decay time t_e. This is the time at which the nonequilibrium energy ΔE decays to 1/e of its initial value, $\Delta E \simeq \exp(-t/t_e)$. The value of t_e is related to the fractional round-trip loss of the mode and the round-trip optical length L of the resonator by

$$t_e = -\frac{L}{c}\ln(1-\gamma)\,, \tag{13}$$

where c is the velocity of light. Usually $\gamma \ll 1$ and the equation may be

approximated by

$$t_e = L/c\gamma \tag{14}$$

The decay time and the quality factor Q of the cavity are related by

$$Q = 2\pi\nu_{12}t_e\,, \tag{15}$$

where Q is the loss rate of the system and depends on the macroscopic properties of the cavity. Any disturbance that decreases Q increases γ and increases ΔN, the population inversion at which the oscillation begins.

From equations (10) and (11) it is evident that the material parameter for the laser condition at a given population inversion is explicitly contained in the $k(\nu_0)$ which is related to the stimulated cross section of emission. This is true both for 3- and 4-level laser systems.

3.2.4. *Rare-earth doped laser glasses*

Trivalent rare-earth ions present a unique instance for which *a priori* calculations can be made from a small number of parameters, which are calculated theoretically and/or derived from simple experiments on small samples. Such predictions are of value in devising materials based on transparent media doped by rare-earth ions. The cross sections and performance of glass lasers can be predicted with quite good accuracy based on such calculations (Reisfeld and Jørgensen, 1977; Reisfeld, 1984a,b).

The main difference between optical spectra of inorganic ions in amorphous materials and crystalline media of comparable composition is the inhomogeneous broadening due to the variety of sites in the former (Riseberg, 1973; Weber, 1981). This is due to the fact that the dopant ions in glasses reside in a variety of environments and experience different perturbing local fields. Thus, instead of identical electronic energy levels, there is a distribution of spectroscopic parameters which depend on the host glass composition and result in different and nonradiative transition probabilities. These variations are evident in absorption and fluorescence spectra as inhomogeneously broadened lines when conventional light sources are used. The decay times of fluorescence from excited states of different sites normally exhibit a nonexponential behavior. However, if fast diffusion of excitation energy occurs among the different sites, then the decay will become exponential with the fastest time constant available among the sites.

Laser-induced-fluorescence line-narrowing (FLN) enables, in some cases, the excitation of a subset of ions having the same energies. In the absence of accidental coincidence of electronic levels, a tunable pulsed laser can be used for determining the electronic levels and transition probabilities of a selected subset of the total ensemble of sites. The intraconfigurational 4f–4f transitions of rare-earth ions are especially suitable in this type of investigation because of small

electron–phonon coupling. The degree of selectivity of the FLN technique depends on the ratio of homogeneous to inhomogeneous widths (Weber et al. 1976; Brawer and Weber, 1981a,b), which is of the order of 10^{-3} for rare earths at low temperatures. Figure 1 of Durville et al. (1983) provides an example of FLN on Eu(III) in phospho-tungstate glasses at 4 K, the excitation being performed into the $^5D_0$ level of the different sites. The three-line $^5D_0 \rightarrow {}^7F_1$ emission is shown as a function of excitation frequency of the $^7F_0 \rightarrow {}^5D_0$ transition and corresponds to the different sites.

Modelling the atomic arrangement in glass is often done using molecular dynamics. In this technique the position of the ions is calculated by numerical integration of Newton's equations of motion using a model interatomic potential function. This method has been applied so far to SiO_2, B_2O_3, BeF_2, $ZnCl_2$, KCl, and multicomponent sodium silicate, sodium borosilicate, and fluoroberyllate glasses (Weber, 1982). While the method is very elegant and promising, its validity is still being tested by comparison with experimentally measured physical properties such as thermodynamic and transport characteristics.

The previously discussed radiative transition probabilities and line strengths are connected to the peak-stimulated emission cross sections of the rare-earth ion in a glass by

$$\sigma_p = \frac{8\pi^3 e^2}{3hc(2J+1)} \frac{(n^2+2)^2}{n} \frac{\lambda_p}{\Delta\lambda_{eff}} S(J, J') , \tag{16}$$

where n is the refractive index, λ_p is the wavelength of the emission peak, and $\Delta\lambda_{eff}$ is the effective linewidth of the emission between states of J and J'.

3.3. *Luminescence efficiency and competing processes*

Luminescence is the emission of light in the ultraviolet, visible, and infrared part of the spectrum as a result of excitation of the system in excess of thermal equilibrium. In condensed matter, luminescence of an excited electronic state is the exception rather than the rule, especially at room temperature and above.

Luminescent emission can be excited by light (photoluminescence), by cathode rays, electric field (electroluminescence), and high temperature (candoluminescence).

In glass, rare-earth luminescence has in general higher quantum efficiencies than the luminescence of the 3d and 4d ions. This is due to the fact that the 4f orbitals are rather isolated from the surrounding medium. The luminescence quantum efficiency is defined as the number of photons emitted divided by the number of photons absorbed, and in most cases is equal to the ratio of the measured lifetime to the radiative lifetime of a given level.

The processes competing with luminescence are radiative transfer to another ion and nonradiative transfers such as multiphonon relaxation and energy transfer

between different ions or ions of a similar nature. The last transfer is also named cross-relaxation.

The radiative transfer consists of absorption of the emitted light from a donor molecule or ion by the acceptor species. In order that such transfer takes place, the emission of the donor has to coincide with the absorption of the acceptor. The radiative transfer can be increased considerably by designing a proper geometry. Such transfers may be important in increasing pumping efficiencies of glass lasers (Reisfeld, 1985a) and luminescent solar concentrators, whereby energy emitted from organic molecules can be absorbed by ions such as Cr(III), Mn(II), or Nd(III), followed by characteristic emission from these ions.

4. Nonradiative processes

The nonradiative processes competing with luminescence are energy loss to the local vibrations of surrounding atoms (called phonons in solids) and to electronic states of atoms in the vicinity, such as *energy transfer*, which may be resonant (including as a special case energy migration between identical systems, which may ultimately emit radiation) or phonon-assisted [the excess energy being dissipated as heat, or, to a much smaller extent, the thermal reservoir supplying low-energy phonons ($kT = 210\,\mathrm{cm}^{-1}$ at 300 K) to a slightly higher level of an adjacent system]. Special cases of energy transfer are cross-relaxation, where the original system loses the energy ($E_2 - E_1$) by obtaining the lower state E_1 (which may also be the ground state E_0) and another system acquires the energy by going to a higher state. Cross-relaxation may take place between the same lanthanide (being a major mechanism for quenching at higher concentration in a given material) or between two differing elements which happen to have two pairs of energy levels separated by the same amount.

The observed lifetime τ and the quantum yield of luminescence η of a given J-level in a given material are connected with the rate W of nonradiative relaxation (in $\mathrm{Hz} \equiv \mathrm{s}^{-1}$),

$$\tau = 1/(\tau_R^{-1} + W)\,, \qquad \eta = \tau/\tau_R\,. \tag{17}$$

In most cases, η is well below 10^{-3} and cannot be readily detected. When cross-relaxation and energy transfer are not the predominant mechanisms, the multiphonon deexcitation is reasonably well described (typically ±30%) with the exponential law

$$W = B \exp(-\alpha\, \Delta E)\,, \tag{18}$$

where B is in Hz and ΔE is the *energy gap* between the luminescent J-level and the closest lower J-level. It is empirically well-known (Reisfeld, 1976a; Reisfeld

and Jørgensen, 1977) that the glasses and crystalline materials most favorable for luminescence tend to have the highest (fundamental frequency) phonon $\hbar\omega$ with as low wave number as possible, providing smaller rates W. Though the parameter α has the dimension of a reciprocal wave number, it is not simply $1/\hbar\omega$, but is related by a small constant a in $\alpha = (a\hbar\omega)^{-1}$, where a is increasing from 0.25 for $LaCl_3$ through 0.4 for aqua ions and the garnet $Y_3Al_5O_{12}$ up to 0.5 for Y_2O_3. Crystalline LaF_3 has $a = 0.5$ and ZBLA glass has $a = 0.38$. Though eq. (18) has a somewhat greater percentage uncertainty than the Judd–Ofelt treatment of τ_R, it is noted that the parameters B and α do not depend on the lanthanide chosen (Reisfeld, 1985b,c).

4.1. *Multiphonon relaxation*

Today, multiphonon relaxation in lanthanide ions is a well-understood process, contrary to other transition metal ions, which still require additional understanding. Excited electronic levels of rare earths R in solids decay nonradiatively by exciting lattice vibrations (phonons). When the energy gap between the excited level and the next lower electronic level is larger than the phonon energy, several lattice phonons are emitted in order to bridge the energy gap. It was recognized that the most energetic vibrations are responsible for the nonradiative decay since such a process can conserve energy in the lowest order. In glasses the most energetic vibrations are the stretching vibrations of the glass network polyhedra; it was shown that these distinct vibrations are active in the multiphonon process, rather than the less energetic vibrations of the bond between the R and its surrounding ligands. It was demonstrated that these less energetic vibrations may participate in cases when the energy gap is not bridged totally by the high-energy vibrations. The experimental results reveal that the logarithm of the multiphonon decay rate decreases linearly with the energy gap, and hence with the number of phonons bridging the gap, when the number of phonons is larger than two. Figure 3 presents the logarithm of the nonradiative relaxation rate versus the number of phonons of the glass-forming material. Figure 4 presents the same dependence; however, two phonons are taken as the origin of the abscissa.

Application of the multiphonon theory to glasses requires the knowledge of the structural units forming the glass. Similar to the electronic spectra in glasses, the vibrational frequencies show inhomogeneous broadening due to the variation of sites. Table 2 shows the average frequencies of the network formers. The vibrations involving the network modifiers are lower by a factor of 2 to 4. Considering the dependence of the multiphonon relaxation rate, W_p, on the phonon occupation number for a p-order multiphonon decay at temperature $T > 0$,

$$W_p = B[n(T) + 1]^p \exp(-\alpha\,\Delta E)\,, \tag{19}$$

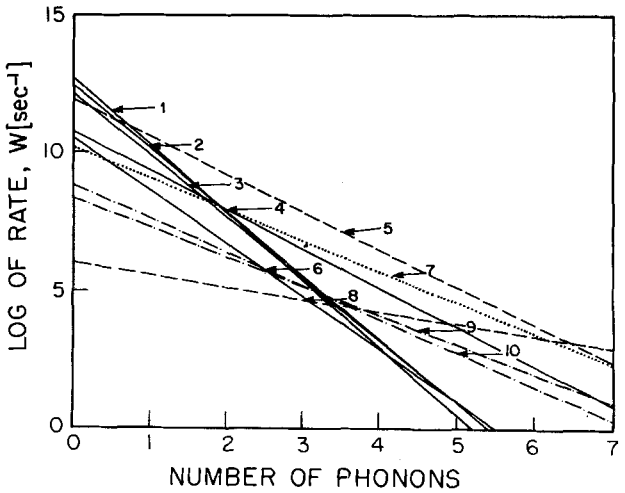

Fig. 3. Dependence of multiphonon relaxation on the number of phonons in the glass former needed to bridge the energy gap between the luminescent J-level and the closest lower-lying level. The curves refer to glasses of the following types: (1) phosphate; (2) borate; (3) silicate; (4) tellurite; (5) fluoroberyllate; (6) germanate; (7) zirconium fluoride (ZBLA); (8) aluminum lanthanide sulfide (ALS) and gallium lanthanide sulfide (GLS); (9) the crystalline hosts $Y_3Al_5O_{12}$(YAG), and (10) LaF_3.

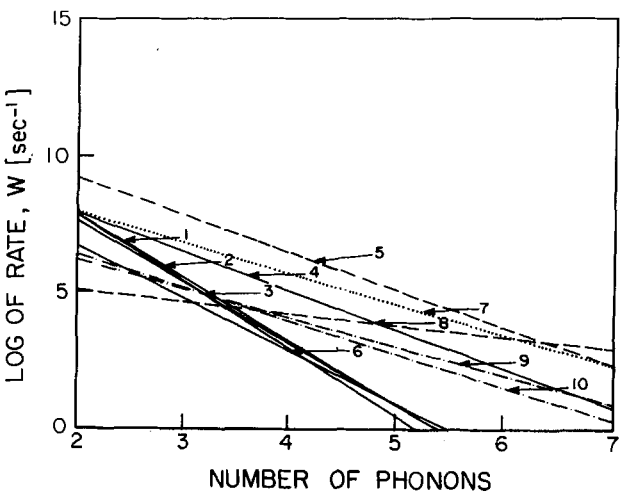

Fig. 4. Dependence of multiphonon relaxation on the number of phonons in the glass former and in two crystalline materials (note that the abscissa starts at 2 phonons). The numbering of the samples is the same as in fig. 3.

TABLE 2
Parameters for nonradiative relaxations in glasses.

Matrix	B (s^{-1})	α (10^{-3} cm)	$\hbar\omega$ (cm^{-1})	a	$\log_{10} B^*$	Ref. *3
tellurite	6.3×10^{10}	4.7	700	0.30	7.97	a
phosphate	5.4×10^{12}	4.7	1200	0.18	7.88	a
borate	2.9×10^{12}	3.8	1400	0.19	7.89	a
silicate	1.4×10^{12}	4.7	1100	0.19	7.89	b
germanate	3.4×10^{10}	4.9	900	0.23	6.74	a
ZBLA *1	1.59×10^{10}	5.19	500	0.38	7.97	c
	1.88×10^{10}	5.77	460–500	0.36	7.89	d, e
LaF_3 (cryst.)	6.6×10^{8}	5.6	350	0.50	7.1	f
ALS, GLS *2	10^{6}	2.9	350	1.0	5.1	a

*1 ZBLA glass: 57 ZrF_4 : 34 BaF_2 : 3 LaF_3 : 4 AlF_3 : 2 RF_3.
*2 ALS glass: 3 Al_2S_3 : 0.872 La_2S_3 : 0.128 Nd_2S_3; GLS glass: 3 Ga_2S_3 : 0.85 La_2S_3 : 0.15 Nd_2S_3.
*3 References:
(a) Reisfeld (1980).
(b) Layne et al. (1977).
(c) Reisfeld et al. (1985a).
(d) Shinn et al. (1983).
(e) Tanimura et al. (1984).
(f) Riseberg and Moos (1968).

where ΔE is the energy gap between the emitting and next lower level

$$\alpha = -\ln(\varepsilon)/\hbar\omega \,, \tag{20}$$

and α and B are dependent on the host but independent of the specific electronic level of R from which the decay occurs.

In calculating theoretically the multiphonon relaxation (Englman, 1979), the electronic matrix elements are separated from the vibrational ones, assuming that the transition is dominated by a small number of promoting modes which consume the energy $\hbar\omega$. The accepting modes provide only for the remaining energy difference $\Delta E_0 - \hbar\omega_{max}$.

The multiphonon decay rate from a given level to the next lower level decreases with the lowering of energy of the stretching frequencies of the glass former. Since, in order to reach the same energy gap, a larger number of phonons is needed in fluoride and in chalkogenide glasses, the nonradiative relaxations are, under equal circumstances, smallest in these glasses.

Table 2 gives B and α of eq. (19) together with the highest phonon energy for a variety of glasses and crystals. For most oxide glasses, α is fairly constant while B differs by several orders of magnitude. Schuurmans and Van Dijk (1984) carefully analyzed this phenomenon, and gave specific reasons to decrease the energy gap by twice the phonon energy, and hence write

$$\begin{aligned} W_{NR} &= B^* \exp[(-\Delta E + 2\hbar\omega)\alpha] \,, \\ \log_{10} B^* &= \log_{10} B - 0.86\alpha\hbar\omega = \log_{10} B - (0.86/a) \,, \end{aligned} \tag{21}$$

TABLE 3

Radiative transition probabilities, branching ratios β, lifetimes, oscillator strengths, and peak cross sections for holmium(III) in ZBLA glass at 300 K [Reisfeld et al. (1985a) when no other reference is given].

Transition	cm^{-1}	A_{ED} (s^{-1})	A_{MD} (s^{-1})	β	τ_{obs} (μs)	τ_{calc} (μs)	$P(10^{-6})$ meas.	$P(10^{-6})$ calc.	σ_p (10^{-20} cm^{-2})
$^5I_7 \rightarrow {}^5I_8$	5150	63	21	1.00	4200 *4	11900	1.95	1.79	0.93 *1
$^5I_6 \rightarrow {}^5I_7$	3550	16	11.5	0.15	–	–	–	1.06	–
$\rightarrow {}^5I_8$	8700	150	–	0.85	2500 *4	2900	1.03	1.03	0.42 *1
$^5I_5 \rightarrow {}^5I_6$	2570	5	5	0.08	–	–	–	0.82	–
$\rightarrow {}^5I_7$	6120	74	–	0.55	–	–	–	0.92	–
$\rightarrow {}^5I_8$	11270	50	–	0.37	–	40	0.16	0.16	0.56 *1
$^5I_4 \rightarrow {}^5I_5$	1870	2.5	1.3	0.07	–	–	–	0.37	–
$\rightarrow {}^5I_6$	4440	21	–	0.37	–	–	–	0.37	–
$\rightarrow {}^5I_7$	7990	26	–	0.46	–	–	–	0.14	–
$\rightarrow {}^5I_8$	13140	6	–	0.10	–	0.9	0.015 *4	0.012	–
$^5F_5 \rightarrow {}^5I_4$	2480	0.04	0.05	0.00	–	–	–	0.01	–
$\rightarrow {}^5I_5$	4350	5	0.01	0.00	–	–	–	0.18	–
$\rightarrow {}^5I_6$	6920	73	1.5	0.04	–	–	–	0.84	–
$\rightarrow {}^5I_7$	10470	350	–	0.19	–	–	–	1.5	1.3
$\rightarrow {}^5I_8$	15620	1430	–	0.77	25	25	2.44	2.43	0.9
$^5S_2 \rightarrow {}^5I_6$	9750	140	–	0.07	–	–	–	0.27	–
$\rightarrow {}^5I_7$	13300	760	–	0.36	–	–	–	0.81	1.93 *2
$\rightarrow {}^5I_8$	18450	1140	–	0.55	105	106 *3	[3.38]	0.63	0.34 *2
$^5F_4 \rightarrow {}^5I_6$	9900	210	–	0.06	–	–	–	0.72	–
$\rightarrow {}^5I_7$	13450	300	–	0.09	–	–	–	0.55	0.93 *2
$\rightarrow {}^5I_8$	18600	2880	–	0.82	105	106 *3	[3.38]	2.8	0.63 *2
$^5F_3 \rightarrow {}^5I_6$	11790	300	–	0.09	–	–	–	0.75	–
$\rightarrow {}^5I_7$	15340	1080	–	0.33	–	–	–	1.37	–
$\rightarrow {}^5I_8$	20490	1700	–	0.53	1.0	1.1	1.22	1.2	0.28 *1
$^5G_6 \rightarrow {}^5I_7$	17120	1500	4	0.12	–	–	–	–	–
$\rightarrow {}^5I_8$	22270	10500	–	0.84	< 0.05	0.004	10.37	10.32	3.05 *1
$^5G_5 \rightarrow {}^5I_6$	15340	580	5	0.09	–	–	–	0.6	–
$\rightarrow {}^5I_7$	18890	2130	–	0.34	–	–	–	2.8	–
$\rightarrow {}^5I_8$	24040	3090	–	0.50	0.2	0.57	2.29	2.23	1.32 *1
$^5G_4 \rightarrow {}^5I_6$	17270	2110	–	0.37	–	–	–	3.15	–
$\rightarrow {}^5I_7$	20820	1630	–	0.29	–	–	–	1.45	–
$\rightarrow {}^5I_8$	25970	600	–	0.11	1.2	1.4	0.50	0.33	0.22 *1
$^3P_1 + {}^3D_3 \rightarrow {}^5I_6$	24240	1660	–	0.38	–	–	–	–	0.29 *4
$\rightarrow {}^5I_7$	27790	1990	–	0.46	–	–	–	–	0.21 *4
$\rightarrow {}^5I_8$	32940	55	–	0.01	50 *4	–	–	–	–

*1 Evaluated from absorption spectrum.

*2 Based on estimated widths of components $^5S_2$ and $^5F_4$ of unresolved emission at 540 and 746 nm.

*3 Calculated, assuming thermalization of the levels $^5S_2$ and $^5F_4$.

*4 Tanimura et al. (1984).

TABLE 4

Radiative transition probabilities, branching ratios β, lifetimes, oscillator strengths, and peak cross sections for erbium(III) in ZBLA glass at 300 K [Reisfeld et al. (1983a) when no other reference given].

Transition	cm^{-1}	A_{ED} (s^{-1})	A_{MD} (s^{-1})	β	τ_{obs} (μs)	τ_{calc} (μs)	$P(10^{-6})$ meas.	$P(10^{-6})$ calc.	σ_p ($10^{-20}cm^2$)
$^4I_{13/2} \rightarrow {}^4I_{15/2}$	6540	86	36	1.00	8100 *2	8065	1.74	1.63	0.58
$^4I_{11/2} \rightarrow {}^4I_{13/2}$	3720	16	8.4	0.18	6000 *2	5200	–	1.1	–
$\rightarrow {}^4I_{15/2}$	10260	111	–	0.82	–	–	0.54	0.51	0.37
$^4I_{9/2} \rightarrow {}^4I_{11/2}$	2320	0.7	1.2	0.01	–	–	–	–	–
$\rightarrow {}^4I_{13/2}$	6040	41	–	0.22	–	–	–	–	–
$\rightarrow {}^4I_{15/2}$	12580	148	–	0.77	–	–	0.29	0.38	0.19
$^4F_{9/2} \rightarrow {}^4I_{9/2}$	2800	2.2	2.5	0.004	–	–	–	–	–
$\rightarrow {}^4I_{11/2}$	5120	53	6.5	0.043	120 *2	110	–	–	–
$\rightarrow {}^4I_{13/2}$	8840	62	–	0.044	–	–	–	–	–
$\rightarrow {}^4I_{15/2}$	15380	1250	–	0.909	170	110	1.86	2.13	1.12
$^4S_{3/2} \rightarrow {}^4F_{9/2}$	3140	0.5	–	0.000	–	–	–	–	–
$\rightarrow {}^4I_{9/2}$	5940	53	–	0.039	–	–	–	–	–
$\rightarrow {}^4I_{11/2}$	8260	28	–	0.021	–	–	–	–	–
$\rightarrow {}^4I_{13/2}$	11980	383	–	0.284	290	343 *1	–	–	–
$\rightarrow {}^4I_{15/2}$	18520	886	–	0.656	–	–	0.46	0.42	0.70
$^2H_{11/2} \rightarrow {}^4S_{3/2}$	750	0.03	–	0.000	–	–	–	–	–
$\rightarrow {}^4F_{9/2}$	3890	13	0.2	0.003	–	–	–	–	–
$\rightarrow {}^4I_{9/2}$	6690	58	5.7	0.014	–	–	–	–	–
$\rightarrow {}^4I_{11/2}$	9010	57	8.2	0.015	–	–	–	–	–
$\rightarrow {}^4I_{13/2}$	12730	92	66	0.036	–	343 *1	–	–	–
$\rightarrow {}^4I_{15/2}$	19270	4110	–	0.932	–	–	4.88	5.39	2.54

*1 Assuming thermalization of $^2H_{11/2}$ with lower-lying $^4S_{3/2}$.

*2 Shinn et al. (1983).

where $0.86 = \log_{10} e^2$. The value of $\log_{10} B^*$ is also presented in table 2 and is seen to differ much less between most glasses (and crystals) than B. One may also compare with fig. 4.

The multiphonon transition rates for lanthanides in a variety of glasses can be obtained from eq. (21) using the tabulated B^*, α, and $\hbar\omega$ in table 3 and the energy difference to the next lower J level ΔE. The good agreement with experiment (typical uncertainties are 0.1 or 0.2 in $\log_{10} W_{NR}$) has been demonstrated for Pr(III) (Eyal et al., 1985); Nd(III) (Lucas et al., 1978), Ho(III) (Tanimura et al., 1984; Reisfeld et al., 1985a), and Er(III) (Reisfeld and Eckstein, 1975a; Shinn et al., 1983; Reisfeld et al., 1983a).

The multiphonon processes compete with luminescence as excitation energy is lost to the local vibrations of the glass formers. Other nonradiative losses arise from energy transfer to the electronic states of atoms in the vicinity of the excited ion. The energy-transfer process may be either resonant or phonon-assisted, where the excess of energy is dissipated as heat. The energy deficiency in nonresonant processes may be supplied by the thermal reservoir of the low-energy phonons ($kT = 210\,\mathrm{cm}^{-1}$ at 300 K) to match the missing energy. Because of thermodynamical considerations the last process is much less efficient. As characteristic examples of observed and radiative lifetimes, branching ratios, etc., the $4f^{10}$ holmium(III) in ZBLA glass is treated in table 3, and $4f^{11}$ erbium(III) in table 4.

4.2. *Cross-relaxations*

A special case of energy transfer is cross-relaxation, where the original system loses the energy $(E_3 - E_2)$ by obtaining the lower state E_2 (which may also be the ground state E_1) and another system acquires the energy by going to a higher state E_2'. Cross-relaxation may take place between the same lanthanide (being a major mechanism for quenching at higher concentration in a given material) or between two differing elements, which happen to have two pairs of energy levels separated by the same amount.

The cross-relaxation between a pair of R ions is graphically presented in fig. 5.

The two energy gaps may be equal or can be matched by one or two phonons. Cross-relaxation has been measured in a variety of ions and it is a dominating factor in nonradiative relaxations at high concentration. The nonradiative relaxation rates can be obtained by analysis of the decay curves of R fluorescence using the formula of the general form where the population number of state i, N_i, is proportional to the intensity of emitted light, I_i:

$$\frac{\mathrm{d}N_i(t)}{\mathrm{d}t} = -\left(\gamma_R + X_i + \sum_{i \neq j} W_{ij}\right) N_i(t) + \sum_{i \neq j} W_{ji} N_i(t)\,. \tag{22}$$

$\mathrm{d}N_i(t)/\mathrm{d}t$ is the decrease of intensity after pulse excitation, γ_R is the reciprocal of

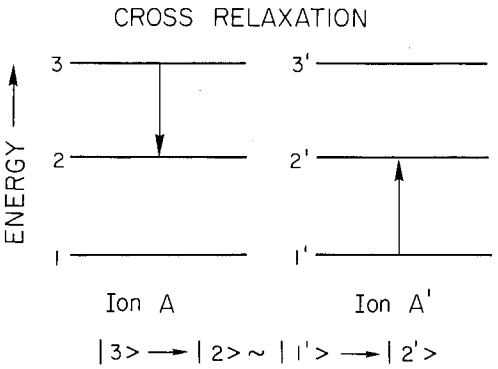

Fig. 5. Scheme for cross-relaxation between two ions of the same, or of different nature.

the lifetime of the excited state in the absence of a cross-relaxation process. ΣW_{ij} is the probability for cross-relaxation, W_{ji} is the probability of the inversed process, and W_{ij} is the rate of cross-relaxation.

Theoretically, the cross-relaxation rate for a dipole–dipole transfer can be obtained from the formula (Reisfeld, 1976a)

$$P_{SA}^{(DD)} = \frac{1}{(2J_S+1)(2J_A+1)} \frac{2}{3} \left(\frac{2\pi}{h}\right)\left(\frac{e^2}{R^3}\right)^2 \left[\sum_t \Omega_{tS} \langle J_S \| U^{(t)} \| J'_S \rangle^2\right] \times \left[\sum_t \Omega_{tA} \langle J_A \| U^{(t)} \| J'_A \rangle^2\right] \bar{S} \,. \tag{23}$$

Here Ω_t are the Judd–Ofelt intensity parameters, $\langle J \| U^{(t)} \| J' \rangle$ is the matrix element of the transition between the ground and excited state of the sensitizer and activator, respectively. [The calculation of these matrix elements in the intermediate-coupling scheme is now a well-known procedure and may be found in Reisfeld (1976a) and Riseberg and Weber (1976)]. $\bar{S}$ is the overlap integral and R is the interionic distance.

The measured lifetime of luminescence is related to the total relaxation rate by

$$\frac{1}{\tau} = \sum W_{NR} + \sum A + P_{CR} = \frac{1}{\tau_0} + P_{CR} \,, \tag{24}$$

where ΣA is the total radiative rate, ΣW_{NR} is the nonradiative rate and P_{CR} is the rate of cross-relaxation between adjacent ions.

The possible cross-relaxation channels for Pr(III), Nd(III), and Ho(III) are outlined in table 5 (Reisfeld, 1985c, Reisfeld and Eyal, 1985).

In order to obtain the critical radii, which are the distances at which the probability for cross-relaxation is equal to the sum of the radiative and multi-phonon probabilities, the decay curves are analyzed with respect to the Inokuti–Hirayama model (Inokuti and Hirayama, 1965).

TABLE 5

Cross-relaxation mechanisms involving the same lanthanide, and critical radii, for praseodymium(III), neodymium(III), and holmium(III) in glasses.

Ion	Glass *	Lifetime		R/cm^3 (10^{20})	Transition $E_3 \rightarrow E_1$		Relaxation path (fig. 5) $E_3 \rightarrow E_2$ and $E_1 \rightarrow E_2'$		R_0 (Å)
		τ_{obs} (μs)	τ_{rad} (μs)		E_3	E_1	E_2	E_2'	
Pr(III)	ZBLA	13	41	3.25	$^3P_0 + {}^3P_1$	$^3H_4$	$^1G_4$	$^1G_4$	8.23 ± 0.18
	ZBLA	60	605	3.25	$^1D_2$	$^3H_4$	$^1G_4$	$^3F_3 + {}^3F_4$	10.0 ± 0.8
Nd(III)	LLP	216	395	2.70	$^4F_{3/2}$	$^4I_{9/2}$	$^4I_{15/2}$	$^4I_{15/2}$	6.58 ± 0.29
	LLP	167	395	5.49	$^4F_{3/2}$	$^4I_{9/2}$	$^4I_{15/2}$	$^4I_{15/2}$	6.50 ± 0.36
	LLP	96	395	8.40	$^4F_{3/2}$	$^4I_{9/2}$	$^4I_{15/2}$	$^4I_{15/2}$	6.74 ± 0.38
Ho(III)	ZBLA	105	330	3.20	$^5S_2 + {}^5F_4$	$^5I_8$	$^5I_4$	$^5I_7$	5.54 ± 0.28
	ZT	12.3	110	0.48	$^5S_2 + {}^5F_4$	$^5I_8$	$^5I_4$	$^5I_7$	3.32 ± 1.3
	ZT	10.2	110	1.90	$^5S_2 + {}^5F_4$	$^5I_8$	$^5I_4$	$^5I_7$	4.21 ± 0.44
	ZT	9.3	110	5.80	$^5S_2 + {}^5F_4$	$^5I_8$	$^5I_4$	$^5I_7$	3.44 ± 0.56

* ZBLA: zirconium barium fluoride glass; LLP: lithium lanthanum phosphate glass; ZT: zinc tellurite glass.

The energy transfer between Cr(III) and Nd(III) (Reisfeld and Kisilev, 1985), and Cr(III) and Yb(III) (Reisfeld, 1983), has been studied extensively by static and dynamic methods. The transfers occur by dipole–dipole mechanisms and are important in increasing the pumping range of Nd(III) and Yb(III) ions.

4.3. *Temperature dependence and lifetime of the excited states*

Huang and Rhys (1950) base their theoretical explanation of the temperature dependence of the nonradiative decay rate on a single-configuration-coordinate model, in which the parabolas representing the ground- and excited-state oscillators both have the same force constants, but whose minima are offset. The use of the time-dependent perturbation theory for calculation of multiphonon emission rates for the rare-earth ions, with no restriction on force constants or offsets, was also provided (Struck and Fonger, 1975; Fonger and Struck, 1978). In this treatment the theoretical data may differ by one order of magnitude from the experimental results. A phenomenological model of multiphonon emission in crystals (Riseberg and Moos, 1968) and in glasses (Reisfeld and Eckstein, 1975a) gives good agreement with experiment when the number of phonons bridging the emitting and terminal levels is more than two. Recently, a modified energy-gap model was developed (Schuurmans and Van Dijk, 1984). Their model assumes that the phonons having single highest frequencies are active in the nonradiative transition.

The expression for the temperature dependence is

$$W_{\mathrm{NR}}(T) = W_{\mathrm{NR}}(0)\left[\frac{\exp(\hbar\omega)/kT}{\exp(\hbar\omega/kT)-1}\right]^{p}, \tag{25}$$

where p is the number of phonons emitted in the transition, and $W_{\mathrm{NR}}(0)$ is the low-temperature multiphonon emission rate.

Experimentally, the multiphonon emission rate of an excited state i to an adjacent lower-lying state j in the absence of energy transfer is given by

$$W_{\mathrm{NR}} = \frac{1}{\tau_{\mathrm{obs}}} - \frac{1}{\tau_i} \tag{26}$$

at a constant temperature. In this formula τ_{obs} is the observed lifetime of state i at the particular temperature, and the subscript NR stands for the nonradiative process.

Expression (26) has been found to account fairly well for the temperature dependence of the nonradiative rate as determined by the use of equation (25) at various temperatures in oxide glasses (Layne et al., 1977; Reisfeld and Eckstein, 1975a; Reisfeld and Hormadaly, 1976) in cases where the highest-energy phonons were active. However, when the energy gap cannot be bridged by only one

frequency phonon, two vibrational modes are responsible for the relaxation (Hormadaly and Reisfeld, 1977; Reisfeld et al., 1978). In instances where less than one phonon is needed to bridge the energy mismatch, the relaxation is slowed down due to a bottleneck created, as shown in the relaxation of Ho(III) in tellurite glass (Reisfeld and Kalisky, 1980a). The temperature dependence of multiphonon relaxation in fluoride glasses was studied for Er(III) (Shinn et al., 1983), for Ho(III) (Tanimura et al., 1984), and for Nd(III) (Lucas et al., 1978). The temperature dependence in these glasses exhibits a similar behavior to the oxide glasses; however, the phonon energies of about 500 cm^{-1}, characteristic for fluoride glasses when put into eq. (25), result in the best theoretical fit.

5. Energy transfer between differing species

5.1. *Possible mechanisms of energy transfer*

Energy transfer between two inorganic ions can occur either by multipolar interaction or an exchange mechanism in dilute systems (Reisfeld and Jørgensen, 1977; Reisfeld, 1973, 1975, 1976a), or by multi-step migration in concentrated systems (Powell and Blasse, 1980). In addition to resonant transfer, phonon-assisted transfer is a quite common phenomenon (Reisfeld, 1976a, 1986).

Usually, energy transfer efficiencies and probabilities determined experimentally for macroscopic systems are applied to some average values and not to actual distances between donor and acceptor ions. The theories for resonant energy transfer were developed by Dexter (1953) and Förster (1959) for multipolar coupling, and by Inokuti and Hirayama (1965) for exchange coupling; the theory for nonresonant energy transfer, where the energy mismatch between the energy levels of the donor and the acceptor ions is compensated by the emission or absorption of phonons, was developed by Miyakawa and Dexter (1970).

The energy transfer mechanism in dilute systems has been summarized by Watts (1975). At high donor concentrations and at elevated temperatures the donor–donor transfer may be appreciable. The fluorescence decay curves of the donors behave differently in the two cases mentioned above. If we write the donor–acceptor transfer rate as a/R^s and the donon–donor rate as b/R^s, where R is the separation between the interacting ions and s equals 6, 8, and 10, for dipole–dipole, dipole–quadrupole, and quadrupole–quadrupole interactions, respectively, then two limiting cases can be considered: (i) $b/a = 0$, where donor–donor interaction is absent, and (ii) $b/a \gg 1$, where donor–donor interaction is predominant. In the former case the decay curve of the donor fluorescence is nonexponential, being the sum of the decay of an isolated donor ion and the energy transfer to various accepted ions characterized by the factor $\exp(-At^{3/s})$. In the opposite limit, which corresponds to rapid donor–donor transfer, the decay is exponential at all times, with a rate equal to the total donor–acceptor transfer

rate averaged over all donors. In most cases falling between these two limits the donor decay is initially nonexponential but becomes exponential in the long-time limit.

The energy-transfer processes in laser materials are discussed thoroughly by Auzel (1980) and Weber (1981). An excellent theoretical treatment of energy-transfer dynamics can be found in an article by Huber (1981). Energy transfer between inorganic ions in glasses has been also summarized recently (Reisfeld, 1984c). The various mechanisms are summarized below.

5.1.1. *Radiative transfer*

Radiative transfer occurs when the absorption spectrum of the acceptor ion overlaps the emission of the donor ion. The emission profile of the donor ion in such a case are concentration- and geometry-dependent and the lifetime of the donor is independent of the concentration.

The probability of such a transfer between the D and A ions at distance R is:

$$W_{SA}(R) = \frac{\sigma_A}{4\pi R^2} \frac{1}{\tau_D} \int g_S(\nu) g_A(\nu)\, d\nu\,, \tag{27}$$

where σ_A is the integrated absorption cross section of an A ion. An example of radiative transfer is germanate glass codoped with Bi(III) and Eu(III) (Boulon et al., 1979).

The excitation spectra of 0.8% Bi(III) germanate glass consist of two broad bands with maxima at 2780 Å and 3190 Å at $T = 4.2$ K and 2860 Å and 3250 Å at room temperature. By pumping in the first band $^1S_0 \rightarrow {}^3P_1$ with a nitrogen laser, it is easy to observe the broad blue fluorescence band (4490 Å at 295 K) due to the $^3P_1 \rightarrow {}^1S_0$ transition and 4650 Å at 4 K due to the $^3P_0 \rightarrow {}^1S_0$ transition. At 4.2 K only the $^3P_0 \rightarrow {}^1S_0$ band has a time constant long enough for accurate measurements ($\tau_0 = 0.7$ ms). A subset of ions in the quasi-continuum of multisites in glass was selected and the fluorescence spectra and decay curves were obtained for various concentrations of Eu(III) acceptor ions up to 5%.

The radiative transfer can be visualized from the dip in the maximum of the $^3P_0 \rightarrow {}^1S_0$ broad band corresponding to the $^7F_0 \rightarrow {}^5D_2$ forced electric dipolar transition. The radiative transfer efficiency η_R can be approximately calculated by comparing the area of the dip to the area of the emission band included in the spectral range of the $^5D_2$ absorption: the rate of the radiative transfer, η_R, is 0.05 with 0.5% Eu(III), and 0.3 with 5% Eu(III), in agreement with eq. (27). η_R is independent of temperature.

5.1.2. *Nonradiative transfer*

The interaction between the donor and the acceptor ion may occur via an exchange interaction when their wave functions overlap; the following expression

for the transfer probability then holds:

$$W_{DA}(R) \propto \exp\left(-\frac{2R}{L}\right) \int g_D(\nu) g_A(\nu)\, d\nu\,, \tag{28}$$

where R is the distance between the two ions, L the effective average Bohr radius, and $g_D(\nu)$ and $g_A(\nu)$ are the normalized absorption and emission spectral shapes of the donor and acceptor ions. The integral presents the spectral overlap.

5.1.3. *Multipolar interaction*

Multipolar interaction has been previously discussed in section 4.2, in connection with cross-relaxation, where the general formula for time evolution was presented. The same formula holds for macroscopic cases of energy transfer. When dealing with the microscopic situation, we have for the resonant nonradiative energy transfer

$$W_{DA}^{R} = (R_0/R)^s \tau_d^{-1}\,, \tag{29}$$

where s equals 6, 8, and 10, for dipole–dipole, dipole–quadrupole, and quadrupole interaction, respectively, and $R_0 \approx g_D(\nu) g_A(\nu)\, d\nu$ according to the Förster–Dexter theory. When there is no diffusion within the donor system, eq. (27) acquires the form given by Inokuti and Hirayama (1965):

$$I(t) = \exp\left[-\frac{t}{\tau_d} - \Gamma\left(1 - \frac{3}{s}\right)\left(\frac{t}{\tau_d}\right)^{3/s}\right], \tag{30}$$

corresponding to a situation where one donor ion is surrounded by a large amount of acceptor ions.

5.1.4. *Phonon-assisted transfer*

Here one has to distinguish between energy transfer among ions of the same nature and between different types of ions. The energy transfer within inhomogeneously distributed ions requires lattice phonons (vibrations) to make up for the energy gap to enable the transfer. The phonon assistance may involve one or more acoustic phonons of energy of several reciprocal centimeters (Holstein et al., 1981). A microscopic treatment of this type of phonon-assisted energy transfer results in a paradoxical situation: one-phonon-assisted transfers are inhibited between sites that have similar coupling strength to the lattice and two-phonon transfers are more probable.

When the energy mismatch is considerably larger than the maximum phonon energy available, multiple-phonon interactions are required for conservation of energy. This has been formulated by Miyakawa and Dexter (1970). The energy-

transfer probability according to their theory is given by

$$N_{DA}^{NR} = (R_0/R)^s \tau_D^{-1}, \quad s = 6, 8, 10. \tag{31}$$

This formula for nonresonant transfer resembles the formula for resonant transfer; however, in this case $R_0^s \simeq \exp(-\beta\,\Delta E)$, where β is related to the coefficient α of multiphonon relaxation by $\beta = \alpha - \ln 2$, α being given by $\alpha = \hbar\omega^{-1}\ln\{[p/S(\bar{n}+1)]-1\}$.

5.1.5. *Energy transfer in the case of interaction between donor ions*

The diffusion of energy in the donor-system ion occurs in concentrated systems and is of the same magnitude as the transfer between donors and acceptors. The general case of diffusion in the donor system has been treated by Yokota and Tanimoto (1967). When energy transfer occurs by a dipole–dipole mechanism, their equation takes the form under uniform distribution

$$N_D(t) = N_D(0)\,e^{-t/\tau} \exp\left[\tfrac{4}{3}\pi^{3/2} N_A (\alpha t)^{1/2} \left(\frac{1 + 10.87x + 15.50x^2}{1 + 8.743x}\right)^{3/4}\right], \tag{32}$$

where $x = D\alpha^{-1/3}t^{2/3}$, $W_{SA} = \alpha R^{-6}$, and D is the diffusion constant.

The survival probability of the excited donor ions $\phi(t)$ is nonexponential at short times t, where the migration is still unimportant. In this limit it approaches the Inokuti–Hirayama function for d–d interaction. For large t, $D(t)$ decays exponentially at a rate determined by the migration. As migration becomes more rapid, the boundary between these two regions shifts to shorter times until, for sufficiently fast migration, the decay appears to be a pure exponential. This long-time behavior is referred to as diffusion-limited relaxation. In the limit, as t goes to infinity, the fluorescence decay function (Inokuti and Hirayama, 1965) becomes

$$\phi(t) = \exp\left(-\frac{t}{\tau} - \frac{t}{\tau_D}\right), \qquad \frac{1}{\tau_D} = 0.51(4\pi N_A \alpha^{1/4} D^{3/4}). \tag{33}$$

The last equation characterizes the regime which is most easily investigated experimentally because the experimental conditions enable analyzing the behavior of decay curves at long times in a more tractable way.

It was shown (Layne, 1975) that the diffusion-limited decay depends on the concentration of sensitizer and activator ions by

$$\phi(t) = \exp\left(-\frac{t}{\tau} - k_2 N_S N_A\, t\right), \tag{34}$$

where k_2 is a constant proportional to α_S and α_A.

Experimental evidence for migration of energy has been given in many papers

recently. Weber (1971) investigated energy transfer between europium and chromium in phosphate glasses and analysed his data in view of the Yokota–Tanimoto theory. He found that the diffusion constant within Eu(III) in $Eu(PO_3)_3$ glass is 6×10^{-10} cm^2 s^{-1} at room temperature.

5.2. *Novel experimental techniques of studying energy transfer*

This section reviews the application of two new experimental methods to study energy transfer in glasses: (a) *time-resolved spectroscopy*, and (b) *fluorescence line-narrowing* (FLN).

A very effective method to study incoherent transport of electronic excitation in glasses is the method of time-dependent selective spectroscopy (Weber, 1981). In this method, a short laser pulse is used to excite selectively ions having a single energy by following the changes of the emission frequency with time. This observation enables the study of the kinetics of migration of energy from originally excited centers.

The technique of FLN, using laser excited luminescence spectroscopy, has contributed to our understanding of glass structure. Since glass is a strongly disordered medium, both absorption and emission spectra exhibit considerable inhomogeneous broadening. FLN allows the excitation of individual sites (Weber, 1981) in the inhomogeneously broadened band, which has a typical width of 100 cm^{-1}.

Applying FLN measurements, Brecher and Riseberg (1976) succeeded in measuring radiative and nonradiative parameters for individual sites of Eu(III) in NaBaZn silicate glass. Other examples of FLN studies in glasses may be found in the papers by Motegi and Shionoya (1973), Takushi and Kushida (1979), Hegarty et al. (1979), and Brecher and Riseberg (1980).

Phospho-tungstate glasses doped by Eu(III) were studied by Durville et al. (1983). The analysis of the experimental data allowed them to locate the Eu(III) residing in holohedrized symmetry in the glass and crystalline domain of the phosphotungstate matrix.

A clear-cut example of the use of time-resolved spectroscopy for studying the energy migration of Yb(III) in silicate glass can be found in the paper by Weber et al. (1976).

The emission of Yb(III) corresponds to the transition between the lowest "ligand field" levels of the $^2F_{5/2}$ and $^2F_{7/2}$ manifolds. Following the laser pulse, the initial line-narrowed luminescence decays, due to radiative decay and nonradiative transfer to other Yb(III) ions, without pronounced broadening. However, luminescence from the acceptor ions results in a rise of the inhomogeneously broadened emission profile, demonstrating that transfer occurs to nearby, but spectrally different sites. The transfer was attributed to multipolar processes with an effective range of about 1 nm.

Time-resolved spectroscopy was also used by Moine et al. (1981) to study

energy transfer between Bi(III) and Eu(III) in germanate glass at liquid helium temperature. At this temperature there is no indication of diffusion of energy within the donor system. The experimental curves of the Bi(III) emission from the $^3P_0$ level to the ground state $^1S_0$ could be fitted by the Inokuti–Hirayama formula, indicating dipole–dipole interaction between the donor Bi(III) ion and acceptor Eu(III) ion.

Basiev (1985) used time-resolved spectroscopy to study the energy migration between Sm(III), Nd(III), Eu(III), and Yb(III) ions in a variety of glasses. He believes that energy migrates by a dipole–dipole mechanism in the ions, with the exception of Eu(III), where he attributes the energy migration to a quadrupole–quadrupole mechanism. Blasse (1985) recently published reviews on energy migration and energy transfer to traps in crystals, with special emphasis on Gd(III), Eu(III), and Tb(III).

5.3. *Energy transfer between trivalent lanthanides*

Energy transfer between trivalent rare earths has been investigated thoroughly in crystals (Blasse, 1984) in connection with their use for phosphors and related compounds. Their sharp lines, mainly arising from the zero-phonon transitions, are ideal for energy transfer studies. In the transfer studies one can derive a distinction between dilute systems, which have been shown to follow the pattern of dipole–dipole interaction, and concentrated systems, the extreme case of which is the stoichiometric material of the pentaphosphate type, suitable for minilasers. The migration of energy in the latter class is mainly diffusion controlled. In glasses, energy transfer between different lanthanides was studied thoroughly in dilute systems (Reisfeld, 1973, 1976a; Reisfeld and Jørgensen, 1977; Weber, 1981).

Energy absorbed by a donor system in a glass which contains both donor and acceptor ions will excite the donor system. If the energy is absorbed to levels higher than the emitting state, the excess energy is lost to the glass matrix as phonons until the emitting level is reached. The excited donors can then return to the ground state by spontaneous emission or by transfer of energy to the nearest acceptor ions. Reisfeld (1984c) discusses energy transfer between UO_2^{+2} and Sm(III), Pr(III), Eu(III), Nd(III), and Ho(III), between Bi(III) and Nd(III), and between Mn(II) and Eu(III). Qualitative evidence of energy transfer between Cr(III), Nd(III), and Yb(III) in lanthanum phosphate glass is also given. Quantitative data of energy transfer between Cr(III) and Nd(III) in lithium lanthanum phosphate glasses (LLP) are presented below.

Some recent additional evidence for a dipole–dipole transfer between Sm(III) and Nd(III) (Joshi, 1978a), and Eu(III) and Nd(III) in sodium borate glass (Joshi, 1978b) was found. In addition, energy transfer from Tb(III) to Sm(III) in barium borate glass as been found to take place by a dipole–dipole mechanism (Agarwal et al., 1984).

Diffusion of energy in the europium system has been discovered to be the

decisive factor in energy transfer from europium to chromium in europium phosphate glass (Weber, 1971), and in the ytterbium system in barium aluminum phosphate glass (Ashurov et al., 1984). Phonon-assisted energy transfer according to the theory of Miyakawa and Dexter was detected by Yamada et al. (1971) for a variety of rare-earth ions in yttrium oxide. Chen et al. (1984) found this transfer between ytterbium and neodymium in phosphate glass. Energy transfer between neodymium and ytterbium in tellurite glass was found to be very efficient (Reisfeld and Kalisky, 1981). Contrary to the assumption of Holstein et al. (1981), discussed previously, a one-phonon-assisted transfer was observed by Chen et al. (1984). The efficient transfer from Nd(III) to Yb(III) in a lead–gallium–zinc fluoride glass agrees with the model of Eyal et al. (1986) for the detailed time evolution.

5.4. *Energy transfer from the uranyl ion to lanthanides*

The uranyl ion (Rabinowitch and Belford, 1964) has been extensively studied in connection with its photophysics (Jørgensen and Reisfeld, 1982a) and luminescence. It has been established that in glasses similarly to crystals the uranyl ion forms a linear molecule with U–O distances of about 1.75 Å, which is about 0.6 Å shorter than the distances to 5 or 6 ligating oxygen atoms from the glass in the equatorial plane. The excited states around $20000\,cm^{-1}$ arise from electron transfer from the highest M.O. (of odd parity) of the 2p oxygen orbitals to the empty orbitals of uranium.

The lowest excited state of the uranyl ion is the only long-lived state. All the higher levels are nonradiatively deexcited to this level, followed by emission in the yellow and green part of the spectrum (Lieblich-Sofer et al., 1978). The oscillator strengths to the lowest levels are about 10^{-4} for the region between 20000 and $25000\,cm^{-1}$ and represent at least four electronic transitions (Jørgensen and Reisfeld, 1983a) from π_u or σ_u orbitals of oxygen 2p orbitals to the empty 5f shell. There are no parity-allowed transitions below $30000\,cm^{-1}$, hence the relatively weak intensity of the electron transfer band of uranyl as compared with transition metal complexes.

In phosphate glasses five emission maxima, peaking at 20530, 19710, 18840, 17950, and $17070\,cm^{-1}$, are obtained. The decay curve can be approximated by two exponential curves with lifetimes of 115 and 367 μs (Lieblich-Sofer et al., 1978). The luminescence undergoes concentration quenching and the maximum efficiencies are obtained at about 0.1 molar concentrations. The best efficiencies at room temperature are observed in borosilicate glasses, where the efficiencies are about 50% at 0.1 mole % (Flint et al., 1983).

Efficient energy transfer from the uranyl group was observed for Eu(III) (Reisfeld et al., 1976a), for Sm(III) (Reisfeld and Lieblich-Sofer, 1979), Nd(III) and Ho(III) (Reisfeld and Kalisky, 1980b), and for Er(III) (Joshi et al., 1977). A comparative study in phosphate glasses on the energy transfer for the uranyl group to a number of rare-earth ions showed that the energy transfer is phonon-

TABLE 6
Efficiency η of the energy transfer [eq. (35)] in glasses from the ion at left to the ion at right.

	oxide concentration				oxide concentration		
	(wt.%)	(wt.%)	η		(mol.%)	(mol.%)	η
Borate glass:	Ce(III)	Tb(III)		LLP glass *:	Cr(III)	Nd(III)	
	0.025	2.0	0.19		0.05	1	0.35
	0.025	3.0	0.32		0.05	2	0.60
					0.05	3	0.75
	Ce(III)	Tm(III)			0.15	0.5	0.47
	0.13	0.05	0.09		0.15	1	0.54
	0.13	0.15	0.17		0.15	2	0.58
	0.13	0.25	0.25		0.15	3	0.79
	0.13	0.50	0.41		0.31	0.5	0.59
	0.13	1.00	0.52		0.31	1	0.76
	Tl(I)	Gd(III)			0.31	2	0.91
	0.01	1.0	0.85		0.31	3	0.92
	0.01	3.0	0.89				
	0.01	5.0	0.91		Cr(III)	Yb(III)	
	0.01	7.0	0.93		0.31	0.5	0.51
					0.31	1	0.64
	Bi(III)	Sm(III)			0.31	2	0.78
	1.0	1.0	0.19		0.31	3	0.88
$NaPO_3$ glass:	uranyl	Nd(III)					
	1	2	0.56				
	uranyl	Sm(III)					
	1	1	0.22				
	uranyl	Eu(III)					
	1	1	0.17				
	uranyl	Ho(III)					
	1	2	0.29				
Germanate glass:	Pb(II)	Eu(III)					
	1.0	2.0	0.25				
	1.0	3.0	0.41				
	1.0	7.0	0.68				
	Bi(III)	Sm(III)					
	1.0	0.5	0.28				
	1.0	1.0	0.43				
	Bi(III)	Eu(III)					
	1.0	0.5	0.20				

* Composition: $10\,Li_2O:25\,P_2O_5:4(La_{1-x-y}Ln_xCr_y)_2O_3$.

assisted with its probability decreasing along the series Nd(III), Sm(III), Eu(III), Pr(III), Tm(III), Dy(III) (Reisfeld, 1980; Reisfeld and Jørgensen, 1982). Efficiencies of transfer are summarized in table 6, from Reisfeld (1984c).

A practical consequence of the energy transfer between UO_2^{+2} and Nd(III) can be applied to LSCs, since the existence of the two ions in a glass increases the absorption range of the spectrum (Reisfeld and Kalisky, 1980b).

5.5. *Energy transfer from thallium(I) and lead(II) to lanthanides*

The first excited states of mercury-like ions having two electrons in the ns shell have been known for many years (Boulon, 1984). Due to strong spin–orbit coupling, the oscillator strengths of the $^1S_0 \rightarrow {}^3P_1$ transitions of Tl(I), Pb(II), and Bi(III) are of the order of magnitude of 0.1; the $^3P_1$ level is split in glasses into three components as the degeneracy is removed in the low-symmetry site. At low temperature, transitions are also observed from the $^3P_0$ state. Even the absorption spectrum of Sb(III) in phosphate glass (Reisfeld et al., 1977a) at room temperature consists of three components peaking at different wavelengths and arising from the transitions $^3P_1(x)$, $^3P_1(y)$, $^3P_1(z) \rightarrow {}^1S_0$. The conclusion was that Sb(III), similarly to heavy metal ions, is situated at C_s or C_2 symmetry in the glass. Energy transfer between Sb(III) and Dy(III) (Reisfeld et al., 1977a), Tl(I) and Gd(III) (Reisfeld and Morag, 1972), and Pb(II) and Eu(III) (Reisfeld and Lieblich-Sofer, 1974) exhibits nonradiative energy transfer in glasses.

Contrary to energy transfer between a couple of rare-earth ions, where the transfer probabilities can be obtained from optical transition probabilities using the Judd–Ofelt approach, in the present case the transfer probabilities cannot be predicted theoretically, as the optical transitions in the donor ions depend strongly on the ligand field and our present theoretical techniques do not allow *a priori* calculation of these transitions in the condensed phase.

Practical aspects of the energy transfer described here may be found in increasing the pumping efficiency of glass lasers or in recently studied luminescent solar concentrators (Reisfeld and Jørgensen, 1982; Reisfeld et al., 1981, 1983b; Kisilev et al., 1982; Reisfeld and Kisilev, 1985).

Our discussion here will include energy transfer between UO_2^{+2} and Nd(III), Ho(III) and Eu(III) in oxide glasses, Bi(III) and Nd(III) and Eu(III) in oxide glasses, Cr(III) and Nd(III) and Yb(III) in lithium lanthanum phosphate glasses (LLP), and Mn(II) and Er(III) in fluoride and oxide glasses.

The formulae for the determination of energy transfer probabilities and efficiencies are obtained from experimentally measured lifetimes of the donor ion with and without addition of the acceptor ion, the decrease of the donor-luminescence quantum yield in the presence of the acceptor ion, and the increase of the acceptor emission when excited via the donor ion as compared to the acceptor emission when exciting the acceptor ion directly. This can be summarized in the following equations:

The efficiency η_{tr} of the energy transfer for measured lifetimes is given by

$$\eta_{tr}^{(1)} = 1 - \frac{\tau_d}{\tau_d^0}, \tag{35}$$

where τ_d^0 is the lifetime of the donor ion in singly doped glasses and τ_d is the lifetime of the donor ion in presence of the acceptor ion.

When the lifetimes are not single exponentials, the average lifetimes are used. The average lifetime τ_{av} is defined as

$$\tau_{av} = \frac{\int_0^\infty tI(t)\,dt}{\int_0^\infty I(t)\,dt}, \tag{36}$$

where $I(t)$ is the emission intensity at a given time t.

The transfer efficiencies τ_{tr} for the decrease of the donor-luminescent efficiency in presence of the acceptor ion are obtained using

$$\eta_{tr}^{(2)} = 1 - \frac{I_d}{I_d^0}, \tag{37}$$

where I_d is the luminescence quantum efficiency of the donor ion in presence of the acceptor ion and I_d^0 is the efficiency of the donor ion in the singly doped glass.

The transfer efficiency can also be calculated from the increase of the acceptor fluorescence using

$$\eta_{tr}^{(3)} = \frac{E_a^d A_a}{E_a^a A_d}, \tag{38}$$

where E_a^a is the emission of the acceptor ion excited at the donor absorption band, E_a^d is the emission of the acceptor ion excited via the acceptor, A_a and A_d are the optical densities of the acceptor and donor at their absorption maxima.

This last equation provides the net transfer, which is the forward minus the backward transfer.

5.5.1. *Optical properties of bismuth(III)*

The optical characteristics of Bi(III)-doped oxide glasses are summarized by Reisfeld et al. (1977a). The absorption and excitation spectra of Bi(III), peaking at 330 nm, arise from the transition $^1S_0 \rightarrow {}^3P_1$ and the fluorescence of Bi(III) arises from the $^3P_1 \rightarrow {}^1S_0$ transition, peaking at about 450 nm. Although this transition is spin-forbidden, it has a high oscillator strength of about 0.1 because of strong spin–orbit coupling. The quantum efficiency of the fluorescence of Bi(III) in germanate glass is about 2%.

At room temperature, energy transfer takes place from the $^3P_1$ level and the

transfer probability from 0.1 wt.% Bi(III) to 1.0 wt.% Nd(III) is $10^6\ s^{-1}$. The same value was obtained for room temperature transfer between Bi(III) and Eu(III) (Reisfeld et al., 1976a).

The concentration dependence of the energy transfer between Bi(III) and Nd(III) reveals that at a concentration of 1.0 wt.% Bi(III) and 0.2 wt.% Nd(III) the pumping efficiency is increased by 175% (Kalisky et al., 1981). The transfer efficiency is given in table 6.

The low-temperature dependence of the above-mentioned bismuth-europium germanate glass and the time-resolved spectroscopy of these glasses has been studied by the Lyon group (Bourcet et al., 1979; Moine et al., 1981).

At liquid helium temperature, Bi(III) could be excited into an inhomogeneously broadened $^1S_0 \rightarrow {}^3P_1$ band in germanate glass and emission was observed from the $^3P_0 \rightarrow {}^1S_0$ transition. A careful analysis of the decay curves of Bi(III) reveals a dipole–dipole energy transfer to europium and absence of energy diffusion within the Bi(III) system.

5.6. *Energy transfer from d-group ions to lanthanides*

5.6.1. *Chromium(III)*

Absorption and emission of Cr(III) arises from the parity-forbidden electronic transitions in the 3d electronic shell. Crystal field split states of Cr(III) in octahedral symmetry are illustrated in the Tanabe–Sugano diagrams. The relative positions of the excited $^4T_2$ and ^2E states depend on the crystal field strength (the subshell energy difference $\Delta = 10\,Dq$). In cases where $Dq/B < 2.3$ (low-field cases) $^4T_2$ is the low state and the emission arises from the $^4T_2$ to $^4A_2$ spin-allowed transition. In the case of $Dq/B > 2.3$ (high field cases), the lowest state is ^2E and the luminescence arises from the spin-forbidden transition from ^2E to $^4A_2$ characteristic for the R-line emission of ruby. The spin-allowed transitions are characterized by broad emission spectra and short lifetimes, contrary to the spin-forbidden emission from the ^2E state (which sometimes is mixed with $^2T_1$ levels) with narrow band and long lifetimes.

All the known emissions of Cr(III) in glasses arise from $^4T_2$. Reasons for this may be: (a) $^4T_2$ lies below the ^2E level; (b) the position of these two levels may be of equal energy; however, the weak ^2E emission may be obscured by the broad emission from $^4T_2$.

The quantum efficiency of the emission arising from ^2E is usually about 100% because of the equal equilibria positions and shape of $^4A_2$ and ^2E levels in the configuration diagrams. The fluorescence efficiency from the ^4T levels varies drastically in various media. Thus, contradictory to the high efficiency of Cr(III) in crystalline fluoride materials (elpasolite), and probably in crystalline aluminum metaphosphate, the efficiency of Cr(III) in glasses is low; but it may be increased by tailoring the glass composition (Kisilev and Reisfeld, 1984). The best efficiencies for $^4T_2 \rightarrow {}^4A_2$ (23%) are obtained for LLP glasses. The reason for the

nonradiative transitions for Cr(III) in glasses is different from the multiphonon relaxation in the lanthanides, as the coupling to the host is much stronger.

5.6.2. *Energy transfer between chromium and neodymium*

The combination of the Cr(III) donor and Nd(III) acceptor is the most common combination for doubly activated laser materials. Cr(III) has strong absorbing bands in a wide spectral range, where powerful flashlamps are available. Nd(III) presents an ideal four-level laser material when doped into a suitable host; however, it has narrow and relatively weak absorption bands.

Lithium lanthanum phosphate glasses doped by Nd(III) were reported to have a reasonable cross section for laser emission (Batygov et al., 1976). Later it was suggested that a Nd laser can be pumped via Cr(III) in $Nd(Al, Cr)_3(BO_3)_4$ crystals (Hattendorf et al., 1978) and several silicate glasses (Edwards and Gomulka, 1979). Advantage of such systems is broad absorption of Cr(III) vide infra. It was shown that efficient energy transfer takes place between Cr(III) and Nd(III) in LLP glass (Avanesov et al., 1979a). However, the lifetime of Cr(III) from which the transfer rates can be determined was not measured because of the low intensity of Cr(III) luminescence. In LLP glass with high Nd concentration the interaction between Cr(III) and Nd(III) is more effective than the nonradiative losses in Cr(III). Härig et al. (1981) have observed CW lasing in LLP glasses doped by Cr(III) and Nd(III) and concluded that the presence of Cr(III) does not lower significantly the slope efficiency of Nd(III) as compared to Nd(III)-only-doped glasses. These authors concluded that presence of Cr(III) can extend the pumping range of the lasers.

In order to evaluate the advantages and disadvantages of codoping Nd(III) with Cr(III) for glass lasers and luminescent solar concentrators (LSC) (Reisfeld 1975, 1976a; Kisilev and Reisfeld, 1984) it is necessary to scan a wide concentration range of both Cr(III) and Nd(III) in order to find the optimal conditions of operation. Energy transfer from Cr(III) to Nd(III), back transfer and luminescent efficiency will strongly depend on the absolute concentration of the two ions and their relative ratio in the glass. Unfortunately, energy transfer and luminescence efficiency proceed in opposite directions and only by detailed determination of each is it possible to predict the optimal composition. Reisfeld and Kisilev (1985) have measured energy transfer as a function of donor and acceptor concentration both by static and dynamic methods. The dependence of the quantum efficiency of Nd(III) on excitation wavelength was determined. The quantum efficiency of Nd(III) when excited to $^4F_{3/2}$ (880 nm) is unity up to a concentration of 2 mole %. At a higher concentration a cross-relaxation (Reisfeld and Jørgensen, 1977) $(^4F_{3/2} \rightarrow {}^4I_{15/2}) = (^4I_{9/2} \rightarrow {}^4I_{15/2})$ takes place and the quantum efficiency is lowered to 0.45 at 3 mole % of Nd(III). Similar results were also obtained by Avanesov et al. (1979b). The excitation at higher wavelength results in lower quantum efficiencies, probably due to additional relaxation $(^4G_{5/2} \rightarrow {}^4I_{15/2}) =$

$2(^4I_{9/2} \rightarrow {}^4I_{15/2})$. For instance, at 1 mole % Nd(III) the quantum efficiency is only 0.5 when excited at 570 nm, as contrasted to 1 when excited at 880 nm.

The most relevant spectroscopic data for Nd(III) in LLP glasses are outlined in table 7. The evaluation of the energy transfer between Cr(III) and Nd(III), both by static and dynamic methods, is presented by Reisfeld and Kisilev (1985). The energy transfer from $^4T_2$ of Cr(III) (excitation at 647 nm) occurs to the lower energy levels of Nd(III) $^4F_{5/2}$ (820 nm) and $^4F_{3/2}$ (880 nm).

Table 8 gives the plate efficiencies of luminescent solar concentrators (Reisfeld and Jørgensen, 1982) consisting of LLP glass doped either by Cr(III) or Nd(III) alone, or simultaneously containing Cr(III) and Nd(III). These data are discussed by Reisfeld (1985c).

TABLE 7

Some spectroscopic data for neodymium(III) in lithium lanthanum phosphate (LLP) glass, with 0.5 mol.% Nd_2O_3, corresponding to 1.4×10^{20} ions/cm^3 or 0.23 molar (moles Nd/litre).

		λ (nm)	ε (M^{-1} cm^{-1})	P ($\times 10^{-6}$)
Absorption:	$^4I_{9/2} \rightarrow {}^4G_{5/2}$	580	5.54	13.4
	$^4I_{9/2} \rightarrow {}^4F_{5/2}$	801	4.40	4.7
	$^4I_{9/2} \rightarrow {}^4F_{3/2}$	874	0.91	1.2
Emission:	$^4F_{3/2} \rightarrow {}^4I_{9/2}$	885	–	–
	$^4F_{3/2} \rightarrow {}^4I_{11/2}$	1057	–	–

TABLE 8

Plate efficiencies η_p of luminescent solar concentrators based on lithium lanthanum phosphate (LLP) glass, doped either by Cr(III), Nd(III), or both.

Cr(III) (mol.%)	Nd(III) (mol.%)	η_{lum}	η_{stokes} *2	η_{abs}	A *3	η_p (%)
0.05	0	0.22	0.65	0.16	16.8	1.7
0.10	0	0.16	0.65	0.27	21.4	2.1
0	1.0	0.64 *1	0.70	0.22	33.8	7.4
0	2.0	0.49 *1	0.70	0.29	31.2	7.5
0.05	1.0	–	–	–	35.0	7.7
0.05	2.0	–	–	0.36	36.2	8.2
0.15	2.0	–	–	0.46	35.8	8.1

*1 Luminescence efficiency is averaged for four absorption peaks (583, 740, 800 and 880 nm) according to their contribution to the total absorption of solar spectrum (AM 1).

*2 Stokes shift is averaged for principal absorption bands according to their contribution to total absorption.

*3 A is the area under the excitation spectrum of 880 nm luminescence of Nd(III).

When comparing the efficiency of energy transfer obtained by the dynamic and by the static method (Reisfeld and Kisilev, 1985), it can be seen that the energy transfer efficiency increases with increasing concentration of Nd(III), unlike the quantum yield of Nd(III) luminescence. The dependence of the transfer efficiency on the Cr(III) concentration is different. The efficiency measured by the dynamic method is increasing, while in the static method it is decreasing in the presence of more Cr(III). Similar differences between the two methods were observed by Edwards and Gomulka (1979).

It can also be seen that the efficiency of energy transfer from Cr(III) to Nd(III) is faster than the nonradiative relaxation of Cr(III) for a given concentration of Cr(III). A similar phenomenon was observed in silicate glasses (Edwards and Gomulka, 1979) and LLP glass (Avanesov et al., 1979b; Härig et al., 1981). This strong interaction between Nd(III) and Cr(III) can perhaps be explained by antiferromagnetic coupling between the two ions, each of them having three unpaired electrons in the inner shells.

From a practical point of view, the static method provides general information on the increase of total Nd(III) luminescence in the presence of Cr(III). However, a more significant increase is obtained only at low Cr(III) concentrations. Since the total efficiency is composed of two factors – energy transfer efficiency and quantum efficiency of Nd(III) – the best results are obtained at these low concentrations of Cr(III) and 1 to 2 mole % of Nd(III), where the concentration quenching of Nd(III) and back transfer of energy from Nd(III) to Cr(III) is still low.

In summary, it is possible to increase the luminescence obtained from Nd(III) in the presence of Cr(III); but even in the optimum conditions of 0.05 mole % of Cr(III) and 2 mole % of Nd(III) the increase is no more than 10%.

A better increase in the efficiency of plates doped by Cr(III) or Nd(III) can be obtained by radiative energy transfer of light from highly luminescent, stable, organic dyes covering the plates (Reisfeld, 1985a).

5.7. *Energy transfer from cerium(III) to other lanthanides*

Contrary to the f→f transitions in the lanthanides of very weak oscillator strengths, the f→d transitions of Ce(III) and Tb(III) have very high intensities and resemble the parity-allowed transitions in mercury-like ions, known as Tl(I), Pb(II), and Bi(III) in glasses.

The 4f→5d transitions in the case of cerium(III) and $4f^8 \rightarrow 4f^7 5d$ of terbium(III) fall within the limit (above 190 nm) of standard spectrophotometers. The excited ^2D term of Ce(III) may be split by deviations from spherical symmetry into at most five levels, the 10 states of ^2D necessarily remaining degenerate two and two, according to the theorem of Kramers valid for an odd number of electrons.

Heidt and Berestecki (1955), Jørgensen (1956), and Jørgensen and Brinen

(1963) found five strong $4f \rightarrow 5d$ bands in aqueous solution. Loh (1966) reported four bands of Ce(III) in CaF_2, SrF_2, and BaF_2 and suggested that they correspond to the four 5d subshells of tetragonally distorted $Ce(III)F_8$. A slightly different interpretation (Jørgensen, 1969) is that the low-energy transition close to 300 nm goes to e_g (which is roughly nonbonding, and not split by spin–orbit coupling in cubic symmetry) and the three transitions close to 200 nm represent the three Kramers doublets t_{2g} strongly influenced by the Jahn–Teller effect (since they are anti-bonding) and by spin–orbit coupling. In gaseous Ce^{+3} the two J-levels of $5d^1$ are situated at 49737 and 52226 cm^{-1}. Hence, one can expect effects of spin–orbit coupling up to some 2000 cm^{-1}. The shift toward lower energy in cerium(III) compounds, relative to Ce^{+3}, and the energy differences between the five Kramers doublets are further discussed in section 7.

In spite of the short radiative lifetimes of the order of 10^{-8} s, both luminescence (frequently Stokes-shifted to the violet or the blue) and energy transfer to other species present in a glass can show remarkably high yields.

Energy transfer from Ce(III) to thulium(III) was reported to take place by dipole–dipole interaction in borate and phosphate glasses (Reisfeld and Eckstein, 1975b). The blue emission of thulium due to $^1D_2 \rightarrow {}^3F_4$ (previously named $^3H_4$) could be increased many times by this transfer. Also the emission of terbium can be greatly enhanced in glasses by energy transfer from Ce(III) (Reisfeld and Hormadaly, 1975). The efficiency of energy transfer between cerium and thulium is independent of temperature, while the transfer between Ce(III) and Tb(III) is increased as the temperature rises from 3 K to 300 K (Boehm et al., 1977). Energy transfer between Ce(III) and Tb(III) in pentaphosphates is also strongly assisted by temperature (Blanzat et al., 1977). This increase is due to the increase of the spectral overlap and phonon assistance. A comparison of the transfer in glass and crystals of similar composition shows that nonradiative processes, such as energy transfer and multiphonon relaxations, are stronger in glasses, due to removal of symmetry restrictions. Because of this reason also the radiative processes are enhanced in glasses.

Energy transfer from Ce(III) to Tb(III) and Tm(III) was also found to take place in fluorophosphate glasses (Kermaoui et al., 1984) and attributed to a diffusion-limited process.

5.8. *Energy transfer from manganese(II) to lanthanides, and the opposite transfer*

Manganese(II) has one electron in each of the d-like orbitals, and thus there is no reason for octahedral symmetry like in chromium(III) by ligand field stabilization. Thus, one can find a variety of compounds in which the coordination number of Mn(II) can acquire values from 4 to 7 (Reisfeld et al., 1984b,c).

Mn(II), as well as Fe(III), has no excited states with configuration $3d^5$ and the same high total spin quantum number $S = 5/2$ as the sextet groundstate ^6S, and

among the $252 - 6 = 246$ excited states, 96 states have $S = 3/2$ (quartets). The first two absorption bands are generally rather broad (Reisfeld et al., 1984c), whereas a sharp absorption band situated somewhere in the interval between 25300 and 21000 cm^{-1} corresponds to some of the components of ^4G lacking ligand field influence. Comparison of this energy difference with 26850 cm^{-1} in gaseous Mn^{+2} and 20520 cm^{-1} in Cr^+ allows a direct evaluation of the nephelauxetic effect, indicating weak covalent bonding with the neighbor atoms of the compound or the glass-forming medium. It is difficult to draw conclusions about the local symmetry of Mn(II) (with the exception of tetrahedral) from the position of the absorption bands below this level. Such conclusions may be drawn to some extent from the emission spectra, showing a considerable Stokes shift below the first quartet. For example, salts of the tetrahedral $MnBr_4^{-2}$ show luminescence of the first quartet (Jørgensen, 1957a) in the green with a quantum efficiency of about 1. On the other hand, the red luminescence of Mn(II) in lanthanum aluminate is ascribed to Mn(II) octahedrally surrounded by oxygen ions (Stevels, 1979). Several sites of Mn(II) were observed in calcium fluorophosphate, emitting in the red. In oxide glasses, a variety of sites is observed from the different emission spectra (Reisfeld and Jørgensen, 1982).

The absorption and fluorescence spectra of Mn(II) in phosphate, silicate, and borate glasses were treated by "ligand field" arguments by Bingham and Parke (1965). These authors concluded that their silicate glasses have tetrahedral $N = 4$ and phosphate $N = 6$, whereas borate glasses contain a mixture. However, an alternative possibility, quite likely to occur also in fluoride glasses, is a heterogeneous mixture of several low-symmetry $N = 7$ or 5, and perhaps nonoctahedral $N = 6$.

The high quantum yield of Mn(II) luminescence in a variety of glasses (Reisfeld and Jørgensen 1982; Reisfeld et al., 1984b) makes them potential materials for luminescent solar concentrators, provided that the low absorption bands arising from the spin-forbidden transitions will be overcome by a high concentration of Mn(II). Fortunately, in a number of manganese-doped glasses the concentration quenching is very low (Reisfeld et al., 1984b).

Energy transfer from Mn(II) to Nd(III) in calcium phosphate glass and from Mn(II) to Er(III) and Ho(III) in silicate glass was found to occur by a dipole–dipole interaction (Parke and Cole, 1971). The same mechanism takes place also for the energy transfer between Mn(II) and Nd(III) in barium borate glass (Kumar, 1977).

The fluorescence spectra and lifetimes of fluoride glasses of molar composition 36 PbF_2, 24 MnF_2 (or ZnF_2), 35 GaF_3, 5 (or 7) $Al(PO_3)_3$, doped by ErF_3, were investigated by Reisfeld et al. (1984c). The emission of Mn(II) in the absence of Er(III) consists of a broad band centered around 630 nm and an integrated lifetime of 1.4 ms. In the presence of Er(III), the intensity and lifetimes are decreased as a result of energy transfer to the $^4F_{9/2}$ level of Er(III). The fluorescence of Er(III) arising from $^4S_{3/2}$ at 543 nm has an integrated lifetime of

0.06 ms in the absence of Mn(II), which decreases to 0.01 ms in the presence of Mn(II) as a result of energy transfer to Mn(II). The 666-nm luminescence of Er(III) due to $^4F_{9/2}$ emission under excitation at 370 nm ($^4G_{11/2}$) is about 20 times weaker than the 543-nm emission when Mn(II) is absent. However, in the presence of Mn(II) this emission becomes 5 times stronger than the 543-nm emission. This intensified emission has a nonexponential time dependence. The longer component corresponds to the transfer of stored energy in Mn(II) to Er(III) while the short-lived component is probably due to cascading down Er(III)→Mn(II)→Er(III) through states above the Stokes threshold of Mn(II). This interpretation is backed up by weaker 543 nm emission and stronger 630 nm broad-band emission when the mixed system is excited in one of the upper excited states of Mn(II) at 395 nm, or of Er(III), as depicted in fig. 6.

Similar mutual energy transfer has also been studied (Reisfeld et al., 1986a) with neodymium(III) and manganese(II) in ZBLA glass. Nd(III) alone not only shows the well-known luminescence from $^4F_{3/2}$ (11400 cm^{-1} above the ground state) to lower ^4I levels with lifetime 0.34 ms (e.g., when excited in the yellow to $^4G_{5/2}$), but also short-lived (0.02 ms) emission from $^2P_{3/2}$ (26100 cm^{-1} above the ground state and 2400 cm^{-1} above the closest lower J-level $^2D_{5/2}$) and 1.5 μs from

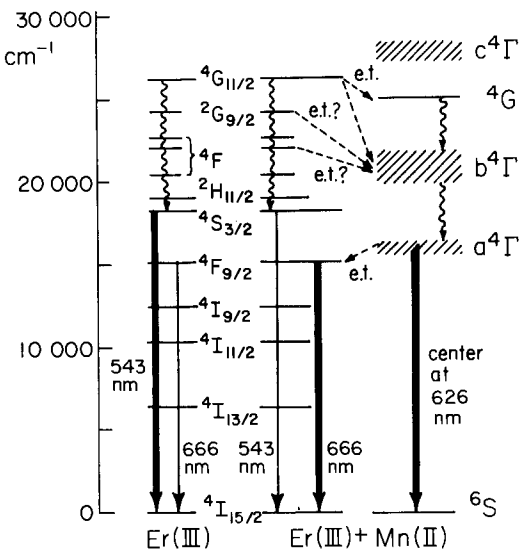

Fig. 6. Scheme for mutual energy transfer between erbium(III) and manganese(II) in a fluoride glass. To the left, the two major luminescent transitions in Er(III) are given as vertical arrows, and rapid nonradiative relaxations as wavy arrows. Simultaneous presence of Er(III) and Mn(II) has been shown (Reisfeld et al., 1984c) to provide the processes of energy transfer (e.t.) indicated. The absorption spectrum of Mn(II) alone shows a sharp band (essentially due to $^6S\rightarrow{}^4G$) and several other quartet states with differing bonding character, producing broad absorption and emission bands, in agreement with the principle of Franck and Condon.

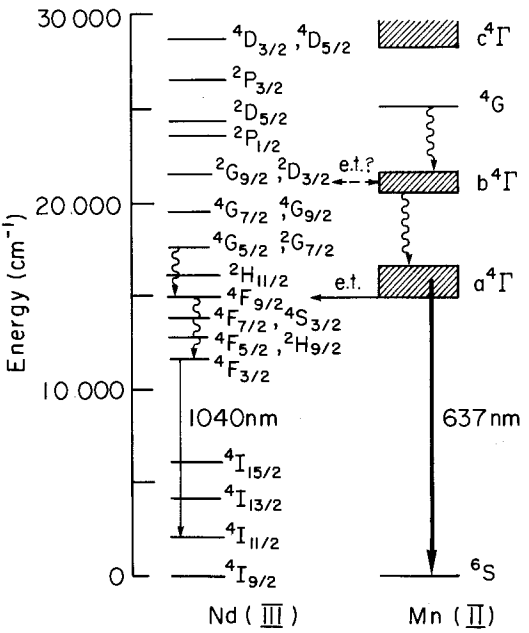

Fig. 7. Luminescence and energy transfer between manganese(II) and neodymium-(III) in ZBLA glass (Reisfeld et al., 1986a). See also fig. 6.

$^4D_{3/2}$ at 28100 cm^{-1} (2000 cm^{-1} above $^2P_{3/2}$). However, in the presence of 1 mole % each of MnF_2 and NdF_3, broad-band emission from the lowest quartet level of Mn(II) is centered at 545 nm. It is interesting that Nd(III) emission monitored at 876 nm, when excited at the sharp Mn(II) band at 404 nm, shows a rise time of about 0.1 ms followed by an approximately exponential decay with a lifetime of 1.5 ms. The latter phenomenon corresponds to an effective storage of energy in the lowest quartet level of manganese(II), releasing energy approximately 8 times more rapidly to Nd(III) than its lifetime 12 ms emitting in the absence of Nd(III) (see also fig. 7).

Comparable work is in progress (in collaboration with Jacoboni) on mutual energy transfer between Mn(II) and Nd(III) in gallium lead fluoride glasses (Reisfeld et al., 1986c). Greatly different Mn(II) sites can be detected as a function of the Mn(II) concentration, much like the case of Mn(II) luminescence in differing phosphate glasses (Reisfeld et al., 1984b).

6. Recent nonoxide materials

Most of the glasses encountered in the laboratory or in daily life are composed of mixed oxides of several elements. The oxides are usually described as the polyanion of a nonmetallic element of high electronegativity (borate, silicate,

phosphate, germanate, tellurite). Also other materials may remain vitreous, but only those that are electronegative can incorporate rare earths. Thus, mixed fluorides are attractive materials for formation of glasses.

6.1. *Fluoride glasses*

One of the incentives to study transparent fluorides may have been the coating of camera lenses by evaporating a thin layer of MgF_2 on them. The goal is to avoid luminous spots by specular reflection of light sources, and the ideal coating material has a refractive index n equal to the square-root of n for the lens glass. The n-values are closely related to electric dipolar polarizabilities (Salzmann and Jørgensen, 1968; Jørgensen 1975). Though $n = 1.39$ for LiF is nearly the value for MgF_2, the former material is less suitable because it is more soluble in rain water. Schröder (1964) found that many anhydrous fluorides form glasses by addition of gaseous HF. Contrary to what one might expect, most of these glasses are stable in humid air, and some even resist boiling water. Most have n below 1.27 and very weak dispersion (variation of n through the visible), corresponding to very high wave numbers of the first ultraviolet transitions with large oscillator strength P. As examples of (molar) composition may be mentioned $5\,LaF_3 : HF$; $2\,LaF : HF$ and $53\,ZrF_4 : 47\,HF$. There are probably strong, symmetric hydrogen bonds, as in FHF^-, known in many salts and in solution. If needed for attenuating nonradiative relaxation, the glasses might be prepared with DF. We have not heard of absorption spectra nor of emission spectra of lanthanides in such glasses.

The areas of composition of mixed fluorides allowing glass formation are much narrower than for conventional mixed oxides, and may need considerable serendipity for being detected. An important category of zirconium fluoride glasses was invented in 1975 at the University of Rennes. An early case (Lucas et al., 1978) has the molar composition $60\,ZrF_4 : 34\,BaF_2 : 6\,NdF_3$, but a certain variability (Lucas, 1985) is feasible; for instance, the zirconium may be replaced by colorless hafnium and thorium, or green uranium(IV). Many spectroscopic studies of europium(III) (Reisfeld et al., 1983c), holmium(III) (Tanimura et al., 1984; Reisfeld et al., 1985a; Jørgensen et al., 1986), and erbium(III) (Reisfeld et al., 1983a; Shinn et al., 1983) have concentrated on ZBLA (zirconium barium lanthanum aluminum) glass with composition $57\,ZrF_4 : 34\,BaF_2 : 4\,AlF_3 : 5\,RF_3$, R usually being some lanthanide added to more La.

Another type of fluoride glass was invented at Université du Maine (Le Mans) in 1979 (Miranday et al., 1981; Reisfeld et al., 1982), with the typical composition $46\,PbF_2 : 30\,GaF_3 : 22\,MF_2 : 2\,RF_3$, where M is manganese(II) or zinc(II). When chromium(III) or nickel(II) is incorporated in such a glass, octahedral chromophores $Cr(III)F_6$ and $Ni(II)F_6$ are clearly indicated from the absorption spectra. Seen from the point of view of the rare earth R, a major difference (table 1) is that Ω_2 is frequently much smaller than for the same R in ZBLA glass. It is likely that both types of glasses represent high and rather variable coordination

numbers N for R. In practice, it is much easier to prepare fluoride glasses with a small admixture of phosphate, such as $36\,PbF_2:35\,GaF_3:24\,(MnF_2$ or $ZnF_2):2\,RF_3:5\,Al(PO_3)_3$ (Reisfeld et al., 1984c) or $37.3\,AlF_3:32\,CaF_2:10\,MgF_2:10\,SrF_2:7\,BaF_2:1\,RF_3:2.67\,AlPO_4$ (Kermaoui et al., 1984). There is no doubt that the presence of 45 oxide/231 fluoride in the former zinc glass is somewhat deleterious for the fluorescence, since 0.1 mole % ErF_3 dissolved in it gives $\tau = 0.10$ ms for $^4S_{3/2}$ and 0.084 ms for $^4F_{9/2}$, to be compared with 0.29 and 0.35 ms for the phosphate-free fluoride glass. A comparable glass with (O/F) = 30/230 was studied by Brecher et al. (1978), containing Nd(III) dispersed in $40\,AlF_3:30\,CaF_2:10\,MgF_2:10\,SrF_2:5\,BaF_2:5\,Ba(PO_3)_2$. Such fluorophosphate glasses are rather distinct from monomeric fluorophosphates. Other homonymous concepts are borosilicate and phosphotungstate (Mack et al., 1985) glasses not referring to distinct heteropolyanions.

Fluorescence line-narrowing of $^4F_{3/2}$ neodymium emission was performed. (As can be seen in table 1, a curious property is that Ω_2 is smaller than the experimental uncertainty.) These studies triggered a theoretical model (Brawer, 1981; Brawer and Weber, 1981a,b) where a large number of fluoride anions and various cations are confined in a big, cubic unit cell and allowed to equilibrate (at a high temperature T) with Coulombic interactions and a reasonable short-range repulsive potential. This model reminds us about the fact that a glass has frozen in the nuclear positions it had at a much higher T, which may be the major reason why absorption bands tend to be more intense in glasses than in regular crystals. The model of Brawer confirms the expectation that the average value of N for europium(III) increases as a function of increasing stoichiometric ratio (F/Eu). Thus, $Be_{100}Na_3EuF_{106}$ (close to vitreous BeF_2 similar to silica) has $N = 7$ for most of the Eu, and 6 and 8 for minorities. The predictions for $Be_{76}Na_{74}EuF_{229}$, $Be_{76}Rb_{74}EuF_{229}$, and $Be_{76}Ca_{37}EuF_{229}$ are a distribution on 7, 8, 9, and 10, with $N = 8$ the most frequent value, whereas the hypothetical glass $Ca_{130}EuF_{263}$ has $N = 10$ more abundant than 9 and 11. Many chemists find it surprising that the average N for beryllium(II) is predicted to fall between 4.3 and 4.5 while the acidic aqueous solution contains exclusively $Be(OH_2)_4^{+2}$ and the alkaline solution $Be(OH)_4^{-2}$. The potentials assumed in Brawer's model have no explicit angular dependence, and it may be argued that Be(II) actually is known to be more uniformly tetrahedral than carbon in aliphatic molecules. However, it must also be recognized that N is mainly (though not exclusively) determined by relative atomic sizes in inorganic compounds (Jørgensen, 1983, 1984) and that fluoride anions are exceptionally small as neighbor atoms, like hydride having $N = 6$ in the NaCl-type LiH to CsH and the perovskites $BaLiH_3$ and $EuLiH_3$ (Messer and Levy, 1965), without any pretention of forming six "chemical bonds". In cubic perovskites, the large cation [here Ba(II) and Eu(II)] has $N = 12$.

From the point of view of luminescent behavior, the cascading down between eight excited J-levels of holmium(III) in ZBLA glass is one of the most spectacular effects in fluoride glasses (fig. 8). The multiphonon relaxation being

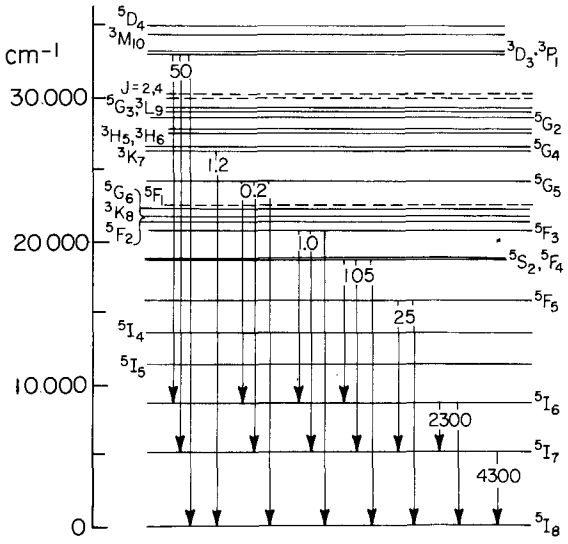

Fig. 8. Luminescent transitions of holmium(III) in ZBLA glass (Tanimura et al., 1984; Reisfeld et al., 1985a). The J-levels known to be involved in luminescence are given to the right, the other J-levels (cf. fig. 1) to the left. The lifetimes at 300 K of the eight emitting levels are given in μs (cf. table 3).

attenuated, it allows perceptible luminescence of J-levels with the next lower J-level at a distance ΔE of about 1900 cm^{-1}. A similarity exists between this case and the classical study (Weber, 1967a) of crystalline $Er_xLa_{1-x}F_3$. Another interesting feature is the mutual energy transfer from higher J-levels of erbium(III) to the lowest quartet level of manganese(II) (the maximum of the broad emission band occurs at 16000 cm^{-1}, going down to the sextet ground state; but it is difficult to know where the Stokes origin is situated) and from the latter quartet to $^4F_{9/2}$, giving narrow Er(III) emission at 15000 cm^{-1} (Reisfeld et al., 1984c) in a PbZnGa fluoride glass containing small amounts of aluminum meta-phosphate. Such energy transfer is also known from erbium-doped crystalline materials such as MnF_2 (Flaherty and DiBartolo, 1973; Wilson et al., 1979), $RbMnF_3$ (Iverson and Sibley, 1980), $RbMg_{1-x}Mn_xF_3$ (Shinn et al., 1982) and several ternary halides (Kambli and Güdel, 1984).

When the manganese(II) concentration is varied in phosphate glasses (Reisfeld et al., 1984b) the emission spectrum shows a complicated structure changing in a way suggesting not only nonequivalent Mn(II) sites, but also strong *antiferromagnetic coupling* between adjacent pairs or clusters, as known from crystalline MnF_2 (Flaherty and DiBartolo, 1973), $RbMnCl_3$, $CsMnCl_3$, $CsMnBr_3$, and Rb_2MnCl_4 (Kambli and Güdel, 1984). These effects invite further study.

A major technological interest in glasses is related to *optical fibers* transmitting infrared or visible signals over tens of kilometers without prohibitive absorption or scattering loss. The conditions for successful operation of such fibers are closely similar to attenuating multiphonon relaxation, where the fundamental stretching of OH and its overtones are one of the major problems. A large part of the recent work on fluoride glasses is directed toward optical fibers, and the relation with our

review is that the light source may be a laser connected directly with the optical fiber consisting of the same glass, except for the admixture of rare earth in the laser. Another problem is the weak-continuum absorption known to exist in the blue in liquid water, and in the near ultraviolet in many gaseous molecules (Jørgensen, 1985) which may impair optical fibers beyond 20000 cm^{-1} (or a lower energy).

The main part of nonoxide glasses studied at present are fluoride glasses. Three international symposia on nonoxide glasses have been held: in Cambridge, 1982, in Troy, NY, 1983, and in Rennes, 1985 (cf. Reisfeld et al., 1985b).

One may ask the question whether chloride, bromide, or iodide glasses may contain rare earths. Certain glasses formed from such heavier halides are indeed known, e.g., with zinc chloride as major constituent, and are comparable to crystalline RX_3 in lanthanide absorption and luminescence spectra. $LaCl_3$ (with trigonal sites having $N = 9$, each chloride having three adjacent La) achieved a great importance early, as can be seen in the book by Dieke (1968); $LaBr_3$ has the lowest known propensity toward multiphonon deexcitation (Riseberg and Moos, 1968), where emission was observed from levels of only 750 cm^{-1} above the next lower level. These materials cannot be used in lasers because of their extreme hygroscopicity.

6.2. *Sulfide glasses*

The elements O, S, Se, Te, and Po, having the atomic number Z two units below that of the noble gases, are called *chalkogens*. When speaking about chalkogenide glasses, oxide is normally disregarded (perhaps influenced by "chalkophilic", the geochemical concept of Goldschmidt). Besides elemental selenium, several glasses are known containing germanium, arsenic, selenium, and tellurium (Reisfeld et al., 1977b) but they are of limited interest for lanthanide luminescence, because they are only transparent in the far infrared. On the other hand, the black glass $Ge_{33}As_{12}Se_{55}$ transmits 950 cm^{-1} radiation readily from a CO_2 laser. In spite of the great stability of crystalline PbS, it is possible to make vitreous $0.9\,As_2O_3 : 0.1\,PbS$, $0.7\,As_2O_3 : 0.3\,PbS$, and $Ge_{0.86}Ca_{0.10}Ho_{0.04}S_{1.88}$ (Reisfeld et al., 1976b).

Flahaut (1979) reviewed crystal structures of binary and ternary rare earth sulfides. This interest in vitreous mixed sulfides started a collaboration with us on their spectra, as reviewed by Reisfeld (1982). The two main categories are $R_xLa_{1-x}Al_3S_6$ and $R_xLa_{1-x}Ga_3S_6$, being transparent in the yellow and having an absorption edge rapidly rising in the green and blue. At this point, it may be noted that reflection spectra of ternary crystalline sulfides such as $BaNd_2S_4$ and $CdEr_xGa_{2-x}S_4$ had been measured (Jørgensen et al., 1965b), quite exceptionally showing a more pronounced nephelauxetic effect than even R_2O_3 whereas binary sulfides tend to be dark colored with the narrow (but weak) absorption bands obscured by a strong background. This distinction of solid sulfides relative to

monomeric complexes of sulfur-containing ligands is also striking in the d-groups (Jørgensen, 1962d, 1968). The dark colors might be ascribed to transitions of d-like electrons to the lowest empty conduction band (like in dark violet $TiCl_3$ or the strong absorption in the near ultraviolet of sky-blue anhydrous, octahedrally coordinated $CoCl_2$) but they are also observed in the (even dilute) solutions of NiS in strong Na^+HS^- with or without As_2S_3 added. These solutions can be filtrated and do not seem colloidal, though the dissolved brownish black species are probably oligomeric. These collective phenomena should not be confused with the electron transfer spectra of tetrahedral V(V), Cr(VI), Mn(VII), Mo(VI), Tc(VII), W(VI), and Re(VII) complexes of O^{-2}, S^{-2}, and Se^{-2} (Müller et al., 1973). Anyhow, *J*-levels can be detected up to 22000 cm^{-1} in crystalline and powdered Dy_2S_3 (Henderson et al., 1967).

Both Yb_2S_3 and $BaYb_2S_4$ are bright yellow, due to straightforward electron transfer bands in the near ultraviolet (Jørgensen 1962c) as in lemon-yellow Yb(III) dithiocarbamates. $Yb_xY_{2-x}O_2S$ (Nakazawa, 1979) emits two bands, having maxima at 15000 and 25000 cm^{-1} (going to $^2F_{5/2}$ and $^2F_{7/2}$) when excited in the broad electron transfer bands, starting with a shoulder at 32000 cm^{-1}. Corresponding emission in $Yb_xLa_{2-x}O_2S$ is shifted to12000 and 22000 cm^{-1}. Such electron transfer spectra were recently studied (Garcia et al., 1984) with maxima between 32500 and 34000 cm^{-1} in $Na_{0.02}Er_{0.02}M_{0.96}Ga_2S_4$ thiogallate (M = Ca, Sr, or Ba) allowing efficient luminescence of erbium(III) from $^4G_{11/2}$ at 26100 cm^{-1} and four *J*-levels in the visible, the smallest ΔE being 1600 cm^{-1} for $^4F_{5/2}$.

It is not an absolute truth that the R–S bonding is weak; at higher temperatures, anhydrous RCl_3 reacts with H_2S to give R_2S_3 and gaseous HCl. However, as is well known from aluminum(III), it is hopeless to precipitate sulfides in aqueous solution. Any use of sulfide glasses containing rare earths will be subject to the kinetic rate of hydrolysis in humid air. Their properties are somewhat enigmatic at the moment; Ω_2 is not nearly as large as one would expect for such relatively covalent bonding (compare with the borate glasses in table 1) and the parameters of the exponential-gap law of multiphonon relaxation are not those expected. However, for *J*-levels well below the background absorption starting (at the best) at 20000 cm^{-1} the yields of luminescence are excellent. In view of what was said above on the thioamphoteric behavior of nickel(II), it may be that minor, strongly colored impurities may be avoided in sulfide glasses, subsequent to further careful studies. For some reason, this problem is much less severe in crystalline thiogallates.

7. Chemical properties of excited states

Photochemical reactions are essentially large nuclear displacements on the $(3N-5)$-dimensional potential hypersurfaces of N nuclei. These are induced at

(or below) ambient temperature by absorption of visible or ultraviolet photons. If these changes conduct the nuclei to a situation of considerably lower free energy (compared to kT of 200 cm^{-1} at ambient T), we have photochemical catalysis, whereas confining the nuclear positions at a relative minimum of the potential hypersurface at a much higher free energy is photochemical storage of energy. These definitions assume the Born–Oppenheimer factorization to be much more significant than a metaphor, and disregard vibrational photochemistry (e.g., high-power lasers dissociating MF_6 molecules to MF_5 and fluorine atoms) without electronic excitation of the kind possible for a single photon.

Contrary to the extensive photochemistry of many d-group complexes (Adamson, 1981, 1983) one might expect the lanthanides to be much less active, and perhaps limited to instances of modified oxidation states, of which Ce(III), Ce(IV) and Eu(II), and Eu(III), are the most familiar cases. Such photochemistry by electron transfer is indeed observed in glasses, and is known from solution chemistry. Most cerium(IV) complexes have strong absorption bands in the near ultraviolet with P from 0.1 to 0.4 (Ryan and Jørgensen, 1966), one to two orders of magnitude stronger than R(III) electron transfer bands (Jørgensen, 1962c); and the photochemical formation of cerium(III) and oxidized ligands is rather similar to the reduction of iron(III) to iron(II) complexes. Since the excited state of the electron transfer band already would have τ_{rad} below 10^{-8} s (and since no luminescence is detected), the capture of an electron from the ligand must be exceedingly rapid. Even in homogeneous aqueous solution, some photochemical reactions are surprisingly rapid. Thus, cerium(III) aqua ions at moderately low pH catalyze the reaction between four iodide anions and one O_2 molecule to form two I_2 [attempts to iodometric titration of cerium(IV) in $Ce_xR_{1-x}O_{1.5+0.5x}$ after dissolution in acid may show the unpleasant result of irreproducible values of x well above 1]. Douglas and Yost (1949) showed that 0.25 molar $EuCl_2$ in 0.3 molar hydrochloric acid can be kept for weeks in the dark, but that sunlight or 366 nm near-ultraviolet spectral lines of mercury lamps produce H_2 bubbles and Eu(III) aqua ions. Interestingly enough, the quantum yield is close to 0.15. The input of energy results in the excited configuration $4f^6 5d$ of Eu(II), losing the 5d electron to the solvent. This rapid non-Franck–Condon evolution of an excited state may be compared to the first excited state of an iodide ion in solution or in crystalline alkali-metal iodides (Jørgensen, 1969, 1975) at the immediate formation upon absorption of an ultraviolet photon having a configuration $5p^5 6s$ like a xenon atom.

Photochromic materials change their color upon illumination. In some cases, a quasi-stationary concentration of an excited state has strong absorption bands, such as triplet–triplet transitions in many aromatic hydrocarbons, or the doublet–doublet transitions of chromium(III) in ruby operating as a three-level laser. In other cases, the color is due to excited states of the reversible or irreversible product of a photochemical reaction. Many organic molecules can undergo such reactions, like rearrangement between *cis*- and *trans*-isomers around double

bonds, or spiropyran rearrangements (Heiligman-Rim et al., 1962). The strongly colored dithizonate complexes used for analytical detection of traces of heavy metals are frequently strikingly photochromic (Meriwether et al., 1965), such as mercury(II) dithizonate changing from orange to dark blue by strong illumination. Most applications of photochromic materials need a relatively short time of reversal (such as sun-glasses and glass roofs of buses; the bleaching has to be almost instantaneous in the case of windshields before a driver, because of the danger inherent in entering, e.g., a dark tunnel) and a large number of feasible cycles.

A famous photochromic silicate glass, containing cerium and europium, was developed at Corning Glass, NY (Stroud, 1965). In the dark, cerium(III) has a broad, intense $4f \rightarrow 5d$ absorption band at 310 nm. After photochemical detachment of an electron, cerium(IV) has a broad band at 250 nm. In view of the notorious variability of cerium(IV) electron transfer bands with the neighbor atoms, it is not certain that this species is enormously different from Ce(IV), in the dark having a band at 240 nm. Anyhow, europium(III) present in the dark state can trap electrons, and provide strong absorption in quasi-equilibrium under illumination, as well as various color centers, one with bands at 440 and 620 nm, and another, thermally more stable, with one maximum at 500 nm. This interplay between Ce(III), Eu(III) and metastable Ce(IV), Eu(II) can also be found in less intensely photochromic glasses (Weyl, 1959), involving bivalent and trivalent iron and manganese. At present it seems that the most common photochromic glass contains finely dispersed (600 nm large) silver halide crystallites (Armistead and Stookey, 1964; Megla, 1966; Araujo, 1985) where the liberated electrons are captured reversibly in the homogeneous glass by Cu(II), which is reduced to copper(I). Yokota (1967) showed that Eu(III) may also trap electrons in a $Li_{12}Al(PO_3)_{15}$ glass containing small amounts of Ag(I) and Eu(III).

On the whole, trivalent lanthanides have a much less developed photochemistry than the uranyl ion UO_2^{+2}, having as first excited state a parity-forbidden ultraweak electron transfer transition with P close to 10^{-5} and τ_{rad} slightly above 1 ms (Jørgensen and Reisfeld, 1982a, 1983a). Photochemical reactions contribute significantly to shorten this lifetime in many uranyl complexes, the highly oxidizing excited state abstracting hydrogen atoms in many unprecedented ways from organic solvents and ligands, and removing electrons from inorganic species such as $Mn(OH_2)_6^{+2}$ and other, moderately reducing complexes. The early observation of bromide, iodide, and thiocyanate quenching uranyl fluorescence even at low concentration, can be rationalized in two alternative (and not mutually exclusive) ways; (a) by a collision between the reducing anion and the excited uranyl ion, or (b) by the formation of complexes of the excited state showing the chemical behavior of a Pearson-soft noble-metal cation such as Au(III) or Pt(IV). The quenching of uranyl fluorescence by silver(I) and thallium(I) in aqueous solution has been shown to involve stoichiometric adducts (Marcantonatos and Deschaux, 1981). These explanations are not as readily

adaptable to glasses and highly viscous solutions. An interesting case is the study (Manor et al., 1985) of the energy transfer between excited uranyl and europium(III) in poly(methylmethacrylate), where the rather violent influence on the organic polymer has important bearings on induced photodegradation of organic colorants and transparent materials by fluorescent species, which is a serious problem for flat-plate luminescent solar concentrators (Reisfeld and Jørgensen, 1982). Anyhow, there are a few unexpected correlations between the behavior of excited states of lanthanides and the uranyl ion, and we start by considering recent progress related to the old problem of the constitution of the cerium(III) aqua ion.

Freed (1931) compared (by photographic techniques) the absorption spectra of dilute Ce(III) solutions and crystalline $[La(OH_2)_9](C_2H_5OSO_3)_3$ containing small concentrations of syncrystallized Ce(III). In both cases, four strong $4f \rightarrow 5d$ transitions were detected [39600 ($\varepsilon = 710$), 41700, 45100, and 47400 cm^{-1}], as later investigated by Heidt and Berestecki (1955) using an electronic spectrophotometer. An intriguing problem (already occupying Freed) is a much weaker band at 33800 cm^{-1} (296 nm) having ε increasing from 18 at 16°C to 25 at 54°C in dilute solution, and being somewhat weaker in the presence of a few molar ClO_4^-. Okada et al. (1981, 1985) demonstrated that the weak band does not occur in absorption in the crystalline ethylsulfate, and hence does not originate in trigonal $Ce(OH_2)_9^{+3}$. However, this solid luminesces at 300 K in a band at 31000 cm^{-1} with a large Stokes shift relative to the first absorption band at 39000 cm^{-1}. The emission band splits into two narrower components at 30000 and 32000 cm^{-1} by cooling to 80 K. Such a separation was first interpreted by Kröger and Bakker (1941) as transitions to the two J-levels of the ground term ^2F separated by 2253 cm^{-1} in gaseous Ce^{+3}. The aqueous Ce(III) solution produces a broader emission band at 28000 cm^{-1} with an observed τ of 45 ns of an exponential decay to be compared with 27 ns for the crystal at 300 K, a value that is not modified by complete deuteriation (Okada et al., 1985). Since $P = 0.01$ for the first absorption band in the crystal, eq. (1) gives $\tau_{rad} = 30$ ns if $e_2 = 2$ and $e_1 = 6$. The interpretation by Okada et al. (1981, 1985) is that during the short lifetime of the excited state in the crystal, one water molecule becomes detached by a photochemical reaction, and that the observed emission is due to $Ce(OH_2)_8^{+3}$. This dissociation must be much more rapid than a few ns, unless the Stokes shift of the undetected (but unavoidable) emission from the intact $Ce(OH_2)_9^{+3}$ is negligible, hiding the initial luminescence by self-absorption. It is conceivable that the emission of the aqua ion in solution occurs at lower energy, because $Ce(OH_2)_8^{+3}$ is much more constrained by the neighbor anions in the crystal, creating other equilibrium Ce–O distances, and the the octa-aqua ion in solution does not have time to attract a ninth ligand, as discussed below. However, it is also conceivable that the modified aqua ion emitting in the crystal in a way still has $N = 9$, but for instance having longer Ce–O distances in the trigonal prism than in the equatorial triangle (or vice versa). Anyhow, the absorption spectrum

of genuine $Ce(OH_2)_9^{+3}$ entails the corollary that the sixth band at 50000 cm^{-1} (Jorgensen and Brinen, 1963) is still due to excitation to 5d and not to 6s.

It is interesting to apply the *angular overlap model* (Jørgensen et al., 1963; Jørgensen, 1971) to the one-electron energy differences between the five 5d orbitals. Since the approximate symmetry of $Ce(OH_2)_9^{+3}$ in ethylsulfate crystals is D_{3h}, the holohedrized symmetry is close to D_{6h}. Whereas the two $4f_\varphi$ orbitals separate in this symmetry, d-like orbitals have the same symmetry types as in the linear symmetry (but not necessarily the order $\delta < \pi \ll \sigma$ expected in MX and linear XMX).

However, the spin–orbit coupling is not negligible in Ce(III); the Landé parameter ζ_{5d} is expected to be somewhat lower than 1100 cm^{-1} since gaseous Ce^{+3} shows $^2D_{3/2}$ at 49737 and $^2D_{5/2}$ at 52226 cm^{-1} above the ground state. Okada et al. (1985) used a parametrized model with the following results for the ethylsulfate crystal:

	$\sigma(\omega = 1/2)$	$\delta(\omega = 3/2)$	$\delta(\omega = 5/2)$	$\pi(\omega = 1/2)$	$\pi(\omega = 3/2)$
calculated	38880	42250	44630	48230	49300
observed	39060	41950	44740	47400	50130

(39)

The calculated spin–orbit separations are indeed $2.16\zeta_{5d}$ for δ and $0.97\zeta_{5d}$ for π, close to the first-order coefficients 2 and 1. However, for some accidental reason, the five absorption maxima are roughly equidistant, and the apparent enhancement of spin–orbit coupling may be due to a small distortion allowing mixing of λ values from linear symmetry. The simplest use of the angular overlap model with the angle $\alpha = 45°$ (Jørgensen et al., 1963) gives anti-bonding effects (only considering Ce–O σ-bonding) with the ratio 2:3:4 for $d\sigma : d\delta : d\pi$, in good agreement with eq. (39).

A surprising side effect is that a nonbonding 5d orbital would be situated close to 29300 cm^{-1}. This may invite the unorthodox comment that the excited Ce(III) state in the ethylsulfate distorts its geometry within a nanosecond in such a way that the luminescence originates from an almost nonbonding 5d electron (much like the 3d electron in the ground state of the blue vanadyl ion). Such extensive rearrangement is rendered more likely by the remarkably strong effects of anti-bonding among the 5d orbitals of Ce(III) aqua ions. The overall anti-bonding of the five d-orbitals in eq (39), assuming a zero-point at 29300 cm^{-1}, is 76800 cm^{-1}. A hypothetical octahedral aqua ion with the same Ce–O distance would have the subshell energy difference $\Delta = 25600$ cm^{-1} within the frame of the angular overlap model, i.e., $6/(2 \times 9)$ times 76800 cm^{-1}, which is not much below the observed $\Delta = 31000$ cm^{-1} for the strongly bound $Ir(OH_2)_6^{+3}$, and very similar to Δ for $IrCl_6^{-3}$. For comparison, the only $4f \rightarrow 5d$ band of $CeCl_6^{-3}$ and $CeBr_6^{-3}$ in

acetonitrile solution (Ryan and Jørgensen, 1966) occurs at 30300 and 29150 cm^{-1}, respectively. Extrapolation from chromium(III) complexes (Glerup et al., 1976), and circumstantial evidence from $4d^6$ rhodium(III) and $5d^6$ iridium(III), suggests that the π-anti-bonding in MX_6^{-3} is about a quarter of the σ-anti-bonding, putting the zero point of nonbonding in CeX_6^{-3} approximately at 25000 cm^{-1}. It may be noted (Jørgensen, 1956) that a strong $4f \rightarrow 5d$ transition develops at 32300 cm^{-1} in concentrated hydrochloric acid, though it only achieves $\varepsilon = 430$ in 12 molar $H_3O^+Cl^-$ whereas 0.0004 molar $CeCl_3$ in ethanol containing 0.3 molar H_2O (0.5 vol.%) already has $\varepsilon = 700$ for a similar band at 32400 cm^{-1}; this shows the far more extensive formation of chloride complexes in nearly anhydrous alcohols (the so-called Katzin effect), cf. Jørgensen (1979).

Blasse and Bril (1967b) studied the luminescence and cathodoluminescence of cerium(III) syncrystallized in YPO_4, $YAl_3B_4O_{12}$, $LaBO_3$, YBO_3, and $Y_3Al_5O_{12}$ and found in all cases a Stokes shift close to 4000 cm^{-1}, including the latter, orange garnet with an absorption band at 22000 cm^{-1} and emission at 18200 cm^{-1}, where one might have expected that the low-symmetry site occupied by Ce(III) would have allowed a roughly nonbonding 5d orbital. Only monazite-type $LaPO_4$ shows a larger Stokes shift from 36200 to 29800 cm^{-1}, though not as large as in the ethylsulfate. $Ce_{0.01}Y_{1.99}O_2S$ and $Ce_{0.01}Lu_{1.99}O_2S$ absorb at 21600 cm^{-1} and emit at 14300 and 15300 cm^{-1}, respectively (Yokono et al., 1981). A borate glass (Reisfeld et al., 1972) containing cerium(III) shows five distinct absorption bands between 32000 and 47200 cm^{-1} and a phosphate glass five broader bands between 33000 and 51000 cm^{-1}. Since such a spectrum is a superposition of the various sites (weighted by their absorption coefficient), it suggests a relatively limited dispersion of the major site, at least in the borate glass.

Though it is not perfectly certain that the luminescence of Ce(III) in the ennea-aqua ethylsulfate is emitted by the same $Ce(OH_2)_8^{+3}$ that produces the weak absorption band at 33800 cm^{-1} in the aqueous solution, it is possible to give a reliable estimate of the concentration of the latter species. The P value of its first transition can at most be some 60% of the ennea-aqua ion [otherwise, τ_{rad} would be shorter than τ reported by Okada et al. (1985)] and hence ε close to 400. Comparison with several cerium(III) complexes of organic ligands (Jørgensen, 1956) suggests that ε cannot be much below 300. It would seem that (4 ± 1)% of the cerium(III) aqua ions are of this species (formed endothermally) at room temperature, whereas the rest is the same trigonal ennea-aqua ion as known from the crystalline ethylsulfate.

It is known from Eigen's technique of temperature jumps that a water molecule remains coordinated to rare earth aqua ions for roughly 10^{-8} s for R = La to Sm and for roughly 10^{-7} s for yttrium and R = Dy to Lu. There is a marked break from europium to terbium. Unfortunately, these results do not tell us everything we want to know. The problem is that the measured rate may refer to one (or a few) particularly mobile ligands. Thus, copper(II) aqua ions exchange water more

rapidly than 10^{-8} s at a rate ten times higher than zinc(II) aqua ions, and 10^4 times more rapid than $Ni(OH_2)_6^{+2}$ with less pronounced covalent bonding. It seems likely (Jørgensen, 1975) that the axis perpendicular to the plane containing $Cu(OH_2)_4^{+2}$ accommodates one or two loosely bound water molecules at significantly longer distances. The spectrum in the visible and near infrared is conditioned by the Franck–Condon principle and shows a distribution (on a time scale of 10^{-13} s) of Cu–O distances quite different from a regular octahedron, and somewhat similar to the well-established tetragonal-pyramidal $Cu(NH_3)_5^{+2}$ in strong aqueous ammonia. The exchange of water within 10^{-8} s takes place on the perpendicular axis in a given moment, and the concerted motion of the 5 (or 6) ligands, interchanging the roles of the three Cartesian axes, is much faster, say 10^{-10} s. By the same token, water exchange rates cannot alone confirm the plausible picture of the concentration of trigonal $R(OH_2)_9^{+3}$ smoothly decreasing from $(96 \pm 1)\%$ for cerium to some low value for lutetium, and the complementary amount of $R(OH_2)_8^{+3}$ having one definite geometry, or several differing symmetries, increasing from some 4% to a high value. The absorption spectra of aqua ions in solution cannot even exclude the presence of some $N = 7$ and 6, though it is excluded that a major part has a center of inversion (which anyhow is only compatible with even N).

From a purely thermodynamical point of view, an excited state $h\nu$ above the ground state is simultaneously *more oxidizing* [the standard oxidation potential $E^0(+e^-)$ of the species containing an additional electron being $(h\nu/1\,eV)$ more positive than in the ground state, having added an electron] and *more reducing* [E^0 of the excited state being $(h\nu/1\,eV)$ less positive for acting as one-electron reductant], making the first excited state of the uranyl ion nearly as oxidizing as free fluorine (Jørgensen and Reisfeld, 1983a). Seen in this perspective, it is rather frustrating that kinetic sluggishness prevents the photolysis of water to two H_2 and one O_2 by visible light in the presence of relatively long-lived excited states of colored species in solution. Since the classical studies of Förster, it is known that the pK values (expressing Brønsted acidity) of excited states of protonated organic molecules can be widely different from the protonated ground state. Hence, it is not surprising that excited states of an aqua ion can be far more acidic than the ground state by being highly oxidizing, chemically polarizable (Pearson-soft) and perhaps having a lower coordination number N, when it is realized (Jørgensen, 1984) that aqua ions of Fe(III), Cu(II), Pd(II), Au(III), Hg(II), and Tl(III) deprotonate much more readily than aqua ions of the same oxidation state and with comparable ionic radii.

Adamson (1981, 1983) introduced the word "thexi state" for an electronic excited state living for sufficiently long time (10^{-7} s seems more than appropriate) for coming into thermal equilibrium with the surrounding condensed matter (with given kT) as far as vibrational states go. If the vibrational quanta are large compared to the ambient kT, the major vibronic state is the lowest belonging to

the excited potential surface. In this way, it is expected that a given "thexi state" has its own personalized chemical behavior quite distinct from the electronic ground state. This remark is certainly confirmed for the excited uranyl ion.

We are so accustomed to the chemistry of two different trivalent rare earths to be so similar [at least if we except propensity for reduction to R(II) or oxidation to R(IV)], that it was not realized earlier that luminescent, excited *J*-levels of R(III) may behave as thexi states. Most work on this subject has been performed quite recently by the group of Marcantonatos at the University of Geneva. We begin the review by the first excited state, $^6P_{7/2}$, of gadolinium(III) aqua ions. Besides the intense line at 32100 cm^{-1}, going directly to the ground state, seven weak lines or shoulders are detected (Vuilleumier et al., 1982) between 31400 cm^{-1} and 27400 cm^{-1}, 100 to 2000 times weaker then the main line. Among these seven satellites, the third-strongest at 30440 cm^{-1} corresponds to coexcitation of a bending frequency 1660 cm^{-1}, and the strongest at 28900 cm^{-1} to an O–H stretching frequency of a water molecule coordinated to the emitting $^6P_{7/2}$ state. Another species emitting at 31400 cm^{-1} can be shown to have lost a proton with $pK = 2.4$ (and hence much more acidic than the ground-state aqua ion with the first $pK = 7.3$) and showing perceptible coexcited bending and stretching (3430 cm^{-1}) frequencies higher than those of the main emitting aqua ion. A third species has a weak shoulder at 31050 cm^{-1} as major emission, again showing a very weak stretching frequency (as high as 3660 cm^{-1}) coexcited. A comparison of these measurements of perchlorates with $GdBr_3$ in bromide solution (Marcantonatos et al., 1982) and extended work suggests that the species emitting at the lowest energy is a dimer with at least one hydroxo bridge. Further thermodynamic arguments (see also Vuilleumier, 1984) show that the excited Gd(III) aqua ion has *N* two units lower than the ground state, and it seems indeed that $N = 6$ and 8, respectively. It is difficult to be certain that less abundant species may not have $N = 9$ in the ground state and $N = 7$ in the excited state, because the lifetime τ is so long (6 ms in H_2O and 10 ms in D_2O, almost the radiative lifetime) that any fluctuation of *N* is expected to be more rapid. Since the nephelauxetic effect is so weakly pronounced in gadolinium(III) compounds (the average energy of $^6P_{7/2}$ changes only from 32197 cm^{-1} in $Gd_xLa_{1-x}F_3$ to 32106 cm^{-1} in $GdCl_3 \cdot 6H_2O$), the shift of 700 cm^{-1} toward lower wave numbers in the excited hydroxo monomer, and of 1050 cm^{-1} in the dimer, is rather formidable, and may be taken as evidence for shorter Gd–O distances and stronger covalent bonding in the excited hydroxo complexes. Both the two sites with $N = 6$ in C-type Gd_2O_3 show a smaller nephelauxetic effect (Antic-Fidancev et al., 1982). The eight states of $^6P_{7/2}$, forming four Kramers doublets, are situated between 31728 and 31913 cm^{-1} for the C_2 site (average 31832 cm^{-1}); and the luminescent state of the S_6 site (having a center of inversion) is situated at 31696 cm^{-1}. It may finally be mentioned that weak emission due to $^6P_{5/2}$ is detected at 32700 cm^{-1} in Gd(III) perchlorate and bromide solutions, and an extremely weak peak at 33300 cm^{-1}

due to $^6P_{3/2}$. These two J-levels are expected to go nonradiatively to $^6P_{7/2}$ with a huge rate, and their observation in emission is due to the latter long-lived state, allowing them to become thermally populated, the two next J-levels being situated at an energy $3\,kT$ and $6\,kT$ higher at 300 K.

The fact that bromide does not quench Gd(III) luminescence may be rationalized if E^0 for Gd(II) is 3.5 V more negative than for Eu(II) aqua ions, in which case 4.0 eV of excitation energy is not sufficient to oxidize Br^-. The same argument for E^0 of Gd(III) being well above +7 V (as derived from the refined spin-pairing energy treatment) would also make the excited state virtually nonreducing, a rare combination. However, it is a fact that nitrate even at concentrations well below 10^{-5} molar quench Gd(III) luminescence (Vuilleumier, 1984). It is beyond discussion that this phenomenon is related to the numerous collisions during a millisecond and is not due to fixation of nitrate to the excited state. NO_3^- has a weak, broad absorption band, having $\varepsilon = 7$ at 312 nm, and the quenching may be due to very efficient energy transfer to this excited state. However, thiocyanate SCN^- is also quite effective for quenching, and this seems to involve a non-Franck–Condon mechanism.

The excited states of europium(III) $^5D_0$ and $^5D_1$ are 2.14 and 2.36 eV above the ground state $^7F_0$ and all three J-levels show quite different reactivity with nitrate in solution (Marcantonatos et al., 1981). The formation constant $[RNO_3(OH_2)_y^{+2}]/[R(OH_2)_x^{+3}][NO_3^-]$ for inner-sphere complex formation for R(III) ground-state ions depends for a great deal on the presence of ions in solution, but has the order of magnitude $0.5\,M^{-1}$ (i.e., litre/mole). The formation "constant" for outer-sphere association without direct RO_2NO or $RONO_2$ contacts varies even more with salt concentration, but tends to be 2 to $4\,M^{-1}$. The visible absorption spectra are sensitive essentially to inner-sphere contact, but measurements of activities give the sum of both. $^5D_0$ aqua ions have a lifetime $\tau = 0.112$ ms, and mono-nitrate complexes have $\tau = 0.138$ ms. The equilibrium between the latter outer-sphere associates and inner-sphere complexes is established in less than 0.01 ms.

$^5D_1$ has so short τ (3 μs) that the water molecules are not exchanged perceptibly with nitrate ligands. Marcantonatos et al. (1984) have studied this state in mixed perchlorate and bromide solutions. The major part of $^5D_1$ occurs as $^*Eu(OH_2)_8^{+3}$, $^*Eu(OH_2)_7Br^{+2}$; and $^*Eu(OH_2)_7^{+3}$ occurs as intermediate species in smaller concentration. At 300 K, the nonexcited Eu(III) is a mixture of 70% $^7F_0$ and 30% $^7F_1$ and there is about ten times more $Eu(OH_2)_8^{+3}$ than $Eu(OH_2)_9^{+3}$ present. An explanation is proposed why strong bromide and other salt solutions (necessarily having lower water vapor pressure than dilute solutions) nevertheless contain a higher percentage of $Eu(OH_2)_9^{+3}$, reaching above 25. On the other hand, the three heavy halides I^-, Br^-, and Cl^-, as well as ClO_3^-, do not penetrate the inner coordination sphere of $^7F_0$ and $^7F_1$ aqua ions. This reluctance can be overcome by sufficiently high chloride concentration, e.g., in solutions of

cerium(III) and neodymium(III), or in alcohols containing very little water and chloride (Jørgensen, 1956), as can be seen from the fact that $RCl_3 \cdot 6H_2O$ for R = Nd and Sm to Tm crystallize with monomeric $R(OH_2)_6Cl_2^+$ groups. The group $La(OH_2)_7Cl_2^+$ in $LaCl_3 \cdot 7H_2O$ forms a striking contrast to $[Al(OH_2)_6]Cl_3$ precipitated in cold, concentrated hydrochloric acid. The propensity for $N = 9$ in lanthanum(III) overrides the weak affinity for chloride.

After the results obtained by the group of Marcantonatos since 1981, one may ask whether the ionic radii of excited *J*-levels of trivalent lanthanides are *smaller* than those of the ground state. There cannot be a great difference in either direction, since coexcited vibrations are absent or exceedingly weak. The formal result that excited states have less total kinetic energy of the electrons, according to the virial theorem (Jørgensen, 1971), and hence expand, has an absolutely minute numerical size. We have to recognize (Jørgensen, 1983) that internuclear distances are optimized in such a way as to give the lowest possible energy of the compound; they are not quantum-mechanical properties of the individual atom. The characteristic feature of highly excited *J*-levels is probably their stronger covalent bonding (involving the empty 5d and 6s orbitals in the LCAO model), making a lower *N* acceptable. Analogous cases exist in a few places in the Periodic Table; mercury(II) is certainly much larger than beryllium(II), but *N* is normally 2 or 4 for Hg(II), but almost exclusively 4 for Be(II); and thallium(III) is somewhat larger than scandium(III) but tends toward the lower *N* values 4 and 6. It may be added that in both cases, Hg(II) and Tl(III) aqua ions are exceptionally acidic.

It is obvious that glasses are not subject to diffusion of reactive species, and to rapid collisions, as are water and other solvents of low viscosity. Nevertheless, it must not be neglected that glasses have been in such a situation at the high temperature they were prepared at (excepting here gel glasses prepared at low *T*, which may build in other nonequilibrium characteristics). Work on aqua ions and mixed aqua-anion complexes is quite instructive for our study of glasses, and also boosts the optimistic hope of analogous precursors in the understanding of aqua ions, which was slowly constructed, mainly by spectroscopic techniques, around the starting point of $Cr(OH_2)_6^{+3}$ and now is reaching enigmatic species like cerium(III) and copper(II) aqua ions.

8. Conclusions

Whereas a low vapor pressure in general restricts gas-phase chemistry of rare earths to a quite low number of compounds, it has been realized in the last forty years that solid state chemistry is a very important and in many aspects a much more innovating counterpart of the earlier solution chemistry of rare earths. As

far as high reactive solids are concerned, and their unexpected variation from one element to the next, the ion-exchange separation developed by Spedding and the availability of metallic elements have provided an enormous impetus to important research. The purpose of the present chapter is to point out the spectroscopic and other physical properties of isotropic glasses as an interesting alternative to crystalline compounds (including substitutionally doped crystals having colorless lanthanum or yttrium compounds as the major constituent). Some chemists are slightly taken back by the nonstoichiometric nature of nearly all glasses (though most minerals are not much better at this point) and may even consider them as a border-line case between genuine chemistry and agglomerates such as rock, lava, or concrete. However, we have anyhow to recognize that very few stoichiometric, crystalline rare-earth compounds contain discrete molecules (with the exception of organometallic compounds with R–C bonds, and certain neutral complexes of chelating ligands forming R–O and R–N bonds). Nearly all binary R_mX_n involve bridging X.

Our main purpose is to compare absorption and luminescence spectra of R(III) in glasses with the behavior in crystalline compounds and in aqueous solution. In one way, it is surprising how close many of the similarities are, and also how technologically attractive glasses can be as laser materials compared to crystals. It may be noted that the largest-scale terawatt lasers, such as the SHIVA and NOVA systems in Livermore, CA, are neodymium(III) glasses. We summarize most of the major results described in this chapter in seven conclusions:

(a) The quantum yield of luminescence of line emission from a higher to a lower J-level of a given lanthanide can be as high as in comparable crystalline materials. The two most important parameters (characterizing the competing process of nonradiative deexcitation) are a large energy difference ΔE between the emitting J-level and the closest lower J-level, and a small phonon energy (indicating the highest fundamental frequency of the neighbor groups in the glass). The classical cases of fluorescence (even in aqueous solution) correspond to the highest known ΔE in gadolinium(III) and the two following ΔE values in europium(III) and terbium(III). Conventional oxide glasses (borate, silicate, phosphate) only fluoresce strongly in these cases, and sometimes in the case of the slightly smaller ΔE of neodymium(III) (in the near infrared), samarium(III), and dysprosium(III). Oxide glasses with low force constants and heavier nuclei (such as germanate and tellurite) show luminescence for lower ΔE. This is even more true for fluoride glasses, showing perceptible fluorescence of many J-levels of neodymium(III), holmium(III), and erbium(III) with ΔE down to slightly below 2000 cm^{-1}. This propensity for luminescence is as high as in crystalline $R_xLa_{1-x}F_3$ and $R_xY_{1-x}F_3$.

(b) The luminescence of fluoride glasses at room temperature is nearly as strong (at least within a factor 2) as at liquid helium, alleviating the need for cooling of the laser.

(c) Technological progress is starting along several new lines, such as direct contact between laser sources and optical fibers (of the same composition, excepting R) for communication, use of hole burning for short-term (typically millisecond) memory, and simultaneously present lanthanides and d-group ions, e.g., neodymium(III) and chromium(III), for glasses intended for flat-plate luminescent concentrators of solar energy.

(d) Energy transfer is *normally* more effective in glasses than in crystals, allowing pumping of lanthanides (with narrow, weak absorption bands) via broad, intense absorption bands of other species present. Other useful aspects of energy transfer occur from the lowest quartet state of manganese(II), storing energy for several milliseconds and transferring it efficiently to luminescent lanthanide *J*-levels.

(e) Chromium(III) occurs in several highly successful laser crystals such as ruby and alexandrite. It is notoriously difficult to obtain a high fluorescence yield of Cr(III) in glasses, though energy transfer to lanthanides can be quite effective. Glass ceramics containing crystallites much smaller than the wavelength of light are known to give very high quantum yields of Cr(III) and might become important for lanthanide luminescence, also because of the favorable thermal conductivity and increased mechanical strength.

(f) The dispersion of individual sites of lanthanides in glass can be studied by the technique of fluorescence line-narrowing. On the whole, the properties of glasses are only weakly influenced by the "ligand field" structure of each *J*-level. Several coordination numbers (say, 7, 8, 9, . . .) seem to occur in most glasses.

(g) Large-scale experimentation with potential new laser materials can to a great extent be replaced by measurement of spectroscopic characteristics on a laboratory scale. Quite unexpectedly, the Judd–Ofelt treatment with only three material parameters is excellent (for the weighted average of glass sites), describing absorption and radiative emission probabilities. The Judd–Ofelt parameters are closely connected with other aspects of chemical bonding to the neighbor atoms.

Acknowledgements

We would like to thank Mrs. Esther Greenberg for the careful help in preparing the manuscript, and Dr. Marek Eyal and Dr. Anna Kisilev for providing valuable data. We also thank Dr. Nissan Spector for extensive information about calculations of *J*-levels and Judd–Ofelt matrix elements in intermediate coupling. We are grateful to Professor Minas D. Marcantonatos for interesting discussions, and to Professor Charles Jacoboni for unique samples of fluoride glasses. Finally, we thank the Swiss National Science Foundation for the grant 2.152–0.83 and their previous grants significantly furthering many of the studies described here.

References

Adamson, A.W., 1981, Comm. Inorg. Chem. **1**, 33.

Adamson, A.W., 1983, J. Chem. Educ. **60**, 797.

Agarwal, A.K., N.C. Lohani, T.C. Pant and K.C. Pant, 1984, J. Solid State Chem. **54**, 219.

Antic-Fidancev, E., M. Lemaitre-Blaise and P. Caro, 1982, J. Chem. Phys. **76**, 2906.

Araujo, R.J., 1985, J. Chem. Educ. **62**, 472.

Armistead, W.H., and S.D. Stookey, 1964, Science **144**, 150.

Ashurov, M.Kh., T.T. Basiev, A.I. Burshtein, Yu.K. Voronkov and V.V. Osiko, 1984, Pisma v Zh. Eksp. & Teor. Fiz. **40**, 98.

Auzel, F., 1980, in: Radiationless Processes, ed. B. DiBartolo (Plenum, New York) p. 213.

Auzel, F., S. Hubert and P. Delamoye, 1982, J. Lumin. **26**, 251.

Avanesov, A.G., Yu.K. Voron'ko, B.I. Denker, G.V. Maksimova, V.V. Osiko, A.M. Prokhorov and I.A. Shcherbakov, 1979a, Sov. J. Quantum Electron. **9**, 935.

Avanesov, A.G., Yu.K. Voron'ko, B.I. Denker, A.A. Kutenkov, G.V. Maksimova, V.V. Osiko, E.I. Sidorova, Yu.P. Timofeev and I.A. Shcherbakov, 1979b, Sov. J. Quantum Electron. **9**, 1323.

Avnir, D., D. Levy and R. Reisfeld, 1984, J. Phys. Chem. **88**, 5956.

Barnes, N.P., D.J. Gettemy, N.J. Levinos and J.E. Griggs, 1979, Proc. LASL Optics Conf.; SPIE J. **190**, 297.

Basiev, T.T., 1985, J. Phys. Colloq. **46**(C7), 159.

Batygov, S.Kh., Yu.K. Voron'ko, B.I. Denker, A.A. Zlenko, A.Ya. Karasik, G.V. Maksimova, V.B. Neustruev, V.V. Osiko, V.A. Sychugov, I.A. Shcherbakov and Yu.S. Kuzminov, 1976, Sov. J. Quantum Electron. **6**, 1220.

Bethe, H., and F.H. Spedding, 1937, Phys. Rev. **52**, 454.

Bingham, K., and S. Parke, 1965, Phys. Chem. Glasses **6**, 224.

Blanzat, B., J.P. Denis and R. Reisfeld, 1977, Chem. Phys. Lett. **51**, 403.

Blanzat, B., L. Boehm, C.K. Jørgensen, R. Reisfeld and N. Spector, 1980, J. Solid State Chem. **32**, 185.

Blasse, G., 1979, in: Handbook on the Physics and Chemistry of Rare Earths, Vol. 4, eds. K.A. Gschneidner Jr. and L. Eyring (North-Holland, Amsterdam) p. 237.

Blasse, G., 1984, Energy Transfer in Insulating Materials, in: Energy Transfer Processes in Condensed Matter, NATO ASI Series B Physics, eds B. DiBartolo and A. Karipidou (Plenum, New York) p. 251.

Blasse, G., 1985, J. Less-Common Met. **112**, 1, 79.

Blasse, G., and A. Bril, 1967a, J. Chem. Phys. **46**, 2579; **47**, 5442.

Blasse, G., and A. Bril, 1967b, J. Chem. Phys. **47**, 5139.

Boehm, L., R. Reisfeld and B. Blanzat, 1977, Chem. Phys. Lett. **45**, 441.

Boehm, L., R. Reisfeld and N. Spector, 1979, J. Solid State Chem. **28**, 75.

Bouderbala, M., G. Boulon, R. Reisfeld, A. Buch, M. Ish-Shalom and A.M. Lejus, 1985, Chem. Phys. Lett. **121**, 535.

Boulon, G., 1984, in: Energy Transfer Processes in Condensed Matter, NATO ASI Series B, Physics, eds B. DiBartolo and A. Karipidou (Plenum, New York) p. 603.

Boulon, G., B. Moine, J.C. Bourcet, R. Reisfeld and Y. Kalisky, 1979, J. Lumin. **18**, 924.

Bourcet, J.C., B. Moine, G. Boulon, R. Reisfeld and Y. Kalisky, 1979, Chem. Phys. Lett. **61**, 23.

Brawer, S.A., 1981, J. Chem. Phys. **75**, 3516.

Brawer, S.A., and M.J. Weber, 1981a, J. Chem. Phys. **75**, 3522.

Brawer, S.A., and M.J. Weber, 1981b, J. Lumin. **24**, 115.

Brecher, C., and L.A. Riseberg, 1976, Phys. Rev. B **13**, 81.

Brecher, C., and L.A. Riseberg, 1980, Phys. Rev. B **21**, 2607.

Brecher, C., L.A. Riseberg and M.J. Weber, 1978, Phys. Rev. B **18**, 5799.

Broer, L.J.F., C.J. Gorter and J. Hoogschagen, 1945, Physica **11**, 231.

Brown, D.C., 1981, High-peak Power Nd:Glass Laser Systems (Springer, Berlin).

Bryant, B.W., 1965, J. Opt. Soc. Am. **55**, 771.

Bukietynska, K., and G.R. Choppin, 1970, J. Chem. Phys. **52**, 2875.

Bukietynska, K., and A. Mondry, 1985, Inorg. Chim. Acta **110**, 1.

Caird, J.A., J.P. Hessler, W.T. Carnall and C.W. Williams, 1981a, J. Chem. Phys. **74**, 805.

Caird, J.A., W.T. Carnall and J.P. Hessler, 1981b, J. Chem. Phys. **74**, 3225.

Carnall, W.T., 1979, in: Handbook on the Physics and Chemistry of Rare Earths, Vol. 3, eds. K.A. Gschneidner Jr. and L. Eyring (North-Holland, Amsterdam) p. 171.

Carnall, W.T., P.R. Fields and K. Rajnak, 1968, J. Chem. Phys. **49**, 4412, 4424, 4443, 4447, 4450.

Carnall, W.T., H. Crosswhite and H.M. Crosswhite, 1977, Energy Level Structure and Transition Probabilities of the Trivalent Lanthanides in LaF_3 (Argonne National Laboratory Report).

Carnall, W.T., J.P. Hessler, H.R. Hoekstra and C.W. Williams, 1978a, J. Chem. Phys. **68**, 4304.

Carnall, W.T., J.P. Hessler and F. Wagner, 1978b, J. Phys. Chem. **82**, 2152.
Carnall, W.T., J.V. Beitz and H. Crosswhite, 1984, J. Chem. Phys. **80**, 2301.
Caro, P., O.K. Moune, E. Antic-Fidancev and M. Lemaitre-Blaise, 1985, J. Less-Common Met. **112**, 153.
Catlow, C.R.A., A.V. Chadwick, G.N. Greaves and L.M. Moroney, 1984, Nature **312**, 601.
Chen, S., S. Mao and F.M. Dai, 1984, Acta Phys. Sin. **33**, 515.
Chicklis, E.P., C.S. Neiman and A. Linz, 1972, Dig. Tech. Papers, 7th Int. Quantum Electronics Conf., 17.
Condon, E.U., and G.H. Shortley, 1953, Theory of Atomic Spectra, 2nd Ed. (University Press, Cambridge).
Dexter, D.L., 1953, J. Chem. Phys. **21**, 836.
Dieke, G.H., 1968, Spectra and Energy Levels of Rare Earth Ions in Crystals (Wiley–Interscience, New York).
Douglas, D.L., and D.M. Yost, 1949, J. Chem. Phys. **17**, 1345; erratum: 1950, **18**, 1687.
Durville, F., G. Boulon, R. Reisfeld, H. Mack and C.K. Jørgensen, 1983, Chem. Phys. Lett. **102**, 393.
Edwards, J.G., and S. Gomulka, 1979, J. Phys. D **12**, 187.
Elliott, J.P., B.R. Judd and W.A. Runciman, 1957, Proc. R. Soc. London Ser. A **240**, 509.
Englman, R., 1979, Non-Radiative Decay of Ions and Molecules in Solids (North-Holland, Amsterdam).
Ensign, J.C., and N.E. Byer, 1972, Phys. Rev. B **6**, 3227.
Eyal, M., E. Greenberg, R. Reisfeld and N. Spector, 1985, Chem. Phys. Lett. **117**, 108.
Eyal, M., R. Reisfeld, C.K. Jørgensen and C. Jacoboni, 1986, Chem. Phys. Lett. **129**, 550.
Feltz, A., 1983, Amorphous and Glass-like Inorganic Solids (Akademie Verlag, Berlin).
Fenske, R.F., 1967, J. Am. Chem. Soc. **89**, 252.
Flahaut, J., 1979, in: Handbook on the Physics and Chemistry of Rare Earths, Vol. 4, eds. K.A. Gschneidner Jr. and L. Eyring (North-Holland, Amsterdam) p. 1.
Flaherty, J.M., and B. DiBartolo, 1973, Phys. Rev. B **8**, 5232.
Flint, C.D., P.A. Tanner, R. Reisfeld and H. Tzehoval, 1983, Chem. Phys. Lett. **102**, 249.
Folcher, G., J. Lambard, C. Kiener and P. Rigny, 1978, J. Chim. Phys. **75**, 875.
Fonger, W.H., and C.W. Struck, 1978, J. Lumin. **17**, 241.
Förster, Th., 1959, Faraday Disc. Chem. Soc. **27**, 7.
Freed, S., 1931, Phys. Rev. **38**, 3122.
Friedrich, J., and D. Haarer, 1984, Angew. Chem. Int. Ed. Engl. **23**, 113.
Garcia, A., R. Ibanez, C. Fouassier and P. Hagenmuller, 1984, J. Lumin. **29**, 389.
Geier, G., and C.K. Jørgensen, 1971, Chem. Phys. Lett. **9**, 263.
Glaser, J., and G. Johansson, 1981, Acta Chem. Scand. A **35**, 639.
Glerup, J., O. Mønsted and C.E. Schäffer, 1976, Inorg. Chem. **15**, 1399.
Gobrecht, H., 1937, Ann. Phys. **28**, 673.
Gobrecht, H., 1938, Ann. Phys. **31**, 181, 755.
Goldschmidt, Z.B., 1978, in: Handbook on the Physics and Chemistry of Rare Earths, Vol. 1, eds. K.A. Gschneidner Jr. and L. Eyring (North-Holland, Amsterdam) p. 1.
Greenberg, E., G. Katz, R. Reisfeld, N. Spector, R.C. Marshall, B. Bendow and R.N. Brown, 1982, J. Chem. Phys. **77**, 4797.
Gruen, D.M., and C.W. DeKock, 1966, J. Chem. Phys. **45**, 455.
Gruen, D.M., C.W. DeKock and R.L. McBeth, 1967, Adv. Chem. Ser. **71**, 102.
Guntherrodt, H., and H. Beck, 1981, Glassy Metals I (Springer, Berlin).
Hammerling, P., A.B. Budgor and A. Pinto, eds, 1985, Tunable Solid State Lasers, Springer Series in Optical Sciences **47** (Springer, Berlin).
Härig, T., G. Huber and I.A. Shcherbakov, 1981, J. Appl. Phys. **52**, 4450.
Hattendorf, H.D., G. Huber and H.G. Danielmeyer, 1978, J. Phys. C **11**, 2399.
Hegarty, J., W.M. Yen, M.J. Weber and D.H. Blackburn, 1979, J. Lumin. **18**, 657.
Heidt, L.J., and J. Berestecki, 1955, J. Am. Chem. Soc. **77**, 2049.
Heiligman-Rim, R., Y. Hirshberg and E. Fischer, 1962, J. Phys. Chem. **66**, 2465,2470.
Henderson, J.R., M. Muramoto, E. Loh and J.B. Gruber, 1967, J. Chem. Phys. **47**, 3347.
Henrie, D.E., R.L. Fellows and G. Choppin, 1976, Coord. Chem. Rev. **18**, 199.
Holstein, T., S.K. Lyo and R. Orbach, 1981, in: Laser Spectroscopy of Solids, Topics in Applied Physics, Vol. 49, eds W.M. Yen and D.M. Selzer (Springer, Berlin) p. 30.
Holzrichter, J.F., 1985, Nature **316**, 309.
Holzrichter, J.F., E.M. Campbell, J.D. Lindl and E. Storm, 1985, Science **229**, 1045.
Hormadaly, J., and R. Reisfeld, 1977, Chem. Phys. Lett. **45**, 436.
Hormadaly, J., and R. Reisfeld, 1979, J. Non-Cryst. Solids **30**, 337.
Horrocks, W. DeW., and D.R. Sudnik, 1981, Accounts Chem. Res. **14**, 384.
Huang, K., and A. Rhys, 1950, Proc. R. Soc. London Ser A **204**, 406.
Huber, D.L., 1981, in: Laser Spectroscopy of Solids, Topics in Applied Physics, Vol. 49, eds W.M. Yen and D.M. Selzer (Springer, Berlin) p. 83.
Inokuti, M., and F. Hirayama, 1965, J. Chem. Phys. **43**, 1978.
Iverson, M.V., and W.A. Sibley, 1980, Phys. Rev. B **21**, 2522.
Jacobs, R.R., and M.J. Weber, 1974, IEEE J. Quantum Electron. QE **10**, 450.
Jenssen, H.P., A. Linz, R.P. Levitt, C.A. Morrison and D.E. Wortman, 1975, Phys. Rev. B **11**, 92.

Jørgensen, C.K., 1955, Acta Chem. Scand. **9**, 540.
Jørgensen, C.K., 1956, Mat. Fys. Medd. Dan. Vidensk. Selsk. **30**, no. 22.
Jørgensen, C.K., 1957a, Acta Chem. Scand. **11**, 53.
Jørgensen, C.K., 1957b, Energy Levels of Complexes and Gaseous Ions (Gjellerup, Copenhagen).
Jørgensen, C.K., 1959, Mol. Phys. **2**, 96.
Jørgensen, C.K., 1962a, Orbitals in Atoms and Molecules (Academic Press, London).
Jørgensen, C.K., 1962b, Solid State Phys. **13**, 375.
Jørgensen, C.K., 1962c, Mol. Phys. **5**, 271.
Jørgensen, C.K., 1962d, J. Inorg. & Nucl. Chem. **24**, 1571.
Jørgensen, C.K., 1963, Adv. Chem. Phys. **5**, 33.
Jørgensen, C.K., 1968, Inorg. Chim. Acta Rev. **2**, 65.
Jørgensen, C.K., 1969, Oxidation Numbers and Oxidation States (Springer, Berlin).
Jørgensen, C.K., 1970, Prog. Inorg. Chem. **12**, 101.
Jørgensen, C.K., 1971, Modern Aspects of Ligand Field Theory (North-Holland, Amsterdam).
Jørgensen, C.K., 1975, Topics Current Chem. **56**, 1.
Jørgensen, C.K., 1976, in: Gmelin's Handbuch der Anorganischen Chemie, Seltenerdelemente, Vol. 39B1, p. 17.
Jørgensen, C.K., 1979, in: Handbook on the Physics and Chemistry of Rare Earths, Vol. 3, eds. K.A. Gschneidner Jr. and L. Eyring (North-Holland, Amsterdam) p. 111.
Jørgensen, C.K., 1982, Chem. Phys. Lett. **87**, 320.
Jørgensen, C.K., 1983, Rev. Chim. Min. **20**, 533.
Jørgensen, C.K., 1984, Topics Current Chem. **124**, 1.
Jørgensen, C.K., 1985, J. Phys. Colloq. **46**(C7), 409.
Jørgensen, C.K., and J.S. Brinen, 1963, Mol. Phys. **6**, 629.
Jørgensen, C.K., and B.R. Judd, 1964, Mol. Phys. **8**, 281.
Jørgensen, C.K., and V. Parthasarathy, 1978, Acta Chem. Scand. A **32**, 957.
Jørgensen, C.K., and R. Reisfeld, 1982a, Structure and Bonding **50**, 121.
Jørgensen, C.K., and R. Reisfeld, 1982b, Topics Current Chem. **100**, 127.
Jørgensen, C.K., and R. Reisfeld, 1983a, J. Electrochem. Soc. **130**, 681.
Jørgensen, C.K., and R. Reisfeld, 1983b, J. Less-Common Met. **93**, 107.
Jørgensen, C.K., and E. Rittershaus, 1967, Mat. Fys. Medd. Dan. Vidensk. Selsk. **35**, no. 15.
Jørgensen, C.K., R. Pappalardo and H.H. Schmidtke, 1963, J. Chem. Phys. **39**, 1422.
Jørgensen, C.K., R. Pappalardo and E. Rittershaus, 1965a, Z. Naturforsch. a **20**, 54.
Jørgensen, C.K., R. Pappalardo and J. Flahaut, 1965b, J. Chim. Phys. **62**, 444.
Jørgensen, C.K., R. Reisfeld and M. Eyal, 1986, J. Electrochem. Soc. **133**, 1961.
Joshi, J.C., N.C. Pandey, B.C. Joshi and J. Joshi, 1977, Indian J. Pure & Appl. Phys. **15**, 519.
Joshi, J.C., J. Joshi, R. Belwal, B.C. Joshi and N.C. Pandey, 1978a, J. Phys. Chem. Solids **39**, 581.
Joshi, J.C., N.C. Pandey, B.C. Joshi, R. Belwal and J. Joshi, 1978b, J. Solid State Chem. **28**, 135.
Judd, B.R., 1962, Phys. Rev. **127**, 750.
Judd, B.R., 1979, J. Chem. Phys. **70**, 4830.
Kalisky, Y., R. Reisfeld and J.S. Bodenheimer, 1981, J. Non-Cryst. Solids **44**, 249.
Kambli, U., and H.U. Güdel, 1984, Inorg. Chem. **23**, 3479.
Karayanis, N., D.E. Wortman and H.P. Jenssen, 1976, J. Phys. Chem. Solids **37**, 675.
Karraker, D.G., 1971, J. Inorg. & Nucl. Chem. **33**, 3713.
Keller, B., K. Bukietynska and B. Jezowska-Trzebiatowska, 1982, Chem. Phys. Lett. **92**, 541.
Kermaoui, A., C. Barthou, J.P. Denis and B. Blanzat, 1984, J. Lumin. **29**, 295.
Kirby, A.F., and R.A. Palmer, 1981, Inorg. Chem. **20**, 1030, 4219.
Kisilev, A., and R. Reisfeld, 1984, Solar Energy **33**, 163.
Kisilev, A., R. Reisfeld and H. Tzehoval, 1982, Book of Abstracts, 4th Int. Conf. on Photochemical Conversion and Storage of Solar Energy, p. 299.
Kisilev, A., R. Reisfeld, E. Greenberg, A. Buch and M. Ish-Shalom, 1984, Chem. Phys. Lett. **105**, 405.
Knights, M.G., W.F. Wing, J.W. Baer, E.P. Chicklis and H.P. Jenssen, 1982, IEEE J. Quantum Electron. QE **18**, 163.
Kogelnik, H., 1966, in: Lasers, ed. A. Levine (Marcel Dekker, New York).
Kreidl, N., 1984, Ceram. Bull. **63**, 1394.
Kröger, F.A., and J. Bakker, 1941, Physica **8**, 628.
Krupke, W.F., 1966, Phys. Rev. **145**, 325.
Krupke, W.F., 1971, IEEE J. Quantum Electron. QE **7**, 153.
Kumar, R., 1977, Chem. Phys. Lett. **45**, 121.
Landry, R.J., J.T. Fournier and C.G. Young, 1967, J. Chem. Phys. **46**, 1285.
Layne, C.B., 1975, Ph.D. Thesis, University of California.
Layne, C.B., W.H. Lowdermilk and M.J. Weber, 1977, Phys. Rev. B **16**, 10.
Lee, L.S., S.C. Rand and A.L. Schawlow, 1984, Phys. Rev. B **29**, 6901.
Lengyel, B.A., 1971, Lasers (Wiley–Interscience, New York).
Levy, D., R. Reisfeld and D. Avnir, 1984, Chem. Phys. Lett. **109**, 593.
Lieblich-Sofer, N., R. Reisfeld and C.K. Jørgensen, 1978, Inorg. Chim. Acta **36**, 259.

Liu, C.S., and R.J. Zollweg, 1974, J. Chem. Phys. **60**, 2384.
Loh, E., 1966, Phys. Rev. **147**, 332.
Lucas, J., 1985, J. Less-Common Met. **112**, 27.
Lucas, J., M. Chanthanasinh, M. Poulain, M. Poulain, P. Brun and M.J. Weber, 1978, J. Non-Cryst. Solids **27**, 273.
Macfarlane, R.M., R.M. Shelby and A. Winnacker, 1985, J. Phys. Colloq. **46**(C7), 537.
Mack, H., G. Boulon and R. Reisfeld, 1981, J. Lumin. **24**, 111.
Mack, H., R. Reisfeld and D. Avnir, 1983, Chem. Phys. Lett. **99**, 238.
Mack, H., R. Reisfeld and C.K. Jørgensen, 1985, Inorg. Chim. Acta **109**, 51.
Mackenzie, J.D., 1964, Modern Aspects of the Vitreous State (Butterworths, London).
Malta, O.L., P.H. Santa-Cruz, G.F. DeSa and F. Auzel, 1985, Chem. Phys. Lett. **116**, 396.
Manor, N., R. Reisfeld, E. Greenberg, E. Banks, I. Nagata and Y. Okamoto, 1985, J. Phys. Chem., submitted.
Marcantonatos, M.D., and M. Deschaux, 1981, Chem. Phys. Lett. **80**, 327.
Marcantonatos, M.D., M. Deschaux and J.J. Vuilleumier, 1981, Chem. Phys. Lett. **82**, 36.
Marcantonatos, M.D., M. Deschaux and J.J. Vuilleumier, 1982, Chem. Phys. Lett. **91**, 149.
Marcantonatos, M.D., M. Deschaux and J.J. Vuilleumier, 1984, J. Chem. Soc. Faraday Trans. II **80**, 1569.
Martin, W.C., R. Zalubas and L. Hagan, 1978, Atomic Energy Levels, the Rare Earth Elements. NSRDS–NBS 60 (National Bureau of Standards, Washington, D.C.).
Mason, S.F., 1979, Accounts Chem. Res. **12**, 55.
Mason, S.F., 1980, Structure and Bonding **39**, 43.
McLellan, G., and E. Shand, 1984, Glass Engineering Handbook, 3rd Ed. (McGraw–Hill, New York).
McMillan, P., 1979, Glass Ceramics (Academic Press, New York).
Megla, G.K., 1966, Appl. Opt. **5**, 945.
Mehta, P.C., and S.P. Tandon, 1970, J. Chem. Phys. **53**, 414.
Meriwether, L.S., E.C. Breitner and C.L. Sloan, 1965, J. Am. Chem. Soc. **87**, 4441.
Messer, C.E., and I.S. Levy, 1965, Inorg. Chem. **4**, 543.
Miranday, J.P., C. Jacoboni and R. DePape, 1981, J. Non-Cryst. Solids **43**, 393.
Miyakawa, T., and D.L. Dexter, 1970, Phys. Rev. B **1**, 2961.
Moeller, T., and W.F. Ulrich, 1956, J. Inorg. & Nucl. Chem. **2**, 164.
Moine, B., J.C. Bourcet, G. Boulon, R. Reisfeld and Y. Kalisky, 1981, J. Phys. (France) **42**, 499.
Moore, D.S., and J.C. Wright, 1981, J. Chem. Phys. **74**, 1626.
Morrison, C.A., and R.P. Leavitt, 1982, in: Handbook on the Physics and Chemistry of Rare Earths, Vol. 5, eds. K.A. Gschneidner Jr. and L. Eyring (North-Holland, Amsterdam) p. 461.
Motegi, N., and S. Shionoya, 1973, J. Lumin. **8**, 1.
Müller, A., E. Diemann and C.K. Jørgensen, 1973, Structure and Bonding **14**, 23.
Nakazawa, E., 1979, J. Lumin. **18**, 272.
Nielson, C.W., and G.F. Koster, 1964, Spectroscopic Coefficients for the p^n, d^n and f^n Configurations (MIT Press, Cambridge, MA).
Nikitin, V.I., M.S. Soskin and A.I. Khizhnyak, 1978, Sov. J. Quantum Electron. **8**, 788.
Oelkrug, D., and W. Kempny, 1976, Ber. Bunsenges. Phys. Chem. **80**, 436.
Ofelt, G.S., 1962, J. Chem. Phys. **37**, 511.
Okada, K., Y. Kaizu and H. Kobayashi, 1981, J. Chem. Phys. **75**, 1577.
Okada, K., Y. Kaizu, H. Kobayashi, K. Tanaka and F. Marumo, 1985, Mol. Phys. **54**, 1293.
Øye, H.A., and D.M. Gruen, 1969, J. Am. Chem. Soc. **91**, 2229.
Pappalardo, R.G., W.T. Carnall and P.R. Fields, 1969, J. Chem. Phys. **51**, 1182.
Parke, S., and E. Cole, 1971, Phys. & Chem. Glasses **12**, 125.
Peacock, R.D., 1973, Mol. Phys. **25**, 817.
Peacock, R.D., 1975, Structure and Bonding **22**, 83.
Pedrini, C., F. Rogemond, F. Gaume and D.S. McClure, 1985, J. Less-Common Met. **112**, 103.
Porcher, P., and P. Caro, 1980, J. Lumin. **21**, 207.
Porter, L.C., and J.C. Wright, 1982, J. Lumin. **27**, 237.
Powell, R.C., and G. Blasse, 1980, Structure and Bonding **42**, 43.
Rabinowitch, E., and R.L. Belford, 1964, Spectroscopy and Photochemistry of Uranyl Compounds (Pergamon Press, Oxford).
Racah, G., 1949, Phys. Rev. **76**, 1352.
Rasmussen, L., and C.K. Jørgensen, 1968, Acta Chem. Scand. **22**, 2313.
Rawson, H., 1980, Properties and Applications of Glass, Glass Science and Technology, Vol. 3 (North-Holland, Amsterdam).
Reisfeld, R., 1972, J. Res. Natl. Bur. Stand. Sect. A **76**, 613.
Reisfeld, R., 1973, Structure and Bonding **13**, 53.
Reisfeld, R., 1975, Structure and Bonding **22**, 123.
Reisfeld, R., 1976a, Structure and Bonding **30**, 65.
Reisfeld, R., 1976b, Radiative and Non-Radiative Processes and Energy Transfer in Vitreous States, Coll. Int. CNRS **255**, 149.
Reisfeld, R., 1980, Multiphonon Relaxation in

Glasses, in: Radiationless Processes, eds. B. DiBartolo and V. Goldberg (Plenum, New York) p. 489.
Reisfeld, R., 1982, Ann. Chim. Fr. **7**, 147.
Reisfeld, R., 1983, J. Less-Common Met. **93**, 243.
Reisfeld, R., 1984a, Inorg. Chim. Acta **95**, 69.
Reisfeld, R., 1984b, J. Electrochem. Soc. **131**, 1360.
Reisfeld, R., 1984c, Energy Transfer between Inorganic Ions in Glasses, in: Energy Transfer Processes in Condensed Matter, eds B. DiBartolo and A. Karipidou (Plenum, New York) p. 521.
Reisfeld, R., 1985a, Chem. Phys. Lett. **114**, 306.
Reisfeld, R., 1985b, J. Less-Common Met. **112**, 9.
Reisfeld, R., 1985c, in: Rare Earths Spectroscopy, eds B. Jezowska-Trzebiatowska, J. Legendziewicz and W. Strek (World Scientific, Singapore) p. 587.
Reisfeld, R., 1986, Int. School on Spectroscopy of Solid State Laser Materials, Erice, Italy, June 1985.
Reisfeld, R., and Y. Eckstein, 1975a, J. Chem. Phys. **64**, 4001.
Reisfeld, R., and Y. Eckstein, 1975b, Appl. Phys. Lett. **26**, 253.
Reisfeld, R., and M. Eyal, 1985, J. Phys. Colloq. **46**(C7), 349.
Reisfeld, R., and J. Hormadaly, 1975, J. Solid State Chem. **13**, 283.
Reisfeld, R., and J. Hormadaly, 1976, J. Chem. Phys. **64**, 3207.
Reisfeld, R., and C.K. Jørgensen, 1977, Lasers and Excited States of Rare Earths (Springer, Berlin).
Reisfeld, R., and C.K. Jørgensen, 1982, Structure and Bonding **49**, 1.
Reisfeld, R., and Y. Kalisky, 1980a, Chem. Phys. Lett. **75**, 443.
Reisfeld, R., and Y. Kalisky, 1980b, Nature **283**, 281.
Reisfeld, R., and Y. Kalisky, 1981, Chem. Phys. Lett. **80**, 178.
Reisfeld, R., and A. Kisilev, 1985, Chem. Phys. Lett. **115**, 457.
Reisfeld, R., and N. Lieblich-Sofer, 1974, J. Electrochem. Soc. **121**, 1338.
Reisfeld, R., and N. Lieblich-Sofer, 1979, J. Solid State Chem. **28**, 391.
Reisfeld, R., and S. Morag, 1972, Appl. Phys. Lett. **21**, 57.
Reisfeld, R., J. Hormadaly and B. Barnett, 1972, Chem. Phys. Lett. **17**, 248.
Reisfeld, R., H. Mack, A. Eisenberg and Y. Eckstein, 1975, J. Electrochem. Soc. **122**, 273.
Reisfeld, R., N. Lieblich, L. Boehm and B. Barnett, 1976a, J. Lumin. **12**, 749.
Reisfeld, R., C.K. Jørgensen, A. Bornstein and H. Berthou, 1976b, Chimia **30**, 451.
Reisfeld, R., N. Roth and L. Boehm, 1977a, Abstract 145, 157th Meeting of Electrochem. Soc. **77**, 375.
Reisfeld, R., A. Bornstein, H. Berthou and C.K. Jørgensen, 1977b, Chimia **31**, 12.
Reisfeld, R., J. Hormadaly and A. Muranevich, 1978, J. Non-Cryst. Solids **29**, 323.
Reisfeld, R., E. Greenberg, A. Kisilev and Y. Kalisky, 1981, in: Photochemical Conversion and Storage of Solar Energy, ed. J.S. Connolly (Academic Press, New York) p. 364.
Reisfeld, R., G. Katz, N. Spector, C.K. Jørgensen, C. Jacoboni and R. DePape, 1982, J. Solid State Chem. **41**, 253.
Reisfeld, R., G. Katz, C. Jacoboni, R. DePape, M.G. Drexhage, R.N. Brown and C.K. Jørgensen, 1983a, J. Solid State Chem. **48**, 323.
Reisfeld, R., N. Manor and D. Avnir, 1983b, Sol. Energy Mater. **8**, 399.
Reisfeld, R., E. Greenberg, R.N. Brown, M.G. Drexhage and C.K. Jørgensen, 1983c, Chem. Phys. Lett. **95**, 91.
Reisfeld, R., A. Kisilev, E. Greenberg, A. Buch and M. Ish-Shalom, 1984a, Chem. Phys. Lett. **104**, 153.
Reisfeld, R., A. Kisilev and C.K. Jørgensen, 1984b, Chem. Phys. Lett. **111**, 19.
Reisfeld, R., E. Greenberg, C. Jacoboni, R. DePape and C.K. Jørgensen, 1984c, J. Solid State Chem. **53**, 236.
Reisfeld, R., M. Eyal, E. Greenberg and C.K. Jørgensen, 1985a, Chem. Phys. Lett. **118**, 25.
Reisfeld, R., C.K. Jørgensen, C. Jacoboni and R. DePape, 1985b, 3rd Int. Symp. on Halide Glasses, Rennes, 1985; Mater. Sci. Forum **6**, 635.
Reisfeld, R., M. Eyal, C.K. Jørgensen, A.H. Guenther and B. Bendow, 1986a, Chimia **40**, 403.
Reisfeld, R., A. Kisilev, A. Buch and M. Ish-Shalom, 1986b, Chem. Phys. Lett. **129**, 446.
Reisfeld, R., M. Eyal, C.K. Jørgensen and C. Jacoboni, 1986c, Chem. Phys Lett. **129**, 392.
Richardson, F.S., 1982a, Chem. Phys. Lett. **86**, 47.
Richardson, F.S., 1982b, Chem. Rev. **82**, 541.
Riseberg, L.A., 1973, Phys. Rev. A **7**, 671.
Riseberg, L.A., and H.W. Moos, 1968, Phys. Rev. **174**, 429.
Riseberg, L.A., and M.J. Weber, 1976, Relaxation Phenomena in Rare Earth Luminescence, in: Progress in Optics, Vol. XIV, ed. E. Wolf (North-Holland, Amsterdam).
Rotenberg, M., R. Bivins, N. Metropolis and J.K. Wooten, 1959, The 3j and 6j symbols (MIT Press, Cambridge, MA).
Ryan, J.L., 1969, Inorg. Chem. **8**, 2053.
Ryan, J.L., and C.K. Jørgensen, 1966, J. Phys. Chem. **70**, 2845.
Ryba-Romanowski, W., Z. Mazurak and B.

Jezowska-Trzebiatowska, 1982, J. Lumin. **27**, 177.
Salzmann, J.J., and C.K. Jørgensen, 1968, Helv. Chim. Acta **51**, 1276.
Satten, R.A., 1953, J. Chem. Phys. **21**, 637.
Schröder, J., 1964, Angew. Chem. **76**, 344.
Schuurmans, M.F.H., and J.M.F. van Dijk, 1984, Physica **123B**, 131.
Serra, O.A., and L.C. Thompson, 1976, Inorg. Chem. **15**, 504.
Shinn, M.D., J.C. Windscheif, D.K. Sardar and W.A. Sibley, 1982, Phys. Rev. B **26**, 2371.
Shinn, M.D., W.A. Sibley, M.G. Drexhage and R.N. Brown, 1983, Phys. Rev. B **27**, 6635.
Spector, N., and J. Sugar, 1976, J. Opt. Soc. Am. **66**, 436.
Spector, N., C. Guttel and R. Reisfeld, 1977, Opt. Pura & Apl. **10**, 197.
Stevels, A.L.N., 1979, J. Lumin. **20**, 99.
Stokowski, S.E., 1982, in: Handbook of Laser Science and Technology, Vol. 1, ed. M.J. Weber (Chemical Rubber Co., Boca Raton, FL) p. 215.
Stroud, J.S., 1965, J. Chem. Phys. **43**, 2442.
Struck, W., and W.H. Fonger, 1975, J. Lumin **10**, 1.
Sugar, J., 1965, J. Opt. Soc. Am. **55**, 1058.
Szymanski, M., 1984, J. Lumin. **29**, 433, 467.
Takushi, E., and T. Kushida, 1979, J. Lumin. **18**, 661.
Tanimura, K., M.D. Shinn, W.A. Sibley, M.G. Drexhage and R.N. Brown, 1984, Phys. Rev. B **30**, 2429.
Thompson, L.C., O.A. Serra, J.P. Riehl, F.S. Richards and R.W. Schwartz, 1977, Chem. Phys. **26**, 393.
Tofield, B.C., and H.P. Weber, 1974, Phys. Rev. B **10**, 4560.
Uhlmann, D., and N. Kreidl, 1980, Glass Science and Technology (Academic Press, New York).
Uhlmann, D., and N. Kreidl, 1983, Glass Science and Technology (Academic Press, New York).
Uhlmann, D., and N. Kreidl, 1984, Glass Science and Technology (Academic Press, New York).
Vogel, W., 1984, Glass Chemistry (Am. Ceram. Soc., Columbus, OH).
Vuilleumier, J.J., 1984, Thesis no. 2126, University of Geneva.
Vuilleumier, J.J., M. Deschaux and M.D. Marcantonatos, 1982, Chem. Phys. Lett. **86**, 242.
Waseda, Y., 1980, The Structure of Non-Crystalline Materials (Cocoa Beach, FL).
Watts, R.K., 1975, Nato Adv. Study Inst. Ser. B **8**, 307, 336.
Weber, M.J., 1967a, Phys. Rev. **157**, 262.
Weber, M.J., 1967b, in: Optical Properties of Ions in Crystals, eds H.M. Crosswhite and H.W. Moos (Wiley–Interscience, New York) p. 467.
Weber, M.J., 1968, Phys. Rev. **171**, 283.
Weber, M.J., 1971, Phys. Rev. B **4**, 2932.
Weber, M.J., 1976, in: Critical Materials Problems in Energy Production, ed. C. Stein (Academic Press, New York).
Weber, M.J., 1979, in: Handbook on the Physics and Chemistry of Rare Earths, Vol. 4, eds K.A. Gschneidner Jr. and L. Eyring (North-Holland, Amsterdam) p. 275.
Weber, M.J., 1981, in: Laser Spectroscopy of Solids, Topics in Applied Physics, eds W.M. Yen and P.M. Selzer (Springer, Berlin).
Weber, M.J., 1982, J. Non-Cryst. Solids **47**, 117.
Weber, M.J., T.E. Varitimos and B.H. Matsinger, 1973, Phys. Rev. B **8**, 47.
Weber, M.J., J.A. Paisner, S.S. Sussman, W.M. Yen, L.A. Riseberg and M. Brecher, 1976, J. Lumin. **12**, 729.
Weber, M.J., J.D. Myers and D.H. Blackburn, 1981, J. Appl. Phys. **52**, 2944.
Weyl, D.A., 1959, Coloured Glasses (Dawsons of Pall Mall, London).
Wheeler, J., and J.K. Thomas, 1982, J. Phys. Chem. **86**, 4540.
Wilson, B.A., W.M. Yen, J. Hegarty and G.F. Imbusch, 1979, Phys. Rev. B **19**, 4238.
Winnacker, A., R.M. Shelby and R.M. Macfarlane, 1985a, Opt. Lett. **10**, 350.
Winnacker, A., R.M. Shelby and R.M. Macfarlane, 1985b, J. Phys. Colloq. **46**(C7), 543.
Wong, J., and C.A. Angell, 1976, Glass Structure by Spectroscopy (Marcel Dekker, New York).
Wybourne, B.G., 1961, J. Chem. Phys. **34**, 279.
Wybourne, B.G., 1975, Spectroscopic Properties of Rare Earths (Interscience, New York).
Xu, Li-Wen, H.M. Crosswhite and J.P. Hessler, 1984, J. Chem. Phys. **81**, 698.
Yamada, N., S. Shionoya and T. Kushida, 1971, J. Phys. Soc. Jpn **30**, 1507.
Yamada, S., and R. Tsuchida, 1953, Bull. Chem. Soc. Jpn **26**, 15.
Yariv, A., 1975, Quantum Electronics (Wiley, New York).
Yokono, S., T. Abe and T. Hoshina, 1981, J. Lumin. **24**, 309.
Yokota, M., and O. Tanimoto, 1967, J. Phys. Soc. Jpn **22**, 779.
Yokota, R., 1967, J. Phys. Soc. Jpn **23**, 129.

Handbook on the Physics and Chemistry of Rare Earths, edited by K.A. Gschneidner, Jr. and L. Eyring

Chapter 59

INORGANIC COMPLEX COMPOUNDS II

L. NIINISTÖ AND M. LESKELÄ *
Department of Chemistry, Helsinki University of Technology, Otaniemi SF-02150 Espoo 15, Finland

Contents

* Present address: Dept. of Chemistry, University of Turku, SF-20500 Turku, Finland.

1. Rare earth phosphates and related phosphor compounds

1.1. *Introduction*

The rare earth phosphates are important in the geochemistry of the rare earths, since two of the main rare earth minerals are binary orthophosphates. The most abundant of these, monazite, has the approximate composition $(Ce, La)PO_4$, while xenotime is primarily an yttrium phosphate. Several other rare earth minerals containing phosphate have been found in the earth (Gmelin, 1984). In addition, the important phosphorus sources apatite and phosphorite contain up to 1% of rare earths.

Besides these anhydrous orthophosphates many other binary rare earth phosphates are known and prepared synthetically. Study of the phase equilibria of the system La_2O_3–P_2O_5, for example, has shown six intermediate compounds having molar ratios of 3:1, 7:3, 1:1, 1:2, 1:3, and 1:5 (fig. 1) (Park and Kreidler, 1984). The great number of compounds is due to the versatile chemistry of elemental phosphorus. In pentavalent state, for example, it not only forms orthophosphate and hydrogenphosphate ions but also polyphosphates, of which the most common for the rare earths are $P_2O_7^{2-}$, $P_3O_9^{3-}$, $P_4O_{12}^{4-}$, and $P_5O_{14}^{3-}$ (Giesbrecht and Perrier, 1960; Jaulmes, 1969; Beucher, 1970). Several representatives of rare earth hydrogenphosphates, phosphites, and hypophosphites have been prepared (Ionov et al., 1973a,b; Chudinova and Balagina, 1979).

Ternary rare earth phosphates are formed with alkali and alkaline earth elements and in these compounds, too, the composition of the phosphate anion can vary (Hong, 1975a; Hong and Chinn, 1976; Koizumi, 1976). From the

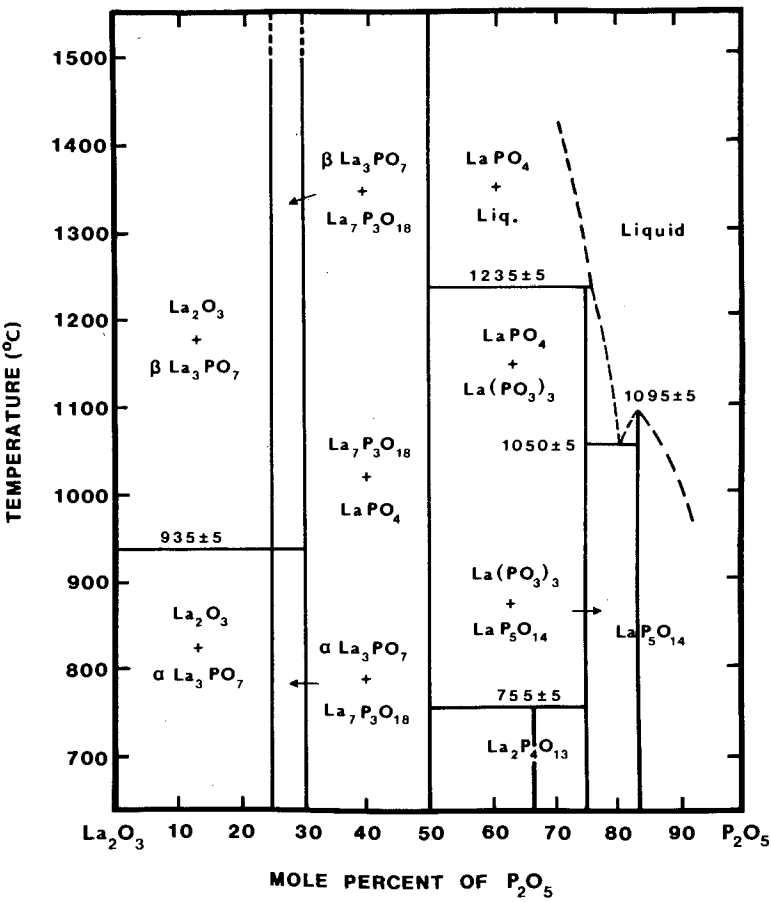

Fig. 1. A phase diagram for the system La_2O_3–P_2O_5 (Park and Kreidler, 1984).

quaternary systems the compounds $M_8^{II}R(PO_4)_6(O, F)_2$, having the apatite structure, are most common (Ito, 1968; Mathew et al., 1979).

A review on the crystal chemistry of rare earth phosphates was recently published by Palkina (1982).

The rare earth phosphates activated with trivalent lanthanides can be used as luminescent materials and neodymium-containing polyphosphates reportedly make efficient laser materials (Palilla and Tomkus, 1969; Albrand et al., 1974; Koizumi, 1976b).

1.2. *Rare earth orthophosphates*

Rare earth orthophosphates, in addition to being found in nature as the minerals monazite, (La, Ce) PO_4, and xenotime, (Y, Er) PO_4, have been synthe-

sized in the laboratory by many methods. The phosphate anion precipitates the rare earth ions from solution. The phosphate source for the precipitation is usually phosphoric acid, but alkali phosphates and hydrogen phosphates can also be used (Schwarz, 1963f; Petushkova et al., 1969a,b; Ropp, 1970; Awazu and Matsunaya, 1974; Tsuhako et al., 1979). The precipitate contains half a molecule of water in the case of the lighter rare earths, and two water molecules in the case of the heavier rare earths (Mooney, 1948; Hikichi, 1978). Rare earth orthophosphate hydrates having 1, 5/3, 2.5, and 3 water molecules have also been reported (Hezell and Ross, 1967; Ropp, 1968a; Petushkova et al., 1969a; Tsagareishvili et al., 1972).

Anhydrous rare earth orthophosphates have been prepared by a fusion method (Duboin, 1888) and by chemical reactions (Mooney, 1950; Schwarz, 1963f). Single crystals have been obtained by hydrothermal crystallization from a mixture of the rare earth hydroxide and phosphoric acid (Anthony, 1957; Carron et al., 1958) and by flux growth from lead phosphate (Feigelson, 1964; Smith and Wanklyn, 1974). The rare earth phosphate phosphors are usually made by a fusion reaction between the rare earth oxide, carbonate, nitrate hydroxide, etc., and $(NH_4)_2HPO_4$ at a temperature of 900–1100°C (Smith, 1967; Palilla and Tomkus, 1969).

The orthophosphates of the cerium subgroup have been found to possess the monoclinic monazite structure (Mooney, 1948; Mooney-Slater, 1962; Schwarz, 1963f), in which the irregularly nine-coordinated rare earth atoms are linked together by isolated, distorted phosphate tetrahedra (fig. 2) (Krstanovic, 1965; Beall et al., 1981). Crystal-structure determinations of numerous samples of monazite having slightly different compositions have been carried out (Parrish, 1939; Finney and Rao, 1967; Ghouse, 1968; Haapala et al., 1969). The space group of monazite has been reported to be $P2_1/n$ but determinations have also been done with a $P2_1/a$ setting (Ueda, 1967; Jaulmes, 1972).

Crystallization of orthophosphates of the cerium subgroup from solution at low temperatures produces hexagonal $RPO_4 \cdot 0.5H_2O$ crystals (Mooney, 1948; Hikichi, 1978). The structure is stable at low temperatures but changes to monazite structure upon heating (Kuznetsov et al., 1969). Characteristic of this structure are the large tunnels running along the *c*-axis (fig. 3). Originally, the hexagonal phase was known only for the hemihydrate and it was suggested that water was needed to stabilize the structure (Mooney, 1950; Mooney-Slater, 1962). However, Vlasse et al. (1982) found no evidence that the presence of water was necessary.

The rare earth phosphates in the middle of the series, containing several water molecules, have also been reported to be hexagonal (Hezel and Ross, 1967; Kuznetsov et al., 1969). In contrast, dysprosium orthophosphate containing 1.5 molecules of water has a unique, orthorhombic structure (Hikichi, 1978).

The phosphates of the yttrium subgroup have the tetragonal zircon structure, which is isomorphic with the corresponding orthovanadates, arsenates, and chromates (Schwarz, 1963f). The crystal structure of xenotime has been deter-

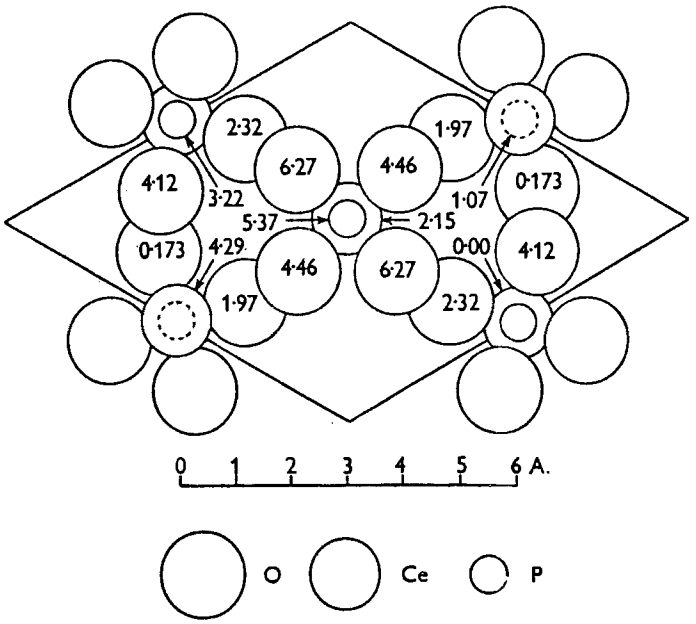

Fig. 2. A projection of the $CePO_4$ structure on the basal plane. The numbers give the z-coordinate in Ångströms (Mooney, 1950).

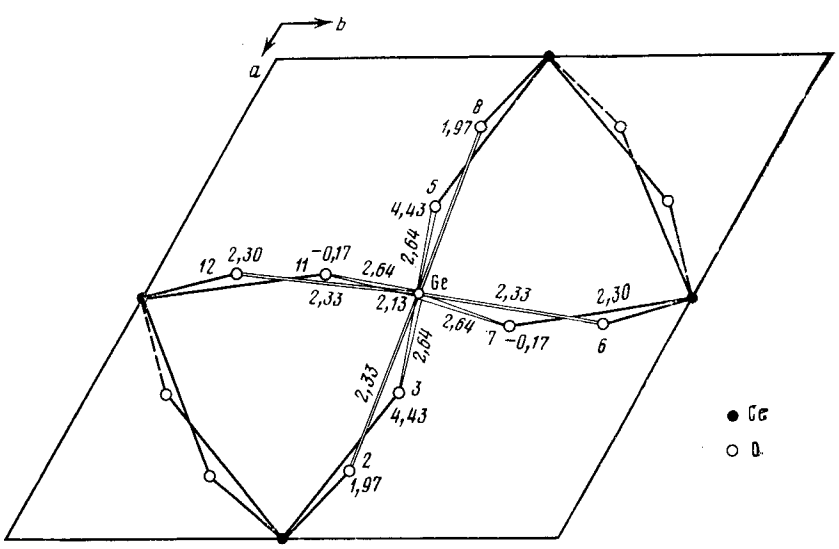

Fig. 3. The environment of Ce^{3+} in the hexagonal $CePO_4 \cdot \frac{1}{2}H_2O$ structure projected on the *ab*-plane (Palkina, 1982).

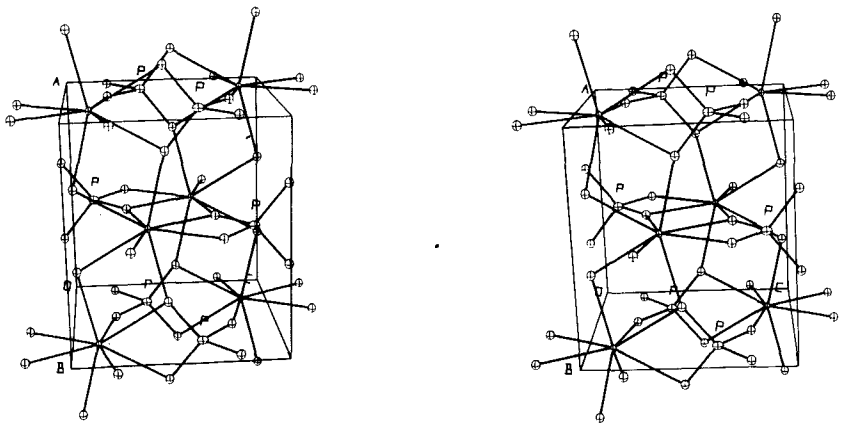

Fig. 4. A stereoview of the polyhedra in the tetragonal RPO_4 structure (Milligan et al., 1983).

mined by several groups (fig. 4) (Vegard, 1927; Durif and Forrat, 1957; Lohmuller et al., 1973; Milligan et al., 1983).

When crystallized from solution, the phosphates of the heavier rare earths contain two water molecules. The dihydrate is found in nature, as the minerals weinschenkite and churchite (Strunz, 1942; Claringsbull and Hey, 1953), which have monoclinic structure. According to Hezel and Ross (1967), the heavier rare earths also have a tetragonal trihydrate with a structure similar to that of zircon where the water molecules are uncoordinated.

Scandium orthophosphate contains two water molecules and is isomorphic with the corresponding iron and aluminum compounds having an orthorhombic crystal lattice (Komissarova et al., 1965a; Eshchenko et al., 1979).

When the rare earth phosphates are precipitated with sodium phosphate, not only binary and ternary phosphates but also hydroxide phosphates can be obtained (Tananaev and Vasileva, 1963). The formula of these compounds may be as complicated as $Pr_{10}(OH)_3(PO_4)_9 \cdot 26H_2O$ (Petushkova et al., 1969b).

Except for scandium, very few hydrogenphosphates are known for the rare earth elements. The complex formation of Ce^{3+} and Ce^{4+} with the $H_2PO_4^-$ has been verified by Lebedev and Kulyako (1978). In solid state, dihydrogenphosphates, $R(H_2PO_4)_3$, with tetragonal structure have been prepared for Sm, Eu, and Gd (Butuzova et al., 1982). Trihydrogen orthophosphates, with formula $H_3R(PO_4)_2 \cdot H_2O$, having orthorhombic structure, have been prepared and studied by Melnikov et al. (1982). Hexagonal $Sc(H_2PO_4)_3$ can be prepared from Sc_2O_3 and large excess of H_3PO_4 or by thermal decomposition of $Sc(PO_3)_3$ (Melnikov and Komissarova, 1969). This hexagonal structure has recently been solved by Smolin et al. (1982) (fig. 5). In solution, other ligands can bond along with hydrogenphosphate to the rare earth ion and a mixed ligand complex is formed (Nazarenko and Polyektov, 1979). Such an interesting compound is

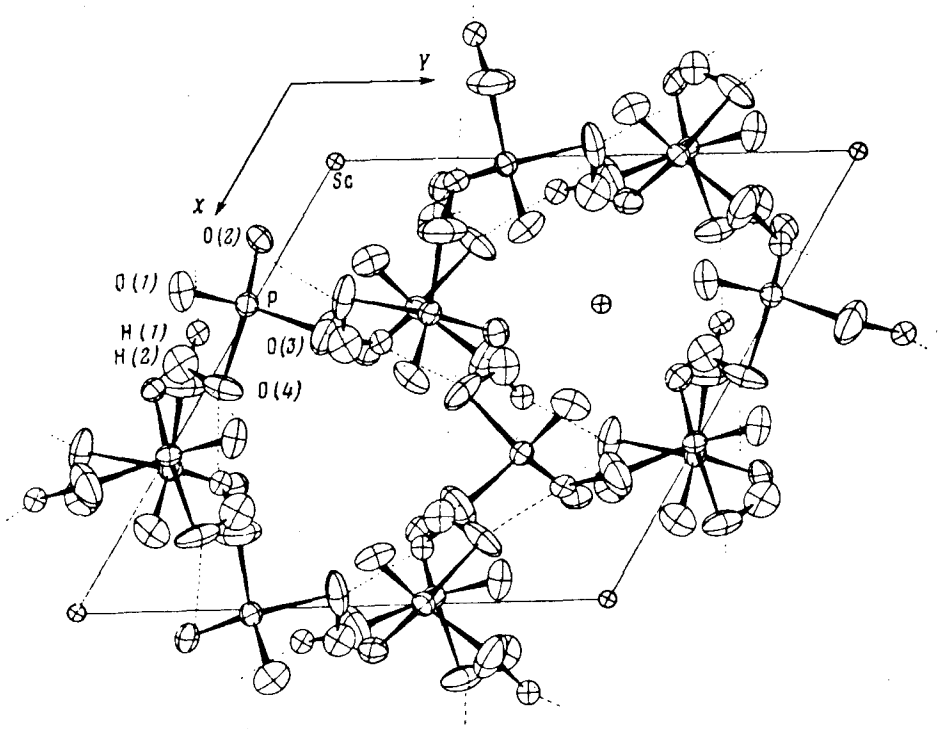

Fig. 5. A perspective view of the $Sc(H_2PO_4)_3$ structure on the *xy*-plane (Smolin et al., 1982).

known for Ce^{4+} in the solid state as well as in solution. The structure of $(CePO_4)_2(HPO_4)_{1-x}(SO_4)_x \cdot 5H_2O$ contains tunnels oriented along the *b*-axis (fig. 6) (Bartl, 1976), and other features which allow it to act as an ion exchanger (König and Psotta, 1978a,b).

1.3. *Condensed rare earth phosphates*

The condensed phosphates contain more than one phosphorus atom in a molecule but with the structure always built up by PO_4 tetrahedra. Whereas in orthophosphates the phosphate tetrahedra are isolated, in condensed phosphates they share corners (but never edges or faces). The larger the O/P ratio in the formula is, the more broken the tetrahedra chains are; and the smaller the O/P ratio is, the more cross-linked the chains are (Hong, 1974b). The condensed phosphates can be divided into three groups: branched or ultraphosphates $[P_nO_{3n-1}]^{(n-2)-}$, cyclic or metaphosphates $[P_nO_{3n}]^{n-}$, and chain or polyphosphates $[P_nO_{3n+1}]^{(n+2)-}$. In addition, there is a group of oligophosphates which contain separate anions: pyrophosphate, tripolyphosphate, etc., but compounds of the rare earths with these anions have been little studied (Palkina, 1978). The

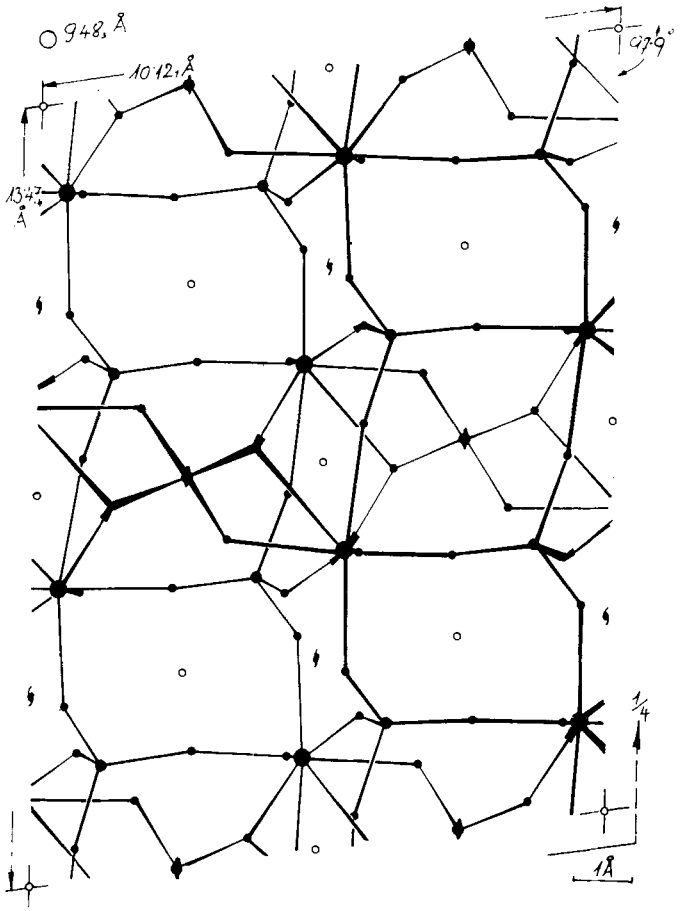

Fig. 6. A perspective view of the structure of $(CePO_4)_2(HPO_4/SO_4)\cdot 5H_2O$ on the *ac*-plane. The projection shows the structural framework with 8- and 4-coordination and the porosity with the O–O distances of 6.1 Å (Bartl, 1976).

temperature dependence of the formation of the different phosphates is shown for cerium in fig. 7.

1.3.1. RP_5O_{14}

The rare earth ultraphosphates – compounds containing branched phosphate anions and also called pentaphosphates (RP_5O_{14}) – can be synthesized both as powder and as single crystals from a solution of rare earth oxide in phosphoric acid allowed to cool from 600–700°C to room temperature. The phosphate anion must be in great excess with respect to the cation in the solution (P/R = 20–40) (Jaulmes, 1969; Hong, 1974a; Chudinova et al., 1977a). RP_5O_{14} can also be prepared via a solid state reaction of R_2O_3 with $(NH_4)_2HPO_4$; different structure

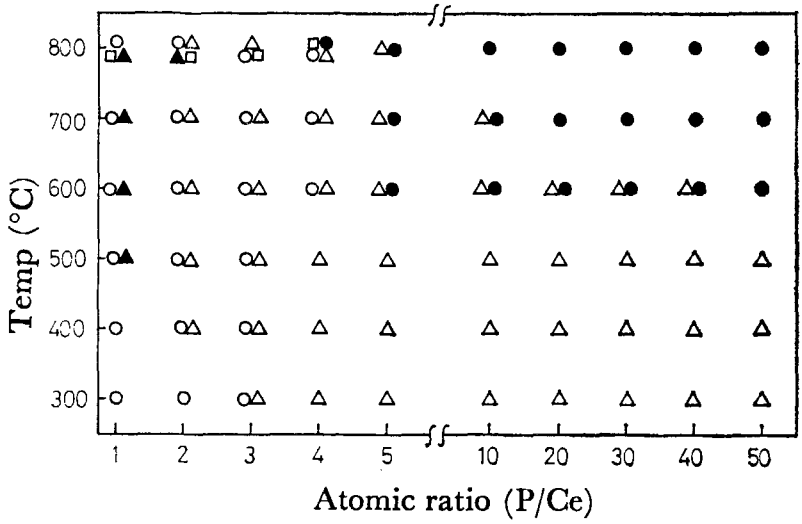

Fig. 7. The formation of cerium phosphates at different temperatures and atomic ratios. ▲: $CePO_4$; ○: CeP_2O_7; □: $Ce(PO_3)_3$; △: $Ce(PO_3)_4$; ●: CeP_5O_{14}. (Tsuhako et al., 1979.)

types are obtained at different temperatures (Sungur et al., 1983). Since NdP_5O_{14} crystals are promising laser materials, there have been attempts to grow them as fibers. Success has been achieved in a controlled gas atmosphere at 450°C (Tofield et al., 1975). The pulling of RP_5O_{14} crystals from a melt is not possible because the compound decomposes before melting.

All ultraphosphates contain PO_4 tetrahedra linked by three vertices to neighboring tetrahedra (fig. 8). The further coordination of the phosphate groups varies, giving rise to three different crystal structures: monoclinic I (La···Tb), monoclinic II (Dy···Lu, Y), and orthorhombic (Dy···Er, Y) (Beucher, 1970;

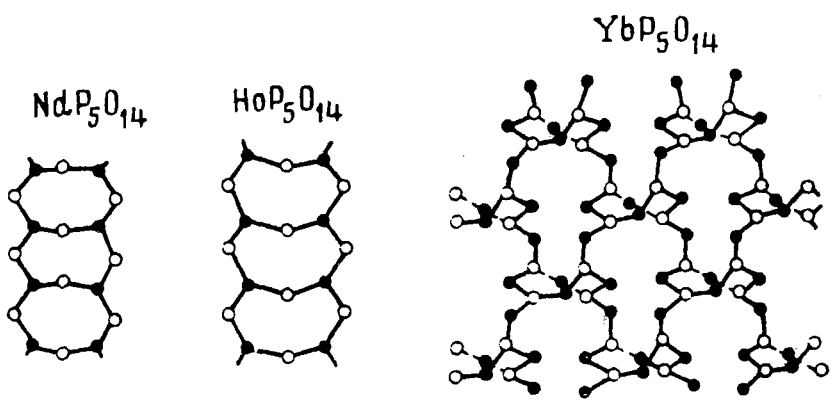

Fig. 8. The structure of the $(P_5O_{14})^{3-}$ anion in NdP_5O_{14}, orthorhombic HoP_5O_{14}, and YbP_5O_{14} (Palkina, 1978).

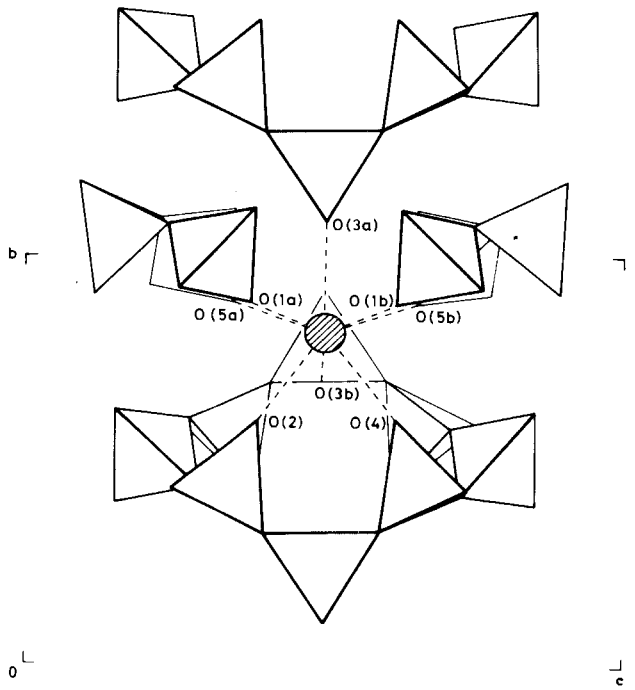

Fig. 9. A perspective view along the *a*-axis showing four phosphate ribbons linked by neodymium in the structure of NdP_5O_{14} (Albrand et al., 1974).

Hong and Pierce, 1974). All the structures contain eight-membered conjugate rings (fig. 9). The monoclinic I structure and the orthorhombic structure differ only in the orientation of the middle tetrahedra, which form common sheets of conjugate rings (Durif, 1971; Tranqui et al., 1972; Hong, 1974c). In the monoclinic II structure each PO_4 ring is not linked with two rings as in the other structures but with four rings, and thus eight- and twenty-membered rings are formed (fig. 10) (Bagieu et al., 1973; Hong and Pierce, 1974; Palkina, 1978). In all rare earth ultraphosphates the cations are eight-coordinated. The isolated polyhedra can best be described as bicapped trigonal prisms. Albrand et al. (1974), however, propose a square antiprismatic coordination for neodymium in NdP_5O_{14}.

Recently, a new type of ultraphosphate has been found for CeP_5O_{14} (Rzaigui et al., 1984; Rzaigui and Ariguip, 1985). Its structure is triclinic and the atomic arrangement can be described as $P_{10}O_{28}$ sheets spreading in the (110) planes. The internal structure of these sheets is mainly a linkage of $P_{12}O_{36}$ rings in which 40% of the phosphorus atoms are branching. Cerium atoms have an eight-fold coordination and the CeO_8 polyhedra have no common oxygen atoms.

According to Schulz et al. (1974), NdP_5O_{14} has an orthorhombic high-temperature form which can be derived from the monoclinic structure. Otherwise, the ultraphosphates decompose to metaphosphates at high temperatures (900–1000°C) (Chudinova et al., 1975; Chudinova and Balagina, 1979).

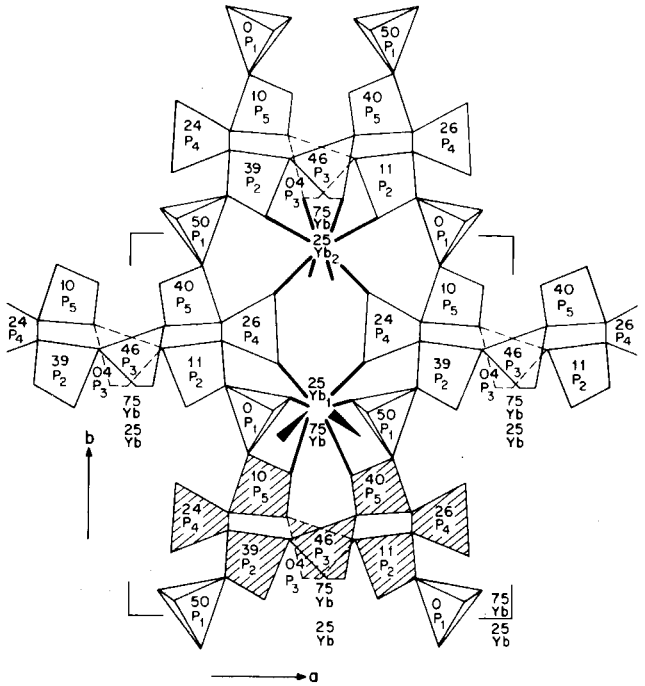

Fig. 10. An *ab*-projection of one phosphate layer in YbP_5O_{14} (Hong and Pierce, 1974).

1.3.2. *RP_3O_9 and $R(PO_3)_3$*

The chemical formula of the rare earth metaphosphates has been presented as RP_3O_9 and $R(PO_3)_3$. The correct name for the first formula would be cyclo-triphosphate and for the second catena-polyphosphate. Most of the metaphosphates described in the literature are catena-polyphosphates, but this is not obvious from either the formulas or the names generally used.

Rare earth catena-polyphosphates (metaphosphates) can be prepared by the following methods: (a) heating of rare earth oxides with phosphoric acid within a specific temperature range (Chudinova et al., 1975, 1977a; Chudinova and Balagina, 1979); (b) roasting of a mixture of R_2O_3 and $NH_4H_2PO_4$ (Chudinova et al., 1978a,b); (c) thermal dehydration of $RP_3O_9 \cdot nH_2O$ precipitated from aqueous solution (Birke and Kempe, 1973a,b); (d) decomposition of ultraphosphate RP_5O_{14} above 900°C with release of P_2O_5 (Bagieu-Beucher and Tranqui, 1970); (e) thermal condensation of dihydrogentriphosphates, $RH_2P_3O_{19}$ (Melnikov et al., 1981b); and (f) crystallizing from a solution of R_2O_3, H_3PO_4, NaF, and P_2O_5 at high temperature (Hong, 1974b). In the preparation of catena-polyphosphate from a mixture of R_2O_3 and H_3PO_4 the P/R ratio should be 2–3. The product is not always pure but may contain ortho- and ultraphosphates (Tsuhako et al., 1979).

In the series of rare earth metaphosphates (polyphosphates), the larger cations form an orthorhombic structure containing helical chains of corner-sharing PO_4 tetrahedra. The PO_8 dodecahedra share edges in a zigzag fashion (fig. 11) (Hong, 1974a). The polyphosphates of the smaller rare earths are monoclinic and the phosphate tetrahedra form chains characteristic of metaphosphates. The rare earth atoms lie at the centers of the isolated oxygen octahedra (fig. 12) (Hong, 1974b).

The smaller rare earth cations form compounds with a composition $R(PO_3)_3$ corresponding to metaphosphate, but according to their crystal structure the correct formula is $R_4(P_4O_{12})_3$ (Bagieu-Beucher, 1976; Smolin et al., 1978). Thus the anions are cyclic polyphosphates. Their structure is cubic, containing eight-membered phosphate rings linked together by RO_6 octahedra (fig. 13) (Mezentseva et al., 1977; Bagieu-Beucher and Guitel, 1978; Chudinova, 1979).

The dehydration of scandium hydrogenphosphate, $Sc(H_2PO_4)_3$, leads to the formation of $Sc(PO_3)_3$. This material decomposes above 1200°C to normal orthophosphate (Melnikov and Komissarova, 1969; Komissarova et al., 1971a; Khrameeva et al., 1971). The monoclinic structure of $Sc(PO_3)_3$ consists of infinite chains of PO_4 tetrahedra, linked together by octahedrally coordinated scandium atoms (fig. 14) (Domanskii et al., 1982).

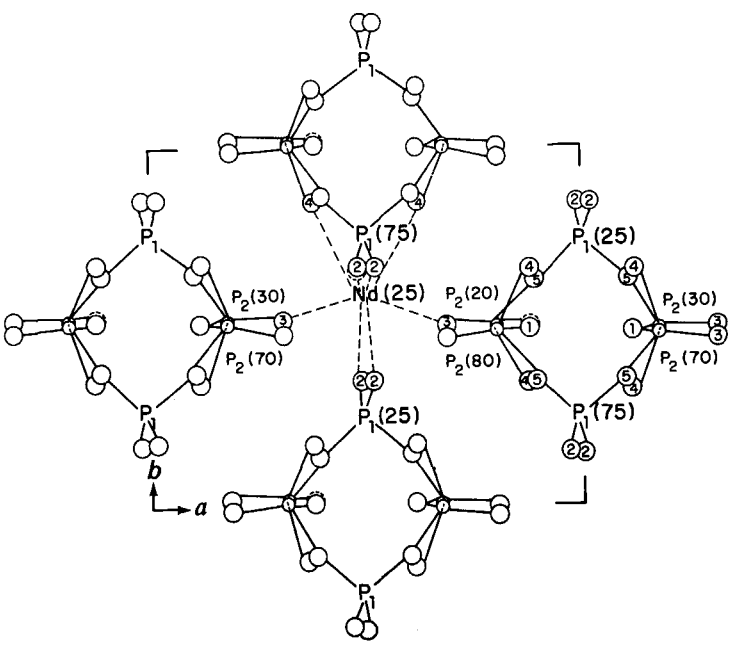

Fig. 11. An *ab*-projection of the NdP_3O_9 structure showing how the PO_4 tetrahedra are connected by Nd atoms (Hong, 1974a).

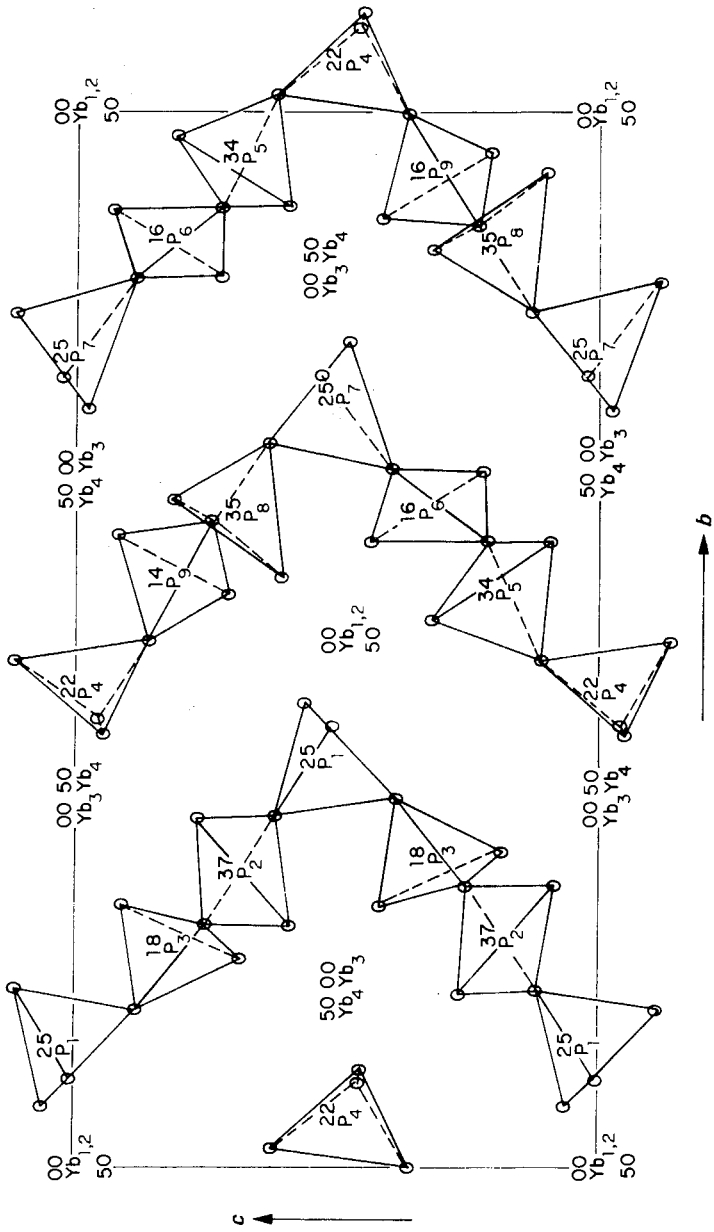

Fig. 12. A *bc*-projection of the arrangement of PO_4 tetrahedra in YbP_3O_9 showing the ribbons running helically along the *c*-axis (Hong, 1974).

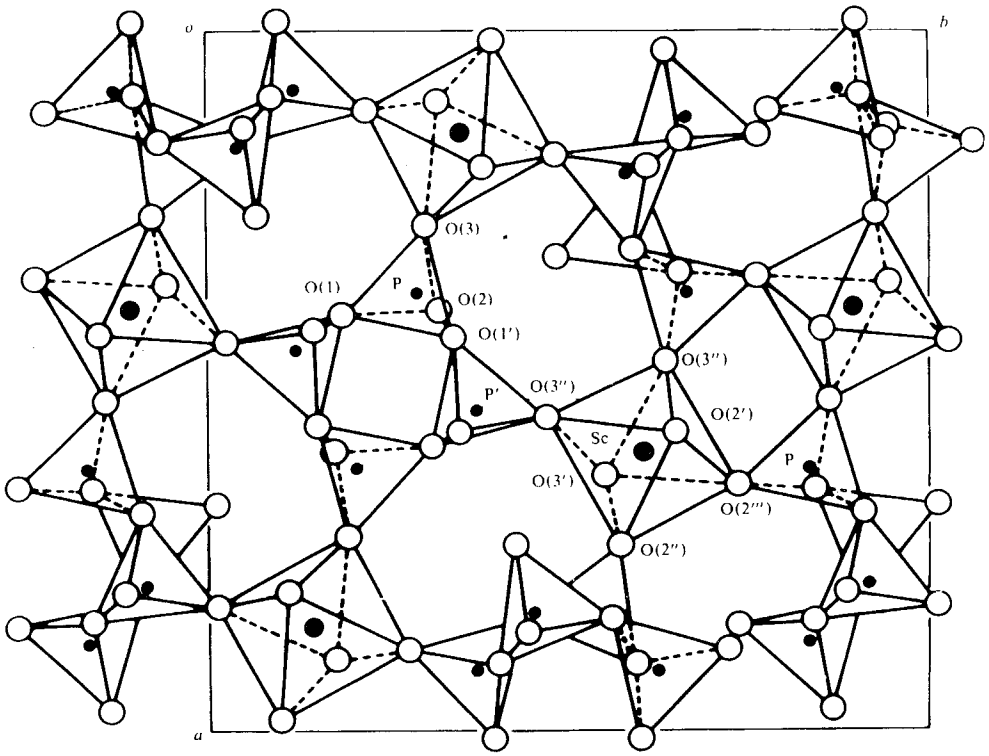

Fig. 13. A projection of the cubic $Sc_4(P_3O_{12})_3$ structure on the *ab*-plane showing the anion rings and regular ScO_6 octahedra (Bagieu-Beucher and Guitel, 1978).

Besides anhydrous compounds $R(PO_3)_3$, hydrates of cyclotri-, cyclotetra-, cyclohexa- and cyclooctaphosphates of rare earth elements have been obtained from aqueous solutions by an exchange reaction with the corresponding sodium phosphate. The precipitation of cyclotriphosphate, having 3 to 5 water molecules, with $Na_3P_3O_9$ has been reported by Birke and Kempe (1973a,b) and Serra and Giesbrecht (1968). The cerium cyclotriphosphate trihydrate, $CeP_3O_9 \cdot 3H_2O$, which is isomorphic with the corresponding La and Pr compounds, has been studied by X-ray diffraction analysis. The hexagonal structure contains flat $P_3O_9^{3-}$ rings and Ce has a tricapped trigonal prismatic coordination to six oxygens of the phosphate rings and to the three oxygens of the water molecules (Bagieu-Beucher et al., 1971).

Compounds having the general formula of metaphosphates but containing hexa- or octaphosphate as anion have been studied by Chudinova et al. (1978c) and Lazarevski et al. (1982). These compounds, precipitated with $Na_6P_6O_{18}$ or $Na_8P_8O_{24}$, may also contain crystal water. The structure is unknown; only the X-ray diffraction powder pattern and IR spectra have been recorded. Europium

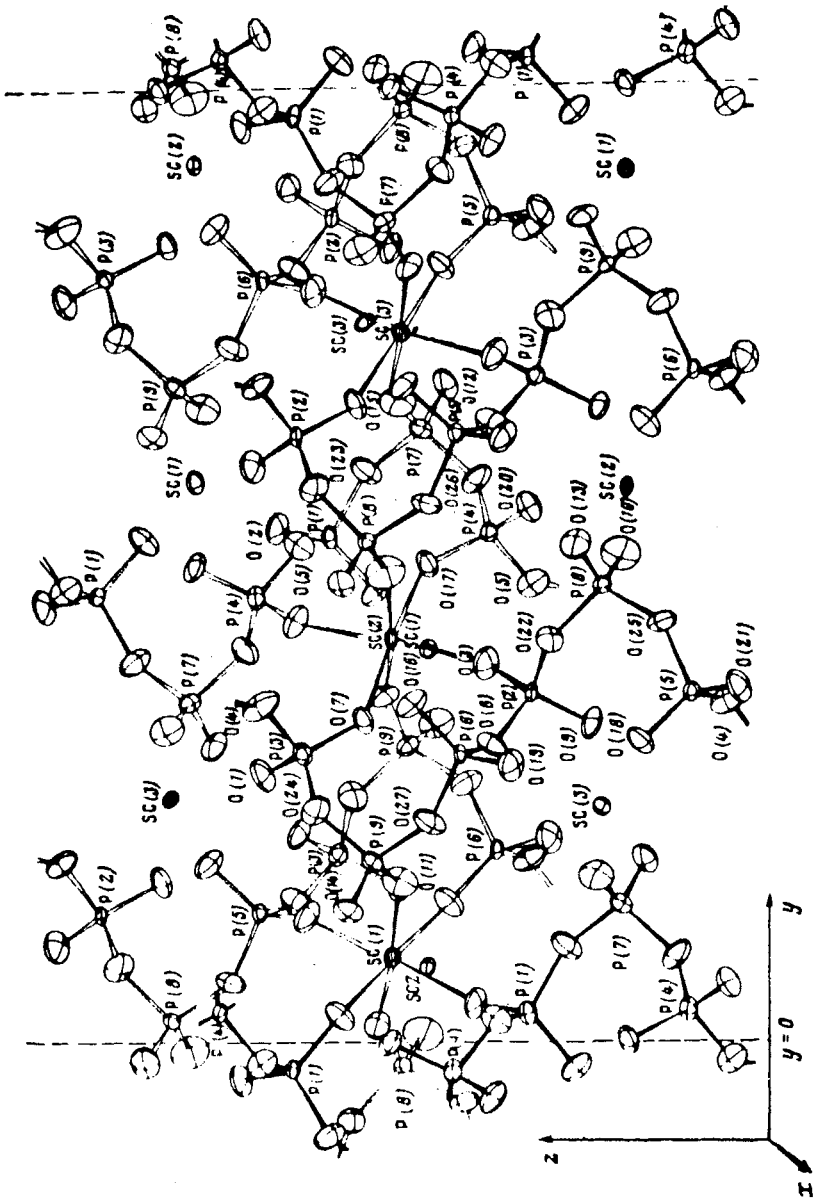

Fig. 14. A perspective view of the crystal structure of $Sc(PO_3)_3$ on the *yz*-plane (Domanskii et al., 1982).

and lanthanum form hydrated polyphosphates having the same O/P ratio as metaphosphates, and for these Ezhova et al. (1978a,b) have investigated the formation, thermal behavior, and IR spectra.

1.3.3. *Other condensed phosphates*

Except for the catena-polyphosphates, the binary condensed phosphates or polyphosphates have been investigated much less thoroughly than the ternary polyphosphates containing alkali as an additional cation. The crystal structures of the rare earth binary polyphosphates are largely unknown. Trivalent rare earth ions react with sodium triphosphate in solution to form insoluble compounds where the molar ratio between R^{3+} and $P_3O_{10}^{5-}$ is 1:1 and 5:3 (Giesbrecht and Audrieht, 1958; Giesbrecht, 1960; Giesbrecht and Melardi, 1963). In the solid state, these compounds contain more than twenty water molecules (Petushkova et al., 1971). The rare earth polyphosphates also form a complex in solution where the ratio $R^{3+}/P_3O_{10}^{5-}$ is 1:2 (Rodicheva, 1981). The separated solid state 1:1 and 5:3 compounds dissolve in excess of sodium triphosphate.

Tetravalent cerium behaves exceptionally upon heating with H_3PO_4. With low P/Ce ratio (1–3) it forms diphosphate, CeP_2O_7, and with a higher proportion of phosphorus it forms catena-polyphosphate, $Ce(PO_3)_4$. Cerium may also reduce to trivalent in this system, with the formation of $Ce(PO_3)_3$ at lower temperatures and the ultraphosphate CeP_5O_{14} at higher temperatures (Tsuhako et al., 1979).

Whereas cerium diphosphate can be prepared from phosphoric acid, the other rare earth diphosphates require the diphosphate anion as starting material (Tananaev et al., 1967; Ukrainskaya et al., 1971). The formula of the diphosphate of the trivalent rare earths is $R_4(P_2O_7)_3$ (Chudinova et al., 1967; Kuznetsov and Vasileva, 1967). In excess, the alkali diphosphates used in the preparation of the diphosphate lead to the formation of double diphosphate. An alternative preparation method for scandium diphosphate (Muck and Petrů, 1971) is the decomposition of scandium hydrogen phosphite, $Sc_2(HPO_3)_3$, at 380–500°C. The crystal structures of the rare earth diphosphates are unknown. Petrů and Muck (1971) have indexed the powder of scandium diphosphate as tetragonal with the axes $a = 6.60$ and $c = 14.02$ Å.

In solid-state studies of R_2O_3–$2P_2O_5$ mixtures, a phase with the composition $R_2P_4O_{13}$ has been found. The X-ray diffraction powder pattern and IR spectrum of this compound have been reported but the detailed structure is unknown (Park and Kreidel, 1984; Agrawal and White, 1985).

In the system R_2O_3–H_3PO_4, hydrogen diphosphate and dihydrogen triphosphate appear as anions forming complexes with R^{3+}, the first anion only with the heavier lanthanides however (Chudinova et al., 1977a,c, 1978d). For the dihydrogen triphosphates a single crystal structure determination has been carried out for $YbH_2P_3O_{10}$. The monoclinic structure consists of short PO_4^{3-} chains, the $P_3O_{10}^{5-}$ ions are symmetric, and the isolated ytterbium atoms have octahedral coordination (fig. 15) (Palkina et al., 1979).

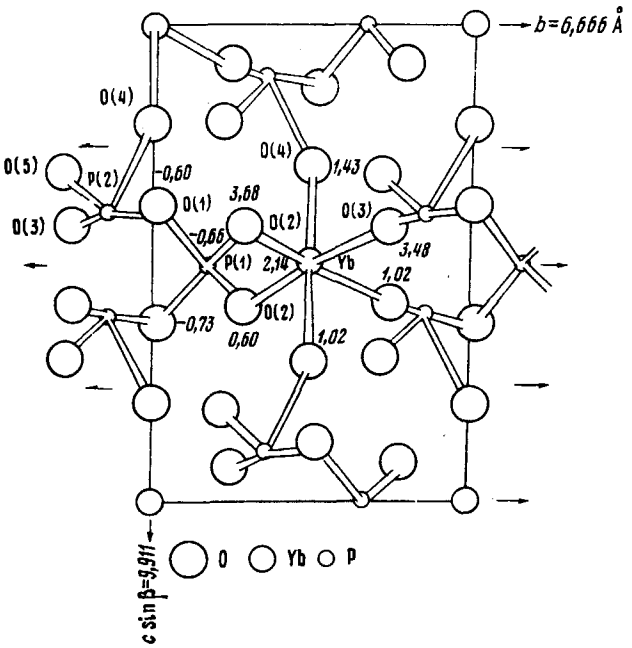

Fig. 15. The structure of triphosphate anion, $P_3O_{10}^{5-}$, and YbO_6 polyhedron in $YbH_2P_3O_{10}$ projected on the *bc*-plane (Palkina, 1982).

Mironova and Tananaev (1982) have reported the preparation of erbium hypophosphate in a study of the interaction in the $Er(NO_3)_3$–$H_4P_2O_6$–H_2O system; orthorhombic $ErHP_2O_6 \cdot 4H_2O$ crystals were separated and their thermal properties characterized. In the structure the hypophosphate anions are connected by hydrogen bridging into infinite –O–P–P–O–H–O–P–P–O– chains (fig. 16), and the ErO_8 polyhedra are distorted tetragonal antiprisms isolated from one another (Palkina et al., 1983a). Later it was shown that the hypophosphate hydrates of Nd, Eu, Er, and Yb are isostructural (Palkina et al., 1983b, 1984a).

1.4. *Rare earth phosphites and hypophosphites*

Of the rare earth phosphites only the scandium compounds have been prepared and studied. $Sc(H_2PO_3)_3$ was prepared by dissolving $Sc(OH)_3$ in H_3PO_3 and distilling off the excess water (Komissarova et al., 1967; Petrů and Muck, 1967). The structure was reported to be rhombohedral. $Sc_2(HPO_3)_3 \cdot xH_2O$ was obtained by dissolving metallic scandium in H_3PO_3 at 60–80°C and leaving the solution to evaporate for several weeks.

The rare earth hypophosphites can be obtained from an aqueous solution of R^{3+} ions and alkali hypophosphite. Except for scandium, the compounds are very soluble in water and therefore they have mainly been studied in solution (Komissarova and Melnikov, 1966; Sheka and Sinyavskaya, 1969; Polyektov et

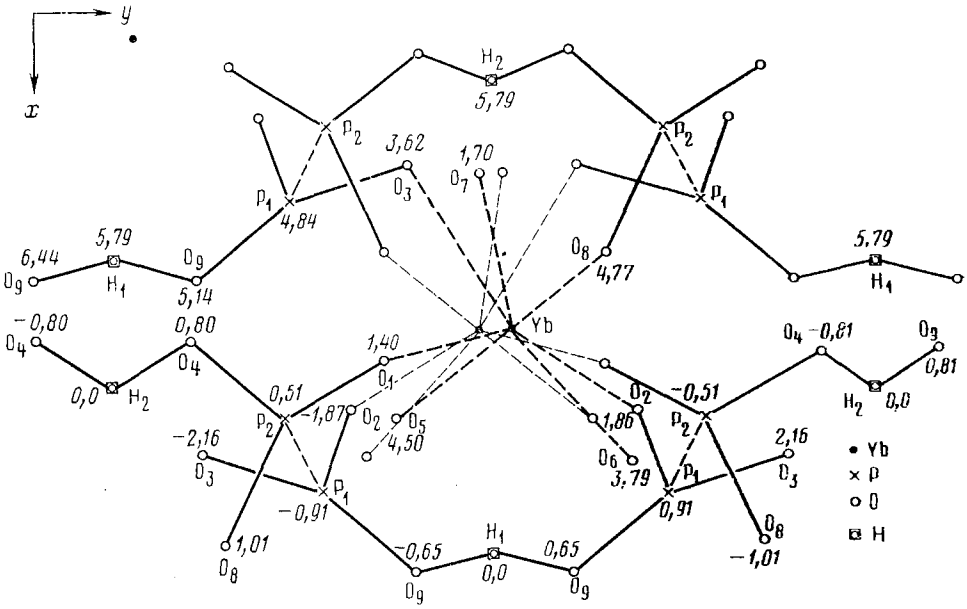

Fig. 16. A projection of the structure of $YbHP_2O_6 \cdot 4H_2O$ on the *xy*-plane (Palkina et al., 1984a).

al., 1970). More recently, Aslanov et al. (1975) have developed a method of synthesizing the hypophosphites in nonaqueous medium.

The lanthanides form two structurally different groups of $R(H_2PO_2)_3$ compounds. The lighter lanthanides (La $\cdots$ Eu) form compounds containing one water molecule and the heavier lanthanides (Gd $\cdots$ Lu) form anhydrous compounds. The crystal systems are triclinic and monoclinic, respectively. The first structure contains three different hypophosphite groups, of which one is tridentate and two are bidentate bridging (Ionov et al., 1973a,b). According to Ionov et al. (1973a), the La and Eu compounds are similar but not isomorphous: some positional parameters of the oxygen atoms differ significantly. The coordination number of R^{3+} in both structures is eight. In $Er(H_2PO_2)_3$ the erbium atoms are octahedrally coordinated and are cross-linked by bidentate bridging H_2PO_2 groups (fig. 17) (Aslanov et al., 1975):

1.5. *Rare earth oxophosphates*

Compounds having a complex anion and excess ionic oxygen are often called oxosalts. Thus the R_2O_3/P_2O_5 ratio in oxophosphates is more than one. For different rare earths and under different conditions the following oxophosphates have been determined: $R_7P_3O_{18}$ ($=7R_2O_3 \cdot 3P_2O_5$) with R = La $\cdots$ Tb; R_3PO_7 ($=3R_2O_3 \cdot P_2O_5$) with R = La $\cdots$ Tm; $R_8P_2O_{17}$ ($=4R_2O_3 \cdot P_2O_5$) with R = Sm $\cdots$ Lu; and $R_{12}P_2O_{23}$ ($=6R_2O_3 \cdot P_2O_5$) with R = Tb $\cdots$ Lu (Serra et al.,

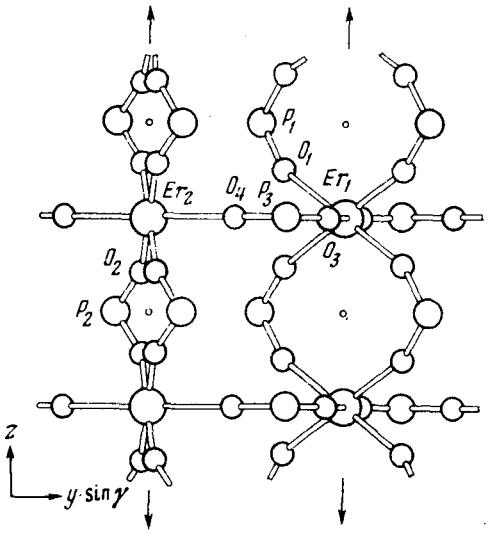

Fig. 17. The crystal structure of erbium hypophosphite, $Er(H_2PO_2)_3$, projected on the *yz*-plane (Aslanov et al., 1975).

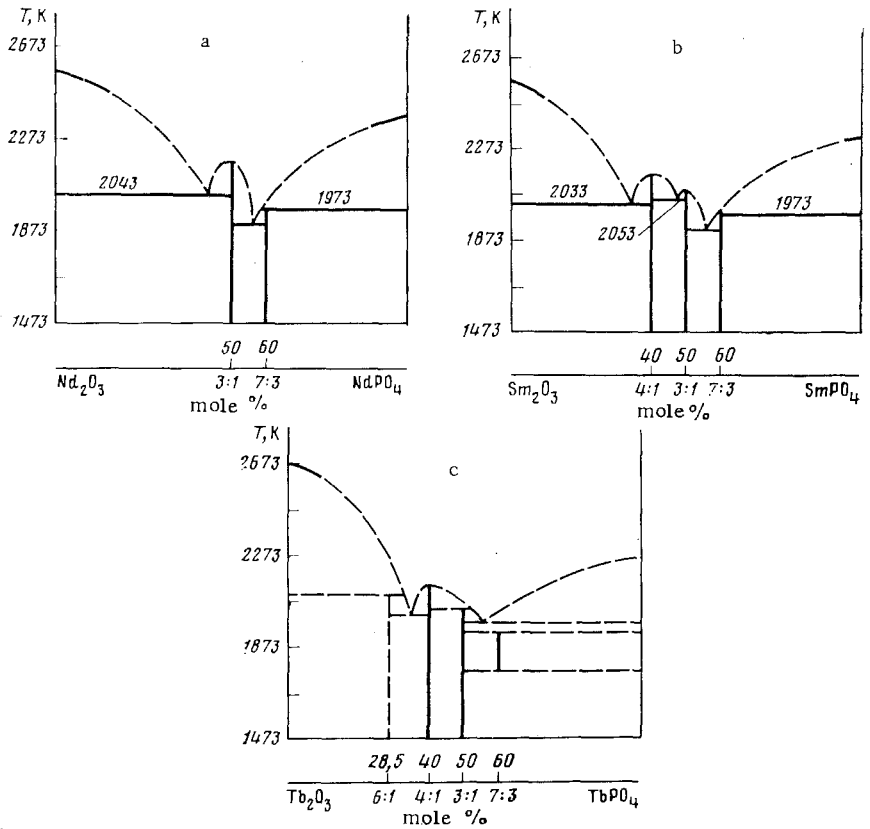

Fig. 18. Phase diagrams for the systems (a) Nd_2O_3–$NdPO_4$, (b) Sm_2O_3–$SmPO_4$, and (c) Tb_2O_3–$TbPO_4$ (Rouanet et al., 1981).

1976a). Phase diagrams of the systems RPO_4–R_2O_3 have been published by Rouanet et al. (1981) (fig. 18).

The rare earth oxophosphates are formed in the thermal decomposition of orthophosphates, RPO_4. The R_3PO_7 phase has also been prepared by solid-state reactions between R_2O_3 and RPO_4 or $NH_4H_2PO_4$ at 800–1200°C (Serra et al., 1976b), and between RPO_4 and Na_2CO_3 at 700–900°C (Kizilyalli and Welch, 1980). The structures of the oxophosphates are unknown: only X-ray diffraction powder data and limited IR, Raman and fluorescence spectroscopic results have been published (Orlovskii et al., 1979; Park and Kreidler, 1984; Agrawal and White, 1985). According to the diffraction data, La_3PO_7 and $La_7P_3O_{18}$ may be monoclinic (Serra et al., 1978).

1.6. *Ternary rare earth phosphates*

In recent years considerable interest has been focused on ternary phosphates of the rare earths and alkali metals, both as prospective laser materials and as phosphors. Two compounds in particular have been studied: polyphosphate $MR(PO_3)_4$ and orthophosphate $M_3R(PO_4)_2$ (Hong and Chinn, 1976; Palkina et al., 1981b). Owing to a confusing usage of formulas and names of the phosphates the first compound is also presented in the form MRP_4O_{12} and called tetrametaphosphate (Hong, 1975b; Koizumi and Nakano, 1978). In reality, there are two structure types corresponding to the stoichiometry $MR(PO_3)_4$, of which the first is a polyphosphate and the second a cyclophosphate containing the $P_4O_{12}^{4-}$ anion (Palkina et al., 1981b).

The preparation of rare earth double polyphosphates has been widely studied by Chudinova et al. (1972, 1975, 1977a,b, 1978d). As starting material they used phosphoric acid, alkali carbonate, and rare earth oxides. The best mixing proportion was $P_2O_5:M_2O:R_2O_3 = 15:5:1$ and the samples were heated several weeks at different temperatures (100–700°C). With lithium all lanthanides form polyphosphate, $LiR(PO_3)_4$, and a RHP_2O_7 phase is obtained for the heavier lanthanides (Chudinova and Vinogradova, 1979). When potassium is present in the system, all lanthanides except La, Tm···Lu form compounds of the type $KRHP_3O_{10}$ at temperatures below 200°C, and $KR(PO_4)_3$ at higher temperatures (fig. 19). Lanthanum crystallizes at higher temperatures as binary ultraphosphate and Tm···Lu as binary tripolyphosphate (Chudinova et al., 1977c, 1978d). In the case of rubidium and cesium the phases formed are $MRHP_3O_{10}$ for Pr···Lu and $MR(PO_3)_4$ for La···Pr (Vinogradova and Chudinova, 1981).

Ternary alkali rare earth polyphosphates are also obtained in the reaction between MPO_3 (M = Li, Na, K, Rb, Cs, Ag, Tl) and RP_3O_9. The reaction temperature depends on the alkali metal (Ferid et al., 1981; Rzaigui and Ariguip, 1981). Phase diagrams have been published for the systems MPO_3–SmP_3O_9 (M = Li, Na, Ag) (Ferid et al., 1984a), MPO_3–LaP_3O_9 (M = Rb, Cs) (Hassen et al., 1984), $TlPO_3$–LaP_3O_9 (Ferid et al., 1984b), and $TlPO_3$–$Ce(PO_3)_3$ (Rzaigui et al., 1983a); an example is presented in fig. 20.

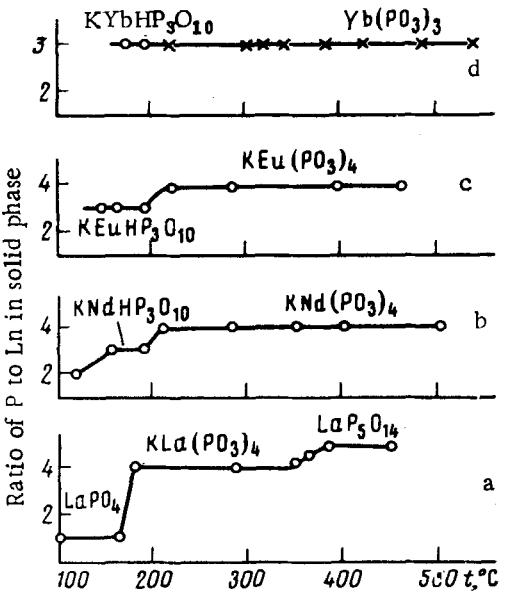

Fig. 19. The composition of the compounds formed in the system K_2O–P_2O_5–R_2O_3–H_2O at the initial ratio of the components P_2O_5 : K_2O : R_2O_3 = 15 : 5 : 1 (Chudinova et al., 1978d).

Litvin et al. (1981a, 1982) have studied the systems M_2O–Nd_2O_3–P_2O_5–H_2O (M = K, Cs), not using an open crucible but carrying out the experiments under partial vapor pressure of water. With low cesium concentrations the products are $Nd(PO_3)_3$ and NdP_5O_{14}, depending on the temperature, and with higher cesium concentrations double polyphosphates are formed. The cubic cyclophosphate, $CsNdP_4O_{12}$, is formed at 350–520°C, the monoclinic polyphosphate ($P2_1/n$) $CsNd(PO_3)_4$ at 520–675°C, and another monoclinic polyphosphate ($P2_1$) above 675°C.

An analogous type of polyphosphate chain with four tetrahedra in the repeat period has been observed in hydrogen polyphosphates with formula $RH(PO_3)_4$ (Chudinova and Balagina, 1979). Under certain experimental conditions these compounds are obtained in the system R_2O_3–H_3PO_4.

Cerium ammonium phosphates can be obtained by heating Ce(III) compounds and CeO_2 with ammonium phosphates at 400°C (Vaivada and Konstant, 1979). The formulas of the compounds prepared by this method are $CeNH_4P_4O_{12}$ and $Ce(NH_4)_2(PO_3)_5$. A summary of the preparation and properties of ammonium cerium condensed phosphates has been published by Rzaigui and Ariguip (1983).

Single crystals of the condensed rare earth double phosphates have been prepared by the flux method. R_2O_3, M_2CO_3, and $NH_4H_2PO_4$, with large excess of the latter two, are mixed, preheated at about 200°C and heated to 900–1000°C, and allowed to cool slowly (Hong, 1975a,b; Koizumi, 1976a,b; Nakano et al., 1979). The flux where the growing occurs is thus a mixture of alkali and phosphorus oxides.

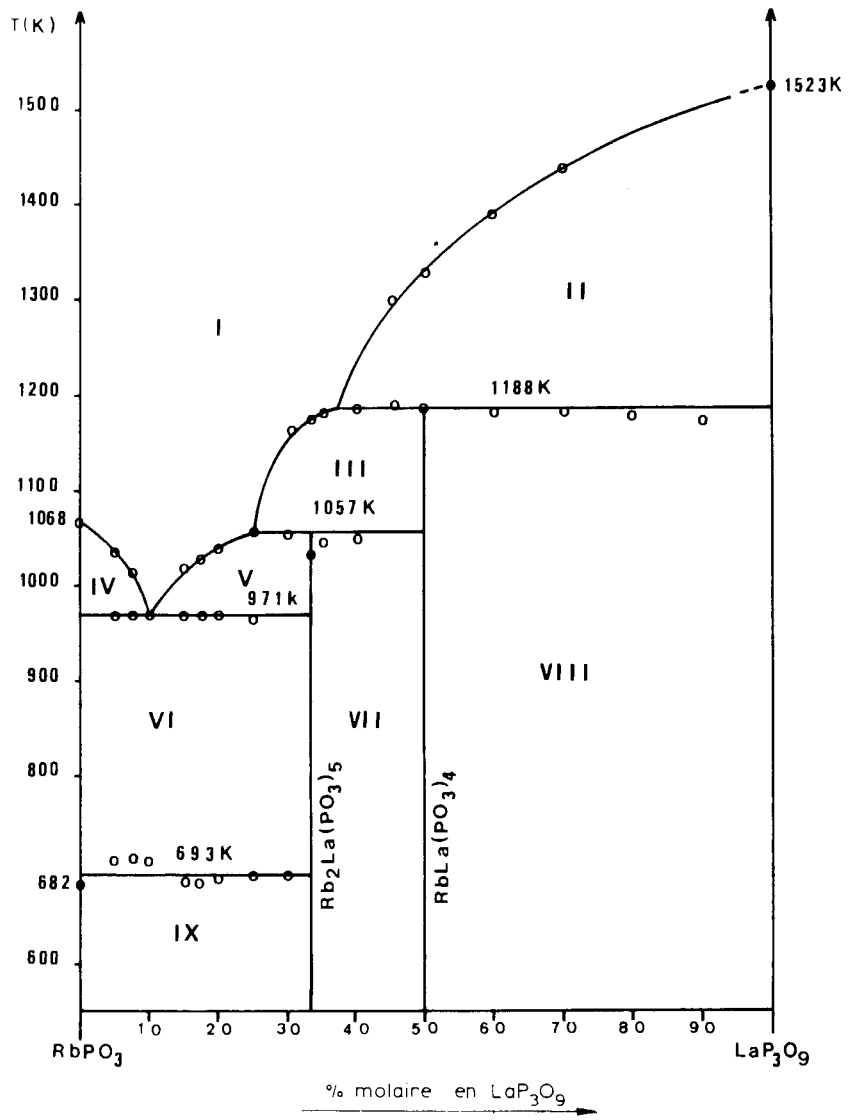

Fig. 20. A phase diagram for the system $RbPO_3$–BaP_3O_9. (I): liquid, (II): liquid + LaP_3O_9; (III): liquid + $RbLa(PO_3)_4$; (IV): liquid + $RbPO_3$; (V): liquid + $Rb_2La(PO_3)_5$; (VI): $RbPO_3$ + $Rb_2La(PO_3)_5$; (VII): $Rb_2La(PO_3)_5$ + $RbLa(PO_3)_4$; (VIII): $RbLa(PO_3)_4$ + LaP_3O_9; (IX): $RbPO_3$ + $Rb_2La(PO_3)_5$. (Hassen et al., 1984.)

The rare earth double orthophosphates, $M_3R(PO_4)_2$, have been prepared by three different methods. The first method involves the heating of K_2CO_3, Nd_2O_3, and $NH_4H_2PO_4$ at a higher temperature (1400°C) than in the preparation of polyphosphate. The high temperature is needed for the conversion to orthophosphate. In the second method, potassium chloride and fluoride are used instead of potassium carbonate and the temperature is lower (Hong and Chinn, 1976). The single crystal preparation requires a slow cooling of the melt. The heating of stoichiometric amounts of RPO_4, M_2CO_3, and MH_2PO_4 at 600–1050°C provides a third route to double orthophosphates (Salmon et al., 1975; Melnikov et al., 1981a).

$Na_3R(PO_4)_2$ has been obtained as single phase in the solid-state reaction between RPO_4 and Na_3PO_4 at 1150°C (Kizilyalli and Welch, 1977). At lower temperatures several phases exist, among them the ternary orthophosphate (Kizilyalli and Welch, 1980). According to Bamberger et al. (1979), the use of MH_2PO_4, M_2HPO_4, $M_4P_2O_7$, or $(MPO_3)_3$, where M = Na, K, gives $M_3R(PO_4)_2$ in the solid-state reaction with R_2O_3.

Alkaline rare earth double phosphate hydrates have been precipitated from solution with sodium phosphate. With large $PO_4^{3-}:R^{3+}$ ratio the compositions $Na_3Gd_4(PO_4)_5 \cdot 12H_2O$ and $Na_3Pr_2(PO_4)_3 \cdot 7H_2O$ are obtained (Petushkova and Tananaev, 1963; Petushkova et al., 1969b). When Na_2HPO_4 is the precipitating agent, the products contain hydrogen: $Na_4H_2Pr_5(PO_4)_7 \cdot 11H_2O$ and $Na_2HYb_2(PO_4)_3 \cdot 6H_2O$ (Tananaev and Vasileva, 1963; Petushkova et al., 1969a).

Ternary triphosphates form in the system RCl_3–$Na_5P_3O_{10}$–H_2O when concentrations are suitable (Petushkova et al., 1971). In systems containing rubidium and cesium the composition (Rb, Cs)RHP_3O_{10} (R = Pr ··· Er), corresponding to the dihydrogen compound, is formed at 200°C (Vinogradova and Chudinova, 1981).

The system $(NH_4)_5P_3O_{10}$–$Nd(NO_3)_3$–H_2O provides two types of double polyphosphates: $NH_4Nd_3(P_3O_{10})_2 \cdot 12H_2O$ and $(NH_4)_3Nd_4(P_3O_{10})_3 \cdot 14H_2O$ (Rodicheva, 1981). With sodium polyphosphate as precipitant, binary polyphosphates ($Na_3Eu(PO_3)_6 \cdot 12H_2O$) are formed as well (Ezhova et al., 1978b). With potassium the stoichiometries $KR(PO_3)_4 \cdot 5H_2O$ and $KR(PO_3)_7 \cdot 10H_2O$ are obtained (Ezhova et al., 1983).

1.6.1. *Structures of ternary condensed phosphates*

The structures of alkali rare earth condensed phosphates can be divided into fourteen different types (table 1). The formation of a particular structure depends on the crystallization conditions as well as on the alkali and rare earth metals concerned (fig. 21). Characteristic of all alkali rare earth ternary polyphosphates is that the structural framework consists of a helical chain of $(PO_3)_\infty$ formed by corner sharing of PO_4 tetrahedra along some axis. Besides the polyphosphates, there are cyclic condensed phosphates containing the cyclic $P_4O_{12}^{4-}$ group.

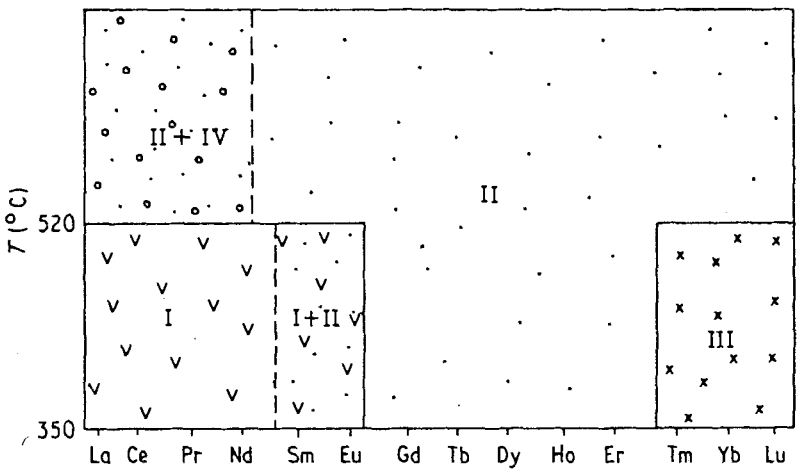

Fig. 21. The different structural types of $CsRP_4O_{12}$, illustrating the relationship between the ionic radii of R^{3+} and the growth temperature. (I): cubic; (II): monoclinic ($P2_1/b$); (III): monoclinic (B2/b); (IV): monoclinic ($P2_1$). (Byrappa and Dorokhova, 1981.)

In $LiNd(PO_3)_4$ the Nd^{3+} and Li^+ ions lie in alternating order between the four $(PO_3)_\infty$ helical chains. NdO_8 dodecahedra and distorted LiO_4 tetrahedra, sharing edges, form linear chains (fig. 22) (Hong, 1975a; Koizumi, 1976a). Likewise in $NaNd(PO_3)_4$, the cations are situated between the four phosphate chains, but here the cation–oxygen polyhedra share faces and form zigzag chains (fig. 23) (Koizumi, 1976b). In the other double polyphosphate structures the $(PO_3)_\infty$ helical chains are connected by the isolated cation polyhedra. In $KNd(PO_3)_4$ the neodymium atoms are eight-coordinated and the potassium atoms occupy irregular interstitial polyhedra (fig. 24) (Hong, 1975b; Palkina et al., 1976a). According to Krutik et al. (1980), in isomorphic $KEr(PO_3)_4$ the coordination number of erbium is six.

The heavier rare earths (Tm $\cdots$ Lu) form potassium phosphates with a structure basically similar to that of the lighter rare earths, but the isolated R^{3+} ions are seven-coordinated (fig. 25) (Palkina et al., 1981a). Two types of rare earth double phosphates have been found with rubidium and cesium. Both structures are monoclinic and contain infinite phosphate chains and isolated RO_8 dodecahedra (Maksimova et al., 1978, 1981, 1982; Dago et al., 1980), but whereas in the first structure type the Rb and Cs atoms are nine- or ten-coordinated, in the second type the coordination polyhedron is irregular (figs. 26, 27) (Koizumi and Nakano, 1978; Palkina et al., 1978a,b; Maksimova et al., 1979). In the first structure the $(PO_3)_\infty$ helical ribbons are connected by cation polyhedra which repeat after four PO_4 tetrahedra, and in the second structure the repeating unit is four PO_4 groups. $TlR(PO_3)_4$ is isomorphic with the first type of rubidium and cesium rare earth polyphosphates (Palkina et al., 1977).

TABLE 1
Summary of the structural data on rare earth phosphates.

Compound	R	Example	a (Å)	b (Å)	c (Å)	Angle (deg)	Z	Space group	Reference
RPO_4	La···Gd	La	6.84	7.06	6.48	$\beta = 103.5$	4	$P2_1/n$	Mooney-Slater, 1962
	Tb···Lu, Y, Sc	Ho	6.89		6.03		4	$I4_1/amd$	Schwarz, 1963f
$RPO_4 \cdot 0.5H_1O$	La···Gd	La	6.94		6.35		3	$P3_121$	Mooney-Slater, 1962
$RPO_4 \cdot 2H_2O$	Tb···Lu, Y	Y	5.61	15.14	6.19	$\beta = 115.0$	4	$A2/a$	Claringsbull and Hey, 1953
$R(H_2PO_4)_3$	Sm···Gd	Eu	16.13		11.83		12		Butuzova et al., 1982
	Sc	Sc	8.27		25.98		6	R3c	Smolin et al., 1982
$R(PO_3)_3$	La···Gd	Nd	11.17	8.53	7.28		4	$C222_1$	Hong, 1974a
	Tb···Lu, Y	Yb	11.22	19.98	10.00	$\beta = 97.3$	12	$P2_1/c$	Hong, 1974b
	Sc	Sc	13.56	19.56	9.69	$\beta = 127.1$	12	Cc	Domanskii et al., 1982
$R(PO_3)_3 \cdot 3H_2O$	La···Pr	Ce	6.77		6.08			$P\bar{6}$	Bagieu-Beucher et al., 1971
$R_4(P_4O_{12})_3$	Yb, Lu, Sc	Sc	14.36				4	$I\bar{4}3d$	Smolin et al., 1978
RP_5O_{14}	La···Gd	Sm	8.75	8.94	13.00	$\beta = 90.5$	4	$P2_1/c$	Tranqui et al., 1974
	Eu···Ho	Ho	8.73	12.71	8.73		4	Pcmn	Durif, 1971
	Er···Lu	Er	12.84	12.72	12.38	$\beta = 91.3$	8	C2/c	Jezowska-Trzebiatowska and Mazurak, 1980
	Ce	Ce	9.23	8.89	7.22	$\alpha = 110.1$ $\beta = 102.7$ $\gamma = 82.1$	2	$P\bar{1}$	Rzaigui et al., 1984
$R(H_2PO_2)_3{}^{\circ}H_2O$	La···Eu	La	8.98	8.08	7.29	$\alpha = 104.8$ $\beta = 99.0$ $\gamma = 109.7$	2	$P\bar{1}$	Ionov et al., 1973a
$R(H_2PO_2)_3$	Gd···Lu	Er	14.40	12.10	5.64	$\beta = 111.3$	4	$B2/m$	Aslanov et al., 1975
$RHP_2O_6 \cdot 4H_2O$	Nd, Eu, Er, Yb	Er	7.19	9.82	11.52		4	Pbnn	Palkina et al., 1983a
$RH_2P_3O_{10}$	Yb	Yb	5.62	6.67	10.01	$\beta = 97.2$	2	A2	Palkina et al., 1979
$HR(PO_3)_4$	Eu, Sm (Bi)	Bi	8.63	8.87	7.06	$\alpha = 112.2$ $\beta = 108.5$ $\gamma = 98.5$	2	$P\bar{1}$	Chudinova and Balagina, 1979
	Gd···Er	Er	9.57	7.10	13.64	$\beta = 101.0$	4	$P2_1/a$	Palkina et al., 1982
$LiR(PO_3)_4$	La···Lu	Nd	16.41	7.04	9.73	$\beta = 126.4$	4	C2/c	Hong, 1975a
$NaR(PO_3)_4$	La···Er	NaNd	9.91	13.10	7.20	$\beta = 90.5$	4	$P2_1/n$	Koizumi, 1976b
$KR(PO_3)_4$	Ce								Linde et al., 1983
$AgR(PO_3)_4$	Sm								Ferid et al., 1984a
$KR(PO_3)_4$	La···Er	Nd	7.27	8.44	8.01	$\beta = 92.0$	2	$P2_1$	Hong, 1975b
	Tm···Lu	Yb	7.76	8.85	14.83	$\beta = 96.4$	2	$P2_1/n$	Palkina et al., 1981a
$KR(PO_3)_4$	Tm···Lu								Dago et al., 1980
$RbR(PO_3)_4$	Nd···Lu	KEr	10.80	8.89	10.28	$\beta = 106.0$	4	$P2_1/n$	Maksimova et al., 1978
$CsR(PO_3)_4$	Na···Lu								Maksimova et al., 1981
$TlR(PO_3)_4$	Ce, Nd								Palkina et al., 1977
$NH_4R(PO_3)_4$	Ce								Rzaigui and Kbir-Ariguip, 1983
$RbR(PO_3)_4$	La···Er								Maksimova et al., 1979
$CsR(PO_3)_4$	La···Er	CsPr	7.16	9.19	8.81	$\beta = 99.4$	4	$P2_1$	Palkina et al., 1978a
$TlR(PO_3)_4$	La								

$CsR(PO_3)_4$	Tm···Lu	Lu	9.96	13.96	20.02	$\gamma = 52.4$	8	B2/b	Byrappa and Dorokhova, 1981
KRP_4O_{12}	La···Er	$KHoP_4O_{12}$	10.55	7.80	12.31	$\beta = 112.6$	4	B2/b	Palkina et al., 1976b
$RbRP_4O_{12}$	Pr···Gd								Koizumi and Nakano, 1977
$NH_4RP_4O_{12}$	La···Nd	NH_4Pr	7.91	12.65	10.68	$\beta = 110.0$	4	C2/c	Masse et al., 1977
$RbRP_4O_{12}$	La···Gd								Palkina et al., 1981c
$TlRP_4O_{12}$	La								
$NH_4RP_4O_{12}$	Ce								
$RbRP_4O_{12}$	La, Nd								Palkina et al., 1981b
$CsRP_4O_{12}$	La···Eu	CsNd	15.23				12	$I\bar{4}3d$	Palkina et al., 1981d
$NH_4R(PO_3)_5$	Ce	Ce	8.59	13.37	11.74	$\gamma = 90.4$	4	Bb	Palkina et al., 1981e
$(NH_4)_2R(PO_3)_5$	Ce	$(NH_4)_2Ce$	7.24	13.31	7.24	$\alpha = 90.4$ $\beta = 107.5$ $\gamma = 90.3$	2	$P\bar{1}$	Rzaigui et al., 1983b
$Tl_2R(PO_3)_5$	Ce								Rzaigui et al., 1983a
$Rb_2R(PO_3)_5$	La								Hassen et al., 1984
$Na_3R(PO_4)_2$	La···Eu	Nd	15.87	13.95	18.47		24	$Pbc2_1$	Salmon et al., 1978
	Gd···Lu	Nd *	29.14	5.57	14.22	$\beta = 92.4$	12	Cc	Parent et al., 1979
	Tm···Lu	Tm	18.43	6.97	15.82		12	Pnmm *or* $Pnm2_1$	Apinitis and Sedmalis, 1978
	Sc	Sc	16.10	9.11	8.93	$\beta = 127.2$	2	Bb	Efremov and Kalinin, 1978
	Tb···Lu	Yb	9.13		21.86		9	$R\bar{3}m$	Apinitis and Sedmalis, 1978
$Na_3R_2(PO_4)_3$	Sc	Sc	8.93		22.34		6	$R\bar{3}c$	Lazoryak et al., 1980
$Na_{4.5}R_{1.5}(PO_4)_3$	Er···Lu	Yb	9.12		21.81		6	$R\bar{3}c$	Salmon et al., 1979
$K_3R(PO_4)_2$	Nd	Nd	9.53	5.63	7.44	$\beta = 91.0$	2	$P2_1/n$	Hong and Chinn, 1976
	Tn···Lu, Y, Sc	Lu	9.60		7.73		3	$P\bar{3}m1$	Efremov et al., 1981
$Rb_3R(PO_4)_2$	Gd···Tb	Gd	19.53	34.45	7.73	$\beta = 90.8$			Melnikov et al., 1981a
	Dy···Lu, Y	Er	5.69		8.12				Melnikov et al., 1981a
	Sc	Sc	10.51	10.07	9.81	$\beta = 104.6$			Melnikov et al., 1981a
$Ag_3R(PO_4)_2$	Sc	Sc	5.16	5.37	12.70		1		Melnikov et al., 1984
$CaKR(PO_4)_2$	Nd	Nd	7.03		6.40		1	$P6_222$	Vlasse et al., 1982
$K_2CsR(PO_4)_2$	Ho···Lu, Y	Ho	9.74	5.65	8.09	$\beta = 90.1$			Melnikov et al., 1983
	Sc	Sc	5.48		7.92				Melnikov et al., 1983
$Ca_8R_2(PO_4)_6O_2$	La···Er	La	9.50		6.96		1	$P6_3/m$	Escobar and Baran, 1982
$M_3R(PO_4)_3$ (M = Ca, Sr, Ba, Eu, Pb)	La···Lu, Y, Sc	$Eu^{II}Gd$	10.12				4	$I\bar{4}3d$	Engle and Kirchberger, 1975
$R_xM_{10-2x}Na_x(PO_4)_6F_2$ ($x = 0\cdots4$; M = Ca, Sr)	La···Sm	Ca, Nd	9.41		6.91		1	$P6_3/m$	Mayer et al., 1974
$R_2M_6Na_2(PO_4)_6F_2$ (M = Ba, Pb)	La···Nd	Ba, La	9.94		7.44		1	$P\bar{6}$	Mathew et al., 1979
$R_3Ba_4Na_3(PO_4)_6F_2$	La···Sm	Nd	9.79		7.28		1	$P\bar{3}$	Mathew et al., 1979
$R_xPb_{10-2x}K_x(PO_4)_6F_2$ ($x = 0\cdots3$)	La···Eu	Pb, La	9.82		7.30		1	$P6_3/m$	Mayer et al., 1980
$R_7O_6(BO_3)(PO_4)_2$	La···Dy	Nd	6.88	17.65	12.45	$\beta = 97.3$	4	$P2_1/n$	Palkina et al., 1984b

* Parameters are given for $Na_3Nd(VO_4)_2$.

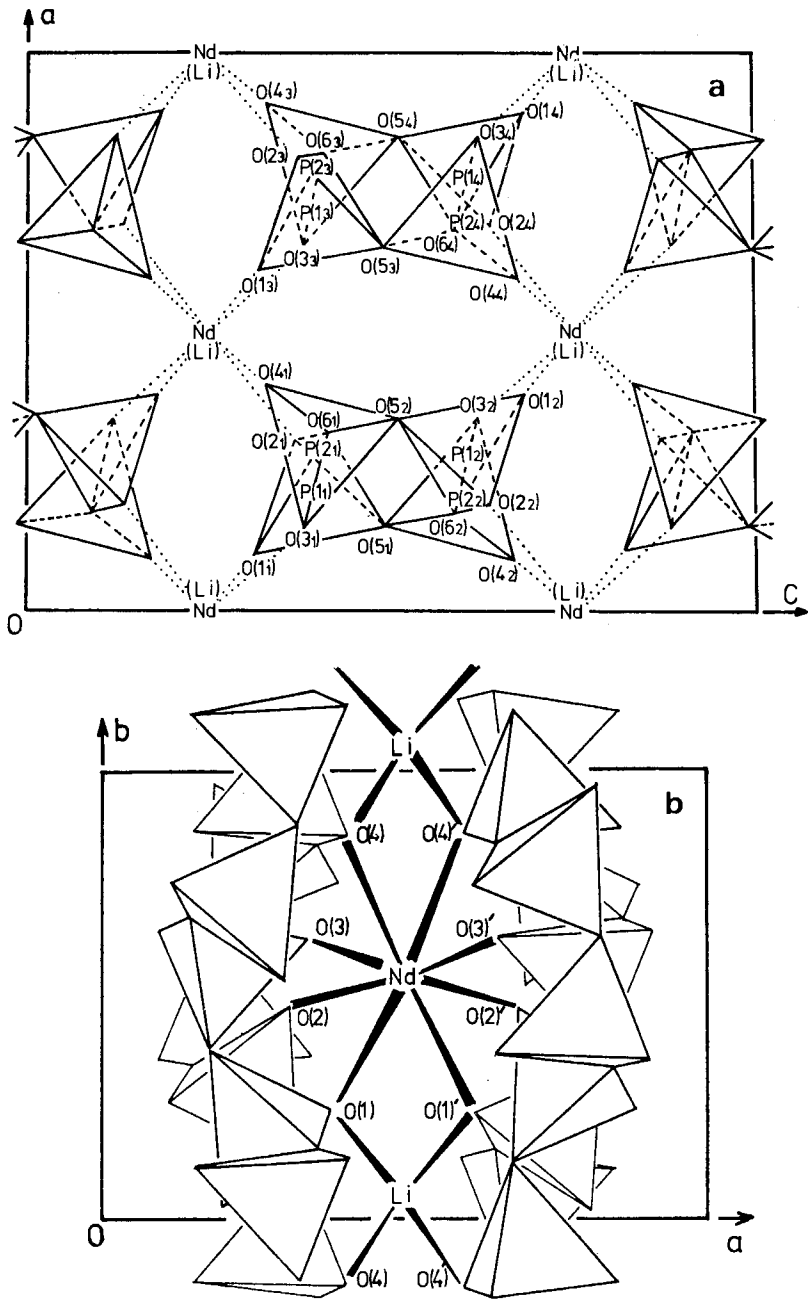

Fig. 22. A projection of the $LiNd(PO_3)_4$ (I2/c) structure along the *b*-axis (a) and a schematic view of the NdO_8–LiO_4 chain projected on the *ab*-plane (b) (Koizumi, 1976a).

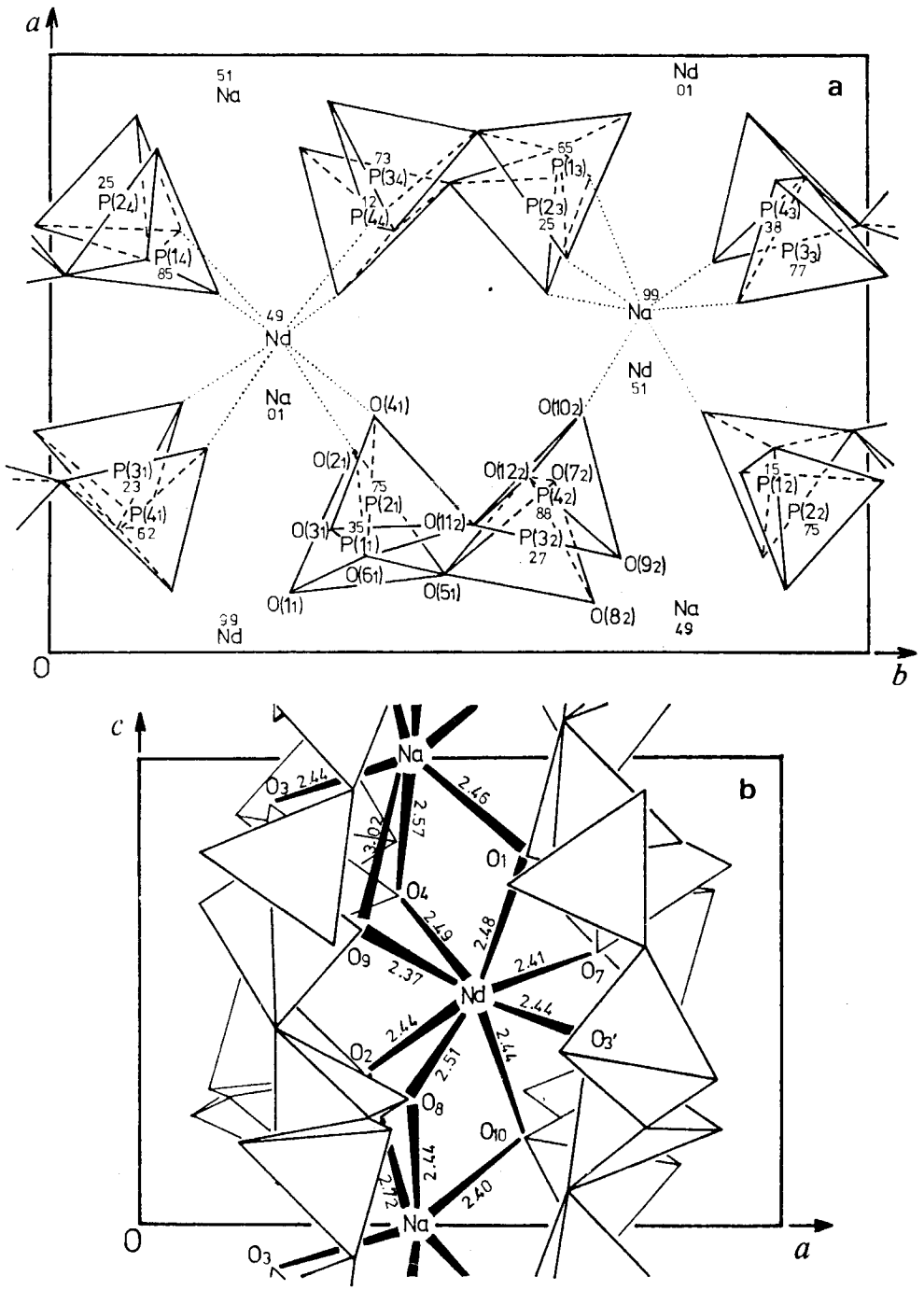

Fig. 23. A projection of the $NaNd(PO_3)_4$ structure along the *b*-axis (a) and a schematic view of the Nd–Nd chain projected on the *ac*-plane (b) (Koizumi, 1976b).

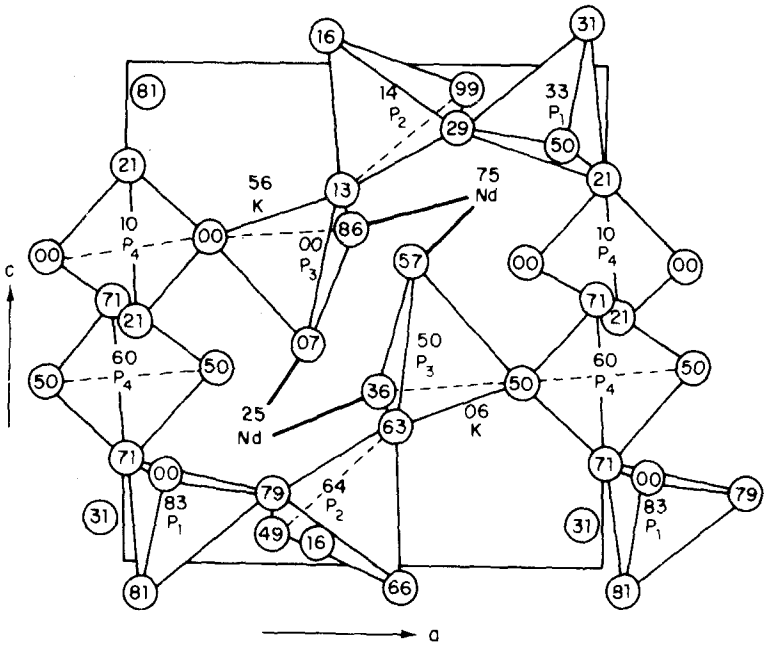

Fig. 24. The crystal structure of $KNd(PO_3)_4$ projected on the *ac*-plane (Hong, 1975b).

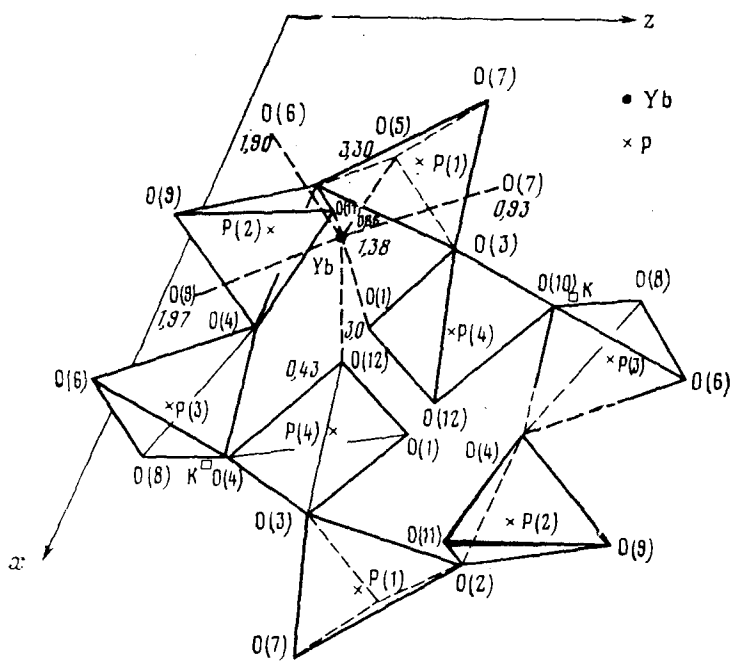

Fig. 25. A projection of the $KYb(PO_3)_4$ structure along the *y*-axis (Palkina et al., 1981a).

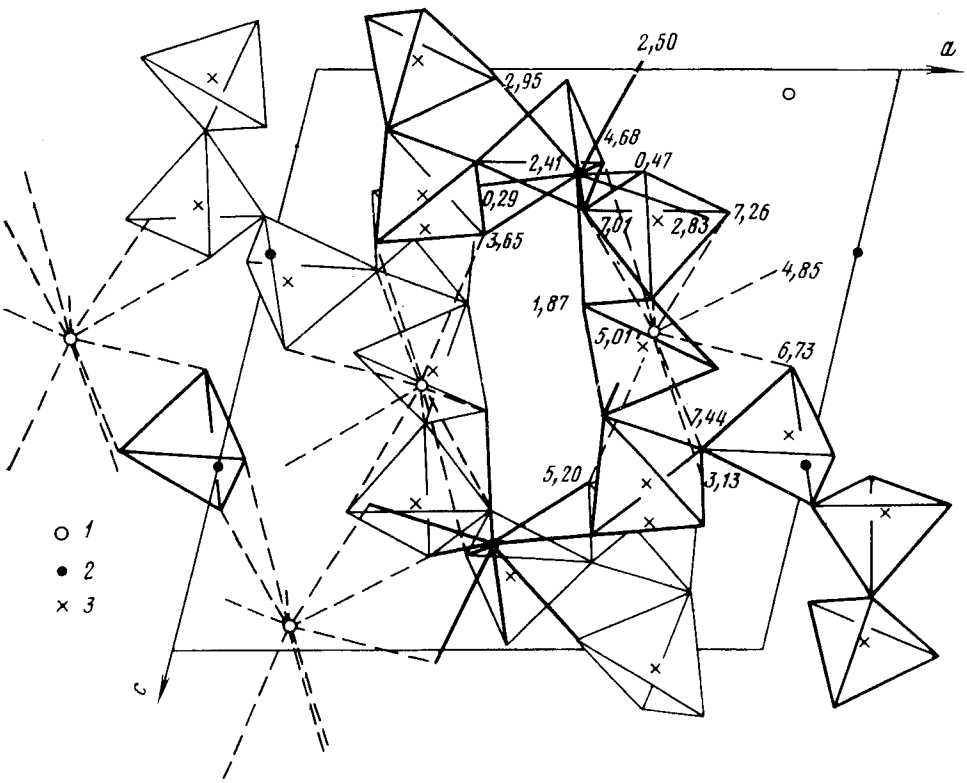

Fig. 26. A projection of the $RbHo(PO_3)_3$ ($P2_1/n$) structure along the *y*-axis. 1: Rb; 2: Ho; 3: P. (Maksimova et al., 1982.)

Byrappa and Dorokhova (1981) have observed the formation of a new monoclinic structure for $CsLu(PO_3)_4$. The same structure was verified for Tm and Yb at 350–520°C. A detailed crystal analysis is in progress.

Polyphosphates containing hydrogen with the composition $RH(PO_3)_4$ crystallize in two forms: triclinic (Sm, Eu) and monoclinic (Gd $\cdots$ Er) (Palkina, 1982). In both structures the distorted RO_7 polyhedra are isolated from one another. The difference in the structures lies in the polyphosphate chains, which in the monoclinic form are crystallographically nonequivalent (fig. 28) (Palkina et al., 1982).

The condensed cyclic phosphates having a cyclic $P_4O_{12}^{4-}$ anion can be divided into three groups on the basis of space group: monoclinic B2/c, monoclinic C2/c and cubic $I\bar{4}3d$ compounds. The first structure type is found for potassium and rubidium compounds, the second for ammonium and rubidium compounds, and the third for cesium compounds (Palkina et al., 1981b). Typical of all the crystals is that they contain the $P_4O_{12}^{4-}$ anion in the form of an eight-membered P_4O_4 ring

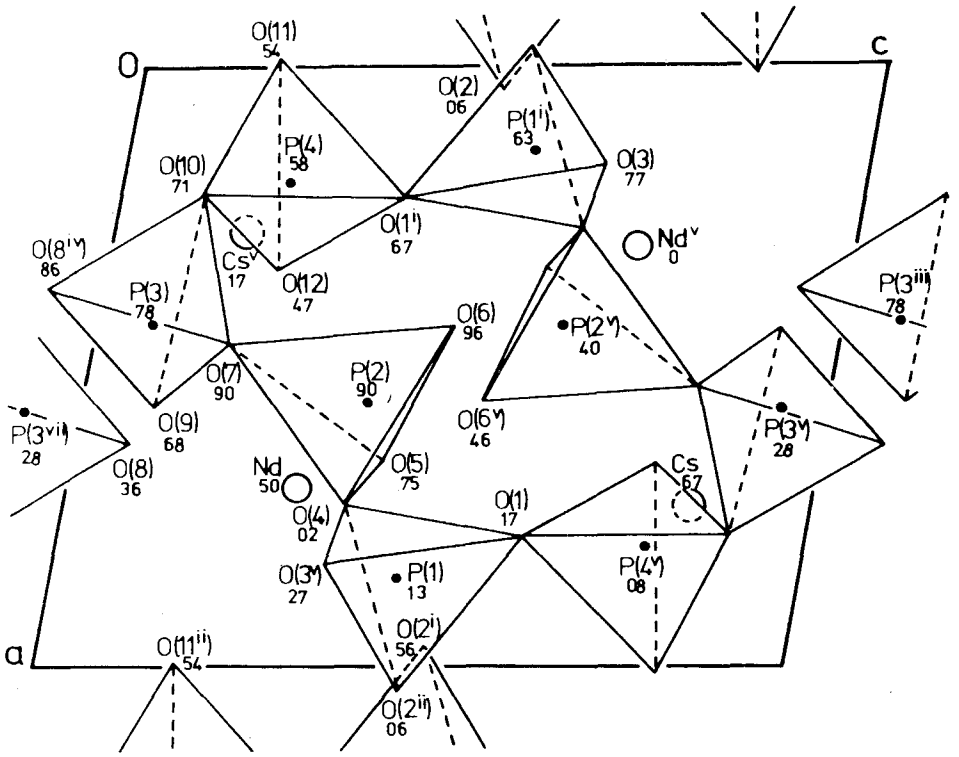

Fig. 27. The structure of $CsNd(PO_3)_4$ ($P2_1$) projected along the *b*-axis (Koizumi and Nakano, 1978).

(Palkina et al., 1976b). The rare earth atoms also have eight-coordination, and the rubidium atoms have an irregular coordination polyhedron (fig. 29) (Koizumi and Nakano, 1977; Litvin et al., 1981b). The second and third structures differ from the first structure only in the coordination of the alkali metal (Masse et al., 1977; Palkina et al., 1981a,d).

The crystal structure of an ammonium cerium condensed phosphate, whose composition corresponds either to $NH_4Ce(PO_3)_5$ (Ce(IV)) or to $NH_4HCe(PO_3)_5$, has been determined by Palkina et al. (1981e). Complex infinite PO_4 tetrahedra chains are held together by the cations and cerium has the coordination number eight.

Condensed ternary phosphates with the stoichiometry $M_2R(PO_3)_5$ ($M = NH_4^+$, Rb, Tl) have been prepared especially for cerium (Rzaigui et al., 1983a,b; Hassen et al., 1984). The triclinic structure contains two independent infinite $(PO_3)_\infty$ chains, one running along the *a*-axis and the other along the *c*-axis. Both have a sequence of five tetrahedra (fig. 30). Cerium atoms exhibit an eight-fold coordination.

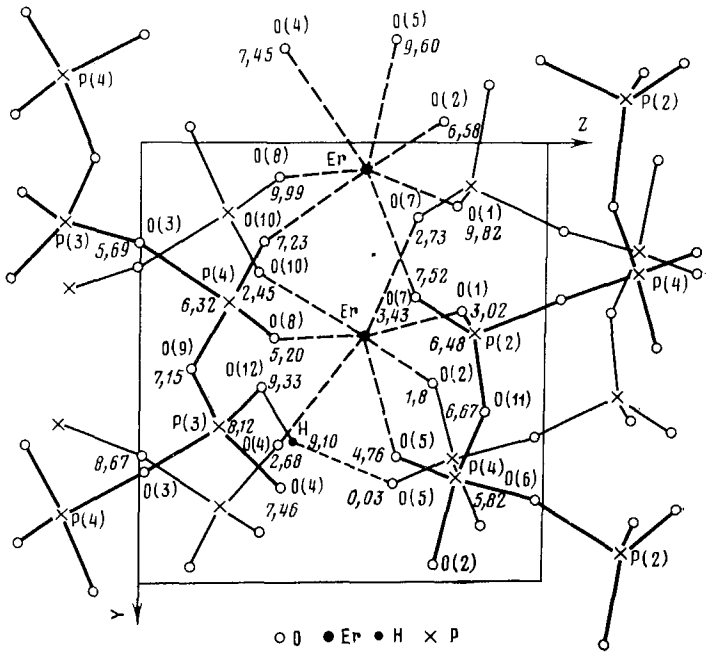

Fig. 28. A projection of the $ErH(PO_3)_4$ structure along the x-axis (Palkina et al., 1982).

1.6.2. *Structures of ternary orthophosphates*

Five different structures have been determined for the compounds $Na_3R(PO_4)_2$. Two of these are low-temperature forms and the other three exist at higher temperatures (fig. 31) (Vlasse et al., 1980a,b). At low temperatures the sodium rare earth orthophosphates from lanthanum to europium form orthorhombic crystals and their structure is similar to that of $Na_3La(VO_4)_2$. The PO_4 tetrahedra are isolated and the cations are arranged in an ordered way (Salmon et al., 1978). There are two arrays of atoms parallel to the b-axis, the first array formed by PO_4 groups and Na atoms, and the second by R and Na atoms. The coordination number of the cations varies: with sodium between five and seven and with the rare earth atoms between six and eight. The structure contains six crystallographically different rare earth atoms (fig. 32). The rare earths from gadolinium to lutetium form a ternary orthophosphate isomorphic with $Na_3Nd(VO_4)_2$ and the structure is monoclinic, with the acentric space group Cc (Vlasse et al., 1980a).

The lighter lanthanides (La···Eu) have a high-temperature form (above 1000°C) with hexagonal glaserite structure, while the sodium phosphates of the heavier lanthanides have a medium-temperature phase and a separate high-temperature phase. The medium-temperature phase (850–1000°C) found for

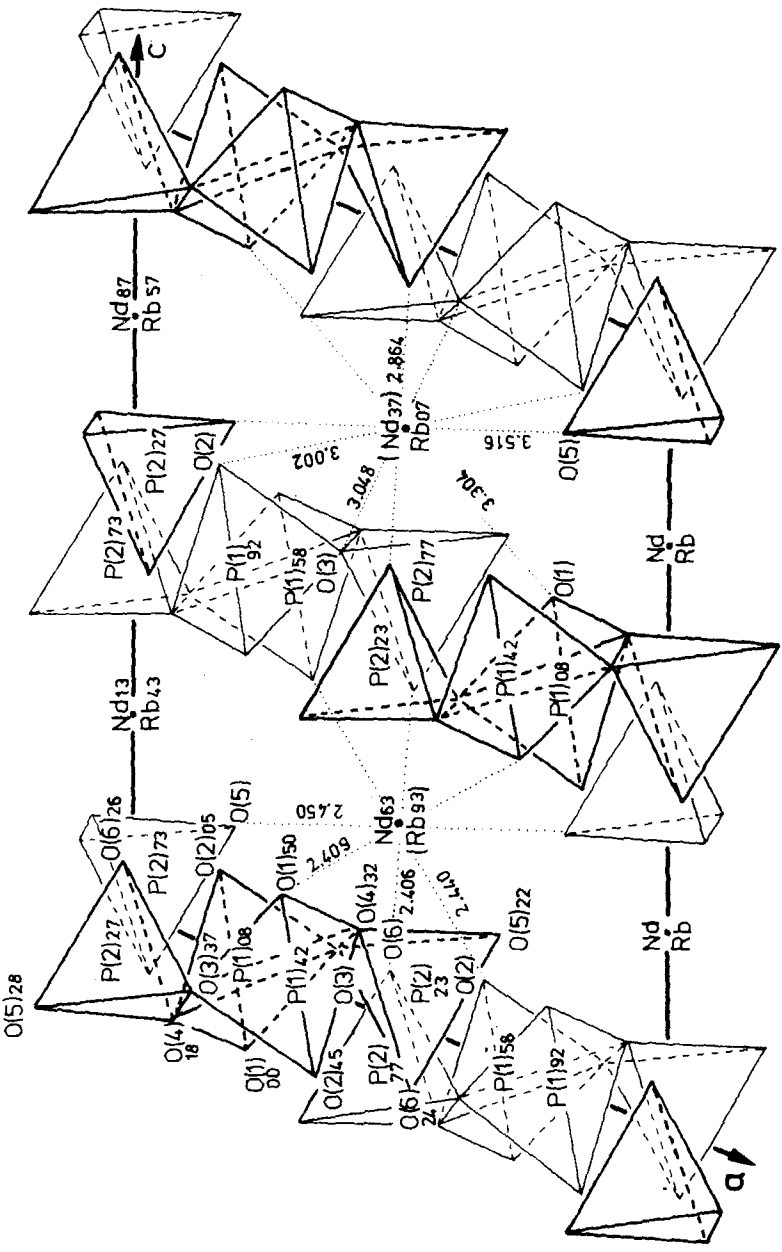

Fig. 29. The atomic arrangement of $RbNdP_4O_{12}$ (C2/c) projected along the *b*-axis. The PO_4 tetrahedra lying at higher level are drawn with thicker lines. (Koizumi and Nakano, 1977.)

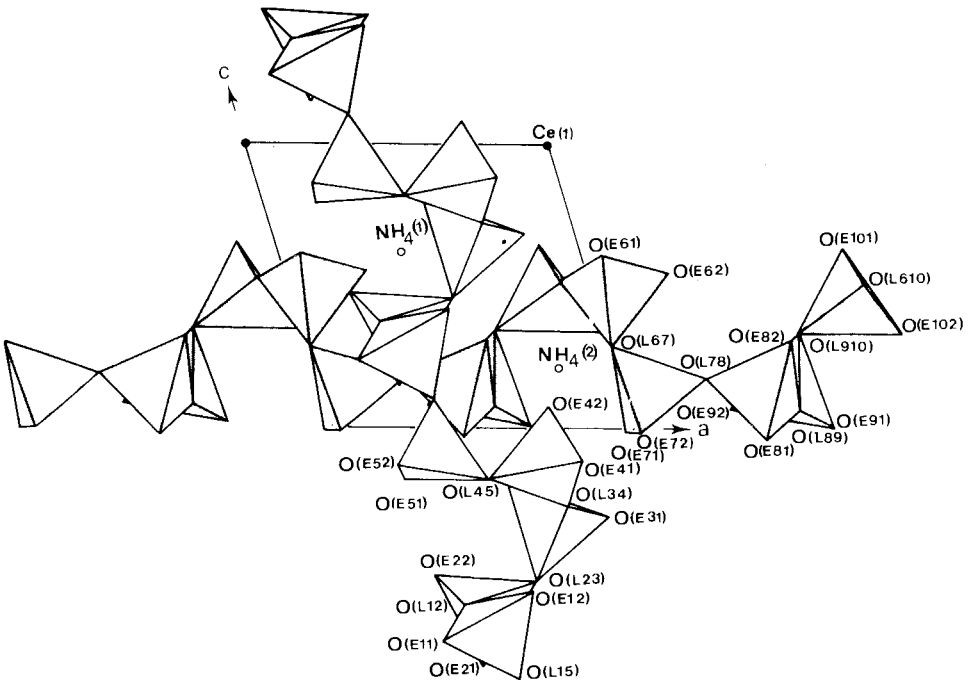

Fig. 30. A projection of the atomic arrangement in $(NH_4)_2Ce(PO_3)_5$ along the *b*-axis (Rzaigui et al., 1983b).

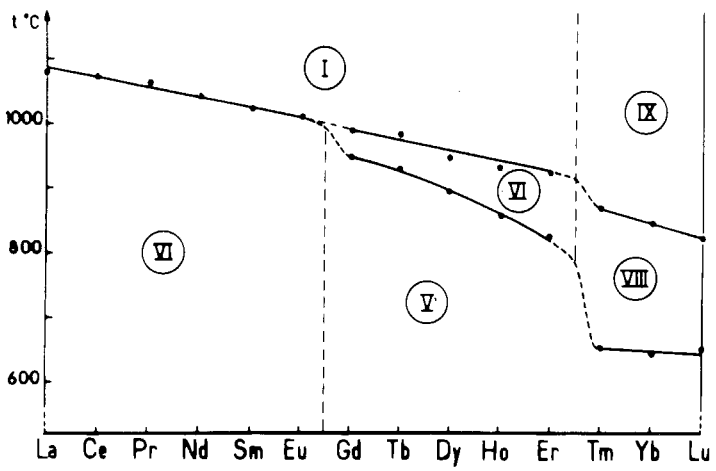

Fig. 31. The thermal behavior of different $Na_3R(PO_4)_2$ phases. (I): glaserite-type; (V): monoclinic $Na_3Nd(VO_4)_2$-type; (VI): orthorhombic $Na_3Nd(PO_4)_2$-type; (VIII): orthorhombic $Na_3Tm(VO_4)_2$-type; (IX): hexagonal $Na_3Yb(PO_4)_2$-type. (Vlasse et al., 1980b.)

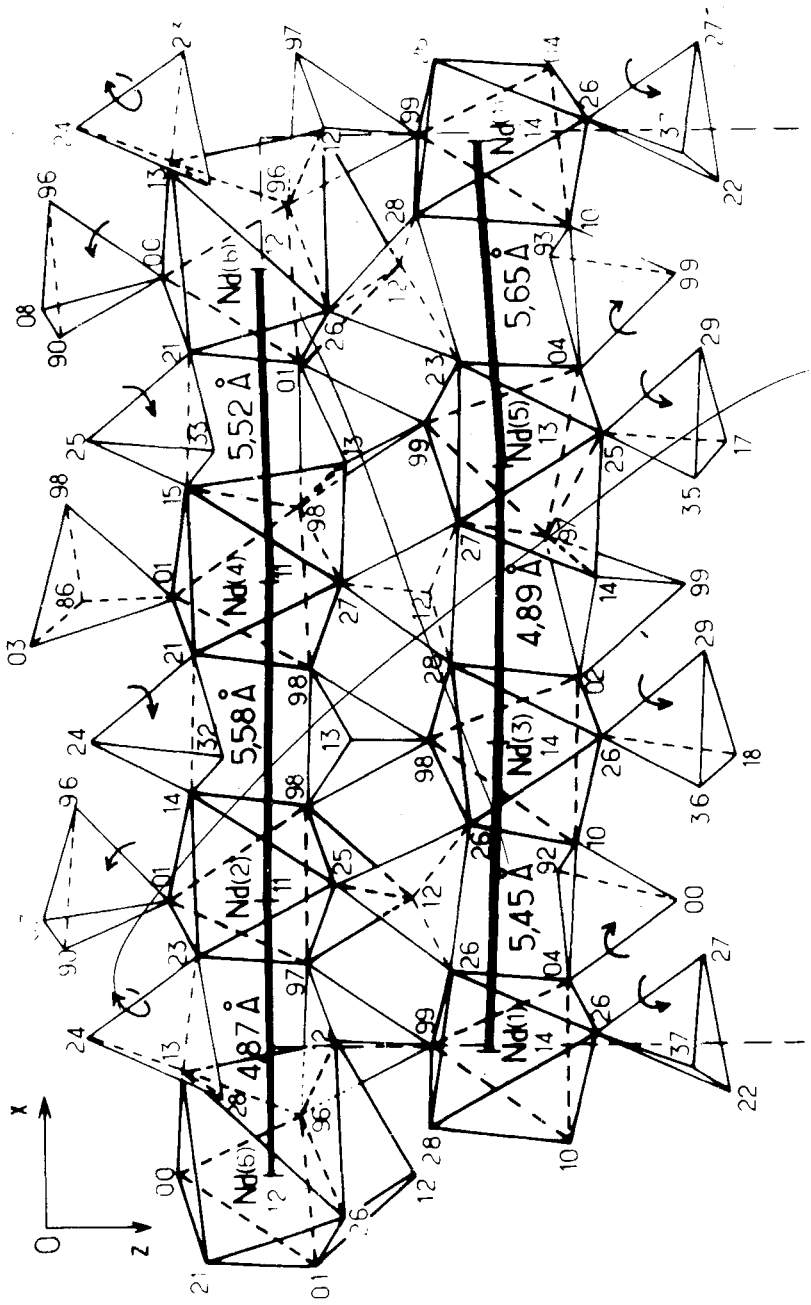

Fig. 32. A representation of NdO_y polyhedra in $Na_3Nd(PO_4)_2$ showing the different Nd–Nd distances along the *a*-axis (Salmon et al., 1978).

R = Gd · · · Er has the same structure as the low-temperature form found for La · · · Eu, and the corresponding high-temperature phase has the known glaserite-like structure. The medium-temperature phase of the sodium phosphate of the heaviest lanthanides (Tm · · · Lu) is formed at 650–850°C. The structure is orthorhombic, but the details of the structure are uncertain (Apinitis and Sedmalis, 1978). The corresponding high-temperature phase is hexagonal and the structure can be derived from $NaZr_2(PO_4)_3$ and the nonstoichiometric $Na_{3(1+x)}R_{2-x}(PO_4)_3$ (Hagman and Kierkegaard, 1968; Salmon et al., 1979; Vlasse et al., 1980a).

$Na_3Sc(PO_4)_2$ is monoclinic and the structure contains a three-dimensional network of corner-sharing PO_4 tetrahedra and ScO_6 octahedra. The sodium atoms are distributed among the chains (Efremov and Kalinin, 1978).

The potassium rare earth orthophosphates have at least two structure types. The lighter lanthanides form monoclinic crystals containing a two-dimensional sheet of RO_7 and PO_4 polyhedra in the *ab*-plane with potassium atoms inserted along the *c*-axis between the sheets (fig. 33) (Hong and Chinn, 1976). The lanthanides at the end of the series form $K_3R(PO_4)_2$ compounds with hexagonal glaserite structure (Melnikov et al., 1976; Efremov et al., 1981). Scandium behaves similarly to the smallest lanthanides (Melnikov et al., 1974).

The rubidium rare earth orthophosphates have three different structures, all of which resemble glaserite. The first structure type is found for gadolinium and

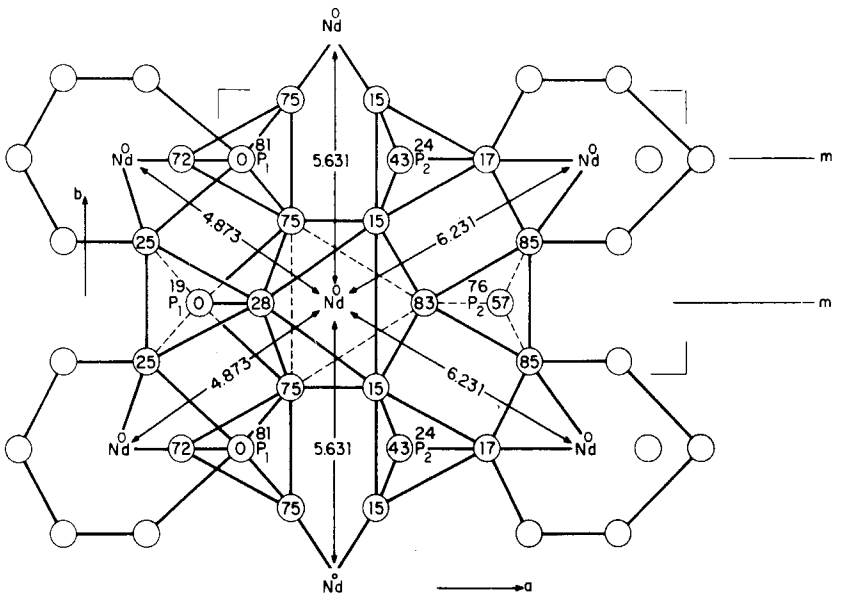

Fig. 33. The crystal structure of $K_3Nd(PO_4)_2$ projected on the *ab*-plane. The Nd–Nd distances are also shown (Hong and Chinn, 1976).

terbium, the second for Dy $\cdots$ Lu, and $Rb_3Sc(PO_4)_2$ has a structure of its own (Melnikov et al., 1981c). The corresponding silver compound, $Ag_3Sc(PO_4)_2$, is reported to be orthorhombic (Melnikov et al., 1984).

Besides the proportion 1:1, the $Na_3PO_4:RPO_4$ compounds can combine in the proportion 1:2. Kryukova et al. (1977) have obtained the corresponding potassium compounds $K_3R_2(PO_4)_2$ as well. The compounds of this type may show nonstoichiometry among the cations, $Na_{3(1+x)}R_{2-x}(PO_4)_3$. Their structure is hexagonal and resembles that of $NaZr_2(PO_4)_3$ and thus also the high-temperature form of $M_3R(PO_4)_2$ (fig. 34) (Salmon et al., 1979; Delmas et al., 1981). The corresponding scandium compound $Na_3Sc(PO_4)_3$, which is a new superionic conductor, has the same structure (Hong, 1979; Lazoryak et al., 1980).

The hexagonal form of RPO_4 contains large tunnels, as described by Mooney (1950). Et-Tabirou and Daoudi (1980) were able to prepare phases like $MCaNd(PO_4)_2$ (M = K, Rb, Cs), with the large alkali ions inserted in the tunnels. The crystal structure of $KCaNd(PO_4)_2$ is thus similar to that of hexagonal RPO_4 except that K atoms occupy the large tunnels in the lattice and the R position is statistically occupied by both Nd and Ca atoms (Vlasse et al., 1982). The corresponding strontium compound $Na_xSr_{3-2x}R_x(PO_4)_2$ is isotypic with pure strontium phosphate (Parent et al., 1981, 1982).

Triple orthophosphate with formula $M_2M'R(PO_4)_2$ (M = K; M′ = Cs) has been prepared for the smaller rare earths (Melnikov et al., 1983). According to X-ray powder diffraction studies their structure is monoclinic, with the exception of scandium, which is hexagonal.

The apatites with general formula $M_{10}(XO_4)_6Y_2$, where X = P, As, V, Mn, Cr, Si, Ge and Y = O, F, Cl, OH, have been widely studied for many divalent cations M. Rare earths occur in minor amounts in all natural apatites, and in synthetic apatites they may be added as partial replacement for M (Mazelsky et al., 1968; Wanmaker et al., 1971). A mixture of the elements mentioned above may also be in the formula. Mixed silicate–phosphate apatites containing rare earths have been synthetically prepared, for example (Ito, 1968). The practical interests of ore exploitation provide the impetus for the studies of rare earths in apatite structures.

Besides occurring or being introduced as minor or trace constituents in apatites, rare earths form apatites $M_8R_2(PO_4)_6Y_2$ in which they have a more dominant role in the stoichiometry. The first of these were synthesized over fifty years ago (Trömel, 1932). The powder pattern has been indexed as hexagonal (Escobar and Baran, 1982b). A systematic study by Mayer et al. (1974) on $R_xM_{10-2x}Na_x(PO_4)_6Y_2$ showed that all rare earth phosphate apatites of this composition can be indexed as hexagonal, but there are several different space groups. The Ca and Sr fluoride apatites crystallize in the space group $P6_3/m$, the $R_2Ba_6Na_2(PO_4)_6F_2$ compounds in the space group $P\bar{6}$, and the $R_3Ba_4Na_3(PO_4)_6F_2$ compounds in the trigonal space group $P\bar{3}$ (Mathew et al., 1979). In the lead rare earth system, $R_2Pb_6Na_2(PO_4)_6F_2$ compounds have the

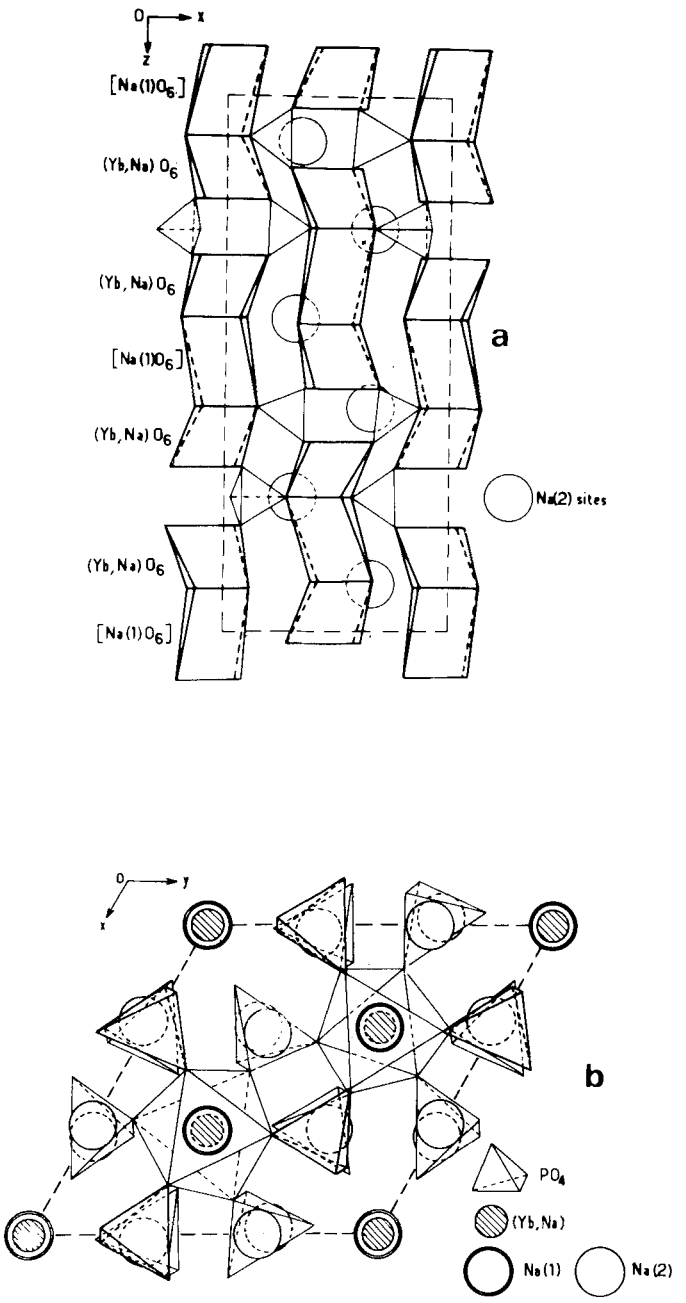

Fig. 34. A projection of 1/3 of the unit cell of the high-temperature form of $Na_{4.5}Yb_{1.5}(PO_4)_3$ along the *c*-axis (a) and a projection along the [120] direction (b) (Salmon et al., 1979).

space group $P\bar{6}$ and the corresponding potassium compounds $P6_3/m$ (Mayer et al., 1980).

The trivalent rare earths form double phosphates with divalent cations, having the formula $M_3R(PO_4)_3$. Their structure is cubic and isomorphic with eulytine $Bi_3(SiO_3)_3$ (Engel, 1972; McCarthy and Pfoertsch, 1981). The divalent cation can also be europium and it is interesting that a mixed valence compound $Eu_3^{II}Eu^{III}(PO_4)_3$ is possible (Engel and Kirchberger, 1975).

1.7. *Orthophosphates with mixed anions*

Isostructural RXO_4 (X = P, V, As) compounds easily form solid solutions with each other. This phenomenom has been studied for yttrium phosphate, and vanadate in particular, with the aim of improving the luminescence properties of YVO_4 by adding some phosphate (Aia, 1967; Ropp and Carroll, 1976).

In section 1.2 mention was made of the formation in solution and solid state of compounds containing HPO_4^- and some other anion (e.g. SO_4^{2-}). A new type of mixed anion phosphate, viz. borate phosphate, has recently been synthesized and structurally characterized by Palkina et al. (1984b). With the lighter lanthanides (La $\cdots$ Dy) isomorphous monoclinic $R_7O_6(BO_3)(PO_4)_2$ compounds are formed, in which seven- and eight-coordinated R atoms lie, together with P and B atoms, in layers parallel to the y-axis. The PO_4 tetrahedra and BO_3 triangles are isolated from each other. The RO_n polyhedra are connected by apexes, edges, and faces and link the layers into a three-dimensional framework.

1.8. *Properties and applications of rare earth phosphates*

The rare earth binary orthophosphates are only sparingly soluble in water and their solubility in phosphoric acid is less than that of $AlPO_4$ and $FePO_4$ (Vasilenko and Chepelevetskii, 1957). The low solubility has been exploited in a process developed for the separation of rare earths during phosphoric acid production (Habash, 1985). The ternary orthophosphates, by contrast, are soluble in water, which is contrary to the behavior of most R^{3+} ternary oxoanion compounds (Kizilyalli and Welch, 1977).

The decomposition reactions of rare earth phosphate minerals promoted by sintering with alkali, alkaline earth, and other compounds have been widely studied (Kizilyalli and Welch, 1980). When the minerals are sintered with alkali compounds the double orthophosphates are formed. With CaO they decompose above 700°C to form calcium phosphate. RPO_4 does not react with SiO_2, and with Al_2O_3 the reaction does not begin until 1800°C (Hikichi et al., 1980a).

The mechanical strength and thermal expansion of the sintered (1500°C) RPO_4 compounds are as follows: compressive strength 2300–3000 kgf/cm^2, bending strength 320–500 kgf/cm^2, and linear thermal expansion coefficients (30–900°C) $5.75–10 \times 10^{-6}$ (Hikichi et al., 1980b). The standard formation enthalpies and

entropies at 298.15 K, and the enthalpies and specific heats at higher temperatures of RPO_4 have been measured by Tsagareishvili et al. (1972) and Orlovskii et al. (1977) (table 2).

The thermoanalytical studies on both binary and ternary rare earth phosphates have focused on the dehydration of hydrates (Petushkova et al., 1969a,b; Hikichi et al., 1978; Zsinka et al., 1978; Horvath et al., 1981). The literature provides very little information on the behavior of rare earth orthophosphates at high temperatures, probably owing to the temperature limits of the equipment. Orthophosphates begin to decompose above 1200°C (Rouanet et al., 1980), and their melting points are about 2000°C ($LaPO_4$: 2050°C, $SmPO_4$: 2040°C, $GdPO_4$: 1950°C, YPO_4: 1980°C) (Tananaev et al., 1978; Hikichi et al., 1980a). The solidification of the orthophosphate liquid leads to the formation of several different oxophosphates (Rouanet et al., 1981).

The condensed rare earth phosphates decompose to orthophosphates, releasing P_2O_5. Ultraphosphates decompose via catena-polyphosphate (Bagieu-Beucher and Tranqui, 1970). The decomposition scheme for $EuH(PO_3)_4$, for example, is:

$$2EuH(PO_3)_4 \xrightarrow{570°C} Eu(PO_3)_3 + EuP_5O_{14} \xrightarrow{970°C} 2Eu(PO_3)_3 \xrightarrow{\sim 1200°C} 2EuPO_4 \,. \quad (1)$$

TABLE 2

(a) The standard enthalpies of formation (kcal mol^{-1}) and entropies (cal deg^{-1} mol^{-1}) for some anhydrous rare earth orthophosphates; (b) experimental enthalpies (kcal mol^{-1}) and mean specific heats (cal deg^{-1} mol^{-1}) for some orthophosphates at elevated temperatures. *

(a)

Compound	$-\Delta H^0_{f(298.15)}$	$S^0_{298.15}$
$LaPO_4$	471	29
$CePO_4$	472	32
$EuPO_4$	452	31
$GdPO_4$	475	32
$ErPO_4$	468	32
$LuPO_4$	465	27
YPO_4	468	25
$ScPO_4$	463	23

(b)

T	$LaPO_4$		$NdPO_4$		YPO_4	
	$H_T - H_{298}$	$\overline{C}_p$	$H_T - H_{298}$	$\overline{C}_p$	$H_T - H_{298}$	$\overline{C}_p$
370	1.931	25.78	1.907	26.78	1.852	26.42
670	10.96	29.32	11.91	30.48	10.87	29.66
966	21.18	31.61	21.92	32.80	21.09	31.68
1270	32.28	33.23	33.97	34.74	31.69	32.85
1595	45.25	34.87	46.50	35.91	44.34	34.13

* Tsagareishvili et al. (1972); Orlovskii et al. (1977).

Before decomposing to $EuPO_4$, $Eu(PO_3)_3$ undergoes a phase transition at 1030°C (Chudinova and Balagina, 1979).

The ternary polyphosphates and orthophosphates have significantly lower melting points than the binary orthophosphates. The ternary phosphates melt at about 900–1100°C, depending on the composition (Vlasse et al., 1980a). The melting may also be incongruent, as is the case for $LiNdP_4O_{12}$ (Nakano and Yamada, 1976).

The temperatures for antiferromagnetic phase transitions for Tb, Dy, and Ho orthophosphates are 2.17, 3.39, and 1.35 K, respectively (Cooke et al., 1973; Smith and Wanklyn, 1974). The magnetic properties and behavior have been determined. Neutron diffraction has been applied in studies of the phase transitions (Millhouse et al., 1980; Petit et al., 1981). The magnetic entropy of certain paramagnetic single crystals, such as $DyPO_4$, changes markedly as the crystal rotates in a magnetic field. Exploiting this anisotropic property, Barclay (1980) has presented a design for a magnetic refrigerator based on $DyPO_4$.

1.8.1. *Luminescence properties of rare earth phosphates*

The rare earth phosphate phosphors $CePO_4$ and $EuPO_4$ were prepared and investigated as early as the 1930's (Lange, 1938; Kroger and Baker, 1941). Intensive study of rare earth phosphors and of activated RPO_4 phosphors has been going on since the mid-60's (Bril and Wanmaker, 1964; Brixner and Fluorney, 1965). Ropp (1968a) has described the spectral properties of R^{3+} in $LaPO_4$, $GdPO_4$, and YPO_4 matrices and compared them with those of oxide phosphors (fig. 35). The change of host does not affect the wavelength but does have a major effect on the total energy efficiency and on the relative intensities of the emission lines. The latter effect is due to the different structures of the phosphate hosts. The brightest phosphors are the rare earth phosphates activated with Eu^{3+}, Tb^{3+}, Gd^{3+}, and Ce^{3+}. The quantum efficiencies are not very high, however, in any of the phosphates.

Ropp (1969) has recorded the reflection spectra of the rare earth phosphates. Only $EuPO_4$ and $TbPO_4$ produce luminescence, and the broad band observed in their spectra is due to charge transfer. The Ce-activated YPO_4 is a fast-decay UV phosphor (Ropp, 1968b). When sensitized with thorium, it becomes much more efficient than the traditional phosphors emitting in UV region (Awazu and Muto, 1969).

The energy transfer from Ce^{3+} to Tb^{3+} has been actively studied in rare earth phosphors (Bourchet et al., 1971, 1974), with the object of obtaining an efficient and durable green phosphor for low-pressure fluorescent lamps. The results obtained with rare earth phosphates are promising (Denis and Loriers, 1970; Murakami et al., 1979; Nichia Denshi Kagaku, 1982).

The activated rare earth phosphate phosphors can be used in all applications developed for phosphors: in fluorescent lamps, cathode-ray tubes, X-ray intensify-

ing screens (D'Silva and Fassel, 1974; Fukuzawa et al., 1977) and, especially as yttrium vanadate-phosphate, high-pressure mercury lamps (Aia, 1967; Kobayashi et al., 1977). Some reports have also been published on the conversion of IR radiation to visible light with rare earth phosphate phosphors (Nakazawa and Shionoya, 1970; Bimberg and Robbins, 1975).

Detailed spectroscopic studies have been made on the rare earth phosphates. The crystal field parameters for YPO_4 and $LuPO_4$ have been calculated using Eu^{3+} and Nd^{3+} as spectroscopic probes (Becher et al., 1968; Ionkina et al., 1973); detailed analyses have been made to discover how the change in structure from monazite to xenotime affects the nearest environment of the activator (Muravev et al., 1981).

The luminescence properties of condensed phosphates and double phosphates, and their possible use as phosphor material have also been investigated. The activator normally used in these studies is Tb^{3+} sensitized with Ce^{3+}. Most of the condensed phosphates studied are catena-polyphosphates (Takezako et al., 1977; Tsujimoto et al., 1977) or ultraphosphates (Blanzat et al., 1977). $LiY(PO_3)_4:Tb^{3+}$; Ce^{3+} is reportedly a bright green phosphor with a brightness exceeding that of the common green phosphor $Zn_2SiO_4:Mn^{2+}$. The luminescence intensity of $LiY(PO_3)_4$ changes little over a wide activator concentration (Tsujimoto et al., 1977). The double orthophosphates can act as hosts for green-emitting Tb^{3+} and Ce^{3+} ions and can be applied in fluorescent lamps (Fava et al., 1978; van den Boom and Seufer, 1979; Bochu et al., 1981). The dependence of excitation and emission wavelengths of Ce^{3+} and Tb^{3+} on the structure of the alkali earth alkaline double and triple orthophosphates has been discussed by Parent et al. (1984). The spectral overlapping between the emission of Ce^{3+} and excitation of Tb^{3+} at 340–400 nm can be altered by changing the contents of the monovalent and divalent cations (Bochu et al., 1981; Le Flem et al., 1983) (fig. 36). The luminescence of Eu^{3+} has been used as a structural probe in alkaline double and triple orthophosphates (Ben Amara et al., 1983).

$LiLa(PO_3)_4$ activated with Ce^{3+}, Eu^{3+}, Tb^{3+}, Bi^{3+}, and Sb^{3+} shows interesting luminescence properties (fig. 37). Only for the Ce^{3+} ion a pronounced concentration quenching is observed. The spectra of pairs of activators differ only slightly from those of isolated activators. Bi^{3+} has a very large Stokes shift in this matrix, whereas Sb^{3+} has a very small one. The efficiency of the luminescence of Sb^{3+} is very high (Blasse and Dirksen, 1982).

1.8.2. *Phosphate lasers*

Neodymium-activated compounds are used as laser materials, the most popular of these at present being $YAG:Nd^{3+}$. The spectroscopic properties of $RPO_4:Nd^{3+}$ have also been investigated with a view to their use as laser materials. The lifetime of the Nd^{3+} emission decreases strongly with increasing activator concentration. However, at 77 K concentration quenching has not been observed (Zverev et al., 1973).

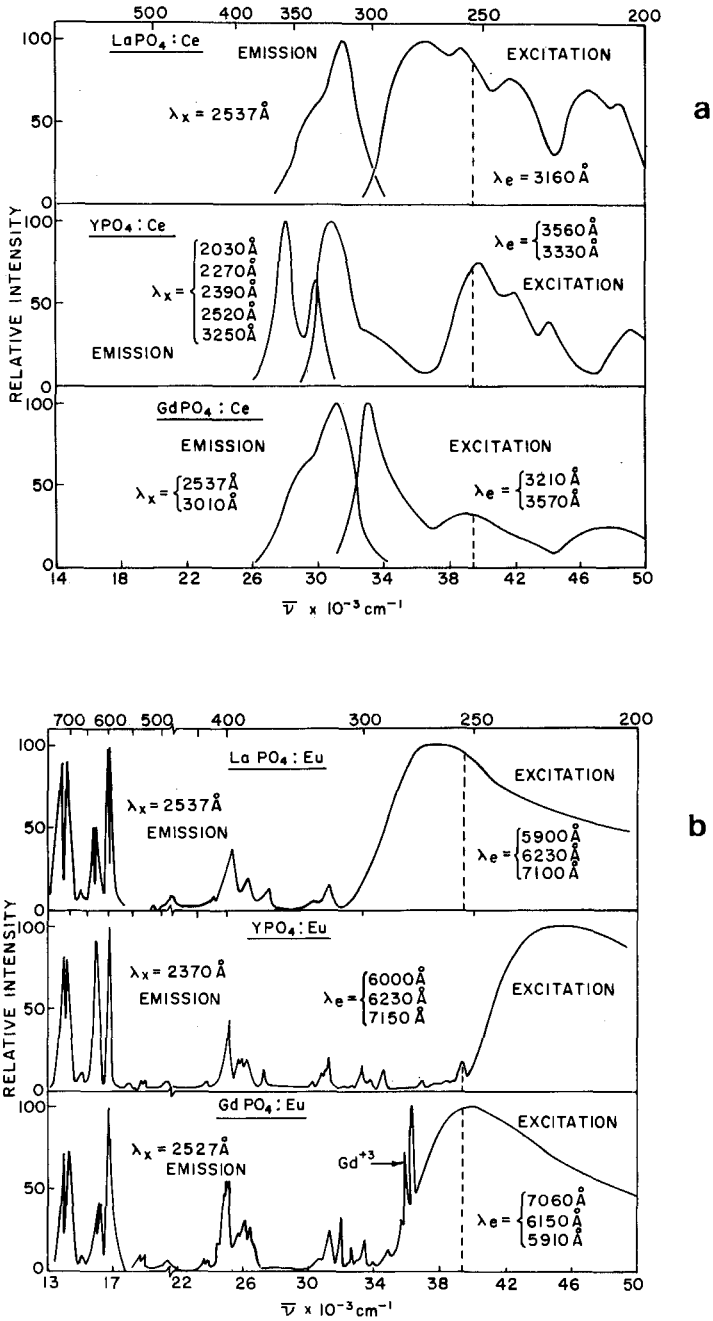

Fig. 35. The excitation and emission spectra of (a) Ce^{3+}-activated, (b) Eu^{3+}-activated, and (c) Tb^{3+}-activated $LaPO_4$, $GdPO_4$, and YPO_4 (Ropp, 1968a).

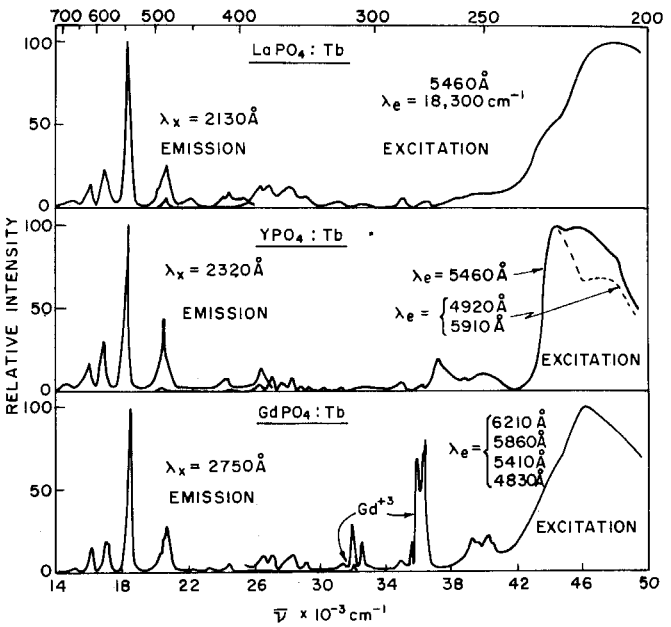

Fig. 35 (*continued*).

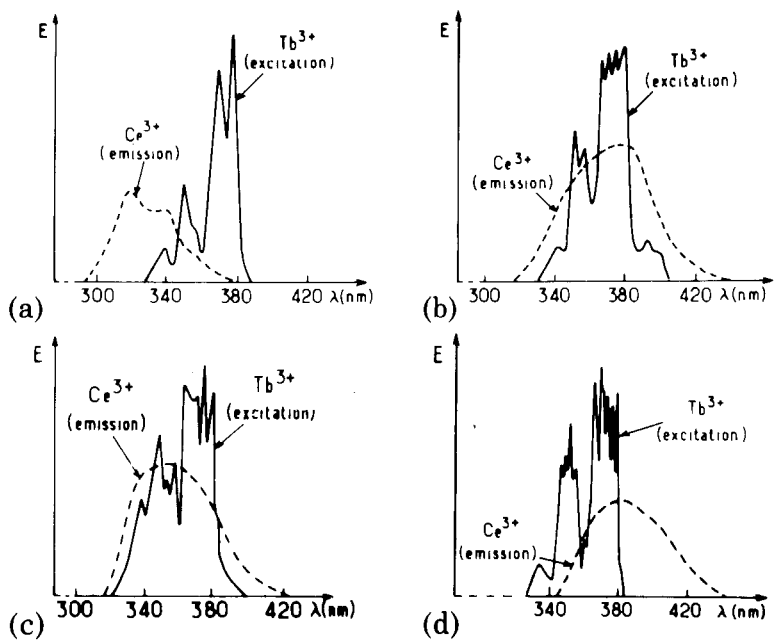

Fig. 36. The overlapping of the normalized Ce^{3+} emission and Tb^{3+} excitation spectra in (a) $La_{1-x-y}Ce_xTb_yPO_4$, (b) $Na_3Ce_{0.65}Tb_{0.35}(PO_4)_2$, (c) $NaSrLa_{0.60}Ce_{0.20}Tb_{0.20}Tb_{0.20}(PO_4)_2$, and (d) $KCaLa_{0.60}Ce_{0.20}Tb_{0.20}(PO_4)_2$ (Le Flem et al., 1983).

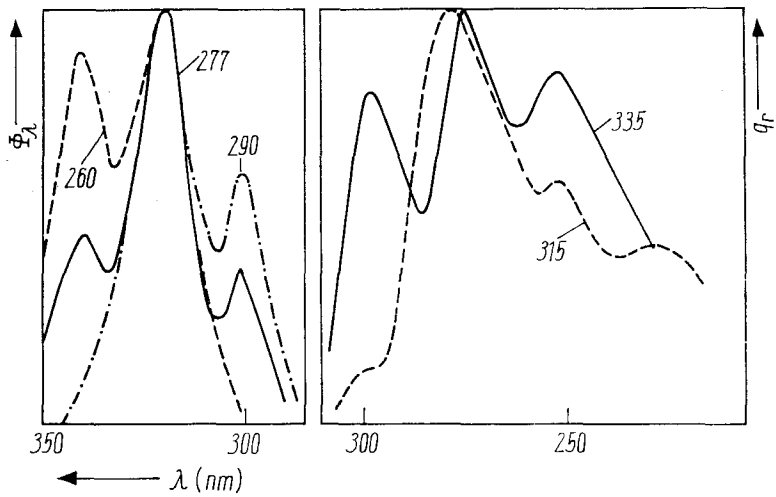

Fig. 37. The excitation (right) and emission (left) spectra of the luminescence of $LiLa_{0.95}Ce_{0.05}P_4O_{12}$. The numbers indicate the monitored emission wavelength (excitation spectrum) and the monitored excitation wavelength (emission spectrum) (Blasse and Dirksen, 1982).

Low-threshold CW laser action has been reported in condensed neodymium phosphates; the high Nd concentration allows the operation of very small lasers, since efficient absorption pump radiation occurs over short distances and the resulting optical gains can be large (Hong, 1975b). The compounds studied thus far are NdP_5O_{14}, $MNd(PO_3)_4$ (M = Li, K, Cs), and $K_3Nd(PO_4)_2$ (Otsuka and Yamada, 1975; Weber and Tofield, 1975; Hong, 1975a,b; Hong and Chinn, 1976; Litvin and Byrappa, 1981). The materials for miniature Nd lasers should have two structural characteristics: (a) isolation of Nd–O polyhedra to avoid concentration quenching, and (b) the absence of local inversion symmetry about the Nd^{3+} ions (Hong and Dwight, 1974). Figure 38 shows the fluorescence spectra of different cesium neodymium condensed phosphates.

Quasi-continuous laser oscillations with very low threshold have also been reported in Sc^{3+}-activated neodymium pentaphosphate(3-) and lanthanum-neodymium pentaphosphate(3-) ($La_{0.5}Nd_{0.5}P_5O_{14}$) (Damen et al., 1973; Danielmeyer, 1973).

Also neodymium lead chloro apatites have been synthesized and their crystals grown with the purpose of obtaining new laser materials (Grisafe and Hummel, 1970; Michel et al., 1975, Joukoff et al., 1978). They are prospective minilaser crystals (Guillot et al., 1980). The condensed phosphates have been evaluated, along with the borates, as hosts for Tb^{3+} laser applications (Colak and Zwicker, 1983).

Table 3 presents the laser properties of some neodymium phosphates. The most intense emission line in all these compounds is about 1.05 μm (Byrappa, 1982).

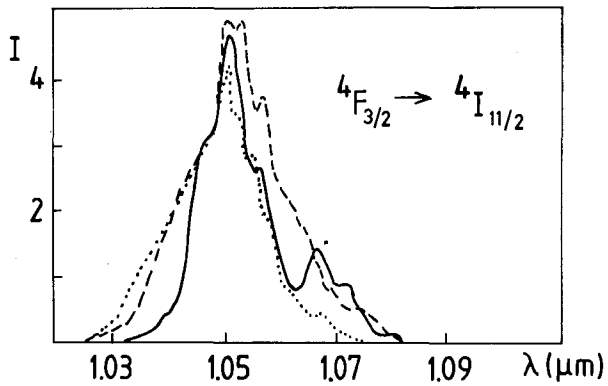

Fig. 38. The fluorescence spectra showing the strongest band in different cesium neodymium phosphates at room temperature. —: cubic $CsNdP_4O_{12}$; – – – –: monoclinic ($P2_1/b$) $CsNd(PO_3)_4$; · · · ·: monoclinic ($P2_1$) $CsNd(PO_3)_4$. (Byrappa, 1982.)

TABLE 3
Laser properties of some neodymium phosphates. *

Compound	Coordination number of Nd	Minimum Nd–Nd distance (Å)	N (10^{21} atoms/cm^3)	Lifetimes (μs)	
				$x = 1.0$	$x = 0.01$
NdP_5O_{14}	8	5.19	3.9	120	320
$LiNd(PO_3)_4$	8	5.62	4.4	120	
$KNd(PO_3)_4$	8	6.66	4.1	100	275
$CsNd(PO_3)_4$ ($P2_1/b$)	8	5.76	3.9	110	370
$CsNd(PO_3)_4$ ($P2_1$)	8	6.69	3.5	115	360
$CsNdP_4O_{12}$	8	6.70	3.5	115	360
$K_3Nd(PO_4)_2$	7	4.87	5.0	21	450
$Na_3Nd(PO_4)_2$	6–8	4.65	5.8	23	360
$KNdP_4O_{12}$	8	6.59	4.0	110	280

* Chinn and Hong (1976); Litvin and Byrappa (1981); Litvin et al. (1982).

1.8.3. *IR and Raman spectra*

Infrared spectroscopy has proved an important tool for determining the different structure types of rare earth phosphates. Several orthophosphate types, as well as condensed phosphate types, can be distinguished (fig. 39) (Hezel and Ross, 1966; Yurchenko, 1978). In condensed rare earth double phosphates, the chain and ring modifications were detected first in spectroscopic studies, and later in crystal structure determinations (fig. 40) (Chudinova et al., 1977c; Madii et al., 1978). Armbruster (1976) has recorded the infrared reflection spectra of YPO_4 and $LuPO_4$ single crystals and made the dispersion analysis of the resulting curves.

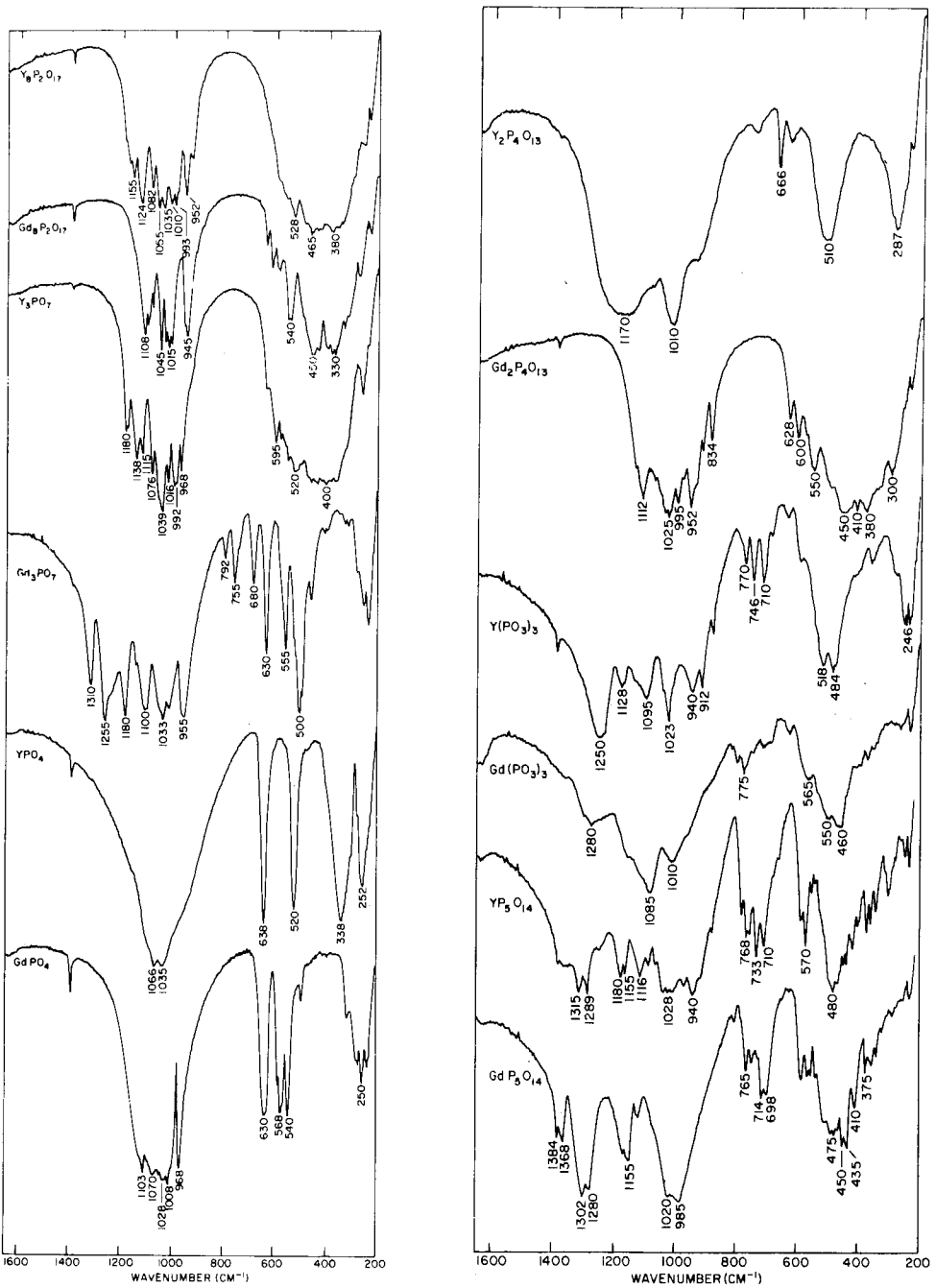

Fig. 39. The IR spectra of the compounds obtained in the Y_2O_3–P_2O_5 and Gd_2O_3–P_2O_5 systems (Agrawal and White, 1985).

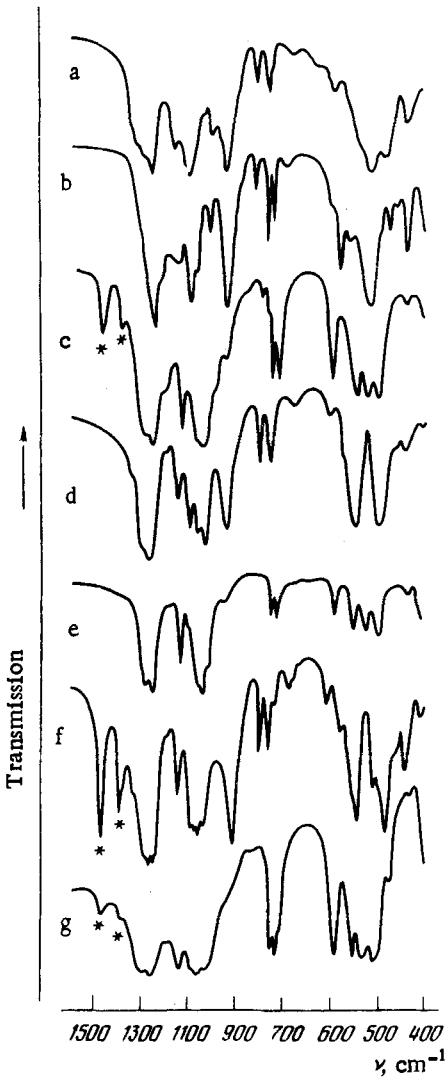

Fig. 40. The IR absorption spectra of ternary rare earth metaphosphates. (a) $HEu(PO_3)_4$; (b) $LiEu(PO_3)_4$; (c) $RbEu(PO_3)_4$; (d) $KEu(PO_3)_4$; (e) $KNdP_4O_{12}$; (f) $KLa(PO_3)_4$; (g) $KLaP_4O_{12}$. (Madii et al., 1978.)

Raman spectroscopy has been used in studies of the rare earth orthophosphates (table 4). The spectra are described by Richman (1966), and the normal coordination analysis calculations of the vibrations of free PO_4^{3-} ion in xenotime structure are presented by Mooney and Toma (1967). Lazarev et al. (1978) have calculated the normal coordinates of YPO_4 crystals and have shown that the resonance splitting of the frequencies of internal vibrations of the complex anion cannot be due to dipole–dipole interaction of the localized vibrators. Begun et al.

TABLE 4
(a) IR and (b) Raman spectra (frequencies in cm^{-1}) of some rare earth orthophosphates with xenotime structure (Yurchenko et al., 1978). *

(a)	$TmPO_4$	280	(305, 320)w	348av	525s		645	(1000)	1065	1135w		
	$TbPO_4$	285	308s	332av	530, 550w	580av	640	1010	1050			
	YPO_4	270	310s	350av	530		640	1030	1060			
	$DyPO_4$	285		344	527, 575		637	1025	1060			
	$LuPO_4$	280	310	350	524		647	1028	1070	1140w		
	$HoPO_4$	290	310w	342	526		637	1032	1056			
	$YbPO_4$	280	310	350	528		647	1020	1065	1140w		

(b)	$TmPO_4$	265	290	328	395			485	580	645	878	1008s	1025w	1062s
	$TbPO_4$							470				986		1040
	YPO_4							480				1010	1040w	1065
	$DyPO_4$						425	490w				990		1057
	$YbPO_4$					420	458	480w	578w	655w		998	1025w	1055
	$LuPO_4$					420		490				1015		1075
	$HoPO_4$						445	480	525w			993	1015w	1050

* av = average; s = strong; w = weak.

(1981) have recorded the Raman spectra of all RPO_4 compounds and interpreted the observed bands.

2. Rare earth arsenates

2.1. *Introduction*

There are many common features to the structural chemistry of rare earth compounds formed by the tetrahedral oxoanions RXO_4, where X is a pentavalent element (P, As, V, Cr). Nevertheless, considerably less structural and other information is available for the rare earth arsenates than for the phosphates and vanadates.

2.2. *Binary arsenates*

Rare earth arsenates can be prepared by firing stoichiometric amounts of rare earth nitrate and ammonium arsenate for several hours at 700–1150°C (Schwarz, 1963f); or they can be precipitated in water solution by Na_2HAsO_4 solution. The product in the case of the lighter lanthanides is anhydrous arsenate, in contrast to

the corresponding phosphate, which is a hydrate. $RAsO_4$ differs from RVO_4 in that the structure is independent of the method of preparation (Escobar and Baran, 1978). The heavier lanthanides, yttrium and scandium, form the hydrated compound $ScAsO_4 \cdot 2H_2O$ in the reaction between $ScCl_3$ and Na_2HAsO_4, or Sc_2O_3 and H_3AsO_4, at 25°C (Ivanov-Emin et al., 1971; Shakhtakhtinskii et al., 1977).

Optically clear $RAsO_4$ crystals were grown from $Pb_2As_2O_7$ flux by slow cooling and recovered by a hot-pouring technique (Smith et al., 1978). Attempts to prepare larger crystals by modifying the flux and the controlling of evaporation by a crystallization seal have been made by Wanklyn et al. (1984). Both monoclinic and tetragonal orthoarsenates were grown.

The structural similarity between YPO_4 and $YAsO_4$ was observed over fifty years ago by Strada and Schwendimann (1934). Most of the rare earth arsenates (Sm $\cdots$ Lu) have been found to have the tetragonal zircon structure (Durif, 1956), whereas the larger rare earths, like the corresponding phosphates, have the monoclinic monazite structure (Carron et al., 1958). The behavior of the neighboring arsenates $NdAsO_4$ and $SmAsO_4$ suggests and $PmAsO_4$ will be dimorphic, but this compound has not been prepared (Escobar and Baran, 1978). At higher pressures (2000–7000 MPa), the arsenates have scheelite structure. The phase transition zircon $\rightarrow$ scheelite has been observed for most arsenates (Sm $\cdots$ Lu, Y). With $PrAsO_4$ and $NdAsO_4$ the monazite $\rightarrow$ scheelite transformation is possible (Stubican and Roy, 1962). The vibrational spectra of $RAsO_4$ recorded by Botto and Baran (1982) are closely similar to those of other RXO_4 compounds (fig. 41). In table 5 a summary of the structural data for rare earth arsenates is given.

The formation of different scandium arsenates in solution has been studied by titration (Chernova et al., 1974). The formation of compounds with $Sc^{3+} : AsO_4^{3-}$ ratios of 1:1, 1:1.5, and 1:3 was confirmed.

Khrameeva et al. (1971) have prepared both anhydrous scandium arsenate, $Sc(AsO_3)_3$, and hydrogenarsenate dihydrate, $Sc(HAsO_4)_3 \cdot 2H_2O$. The former compound is very soluble in water, and the latter hydrolyzes to $ScAsO_4 \cdot 2H_2O$. The $Sc(AsO_3)_3$ compound decomposes upon heating to $ScAsO_4$ at 800–900°C. The decomposition of $Sc(H_2AsO_4)_3 \cdot 2H_2O$ is a multistep process and the following intermediate products have been obtained: $Sc(H_2AsO_4)_3 \cdot H_2O$, $Sc(H_2AsO_4)_3$, $Sc_2(H_2As_2O_7)_3$, $Sc(AsO_3)_3$, and $ScAsO_4$ (fig. 42).

The same group (Khrameeva et al., 1973) has also used IR and NMR spectroscopy to study $Sc_2(HAsO_4)_3 \cdot nH_2O$ ($n = 0, 1, 2$) and $Sc_4(As_2O_7)_3$. Starting material in this study was $Sc_2(HAsO_4)_3 \cdot 2H_2O$, which yielded the other compounds upon heating in air. $Sc_4(As_2O_7)_3$ was found to be the most stable of the compounds; its thermal stability range extended from 330 to 650°C.

Scandium arsenate dihydrate $ScAsO_4 \cdot 2H_2O$ is isomorphic with the corresponding phosphate, differing from it only in the somewhat higher solubility in water and reduced thermal stability (Komissarova et al., 1971c).

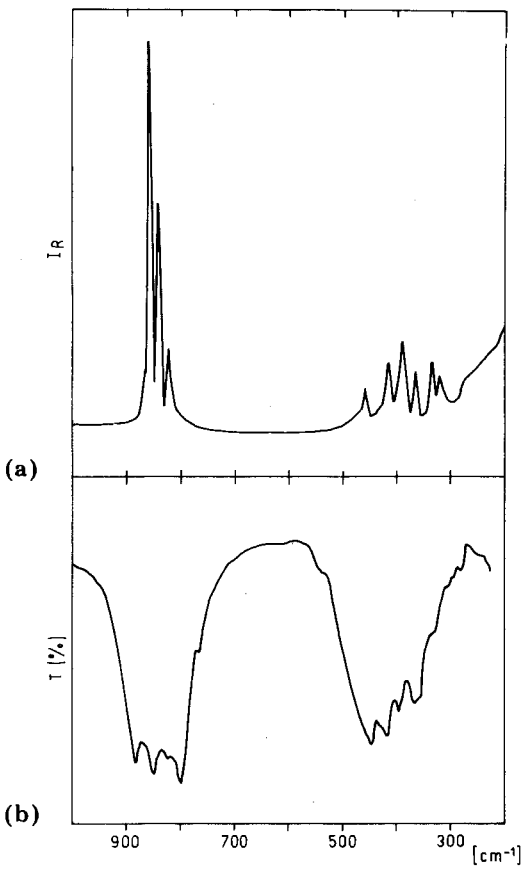

Fig. 41. The vibrational spectra of $LaAsO_4$. (a) Raman spectrum, (b) IR spectrum. (Botto and Baran, 1982.)

TABLE 5
Summary of structural data for rare earth arsenates.

Compound	R	Example	a (Å)	b (Å)	c (Å)	β (deg)	Z	Space group	Ref.
$RAsO_4$	La · · · Nd	Ce	7.02	7.15	6.59	104.3	4	$P2_1$	a
	Sm · · · Lu, Y, Sc	Eu	7.17		6.35		4	$I4_1/amd$	b
$RAsO_4 \cdot 2H_2O$	Sc	Sc	5.64	10.47	9.36				c

(a) Botto and Baran (1982).
(b) Durif and Forrat (1957).
(c) Komissarova et al. (1971c).

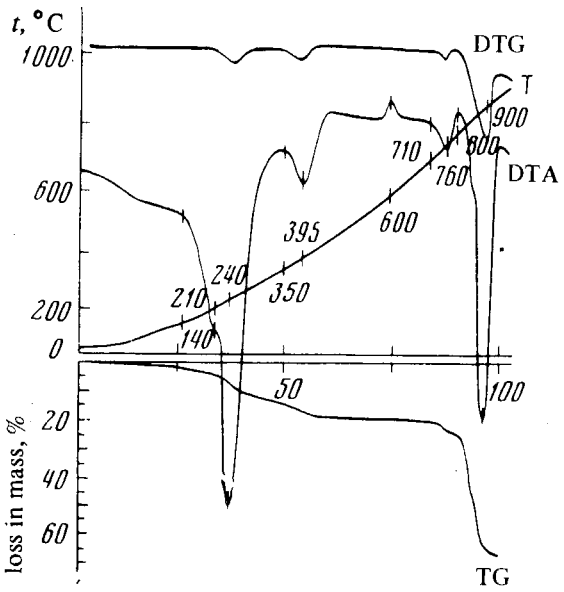

Fig. 42. The TG, DTG, and DTA curves for $Sc(H_2AsO_4)_3 \cdot 2H_2O$. Heating rate 10°C/min (Khrameeva et al., 1971).

2.3. *Double and triple arsenates*

Like the corresponding phosphates, $Na_3R(AsO_4)_2$ compounds have two low-temperature forms: orthorhombic $Na_3Nd(PO_4)_2$ type and monoclinic $Na_3Nd(VO_4)_2$ type (fig. 43). The region of the first type in the rare earth series is narrower in arsenates (La · · · Nd) than in phosphates (La · · · Eu) (Vlasse et al.,

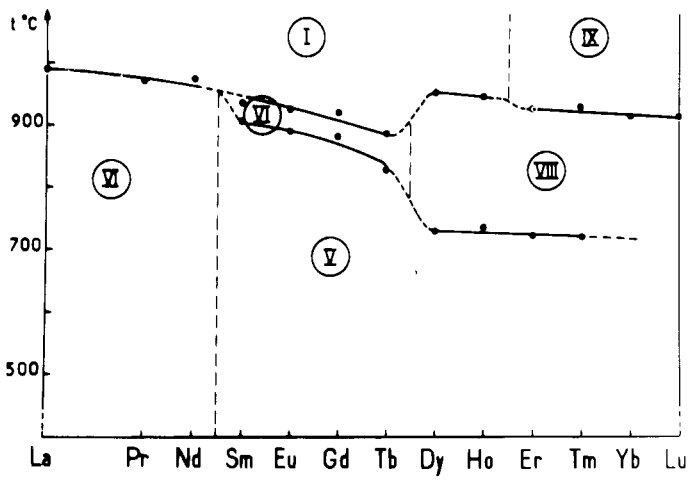

Fig. 43. The thermal behavior of the $Na_3R(AsO_4)_2$ phases. Abbreviations have been presented in fig. 31 (Vlasse et al., 1980b).

1980b). The four higher-temperature forms of sodium rare earth arsenates are likewise similar to those of phosphates. $Na_3R(AsO_4)_2$ (R = La $\cdots$ Nd) have a glaserite-type high-temperature form. The rare earths from Sm to Tb have an orthorhombic intermediate phase identical in structure with orthorhombic $Na_3Nd(PO_4)_2$, and a high-temperature phase of glaserite-type. The medium-temperature phase of arsenates from Dy to Lu is the same as observed for $Na_3Tm(PO_4)_2$. The high-temperature phase of $Na_3Dy(AsO_4)_2$ and $Na_3Ho(AsO_4)_2$ is hexagonal glaserite-type, and compounds of Er $\cdots$ Lu have hexagonal $Na_3Yb(PO_4)_2$ structure (Parent et al., 1980b).

K_2CO_3 (or Rb_2CO_3), H_3AsO_4, and $RAsO_4$ react in solid state at 500°C to give $K_3R(AsO_4)_2$ (Kalinin et al., 1978). Most of the trigonal structures obtained can be considered as derived from the mineral glaserite (Melnikov and Komissarova, 1981).

Two sodium scandium arsenates, $Na_3Sc_2(AsO_4)_3$ and $Na_2HSc_2(AsO_4)_3 \cdot 1.5H_2O$, have been synthesized by Ivanov-Emin et al. (1971). Their IR spectra and X-ray diffraction patterns have been recorded but the structures are unknown.

Ternary rare earth arsenates having hexagonal apatite structure have been prepared by Escobar and Baran (1982a). As with phosphates and vanadates their composition can vary widely.

Recently, Nabar and Sakhardande (1985a,b) have studied the triple orthoarsenates with general formula $MRTh(AsO_4)_3$ where M = Ca, Cd. The X-ray diffraction and IR spectroscopic studies have revealed that, like the binary orthoarsenates, they have two structure types: monoclinic monazite (La $\cdots$ Nd) and tetragonal zircon (Sm $\cdots$ Tm, Y). Some of the compounds show dimorphism at high temperatures (>900°C): a monazite → scheelite transition.

2.4. *Properties of rare earth arsenates*

2.4.1. *Chemical properties*

Because the rare earth arsenates are very insoluble, Na_3AsO_4 can be used in the quantitative determination of rare earth ions (Shakhtakhtinskaya and Iskenderov, 1973, 1975; Shakhtakhtinskii et al., 1977).

Ce(IV) forms hydrogenarsenate dihydrate when precipitated with Na_2HAsO_4. Its dehydration, intercalation reactions, ion exchange properties, and possible use in radiochemical applications have extensively been studied by Zsinka et al. (Zsinka et al., 1974; Zsinka and Szirtes, 1974; Szirtes and Zsinka, 1974; Korney et al., 1977, 1978a,b; Szirtes et al., 1984).

The thermal stability of rare earth arsenate dihydrates, the formation of $RAsO_4$ phases of various structures, and the melting of $RAsO_4$ have been studied by Angapova and Serebrennikov (1973a,b). The melting points of $RAsO_4$ are between 1830 and 2000°C, increasing with increasing atomic number.

2.4.2. *Physical properties*

While rare earth phosphates and vanadates are extensively investigated, the literature on the properties of analogous arsenates is rather sparse. $TbAsO_4$, $DyAsO_4$, and $TmAsO_4$ are most interesting because of their structural and magnetic transitions at low temperatures.

Due to the Jahn–Teller effect $TbAsO_4$ transforms to a structure of low symmetry at 27.7 K and $DyAsO_4$ at 11.2 K (Klein et al., 1971; Hudson and Magnum, 1971; Will et al., 1971b; Goebel and Will, 1972a,b; Wappler, 1974). Both structures have been studied by X-ray and neutron diffraction techniques. After the transition the unit cell of $DyAsO_4$ is $a = 7.06$ Å, $b = 7.03$ Å, $c = 6.30$ Å (Imma) and that of $TbAsO_4$ $a = 10.12$ Å, $b = 9.95$ Å, $c = 6.31$ Å (Fddd) (Long and Stager, 1977).

group of $P2_12_12_1$ (Will et al., 1971a; Schaefer and Will, 1971; Goebel and Will, 1972c). In $TbAsO_4$ the corresponding magnetic transition from paramagnetic to the antiferromagnetic state occurs at 1.50 K (Becher et al., 1972; Klein, 1973). Below the transition temperature, $TbAsO_4$ is an Ising ferromagnet with induced magnetic moments (Mueller et al., 1983). $TmAsO_4$ undergoes a magnetically controllable Jahn–Teller distortion at 6 K (Magnum et al., 1971; Battison et al., 1976). This transition and the connected electronic properties of $TmAsO_4$ have also been studied by Mössbauer spectroscopy (Hodges et al., 1982), NMR spectroscopy, and high resolution optical absorption spectroscopy in the magnetic field (Bleaney et al., 1983, 1984).

The dielectric measurements of $RAsO_4$ crystals have shown them to be ferroelectric, with Curie temperatures in the region of 25–55°C (fig. 44) (Ismail-zade et al., 1980).

2.4.3. *Spectroscopical properties*

The luminescence properties of Eu^{3+} in $RAsO_4$ have been reported already in 1966 but the arsenates have not found use in lamps as luminescent materials (Wanmaker et al., 1966). The IR excited visible luminescence has been obtained with Yb^{3+} and Er^{3+} in arsenates but the conversion efficiency is much lower than that obtained in some fluorides (Sommerdijk et al., 1971). The rare earth $YAsO_4$ host lattice interactions have been reviewed and the crystal field parameters for various R^{3+} ions in this site symmetry have been presented (Wortman et al., 1976). Vishwamittar (1974a,b) has studied the crystal field parameters of Er^{3+} in zircon-type arsenate structures. The multiphonon relaxation rates of excited states of R^{3+} ions in yttrium arsenate have been investigated by Reed and Moos (1973a,b).

Vibrational spectroscopies have been employed in characterization of different structure types of $RAsO_4$. Raman scattering investigations have been made at low

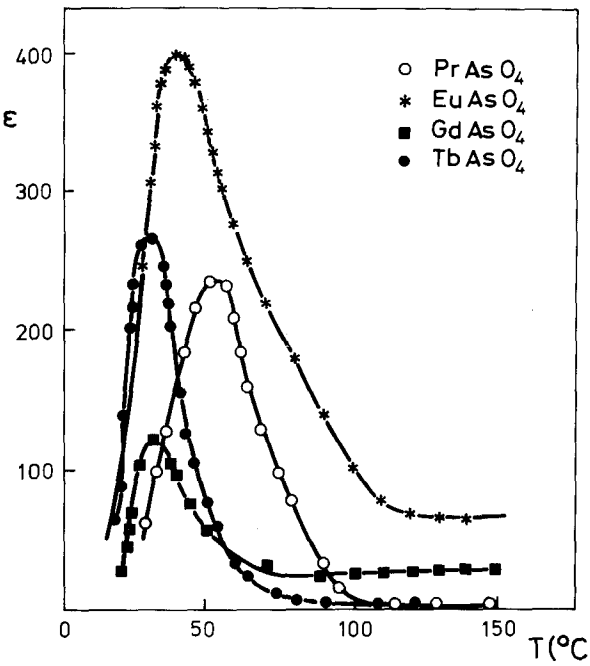

Fig. 44. The dielectric constant versus temperature for the $RAsO_4$ compounds (after Ismail-zade et al., 1980).

temperatures to indicate the phase transitions occurring in Tb, Dy, and Tm arsenates (D'Ambrogio et al., 1971; Harley et al., 1971, 1972; Elliot et al., 1972).

EPR measurements of several R^{3+} ions (e.g., Gd^{3+}, Dy^{3+}, Tb^{3+}, Er^{3+}, Tm^{3+}, Yb^{3+}) in tetragonal $RAsO_4$ (R is usually Y) have been carried out. The *g*-factors, hyperfine constants, magnetic interaction, symmetry parameters, and pair interactions of R^{3+} ions were determined in these studies (Schowalter, 1971; Kalbfleisch, 1972; Hillmer et al., 1972; Schwab, 1975; Schwab and Hillmer, 1975; Mehran et al., 1979).

3. Rare earth sulfites

3.1. *Introduction*

Because of their low solubility, most lanthanide sulfite phases have been prepared only as amorphous or polycrystalline powders. As a result, their structural characterization is incomplete and based mainly on the interpretation of infrared spectra. In the past, studies on lanthanide sulfites have been directed mainly to the synthesis and identification of binary and more complex ternary sulfites. As well, there are a few studies dealing with solubility and solution equilibria. In more recent years, the emphasis has been on thermal properties.

Thermal degradation of lanthanide sulfites is complicated, particularly in inert and reducing atmospheres. In a reducing environment oxysulfides are formed, offering a convenient route to oxysulfide phosphors. The Ce(III) sulfite–sulfate compounds appear to have an interesting application in thermochemical cycles.

A recent volume of the Gmelin Handbook (Gmelin, 1981a) gives a survey of studies on lanthanide sulfites and references to the literature up to 1980, with emphasis on more recent years. In addition, there are two reviews of limited scope (Niinistö, 1973; Leskelä, 1980a). A recent review by Verma (1985) on metal sulfites also briefly discusses the lanthanides.

3.2. *Binary sulfites*

Lanthanide sulfite hydrates were first studied in 1843 by Berthier, who prepared $Ce_2(SO_3)_3 \cdot 3H_2O$. However, a systematic study was not carried out until a full century later when Vickery (1955) prepared the complete series of binary compounds and studied their solution equilibria. Applying spectrophotometric, titrimetric, and ion exchange techniques, Vickery found evidence for the formation of a trisulfito complex $[Ln(SO_3)_3]^{3-}$ in the pH range 5.5–6.1. This complex can also be separated by liquid–liquid extraction with C_{10}–C_{12} alkylamines, as Simonova et al. (1973) showed for La^{3+} and Tb^{3+} using an excess of Na_2SO_3 in the pH range 5–5.5. In more acidic solutions (pH = 1.6–2.0) the 1:1 complex is formed (Mayer and Schwartz, 1950). The formation constant for $CeSO_3^+$ at 25°C extrapolated to ionic strength $I = 0$ has a value $\lg K_1 = 8.04$.

In the solid state, all rare earths, including scandium, form binary sulfites corresponding to the general formula $R_2(SO_3)_3 \cdot nH_2O$. There has been considerable disagreement among authors as regards the value of n; thus Cleve (1874), one of the earliest researchers in the field, gives n the value 3 for erbium sulfite, whereas Vickery (1955) reports this phase to contain 8 moles of water. We now know that the discrepancies are largely due to the existence of two series of hydrates: the long familiar trihydrates and the more recently discovered hexahydrate series (Koskenlinna and Niinistö, 1975). The extreme values of n (11 or 12) reported by Sarkar (1926) are probably due to his preparative method; in the presence of alkali or ammonium ions it is not always the binary sulfite that is formed but a ternary phase may be precipitated.

3.2.1. *The trihydrate series*

The normal method of preparing lanthanide sulfites is to dissolve an aqueous suspension of the oxide by passing SO_2 gas through the solution. The solid binary sulfite is precipitated by reducing the SO_2 pressure, either by introducing a vacuum or by increasing the temperature. Oxidation by atmospheric oxygen is prevented by working in nitrogen atmosphere and applying a paraffin layer to the top of the solution (Niinistö and Koskenlinna, 1973). Under these preparative conditions, at temperatures above 20°C all rare earths except scandium and

lanthanum precipitate as trihydrates (Niinistö and Koskenlinna, 1973; Koskenlinna and Niinistö, 1975; Moskalenko et al., 1975a, 1976a, 1977a). As established long ago by Cleve (1874), lanthanum sulfite contains four molecules of water. Recent studies indicate that scandium forms a pentahydrate in a wide temperature range (Leskelä et al., 1987).

The solubilities of the binary sulfites are very low but show a slightly increasing trend with increasing atomic number. For the solubility of the lanthanum and ytterbium compounds, Vickery (1955) gives the values 0.2 g/l and 0.6 g/l, respectively. Aleksandrovich and Serebrennikov (1962) obtained still lower values: their solubility product for $La_2(SO_3)_3 \cdot 4H_2O$ ($K_s = 1.5 \times 10^{-22}$) corresponds to a solubility of only 0.01 g/l. Ermolaev and Kudrina (1970) have studied the solubility of $La_2(SO_3)_3 \cdot 4H_2O$, too. But since their studies were made in solutions containing Na^+ and NO_3^- ions, the formation of complex species cannot be excluded. Nevertheless, fig. 45 shows that the solubility decreases with increasing temperature, as in the case of the rare earth sulfates.

Because of the low solubility, the crystalline size is small and typically only X-ray powder methods have been used for characterization of the precipitated phases. The medium heavy lanthanides have indeed yielded crystals suitable for unit cell determination by single-crystal techniques, but the size and quality of the crystals have never been sufficient for a full structural analysis. The sulfite trihydrates of rare earths from Sm to Dy are isostructural and form triclinic crystals. The measured and calculated densities indicate two formula units in a cell, which in the case of Sm has the dimensions $a = 9.528(3)$ Å, $b = 8.798(5)$ Å, $c = 6.647(2)$ Å, $\alpha = 105.07(3)°$, $\beta = 94.91(3)°$ and $\gamma = 90.50(5)°$ (Koskenlinna and Niinistö, 1975). According to X-ray powder diagrams the heavier rare earths form another isostructural series (Moskalenko et al., 1975a); Sc and Y trihydrates give

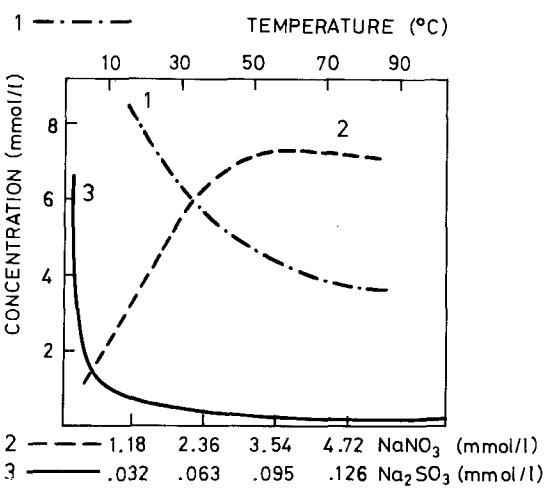

Fig. 45. Solubility of $La_2(SO_3)_3 \cdot 4H_2O$ as function of: (1) temperature (– · –), (2) $NaNO_3$ (– – –), and (3) Na_2SO_3 (—) concentrations. (After Ermolaev and Kudrina, 1970.)

no sharp diffraction pattern (Moskalenko et al., 1976a). On the other hand, Leskelä et al. (1987) have prepared $Sc_2(SO_3)_3 \cdot 5H_2O$ as well-crystallized powder.

3.2.2. *The hexahydrates*

The existence of higher sulfite hydrates was conclusively shown for Sm, Eu, and Gd by a slow crystallization process at 20°C (Koskenlinna and Niinistö, 1975). The excess of SO_2 was removed by extraction into an ether layer and after several days small needle-shaped crystals appeared at the water–ether interface. A slightly different preparative approach was employed by Moskalenko et al. (1977b), who studied the formation of hexahydrates where R was Pr–Eu; later the Gd compound was prepared at 5–10°C (Moskalenko et al., 1977c).

The hexahydrated Sm–Gd sulfites are isostructural and form monoclinic crystals. Though X-ray study is hampered by their minute size, unit cell dimensions have been determined for $Sm_2(SO_3)_3 \cdot 6H_2O$: $a = 20.736(12)$ Å, $b = 7.104(5)$ Å, $c = 16.498(14)$ Å, and $\beta = 110.84(6)°$ (Koskenlinna and Niinistö, 1975).

3.2.3. *Lower hydrates and anhydrous phases*

With the exception of the $La_2(SO_3)_3 \cdot 4H_2O$ phase, the other hydrates have been reported only as intermediates during the thermal decomposition of solid tri- or hexahydrates, discussed in section 3.3.2. The anhydrous phases have usually been prepared by thermal dehydration and characterized by X-ray powder diffraction. The degree of crystallinity is low for the phases obtained and the powder patterns of anhydrous $R_2(SO_3)_3$ contain only a few peaks (Niinistö and Koskenlinna, 1973; Moskalenko et al., 1975b, 1977a). There is, however, a recent report of the preparation of anhydrous $Nd_2(SO_3)_3$ by precipitation from aqueous solution at 95°C (Leskelä et al., 1985); this might offer a route to products having better crystallinity.

3.3. *Properties of the binary sulfites*

Besides the X-ray diffraction measurements discussed above, determinations have been made of IR spectroscopic and thermal properties of the sulfites.

3.3.1. *IR spectroscopy*

IR spectroscopy has been used as a tool for characterization in the recent synthetic studies carried out by Koskenlinna and coworkers, and by Moskalenko et al. The most interesting region for structural studies is in this case just below 1000 cm^{-1}, where the vibrations ν_1 and ν_3 due to the S–O stretchings occur (fig. 46). Although simple criteria have been elicited to explain the main features of sulfite structures from their IR spectra (Nyberg and Larsson, 1973), the interpretation is not straightforward for the rare earth sulfites, owing to the large number of bands. For instance, the IR spectrum of $Y_2(SO_3)_3 \cdot 3H_2O$ contains five bands in the region 1100–800 cm^{-1} and a further six absorptions between 670 cm^{-1} and

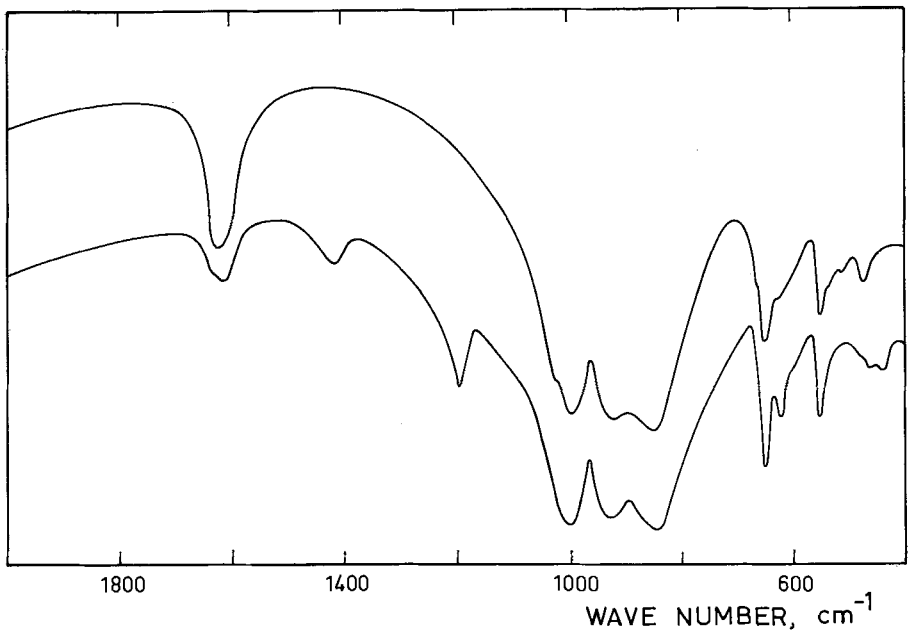

Fig. 46. Infrared absorption spectra of $Gd_2(SO_3)_3 \cdot 3H_2O$ (above) and its partially deuterated analogue (below) in the region 2000–400 cm^{-1} (Koskenlinna and Niinistö, 1975).

470 cm^{-1} (Moskalenko et al., 1976a). Although the main features of coordination cannot be conclusively deduced, IR spectroscopy at the least provides an additional means for the characterization of the solid phases and a method for monitoring thermal decompositions (Koskenlinna and Niinistö, 1973; Moskalenko et al., 1975b; Peterson et al., 1983).

3.3.2. *Thermal decomposition*

Several competing reactions are possible during the thermal decomposition of rare earth sulfites. The thermal stabilities of lanthanum sulfite hydrate and samarium sulfite trihydrate studied in nitrogen up to 450°C (Castellani Bisi and Cola, 1962) indicate that the disproportionation of sulfite to sulfate and sulfide and the dissociation reaction to sulfur dioxide and lanthanide oxide occur simultaneously. In a later study (Castellani Bisi and Clerici, 1963), where the temperature range was extended to 800°C, no disproportionation was found to occur for sulfites of scandium and yttrium; the decomposition products were sulfates and oxides of sulfur. Disproportionation and dissociation reactions are also important in the decomposition of neodymium sulfite.

Grizik and Abdullina (1971) observed anhydrous lanthanum sulfite as an

intermediate product during the thermal decomposition of lanthanum thiosulfate tetrahydrate in vacuum and in air and proposed that the decomposition of $La_2(SO_3)_3$ proceeds via $La_2O(SO_4)_2$ to $La_2O_2SO_4$ and finally to La_2O_3.

More recently, systematic studies have been carried out for both tri- and hexahydrate series of rare earths in inert, oxidative, and reducing atmospheres. We shall first discuss the thermal degradation in inert and oxidative environments.

3.3.2.1. *Inert and oxidative environments.* Comparison of TG/DTA data recorded in oxidative and in inert atmospheres under the same experimental conditions (fig. 47) reveals a similar first step, dehydration, and similar final product, the sesquioxide. The intermediate steps differ, however, and do not always correspond to definitive compositions. For instance, in air the (di)oxosulfate phase $R_2O_2SO_4$ clearly appears as a stable intermediate, whereas in nitrogen the weight loss proceeds further to the apparent R_2S_3 composition. However, X-ray study has shown that also in this case R–O bonds are retained and the phase is actually a mixture of $R_2O_2SO_4$ and R_2O_3 (Koskenlinna et al., 1985). As can be seen in fig. 48 for $Er_2(SO_3)_3 \cdot 3H_2O$ in air, the experimental conditions strongly affect the ratio of the competing disproportion, dissociation, and oxidation reactions. Since all reaction steps involve gaseous products, EGA would be a valuable tool for elucidation of the reaction mechanism; preliminary results (Koskenlinna et al., 1985) have already indicated for instance, that SO_2 is released simultaneously with water, demonstrating the instability of the anhydrous sulfite in thermal degradation.

Scandium, cerium, and neodymium behave somewhat differently, though not enough detailed thermoanalytical data are available for final conclusions. Moskalenko et al. (1976a) compared the thermal behavior of $Sc_2(SO_3)_3 \cdot 3H_2O$ in air with that of Y and La sulfites and noted the low stability of the anhydrous phase, in contrast with the surprisingly wide temperature region where the (di)oxysulfate existed. The latter phase was amorphous to X-rays and thus final confirmation of its presence was not obtained.

Cerium sulfite trihydrate oxidizes in air via two intermediate sulfite–sulfate compounds (Leskelä et al., 1985), of which the first, $Ce_2(SO_3)_2SO_4$, was originally reported by Peterson et al. (1983). When the second, $Ce_2SO_3(SO_4)_2$, phase is heated further it does not seem to form the (di)oxosulfate but to decompose directly to CeO_2 (cf. fig. 49). In nitrogen the (di)oxosulfate is formed under some experimental conditions and this provides a new synthetic route to $Ce_2O_2SO_4$. Because of several competing reactions, the experimental conditions play an important role in the decomposition of $Ce_2(SO_3)_3 \cdot 3H_2O$, as of the other lanthanide sulfites.

Probably because of the difficulties in synthesizing the neodymium sulfite trihydrate, the Nd compound has not been included in earlier investigations. Data for the hexahydrate, however, have been reported by Moskalenko et al. (1977b) and Leskelä et al. (1985); the latter study includes the anhydrous phase as well.

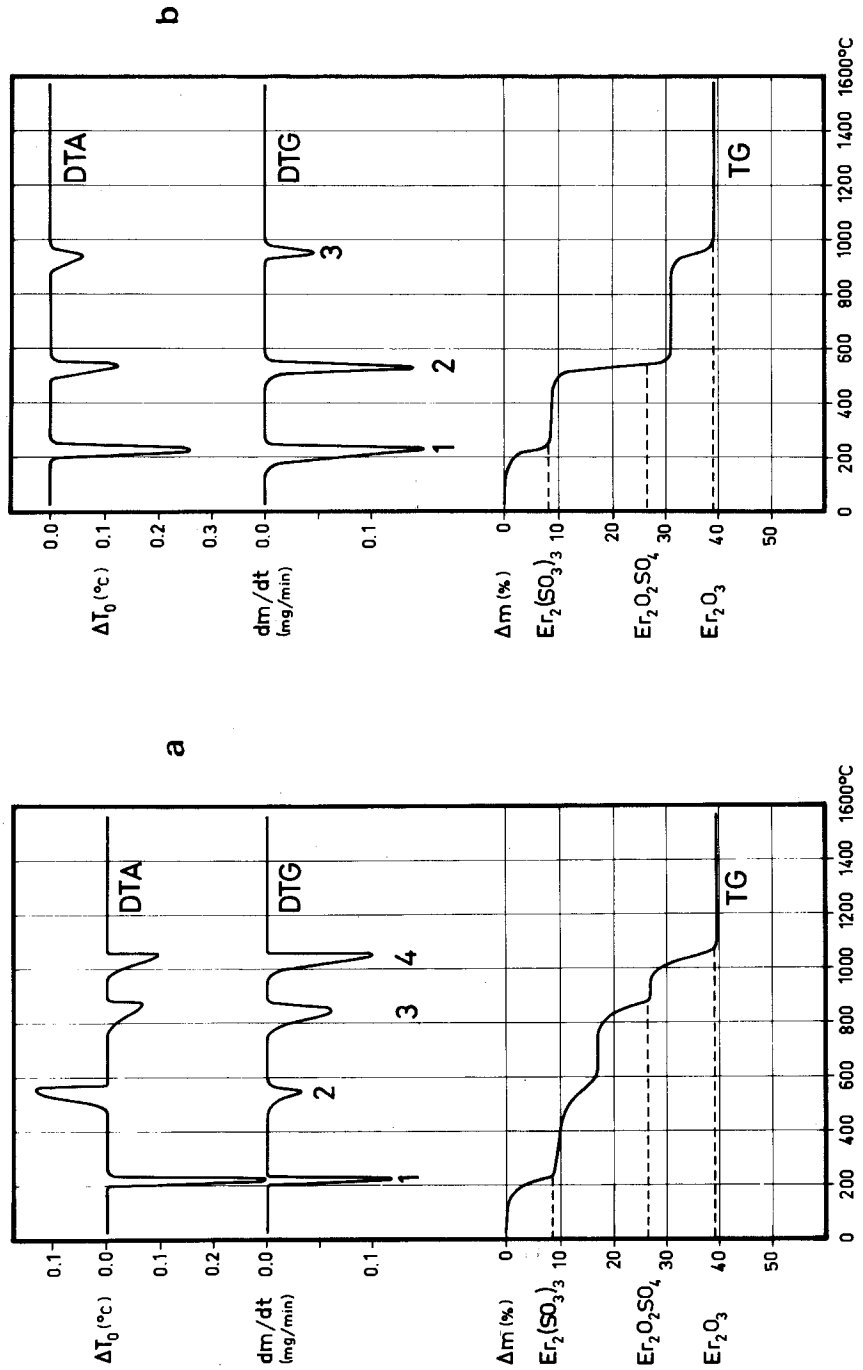

Fig. 47. TG, DTG, and DTA curves for $Er_2(SO_3)_3 \cdot 3H_2O$ recorded under the same experimental conditions in air (a) and in nitrogen (b) (Koskenlinna et al., 1985).

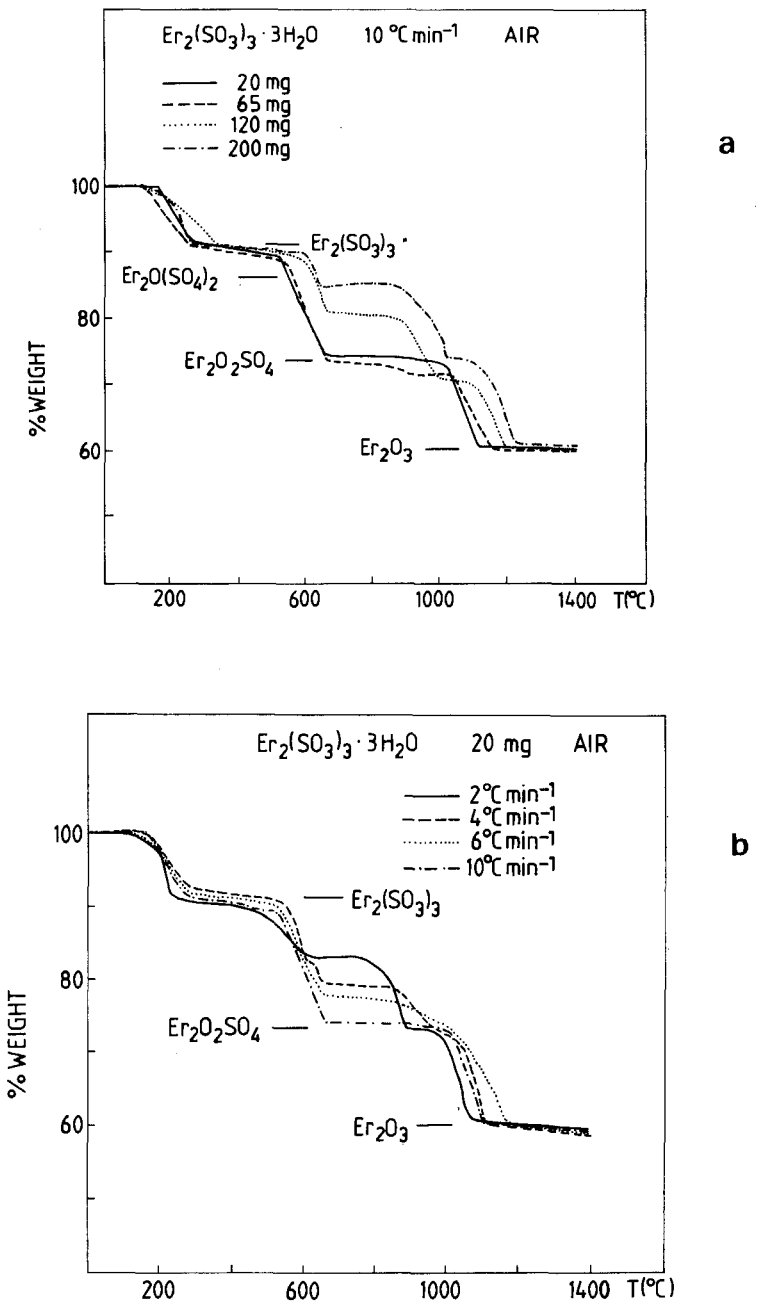

Fig. 48. Effect of sample weight (a) and heating rate (b) on the thermal decomposition of $Er_2(SO_3)_3 \cdot 3H_2O$ (Koskenlinna et al., 1985).

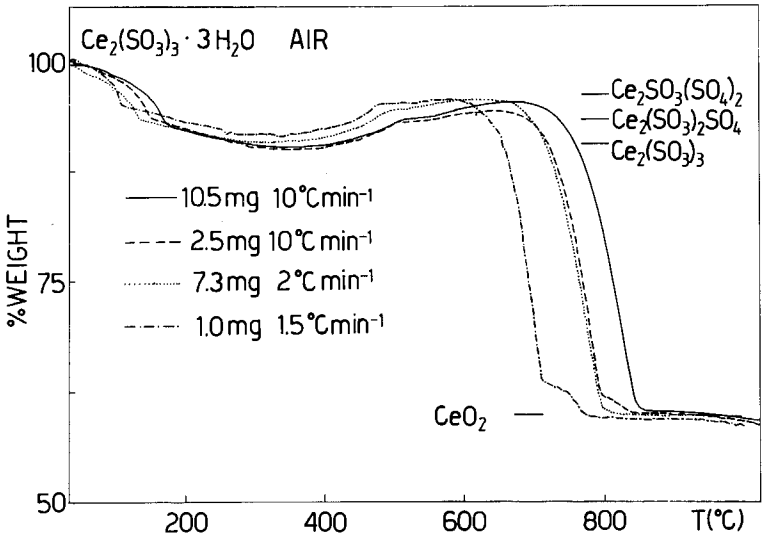

Fig. 49. TG curves of $Ce_2(SO_3)_3 \cdot 3H_2O$ recorded under various experimental conditions in a dynamic air atmosphere. The levels on the right correspond to calculated compositions (Leskelä et al., 1985).

Again, experimental conditions play a central role and lead in some instances to unexpected shapes of the TG curves (Leskelä et al., 1985).

Comparison of the TG data of $Gd_2(SO_3)_3 \cdot 3H_2O$ and $Gd_2(SO_3)_3 \cdot 6H_2O$ (Koskenlinna and Niinistö, 1975; Moskalenko et al., 1977c) shows that the hexahydrate starts to decompose near room temperature and that the stability of the intermediate hydrates is low; the trihydrate phase, nevertheless, appears as a distinct intermediate (fig. 50).

3.3.2.2. *Reducing atmosphere.* It is of special impact for TG studies in reducing atmosphere that the oxosulfides formed are important phosphor materials. The preparative methods for activated rare earth oxosulfides, especially the use of sulfites as starting material, have been reviewed by Leskelä (1980a) and in a broader way by Gmelin (1983).

Several methods of preparation are available for the oxosulfides (Gmelin, 1983; Leskelä, 1980b; Niinistö, 1984a). Koskenlinna and Niinistö (1973) have studied the reduction of rare earth sulfites with H_2S or CO; later, Koskenlinna et al. (1976a) have published a detailed procedure for the synthesis of Eu^{3+}: Y_2O_2S phosphors while Leskelä (1980b) prepared terbium activated R_2O_2S (R = La, Gd, Y). Luckey (1972) has published a similar method, starting mainly from ternary sulfites (cf. Koskenlinna et al., 1976b). More recently, Moskalenko et al. (1980) confirmed that the rare earth sulfites are suitable starting materials for the reduction process.

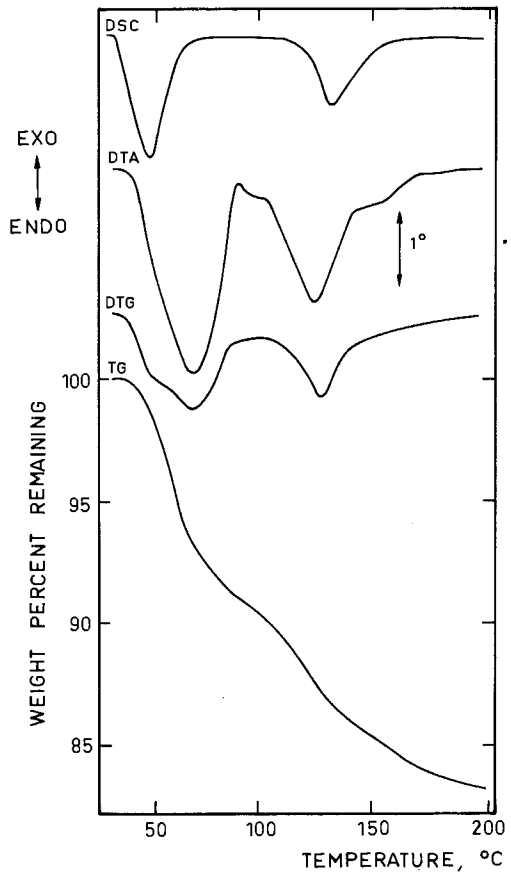

Fig. 50. DSC, DTA, DTG, and TG curves for $Gd_2(SO_3)_3 \cdot 6H_2O$ recorded in air up to 200°C (Koskenlinna and Niinistö, 1975).

The sulfite process involves several steps (fig. 51), none of which requires extreme conditions. The main step, reduction, can be carried out around 500°C (fig. 52). When europium-activated oxysulfides are prepared by this method, there is a danger that part or all of the Eu is reduced to divalent state. This can be avoided by selecting a proper temperature range for the isothermal reduction, as shown by Leskelä and Niinistö (1980a) in TG experiments where Mössbauer spectroscopy was used to analyze the Eu^{2+} content.

3.3.2.3. *Thermochemical cycle.* Peterson et al. (1983) have recently described an interesting thermochemical cycle involving $Ce(III)(SO_3)_2SO_4$ and its tetrahydrate. The synthesis and characterization of the compound were reported by the same group earlier (Peterson et al., 1980) and it was during the detailed thermal decomposition studies that a thermochemical cycle for splitting sulfur dioxide into sulfur and oxygen was assessed.

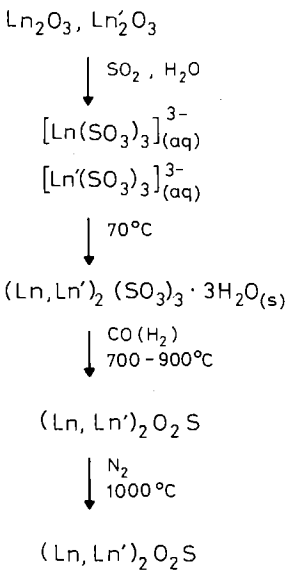

Fig. 51. Preparation of activated oxosulfides by the reduction of sulfites. The matrix lanthanide is indicated by Ln and the activator by Ln' (Niinistö, 1984a).

According to the TG and EGA data, which were supplemented by chemical analyses and IR and X-ray studies, $Ce(SO_3)_2SO_4 \cdot 4H_2O$ thermally decomposes to yield H_2O, S_2, SO_2, and O_2 as gaseous products, with $Ce_2O(SO_4)_2$, $Ce_2O_2(SO_4)_2$, and $CeOSO_4$ as solid intermediates, and CeO_2 as the end product.

The thermoanalytical data provided the basis for the thermochemical cycle presented in fig. 53. Stoichiometry of the cycle gives as net reaction the splitting of one mole of SO_2 into $\frac{1}{2}S_2$ and O_2 when 4 moles of CeO_2 is used as starting material. The fact that the measured yield of S and O_2 was some one third less, was attributed to the direct decomposition of $Ce_2(SO_3)_2SO_4$ into $Ce_2O_2SO_4$ and $2SO_2$, a mechanistically favored reaction which does not involve any change in the oxidation state of sulfur.

3.4. *Ternary sulfites*

The ternary systems of rare earth sulfites have been studied far less than the binary systems. Cuttica (1923), using alkali metals, was the first to prepare ternary sulfites, and shortly thereafter Canneri and Fernandes (1925) prepared uranyl and copper(I) sulfites of some cerium group metals.

Cuttica's method of preparation was to add alkali sulfite to a lanthanide solution prepared by passing SO_2 through a lanthanide carbonate suspension. Cuttica assumed that R^{3+} was associated with the hydrogensulfite ion as $R(HSO_3)_3$, but Vickery (1955) has presented evidence for the existence of $[R(SO_3)_3]^{3-}$ as a predominant species in this pH range. Vickery was consequently

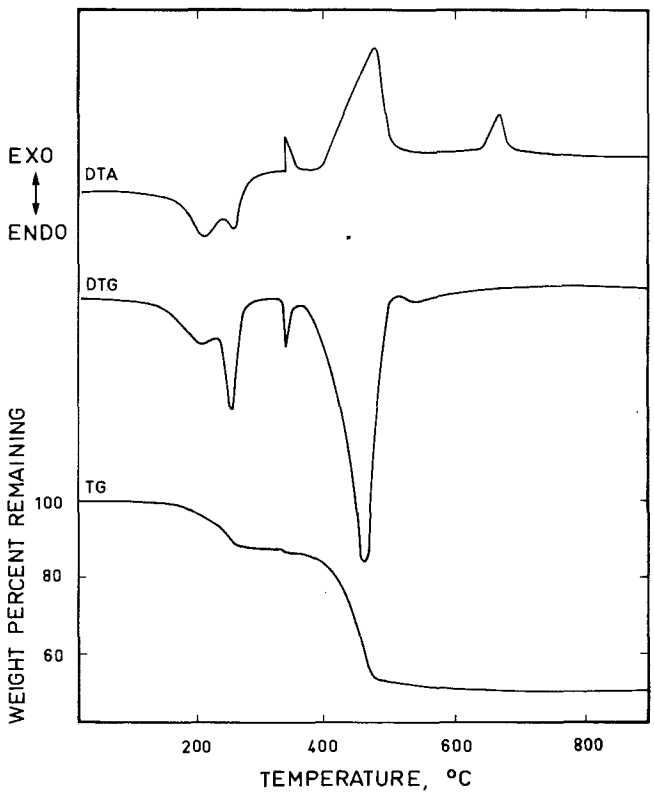

Fig. 52. Thermoanalytical curves in carbon monoxide for $(Eu,Y)_2(SO_3)_3 \cdot 3H_2O$ showing the formation of Eu-activated Y_2O_2S by reduction at 500°C (Koskenlinna et al., 1976a).

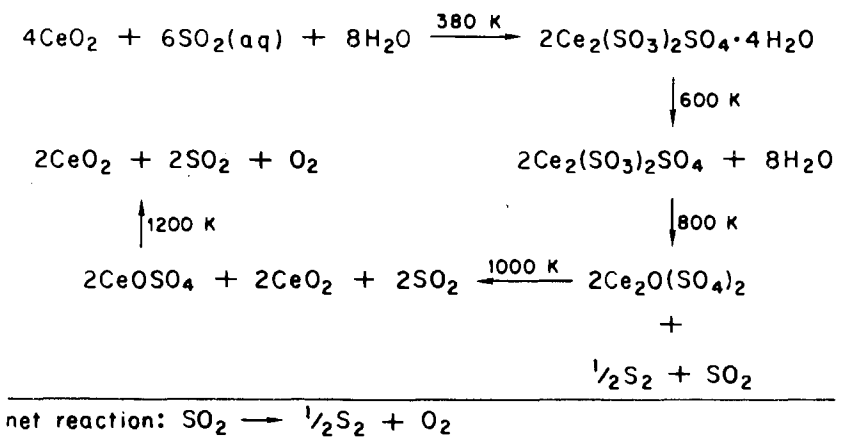

Fig. 53. Thermochemical cycle for splitting sulfur dioxide (Peterson et al., 1983).

able to precipitate the sodium compound of neodymium, $Na_3Nd(SO_3)_3$. He also prepared other ternary compounds, but their properties were described only briefly.

More recently, the ternary compounds of ammonium and sodium with some lanthanides have been prepared and characterized by X-ray, IR spectroscopic, and thermoanalytical methods.

3.4.1. *Ternary sulfites with ammonium ion*

Systematic investigation of the solid phases formed in the system R^{3+}–NH_4^+–SO_2–H_2O (Erämetsä et al., 1972) has shown the composition of the major solid phase to correspond to the trisulfite complex found by Vickery in solution. When R is Sm, Gd, or Dy, $(NH_4)_3R(SO_3)_3 \cdot H_2O$ may be prepared as crystalline precipitate. X-ray powder diffraction studies indicated that this compound has two crystalline modifications: the low-temperature α-form, best obtained around room temperature, and the high temperature or β-form, crystallized at temperatures 50°C higher.

Besides the 1:3 lanthanide/sulfite ratio the solid phase may have 1:1 or 4:9 composition, depending on concentrations and temperature. The anhydrous compound $NH_4R(SO_3)_2$ and its hydrates ($2H_2O$ for Sm and Gd, $3H_2O$ for Dy) have been prepared and characterized by chemical analysis, optical microscopy and X-ray powder diffraction. The more complex composition $(NH_4)_6R_4(SO_3)_9 \cdot 6H_2O$ was obtained only for Gd.

Because of the low solubility of the ternary sulfites, the crystals are usually too small for study by single-crystal X-ray methods. However, crystallization experiments in the temperature range 75–95°C have yielded small needle-shaped ($0.02 \times 0.02 \times 0.15$ mm) crystals for the high-temperature (β) polymorph of $(NH_4)_3Dy(SO_3)_3 \cdot H_2O$ (Niinistö and Larsson, 1973). The monoclinic unit cell dimensions were obtained from Weissenberg photographs and refined from Guinier data to $a = 8.863(6)$ Å, $b = 15.919(5)$ Å, $c = 9.467(5)$ Å, $\beta = 117.38(5)°$. With the centrosymmetric space group P2/m, Patterson and Fourier syntheses gave the positions of Dy, S and N atoms. A least-squares refinement with isotropic temperature factors yielded an *R*-value of 12.7%. Oxygen atom positions could not be found and careful examination of long-exposure films revealed weak superstructure reflections, indicative of a four-fold *b*-axis.

The substructure of β-$(NH_4)_3Dy(SO_3)_3 \cdot H_2O$ is shown as a projection in fig. 54, where the calculated Dy–S distances of 3.40 and 3.41 Å indicate that the bonding of sulfite groups to dysprosium takes place through oxygen. IR spectra provide further support for this bonding mode (Niinistö and Larsson, 1973).

3.4.2. *Ternary sulfites with sodium*

Moskalenko et al. (1976b,c, 1978) have studied systematically the formation and properties of sodium sulfites of type $NaR(SO_3)_2 \cdot nH_2O$, where *n* is 0, 1 or 2. Three different isostructural groups were found among the hydrates: (a) $NaR(SO_3)_2 \cdot 2H_2O$ (R = La), (b) $NaR(SO_3)_2 \cdot 2H_2O$ (R = Pr $\cdots$ Eu), and (c)

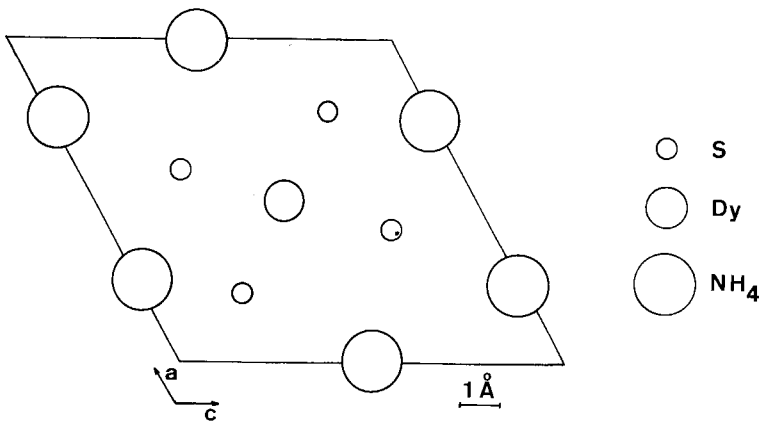

Fig. 54. Substructure of β-$(NH_4)_3Dy(SO_3)_3 \cdot H_2O$ projected down the *b*-axis (Niinistö, 1973).

$NaR(SO_3)_2 \cdot H_2O$ (R = Ho · · · Lu). The anhydrous ternary sulfites $NaR(SO_3)_2$ were prepared by thermal decomposition of the hydrates and were found, on the basis of X-ray powder diffraction patterns, to form three different structure types: La, Pr–Eu, and Ho–Lu.

Besides crystallographic studies by X-ray powder diffractometry and optical microscopy, the compounds have been characterized by IR spectroscopy and thermal analysis. In particular, the IR absorption spectra of the compounds $NaR(SO_3)_2 \cdot 2H_2O$ (R = Pr · · · Eu), have proved to be complex. The great number of bands (up to six in the S–O stretching region) was attributed to the distortion of sulfito groups and their different bonding modes (Moskalenko et al., 1978). The spectra of other ternary sulfites are also complicated, but resemble those of binary sulfites (cf. figs. 46 and 55).

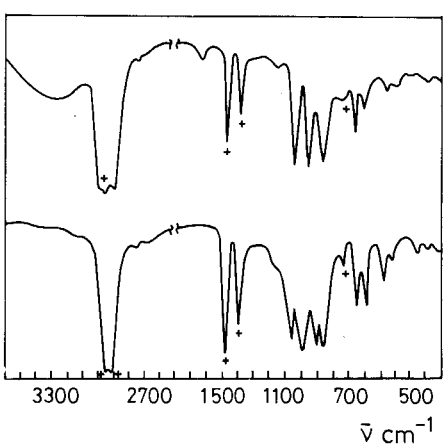

Fig. 55. Infrared spectra of $NaLu(SO_3)_2 \cdot H_2O$ (above) and its dehydration product $NaLu(SO_3)_2$ (below). The peaks due to paraffin are marked by +. (After Moskalenko et al., 1976b,c.)

TG and DTA curves show that when $NaR(SO_3)_2 \cdot nH_2O$ is heated in air the first step is dehydration, which is completed by 200°C. Further heating produces, through an exothermic oxidation process, a mixture of $R_2O_2SO_4$ and Na_2SO_4 at about 450°C; the final product is the sesquioxide formed at temperatures above 900°C. The overall thermal decomposition scheme in air for the $NaR(SO_3)_2 \cdot H_2O$ ($R = Ho \cdots Lu$) series can be written, omitting the gaseous products, as follows: $2NaR(SO_3)_2 \cdot H_2O \rightarrow 2NaR(SO_3)_2 \rightarrow R_2O_2SO_4 + Na_2SO_4 \rightarrow R_2O_3 + Na_2SO_4$ (Moskalenko et al., 1976c).

4. Rare earth sulfates

4.1. *Introduction*

The sulfates are probably the most frequently studied group of inorganic complex compounds formed by the rare earths. Ever since the discovery of the rare earths, the sulfates have also played an important role in separation processes. Even today, the low solubilities of the sodium double sulfates are exploited for the precipitation of the rare earths from monazite and xenotime in the acid process (Hedrick, 1985).

Probably hundreds of individual binary, ternary, and more complex compounds have been synthesized in solution, in the solid state (through decomposition or sintering) and in melts; the compounds have been characterized by spectroscopic and thermal techniques, and now are being studied increasingly by single-crystal X-ray diffraction methods. The first crystal structures of the binary and ternary compounds were determined in the 1960's and 1970's, respectively, but already well over 50 structural determinations have now been published. Attempts have been made to correlate the structures with spectroscopic and other properties.

As there are probably thousands of primary articles dealing with some aspect of the chemistry and physics of the rare earth sulfates, this review will aim only at a selective coverage of the literature, with emphasis on recent reports. The Gmelin–Kraut handbook (1928–1932), predecessor of the present edition of the *Gmelin Handbook*, provides good coverage of the earlier literature, as do the handbooks by Mellor (1965a) and Pascal (1959). Comprehensive coverage up to the late 1970's, with over 300 pages of text and numerous illustrations and references, is provided by Gmelin (1981b); this is unquestionably the best single source of information on the rare earth sulfates.

In addition to the handbooks, a number of reviews and theses of more limited scope have recently appeared. The overviews of Niinistö (1983, 1984b) discuss the structural and thermochemical aspects of rare earth sulfates, while the thesis by Lindgren (1977e) provides a summary of the structural chemistry of Ce^{3+} and Ce^{4+} sulfates. The review by Voronkov et al. (1982) is also specialized in that it

discusses the structures of sulfates (and selenates) of the trivalent elements including scandium but not the larger rare earths.

4.2. *Binary rare earth sulfates*

The preparation and properties of solid binary sulfates of the type $R_2(SO_4)_3 \cdot nH_2O$ ($n = 0$–12) have been widely studied and an enormous amount of data has been accumulated (Gmelin, 1981b). In contrast, solution studies are relatively few in number and in part contradictory.

4.2.1. *Sulfato complexes in solution*

The solubilities of $R_2(SO_4)_3$ in water are moderate for the lanthanides, ranging from approximately 0.04 mol/l to 0.5 mol/l at 25°C (Holleck and Noddack, 1937; Spedding and Jaffe, 1954). Scandium has a significantly higher molar solubility (Komissarova et al., 1971b). The characteristic feature of the solubility curves is that they pass through a minimum in the $Z = 62$ to 63 region (Sm, Eu) and that at higher temperatures the solubilities are lower. For the solubility and temperature dependence of $La_2(SO_4)_3$, for instance, see de Saja et al. (1977).

Although the values for the equilibrium constants vary considerably (Sillén and Martell, 1964, 1971), research groups have agreed on the formation of the monosulfato complex RSO_4^+ as the predominant species in aqueous solutions containing R^{3+} and SO_4^{2-}; but the presence of the disulfato complex cannot be neglected, especially at higher sulfato concentrations (Hale and Spedding, 1972). The main question that has been debated is whether the anion enters the inner (contact) sphere of coordination or remains in the outer (solvent separated) sphere. No X-ray diffraction studies have been reported for sulfate solutions, owing to the difficulty in obtaining concentrated solutions. On the basis of the basicity of the sulfato ligand, however, Choppin and Bertha (1973) have predicted inner-sphere complexation. Their thermodynamic data (DeCarvalho and Choppin, 1967) as well as well as those of Hale and Spedding (1972) also favor predominantly inner-sphere complexation. Recent thermodynamic and spectroscopic studies, however, provide support for the outer-sphere model (Ashurst and Hancock, 1977). Very recent evidence in favor of the inner-sphere complex formation comes from the luminescence lifetime studies in the system Eu^{3+}–SO_4^{2-}–H_2O (Tanaka and Yamashita, 1984) and by analogy from XRD studies in aqueous selenate solutions (Johansson et al., 1985). In contrast to the trivalent lanthanides, scandium (Komissarova, 1980) and tetravalent cerium have a tendency for hydrolysis and formation of polynuclear species.

4.2.2. *Preparation and stoichiometries of the solid compounds*

The classical preparative method of dissolving rare earth oxides or carbonates in diluted sulfuric acid (3 M or lower) and evaporating at room temperature (e.g., Wendlandt, 1958; Brauer, 1980) yields the octahydrated sulfate for all rare earths

except La and Ce, which crystallize under these conditions as nonahydrates (Hunt et al., 1954; Alonso et al., 1973). When more acidic solutions are used, the lighter rare earths (La $\cdots$ Nd) tend to form pentahydrates (Biltz, 1911). Scandium also forms this phase, though with a different structure (Komissarova et al., 1965b; Niinistö et al., 1975).

Besides the pentahydrate, two other phases have been well established for Ce(III), viz. the nonahydrate (Dereigne and Pannetier, 1968) and the tetrahydrate (Dereigne et al., 1972). While the octahydrates are also known for La and Ce, their crystallization requires special techniques (de Saja et al., 1978) and they have a different structure from $R_2(SO_4)_3 \cdot 8H_2O$ (Pr $\cdots$ Lu, Y) (Aslanov et al., 1973b). The thorough investigations into the stabilities and solubilities of various Ce^{3+} sulfate hydrates by Koppel (1904) and by Schröder (1938) serve as the best guides when choosing the crystallization conditions for the sulfate hydrates (fig. 56).

The anhydrous phases have been prepared by dehydration at high temperatures (350°C: Postmus and Ferraro, 1968; 600°C: Surgutskii and Serebrennikov, 1964) and by crystallization from melts formed by thermal decomposition of $LiR(SO_4)_2$ (Sirotinkin et al., 1976a). The latter procedure has been used for the growing of crystals of $Er_2(SO_4)_3$ and $La_2(SO_4)_3$ by slow cooling of melts from an initial temperature exceeding 700°C (Sirotinkin et al., 1981; Sirotinkin and Pokrovskii, 1982a). Thermoanalytical curves for $R_2(SO_4)_3 \cdot nH_2O$, discussed in detail in section 4.3.2, indicate a broad stability range for $R_2(SO_4)_3$, which facilitates the use of thermal techniques for their preparation.

In addition to the firmly established phases with known structures (see section 4.2.3), viz. $R_2(SO_4)_3 \cdot 9H_2O$ (R = La, Ce), $R_2(SO_4)_3 \cdot 8H_2O$ (R = La, Ce; R = Pr $\cdots$ Lu, Y), $R_2(SO_4)_3 \cdot 5H_2O$ (R = La $\cdots$ Nd), and $Ce_2(SO_4)_3 \cdot 4H_2O$ and the anhydrous sulfates, there are reports on the existence of a number of other hydrates (Gmelin, 1981b). Koppel (1904) has found that $Ce_2(SO_4)_3 \cdot 12H_2O$ crystallizes near 0°C; and a recent study on the crystal structure of $La_2(SeO_4)_3 \cdot 12H_2O$ provides indirect evidence for the existence of the dodecahydrate (Karvinen and Niinistö, 1986). On the basis of TG dehydration curves, it has been suggested that Yb forms the 11-hydrate under the same conditions as the octahydrates are formed (Wendlandt, 1958); however, this finding has not been supported by more recent experiments (Hiltunen and Niinistö, 1976a).

Spasibenko (1974) and Spasibenko and Popova (1981) have found evidence for the existence of 10-, 7.5-, and 5.5-hydrates of cerium(III) sulfate in addition to the 8- and 5-hydrates, but the new phases have not yet been adequately characterized. Recently, Govorukhina et al. (1984) have studied the system Ce^{3+}–SO_4^{2-}–H_2O and separated, in addition to the well-established phases, the mono- and dihydrates for $Ce_2(SO_4)_3$ and the phases containing sulfuric acid $Ce_2(SO_4)_3 \cdot 3H_2SO_4 \cdot nH_2O$ ($n = 0, 2, 5$). X-ray diffraction studies indicate that both $Ce_2(SO_4)_3 \cdot 4H_2O$ and $Ce_2(SO_4)_3 \cdot 2H_2O$ crystallize in two polymorphic

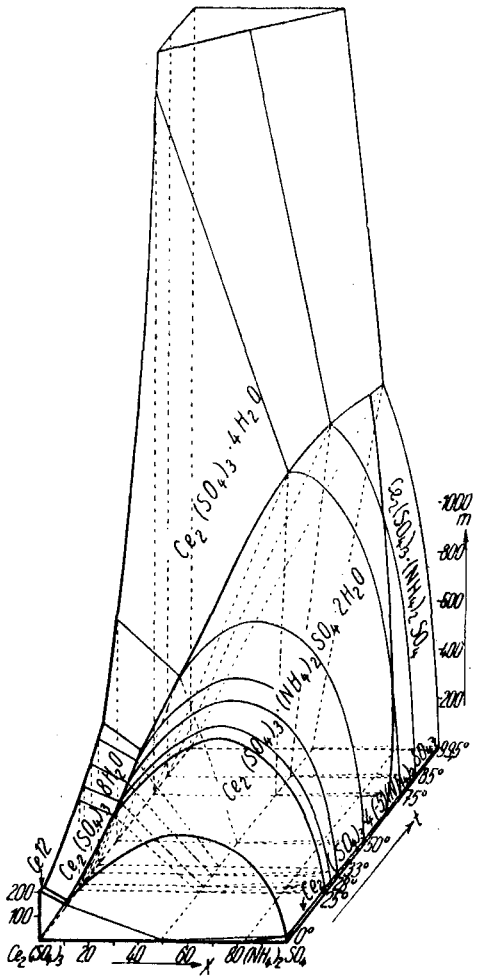

Fig. 56. A solubility diagram of the system $(NH_4)_2SO_4$–$Ce_2(SO_4)_3$–H_2O showing the stability range for binary cerium sulfate hydrates and for the ternary phases (Schröder, 1938).

forms. Although these phases have been characterized by powder diffractometry and by IR and thermoanalytical methods, crystal structure determinations would be desirable to establish the position of the new phases in the crystal chemistry of the rare earth sulfates.

4.2.3. *Structures of the binary rare earth sulfates*

The first X-ray diffraction study to establish unambiguously the coordination around the lanthanide ion was carried out for $Ce_2(SO_4)_3 \cdot 9H_2O$ at the end of the 1960's (Dereigne and Pannetier, 1968). The results were extraordinary, as they indicated the presence of two crystallographically independent highly coordinated cerium ions, 12-coordinated exclusively by sulfate oxygen atoms and the other

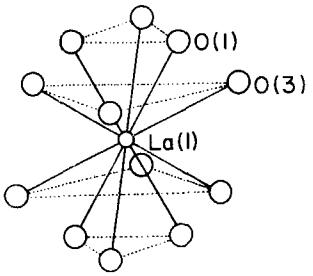

Fig. 57. The coordination around La^{3+} in the structure of $La_2(SO_4)_3 \cdot 9H_2O$, isostructural with the cerium compound (Gebert Sherry, 1976).

9-coordinated by six water molecules and three sulfate oxygens in a trigonal prismatic arrangement. The remaining three water molecules were held in the structure by hydrogen bonds. Figure 57 depicts the coordination around La^{3+} in the isostructural $La_2(SO_4)_3 \cdot 9H_2O$ (Gebert Sherry, 1976).

As summarized in table 6, X-ray studies have established the structures of all stable sulfate hydrates as well as those of the anhydrous phase. The table indicates that, in the case of the octahydrate structure (Pr $\cdots$ Lu, Y), several structural determinations have been performed over the years. Following the first, incomplete analysis by Fitzwater and Rundle (1952), Aslanov et al. (1972) established the octacoordination around Nd^{3+}, and later analyses of variable accuracy performed on the isostructural compounds agree on that as well as on many other structural details. Apparently still unsettled is the proper space group: C2/c or Cc. Most authors have preferred the centrosymmetric one, but Gebert Sherry (1976), while determining the structure of $Pr_2(SO_4)_3 \cdot 8H_2O$, performed a piezoelectric test for the Nd, Eu, Gd, Tb, Dy, and Ho compounds and observed a strong to weak effect. The results for Pr were ambivalent, since the fresh, clear crystals showed conductance and those kept in air did not. Gebert Sherry also tested the C2/c possibility, but preferred the noncentrosymmetric choice even though it gave some unsatisfactory S–O bond lengths with large standard deviations.

In the structure of $R_2(SO_4)_3 \cdot 8H_2O$ (R = Pr $\cdots$ Lu, Y), as well as of $Ce_2(SO_4)_3 \cdot 4H_2O$ (Dereigne et al., 1972), all water molecules are coordinated to the central ion. This is not the case in the structures of $La_2(SO_4)_3 \cdot 8H_2O$ (Aslanov et al., 1973b) and $Nd_2(SO_4)_3 \cdot 5H_2O$ (Larsson et al., 1973), where part of the water molecules remain outside the coordination sphere of the R^{3+} ion and are kept in the structure by hydrogen bonds. In particular, the "noncoordinated" water molecule in $Nd_2(SO_4)_3 \cdot 5H_2O$ seems to be tightly bound in a suitable hole of the structure (cf. figs. 58 and 59).

When the structures are arranged according to coordination number (as in table 9, section 4.4.1; this table also includes data for the ternary or double sulfates to be discussed in section 4.4), a trend becomes apparent. The highest coordination numbers (CN) are found for La and Ce, which have in all cases CN = 9; moreover, the compound $R_2(SO_4)_3 \cdot 9H_2O$ (R = La, Ce) has a second coordina-

TABLE 6
Summary of structure determinations of binary R^{3+} sulfates.

Compound	Cell parameters					Z	Space group	R-value (%)	Reference
	a (Å)	b (Å)	c (Å)	β (deg)	γ (deg)				
$La_2(SO_4)_3 \cdot 8H_2O$	6.898	17.366	9.554	133.8		2	$P2_1/c$	12.6	Aslanov et al., 1973b
$La_2(SO_4)_3 \cdot 9H_2O$	10.98		8.13			2	$P6_3/m$	24.0	Hunt et al., 1954
$La_2(SO_4)_3 \cdot 9H_2O$	11.009		8.076			2	$P6_3/m$	6.3	Gebert Sherry, 1976
$Ce_2(SO_4)_3 \cdot 4H_2O$	13.390	7.247	18.328	134.20		4	$P2_1/c$		Dereigne et al., 1972
$Ce_2(SO_4)_3 \cdot 5H_2O$	15.732	10.361	9.612		119.75	4	B2/b	13.5	Ahmed Farag et al., 1973a
$Ce_2(SO_4)_3 \cdot 9H_2O$	10.997		8.018			2	$P6_3/m$	18.3	Dereigne and Pannetier, 1968
$Pr_2(SO_4)_3 \cdot 8H_2O$	13.675	6.832	18.426	102.8		4	Cc	4.7	Gebert Sherry, 1976
$Pr_2(SO_4)_3 \cdot 8H_2O$	13.694	6.803	18.061	102		4	C2/c	12	Ahmed Farag et al., 1981
$Nd_2(SO_4)_3$	21.72	6.904	6.673		109.78	4	B2/b	4.6	Sirotinkin et al., 1977a
$Nd_2(SO_4)_3 \cdot 5H_2O$	15.702	9.586	10.262	120.05		4	C2/c	6.9	Larsson et al., 1973
$Nd_2(SO_4)_3 \cdot 8H_2O$	13.76	7.20	18.65	102		4		22	Fitzwater and Rundle, 1952
$Nd_2(SO_4)_3 \cdot 8H_2O$	13.65	18.42	6.80		102.1	4	B2/b	10.6	Aslanov et al., 1972
$Sm_2(SO_4)_3 \cdot 8H_2O$	13.43	6.72	18.13	102.8		4	C2/c	12.4	Podberezskaya and Borisov, 1976
$Ho_2(SO_4)_3 \cdot 8H_2O$	13.42	6.69	18.19	102.10		4	C2/c	7.5	Mascarenhas and Folgueras, 1975
$Er_2(SO_4)_3$	12.442	9.001	9.837			4	Pbcn	8.6	Sirotinkin et al., 1981
$Yb_2(SO_4)_3 \cdot 8H_2O$	13.417	6.642	18.110	101.98		4	C2/c	4.2	Hiltunen and Niinistö, 1976a

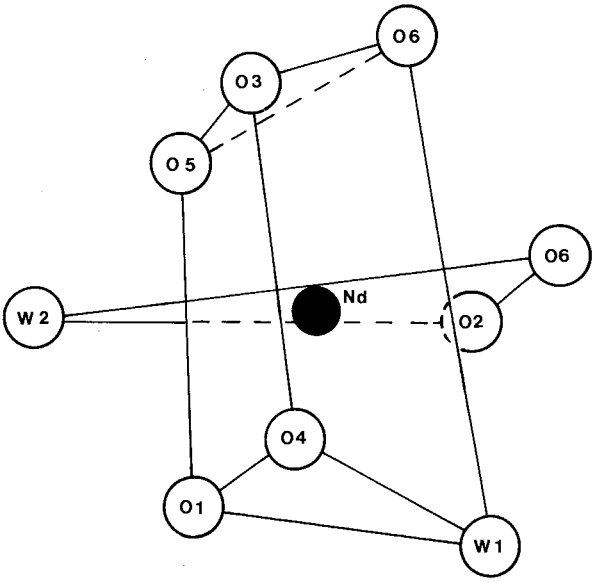

Fig. 58. The coordination around Nd^{3+} in the structure of $Nd_2(SO_4)_3 \cdot 5H_2O$ (Larsson et al., 1973).

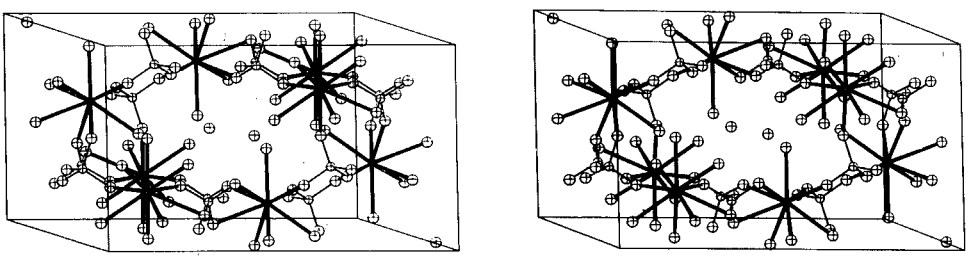

Fig. 59. The unit cell contents of $Nd_2(SO_4)_3 \cdot 5H_2O$ (Larsson et al., 1973).

tion site with an unusually high CN of 12. The anhydrous $Er_2(SO_4)_3$, on the other hand, has a CN of 6, which is exceptionally low for a rare earth other than scandium. Although many of the structural details are not very accurate, owing to the insufficient number of reflections and poor crystal quality, it seems that $R_2(SO_4)_3$ (R = Tb $\cdots$ Lu, Y) is isostructural with β-LiLu$(SO_4)_2$ (Sirotinkin et al., 1981). The other anhydrous sulfates fall into two structural groups, lanthanum belonging to the first group and Ce $\cdots$ Gd to the second (Sirotinkin and Pokrovskii, 1982a). The division between the groups is somewhat idealized because high and low temperature polymorphs exist (Gmelin, 1981b). The structure of $Nd_2(SO_4)_3$ has been solved (Sirotinkin et al., 1977a) but only indexed powder data [$a = 18.897(5)$ Å, $b = 8.948(5)$ Å, $c = 12.399(4)$ Å, $\gamma = 115.43(3)°$, space group Bb or B2/b] are available for $La_2(SO_4)_3$ (Sirotinkin and Pokrovskii, 1982a).

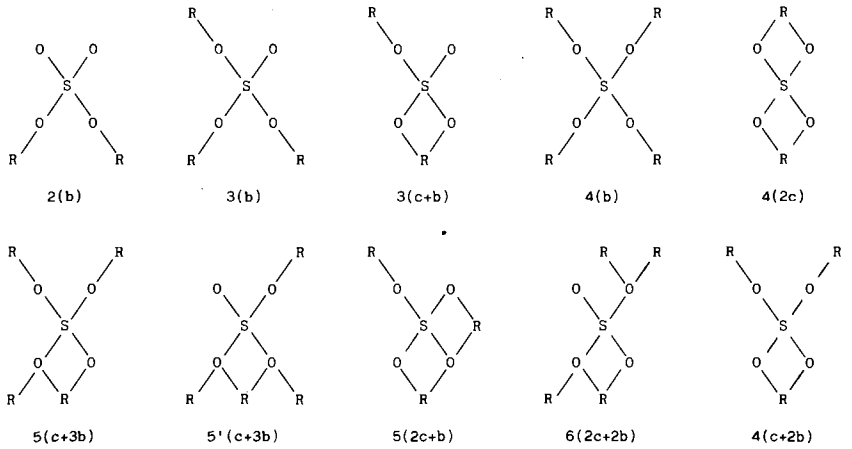

Fig. 60. Different coordination modes of the sulfato ligand in rare earth sulfate structures (after Ponomarenko et al., 1978).

In all structures the coordination polyhedron around the central R^{3+} ion is a distorted or intermediate form of the idealized geometric possibilities (cf. fig. 58). This is understandable in the light of the different ligands present (SO_4 and H_2O) and the different bonding modes which the sulfato group exhibits. Ponomarenko et al. (1978) have compared the coordination modes of sulfate groups in rare earth sulfate structures, including some urea-substituted hydrates, and classified the coordination types into 10 classes (fig. 60). Usually, two or more bonding types are present in a sulfate structure: for instance in $R_2(SO_4)_3 \cdot 8H_2O$ ($Pr \cdots Lu, Y$) the types are 2(b) or 3(b).

Finally, it is interesting to note the similarities between the structural chemistries of the lanthanides and actinides. Crystal structure determinations of $Am_2(SO_4)_3 \cdot 8H_2O$ (Burns and Baybarz, 1972) and $U_2(SO_4)_3 \cdot 9H_2O$ (Bullock et al., 1980) have shown that these compounds are isostructural with $R_2(SO_4)_3 \cdot 8H_2O$ ($R = Pr \cdots Lu, Y$) and $R_2(SO_4)_3 \cdot 9H_2O$ ($R = La, Ce$), respectively.

4.3. *Properties of the binary rare earth sulfates*

Besides their preparation and X-ray crystal structures, studies have been made on several other aspects of the rare earth sulfates, both physical and chemical. Here we shall focus on the vibrational spectra and thermal properties and make only brief mention of the other properties.

4.3.1. *Vibrational spectra*

Vibrational spectra have been reported in the literature for both hydrated and anhydrous rare earth sulfates. Thus, Petrov et al. (1967) have recorded and

discussed the IR spectra for the isostructural series $R_2(SO_4)_3 \cdot 5H_2O$ (R = La $\cdots$ Nd) and the Raman spectrum for $Ce_2(SO_4)_3 \cdot 5H_2O$. The same group (Petrov et al., 1970) has also studied the more highly hydrated sulfates $La_2(SO_4)_3 \cdot 9H_2O$ and $R_2(SO_4)_3 \cdot 8H_2O$ (R = La, Nd $\cdots$ Lu, Y), including deuterated $Nd_2(SO_4)_3 \cdot 8D_2O$. An attempt was made to correlate the spectra of $La_2(SO_4)_3 \cdot 9H_2O$ and $La_2(SO_4)_3 \cdot 8H_2O$ with the crystal structures; for the latter compound, however, only space group information was available.

The most comprehensive study on hydrated and anhydrous rare earth sulfates is that carried out by Postmus and Ferraro (1968), who also covered the far-IR region up to 80 cm^{-1}. Sulfates of stable rare earths were included in the study as octahydrates (or other higher hydrates obtained by crystallization), dihydrates, and anhydrous salts. The latter two phases were obtained respectively by partial and total dehydration of the octahydrates. Deuterated compounds were also prepared.

In the hydrated sulfates, the O–H stretching vibrations are present in the 3080–3500 cm^{-1} region and the bending vibrations around 1640 cm^{-1}. The absorptions in the 800–400 cm^{-1} region can be assigned to sulfate ν_4 vibrations and vibrational modes of coordinated water (fig. 61) and those in the 170–300 cm^{-1} region to various types of $\nu_{(OH\cdots O)}$ vibrations.

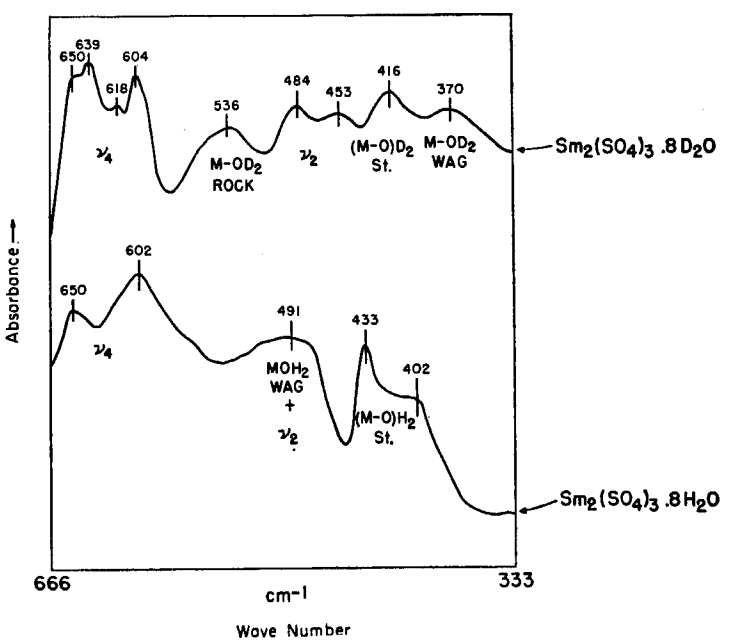

Fig. 61. A comparison of the spectra of $Sm_2(SO_4)_3 \cdot 8H_2O$ and $Sm_2(SO_4) \cdot 8D_2O$ (Postmus and Ferraro, 1968).

The complex patterns appearing in the data for the sulfate fundamentals, especially for the ν_3 and ν_4 vibrations of anhydrous sulfates, indicated that they had lost their degeneracy completely, leading to a symmetry C_{2v} or less. The higher and intermediate hydrates appeared to have symmetry C_{3v}, probably C_{2v}. Table 7 lists as examples the sulfate fundamentals observed for $La_2(SO_4)_3 \cdot nH_2O$ ($n = 9, 4, 0$) and $Ho_2(SO_4)_3 \cdot nH_2O$ ($n = 8, 2, 0$). There seem especially to be differences in the spectra of the anhydrous compounds (fig. 62) and it may be that they are related to the three structure types found for these compounds (see section 4.2.3).

The IR spectra of anhydrous sulfates, prepared by dehydration at ≥500°C, have also been recorded by Lipis et al. (1971), who noted the possibility of polymorphic transitions, which could complicate the interpretation and comparison of the spectra. The IR and Raman spectra of individual sulfates have been given in the literature in several instances (Gmelin, 1981b). Abenoza et al. (1977), for example, have recorded and interpreted in detail the Raman spectra of nonahydrated and nonadeuterated lanthanum sulfate. The collection of spectra of inor-

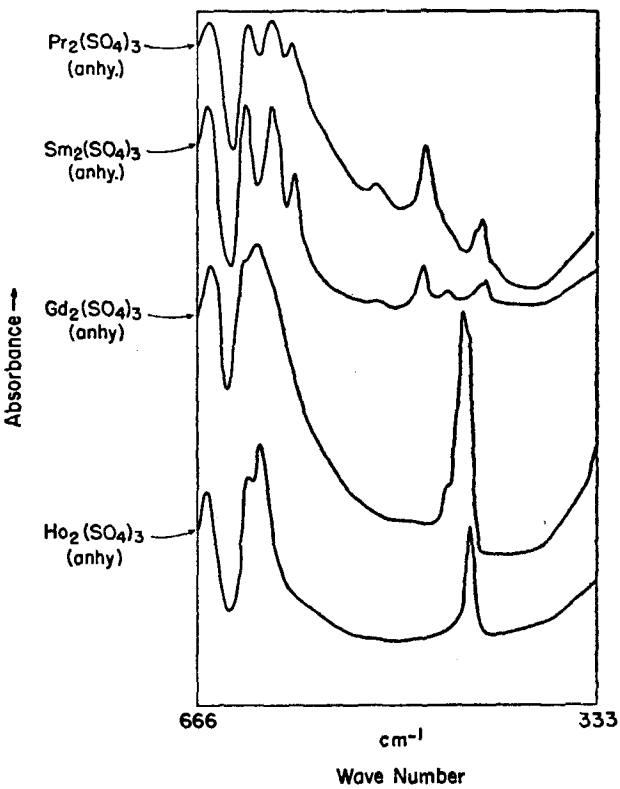

Fig. 62. A comparison of the spectra of anhydrous $R_2(SO_4)_3$ (R = Pr, Sm, Gd, Ho) in the region 666–333 cm^{-1} (Postmus and Ferraro, 1968).

TABLE 7
Observed sulfate fundamentals in the IR spectra of $R_2(SO_4)_3 \cdot nH_2O$ (R = La, Ho) (Postmus and Ferraro, 1968). *

	ν_3	ν_1	ν_4	ν_2 **
$La_2(SO_4)_3 \cdot 9H_2O$	1175 vs, 1050 vs	984 vs, sp	658 w, 645 vs 599 vs	
$La_2(SO_4)_3 \cdot 4H_2O$	1150 vs, 1115 vs 1085 sh, 1040 s	990 s	650 s, 602 s	
$La_2(SO_4)_3$	1150 s, b, 1100 sh 1050 m	1110 m	667 s, 651 s 621 s, 603 vs, 587 s	469 m, 444 vw 420 m
$Ho_2(SO_4)_3 \cdot 8H_2O$	1200 sh, 1140 vs 1085 vs	997 vs	680 sh, 651 s 607 vs	
$Ho_2(SO_4)_3 \cdot 2H_2O$	1250 sh, 1200 sh 1149 w, 1098 vs	1005 sh, 980 sh	659 s, 627 sh 608 vs, 601 sh	
$Ho_2(SO_4)_3$	1300 sh, 1240 sh 1120 s, b	not observed	657 s, 622 sh 612 vs, 558 vw	432 s

* b = broad; m = medium; s = strong; sh = shoulder; sp = sharp; vs = very strong; vw = very weak; w = weak.
** mixed with $R-OH_2$ wagging mode in higher hydrates; listed here only for the anhydrous compounds.

ganic compounds by Nyquist and Kagel (1971) contains also a number of spectra of R^{3+} sulfates recorded up to the far-IR region.

4.3.2. *Thermal decomposition*

The octahydrate series divided structurally into two parts (La $\cdots$ Ce and Pr $\cdots$ Lu, Y) provides an opportunity for comparative thermoanalytical studies in which the effects of crystal structure and central ion size are studied. The octahydrates have been widely investigated by thermoanalytical techniques. The early comprehensive studies by Wendlandt and coworkers using TG and DTA techniques (Wendlandt, 1958; Wendlandt and George, 1961; Nathans and Wendlandt, 1962) have been more recently complemented by the simultaneous TG/DTA study of Bukovec et al. (1975). These latter authors have also used DSC to determine the dehydration enthalpies. Individual rare earth sulfate hydrates have also frequently been investigated. For example, a recent study employed high-resolution luminescence spectroscopy to monitor the decomposition products of $Eu_2(SO_4)_3 \cdot 8H_2O$ during TG experiments (Brittain, 1983).

Thermal decomposition of sulfate octahydrates in air starts with dehydration and proceeds via oxysulfate to sesquioxide as the end product.

$$R_2(SO_4)_3 \cdot 8H_2O(s) \rightarrow R_2(SO_4)_3(s) + 8H_2O(g)\,, \qquad (2)$$

$$R_2(SO_4)_3(s) \rightarrow R_2O_2SO_4(s) + 2SO_3(g)\,, \tag{3}$$

$$R_2O_2SO_4(s) \rightarrow R_2O_3(s) + SO_2(g)\,. \tag{4}$$

The other sulfate hydrates, viz. the nona- and pentahydrate series, behave in a similar way, with a slight difference in the dehydration mechanism. $Ce_2(SO_4)_3 \cdot 8H_2O$ and other cerium sulfate hydrates differ by decomposing from the anhydrous sulfate directly to oxide CeO_2 without step (3). Likewise, $Sc_2(SO_4)_3 \cdot 5H_2O$ decomposes without the oxosulfate intermediate (Komissarova et al., 1965b).

The decomposition schemes and the trends observed in decomposition temperatures have been discussed to some extent by Wendlandt and coworkers and by Bukovec et al. (1975). Pokrovskii and Kovba (1976) have given decomposition temperatures for anhydrous sulfates, and more recently, Niinistö et al. (1982, 1984) have given experimental data for the complete series $R_2(SO_4)_3 \cdot 8H_2O$ (R = La $\cdots$ Lu, Y) taking into account the experimental conditions, which may influence the observed temperatures for reactions (2)–(4) markedly, in some cases by several hundred degrees (fig. 63).

As seen in figs. 64 and 65, which summarize the results for reactions (3) and (4), the temperatures for the decomposition of anhydrous $R_2(SO_4)_3$ show a U-shaped trend, whereas for reaction (4) the temperatures are descending. Figure 65 also shows that the stability range of the oxosulfate $R_2O_2SO_4$ phase becomes

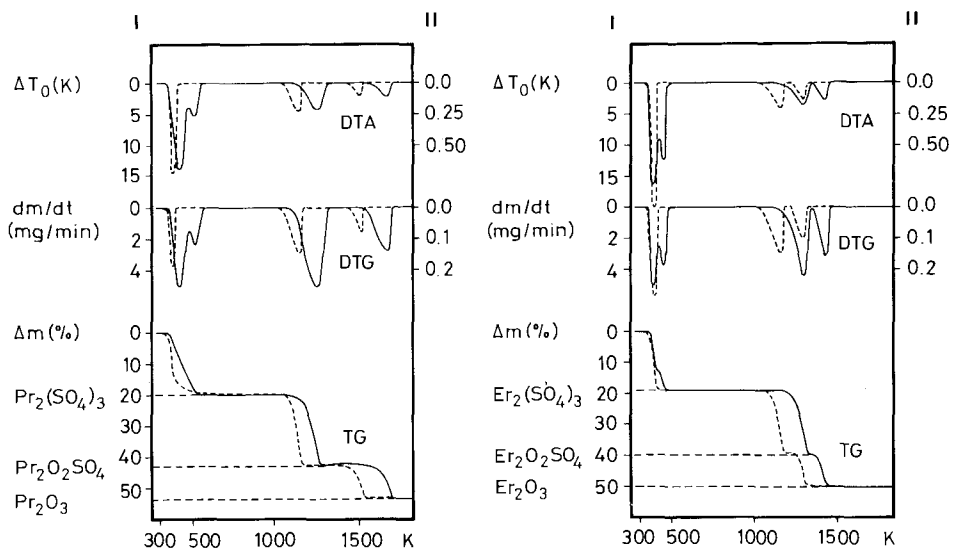

Fig. 63. TG, DTA, and DTG curves for the thermal decomposition of $R_2(SO_4)_3 \cdot 8H_2O$ (R = Pr, Er) measured in air under two different experimental conditions (Niinistö et al., 1982). (I): 200 mg, 10°C/min; (II): 20 mg, 2°C/min.

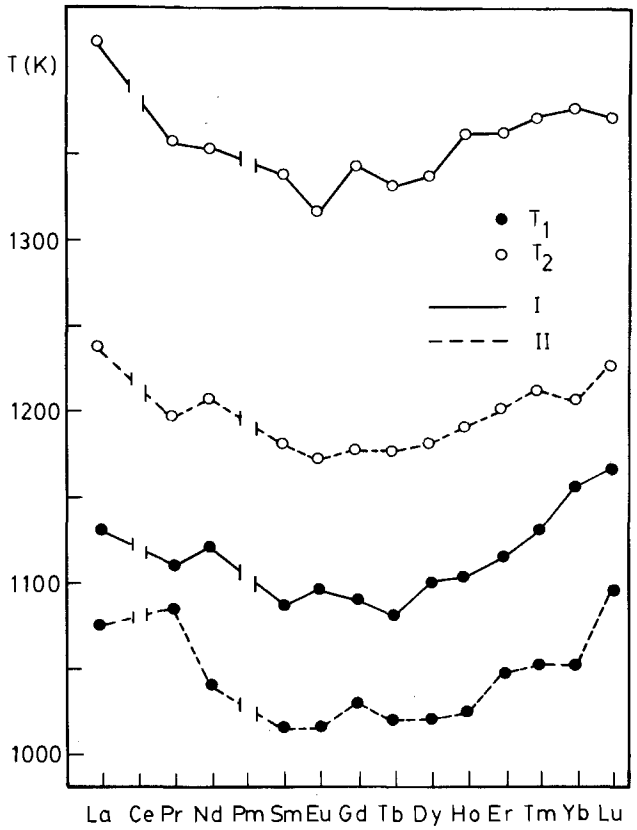

Fig. 64. The initial (T_1) and final (T_2) temperatures for the reaction $R_2(SO_4)_3(s) \rightarrow R_2O_2SO_4(s) + 2SO_3(g)$ measured under two different experimental conditions I and II (Niinistö et al., 1984).

very narrow for the heavier rare earths. The same trend has been observed for the decomposition process $R_2O_2S \rightarrow R_2O_2SO_4 \rightarrow R_2O_3$ (Leskelä and Niinistö, 1980b). In general, the decomposition temperatures for the anhydrous rare earth sulfates are high in comparison with those of sulfates of main group or transition metal elements, as Tagawa (1984) has shown in a recent comparative study.

The kinetics of dehydration and decomposition have been studied for the Pr sulfate. Bukovec et al. (1980a) found that the decomposition of anhydrous $Pr_2(SO_4)_3$ follows a linear law up to $\alpha = 0.5$. Niinistö et al. (1982) used the Coats–Redfern method for determining the apparent reaction order for the dehydration of $Pr_2(SO_4)_3 \cdot 5H_2O$. The dehydration steps are difficult to resolve owing to the limited stability of the intermediate hydrates, but the use of kinetic calculations or a quasi-isothermal heating mode (Paulik and Paulik, 1981) shows the existence of the dihydrate and monohydrate. The relation between the dehydration mechanism of $Pr_2(SO_4)_3 \cdot 5H_2O$ and its structure has been discussed (Niinistö et al., 1982) and comparisons have been made with $CsPr(SO_4)_3 \cdot 4H_2O$, which likewise has differently bound water (Bukovec et al., 1979b). Recently,

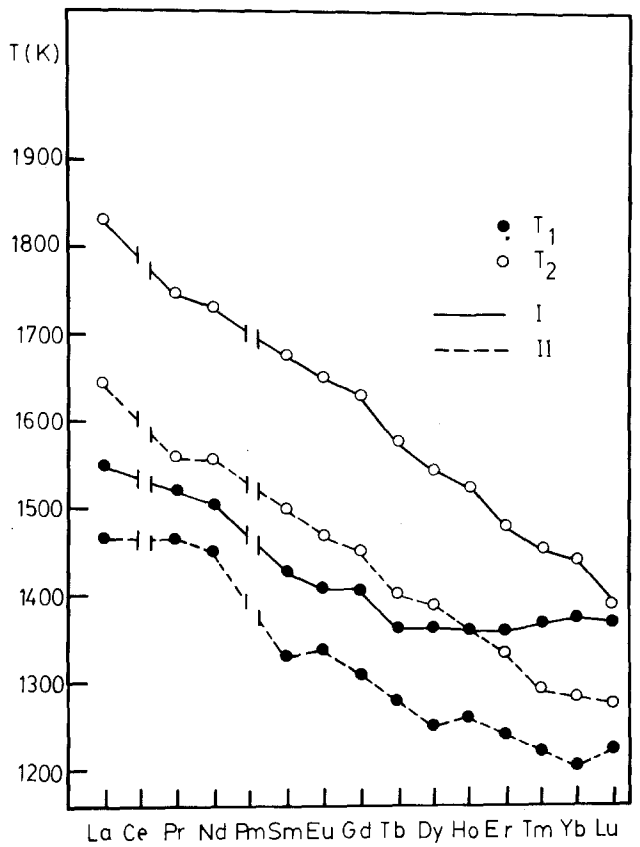

Fig. 65. The initial (T_1) and final (T_2) temperatures for the reaction $R_2O_2SO_4(s) \rightarrow R_2O_3(s)$ measured under two different experimental conditions I and II (Niinistö et al., 1984).

Martin et al. (1984) studied the kinetics of thermal dehydration of $Ce_2(SO_4)_2 \cdot n(H,D)_2O$ ($n = 5$, 8, 9). The study confirmed the earlier results (de Saja et al., 1981) on the three-step dehydration mechanism for $Ce_2(SO_4)_3 \cdot 5H_2O$ with di- and monohydrates as intermediates.

4.3.3. *Other properties and applications*

The paramagnetic properties of many R^{3+} ions have led to a large number of studies on the sulfate lattice (Gmelin, 1981b). Only a few examples can be given here. Single crystals of $R_2(SO_4)_3 \cdot 8H_2O$ doped with Gd^{3+} at 0.1% atomic level have been studied by ESR spectroscopy (Malhotra et al., 1978). Low-temperature studies indicate that two sites are present (Misra and Mikolajczak, 1979). For a detailed ESR study on Tm^{3+} (0.5%) in $Y_2(SO_4)_3 \cdot 8H_2O$, see Stöhr and Gruber (1975). $Gd_2(SO_4)_3 \cdot 8H_2O$ is also a possible magnetic refrigerant near 2 K (Pratt et al., 1977; Steyert, 1978).

Most rare earth nuclides, and especially ^{151}Eu, are suitable for Mössbauer

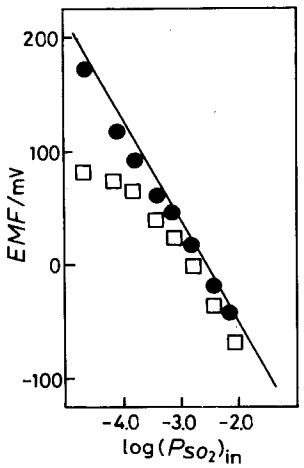

Fig. 66. The variation in EMF for Na_2SO_4–$Y_2(SO_4)_3$–SiO_2 (●) and Na_2SO_4 (□) solid electrolytes with a $NiSO_4$–NiO solid reference electrode at 973 K. The solid line has been calculated according to Gauthier and Bale (1983). (Imanaka et al., 1985.)

spectroscopic studies (Greenwood and Gibb, 1971); R^{3+} sulfates and $EuSO_4$ have been studied by this technique. According to Ehnholm et al. (1970), ^{151}Eu in $EuSO_4$ shows a very large isomer shift of (14.5 ± 0.1) mm/s (compared with Eu^{3+} in Sm_2O_3).

With the exception of cerium, which will be discussed in section 4.6, the applications of rare earth sulfates are few in number. $Y_2(SO_4)_3$–Na_2SO_4(I) solid solutions show ionic conductivity (Höfer et al., 1978) and very recently an interesting application of this solid electrolyte system was described by Imanaka et al. (1985) for the detection of SO_2 gas. The addition of $Y_2(SO_4)_3$ to a Na_2SO_4–SiO_2 system improves the EMF characteristics considerably (fig. 66).

The anhydrous sulfates are not very satisfactory luminescent materials but oxosulfates $R_2O_2SO_4$ prepared from them have been studied as possible phosphor host materials (Haynes and Brown, 1968; Porcher et al., 1983). See also section 4.6.

4.4. *Ternary rare earth sulfates*

A large number of compounds can be prepared in the system M_2SO_4–$R_2(SO_4)_3$–H_2O by varying the concentrations, excess of acid, and temperature. As examples of ternary phase diagrams, the investigations by Schröder (1938) may be mentioned (fig. 56). Examples of more recent aqueous equilibrium studies include phase diagrams of $Gd_2(SO_4)_3$–M_2SO_4–H_2O systems at 25–100°C, where M^+ is an alkali or ammonium ion (Shevchuk et al., 1981; Storozhenko et al., 1981; Storozhenko and Shevchuk, 1981). Equilibria at higher temperatures (150–200°C) have also been investigated (e.g., Belokoskov et al., 1975b; Bondar et al., 1982a). Likewise, anhydrous compounds can be prepared from melts or sintering in the system M_2SO_4–$R_2(SO_4)_3$, where M is usually a monovalent alkali ion.

The structures of the ternary rare earth sulfates were unknown until the beginning of the 1970's, when the first X-ray determinations were made for $NH_4Sm(SO_4)_2 \cdot 4H_2O$ (Niinistö, 1973; Eriksson et al., 1974) and for $K_6Pr_4(SO_4)_9 \cdot 8H_2O$ (Ahmed Farag et al., 1973b). Data on solubilities, crystal habits, and thermal stabilities have been available much longer, since the compounds have been used for the separation and purification of rare earths both in the laboratory (Pearce et al., 1946a) and in industry (Callow, 1967).

4.4.1. *Lithium compounds*

With the exception of $LiSc(SO_4)_2 \cdot 2H_2O$ (Komissarova et al., 1970c) the known lithium compounds are anhydrous. Sirotinkin et al. (1976a,b) have carried out a detailed study on the system Li_2SO_4–$R_2(SO_4)_3$ (R = Pr · · · Lu), and found by powder diffraction studies three structural types for $LiR(SO_4)_2$: (a) Pr, (b) Nd · · · Er, and (c) Tm · · · Lu. There is a polymorphism of forms and, for example, the high-temperature modification of $LiNd(SO_4)_2$ (α-form) is isostructural with $LiPr(SO_4)_2$.

The crystals of $LiPr(SO_4)_2$ are monoclinic, with space group $P2_1/b$ (Sirotinkin et al., 1978a). Tetragonal lattice parameters have been assigned for the second structure type, but complete structural determination of $LiEu(SO_4)_2$ by single-crystal methods revealed it to be orthorhombic, with space group Pnn2 (Sirotinkin et al., 1977b). $LiLu(SO_4)_2$, which also crystallizes in the orthorhombic system, has been determined as an example of the third type (see table 8). In the series $LiPr(SO_4)_2$–$LiEu(SO_4)_2$–$LiLu(SO_4)_2$, representing the three structure types, the coordination number changes from 9 through 8 to 6 (table 9).

As well as the crystal structures, Sirotinkin et al. (1976a) have studied the thermal decomposition of $LiR(SO_4)_2$, which proceeds as follows with the evolution of SO_2 and oxygen:

$$LiR(SO_4)_2 \rightarrow \text{melt} \rightarrow R_2(SO_4)_3 \rightarrow \text{melt} \rightarrow R_2O_2SO_4 \rightarrow \text{melt} + R_2O_3 \,. \qquad (5)$$

The temperatures of incongruent melting of $LiR(SO_4)_2$ vary from 720°C (Pr) through a maximum at 788°C (Gd) to 655°C (Lu). The thermal behavior of $LiR(SO_4)_2$ under a high pressure (60–90 kbar) has recently been studied by the same group (Sirotinkin and Pokrovskii, 1982b).

4.4.2. *Sodium compounds*

Although the observed stoichiometries are limited to $NaR(SO_4)_2 \cdot nH_2O$ (n = 0, 1) and $Na_3Sc(SO_4)_3 \cdot 5H_2O$, several different structure types are represented among the sodium sulfatometallates(III).

According to Chizhov et al. (1980) the anhydrous series $NaR(SO_4)_2$ can be divided on the basis of the structures into five subgroups: (a) La, Ce; (b) Pr · · · Gd; (c) β-Tb; (d) α-Tb · · · Er, Y; and (e) Tm · · · Lu. The crystal structures have been solved for the representatives of all subgroups but (c) and (e) (see table

TABLE 8
Summary of structure determinations of ternary R^{3+} sulfates.

Compound	Cell parameters						Z	Space group	R-value (%)	Reference
	a (Å)	b (Å)	c (Å)	α (deg)	β (deg)	γ (deg)				
Lithium compounds:										
$LiPr(SO_4)_2$	13.69	7.005	6.692			105.25	4	$P2_1/b$	6.4	Sirotinkin et al., 1978a
$LiEu(SO_4)_2$	7.632	5.566	5.566				2	Pnn2	5.0	Sirotinkin et al., 1977b
$LiLu(SO_4)_2$	12.575	9.051	9.138				6	Pbcn	7.6	Sirotinkin et al., 1981
Sodium compounds:										
$NaLa(SO_4)_2$	7.081	6.765	6.465	102.25	91.20	76.71	2	$P\bar{1}$	2.9	Chizhov et al., 1981
$NaNd(SO_4)_2$	6.960	6.342	7.215	96.30	98.95	90.93	2	$P\bar{1}$	5.5	Sirotinkin et al., 1978b
$NaEr(SO_4)_2$	4.673	9.575	6.861			96.71	2	$P2_1/b$	6.6	Sirotinkin et al., 1978b
α-$NaTm(SO_4)_2$	4.669	10.143	6.837			110.40	2	$P2_1/m$	6.0	Chizhov et al., 1982
$NaCe(SO_4)_2 \cdot H_2O$	7.0134		12.920				3	$P3_121$	4.7	Lindgren, 1977d
Potassium compounds:										
$KPr(SO_4)_2$	6.94	5.39	8.47	91.46	93.85	88.55	2	$P\bar{1}$	4.8	Degtyarev et al., 1978a
$KNd(SO_4)_2$	6.919	5.307	9.053	92.06	96.87	90.80	2	$P\bar{1}$		Degtyarev et al., 1977a,b
$KEr(SO_4)_2$	5.435	13.342	8.738		92.80		4	$P2_1/n$	4.4	Sarukhanyan et al., 1985a
$K_3Yb(SO_4)_2$	10.39	8.99	14.65			124.25	4	Bb	5.8	Degtyarev et al., 1978b
$KTb(SO_4)_2 \cdot H_2O$	10.18	10.35	8.38			120	4	$P2_1/b$	11.2	Lyutin et al., 1974
$KLu(SO_4)_2 \cdot 2H_2O$	10.583	7.748	10.014		97.36		4	$P2_1/c$	5.1	Sarukhanyan et al., 1985b
$K_6Pr_4(SO_4)_9 \cdot 8H_2O$	18.48	31.26	6.95			101.6	4	B2/b	11	Ahmed Farag et al., 1973b
Rubidium compounds:										
$RbEu(SO_4)_2$	13.483	5.372	9.444		102.40		4	C2/c	2.7	Sarukhanyan et al., 1983
$RbDy(SO_4)_2$	9.427	13.101	5.316				4	Pnna	3.2	Sarukhanyan et al., 1984d
$RbLu(SO_4)_2$	8.772	5.083	7.590		95.7		2	$P2_1/c$	3.7	Sarukhanyan et al., 1984b
$RbGd(SO_4)_2 \cdot H_2O$	10.265	8.370	10.443		119.49		4	$P2_1/c$	3.3	Sarukhanyan et al., 1984a
$RbHo(SO_4)_2 \cdot H_2O$	10.361	17.775	8.320			149.90	4	$P2_1/b$	3.7	Prokofev, 1981
$RbHo(SO_4)_2 \cdot H_2O$	10.210	8.298	10.404		119.63		4	$P2_1/c$	3.7	Sarukhanyan et al., 1984a
$RbYb(SO_4)_2 \cdot H_2O$	10.124	8.255	10.333		119.82		4	$P2_1/c$	6.5	Sarukhanyan et al., 1984a
$RbPr(SO_4)_2 \cdot 4H_2O$	6.622	18.997	8.740		96.16		4	$P2_1/c$	3.2	Iskhakova et al., 1981a

Cesium compounds:										
$CsLa(SO_4)_2$	7.929	5.483	17.153		91.46		4	$P2_1/n$	6.6	Bukovec et al., 1980c
$CsPr(SO_4)_2$	9.497	14.106	5.457				4	Pnna	2.3	Bukovec et al., 1978
$Cs_3Yb(SO_4)_3$	16.04		9.479				6	R3c	4.7	Samartsev et al., 1980a
$CsLa(SO_4)_2 \cdot 4H_2O$	6.734	8.874	19.16			94.13	4	$P2_1/b$	11.3	Safyanov et al., 1975
$CsPr(SO_4)_2 \cdot 4H_2O$	6.671	19.054	8.839		94.55		4	$P2_1/c$	2.0	Bukovec and Golič, 1975
$CsLu(SO_4)_2 \cdot 4H_2O$	6.670	18.497	8.637		94.23		4	$P2_1/c$	3.9	Bukovec et al., 1979b
Ammonium compounds:										
$NH_4La(SO_4)_2$	7.138	5.425	9.317		98.85		2	$P2_1/m$	2.7	Sarukhanyan et al., 1984c
$NH_4Sm(SO_4)_2 \cdot 4H_2O$	6.582	18.886	8.736		96.88		4	$P2_1/c$	4.6	Eriksson et al., 1974
$(NH_4)_5La(SO_4)_4$	8.109	9.491	12.280	83.22	70.71	69.66	2	$P\bar{1}$	5.4	Niinistö et al., 1980a
$(NH_4)_5Pr(SO_4)_4$	8.061	22.976	9.431		109.71		4	Cc	2.5	Iskhakova et al., 1981b
$(NH_4)_6Tb_4(SO_4)_9 \cdot 2H_2O$	9.008	18.323	21.39		95.33		4	C2/c	5.8	Iskhakova et al., 1985
Other compounds:										
$(H_3O)Ce(SO_4)_2 \cdot H_2O$	9.359	9.926	8.444		96.53		4	$P2_1/n$	4.7	Gatehouse and Pring, 1981
$TlPr(SO_4)_2 \cdot H_2O$	7.153	11.725	10.416		95.25		4	$P2_1/n$	3.8	Iskhakova and Trunov, 1985
$TlLa(SO_4)_2 \cdot 2H_2O$	7.216	11.853	10.486		92.05		4	$P2_1/n$	3.5	Kaučič et al., 1985

TABLE 9

The crystal structures of rare earth sulfates arranged according to the coordination number (CN) of the R^{3+} ion. The isostructural relationships are given in brackets and in footnotes. For references, see tables 6 and 8.

CN = 6:		**CN = 9:**	
$Er_2(SO_4)_3$	(Tb–Lu, Y)	$Nd_2(SO_4)_3$	(Ce–Gd)
$Sc_2(SO_4)_3 \cdot 5H_2O$	[a]	$Ce_2(SO_4)_3 \cdot 4H_2O$	[d]
$LiLu(SO_4)_2$	(Tm–Lu)	$Nd_2(SO_4)_3 \cdot 5H_2O$	(La–Nd)
$Cs_3Yb(SO_4)_3$	(Tm–Lu)	$La_2(SO_4)_3 \cdot 8H_2O$	(La, Ce) [d]
		$Ce_2(SO_4)_3 \cdot 9H_2O$	(La, Ce)[e]
CN = 7:		$LiPr(SO_4)_2$	(La–Pr) [f]
$K_3Yb(SO_4)_3$	[Nd(β-form)–Lu, Y]	$NaNd(SO_4)_2$	(Pr–Gd)
		$NaCe(SO_4)_2 \cdot H_2O$	
CN = 8:		$K_6Pr_4(SO_4)_9 \cdot 8H_2O$	[g]
		$NH_4La(SO_4)_2$	(La–Pr)
$Nd_2(SO_4)_3 \cdot 8H_2O$	(Pr–Lu, Y)	$NH_4Sm(SO_4)_2 \cdot 4H_2O$	(La–Tb)
$LiEu(SO_4)_2$	(Nd–Er)	$(NH_4)_6Tb_4(SO_4)_9 \cdot 2H_2O$	[h]
$NaTm(SO_4)_2$	(Tm–Lu)	$CsLa(SO_4)_2$	
$NaEr(SO_4)_2$	[Tb(β-form)–Er, Tm(α-form)]	$(H_3O)Ce(SO_4)_2 \cdot H_2O$	
$KPr(SO_4)_2$	(La–Tb)	$TlPr(SO_4)_2 \cdot 2H_2O$	(La–Pr)
$KNd(SO_4)_2$	(Nd–Tb)		
$KEr(SO_4)_2$	(Dy–Er)	**CN = 10:**	
$KTb(SO_4)_2 \cdot H_2O$	(Gd–Lu, Y) [b]	$NaLa(SO_4)_2$	(La, Ce)
$KLu(SO_4)_2 \cdot 2H_2O$	(Ho–Lu)	$(NH_4)_5La(SO_4)_5$	
$RbEu(SO_4)_2$	(La–Tb)	$(NH_4)_5Pr(SO_4)_5$	(La–Pr)
$RbLu(SO_4)_2$	(Dy–Lu)		
$CsPr(SO_4)_2$	[c]	**CN = 12:**	
$CsLu(SO_4)_2 \cdot 4H_2O$		$La_2(SO_4)_3 \cdot 9H_2O$	(La–Ce) [e]

[a] The structure of the isostructural selenate has been determined (Valkonen et al., 1975).
[b] Isostructural with $RbHo(SO_4)_2 \cdot H_2O$ (Gd–Lu, Y).
[c] Isostructural with $RbDy(SO_4)_2$ (Pr–Er).
[d] Two coordination sites with CN = 9 each.
[e] Two coordination sites having CN = 9 and 12.
[f] Isostructural with the corresponding Rb and Cs compounds.
[g] Two coordination sites with CN = 8 each.
[h] Two coordination sites having CN = 8 and 9.

8). Similarly to the lithium structures, the coordination number of the central ion gradually decreases from ten in $NaLa(SO_4)_2$ to eight in the isostructural compounds $NaEr(SO_4)$ and α-$NaTm(SO_4)_2$.

Judging from the published powder patterns of $NaR(SO_4)_2 \cdot H_2O$ compounds (e.g., Zaitseva et al., 1964; Belousova et al., 1968; Storozhenko et al., 1983), the compounds La $\cdots$ Er, Y are probably isostructural; however, only the structure of $NaCe(SO_4)_2 \cdot H_2O$ is known (Lindgren, 1977d). It forms trigonal crystals in the acentric space group $P3_121$ (cf. table 8) and the cerium atom is nona-coordinated by eight sulfate oxygens and one water molecule (see fig. 67, and table 13, §4.5.1).

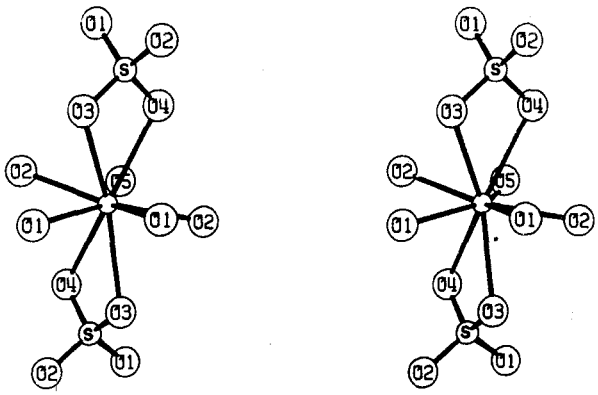

Fig. 67. The coordination around Ce^{3+} in the structure of $NaCe(SO_4)_2 \cdot H_2O$ (Lindgren, 1977d).

A preliminary report describing the crystal structure of $Na_3Sc(SO_4)_3 \cdot 5H_2O$ has appeared (Sizova et al., 1974). The crystals are hexagonal, with $a = 9.555(6)$ Å, $c = 9.915(5)$ Å, and $Z = 2$; the space group is $P6_3$ (Komissarova et al., 1971b). Scandium has an octahedral coordination as expected. The ScO_6 octahedra are joined by bridging sulfato tetrahedra resulting in an infinite column $[Sc(SO_4)_3]_n^{3n-}$. In this respect, the structure closely resembles that of $(NH_4)_3Sc(SeO_4)_3$ (Valkonen and Niinistö, 1978), see section 5.

The vibrational spectra and thermal behavior of $NaR(SO_4)_3 \cdot nH_2O$ ($n = 0, 1$) compounds have been studied, although not systematically. For instance, Lipis et al. (1970, 1971) have recorded and discussed the IR spectra for both the anhydrous and monohydrated compounds of the medium heavy lanthanides. Storozhenko (1983a) recently published the TG and DTA curves for $NaGdSO_4 \cdot H_2O$, showing incongruent fusion to take place at 857°C. The Ce(III) compound seems to behave differently upon heating (Belokoskov et al., 1975a).

Lately, there has been interest in using $NaR(SO_4)_2$ or $NaR(SO_4)_2 \cdot H_2O$ as a matrix in luminescence studies. Thus, Pilipchuk et al. (1980) made a survey of the luminescence spectra of Eu^{3+} in the $MEu(SO_4)_2$ series where $M = Li \cdots Cs$, with the intention of obtaining structural information on the environment of Eu. Brewer and Nicol (1981) studied the energy transfer from Ce^{3+} to Nd^{3+}, Ho^{3+}, and Er^{3+} in $NaR(SO_4)_2 \cdot H_2O$, while Zhiran and Blasse (1984) found for the same matrix that Ce^{3+}, Gd^{3+}, and Tb^{3+} are efficient emitters and that transfer between Gd^{3+} ions occurs with high probability.

4.4.3. *Potassium compounds*

The number of known potassium-containing phases is large, especially in the case of the anhydrous sulfates that can have nonstoichiometric composition (Gmelin, 1981b). Six types of anhydrous compounds have been prepared: $KR(SO_4)_2$, $K_3R(SO_4)_3$, $K_{6+3n}M_{4-n}(SO_4)_9$ ($n \sim 0.4$), $K_6M_4(SO_4)_9$, $K_7R_3(SO_4)_8$, and $K_5R(SO_4)_4$. Only representatives of the first two types have been structurally

characterized (see table 8), and in addition, the structure of $K_5R(SO_4)_4$ (R = La $\cdots$ Sm) is known (Trunov et al., 1977) on the basis of its being isostructural with $K_5La(MoO_4)_4$ (Efremov and Trunov, 1974).

The anhydrous $KR(SO_4)_2$-type sulfates can be synthesized by a solid-state method, and X-ray diffraction studies have shown them to have five structural subgroups along the lanthanide series: (a) La $\cdots$ Pr, (b) Nd $\cdots$ Tb, (c) Dy $\cdots$ Er, (d) Tm, and (e) Yb $\cdots$ Lu (Sarukhanyan et al., 1985a). Published X-ray powder data for La $\cdots$ Tb also show the structural break between Pr and Nd, although both groups are triclinic (Degtyarev et al., 1977a,b). Structures are known for representatives of the first three groups (table 8). Scandium forms the $KR(SO_4)_2$ phase, too, and according to powder diffraction patterns has a monoclinic unit cell isostructural with $KFe(SO_4)_2$ (Perret, 1970).

Vibrational frequencies and thermal data are available for the series $KR(SO_4)_2$ (R = Pr $\cdots$ Yb) (Vazhnov et al., 1980; Degtyarev et al., 1977a). Thermal degradation of $KR(SO_4)_2$ produces a mixture of $K_7R_3(SO_4)_8$ and $R_2(SO_4)_3$ in the case of Pr and Nd, while the heavier rare earths and Y produce the nonstoichiometric compound $K_{6+3n}R_{4-n}(SO_4)_9$ and $R_2(SO_4)_3$ (Degtyarev et al., 1977a). The decomposition temperatures for $KR(SO_4)_2$ range from 930°C (Pr) to 480°C (Lu) but Y has the lowest temperature (420°C).

There are also a large number of different structures in the series $K_3R(SO_4)_3$; for in addition to the three structural types, polymorphic transitions are possible at relatively low temperatures (Degtyarev et al., 1978c, 1980a). The IR spectra have been recorded for R = La $\cdots$ Yb (Vazhnov et al., 1983), but only the structure of the monoclinic $K_3Yb(SO_4)_3$ compound (isostructural with Tm and Lu compounds) is known from X-ray studies (table 8). The YbO_7 polyhedra form six-membered rings joined together by sulfato tetrahedra into a three-dimensional network in which three crystallographically different potassium atoms with eight (K_1), nine (K_2), or eleven (K_3) oxygens around them are incorporated into cavities (Degtyarev et al., 1978b). For a fragment of this structure, see fig. 68.

The two other structure types (La $\cdots$ Nd, Sm $\cdots$ Er, Y) similarly crystallize in the monoclinic system. Scandium forms the $K_3R(SO_4)_3$ phase, too, but probably with a different structure. Characterization of the $K_3Sc(SO_4)_3$ crystals by optical crystallography indicated monoclinic symmetry (Ivanov-Emin et al., 1966). Recently, the powder pattern of the high-temperature polymorph of $K_3Sc(SO_4)_3$ was indexed with hexagonal unit cell parameters, as part of a systematic study of the M_2SO_4–$Sc_2(SO_4)_3$ system where M = K, Rb, Cs (Korotnaya et al., 1983).

Crystal data are available for the $K_{6+3n}M_{4-n}(SO_4)_9$ ($n = \sim 0.4$) series (Degtyarev et al., 1979), and also congruent melting points, which are somewhat above 1000°C. Crystals having stoichiometric composition $K_4R_2(SO_4)_5$ have also been reported (Pospelova et al., 1970).

The complex phases $K_6R_3(SO_4)_9$ and $K_7R_3(SO_4)_8$ (Degtyarev et al., 1978c) are formed in several systems by thermally induced transformations, and in the case of $K_6R_4(SO_4)_9$ by thermal dehydration of the corresponding octahydrate

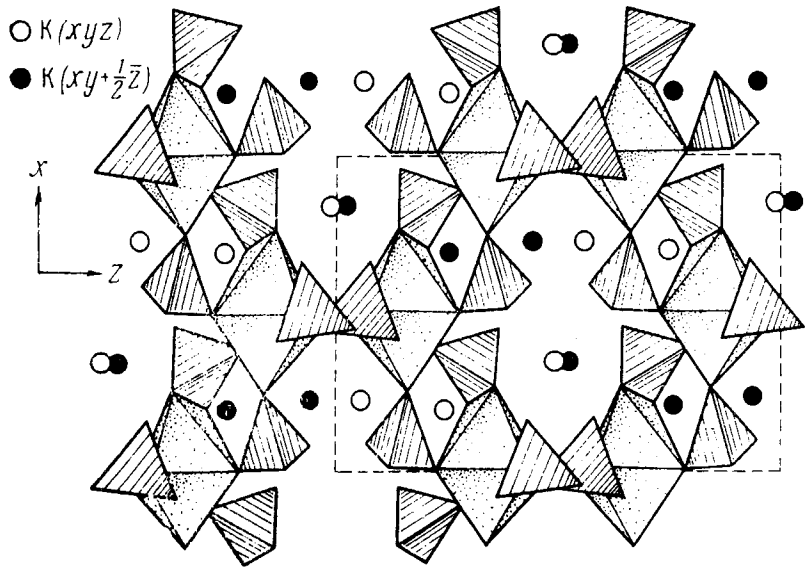

Fig. 68. A fragment of the crystal structure of $K_3Yb(SO_4)_3$ (Degtyarev et al., 1978).

(Pospelova et al., 1970). The compounds $K_6R_4(SO_4)_9$ (R = Sm···Lu, Y) are isostructural; and for $K_7R(SO_4)_3$ isostructurality extends from La to Nd, according to Degtyarev and Pokrovskii (1984), who recently studied the thermal stability of the phases. The orthorhombic unit cell for $K_7Pr_3(SO_4)_8$ is very large as $Z = 6$ (Degtyarev et al., 1980b).

$KR(SO_4)_2 \cdot H_2O$ crystallizes in the monoclinic system and the isostructural sequence may extend from La to Ho, according to Iskhakova et al. (1971), who prepared the crystals at 50°C and studied them by optical crystallography. IR spectroscopic studies were reported in another paper (Petrov et al., 1971). Thermal and thermodynamic data for the Eu compound have been reported by Ilyashenko et al. (1973). Crystal structure determination on $KTb(SO_4)_2 \cdot H_2O$ showed that the compounds are indeed monoclinic (table 8). The coordination number for Tb^{3+} has been given as 8 (Lyutin et al., 1974). The unit cell dimensions (table 8) indicate that the potassium and rubidium compounds are isostructural, as suggested by Sarukhanyan et al. (1982). The structure of $KLu(SO_4)_2 \cdot 2H_2O$ has recently been solved (Sarukhanyan et al., 1985b) and compared with the structure of $KLu(SO_4)_2 \cdot H_2O$ derived on the basis of its being isostructural with $RbGd(SO_4)_2 \cdot H_2O$ (fig. 69). See also section 4.4.4.

One of the very first structural determinations on ternary rare earth sulfates was that performed on $K_6Pr_4(SO_4)_9 \cdot 8H_2O$; unfortunately, only the abstract has been published (Ahmed Farag et al., 1973b). The structure incorporates two crystallographically different Pr atoms, each with a CN of 9 (tables 8 and 9). The main structural features predicted on the basis of the IR spectra (Petrov et al., 1971)

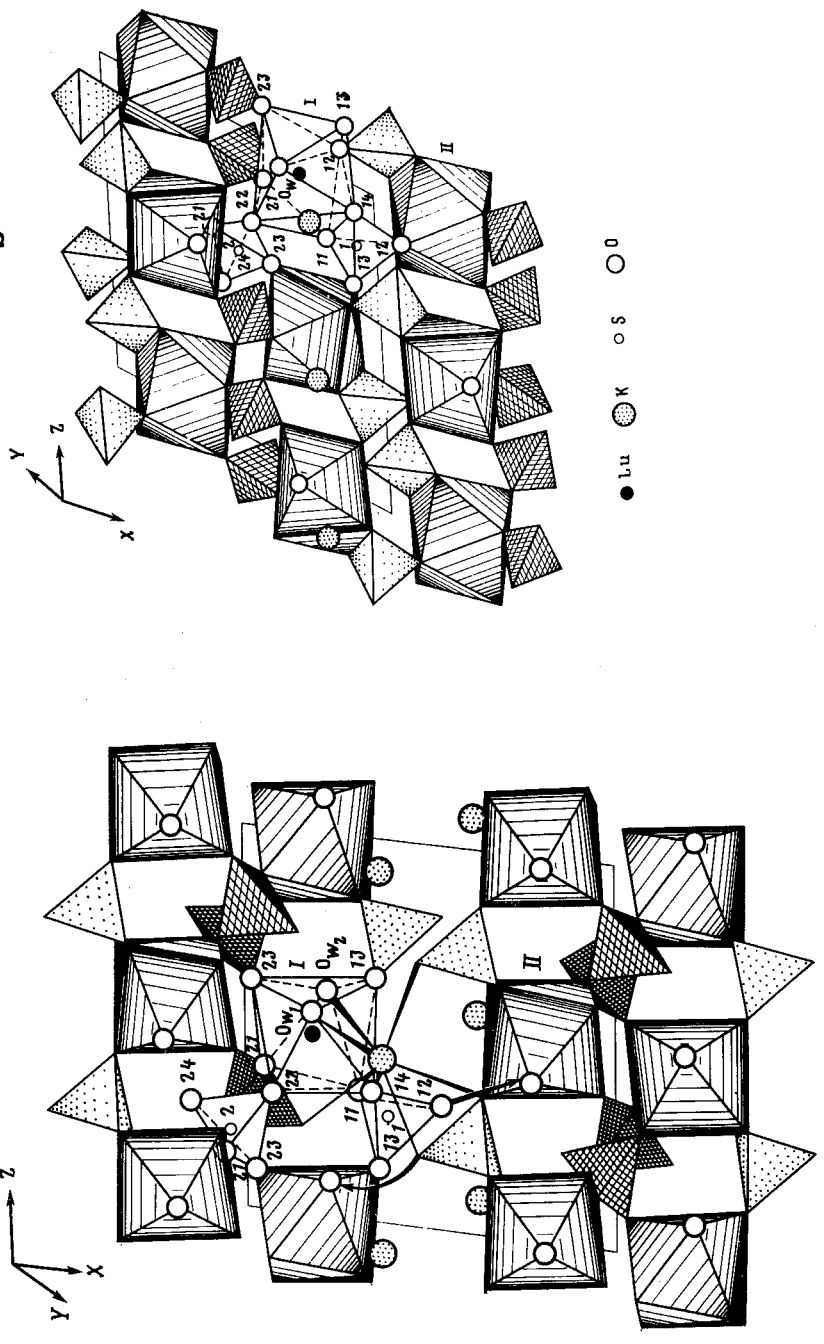

Fig. 69. A comparison of the structures of $KLu(SO_4)_2 \cdot 2H_2O$ (a) and $KLu(SO_4)_2 \cdot H_2O$ (b); both are projected on the *xz*-plane. (Sarukhanyan et al., 1985b.)

seem to be in agreement with the actual structure; the role of water molecules was not obvious from the spectra, however.

For the series $K_5R(SO_4)_4$ ($R = La \cdots Sm$), preparative details are given (Iskhakova et al., 1971) and also IR spectra (Petrov et al., 1971) and X-ray and thermal data (Trunov et al., 1977). The hexagonal unit cell dimensions are based on the isostructural relationship to $K_5La(MoO_4)_4$ and palmierite $K_2Pb(SO_4)_2$.

4.4.4. *Rubidium compounds*

Owing to the similar ionic radii of the cations, the Rb compounds are often isostructural with the potassium or ammonium sulfates, and sometimes also with Cs compounds.

Thus, in analogy with potassium sulfates, the anhydrous phases $RbR(SO_4)_2$, $Rb_3R(SO_4)_3$, $Rb_{6+3n}M_{4-n}(SO_4)_9$, and $Rb_7R_3(SO_4)_8$ can be prepared in the system Rb_2SO_4–$R_2(SO_4)_3$ (Komissarova et al., 1970b; Prokofev et al., 1979). Also known is $Rb_5R_3(SO_4)_7$ (Prokofev et al., 1979). A complete structural analysis has been carried out only for the representatives of the first series $RbR(SO_4)_2$ (cf. table 8).

The $RbR(SO_4)_2$ compounds can be prepared either by isothermal evaporation of an Rb_2SO_4–$R_2(SO_4)_3$ aqueous solution at 70°C or by a solid-state synthesis. The former method can be applied only for the lighter rare earths ($La \cdots Eu$); for with the heavier rare earths the monohydrate forms under these conditions (Sarukhanyan et al., 1982, 1984d). The recent studies by Prokofev et al. (1979) and Sarukhanyan et al. (1983, 1984b,d) have established the existence of three main structure types: (a) monoclinic ($La \cdots Tb$), (b) orthorhombic ($Pr \cdots Er$), and (c) monoclinic ($Dy \cdots Lu$). In addition, unpublished data indicate that lanthanum and cerium form still another polymorph (Prokofev, 1980). Owing to its smaller ionic size, scandium probably forms a sulfate with a different structure; and indeed a hexagonal structure has been proposed on the basis of powder diffraction patterns (Ivanov-Emin et al., 1966; Erämetsä and Haukka, 1968).

The crystal structure determination of one representative of each type (a)–(c) allows us to make a comparison between the structures (table 8).

The coordination mode of the sulfate groups and the coordination number for the lanthanide (CN = 8) remain unchanged, as does the layered type of structure. The average R–O length shortens in accordance with the ionic radii and is 2.43, 2.40, and 2.32 Å for the Eu, Dy, and Lu compounds, respectively. In the Lu compound, however, coordination polyhedron changes from the antiprism of the Eu and Dy compounds to a geometry best described as a dodecahedron (Sarukhanyan et al., 1984b) (fig. 70). It may also be noted that $RbDy(SO_4)_2$ is isostructural with $CsPr(SO_4)_2$ and the coordinates can be directly compared after a shift of origin (Bukovec et al., 1978).

For scandium, the 1:1 compound $RbSc(SO_4)_2$ can be prepared both by a solution (Komissarova et al., 1970b) and by a solid-state (Korytnaya et al., 1980)

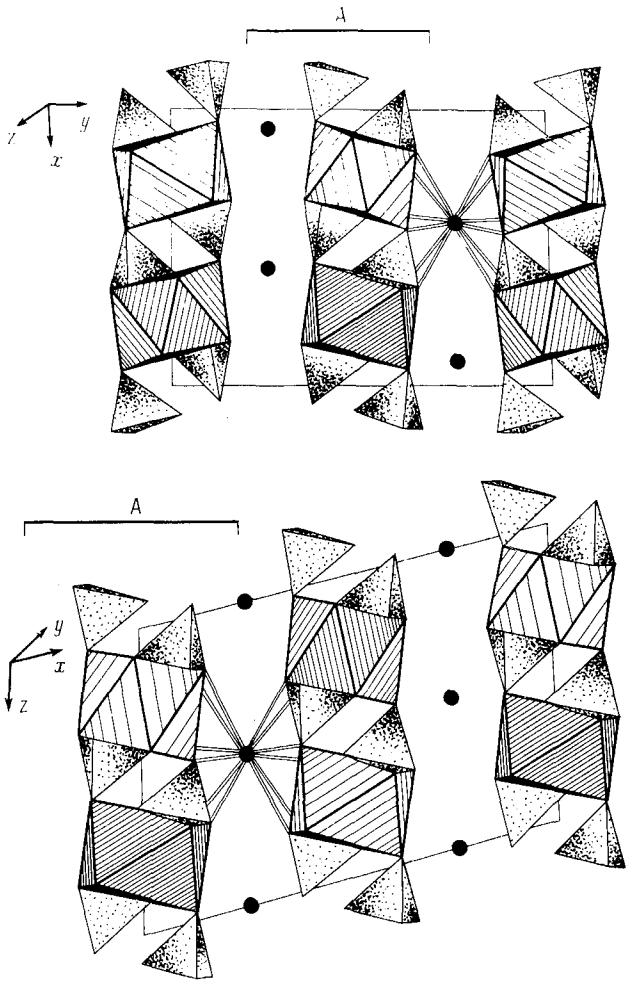

Fig. 70. A comparison of the crystal structures of $RbDy(SO_4)_2$ (above) and $RbEu(SO_4)_2$ (below) (Sarukhanyan et al., 1984d).

method. The compound forms hexagonal crystals (space group P321) with $a = 5.03$ Å and $c = 8.25$ Å (Erämetsä and Haukka, 1968).

Although the monoclinic $Rb_3Sc(SO_4)_3$ can be prepared in aqueous solution at 25°C (Komissarova et al., 1970b), the corresponding sulfates of the other rare earths have been synthesized only by a solid-state, high-temperature reaction (Samartsev et al., 1978; Prokofev et al., 1979). Several structure types and polymorphisms occur, and in some cases the unit cell dimensions and space groups have been determined. The crystal system, hexagonal, appears to be common in the lanthanide series but the space group is different in three subseries: (a) Ce···Nd ($R\bar{3}$), (b) Sm···Eu (R3c), and (c) Gd···Lu, Y (P3).

The second type is isostructural with $Cs_3R(SO_4)_3$ (R = Tm, Yb, Lu) (Samartsev et al., 1978). Scandium appears to form monoclinic crystals (Komissarova et al., 1970b).

As can be seen in fig. 71, the equilibrium diagram of the Rb_2SO_4–Gd_2O_3 system is very complicated. X-ray powder patterns are available for the anhydrous phases, and $Rb_{6+3n}Gd_{4-n}(SO_4)_9$ has been indexed with a large monoclinic (B2/b) cell (Prokofev et al., 1979). The corresponding phase equilibrium diagram of Sc (fig. 72) is much simpler and a thermoanalytical study did not reveal any polymorphic transitions but instead an incongruent melting of $RbSc(SO_4)_2$ at 950°C (Korytnaya et al., 1980).

Evaporation of an aqueous system containing Rb_2SO_4 and $R_2(SO_4)_3$ at room temperature results in the precipitation of $RbR(SO_4)_2 \cdot 4H_2O$ for all rare earths except La and Ce, which lead to the anhydrous phase (Iskhakova and Plyushchev, 1973). The heavier rare earths (Ho···Lu) do not seem to form stable compounds; for instance, $RbHo(SO_4)_2 \cdot 4H_2O$ has been reported to effloresce rapidly in air at 25°C (Pavlov-Verenkin, 1970). If the crystallization is carried out at higher temperature (70°C) the rare earths from Gd to Lu form the monohydrate phase (Sarukhanyan et al., 1982).

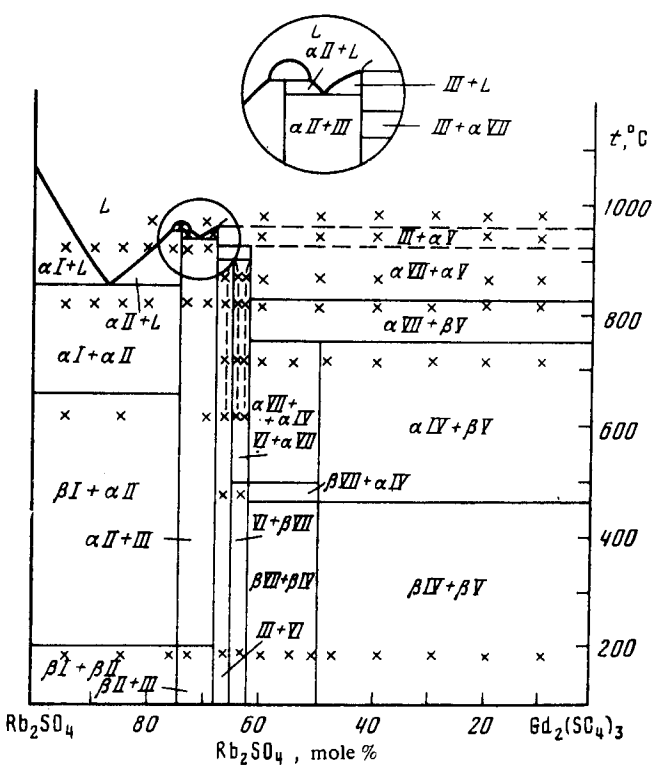

Fig. 71. A phase equilibrium diagram of the $Rb_2(SO_4)_3$–$Gd_2(SO_4)_3$ phase. (L): liquid phase; (I): Rb_2SO_4; (II): $Rb_3Gd(SO_4)_3$; (III): $Rb_{6+3n}Gd_{4-n}(SO_4)_9$; (IV): $RbGd(SO_4)_2$; (V): $Gd_2(SO_4)_3$; (VI): $Rb_4Gd_2(SO_4)_5$; (VII): $Rb_5Gd_3(SO_4)_7$. (Prokofev et al., 1979.)

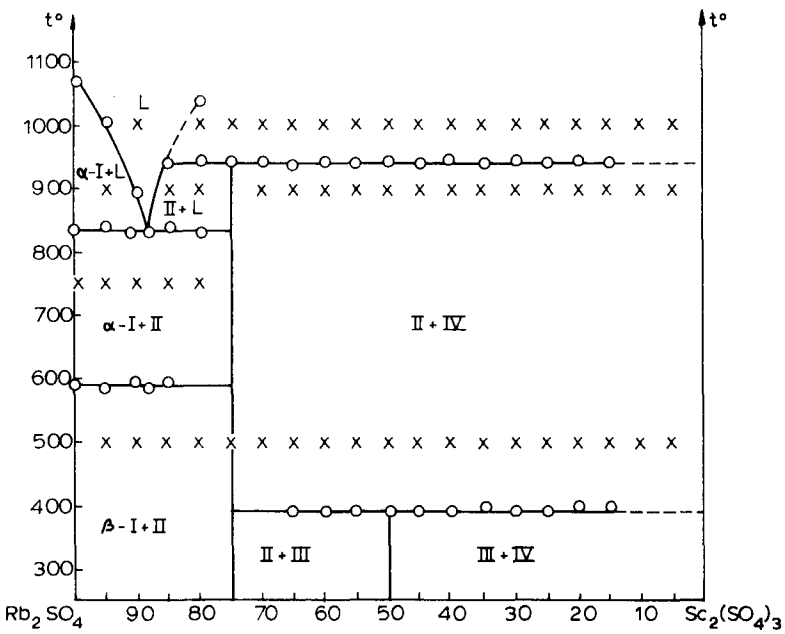

Fig. 72. A phase equilibrium diagram of the $Rb_2(SO_4)_2$–$Sc_2(SO_4)_3$ system. (I): Rb_2SO_4; (II): $Rb_3Sc(SO_4)_3$; (III): $RbSc(SO_4)_2$; (IV): $Sc_2(SO_4)_3$. × indicates points of rapid cooling. (Korytnaya et al., 1980.)

$RbR(SO_4)_3 \cdot 4H_2O$ (R = Pr · · · Tm) form isostructural crystals (Iskhakova and Plyuschev, 1973) which are also isostructural with the monoclinic ($P2_1/c$) ammonium (Erämetsä and Niinistö, 1971) and the cesium (Bukovec and Golič, 1975) compounds. Unit cell data are available for the series $RbR(SO_4)_2 \cdot 4H_2O$ (R = Pr · · · Dy) (Iskhakova et al., 1979). The crystal structure of $RbPr(SO_4)_2 \cdot 4H_2O$ has been determined and compared with that of $Pr_2(SO_4)_3 \cdot 8H_2O$ (Iskhakova et al., 1981a); for crystal-structure determinations of the isostructural NH_4 and Cs compounds, see table 8.

$RbR(SO_4)_2 \cdot H_2O$ (R = Gd · · · Lu) also form monoclinic crystals ($P2_1/c$); the structures of the isomorphous Gd, Ho, and Yb compounds have been determined (Prokofev, 1981; Sarukhanyan et al., 1984a) (table 8). The two structural determinations of the Ho compound were based on different unit cell choices but the bond lengths and other structural details are in general agreement. R^{3+} has eight oxygen atoms at distances less than 2.60 Å and the coordination polyhedron has been described as a distorted tetragonal antiprism (Sarukhanyan et al., 1984a). Prokofev (1981) considers a seven-coordinated polyhedron possible as well, because one of the R–O distances is more than 0.15 Å longer than the others. It may be noted that the $RbR(SO_4)_2 \cdot H_2O$ phase is isostructural with the

potassium compounds and $KRb(SO_4)_2 \cdot H_2O$ has been analyzed to have an eight-coordinated structure (Lyutin et al., 1974).

Considerable amounts of IR spectroscopic and thermoanalytical data are available for the Rb compounds, especially the $RbR(SO_4)_2 \cdot 4H_2O$ series (Gmelin, 1981b). Lipis et al. (1970, 1971) have studied both the tetra- and monohydrate series, using deuterated as well as normal compounds; and Iskhakova et al. (1979) have reported the spectra of $RbR(SO_4)_2 \cdot 4H_2O$ for Gd and Tb. Thermal behavior of the tetrahydrate series will be discussed in sections 4.4.5 and 4.4.6 in connection with the isostructural Cs and NH_4 compounds. For the $RbR(SO_4)_2$ compounds, investigations have been made of their IR spectra (Remizov et al., 1969; Lipis et al., 1971; Couchot et al., 1971) and thermoanalytical properties (Prokofev et al., 1979; Korytnaya et al., 1980). DTA results indicate the existence of high-temperature polymorphs for several lanthanides (Prokofev et al., 1979).

4.4.5. *Cesium compounds*

During the past few years considerable interest has been focused on the study of cesium-containing sulfates. Recent studies include phase equilibrium, X-ray diffraction, IR spectroscopic, and thermoanalytical investigations.

$CsR(SO_4)_2$ compounds are most simply prepared by dehydration of $CsR(SO_4)_2 \cdot 4H_2O$ at 300°C (Bukovec et al., 1979a, 1980d). They can also be prepared by a prolonged sintering of the 1:1 sulfate mixture at 550°C, in a process that includes grinding and compressing of disks at 50 h intervals (Samartsev et al., 1977) (fig. 73). $CsSc(SO_4)_2$ can be prepared in a similar way (Korytnaya et al., 1980, 1983), or precipitated from an aqueous solution of Cs_2SO_4 in a wide concentration range (Komissarova et al., 1970b). With use of higher temperatures, the method of precipitation from aqueous solution is also possible for the other rare earths; thus Bondar et al. (1982a) have prepared $CsCe(SO_4)_2$ at 150 and 200°C. Single crystals of $CsR(SO_4)_2$ have been prepared from melt (Samartsev et al., 1979) and from aqueous solutions of $CsR(SO_4)_2 \cdot 4H_2O$ containing sulfuric acid, at elevated temperatures (300°C) (Bukovec et al., 1978, 1980c).

$CsR(SO_4)_2$ decomposes at temperatures ranging from 795°C (Sm) to 1050°C (Y) (Samartsev et al., 1977; Korytnaya et al., 1980). Upon heating, polymorphic transitions occur in several cases around 400°C, and for Gd also at 710°C (fig. 73). The compounds crystallize in at least four structure types. The values given by various authors (table 10) are not in complete agreement, perhaps because different polymorphs have been investigated. It appears, however, that the two unit cells given for $CsLa(SO_4)_2$ are related, since the volumes differ by a factor of exactly two.

Both $CsPr(SO_4)_2$ and $CsLa(SO_4)_2$ have a layer structure, where sulfate groups join together the 8- and 9-coordinated polyhedra, respectively (Bukovec et al., 1978, 1980a). In $CsPr(SO_4)_2$, the coordination polyhedron of R^{3+} is regular, with R–O distances ranging from 2.46 to 2.59 Å, and can be described as an antiprism

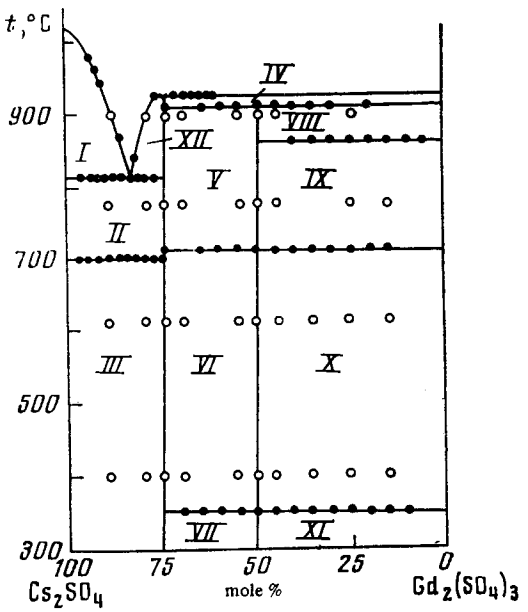

Fig. 73. A phase equilibrium diagram of the Cs_2SO_4–$Gd_2(SO_4)_3$ system. (I): L + α-Cs_2SO_4; (II): α-Cs_2SO_4 + Cs_3Gd $(SO_4)_3$; (III): β-Cs_2SO_4 + $Cs_3Gd(SO_4)_3$; (IV): $Cs_3Gd(SO_4)_3$ + α-$Gd_2(SO_4)_3$; (V): $Cs_3Gd(SO_4)_3$ + α-$CsGd(SO_4)_2$; (VI): $Cs_3Gd(SO_4)_3$ + β-$CsGd(SO_4)_2$; (VII): $Cs_3Gd(SO_4)_3$ + γ-$CsGd(SO_4)_2$; (VIII): α-$CsGd(SO_4)_2$ + α-$Gd_2(SO_4)_3$; (IX): α-$CsGd(SO_4)_2$ + β-$Gd_2(SO_4)_3$; (X): β-$CsGd(SO_4)_2$ + β-$Gd_2(SO_4)_3$; (XI): γ-$CsGd(SO_4)_2$ + β-$Gd_2(SO_4)_3$; (XII): L + $Cs_3Gd(SO_4)_3$ (Samartsev et al., 1977).

(fig. 74). In the La compound the coordination polyhedron is more irregular (La···O range: 2.48–2.80 Å) and an analysis of it has not been attempted. In both structures the Cs ions are situated between the layers (fig. 75) and have a large number of short contacts to sulfate oxygens.

A comparison of the lattice parameters and the space group of $CsSc(SO_4)_2$ with the corresponding values of $KAl(SO_4)_2$ (Manoli et al., 1970) suggests that the compounds are isostructural and thus Sc^{3+} is octahedrally coordinated, forming sulfate bridged layers. According to Korytnaya et al. (1983) the high-temperature form of α-$CsSc(SO_4)_2$ probably has a similar structure.

The tetrahydrates of $CsR(SO_4)_2$ (R = La···Lu, Y) are likewise frequently studied, and unit cell and IR data are both available (Bukovec et al., 1977). Complete structural determinations have been carried out (table 8) and confirm the isostructurality with the corresponding NH_4 (Eriksson et al., 1974) and Rb (Iskhakova et al., 1975) compounds. It is interesting that the smaller ionic size of Lu causes the coordination of sulfate groups to change slightly relative to the Pr compounds (Bukovec et al., 1979b). The unit cell size and space group are not

TABLE 10

Comparison of unit cell data for anhydrous cesium sulfates of type $CsR(SO_4)_2$ and $Cs_3R(SO_4)_3$.

Compound	Cell parameters						V (Å^3)	Crystal system	Space group	Reference
	a (Å)	b (Å)	c (Å)	α (deg)	β (deg)	γ (deg)				
$CsR(SO_4)_2$:										
La	7.944	9.532	5.359	90.65	89.60	113.68	372.3	tricl.	$P\bar{1}$	Samartsev et al., 1979
	7.929	5.483	17.153		91.46		745.5	monocl.	$P2_1/n$	Bukovec et al., 1980c
Pr	9.497	14.106	5.457				731.0	orthorh.	Pnna	Bukovec et al., 1978
	9.409	7.881	5.390			113.22	367.2	monocl.	B2	Samartsev et al., 1980b
Gd	9.408	7.746	5.366			113.23	359.3	monocl.	B2	Samartsev et al., 1980b
Yb (β-form)	9.242	7.656	5.140			95.95	361.6	monocl.	Pb *or* P2/b	Samartsev and Pokrovskii, 1982
Sc	5.107		8.705				196.6	hex.	P231	Bashkov et al., 1972
	5.090		8.682					hex.		Couchot et al., 1971
	5.095		8.725					hex.		Erämetsä and Haukka, 1968
Sc (α-form)	8.951		8.860				615	hex.		Korytnaya et al., 1983
$Cs_3R(SO_4)_3$:										
La	16.614		8.320				1984.5	hex.	$R\bar{3}$ *or* R3	Samartsev et al., 1979
Nd	15.94		9.320					hex.	$P\bar{3}c1$ *or* P3c1	Samartsev et al., 1980c
Gd	27.333	10.139	10.099		106.83		2669.1	monocl.	Cc	Shevchuk et al., 1983
Yb	16.04		9.479					hex.	R3c	Samartsev et al., 1980a

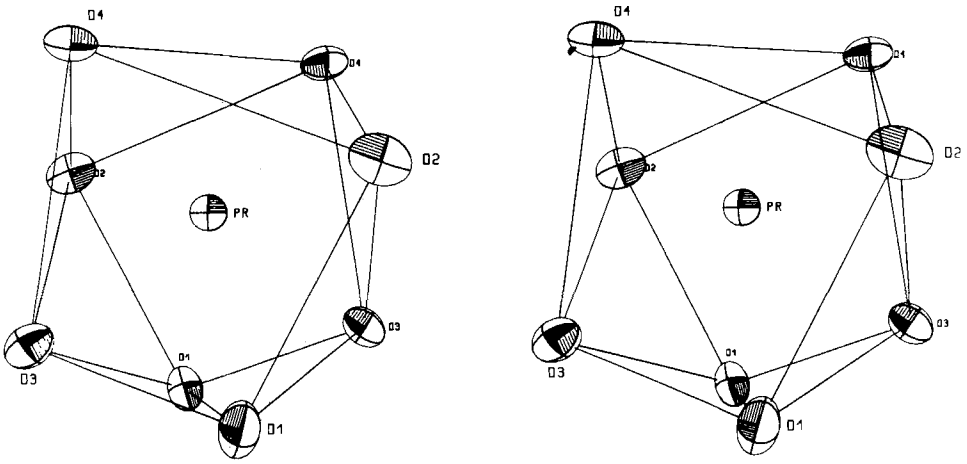

Fig. 74. The square antiprismatic coordination around Pr^{3+} in the structure of $CsPr(SO_4)_2$ (Bukovec et al., 1978).

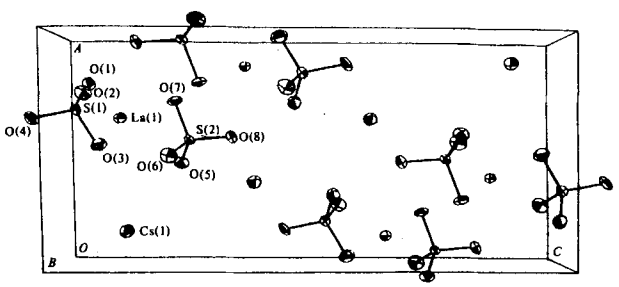

Fig. 75. A perspective view of the unit cell of $CsLa(SO_4)_2$ showing the layer-like structure (Bukovec et al., 1980a).

affected (table 8) but, evidently due to steric reasons, the S(2) sulfate group in $CsLu(SO_4)_2 \cdot 4H_2O$ is rotated, placing the oxygen atom O(8) away from the inner coordination sphere of Lu and resulting in a lower coordination number (8 versus 9 for Pr). A parallel case has been reported earlier for the structures of $(NO)_2[R(NO_3)_5]$ (R = Sc, Y), see chapter 56, section 6.4.1, of Volume 8 of this Handbook.

The thermal behavior of the $CsR(SO_4)_2 \cdot 4H_2O$ series has been studied in detail by Bukovec et al. (1979a, 1980b) and others (Iskhakova et al., 1973; Storozhenko, 1983b). Dehydration experiments indicate that stable monohydrates are formed for Pr···Gd around 100°C (Bukovec et al., 1979a). The dehydration mechanism is explained in terms of the crystal structure, where one of the water molecules is not coordinated to the lanthanide but held in the structure by

hydrogen bonds (Bukovec at al., 1979b). The mechanism of the dehydration may be compared with that of the corresponding Rb compounds, e.g., Sm (Erämetsä and Niinistö, 1971) and Dy (Zaitseva et al., 1972), where the monohydrate also appears as a stable intermediate, although the mechanism is strongly dependent on experimental conditions (Eriksson et al., 1974). In view of the suggested relationship between structure and dehydration mechanism (Bukovec et al., 1979b), it would be interesting to study, using the high-temperature X-ray diffraction method, whether or not the dehydration intermediate $CsR(SO_4)_2 \cdot H_2O$ has the same structure as the well characterized $RbR(SO_4)_2 \cdot H_2O$ phase. A comparison of the available X-ray powder patterns of $RbHo(SO_4)_2 \cdot H_2O$ (Sarukhanyan et al., 1982) and $CsNd(SO_4)_2 \cdot H_2O$ (Bukovec et al., 1979a) does not seem to give immediate support to isostructurality but different structure types and polymorphism may exist in both series.

Of the other hydrates of the 1:1 compounds, $CsSc(SO_4)_2 \cdot 12H_2O$ appears particularly interesting because it is the only known rare earth sulfate having the alum structure (Bashkov et al., 1972). Its thermal stability is low and it has been prepared only at 0°C. The indexed powder pattern indicates that the unit cell parameter $a = 12.51$ Å and the volume $V = 1957$ Å^3. All other scandium compounds with Cs are anhydrous, viz. $CsScSO_4$ and $Cs_3Sc(SO_4)_3$ (Komissarova et al., 1970b).

Like the $CsR(SO_4)_2$ series, the $Cs_3R(SO_4)_3$ series comprises several structure types (table 10), in addition, the Sc compound probably has a monoclinic structure of its own (Komissarova et al., 1970b). Only the structure of $Cs_3Yb(SO_4)_3$ is known from single-crystal studies (Samartsev et al., 1980a). In this compound, Yb has the unusually (table 9) low coordination number of six, and the Yb–O distances are short, ranging from 2.14 to 2.23 Å. The structure consists of infinite chains of $[Yb(SO_4)_3]_n^{3n-}$ parallel to the z-axis (fig. 76), with Cs atoms located between the chains, each with nine neighbors at a range of 2.97–3.64 Å.

4.4.6. *Ammonium compounds*

Ammonium compounds are among the most frequently studied sulfatometallates of the rare earths (Pascal, 1959), even though their chemistry is limited to lower temperatures than that of alkali compounds. The $NH_4R(SO_4)_2 \cdot 4H_2O$ series has been used in fractional crystallization processes for separation of the lighter and heavier rare earth elements and even of individual elements within groups. The solubility diagrams have been presented for several R_2SO_4–$(NH_4)_2SO_4$–H_2O systems (e.g., Ce^{3+}; Schröder et al., 1938).

Besides the 1:1 compound tetrahydrates, the anhydrous phase (Sarukhanyan et al., 1984c) and the intermediate hydrates are known; the latter are of low stability, however. Of other compositions, the $(NH_4)_5R(SO_4)_4$ (R = La $\cdots$ Pr) (Iskhakova et al., 1981b; Niinistö et al., 1980a) and $(NH_4)_6R_4(SO_4)_9 \cdot 2H_2O$ (R = Tb $\cdots$ Er) series (Iskhakova et al., 1985) have been structurally character-

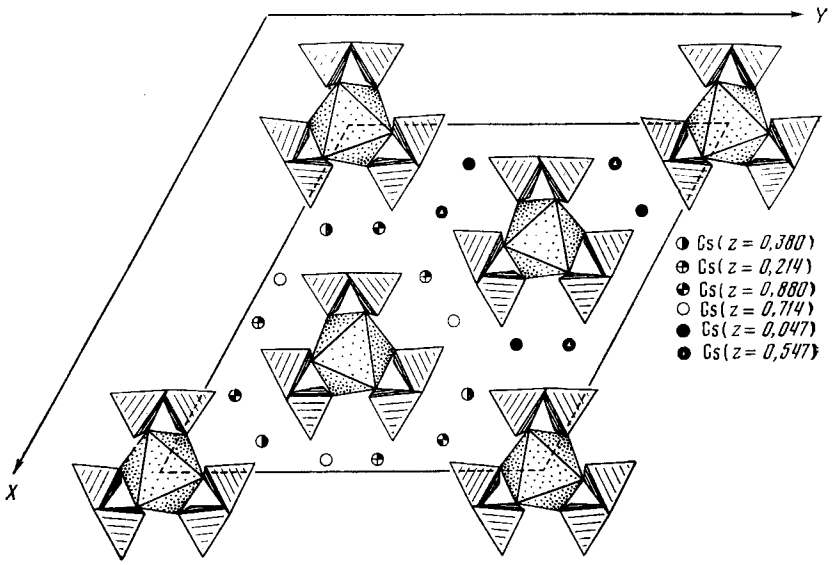

Fig. 76. A projection of part of the structure of $Cs_3Yb(SO_4)_3$ on the *xy*-plane (Samartsev et al., 1980a).

ized. Scandium forms at least two anhydrous phases, $NH_4Sc(SO_4)_2$ and $(NH_4)_3Sc(SO_4)_3$ (Erämetsä and Haukka, 1966; Bashkov et al., 1972), of which $NH_4Sc(SO_4)_2$ is isostructural with the Rb and Cs compounds (Couchot et al., 1971) and $(NH_4)_3Sc(SO_4)_3$ appears to have a different structure (Erämetsä and Haukka, 1966). The existence of an ammonium scandium alum has been claimed, but the compound has not been isolated (Purkaystha and Dutta, 1963).

The $NH_4R(SO_4)_2 \cdot 4H_2O$ (R = La $\cdots$ Tb) series forms isostructural crystals (Eriksson et al., 1974; table 8). It is not certain how far the isostructural character extends among the heavier rare earths, since the published powder patterns for the Dy $\cdots$ Ho region are not in agreement. Thus, Iskhakova et al. (1975) have reported that the Ho compound is isostructural with Tb, while Belousova et al. (1970) have published XRD patterns for Dy and Y which are similar to each other but different from those for the La $\cdots$ Tb compounds. A crystal structure analysis of $NH_4U(SO_4)_2 \cdot 4H_2O$ has revealed that it is isostructural with the corresponding rare earth series (Bullock et al., 1980). $NH_4Sm(SO_4)_2 \cdot 4H_2O$ was among the first "double" sulfates studied by single-crystal X-ray diffraction techniques (Niinistö, 1973; Eriksson et al., 1974). The samarium ion is nine-coordinated by six sulfate oxygens and three water molecules; the coordination polyhedron is an intermediate one and can equally well be described as a monocapped square antiprism or a tricapped trigonal prism (fig. 77). The sulfato groups join the SmO_9 polyhedra into chains with the ammonium ions and "noncoordinated" water molecules located between them (fig. 78).

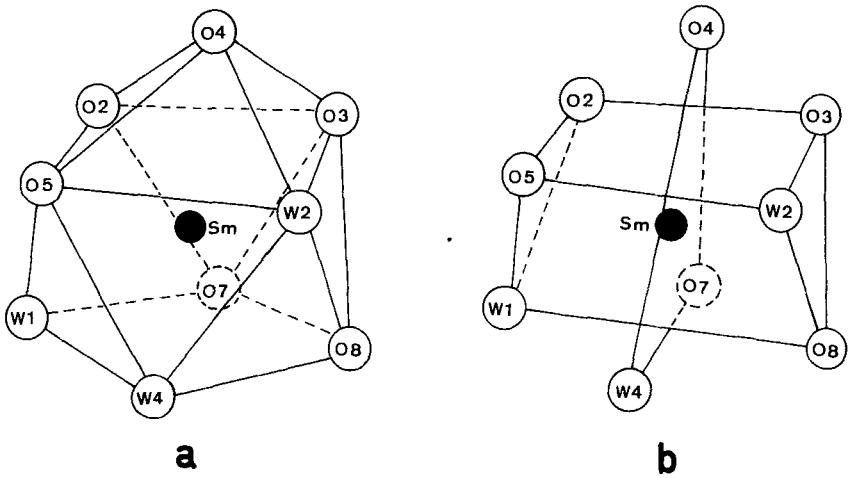

Fig. 77. The coordination around Sm^{3+} in the structure of $NH_4Sm(SO_4)_2 \cdot 4H_2O$. (a) monocapped square antiprism; (b) tricapped trigonal prism. (Niinistö, 1973; Eriksson et al., 1974.)

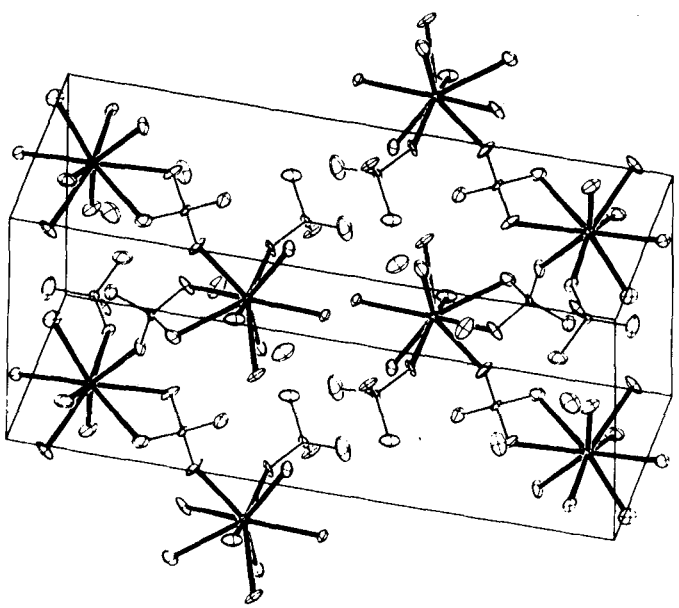

Fig. 78. A perspective view of the structure of $NH_4Sm(SO_4)_2 \cdot 4H_2O$ showing the unit cell packing (Eriksson et al., 1974).

The characteristic features of high CN for R^{3+} and bridging SO_4 groups are also encountered in the structures of $NH_4La(SO_4)_2$ and $(NH_4)_5R(SO_4)_4$ (R = La, Pr). The $(NH_4)_5La(SO_4)_2$ compound was found to crystallize in space group $P\bar{1}$, while for the Pr compound space group Cc was assigned (table 8). The structures are essentially the same, with R^{3+} having a CN of 10 and the relatively large number of ammonium ions situated in holes of the structure (fig. 79). In this case the coordination polyhedron is also distorted and after an analysis of the various possibilities the bicapped dodecahedron and bicapped square antiprism were considered equally possible (Niinistö et al., 1980a).

$NH_4La(SO_4)_2$, which is isostructural with the Ce···Pr compounds, has been prepared by evaporation of an aqueous solution containing $(NH_4)_2SO_4$ and $La_2(SO_4)_3$ at 70°C (Sarukhanyan et al., 1984c). The centrosymmetric choice of the two possible space groups ($P2_1/m$ and $P2_1$) gave a satisfactory solution including hydrogen atom positions. La has a CN of nine in a capped trigonal prismatic arrangement, where two of the La···O distances (2.90 Å) are significantly longer than the others (2.42–2.56 Å), leading to a distorted polyhedron. Although temperature parameters are not reported, it appears that the ammonium ion is firmly situated in a hole of the structure. Judging from the distances and hydrogen atom positions, several hydrogen bounds are formed, including some bifurcated ones (Sarukhanyan et al., 1984c) (fig. 80).

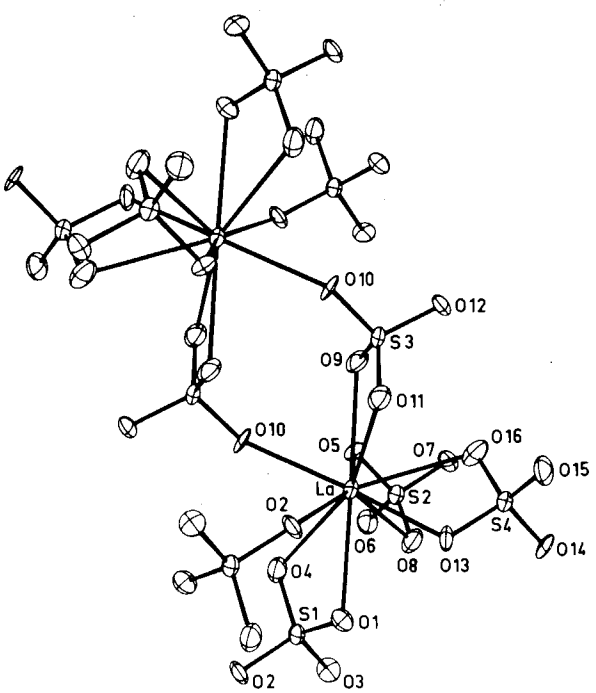

Fig. 79. A perspective view of the structure of $(NH_4)_5La(SO_4)_4$ (Niinistö et al., 1980a).

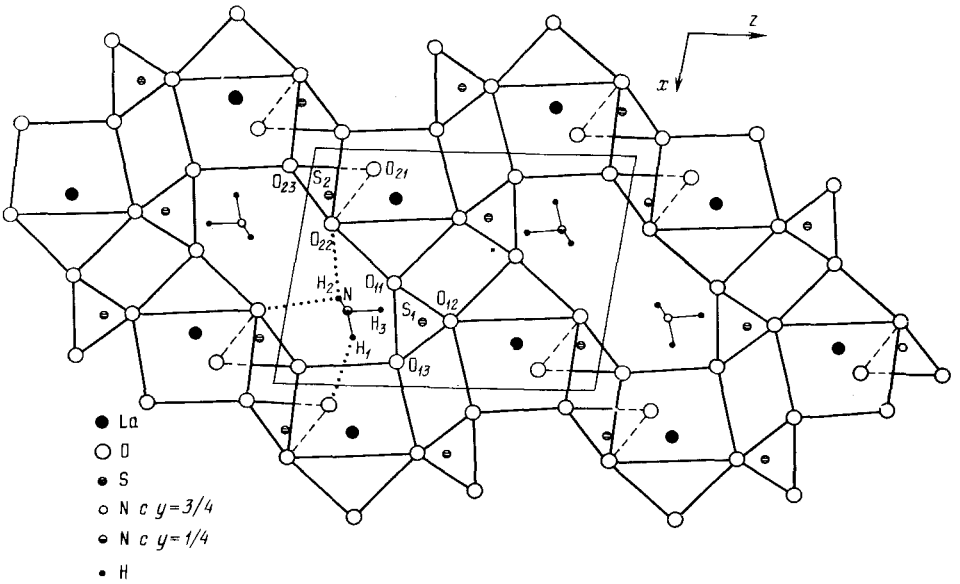

Fig. 80. A projection of the structure of $NH_4La(SO_4)_2$ on the *xz*-plane (Sarukhanyan et al., 1984c).

$(NH_4)_6Tb_4(SO_4)_9 \cdot 2H_2O$ has two crystallographically different Tb^{3+} ions in the structure with CNs of 9 and 8 (tables 8, 9). The water molecules are all firmly coordinated to Tb^{3+} (Tb–O(H_2O) = 2.35 Å) and the NH_4^+ ions are located in holes of the structure (Iskhakova et al., 1985).

The thermoanalytical behavior of the ammonium compounds, especially that of the $NH_4R(SO_4)_2 \cdot 4H_2O$ series, has also been studied. Unlike the situation in alkali sulfatometallates, the monovalent cation is expelled at relatively low temperature and the anhydrous sulfate is formed (fig. 81). In air the thermal degradation sequence is as follows: $2NH_4R(SO_4)_4 \cdot 4H_2O \rightarrow 2NH_4R(SO_4)_2 \rightarrow R_2(SO_4)_2 \rightarrow R_2O_2SO_4 \rightarrow R_2O_3$ (Erämetsä and Niinistö, 1971). Under most experimental conditions the first step, dehydration, appears to proceed through the monohydrate (Belousova et al., 1970; Erämetsä and Niinistö, 1971; Iskhakova et al., 1975; Storozhenko, 1983b), in which respect the behavior of the ammonium compounds is similar to that of the Rb and Cs sulfates.

There are a few reports on the magnetic properties of $NH_4R(SO_4)_2 \cdot 4H_2O$, both undoped and doped with Gd^{3+}. Unfortunately, the study on $NH_4Ce(SO_4)_2 \cdot 4H_2O$ (Singhal, 1973) was carried out before the structure of the compound was known, so the structural conclusions are not valid. The ESR results for Gd^{3+}-doped $NH_4Nd(SO_4)_2 \cdot 4H_2O$ single crystals have been interpreted in terms of two magnetically nonequivalent complexes with tetragonal symmetry (Malhotra et al., 1974).

For the IR spectrum of $NH_4Sm(SO_4)_2 \cdot 4H_2O$ and its assignment, see table 11

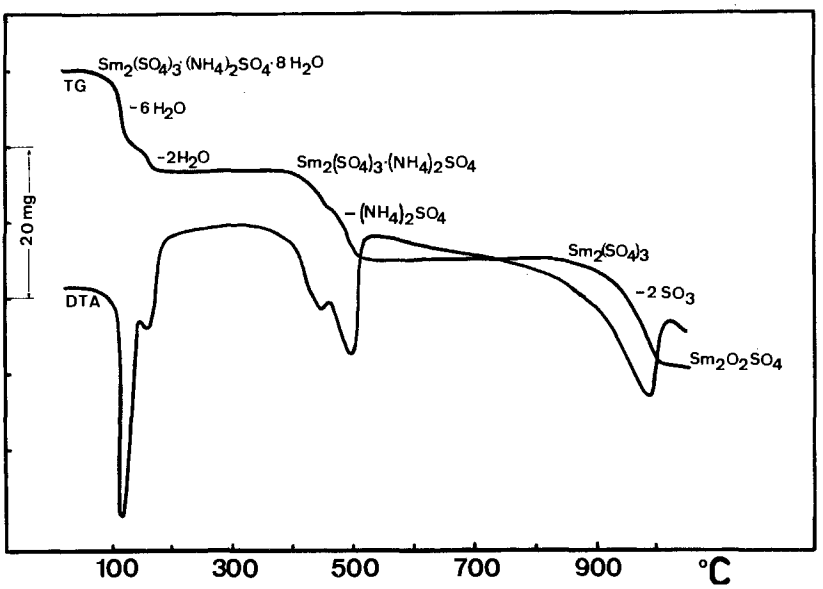

Fig. 81. The thermal decomposition of $NH_4Sm(SO_4)_2 \cdot 4H_2O$ in air (Erämetsä and Niinistö, 1971).

TABLE 11
IR spectrum of $NH_4Sm(SO_4)_2 \cdot 4H_2O$ (4000–400 cm^{-1}) and its assignment (Eriksson et al., 1974). *

Observed frequency	Assignment
3400 s, b	$\nu(H_2O)$
3130 vs	$\nu_3(NH_4)$
1670 sh, 1625 m	$\delta(H_2O)$
1390 vs	$\nu_4(NH_4)$
1190 s, 1120 vs, b	$\nu_3(SO_4)$
975 m	$\nu_1(SO_4)$
660 s, 645 s, 605 sh, 585 s	$\nu_4(SO_4)$
475 w	$\nu_2(SO_4)$, Sm–OH_2 wagging
410 vw	Sm–OH_2 stretching

* b = broad; m = medium; s = strong; sh = shoulder; vs = very strong; vw = very weak; w = weak.

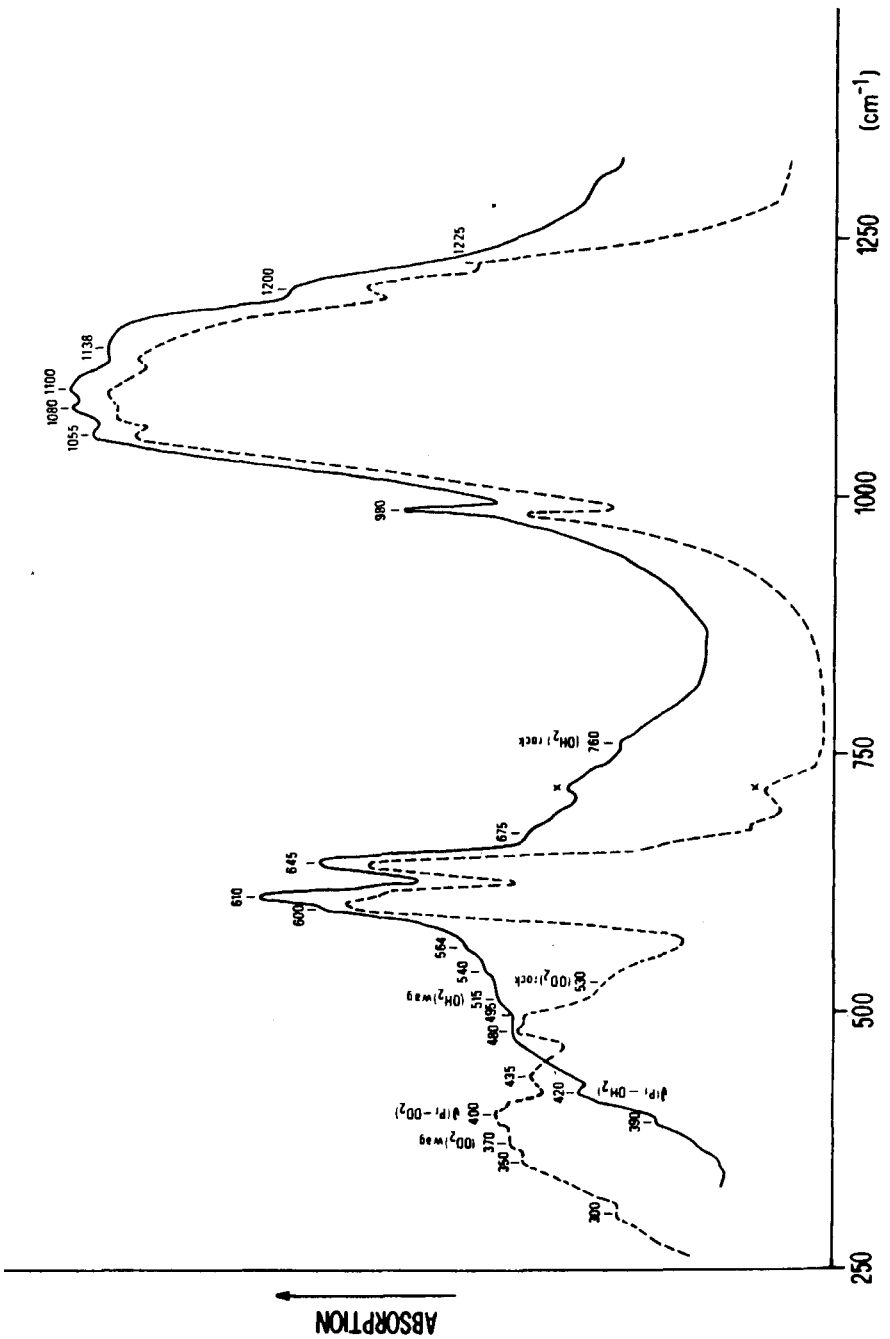

Fig. 82. The IR spectra of $CsPr(SO_4)_2 \cdot 4H_2O$ (—) and $CsPr(SO_4)_2 \cdot 4D_2O$ (– – –) (Bukovec et al., 1977).

(Eriksson et al., 1974). Other published spectra are generally in good agreement (Gmelin, 1981b) but structural interpretations vary (Ilyashenko et al., 1969). The IR spectra of the isostructural Cs compound and its deuterated form are shown for comparison in fig. 82.

4.4.7. *Compounds with other cations*

Some mono-, di-, and tetravalent cations combine with the rare earths to form ternary sulfates. Tl^+, Ag^+, Cd^{2+}, and Sn^{4+} compounds have been reported (Pascal, 1959), and more recently Ce^{3+} sulfates containing H_3O^+ or Ti^{4+} (probably as TiO^{2+} ion) as counterions (Belokoskov et al., 1979; Gatehouse and Pring, 1981). For a recent study of the $La_2(SO_4)_3$–$Ag_2(SO_4)_3$ system, see Campbell et al. (1983).

It is also possible to have more complicated inorganic ions to balance the charge of a sulfatometallate. The neodymium compounds with hydrazinium and hydroxylammonium counterions have been synthesized and characterized by thermoanalytical methods (Bukovec, 1985; Bukovec and Bukovec, 1985). Sakamoto (1984) has reported the preparation and properties of a series of La compounds with cobalt ammine complex cations, e.g., $[Co(NH_3)_6][La(SO_4)_3] \cdot H_2O$.

Three structures have been studied by X-ray single-crystal diffraction methods: the isostructural Tl compounds $TlR(SO_4)_2 \cdot 2H_2O$ (R = La, Pr), and $(H_3O)Ce(SO_4)_2 \cdot H_2O$ (table 8). The crystals of $TlR(SO_4)_2 \cdot 2H_2O$ (R = La, Pr) can be grown at room temperature from aqueous solution, confirming the earlier studies on the Pr compound by Zambonini and Restaino (1931). A characteristic feature of the structure is that nearly all cations lie on planes parallel to (100) that pass through the screw axis (fig. 83). The lanthanide ion is nonacoordinated by seven sulfate and two water oxygens, and the coordination polyhedron has been described as a distorted tricapped prism (Iskhakova and Trunov, 1985).

The synthesis of $(H_3O)Ce(SO_4)_2 \cdot H_2O$ requires a strongly acidic solution (Gatehouse and Pring, 1981). Details of the crystal data and structure are presented in tables 8 and 13 (see also section 4.5).

4.5. *Sulfates of tetravalent and divalent rare earths*

4.5.1. *Ce(IV) sulfates*

Owing to its large charge/ionic radius ratio, Ce^{4+} has a pronounced tendency for hydrolysis and forms a number of oxo- and hydroxosulfates, some analoguous to Ti^{4+} and Th^{4+} compounds (Lundgren, 1956) (see section 4.6). Nevertheless, many "normal" sulfates are known as well (Gmelin, 1981b) and some of them have been structurally characterized. Table 12 summarizes the structural information available and table 13 presents a comparison of the Ce···O distances in Ce^{4+} and Ce^{3+} sulfates; the comparison includes the oxo- and hydroxosulfates of tetravalent cerium.

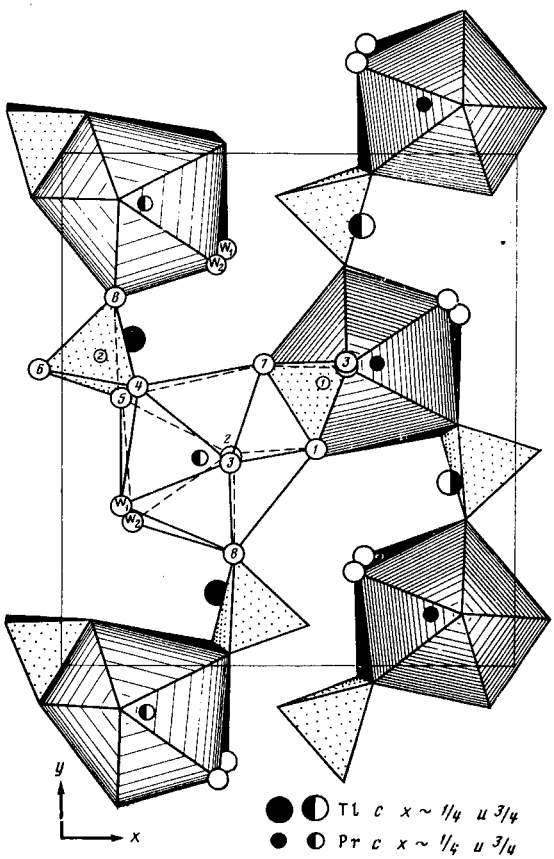

Fig. 83. A projection of the structure of $TlPr(SO_4)_2 \cdot 2H_2O$ on the *xy*-plane. For clarity, some polyhedra have been omitted. (Iskhakova and Trunov, 1985.)

TABLE 12
Summary of structure determinations of Ce(IV) sulfates.

Compound	Cell parameters				Z	Space group	*R*-value (%)	Ref.
	a (Å)	*b* (Å)	*c* (Å)	γ (deg)				
$Ce(SO_4)_2$	9.325	8.891	13.39		8	Pbca	12.0	a
$Ce(SO_4)_2 \cdot 4H_2O$	14.5994	11.0064	5.6601		4	Pnma	4.0	b
$CeOSO_4 \cdot H_2O$	11.983	8.267	4.332		4	$P2_12_12_1$		c
$CeOSO_4 \cdot H_2O$	11.987	8.272	4.331		4	$P2_12_12_1$	3.0	d
$Ce_2(OH)_2(SO_4)_3 \cdot 4H_2O$	15.583	13.448	6.748	95.39	4	A2/a	4.3	e
$Ce_6O_4(OH)_4(SO_4)_6$	10.661		10.288		2	I4/m		f

(a) Rogachev et al. (1974).
(b) Lindgren (1977b).
(c) Lundgren (1953).
(d) Lindgren (1976).
(e) Lindgren (1977c).
(f) Lundgren (1957).

TABLE 13
A comparison of oxygen coordination to Ce(III) and Ce(IV) in the sulfate structures.

Compound	Coordination polyhedron				Ce–O distance		Ref.
	CN	Number of oxygens from:					
		SO_4	H_2O	OH, O	Mean	Range	
Ce(III):							
$Ce_2(SO_4)_3 \cdot 4H_2O$	9	6	3	–	2.59	2.22–3.10	a
	9	7	2	–		2.22–3.10	
$Ce_2(SO_4)_3 \cdot 5H_2O$	9	5	4	–		2.39–2.82	b
$Ce_2(SO_4)_3 \cdot 9H_2O$	9	3	6	–	2.51	2.51–2.52	c
	12	12	–	–	2.71	2.59–2.82	
$(H_3O^+)Ce(SO_4)_2 \cdot H_2O$	9	8	1	–	2.54	2.45–2.63	d
$NaCe(SO_4)_2 \cdot H_2O$	9	8	1	–	2.53	2.48–2.58	e
Ce(IV):							
$Ce(SO_4)_2$	8	8	–	–	2.23	2.07–2.38	f
$Ce(SO_4)_2 \cdot 4H_2O$	8	4	4	–	2.36	2.29–2.39	g
$CeOSO_4 \cdot H_2O$	8	4	1	3	2.36	2.19–2.59	h
$Ce_2(OH)_2(SO_4)_3 \cdot 4H_2O$	8	4	2	2	2.33	2.22–2.41	i
$Ce_6O_4(OH)_4(SO_4)_6$	8	–	–	8	2.34	2.22–2.39	j

(a) Dereigne et al. (1972).
(b) Ahmed Farag et al. (1973a).
(c) Dereigne and Pannetier (1968).
(d) Gatehouse and Pring (1981).
(e) Lindgren (1977d).
(f) Rogachev et al. (1974).
(g) Lindgren (1977b).
(h) Lindgren (1976).
(i) Lindgren (1977c).
(j) Lundgren (1957).

According to Trofimov and Belakoskov (1968) and Trofinov (1968), eight solid phases are formed in the system CeO_2–SO_3–H_2O between 25 and 200°C. Both neutral sulfates $Ce(SO_4)_2$ and $Ce(SO_4)_2 \cdot 4H_2O$ have been studied in detail. Possibly the anhydrous $Ce(SO_4)_2$ has two crystal modifications. The orthorhombic (Pbcc) polymorph (tables 12, 13) has been the object of a complete structural determination (Rogachev et al., 1974), while only approximate unit cell dimensions ($a = 13.7$ Å, $b = 15.8$ Å, $c = 9.19$ Å, and $\beta = 140°$) are known for the monoclinic (C2/c or Cc) form (Rogachev et al., 1983).

Likewise, $Ce(SO_4)_2 \cdot 4H_2O$ exhibits dimorphism. The orthorhombic modification (Fddd) ($a = 26.59$ Å, $b = 11.93$ Å, $c = 5.73$ Å) (Singer and Cromer, 1959) and another orthorhombic form (Pnma) are prepared by hydrothermal methods (Lindgren, 1977b). The crystal structure of the latter modification has been solved (tables 12, 13; fig. 84) and shown to have a layer-like structure with CeO_8 polyhedra.

The ternary sulfate systems containing Ce^{4+} have been studied frequently. Although the total number of solid phases in each CeO_2–M_2SO_4–H_2SO_4–H_2O system (M = alkali metal or ammonium) is large (Gmelin, 1981b), there are not

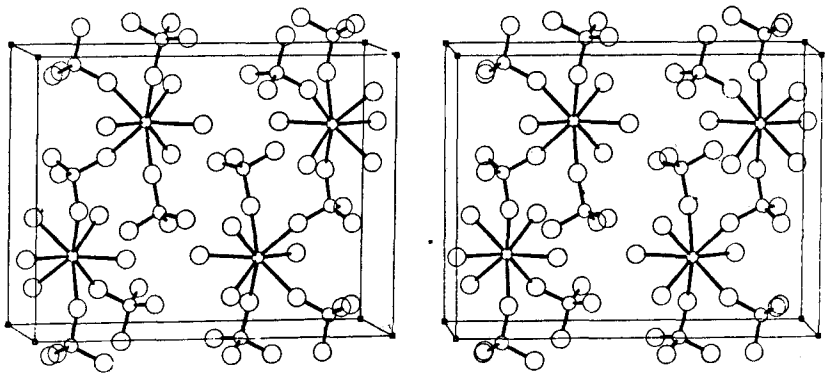

Fig. 84. A stereoscopic view of the structure of $CeSO_4 \cdot 4H_2O$ (Lindgren, 1977b).

so many oxo- and hydroxocompounds (to be discussed in section 4.6) as in the binary system. For instance, Rogachev et al. (1979) isolated four Cs-containing compounds and Nikitina and Bondar (1983) an additional four. None of these compounds contains oxo- or hydroxogroups. In some cases, however, the stoichiometries are so close that the compounds may well be identical: e.g., $Cs_4Ce_3(SO_4)_8 \cdot nH_2O$ where $n = 14$ (Nikitina and Bondar, 1983), or $n = 15$ Rogachev et al., 1979). For a thermal study of some of the compounds, see Bondar et al. (1982b).

Ce(IV) sulfate is widely used as a catalyst for various reactions, for instance grafting acrylamide on alkali lignin (Meister et al., 1984) and the Belousov–Zhabotinskii oscillating reaction (Winfree, 1984). It can be also used as a strong oxidant for several classes of organic compounds (Rao et al., 1983).

4.5.2. *Sulfates of Sm(II), Eu(II), and Yb(II)*

Eu^{3+}/Eu^{2+} normal potential is sufficiently low to allow the preparation of $EuSO_4$ by reduction of $Eu_2(SO_4)_3$ with zinc (Cooley et al., 1946) but for $SmSO_4$ and $YbSO_4$ an electrochemical reduction process has been utilized (Asprey et al., 1964).

$SmSO_4$ and $EuSO_4$ are isostructural with $SrSO_4$ and $BaSO_4$ but $YbSO_4$ has a different structure (table 14). $YbSO_4$ probably contains a small amount of water of crystallization (up to 0.5 mol) (Asprey et al., 1964). There are also reports on the existence of another polymorph for $EuSO_4$ (McCoy, 1936) but structural details are lacking.

Apart from the synthesis and crystal structure, the chemistry and physics of the RSO_4 series have been little studied (Gmelin, 1981b). The Mössbauer spectra of $^{151}EuSO_4$ and $^{153}EuSO_4$, however, have been investigated by several groups (e.g., Enholm et al., 1970).

TABLE 14
A comparison of unit cell data of RSO_4 (R = Sm, Eu, Yb).

Compound	Space group	a (Å)	b (Å)	c (Å)	Reference
$SmSO_4$	Pnma	8.45	5.38	6.91	Asprey et al., 1964
$EuSO_4$	Pnma	8.382	5.333	6.870	Asprey et al., 1964
		8.333	5.326	6.861	Mayer et al., 1964
		8.364	5.356	6.871	Sklyarenko et al., 1965
$YbSO_4$ *	$P6_222$	7.025		6.428	Asprey et al., 1964
		7.004		6.433	

* Single-crystal data from two crystals.

4.6. *Hydroxo- and oxosulfates*

As discussed earlier, hydroxo- and oxocompounds may be formed in aqueous systems when the acidity of the solution is low. Especially Sc^{3+} and Ce^{4+} ions tend to hydrolyze easily. Thermal decomposition under controlled conditions offers another route to the oxocompounds, most notably to $R_2O_2SO_4$.

4.6.1. *Hydroxosulfates*

The system $Sc_2(SO_4)_3$–MOH–H_2O has been studied for M = Li $\cdots$ Cs, NH_4, Tl (Shatskii et al., 1974a,b; Komissarova et al., 1974). The solid phases, $Sc(OH)SO_4 \cdot 2H_2O$, $Sc_3O_2(OH)_3SO_4 \cdot 4.5H_2O$, $Sc_4(OH)_{10}SO_4 \cdot 2H_2O$, $Sc_8(OH)_{22}SO_4 \cdot 2H_2O$, and $MSc_3(OH)_6(SO_4)_2 \cdot nH_2O$ ($n = 1$ for Na, K, NH_4, Rb, Tl, and $n = 2$ for Cs), were characterized by chemical analyses, X-ray diffraction, IR and PMR spectroscopy, and thermoanalytical techniques. The structures of $MSc_3(OH)_6(SO_4)_2 \cdot H_2O$ (M = Na, K, Rb, NH_4, Tl) were found to be isostructural with alunite (Shantskii et al., 1977).

The structures of three hydroxosulfates, $PrOHSO_4$, $Ce_2(OH)_2(SO_4)_3 \cdot 4H_2O$, and $Ce_6O_4(OH)_4(SO_4)_6$ have been solved from single-crystal X-ray diffraction data.

$PrOHSO_4$ crystals were prepared by hydrothermal methods from $Pr(OH)_3$ and Pr sulfate at 450–500°C and at a water pressure of 12000 atm (Fahey et al., 1979). The crystals are monoclinic ($P2_1/c$) with $a = 4.488$ Å, $b = 12.495$ Å, $c = 7.091$ Å and $\beta = 111.08°$. The structure consists of $Pr(OH)^{2+}$ double chains arranged parallel to [100]. The coordination polyhedron around Pr can be described as a slightly distorted monocapped square antiprism. The Pr–O(OH) distances are 2.451, 2.537, and 2.541 Å while the Pr–O(SO_4) distance range is broader or from 2.383 to 2.840 Å.

In the structure of $Ce_2(OH)_2(SO_4)_3 \cdot 4H_2O$ (Lindgren, 1977c), the Ce(IV) ions are connected to each other by double hydroxyl bridges, the Ce–Ce and OH^-–OH^- distances being 3.769 and 2.481 Å, respectively. Besides the two

bridging hydroxyl oxygens and two water oxygens, the CeO_8 coordination polyhedron contains four oxygens from bridging sulfate groups which join the polyhedra into a three-dimensional network (tables 12, 13).

$Ce_6O_4(OH)_4(SO_4)_6$ is isostructural with $U_6O_4(OH)_4(SO_4)_6$ and contains hexameric $[Ce_6O_6(OH)_4]^{12+}$ complex ions (Lundgren, 1957). The mean Ce–Ce and Ce–O distances are 3.80 and 2.33 Å, respectively, or very close to the values found for CeO_2 (see also tables 12 and 13). The arrangement of six cerium atoms and eight oxygen atoms around each of them is very regular. The cerium atoms form an octahedron and the oxygen atoms are at the corners of a square antiprism.

4.6.2. *Oxosulfates*

Two types of oxosulfates have been reported for the trivalent rare earths: $R_2O(SO_4)_2$ and $R_2O_2SO_4$. The first compound, however, has not been fully characterized but found only as an unstable intermediate during thermal decomposition processes (Gmelin, 1981b).

On the other hand, the (di)oxosulfate $R_2O_2SO_4$ has been known since the turn of the century (Mellor, 1965a) and owing to its interesting physical properties it has been studied frequently. The most convenient way of preparation is the thermal decomposition of $R_2(SO_4)_3$ (see section 4.3.2) but many other sulfur-containing compounds yield the oxosulfate when heated in air or oxygen. $Sc_2O_2SO_4$ cannot be prepared by this simple procedure, however, and the thermal synthesis of $Ce_2O_2SO_4$ is not straightforward (Leskelä, 1985; Leskelä et al., 1985).

The $R_2O_2SO_4$ series ($R = La \cdots Lu, Y$) forms isostructural orthorhombic (I222) crystals (Ballestracci and Mareschal, 1967). The structure of the lanthanum compound ($a = 4.2681$ Å, $b = 4.1938$ Å and $c = 13.720$ Å) has been refined from X-ray powder diffraction data by Fahey (1976). The refinement confirmed the earlier results by Ballestracci and Mareschal (1967) concerning the $(RO)_n^{n+}$-type layer structure and showed that the lanthanum atom is coordinated by four oxygens from the $(RO)_n^{n+}$ layer and two oxygens from different sulfate groups. The R–O distances are 2.40 and 2.41 Å in the $(RO)_n^{n+}$ layer and 2.36 Å when sulfate oxygens are involved. The point symmetry around lanthanum is C_2.

Thermal, magnetic and spectral properties of $R_2O_2SO_4$ have been studied frequently (Gmelin, 1981b; see also section 4.3.2). Since the compounds have the $(RO)_n^{n+}$-type layer structure found in many effective phosphor materials, their fluorescence spectra are of interest and have been studied by Haynes and Brown (1968) and Porcher et al. (1983). The latter group has recorded the spectra of Eu-activated $R_2O_2SO_4$ (R = La, Gd, Y) at 4.2, 77, and 300 K and calculated the crystal field parameters.

Hydrothermal hydrolysis of a Ce(IV) sulfate solution yields single crystals of $CeOSO_4 \cdot H_2O$ (Lundgren, 1953). The crystal structure has been refined by Lindgren (1976) and shown to contain $(CeO^{2+})_n$ strings. Ce(IV) is eight-

coordinated, having a square antiprismatic coordination polyhedron. The Ce–Ce distance is exceptionally short or 3.570(1) Å, which is less than in the cerium metal. For other details of the structure, see tables 12 and 13.

5. Rare earth selenates and selenites

5.1. *Introduction*

Due to the fact that the sulfate and selenate oxyanions have the same spatial configuration, the corresponding rare earth compounds are isostructural with only a few exceptions. Their physical and chemical properties are also largely similar. On the other hand, the relationship between rare earth sulfites and selenites is not as close as one would expect. Besides the larger size of the selenite ion, possible factors leading to structural and other differences between the sulfites and selenites include the different relative stabilities of the tetra- and hexavalent states and the lower stability of the selenium–selenium bond compared to the sulfur–sulfur bond. The first factor is responsible for the different observed thermal decomposition mechanisms while the latter contributes, for instance, to the formation of a diselenite ion which has an oxygen-bridged structure. This is much different from the disulfite ion, which is nonsymmetrical and contains a sulfur–sulfur bond.

The literature and applications of rare earth selenates and selenites are not nearly as extensive as those of their sulfur-containing counterparts. The selenates have been known for more than a hundred years and studied frequently. The first rare earth selenites were also prepared by Berzelius, Cleve, Nilson and other pioneers in studying the chemistry of the rare earths in the 19th century but systematic studies have been carried out only recently. Thorough discussions of the early studies are contained in the handbooks of Gmelin-Kraut (1928–1932), Mellor (1965b), and Pascal (1959). These seem to be the only comprehensive reviews on the topic, but a brief report (Niinistö, 1984b) and two theses (Paralkar, 1978; Ajgaonkar, 1981) discuss the data of the binary and ternary rare earth selenates, respectively. The thesis of Valkonen (1979) focuses on the structural chemistry of the scandium selenates and selenites.

5.2. *Binary rare earth selenates*

5.2.1. *Preparation and structures*

H. Töpsöe and P.T. Cleve were the first to study the formation and properties of rare earth selenates in 1873. Later J. Meyer and J.A.N. Friend and coworkers contributed to the preparative chemistry of these compounds by determining solubilities and constitution of the solid phases. For references of these early

investigations concerning the rare earth selenates, see Gmelin-Kraut (1928–1932), Mellor (1965b), or Pascal (1959).

Beginning in the late 1960's, Giolito and Giesbrecht with coworkers undertook a systematic study of the formation and properties of binary and ternary selenates of the rare earths. They have mainly used thermoanalytical and IR spectroscopic methods to characterize the solid compounds. At about the same time single-crystal X-ray diffraction data have become available from other laboratories. Extensive thermoanalytical studies have also been carried out by Nabar and coworkers.

Solution studies are few in number. Solubility data indicate that the solubilities of the rare earth selenates are generally significantly higher than those of the sulfates (Pascal, 1959). Enthalpies of formation for some members of the penta- and octahydrate series have also been published (Smolyakova et al., 1973). The heats of formation of $Sm_2(SeO_4)_3$-based solid solutions have been determined calorimetrically (Serebrennikov et al., 1984); the same group has also studied other $R_2(SeO_4)_3$–$R'_2(SeO_4)_3$ solid solutions. The inner sphere complex formation between the lanthanides including yttrium and selenate ions has been established recently by X-ray diffraction studies in solution (Johansson et al., 1985; Johansson and Wakita, 1985), as shown in fig. 85. Of the formation constants, however, only the stability constant for the scandium selenate complex appears to be known (Sillén and Martell, 1971).

The free selenate ion has the same I_d symmetry as the sulfate but is approximately 10% larger (Se–O = 1.64 Å versus 1.49 Å for S–O; Johanssen, 1974; Gibbs et al., 1976). Due to the similarity, it is not surprising to find the same stoichiometries and structural features as discussed in section 4.

Thus, the main series of selenates, the octahydrates $R_2(SeO_4)_3 \cdot 8H_2O$ (R = Pr–Lu, Y), is isostructural with the corresponding sulfate series (Rosso and Perret, 1970; Hiltunen and Niinistö, 1976a,b). The preparation of the crystalline compounds can be carried out by similar methods, viz. dissolving rare earth oxide, hydroxide, carbonate or chloride in selenic acid and letting the solution evaporate at room temperature.

Besides the octahydrates, the pentahydrate series has been characterized by single-crystal X-ray diffraction methods. Unit cell data are available (Mascarenhas and Folgueras, 1975) and in the case of the cerium compound the structure has been determined (Aslanov et al., 1973a). The space group is $P2_1/c$ versus $C2/c$ in the corresponding sulfates. It contains two crystallographically different cerium atoms with coordination numbers 9 and 8, for which the Ce–O bond distances range from 2.36 to 2.79 Å and from 2.36 to 2.57 Å, respectively. As in the case of $Nd_2(SO_4)_3 \cdot 5H_2O$ (Larsson et al., 1973) one of the water molecules is not coordinated but instead is held in the structure by hydrogen bonds.

Scandium forms only the pentahydrate (Tetsu et al., 1971), which is isostructural with the corresponding sulfate (Niinistö et al., 1975). The scandium atoms are

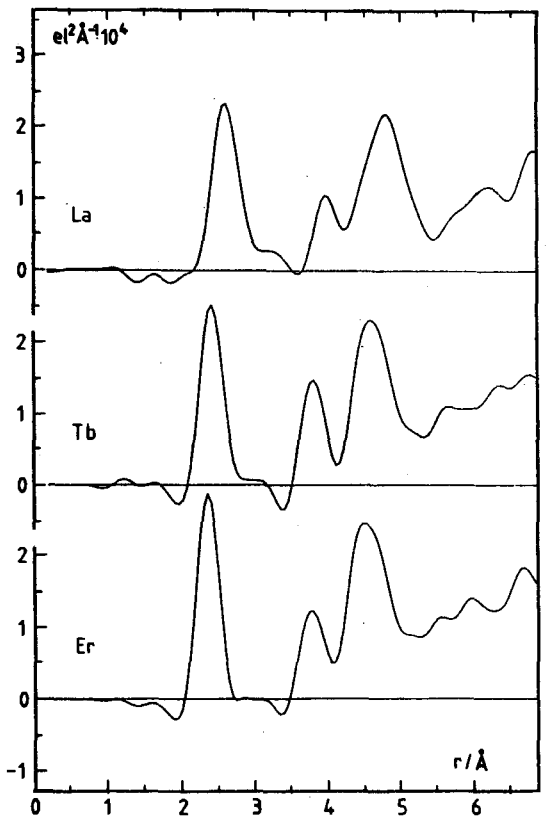

Fig. 85. The X-ray diffraction radial distribution curves for three lanthanide selenate solutions after elimination of light atom interactions. The three peaks correspond to R–O, R–Se, and R–O (outer-coordination sphere) distances. (Johansson et al., 1985.)

octahedrally coordinated as in most of its compounds (Valkonen et al., 1975; Valkonen, 1979). All of the water molecules are coordinated to the scandium atoms, which are joined into a three-dimensional network by bridging tridentate selenate groups (fig. 86).

Table 15 summarizes the structural information which is available from single-crystal X-ray studies. Two interesting structures, which do not yet have counterparts among the sulfates, are apparent: $Eu_2(SeO_4)_3 \cdot 8H_2O$ (second modification) and $La_2(SeO_4)_3 \cdot 12H_2O$. For the europium compound, only the unit cell data and the positions of the europium atoms have been determined (Aslanov and Ahmed Farag, 1974).

Lanthanum selenate dodecahydrate can be crystallized from aqueous solutions near 0°C but the crystals are unstable towards dehydration (Karvinen and Niinistö, 1986). A structural analysis shows that half of the water molecules are not coordinated to lanthanum but are held between the layers by hydrogen bonds. There are five selenate and three water oxygens around lanthanum at normal

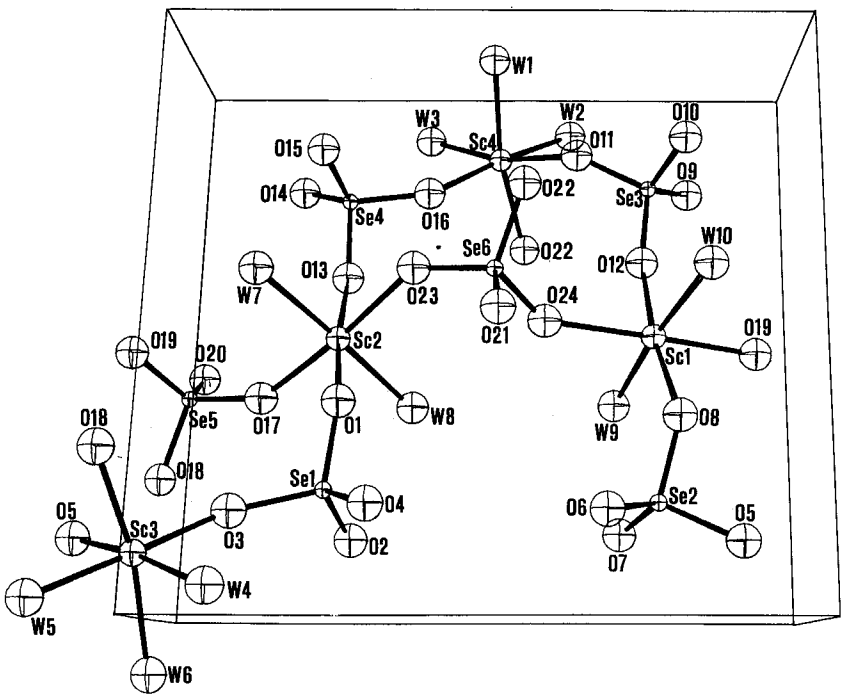

Fig. 86. A perspective view of the structure of $Sc_2(SeO_4)_3 \cdot 5H_2O$ showing the unit cell packing (Valkonen et al., 1975).

TABLE 15
Summary of structural data on rare earth selenates.

Compound	Cell parameters						Z	Space group	R-value (%)	Ref.
	a (Å)	b (Å)	c (Å)	α (deg)	β (deg)	γ (deg)				
$La_2(SeO_4)_3 \cdot 12H_2O$	10.669	20.393	10.744		110.12		4	C2/c	11.1	a
$Eu_2(SeO_4)_3 \cdot 8H_2O$ *	17.69	13.83	6.89			98.5	4	A2/a *or* Aa	–	b
$Yb_2(SeO_4)_3 \cdot 8H_2O$	13.704	6.831	18.507		101.90		4	C2/c	4.1	c
$Ce_2(SeO_4)_3 \cdot 5H_2O$	9.82	14.05	10.69			92.0	4	$P2_1/a$	9.2	d
$Sc_2(SeO_4)_3 \cdot 5H_2O$	11.225	11.804	5.766	91.35	100.10	89.03	2	P1	8.4	e
$Sc_2(SeO_4)_3$	8.899	9.212	15.179		124.83		4	$P2_1/c$	3.8	f
$ScH(SeO_4)_2 \cdot 2H_2O$	8.708	5.632	9.105		101.64		2	C2/m	5.4	g
$(NH_4)_3Sc(SeO_4)_3$	15.567		9.871				6	R3	6.3	h

* Incomplete structural analysis, see the text for details.

(a) Karvinen and Niinistö (1986).
(b) Aslanov and Ahmed Farag (1974).
(c) Hiltunen and Niinistö (1976b).
(d) Aslanov et al. (1973a).
(e) Valkonen et al. (1975).
(f) Valkonen (1978a).
(g) Valkonen (1978b).
(h) Valkonen and Niinistö (1978).

bonding distances (2.42–2.65 Å). In addition, one oxygen is at the significantly larger distance of 3.06 Å.

Two further phases of scandium have been characterized structurally. $Sc_2(SeO_4)_3$ and $ScH(SeO_4)_2 \cdot 2H_2O$ (Valkonen, 1978a,b). Both structures contain octahedrally coordinated scandium ions with Sc–O bond ranges of 2.07–2.11 Å and 2.05–2.12 Å, respectively. Unfortunately, for the latter compound quality of the diffraction data did not allow the detection of hydrogen atom positions but the water content was established by thermogravimetric analysis.

5.2.2. *Thermal decomposition*

Several groups have studied the thermal decomposition of rare earth selenate hydrates $R_2(SeO_4)_3 \cdot nH_2O$ using the TG and DTA (or DSC) techniques, either separately or simultaneously. In some cases it seems that starting materials have not been sufficiently characterized or systematized because unusual stoichiometries have been reported.

Giolito and Giesbrecht (1969) investigated $R_2(SeO_4)_3 \cdot nH_2O$ (R = La $\cdots$ Lu, Y) by thermogravimetry (TG) in air up to 1000°C and noted that the dehydration is in most cases a multistep process which starts around 100°C and leads to the formation of the anhydrous selenate by 400°C. Partial decomposition of the selenate was noted even at these temperatures. Comparable dehydration temperatures have been reported by Nabar and Paralkar (1976a,b), Hajek et al. (1979), and Niinistö et al. (1982). The latter authors and Sonninen (1981) compared the dehydration of the $R_2(SeO_4)_3 \cdot 5H_2O$ series with the corresponding sulfates.

Simultaneous TG/DTA data are also available for the scandium selenate pentahydrate, which is completely dehydrated by 130°C (Tetsu et al., 1971). The dehydration temperatures obtained by various authors are not directly comparable because different experimental conditions have been used. Under similar conditions, however, there appears to be a linear relationship between the DTA peak temperatures and the atomic number of the rare earth in the series $R_2(SeO_4)_3 \cdot 8H_2O$ (R = Rb $\cdots$ Lu) (Nabar and Paralkar, 1976b).

The relationship between the structure and dehydration mechanism for the pentahydrate series has been discussed by Niinistö et al. (1982). A further case of an obvious structure–thermal-stability correlation is provided by the dehydration of the highly hydrated selenate phase $La_2(SeO_4)_3 \cdot 12H_2O$ (Karvinen and Niinistö, 1986). Its dehydration starts around 50°C and at 80°C a distinct plateau in the weight loss curve is reached which corresponds to the formation of the more stable octahydrated phase.

The thermal degradation reactions following the dehydration are complex. Nabar and Paralkar (1976a,b) and Hajek et al. (1979) have concluded that the anhydrous selenate(VI) decomposes first to selenite(IV) and then to (di)-oxoselenite(IV) $R_2O_2SeO_3$ through an unstable intermediate $R_2O(SeO_3)_2$. The final product obtained by heating in air at temperatures usually well over 1000°C

is the sesquioxide. The decomposition scheme can be summarized as follows:

$$R_2(SeO_4)_3 \rightarrow R_2(SeO_3)_3 + 1\tfrac{1}{2}O_2\,, \tag{6}$$

$$R_2(SeO_3)_3 \rightarrow R_2O(SeO_3)_2 + SeO_2\,, \tag{7}$$

$$R_2O(SeO_3)_2 \rightarrow R_2O_2SeO_3 + SeO_2\,, \tag{8}$$

$$R_2O_2SeO_3 \rightarrow R_2O_3 + SeO_2\,. \tag{9}$$

On the other hand, Giolito and Giesbrecht have suggested that an oxoselenate(VI) is formed in analogy with the sulfate decomposition scheme.

As can be seen in fig. 87, it is obviously not possible to deduce the decomposition scheme from the observed weight losses. The plateaus on the TG curve are not distinct and do not correspond to any single intermediate compounds as indicated by the calculated levels. Furthermore, the experimental conditions including the atmosphere, heating rate, and sample size affect the shape of the curves greatly. Therefore, additional analytical data are needed for the interpretation of the TG data. In the case of $Sc_2(SeO_4)_3 \cdot 5H_2O$, Tetsu et al. (1971) have

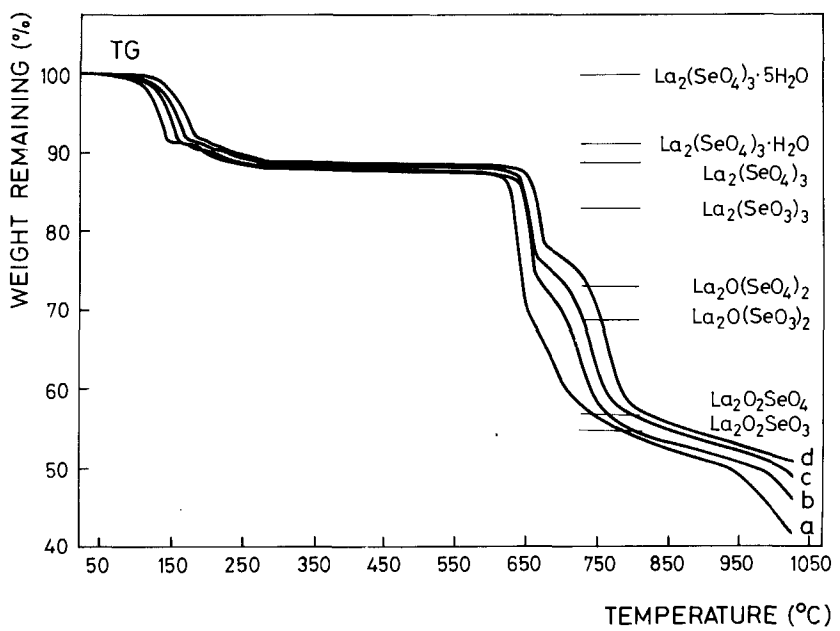

Fig. 87. The thermogravimetric curves of $La_2(SeO_4)_3 \cdot 5H_2O$ recorded in air with different heating rates. a: 2, b: 5, c: 10, and d: 20 deg min^{-1}. (Karvinen et al., 1987.)

utilized the results of quantitative chemical analyses [Se(IV)/Se(VI)], X-ray diffraction, and IR studies to corroborate the suggested mechanism:

$$Sc_2(SeO_4)_3 \cdot 5H_2O \rightarrow Sc_2(SeO_4)_3 \rightarrow Sc_2(SeO_3)_3 \rightarrow Sc_2O_2SeO_3 \rightarrow Sc_2O_3 \,. \quad (10)$$

Thermoanalytical results obtained for scandium usually are not directly applicable to other rare earth systems. Nevertheless, it would be plausible to assume that the thermodynamically more stable Se(IV) plays a dominant role in the decomposition of $La_2(SeO_4)_3$ and other anhydrous lanthanide selenates. There is general agreement among most researchers. The recent, unpublished data by Karvinen et al. (1987) indicate that the presence of $La_2O_2SeO_4$ cannot be altogether excluded. This finding is in agreement with the earlier report by Giolito and Giesbrecht (1969). It is interesting to note that Leskelä and Hölsä (1985) have also discussed the presence of $La_2O_2SeO_4$ when studying the decomposition of $LaH(SeO_3)_2 \cdot 2\frac{1}{2}H_2O$ (see section 5.4.2).

5.2.3. *Spectroscopic and magnetic properties*

Following the IR studies by Giolito and Giesbrecht (1969), several authors have recorded the spectra of the octahydrate series and compared the number and position of the peaks with those recorded for the isostructural sulfates. Petrov et al. (1970) and Hajek et al. (1979) made use of the available structural information to aid in the interpretation of the spectra. The former group also compared the spectra with those of the deuterated compounds. From the structural point of view especially interesting is the region around $1000\,cm^{-1}$ where the selenate Se–O stretching fundamentals ν_1 and ν_3 appear (fig. 88). The IR spectra of $Sc_2(SeO_4)_3 \cdot 5H_2O$ have been recorded in connection with the thermal decomposition and structural studies (Tetsu et al., 1971, and Niinistö et al., 1975, respectively).

Raman spectra of the selenate hydrates $R_2(SeO_4)_3 \cdot nH_2O$ show features similar to those in the IR spectra (Gupta et al., 1982). Unfortunately, the authors have used compounds with variable water content ($n = 3$ for Dy, 6 for Sm, 7 for Gd and Y) and thus, a direct comparison between the spectra and those of the octahydrated compounds is not possible.

By analogy with the sulfate studies (see section 4.4.3), magnetic studies have also been carried out. Neogy and Nandi (1982) concluded that the crystal field around Yb^{3+} in the structure of ytterbium selenate octahydrate is of tetragonal symmetry at least to the first approximation. However, the authors did not compare their model with the actual crystal structure of the ytterbium compound described in the literature (table 15). In a later study, the magnetic behavior of Dy^{3+} was studied and the effects of J–J mixing were noted (Neogy and Nandi, 1983).

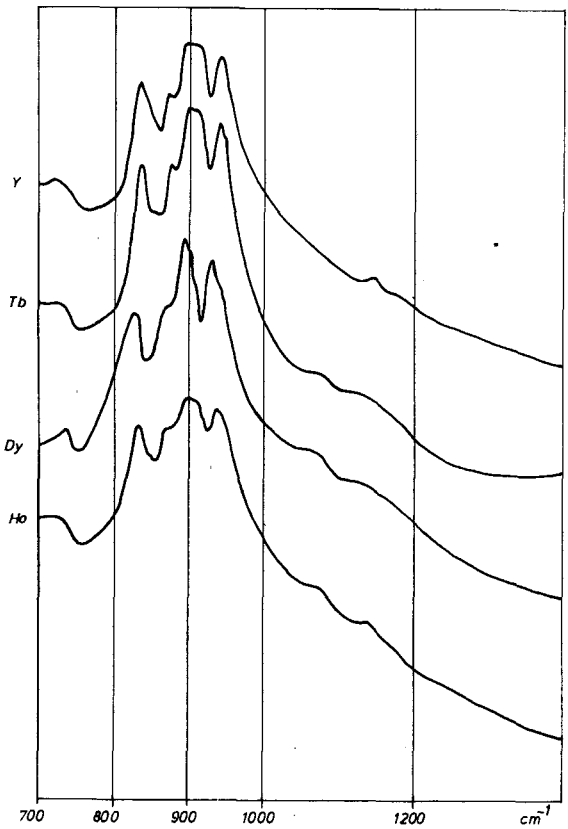

Fig. 88. The infrared spectra of $R_2(SeO_4)_3 \cdot 8H_2O$ (R = Y, Tb $\cdots$ Ho) in the region 700–1300 cm^{-1} (Hajek et al., 1979).

5.3. *Ternary rare earth selenates*

Structural studies on ternary rare earth complexes of the type where M is a monovalent cation (alkali or ammonium ion) are very scarce; but on the other hand, the compounds are similar structurally to the ternary sulfates in many cases. Thus, Nabar and Ajgaonkar (1982b) have studied the unit cell data for the $RbR(SeO_4)_2$ series (R = La $\cdots$ Nd), finding that the compounds are isostructural with $CsLa(SO_4)_2$, whose structure has been determined earlier by Bukovec et al. (1980c). Similarly, the $CsR(SeO_4)_2 \cdot 4H_2O$ series (where R = La $\cdots$ Sm) has been found to be isostructural with the corresponding sulfates by Nabar and Ajgaonkar (1985). Several other isostructural cases probably exist.

The only ternary rare earth selenate which has been fully characterized by a single-crystal X-ray diffraction study appears to be the triammonium scandium selenate $(NH_4)_3[Sc(SeO_4)_3]$, which corresponds to the complex anion $[Sc(SeO_4)_3]^{3-}$ (Valkonen and Niinistö, 1978; table 15). The crystal structure

belongs to the rhombohedral space group R3 and is probably isostructural with that of the corresponding sulfate. The coordination around Sc is octahedral but the joining of the octahedra is unusual in that the selenate groups connect the ScO_6 octahedra into infinite columns $[Sc(SeO_4)_3]_n^{3n-}$ (fig. 89). The ammonium ions are held in position between the columns and kept there by hydrogen bonds.

Although the existence of the ternary selenates has been known since the last century, the first systematic studies on their properties have been carried out recently. These studies focused on their thermal stabilities are are summarized in table 16. In all cases the decomposition mechanism has been explained by the

TABLE 16
Thermoanalytical studies on ternary rare earth selenates.

Compound	R	n	Reference
$LiR(SeO_4)_2 \cdot nH_2O$	La	4	Ionashiro and Giolito, 1980
	Eu	2.5	Ionashiro and Giolito, 1982b
	Ho	4	Nabar and Paralkar, 1980b
$NaR(SeO_4)_2 \cdot nH_2O$	La	2.5	Ionashiro and Giolito, 1980
	Ce, Pr	2	Giolito and Ionashiro, 1981a,b
	Nd, Sm	2	Ionashiro and Giolito, 1982a
	Sm, Ho	3	Nabar and Paralkar, 1980a, b
	Eu	3	Ionashiro and Giolito, 1982b
$Na_3R(SeO_4)_3 \cdot nH_2O$	Gd, Tb, Ho	1	Nabar and Khandekar, 1984
$KR(SeO_4)_2 \cdot nH_2O$	La	4.5	Ionashiro and Giolito, 1980
	Ce	4	Giolito and Ionashiro, 1981a
	Pr	3.5	Giolito and Ionashiro, 1981b
	Nd, Eu	3.5	Ionashiro and Giolito, 1982a, b
	Sm	2.5	Ionashiro and Giolito, 1982a, b
	Sm, Ho	4	Nabar and Paralkar, 1980a, b
$RbR(SeO_4)_2 \cdot nH_2O$	La	4	Ionashiro and Giolito, 1980
	Ce	4	Giolito and Ionashiro, 1981a
	Ce	0	Nabar and Ajgaonkar, 1982a
	Pr	1.5	Giolito and Ionashiro, 1981b
	Nd	0.5	Ionashiro and Giolito, 1982a
	Sm, Eu	2.5	Ionashiro and Giolito, 1982a, b
	Ho, Yb	1	Nabar and Ajgaonkar, 1981b
$CsR(SeO_4)_2 \cdot nH_2O$ *	La	0.5	Ionashiro and Giolito, 1980
	La, Pr $\cdots$ Sm	4	Nabar and Ajgaonkar, 1985
	Ce	0	Nabar and Ajgaonkar, 1982a
	Ce	0.5	Giolito and Ionashiro, 1981a
	Ce	2	Nabar and Ajgaonkar, 1982a
	Pr	0	Giolito and Ionashiro, 1981b
	Eu	1	Ionashiro and Giolito, 1982b
	Ho, Yb	3	Nabar and Ajgaonkar, 1981a
$NH_4R(SeO_4)_2 \cdot nH_2O$	Sm, Ho	4	Nabar and Paralkar, 1980a, b

* In addition, two complex cesium compounds $[2Cs_2SeO_4 \cdot 3Nd_2(SeO_4)_3 \cdot 7H_2O$ and $2Cs_2SeO_4 \cdot Sm_2(SeO_4)_3 \cdot 4H_2O]$ have been prepared and studied by Ionashiro and Giolito (1982a).

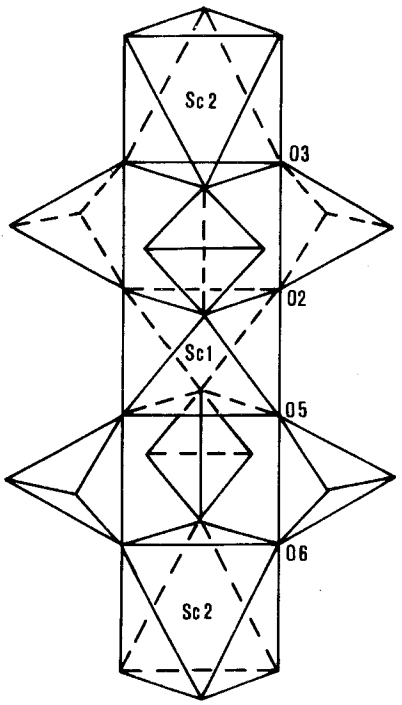

Fig. 89. The basic building unit $[Sc(SeO_4)_3]_n^{3n-}$ column in the structure of $(NH_4)_3Sc(SeO_4)_3$ (Valkonen and Niinistö, 1976).

presence of only Se(IV) compounds in analogy with the proposed mechanism for the thermal decomposition of binary selenates by Nabar and Paralkar (1976a,b). As an example the TG/DTA curves of $Na_3Gd(SeO_4)_3 \cdot H_2O$ are depicted in fig. 90.

5.4. *Rare earth selenites*

J.J. Berzelius (1818), discoverer of both the elements selenium and cerium, combined them into basic and normal selenites, thus becoming the first researcher in this field. Later, other famous Swedish rare earth investigators, P.T. Cleve (1874) and L.F. Nilson (1875), as well S. Jolin (1874) in France prepared a number of selenites, including the hydrogenselenites. The anhydrous selenites were prepared by Espil (1911). It is surprising to note that after this initial active research period nearly a century passed before the studies were continued in Brazil by Giesbrecht et al. (1962, 1968) and Giesbrecht and Giolito (1967).

5.4.1. *Preparative and structural studies*

In an aqueous solution of selenium dioxide, $HSeO_3^-$, SeO_3^{2-}, and $Se_2O_5^{2-}$ exist in a pH- and concentration-dependent equilibrium. Consequently, three main types of solid compounds exist: hydrogenselenites, normal selenites, and disele-

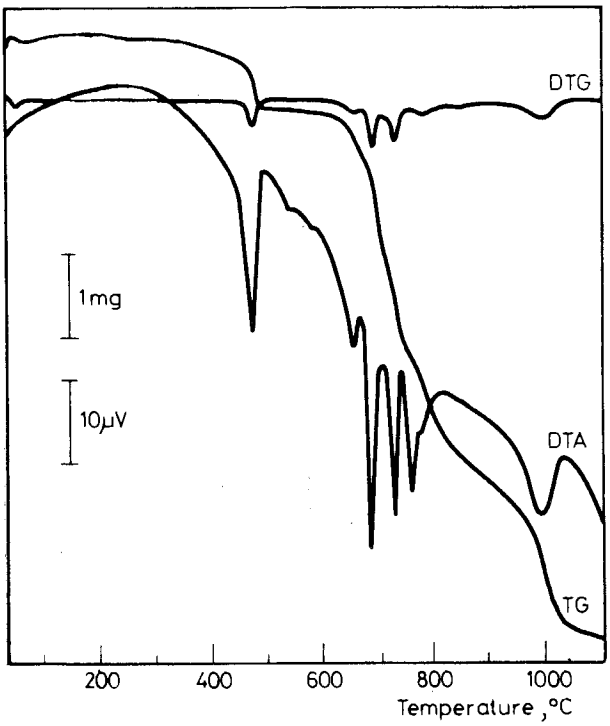

Fig. 90. The thermoanalytical curves of $Na_3Gd(SeO_4)_3 \cdot H_2O$. Sample weight: 21.3 mg; heating rate: 10° min^{-1} (Nabar and Khandekar, 1984).

nites. In addition, hydroxo- and oxoselenites are known. The hydrogenselenites, which can be easily precipitated from an acidic aqueous solution, have been studied most extensively. They form two series: the mono- and trihydrogenselenites, corresponding to the compounds $RH(SeO_3)_2 \cdot nH_2O$ and $R(HSeO_3)_3 \cdot nH_2O$, respectively. The latter series seems to be limited to the lighter rare earths and scandium only.

Because of the small crystal size of these compounds, X-ray diffraction studies have been performed in only a few instances. Immonen et al. (1976) were able to show that the monohydrogenselenites $RH(SeO_3)_2 \cdot 2\frac{1}{2}H_2O$ (R = Pr $\cdots$ Lu, Y) form isostructural crystals with the space group $P2_1$ or $P2_1/m$. They determined the unit cell dimensions for the whole series. For instance, the last member of the series $LuH(SeO_3)_2 \cdot 2\frac{1}{2}H_2O$ has a cell of dimensions: $a = 7.089(3)$ Å, $b = 6.675(5)$ Å, $c = 16.663(6)$ Å, and $\beta = 101.10(5)°$. Under the experimental conditions used, no variations in the composition were found, contrary to some of the earlier reports (table 17).

Much less structural information is available for the normal selenites $R_2(SeO_3)_2 \cdot nH_2O$, where according to Petrov et al. (1973) n has a value of 3 for La $\cdots$ Eu but 7 for Gd. Other water contents have also been reported (Savchenko

TABLE 17
The content of water, n, in solid hydrogen selenites of type $RH(SeO_3)_2 \cdot nH_2O$.

Sc	Y	La	Ce	Pr	Nd	Sm	Eu	Gd	Tb	Dy	Ho	Er	Tm	Yb	Lu	Ref.
				1.5		2										a
			2													b
	1.5		2.5	4								1.5				c
				1.5												d
								3								e
	2	1.5	0	2	2	2	2.5	2	2.5	2.5	2.5	2.5	2.5	2.5	2.5	f
	2				1.5	2		2								g
			0													h
				2.5												i
0.5																j
				2.5	2.5	2.5	2.5	2.5	2.5	2.5	2.5	2.5	2.5	2.5	2.5	k

(a) Cleve (1874, 1885).
(b) Jolin (1874).
(c) Nilson (1875).
(d) von Scheele (1898).
(e) Benedicks (1900).
(f) Giesbrecht et al. (1968).
(g) Savchenko et al. (1968).
(h) Markovskii and Safina (1968).
(i) Maier et al. (1969).
(j) Komissarova and Znamenskaya (1974).
(k) Immonen et al. (1976).

et al., 1968). IR spectra and X-ray line diagrams have been published, the latter showing a difference between the tri- and heptahydrates.

Scandium selenites have been studied in more detail than those of the other rare earths. The preparative conditions have been established by Znamenskaya and coworkers for the normal selenite $Sc_2(SeO_3)_3 \cdot 5H_2O$, hydrogen containing compounds $ScH(SeO_3)_2 \cdot H_2O$ and $Sc(HSeO_3)_3$, diselenite $Sc_2(Se_2O_5)_3$, as well as hydroxo- and oxoselenites $Sc(OH)SeO_3 \cdot nH_2O$, $Sc_4(OH)_2(SeO_3)_5 \cdot nH_2O$, and $Sc_2O(SeO_3)_2 \cdot 3H_2O$ (Znamenskaya et al., 1972, 1979; Znamenskaya and Komissarova, 1973; Komissarova and Znamenskaya, 1974). IR and PMR spectra for the different compounds listed are characteristic of each type, indicating a different structure in each case (table 18).

The structure of scandium trihydrogenselenite has been determined (Valkonen and Leskelä, 1978). The compound forms monoclinic crystals in the acentric space group Cc. The unit cell has the following dimensions: $a = 11.130(2)$ Å, $b = 9.506(4)$ Å, $c = 7.598(2)$ Å, and $\beta = 97.59°$. The structure consists of ScO_6 octahedra joined by bridging selenite groups (fig. 91). The Se–O bonds involving the hydrogen atoms show a significant elongation, and range from 1.76 to 1.79 Å versus 1.64–1.70 Å for the other bonds.

Two other interesting rare earth selenite compounds have been characterized structurally. The first one, $PrH_3(SeO_3)_2(Se_2O_5)$, which contains simultaneously the selenite, hydrogenselenite, and diselenite groups, shows that the solution equilibria can be "frozen" into a solid compound. Without an X-ray structural analysis it would have been extremely difficult to deduce the correct formula of the complex.

TABLE 18

Infrared absorption frequencies (cm^{-1}) of scandium selenites. The assignments are based on the C_{3v} and C_{2v} symmetries of the selenite and diselenite ions, respectively (Znamenskaya et al., 1979). *

$Sc_2O(SeO_3)_2 \cdot 3H_2O$	$Sc_2(SeO_3)_3 \cdot 5H_2O$	$Sc_2(SeO_3)_3 \cdot 5D_2O$	$ScH(SeO_3)_2 \cdot H_2O$	$Sc(HSeO_3)_3$	$Sc_2(Se_2O_3)_3$	Assignment
			270 mw	275 s	270 s	
				285 s	293 s	
	310 m		305 m	308 s, sh	308 s	
330 m	330 m	–	325 s		330 m	ν_4[O–Se–O(H)]
			340 s	350 w, sh	–	
	370 w			365 m	360 sh	
			390 s	385 m	385 w, sh	
410 m, b	420 w	415 m	430 s	430 m	–	ν_2(O–Se–O)
	460 w			450 m		
–	–	–	–	–	435 w	ν_{as}(Se–O–Se)
					450 m	
475 s		495 w	490 m	485 mw		
500 s, sh	525 m	530 m	505 m		525 s	ν(Sc–O)
–	–	–	–	–	575–660 s, b	ν_s(Se–O–Se)
		565 w?				
		650 w				
635 m	–	–	–	655 s	–	δ(Se–OH)
				675 s, sh		
			700 s			
750 vs	730 s	725 s	735 s	730–810 s	–	ν_3(Se–O)
	775 s	780 s	780 vs			
	–	–	–	–	790–940 s, b	ν(SeO_2)(Se_2O_5)
				835 s		
870 s	870 m, sh	855 m	870 s, sh	870 s	–	ν_1(Se–O)
			880 s	885 s		
–	–	920 m	–	–	–	δ(D_2O)
		1220 w				
			920 s	920 m		
–	–	–	1190 w	1110 m	–	δ(O–Se–OH)
			1220 w	1265 m		
1650 w	1650 w	–	1660 m	–	–	δ(H_2O)
		2300 s				
–	–	2400 s	–	–	–	ν(OD)
		2470 m				
		2630 m				
2350 vw, b	2350–2380 w		2400 w, b	2450 w		
3200–3400 s, b	3100–3420 s, b		3260 s	3200–3270 m, b		ν(OH)
	3530 w, sh	–	3350 s		–	

* b = broad; m = medium; s = strong; sh = shoulder; v = very, w = weak.

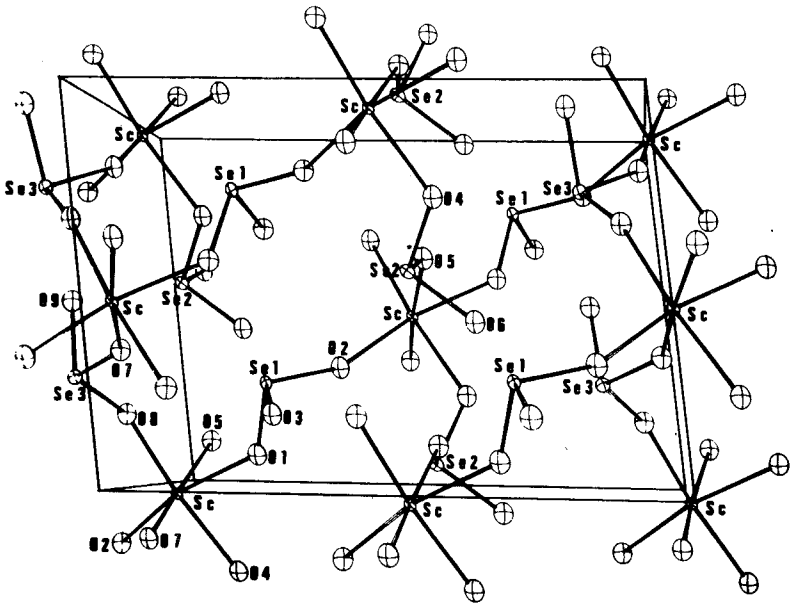

Fig. 91. The unit cell contents of $Sc(HSeO_3)_3$ (Valkonen and Leskelä, 1978).

X-ray data indicate that $PrH_3(SeO_3)_2(Se_2O_5)$ has a monoclinic crystal structure belonging to the space group $P2_1/c$ and a unit cell of dimensions: $a = 12.933(3)$ Å, $b = 7.334(2)$ Å, $c = 10.811(2)$ Å, and $\beta = 91.68(1)°$ (Koskenlinna and Valkonen, 1977). The praseodymium atom has a coordination number of nine, bonding to six diselenite oxygens and three selenite oxygens. The formation of PrO_9 polyhedra and their joining into a double-layered structure involves several interesting features such as bridging tridentate diselenite groups and triply coordinated oxygens (fig. 92).

The second compound belongs to a new series prepared recently and characterized by X-ray diffraction, IR spectroscopy, and thermal analysis (Niinistö et al., 1980b). It was discovered that when the crystallization of rare earth selenites occurs from a solution containing nitric acid, a mixed anion complex forms. The complex contains both coordinated nitrate and diselenite ligands and has a formula $RNO_3(Se_2O_5)\cdot 3H_2O$, where R is Pr$\cdots$Lu or Y. The crystal system is orthorhombic with the space group $P2_12_12_1$. Unit cell data are available for the whole series and, for instance, the yttrium compound has a cell with $a = 6.216(1)$ Å, $b = 7.100(2)$ Å, and $c = 20.689(6)$ Å.

A single-crystal study of the yttrium compound by Valkonen and Ylinen (1979) revealed that the water molecules are all also coordinated to the rare earth ion. Its coordination number is eight and the polyhedron formed around yttrium is nearly a regular square antiprism. The structure is depicted in fig. 93, and the unusual tetradentate coordination of the diselenite ligand is illustrated in fig. 94.

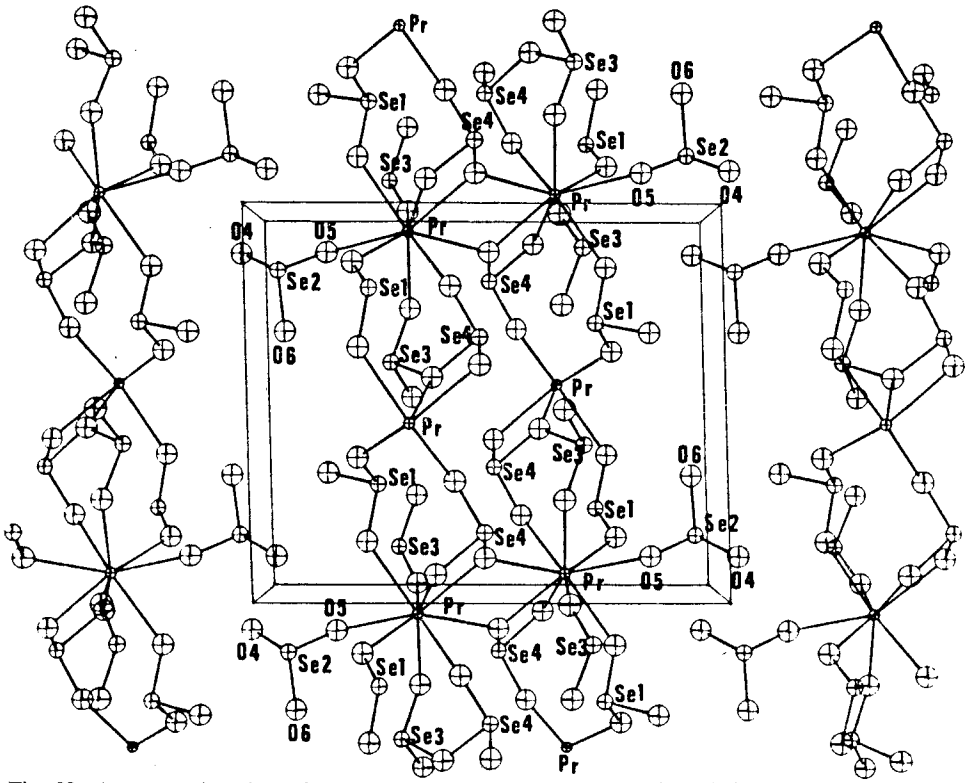

Fig. 92. A perspective view of the double-layer structure of $PrH_3(SeO_3)_2(Se_2O_5)$ along the *b*-axis (Koskenlinna and Valkonen, 1977).

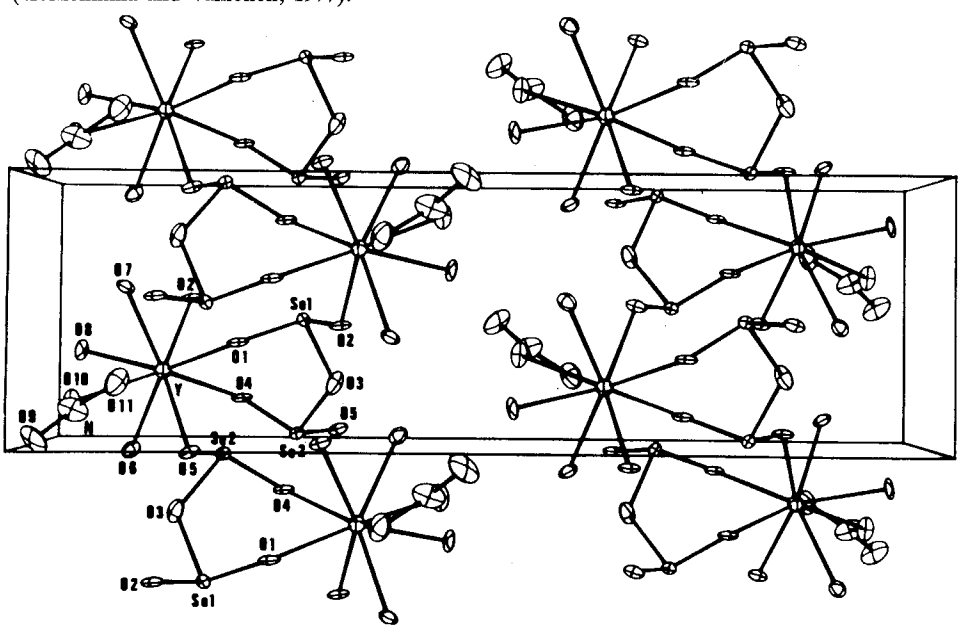

Fig. 93. A perspective view of the unit cell contents of $YNO_3(Se_2O_5)\cdot 3H_2O$ showing the packing of the chains (Valkonen and Ylinen, 1979).

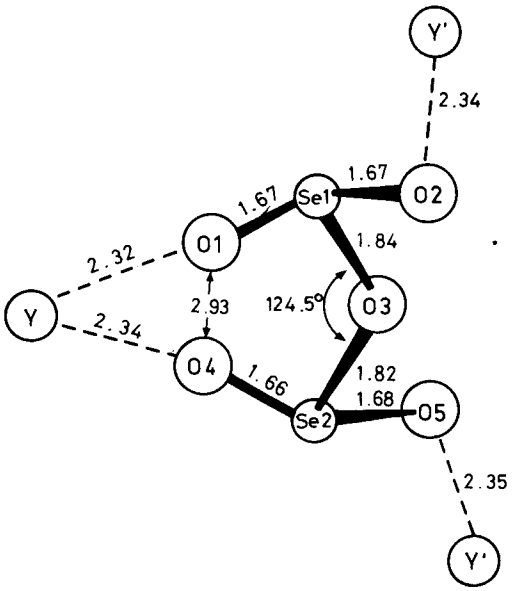

Fig. 94. The coordination of the diselenite ion in the structure of $YNO_3(Se_2O_5)\cdot 3H_2O$ (Niinistö and Koskenlinna, 1987).

In spite of the three quite different types of ligands, the Y–O bond length variations are relatively small, viz. 2.32–2.35 Å ($Se_2O_5^{2-}$), 2.37–2.44 Å (H_2O) and 2.46 Å (NO_3^-).

Ternary rare earth selenites are also known, although the number of studies on them is still very limited. Giesbrecht and Giolito (1967) reported the precipitation of amorphous sodium yttrium selenite $NaY(SeO_3)_2\cdot 3H_2O$ by mixing yttrium chloride and sodium selenite solutions. A systematic study of the formation of the sodium, potassium, and ammonium compounds was carried out by Erämetsä et al. (1973). Besides the composition of the $MR(SeO_3)_2\cdot nH_2O$ (M = Na, K, or NH_4; $n = 2$ or $2\frac{1}{2}$) phases they recorded the X-ray powder diffraction patterns for the different structural types and studied the compounds by IR spectroscopic and thermoanalytical techniques. A detailed study on the formation of scandium ternary selenites of the type $MSc(SeO_3)_2\cdot nH_2O$ (M = Li $\cdots$ Cs or NH_4; n = 1–2.5) is also available (Znamenskaya et al., 1977).

5.4.2. *Spectroscopic and thermoanalytical studies and applications*

The IR spectra of rare earth selenites have been studied only occasionally. Besides the spectra of the various scandium compounds (table 18; see also Znamenskaya et al., 1978), data are available for hydrogenselenites (Giesbrecht et al., 1968), selenite hydrates (Petrov et al., 1973), $KGd(SeO_3)_2\cdot 2H_2O$ (Erämetsä et al., 1973), and $YNO_3(Se_2O_5)\cdot 3H_2O$ (Niinistö et al., 1980b).

Thermal decomposition of rare earth selenites or hydrogenselenites in air does not show unexpected features; it proceeds through the anhydrous selenite to

oxoselenite $R_2O_2SeO_3$ and then finally to the sesquioxide (Giesbrecht et al., 1962; Savchenko et al., 1968; Maier et al., 1969). Scandium compounds behave similarly to the lanthanide compounds (Znamenskaya and Komissarova, 1973), but the thermal decomposition scheme of the cerium compounds is more complex and difficult to interpret due to the occurrence of overlapping reactions (Markovskii and Safina, 1968).

The presence of an additional cation also makes the thermogram more complex, as seen for the alkali rare earth selenites (Erämetsä et al., 1973) and the corresponding scandium compounds, which also contain variable amounts of hydrogen (Znamenskaya et al., 1978). Below 1000°C the end products contain the alkali ion. The extra cation is volatilized at relatively low temperatures or below 600°C only in the case of ammonium compounds (Erämetsä et al., 1973).

The difference between the thermal behavior of the selenite and sulfite compounds becomes more obvious by comparing the thermal degradation in reducing atmospheres. Whereas the reduction of rare earth sulfites yields the oxosulfide phase R_2O_2S (Koskenlinna and Niinistö, 1973), thermal decomposition of the hydrogenselenites in hydrogen or carbon monoxide leads to the formation of an oxoselenite with a more complicated composition $R_4O_4Se_3$ (Immonen et al., 1976).

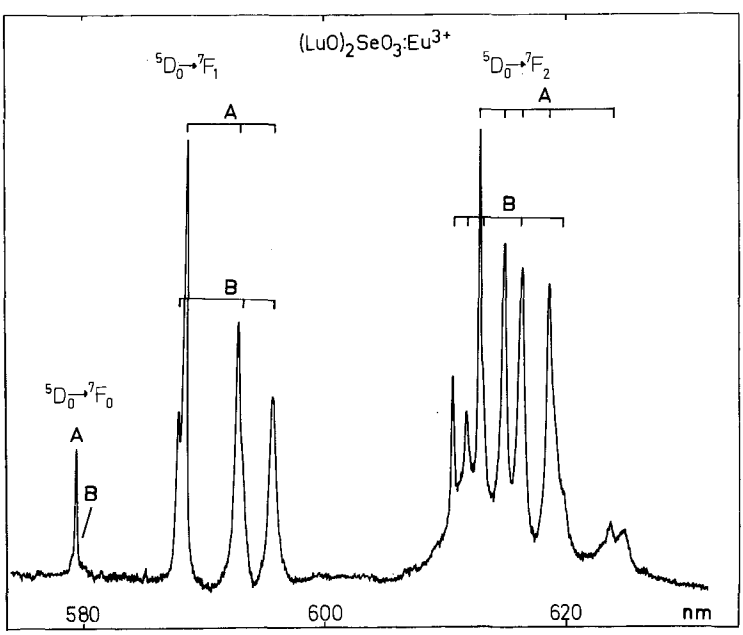

Fig. 95. A part of the UV-excited luminescence spectrum of $La_2O_2SeO_3:Eu^{3+}$ at 77 K (Hölsä and Leskelä, 1985).

The oxoselenite phases $R_2O_2SeO_3$ (R = La, Gd, Lu, or Y), which appear as intermediate compounds during the thermal decomposition of the corresponding hydrogenselenites, have recently been investigated as host matrices for Eu^{3+} luminescence (Leskelä and Hölsä, 1985). The spectra of $Lu_2O_2SeO_3:Eu^{3+}$ (fig. 95) indicate that at least two different lanthanide sites are present (Hölsä and Leskelä, 1985) and that the structure is probably very similar to other oxocompounds which contain the $(RO)_n^{n+}$ structural unit (Caro, 1968).

Another possible application has emerged recently. Cerium(IV) selenite, prepared previously by Markovskii and Safina (1968), shows promising ion exchange properties, especially toward Hg(II) (Rawat et al., 1984; Husain et al., 1984).

6. Oxohalogen rare earth compounds

6.1. *Introduction*

Of the rare earth compounds with halogen-containing oxoanions, the perbromates have not yet been prepared and the chlorites and chlorates have been studied only sporadically; the other bromates and the iodates, perchlorates, and periodates are widely discussed in the literature. A comprehensive review on the oxohalogen compounds of Cl, Br, and I with the rare earths has appeared in the late 1970's (Gmelin, 1977, 1978). The oxofluorides have been discussed in an earlier volume (Gmelin, 1976); only the ROF and related types of compounds are known and they fall outside the scope of this review. The TG and DTA data on rare earth perchlorates and iodates are discussed in Solomosi's comprehensive book (1977) on the structure and stability of solid halogen oxoacid compounds; however, many important papers have been published since its appearance.

A number of different factors have directed attention to the oxohalogen rare earth compounds and classes of compounds. For instance, the perchlorates have mainly in solution been studied for their coordination types, while the iodates have been studied for their solid state properties. Because of the great number of papers published in this area, the present review will focus almost exclusively on the investigations of solid compounds. A brief account of perchlorate solutions, which are of central importance in rare earth complexation studies, is given in section 6.3.

6.2. *Rare earth chlorites and chlorates*

Solid rare earth chlorites can be synthesized only at lowered temperatures because at room temperature the concentrated solution decomposes before crystallization. Anhydrous chlorites are known for scandium and cerium. $Sc(ClO_2)_3$ is formed only in a reaction of aqueous suspension of $Sc(OH)_3$ with gaseous ClO_2. The formation of a complex in solution has been confirmed by

chemical reactions but the product decomposes too easily to be isolated in solid form. $Ce(ClO_2)_3$ is formed during the reaction of $Ce(NO_3)_3$ with $NaClO_2$, as an intermediate product, before Ce^{3+} oxidizes to Ce^{4+}. Pure $Ce(ClO_2)_3$ can be prepared only in the presence of hydrazine (Barbier-Melardi, 1954).

Compounds of the type $R(ClO_2)_3 \cdot nH_2O$ have been obtained with La, Pr, Nd, Sm, Tb, and Y by reaction of $R(NO_3)_3$ with $NaClO_2$ in aqueous solution (Castellani Bisi and Clerici, 1963a). The water content may vary between 0.5 and 4 moles, depending on the rare earth. At 15°C $La(ClO_2)_3$ crystallizes as the tetrahydrate and close to 0°C as the trihydrate. The only chlorite whose structure has been studied is $La(ClO_2)_3 \cdot 3H_2O$, which crystallizes in the hexagonal space group $P\bar{6}2c$. Lanthanum has a ninefold coordination in which three pairs of oxygen atoms from the ClO_2^- groups form a trigonal prism around it and three oxygen atoms from the water molecules act as capping atoms. The structure is held together by hydrogen bonds (Coda et al., 1965).

The rare earth chlorates have not been studied to the same extent as the bromates and iodates. Rare earth chlorates of the type $R(ClO_3)_3 \cdot nH_2O$ ($n = 4 \cdots 10$) may be obtained by dissolving rare earth oxides in chloric acid at 0°C and crystallizing at a pH of 6–7 above P_2O_5 at the same temperature. A second preparation approach is the reaction of $R_2(SO_4)_3$ and $Ba(ClO_3)_2$ in aqueous solution, where barium sulfate is precipitated and filtered out. $R(ClO_3)_3 \cdot nH_2O$ crystals grow upon evaporation of the filtrate (Yakunina and Serebrennikov, 1970). In the first preparation method the n is 4 or 5, and in the second method 8 or 10 (Sarkar, 1926; Yakunina and Serebrennikov, 1970). Lanthanum also forms a dihydrate (Smirnov and Volkov, 1974).

The rare earth chlorate hydrates lose water between 80 and 170°C. The anhydrous $R(ClO_3)_3$ phase is not stable however, but decomposes readily above 160°C to oxychloride. The kinetics of the decomposition reaction have been studied by Yakunina and Serebrennikov (1974). Anhydrous $Nd(ClO_3)_3$ has been obtained by an exchange reaction between $Ba(ClO_3)_2$ and $Nd_2(SO_4)_3$ (Rocchiccioli, 1960).

The IR spectra of rare earth chlorates have been recorded by Duveau (1943). The stability constants, formation enthalpies, and entropies of Eu and Tb chlorate complexes of the type $[RClO_3]^{2+}$ in solution have been determined by Roulet and Chenaux (1972). At 20°C the values of K_1 are 1.2 and 1.0 for the Eu and Tb complexes, respectively.

6.3. *Rare earth perchlorates*

Numerous investigations have been carried out on rare earth perchlorate solutions. The properties of the solutions – molal heat capacities, densities and molal volumes, viscosities, heats of dilution, activity coefficients, conductances, transfer numbers, etc. – are well known (Spedding et al., 1974; 1975a,b, 1977a,b). Information on the structures of solvated metal ions can often be obtained from

the study of their perchlorate solution because of the weak tendency of the perchlorate ion to form inner-sphere complexes. IR and fluorometric investigations of the solvation have been carried out (Bünzli and Yersin, 1979, 1982). Investigations have also been made on complex formation with a variety of organic ligands in rare earth perchlorate solutions. The products have been studied by IR, Raman, and NMR spectrometry, and by ultrasonic measurements (e.g., Gushikem et al., 1972; Scholer and Merbach, 1975; Catton et al., 1978; Jezowska-Trzebiatowska et al., 1978; Bünzli et al., 1979). In the present review only the solid rare earth perchlorates will be discussed in detail; the solid rare earth complexes with organic ligands where perchlorate acts only as a counter anion (Ciampolini et al., 1978, 1979 and 1980) are not discussed here.

Rare earth perchlorate hydrates $R(ClO_4)_3 \cdot nH_2O$ are obtained by dissolving $R(OH)_3$ or $R_2(CO_3)_3$ in perchloric acid or by reaction of $R_2(SO_4)_3$ with $Ba(ClO_4)_2$ in aqueous solution. Evaporation is made above H_2SO_4. The perchlorates of La $\cdots$ Nd, Y have been reported to contain 8 water molecules and the perchlorates of Sm and Gd 9 molecules (Slavkina et al., 1963). A third way to prepare perchlorates is by the dissolution of R_2O_3 in perchloric acid, followed by evaporation of the solution and drying with P_2O_5. The products obtained by this method are pentahydrates in the case of Sm and Gd and hexahydrate in the case of Nd (Nosova, 1966; Krishnamurty and Soundararajan, 1967; Davidenko et al., 1972). Glaser and Johansson (1981) have synthesized hexahydrates which form an isomorphic series extending from La to Er.

Thermoanalytical studies of perchlorate hydrates show that the octa- and enneahydrates begin to dehydrate at 60–90°C; the dehydration is complete at 170–270°C, depending on the rare earth (fig. 96) (Slavkina et al., 1963). The dry perchlorate decomposes to ROCl at 170–460°C, with the lowest temperature for Sc and the highest for La. The large difference in temperature is at least partially due to the different heating rates used (Steinberg and Shidlovsky, 1964; Belkova et al., 1965). The effect of pressure on the decomposition has been studied by Cucinotta et al. (1976).

Scandium perchlorate hexa- and heptahydrates can be crystallized from a solution prepared by dissolving Sc_2O_3, $Sc(OH)_3$, or $Sc_2(CO_3)_3$ in $HClO_4$ (Kilpatrick and Pokras, 1953). The needle-shaped crystals are hygroscopic and their X-ray powder pattern can be indexed with a tetragonal cell of dimensions $a = 8.55$ Å, $c = 5.77$ Å (Petrů and Kutek, 1963). $Sc(ClO_4)_3 \cdot 7H_2O$ decomposes to hexahydrate at 105°C and possibly to $ScOHClO_4$ at 150°C. The decomposition reaction at 200–300°C produces ScOCl. The behavior of yttrium perchlorate heptahydrate is analogous to that of the scandium compound (Petrů and Kutek, 1964).

Pure, solid Ce(IV) perchlorates are not known but the existence of several hydroxide perchlorates has been confirmed (Fichter and Jenny, 1923; Zinovev and Schirova, 1960). In solution the Ce(IV) perchlorates have been identified and studied.

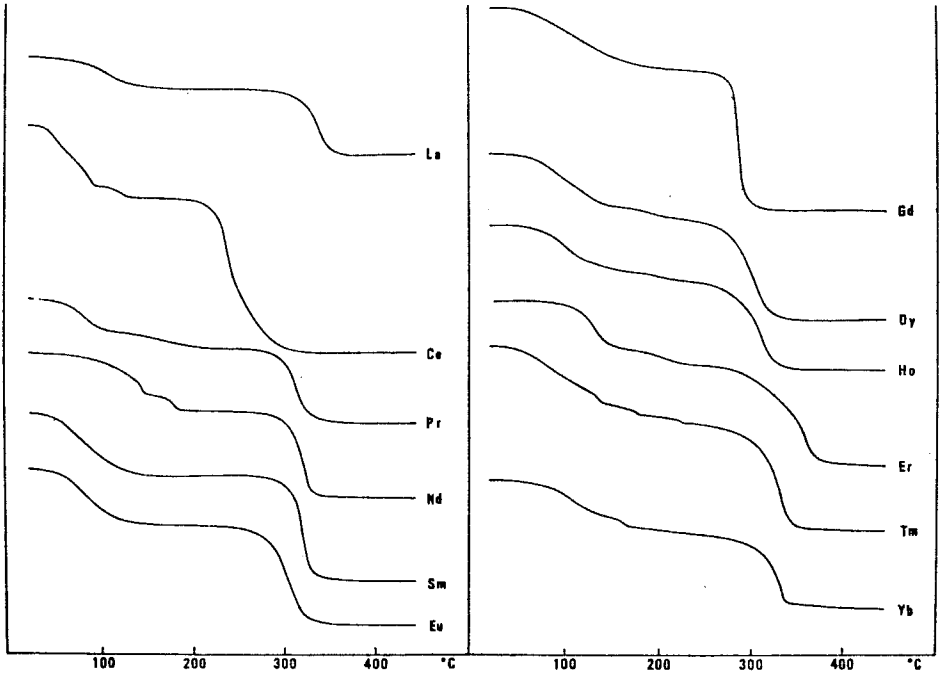

Fig. 96. The TG curves on the thermal decomposition of selected rare earth perchlorate hydrates. Heating rate 5° min^{-1}. (Cucinotta et al., 1976.)

The single crystals of rare earth perchlorates grown by Glaser and Johansson in slightly acidic solution at room temperature or below, proved to be hexahydrates. The crystals were stored in contact with a saturated solution of $R(ClO_4)_3$. The crystal structure is cubic, belonging to the space group Fm3m. The metal ion is coordinated to six water molecules. The structure can be described as a cubic, close-packed arrangement of $R(H_2O)_6^{3+}$ ions, with the perchlorate groups occupying all available octahedral holes. Some of the perchlorate ions show rotational disorder (fig. 97) (Glaser and Johansson, 1981).

Preparation of anhydrous rare earth perchlorates from the corresponding hydrates is difficult. The lighter lanthanides can be dehydrated in vacuum by using a very slow heating rate: heating of 3–4 days to 150°C (Slavkina et al., 1963). A second method of dehydration is to boil a perchlorate hydrate with triethylformiate in ethylacetate or with acetonitrile. This method is effective for the heavier lanthanides (Foster et al., 1972; Birnbaum and Stratton, 1973). Still another method of perparation is the reaction of RCl_3 and $AgClO_4$ in acetonitrile (Birnbaum and Stratton, 1973). The crystallographic properties of $R(ClO_4)_3$ are not known.

The thermal decomposition of rare earth perchlorates has been studied in air, nitrogen, and vacuum. $R(ClO_4)_3$ decomposes at 240–460°C. At 500°C the product

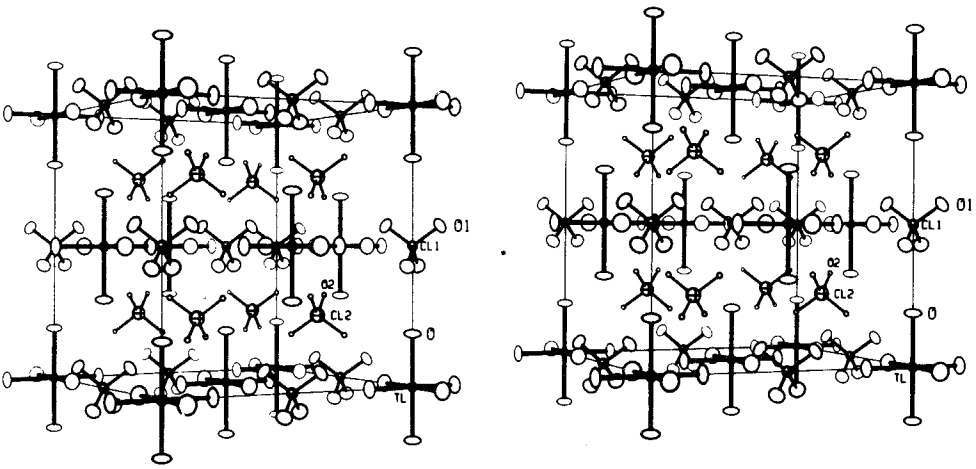

Fig. 97. A stereoscopic view of the cubic unit cell of $Tl(ClO_4)_3 \cdot 6H_2O$ isomorphic with rare earth perchlorate hexahydrates (Glaser and Johansson, 1981).

is ROCl, except in the case of cerium where it is CeO_2 (Steinberg and Shidlovsky, 1962; Belkova and Alekseenko, 1965). The kinetic parameters of the decomposition reactions have been determined.

The rare earth perchlorates are highly soluble in water. The molal concentration (mol/kg) obtained for a saturated solution at 25°C decreases from $La(ClO_4)_3$ (4.76) to $Dy(ClO_4)_3$ and thereafter increases slightly to $Lu(ClO_4)_3$ (4.63) (fig. 98) (Spedding and Rard, 1974). The solubility of perchlorate heptahydrates at 25°C varies between 63.9 and 67.4 wt.%. The enthalpies of the dissolution have been determined (Starostin and Leontov, 1972).

The solubility of rare earth perchlorates has also been studied in perchloric acid, thiourea water, urea water, and benzamide water systems (Korshunov et al., 1971; Karnaukhov et al., 1977; Ashikhnina et al., 1977; Osipova and Runov, 1981; Shchenev and Runov, 1981a,b). The solid compounds obtained were investigated by IR spectroscopy, differential thermal analysis, and X-ray powder diffraction. $R(ClO_4)_3$ also dissolves in ammonia; and $R(ClO_4)_3 \cdot nNH_3$ and $R(ClO_4)_3 \cdot nNH_3 \cdot mH_2O$ ($n = 3$–9; $m = 3.5$–4) compounds have been synthesized (Petrov et al., 1977). The compound $R(ClO_4)_3 \cdot NH_3$, where R = Sm · · · Lu, has been reported to be tetragonal. The unit cell dimensions for $Eu(ClO_4)_3 \cdot 9NH_3$ are $a = 14.88$ Å, $c = 11.56$ Å and there are four formula units in the unit cell (Sakanov et al., 1977).

Rare earth perchlorates form dioxane adducts with composition $R(ClO_4)_3 \cdot 9H_2O \cdot 4C_4H_8O_2$ (Vicentini et al., 1961). According to powder diffraction studies, the lattice is orthorhombic and possible space groups are Pmmm and P2mm. Unit cell dimensions for the lanthanum compound are $a = 16.07$ Å, $b = 17.87$ Å, and $c = 19.50$ Å (de Camargo and Valarelli, 1963).

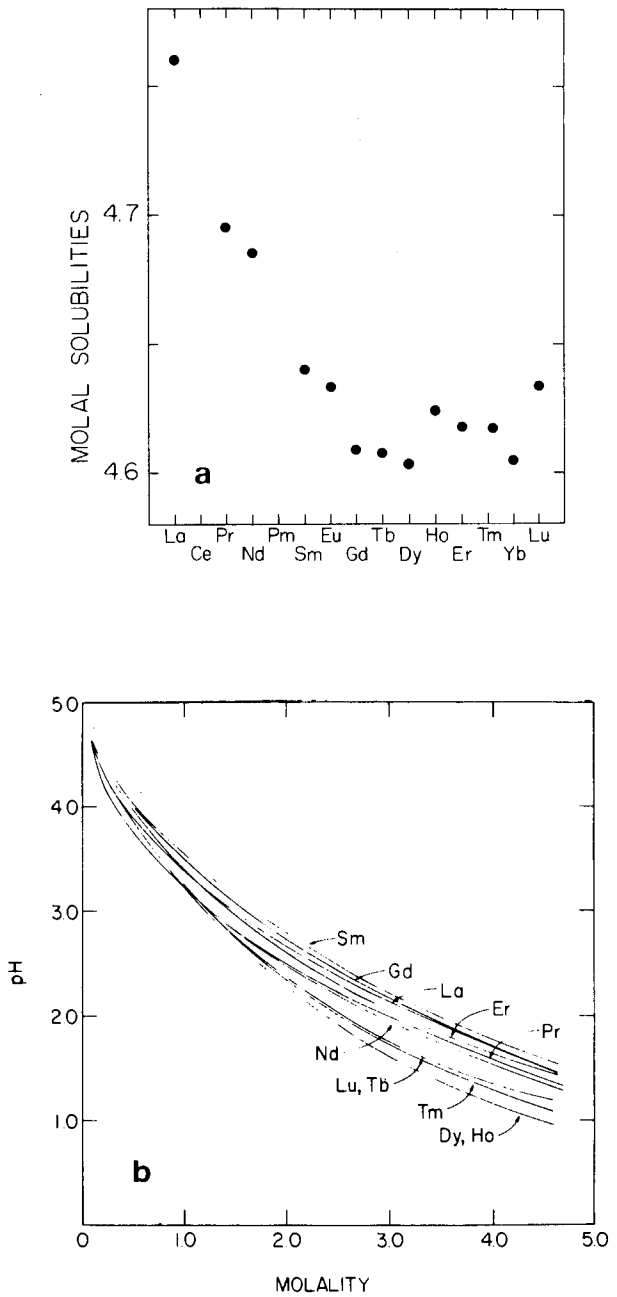

Fig. 98. The solubilities of the aqueous rare earth perchlorates at 25°C (a) and pH's of the solutions as a function of the molality (b) (Spedding and Rard, 1974).

6.4. *Rare earth bromates*

The rare earth bromates crystallize as enneahydrates, except for the scandium bromate, which contains six water molecules (Petrů and Dusek, 1968). The usual way to prepare the bromates is to add solid barium bromate or its water suspension to a rare earth sulfate solution with heating. $BaSO_4$ is filtered off and $R(BrO_3)_3 \cdot 9H_2O$ crystallizes upon cooling (James, 1908; James and Langelier, 1909). The crystallization can be carried out at room temperature and in air atmosphere, except for cerium, which requires the use of vacuum to avoid oxidation to Ce(IV). The use of $BaSO_4$ precipitation in the preparation of bromates has some drawbacks: free bromine or hydroxide-containing rare earth sulfates may form, and part of the rare earth may coprecipitate with $BaSO_4$ (Kremers and Moeller, 1944; Pearce et al., 1946b). These disadvantages can be avoided in some degree by using as concentrated a solution as possible and keeping it continually neutral (Harris, 1931; Mayer and Glamer, 1967). A second method of preparation is to use a rare earth perchlorate solution instead of sulfate in the precipitation, in which case the bromate source is $KBrO_3$ (Kremers and Moeller, 1944; Davidenko et al., 1972; Albertsson and Elding, 1977). In a third method, $R(OH)_3$ is dissolved in bromic acid and the solution slowly evaporated (Staveley et al., 1968).

Since the rare earth bromates easily form well-crystallized precipitates, they were earlier used in fractional crystallization processes aiming at the separation of individual rare earths (Gmelin, 1978). Single crystals of $R(BrO_3) \cdot 9H_2O$ have been grown from a solution containing an excess of BrO_3^- ions (Jantsch and Ohl, 1911; Helmholz, 1939). Slow evaporation of the water solution after $BaSO_4$ filtration also produces single crystals of good enough quality for X-ray studies (Gallucci et al., 1982).

$Sc(BrO_3)_3 \cdot 6H_2O$ can be synthesized similarly to the other rare earth borate hydrates. Thermal decomposition of enneahydrates occurs via intermediate phases. Tetrahydrates have been determined for La···Eu, trihydrates for Dy···Tm, Y, and dihydrates for La···Tb compounds (James and Langelier, 1909; Petrů and Dusek, 1968; Yakunina et al., 1969a, 1970).

The first publications of rare earth bromate enneahydrates correctly described the crystals as hexagonal (James and Langelier, 1909; Jantsch and Ohl, 1911). The hexagonal angle was demonstrated microscopically by Spedding and Bear in 1933; and in the first structure determination, published in 1939, Helmholz confirmed the hexagonal structure and suggested the space group $P6_3mc$. Later, the space group was corrected to $P6_3/mmc$ (Sikka, 1969; Albertsson and Elding, 1977; Gallucci et al., 1982). The structure, which is isomorphous over the whole lanthanide series, consists of columns of bromate groups and columns of hydrated rare earth ions, linked together by hydrogen bonds from the water molecules. The rare earth ions are coordinated to nine water molecules forming a tricapped trigonal prism (fig. 99) (Albertsson and Elding, 1977). See also section 10.

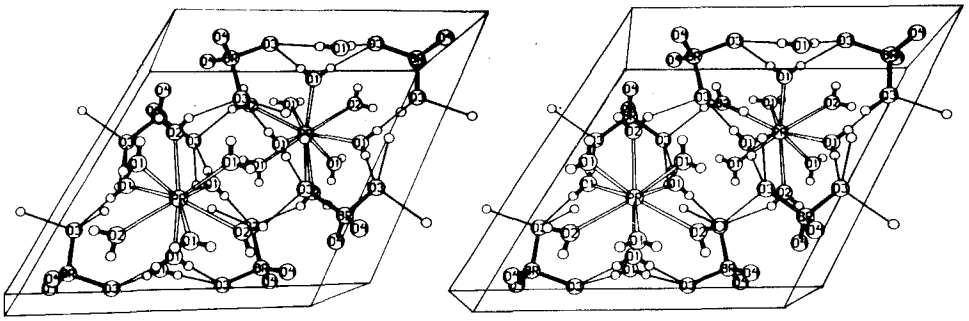

Fig. 99. A stereoscopic view of the unit cell of $Pr(BrO_3)_3 \cdot 9H_2O$ (Albertsson and Elding, 1977).

Optical measurements of $R(BrO_3)_3 \cdot 9H_2O$ crystals have revealed there to be some mosaic structure (Schumann, 1952). According to Poulet et al. (1975) the ordering of the oxygen atoms points to a pseudohexagonal structure. At lower temperatures (40–70 K) the structure of bromates reverts to lower symmetry. This has been detected for Nd and Gd compounds both by IR and Raman spectroscopy, and by optical and calorimetrical measurements (Poulet et al., 1975). According to Hellwege (1953) and Kahle (1959) there are two phase transformations at low temperatures. The structure changes via pseudohexagonal and monoclinic to triclinic.

Thermal decomposition of rare earth bromate enneahydrates begins as low as 50°C, where lower hydrates are formed. At higher temperatures $R(BrO_3)_3$ appears. In vacuum the enneahydrate loses water at room temperature (Hellwege and Johson, 1954). The preparation of pure $R(BrO_3)_3$ by dehydration is only possible for the larger lanthanides. The other anhydrous bromates have been obtained by evaporation of an aqueous solution of $R(BrO_3)_3$ in vacuum at 40–100°C and heating of the dry residue at the same temperatures in the presence of P_4O_{10} (Mayer and Glasner, 1967; Yakunina et al., 1970).

The thermal decomposition of anhydrous bromates, $R(BrO_3)_3 \rightarrow ROBr + Br_2 + 4O_2$, is complete around 280°C (Bancroft and Gesser, 1965; Mayer and Glasner, 1967). The kinetics have been studied by Yakunina et al. (1970). The oxybromide phase is stable over several hundred degrees and decomposes to oxide only at 700–1300°C, depending on the rare earth (Hölsä et al., 1980).

The physical properties of the rare earth bromate hydrates have been studied by several groups and can be summarized as follows: the melting points of the enneahydrates vary between 37 and 80°C (Petrů and Dusek, 1968), the formation enthalpies between 3490 and 3590 kJ/mol (Schumm et al., 1973). The specific heat of $Gd(BrO_3)_3 \cdot 9H_2O$ increases from 0.05 J/g K at 20 K to 0.32 J/g K at 100 K, exhibiting a clear jump at 66 K, where the structure changes (Poulet et al., 1975). The rare earth bromates are readily soluble in water: the concentrations of the saturated solution vary between 1.2 and 2.3 mol/kg H_2O (Staveley et al.,

1968). According to Petrů and Dusek, $Sc(BrO_3)_3 \cdot 3H_2O$ is hygroscopic (1965). On the other hand, bromates are almost insoluble in alcohols (Jantsch and Ohl, 1911).

The IR spectra of $R(BrO_3)_3 \cdot 9H_2O$ show absorption frequencies at 450–600 cm^{-1}, 1625–1640 cm^{-1} and 1665–1670 cm^{-1} for $\delta(H_2O)$, at 3300–3600 cm^{-1} for $\nu(OH)$, at 850 cm^{-1} for $\nu_3(BrO_3^-)$, and at about 460 cm^{-1} for $\nu_2(BrO_3^-)$ (Yakunina et al., 1969a; Poulet et al., 1975).

6.5. *Rare earth iodates*

The interesting physical properties of some of the rare earth iodates have led to systematic studies on this class of rare earth complexes. Altogether 82 binary rare earth iodates have been reported in the literature. Fourteen groups of isostructural crystalline compounds of the type $R(IO_3)_3 \cdot nH_2O$ with $n = 0 \cdots 6$, consisting of 62 individual compounds, have been studied by Nassau et al. (1974, 1975). In addition, there are reports for 15 amorphous compounds, for four compounds with a complex composition, and for the compound $La_5(IO_6)_3$.

6.5.1. *Iodate hydrates*

Rare earth iodate hydrates can be precipitated with iodic acid or lithium iodate from rare earth nitrate solution (Rimbach and Schubert, 1909; Yakunina, 1969b; Hajek and Hradilova, 1971b). The products are dried in air and can be recrystallized by several different methods (Nassau et al., 1974). The most important hydrates and their preparation conditions are presented in table 19.

TABLE 19
Crystallization conditions for the different rare earth iodate hydrates, $R(IO_3)_3 \cdot nH_2O$ (Nassau et al., 1974, 1975).

n	Structure type	Y	La	Ce	Pr	Nd	Sm	Eu	Gd	Tb	Dy	Ho	Er	Tm	Yb	Lu
0.5	–		a	a												
1	–			a	a	a	a									
2	I													a	a	ab
2	II	abc				b	bd	abc	acd	ac	ac	a	a			
4	–	bd							d	bd	b	bd	bd	d	bd	cd
5	II		cd		cd											
5	I			bcd	bd	bcde	b									
6	–		bd *													

a: crystallization in boiling water.
b: precipitation at room temperature.
c: evaporation at normal or reduced pressure.
d: crystallization in acetic acid.
e: cocrystallization of acidic iodate $R(IO_3)_3 \cdot HIO_3$.
*: also reported to be amorphous.

As the table shows, the iodates may contain 0.5, 1, 2, 4, 5, and possibly 6 water molecules. The di- and pentahydrates have two polymorphic modifications. The hemi-, mono- and dihydrates can all be crystallized from a boiling aqueous solution. The hemihydrate may contain traces of monohydrate. $Sc(IO_3)_3 \cdot H_2O$, on the contrary, is formed upon heating of dihydrate in nitrogen (Nassau and Shiever, 1975). All rare earths except lanthanum form iodate dihydrates, with structures of three kinds: type I (triclinic) for Tm $\cdots$ Lu, type II (triclinic) for Nd $\cdots$ Er, Y, and type III for scandium (which has a unique and unknown structure) (Abrahams et al., 1976a). The higher hydrates can be synthesized at room temperature and crystallized by slow evaporation. Crystalline tetrahydrate has been encountered for the smaller rare earths and the amorphous phase has been prepared for the larger ones (Ephraim and Roy, 1929; Yakunina et al., 1969b). Lanthanum and praseodymium form monoclinic iodate pentahydrates. The second pentahydrate has been prepared for Ce $\cdots$ Sm but its crystal structure is unknown (Abrahams et al., 1976a).

Amorphous hexahydrate is known for the lanthanum and neodymium iodates. Both are very unstable: decomposition begins at about 50°C and the total dehydration occurs in two stages between 50 and 350°C (Hajek and Hradilova, 1971b).

Besides the hydrates listed in table 19 there are hydrates with 1.5, 2.5, 3, and $3\frac{1}{3}$ water molecules. The existence of amorphous trihydrate seems probable, although the same analytical result is obtained for a 1:1 mixture of di- and tetrahydrate (Nassau et al., 1975). All the trihydrates have been synthesized from nitrates by iodic acid precipitation (Harmelin, 1966; Odehnal, 1972). The 1.5 and 2.5 hydrates have been reported for lanthanum and scandium iodates, but their existence is somewhat uncertain (Hajek and Hradilova, 1971b). Bosch-Reig et al. (1970) describe a $3Pr(IO_3)_3 \cdot 10H_2O$ compound, i.e., $3\frac{1}{3}$ hydrate, which in DTA was found to lose water near 100°C and to form the anhydride; specific characterization is otherwise lacking.

Rare earth(IV) iodate hydrates are only known for cerium and are obtained by oxidizing $Ce(NO_3)_3$ in nitric acidic solution with excess of HIO_3 (Ibers, 1956).

Promethium forms violet rose iodate hydrates, $Pm(IO_3)_3 \cdot nH_2O$, with variable water content $n = 2 \cdots 9$ (Scherer, 1968; Weigel, 1969). According to Abrahams et al. (1976a) it also forms a monohydrate, which is isomorphic with the other rare earth iodate monohydrates.

The unit cells are known for the rare earth iodate hemi-, mono-, di-, and pentahydrates. The hemihydrates are orthorhombic ($P2_12_12_1$) (Abrahams et al., 1977) and the monohydrates crystallize in the acentric monoclinic space group $P2_1$. The crystal structure of $Nd(IO_3)_3 \cdot H_2O$ (Liminga et al., 1975) contain three independent IO_3^- ions sharing oxygen atoms to form a three-dimensional network (fig. 100). Two of the iodine atoms have seven- and the third has six-coordination. The water molecule links the three independent iodate groups together. The Nd^{3+} ion occupies a distorted bicapped trigonal prism (fig. 101). A different, acentric but orthorhombic ($C222_1$) structure has been determined for the cerium

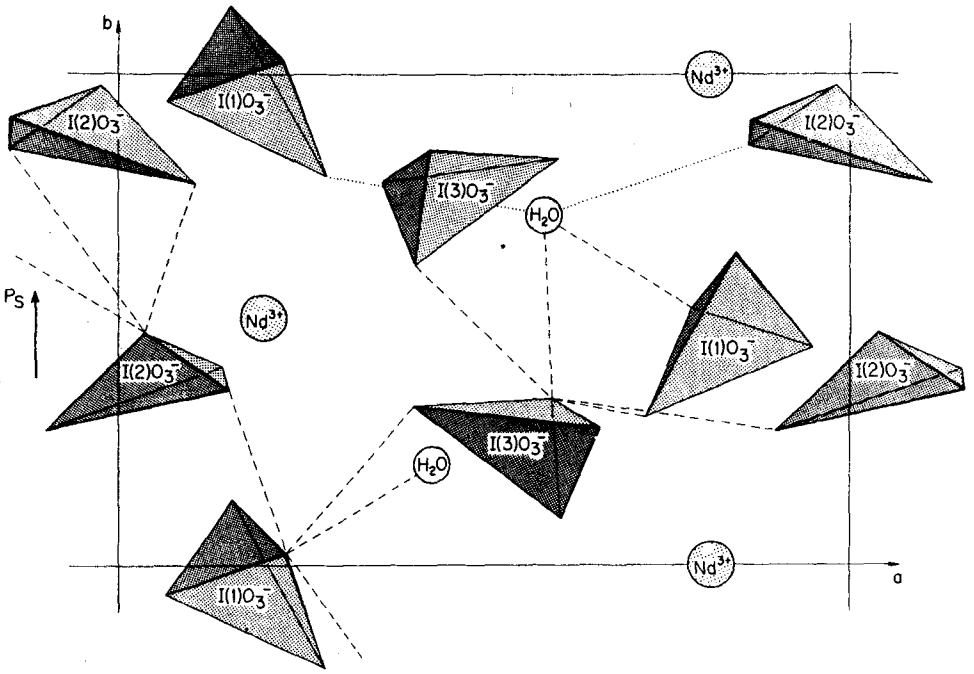

Fig 100. The orientation of IO_3^- and Nd^{3+} ions and H_2O in $Nd(IO_3)_3 \cdot H_2O$ with respect to the polar axis (Liminga and Abrahams, 1976).

monohydrate, which is formed by spontaneous hydration of $Ce(IO_3)_3$ in air (Abrahams et al., 1977). Both the dihydrate phases are triclinic. Of the two pentahydrates, the first structure (La, Pr) is monoclinic and the second (Ce, Nd, Sm) has not yet been characterized by X-ray methods (Abrahams et al., 1977).

Fourvalent cerium forms $Ce(IO_3)_4 \cdot H_2O$ which is monoclinic ($P2_1/n$), containing trigonal IO_3^- groups with two of the oxygen atoms coordinated to cerium (fig. 102). Cerium has eight-coordination with one significantly longer Ce–O distance (2.82 Å), while iodine has octahedral coordination with three short and three long I–O distances (Ibers and Cromer, 1958).

The thermal decomposition of rare earth iodate hydrates is summarized by Nassau et al. (1974, 1975) in the following way. Lanthanum iodate hexahydrate begins to decompose below 70°C, losing water slowly up to 490°C, where the anhydrous plateau is reached. The penta- and tetrahydrates change to amorphous form at 70 and 80°C, respectively, after which they slowly lose water up to 360 and 380°C. Iodate dihydrate is stable up to 250°C (fig. 103). The monohydrate decomposes to hemihydrate or anhydrous iodate at 120°C, and the hemihydrate is dehydrated only at 300°C. The decomposition temperatures are not strongly dependent on the rare earth. The anhydrous phases found for each rare earth are shown in table 20.

The $R(IO_3)_3$ phases of all rare earths except La decompose to oxide at about

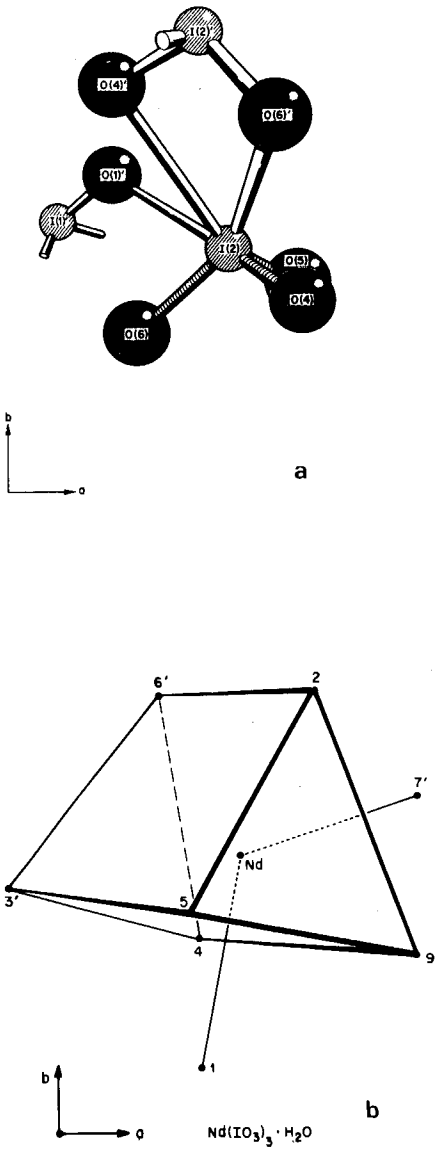

Fig. 101. The nearest-neighbor environment of I(1) (a) and the Nd^{3+} coordination polyhedron (distorted bicapped trigonal prism) (b) in $Nd(IO_3)_3 \cdot H_2O$ (Liminga et al., 1975).

500°C. The temperature is about the same for all structure types. $La(IO_3)_3$ behaves exceptionally in oxidizing to periodate, $La_5(IO_6)_3$, at 520°C (Yakunina et al., 1969b).

The solubilities of thirteen rare earth iodates in aqueous and aqueous alcoholic solvent mixtures at 25°C have been measured. Methanol and ethanol were used as alcoholic components (Miyamoto et al., 1985).

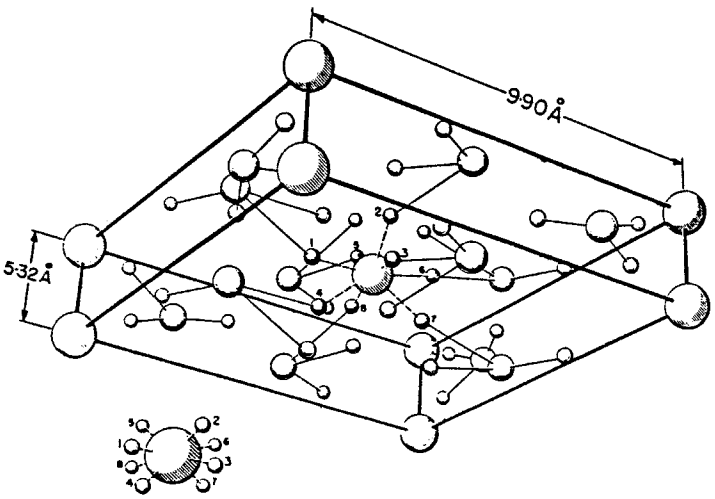

Fig. 102. A perspective drawing of the unit cell of $Ce(IO_3)_4$. The inset is a view of the Ce atom at the center of the cell as one looks along the [110] axis. In decreasing order of size the atoms shown are Ce, I, and O. (Ibers and Cromer, 1958.)

TABLE 20
The different structure types of rare earth iodates (Nassau et al., 1974, 1975; Abrahams et al., 1976a; Nassau, 1976).

	Structure type					
R	I	II	III	IV	V	VI
La				×		×
Ce, Pr	×		×	×	×	
Nd, Sm	×		×		×	
Eu · · · Tm, Y	×					
Yb, Lu	×	×				

6.5.2. *Anhydrous iodates*

The anhydrous rare earth iodates can be prepared in several ways: dehydration of iodate hydrates, crystallization in boiling nitric acid solution, refluxing of oxide in iodic acid, drying of iodate solution at higher temperature (105–180°C), and thermal treatment of acidic iodate $R(IO_3)_3 \cdot HIO_3$ (Chloupek et al., 1932; Pincott and Barnes, 1968; Nassau et al., 1974, 1975).

The anhydrous rare earth iodates exhibit six different structure types, designated here and in table 20 by Roman numerals I–VI. In addition to those included in table 20, anhydrous iodates are formed by Sc^{3+} and Ce^{4+}. The structure types I and II are monoclinic; the others are unknown. Polycrystalline samples of types III–VI have been prepared and their X-ray diffraction patterns reported (Abrahams et al., 1976a).

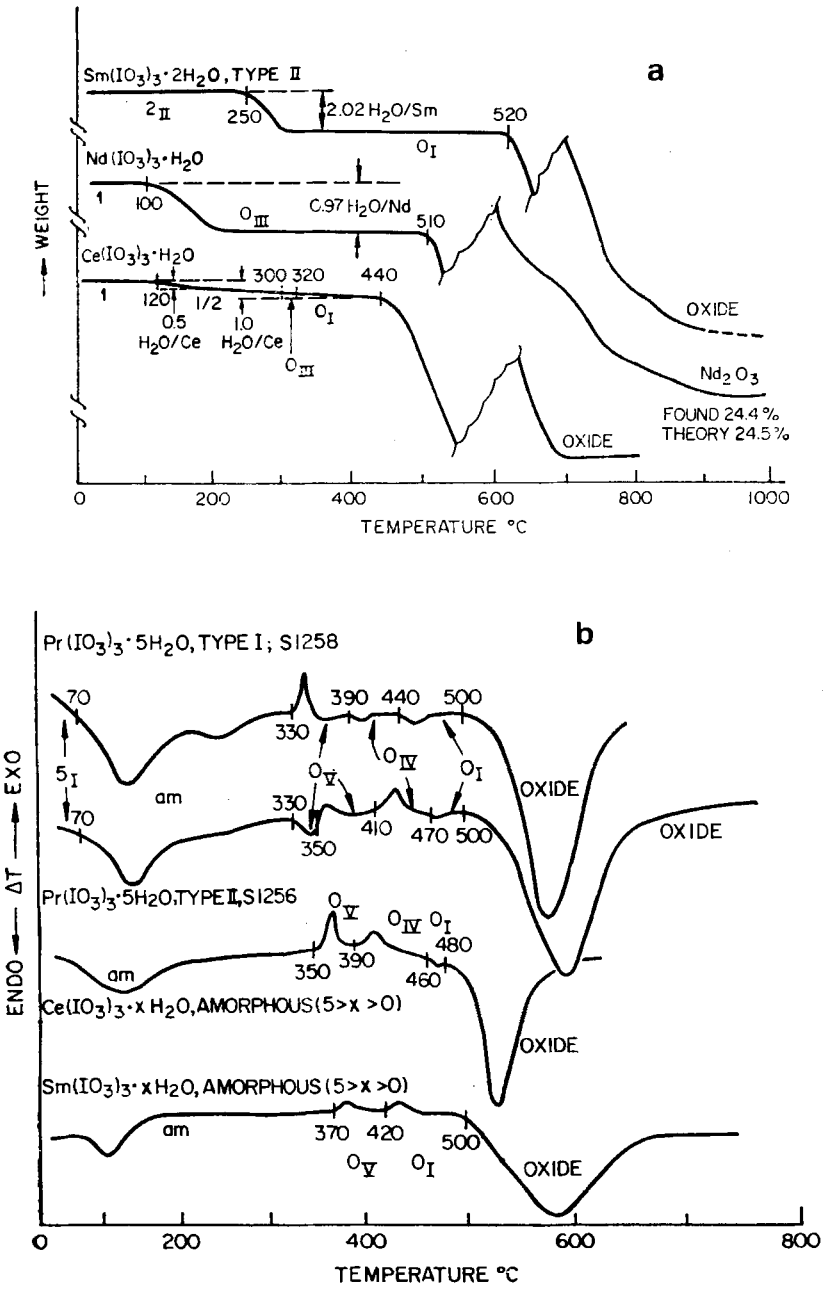

Fig. 103. The TG (a) and DTA (b) curves for selected rare earth iodate hydrates (Nassau et al., 1975).

The formation of anhydrous iodates from iodate hydrates is schematized in fig. 104. As can be seen, the anhydrous phase that forms is strongly dependent on the starting hydrate phase.

In the structure of $Gd(IO_3)_3$, iodate ions form a three-dimensional network based on shared oxygen atoms, with the Gd^{3+} ion located within a distorted dodecahedron of oxygen atoms. The three independent IO_3^- ions form trigonal pyramids (fig. 105) (Liminga et al., 1977).

Anhydrous scandium iodate has three polymorphic modifications. α- and β-forms are formed by dehydration of dihydrate, while the γ-form can be prepared either from the β-form at 450°C or from the boiling water or nitric acid solution of $Sc(IO_3)_3$. The structures of the phases have not been determined (Nassau and Shiever, 1975).

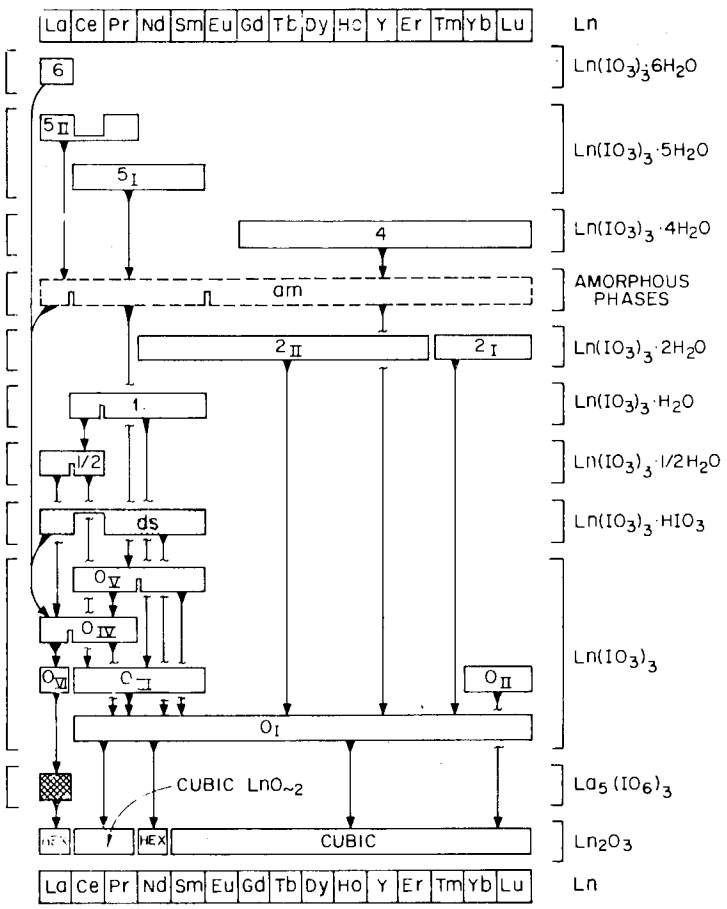

Fig. 104. The occurrence of the lanthanide iodates. Rectangles indicate groups of isostructural compounds and arrows indicate decomposition paths heating in N_2. (Nassau et al., 1975.)

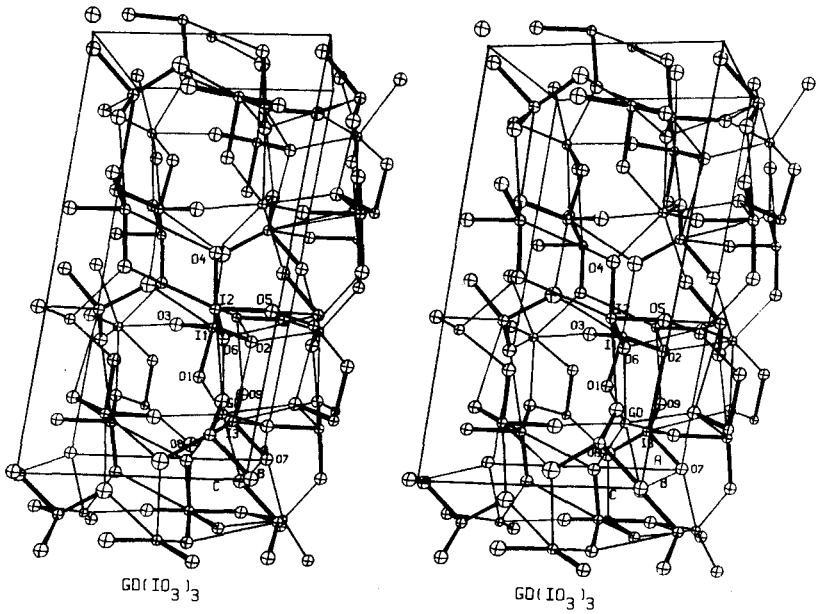

Fig. 105. A stereoscopic view of the structure of $Gd(IO_3)_3$ (type I) (Liminga et al., 1977).

Ce(IV) forms $Ce(IO_3)_4$, which can be crystallized from boiling nitric acid solution (Staritzky and Cromer, 1956; Nassau et al., 1975). The compound is tetragonal, with space group $P4_2/n$. Two oxygen atoms from each trigonal pyramidal IO_3^- group are coordinated to cerium. The coordination polyhedron around cerium is distorted antiprism and is closely related to that found in $Ce(IO_3)_4 \cdot H_2O$. The coordination number of iodine is five (Cromer and Larson, 1956; Staritzky and Cromer, 1956; Azarova et al., 1972).

6.5.3. *Acidic and other iodates of complex composition*

In earlier studies on the system $La(IO_3)_3$–HIO_3–H_2O no hydrogen-containing iodates were found (Lyalina and Soboleva, 1975); but more recently two acidic rare earth iodates have been prepared and characterized in the course of a search for new nonlinear optical materials among the transition metal iodates (Nassau et al., 1975; Abrahams et al., 1976b). When $R(IO_3)_3$ is dissolved in nitric acid and evaporated, nonstoichiometric $R(IO_3)_3 \cdot nHIO_3$ ($n = 0.82$–0.92) is formed. Addition of HIO_3 to the solution causes the formation of stoichiometric acidic iodates (Nassau et al., 1975). The type $R(IO_3)_3 \cdot HIO_3$ is formed by La $\cdots$ Sm and the type $3R(IO_3)_3 \cdot HIO_3 \cdot 7H_2O$ by La.

$Pr(IO_3)_3 \cdot HIO_3$ is known to be monoclinic ($P2_1/a$) but a detailed structure analysis has not been carried out. The crystals are biaxial with refraction indices in the range 1.92–1.97 with $2V = 50°$. All pyro- and piezoelectric coefficients are zero due to the centrosymmetricity of the crystal (Abrahams et al., 1976b).

$3La(IO_3)_3 \cdot HIO_3 \cdot 7H_2O$ crystals have been grown in silica gels wetted with acetic acid, from 0.5 M $La(NO_3)_3$ and HIO_3 solutions. The growth may take several months. In the structure, five independent IO_3^- ions with trigonal–pyramidal conformation having 2, 3, or 4 additional oxygen atoms at longer distances form a three-dimensional network. One independent La atom has eight-coordination and the other ten-coordination. Each of the coordination polyhedra is based on a trigonal prism, having an additional 2 or 4 oxygen atoms (fig. 106). There is an extensive hydrogen-bonding system and an acidic proton is present as H_3O^+ (Abrahams and Bernstein, 1978).

In a recent study of the three-component system $La(IO_3)_3$–HIO_3–H_2O at 25°C, lanthanum iodate trihydrate and two previously unknown lanthanum hydrogen iodates, $3La(IO_3)_3 \cdot 2HIO_3 \cdot 6H_2O$ and $2La(IO_3)_3 \cdot 3HIO_3 \cdot 6H_2O$, were isolated (Tarasova et al., 1985).

$RIO_3 \cdot HIO_3$ decomposes to anhydrous iodate type I above 300°C, or in the case of lanthanum to the iodate type IV (Nassau et al., 1975). According to Tarasova et al. (1985), the loss of iodic acid in lanthanum compounds is a two or three stage process.

The preparation and properties of rare earth hydroxide iodates have not been systematically studied. $Ce(OH)_3IO_3$ is formed by addition of aqueous KIO_3 to Ce(IV) in dilute nitric acid solution at a pH of 2.5 (Shvedov and Musaev, 1959); the compounds $Nd(OH)(IO_3)_2 \cdot nH_2O$ and $Nd(OH)_2IO_3 \cdot nH_2O$ are precipitated from a neutral $Nd(NO_3)_3$ solution with aqueous KIO_3 (Pruitt et al., 1962). An

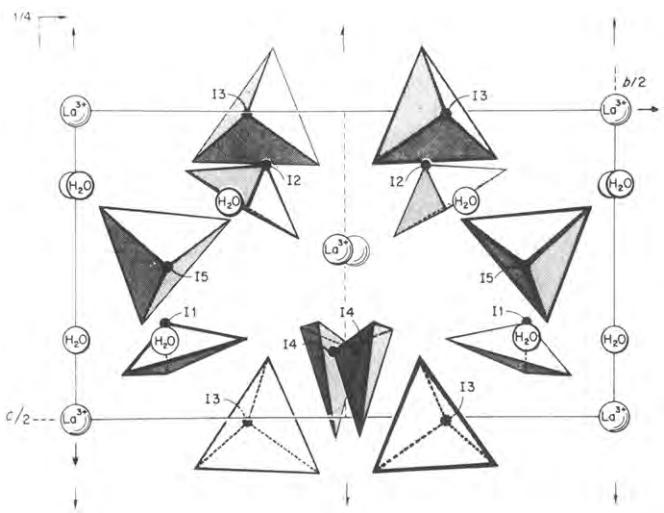

Fig. 106. The arrangement of La^{3+}, IO_3^-, and H_2O in two asymmetric units of the $3La(IO_3)_2 \cdot HIO_3 \cdot 7H_2O$ structure. The symmetry operations are given. (Abrahams and Bernstein, 1978.)

oxide-iodate with composition $TbO_2 \cdot Tb(IO_3)_3 \cdot 2H_2O$ has been reported by Pincott and Barnes (1968). The crystal structure of the material revealed not the expected mixed valent compound but a hydroxide iodate of Tb(IV) or a distorted, nonstoichiometric phase containing Tb^{3+} and Tb^{4+} but retaining the $Tb(IO_3)_3 \cdot 2H_2O$ structure (Barnes, 1977). In the structure, Tb ions are eight-coordinated to seven oxygen atoms, each of a different doubly or triply bridging iodate group, and to one nonbridging hydroxide group (fig. 107).

6.5.4. *Properties of rare earth iodates*

The anhydrous rare earth iodates of structure type III and those dehydrated from monohydrates are hygroscopic. The solubility of $R(IO_3)_3$ (R = La, Ce, Sm, Eu) in water varies between 0.3 and 2.6 mmol/dm^3, being lowest for samarium and highest for cerium (Chloupek et al., 1932; Monk, 1951b; Laurie and Monk, 1963; Shklovskaya et al., 1977). The properties of the water solutions have been studied by Firsching and Paul (1966).

The iodate hydrates are highly soluble in dilute acids but insoluble in alkali hydroxide solutions (Hajek and Hradilova, 1971b). The solubility of hydrated iodates in neutral inorganic salt solutions increases with increasing salt concentration. A series of salts with an increasing solubility effect is $KCl < MgCl_2 \ll MgSO_4 < K_2SO_4$ (Pearce and Oelke, 1938; Newton and Arcand, 1953). The solubility in organic solvents is low (Monk, 1951a).

The formation enthalpies ΔH^0_{298} of $R(IO_3)_3$ compounds vary between -1300 and -1400 kJ/mol and the free energy ΔG^0_{298} is about -1130 kJ/mol (Schumm et al., 1973).

The IR spectra of rare earth iodates have been recorded by many research

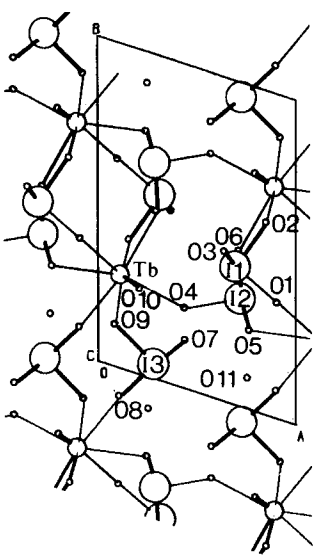

Fig. 107. The structure of terbium(IV) hydroxide iodate; projection along [011]. (Barnes, 1977.)

groups. The following frequencies are found: (O–I–O) and lattice vibrations at 210, 230, 250, and 270 cm^{-1}; ν_4(O–I–O) at 340 cm^{-1}; ν_2(O–I–O) at 360, 390, and 400 cm^{-1}; ν(R–O) at about 500–600 cm^{-1}; ν_1 and ν_3(I–O) at 760–830 cm^{-1}; $\delta(H_2O)$ at 1620 cm^{-1}; hydrogen bonding at 2380 and 2480 cm^{-1}; and ν(OH) at 3300–3600 cm^{-1} (Yakunina et al., 1969b; Hajek and Hradilova, 1971b). As an example of the spectra, fig. 108 presents the results obtained by Nassau et al. (1974).

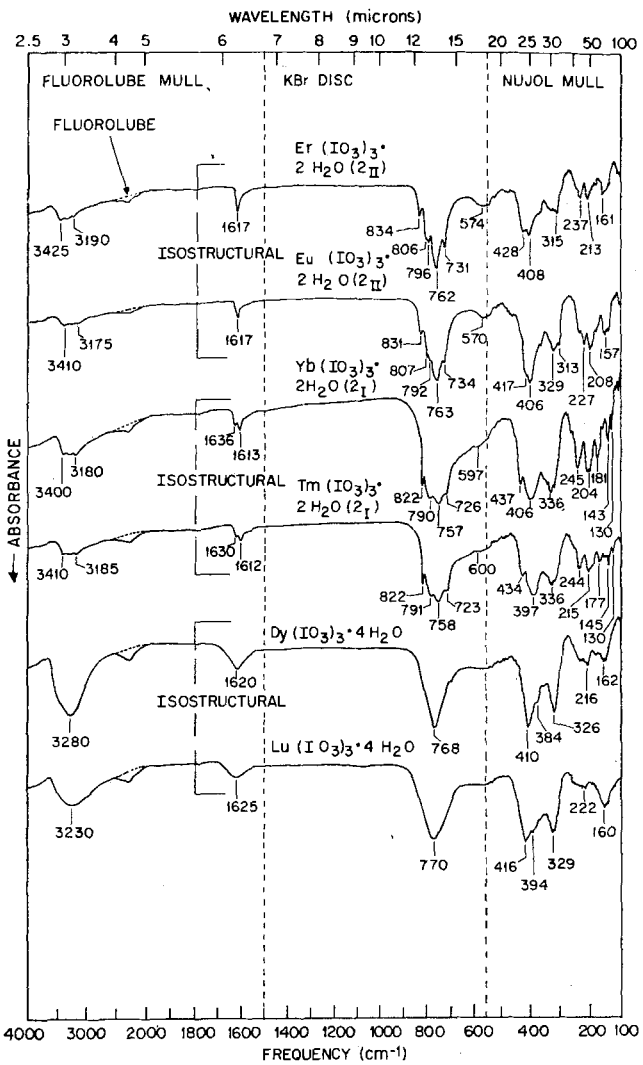

Fig. 108. The IR absorption spectra of some lanthanide iodate hydrates in the region 4000–100 cm^{-1} (Nassau et al., 1974).

Interesting and useful coupling between optical, magnetic, elastic, and dielectric properties is expected for the compounds $R(IO_3)_3 \cdot nH_2O$ (Abrahams et al., 1973). These have been studied by Abrahams et al. (1976), Abrahams and Bernstein (1978), and Liminga et al. (1975, 1977).

6.6. *Rare earth periodates*

Lanthanum periodate $LaIO_5 \cdot 2H_2O$ was prepared for the first time in 1874, by Cleve, in a water solution of $La(CH_3COO)_3$ and H_3IO_5. For yttrium, the same reaction yielded $3Y_2O_3 \cdot 2I_2O_7 \cdot 6H_2O$ and $YIO_5 \cdot 4H_2O$, according to the chemical analysis. Later, Bahl and Singh (1939) synthesized $Y_4I_2O_{13} \cdot 11H_2O$ as coproduct with $YIO_5 \cdot 4H_2O$ and they never did succeed in preparing $3Y_2O_3 \cdot 2I_2O_7 \cdot 6H_2O$. The periodate that Sahney et al. (1946) obtained by reaction of $Na_2H_3IO_6$ in a $La(NO_3)_3$ solution in slightly acidic conditions was confirmed by magnetic measurements to be $La_2H_2I_2O_{11} \cdot 3H_2O$ and not $LaIO_5 \cdot 2H_2O$. However, the tri- and tetrahydrates of $LaIO_5$ have been obtained in a water solution of $Na_2H_3IO_6$ and $R(NO_3)_3$ (Varfolomeev et al., 1971; Odehnal, 1972). The tetrahydrate, $RIO_5 \cdot 4H_2O$, is known for all rare earths (Varfolomeev et al., 1972, 1973). As an alternative iodine source in the preparation of the tetrahydrates the acid $HIO_4 \cdot 2H_2O$ can be used. Recently, Varfolomeev (1985) has reviewed the chemistry of the rare earth iodates and periodates.

According to Kyrki and Lokio (1971), most of the rare earth periodates are really hexaoxoiodates containing the $H_2IO_6^{3-}$ ions, and $RIO_5 \cdot 4H_2O$ should be formulated as $RH_2IO_6 \cdot 3H_2O$, and $La_2H_2I_2O_{11} \cdot 3H_2O$ as $2LaH_2IO_6 \cdot H_2O$. Periodic acid or its di- or trisodium salt reacts with rare earth perchlorate in the molar ratio 1:1 at a pH of 1.9–2.6 to $RH_2IO_6 \cdot nH_2O$, which by drying can be converted to the phase $RH_2IO_6 \cdot 3H_2O$ (Kyrki and Lokio, 1971). Crystal water amounts of 1, 5, 9, and 13 have also been reported (Hajek and Hradilova, 1971a). The hexaoxoiodate formula ($ScH_2IO_6 \cdot 6H_2O$) has even been proposed for scandium, though only on the basis of its IR spectrum (Petrů et al., 1970).

Depending on the periodate source used as starting material, $PrH_2IO_6 \cdot xH_2O$ may contain 1.5, 3, or 5 water molecules. $Pr(ClO_4)_3$ reacts with $Na_2H_3IO_6$ to form the trihydrate, with H_5IO_6 to form the pentahydrate (Lokio, 1971). The $2Pr_2O_3 \cdot 3I_2O_7 \cdot 24H_2O$ phase obtained by Ephraim and Ray (1929) did not appear in the systematic experiments of Lokio and Kyrki, which have been summarized by Lokio (1974a). Tetravalent cerium forms periodates with the formula $CeHIO_6 \cdot nH_2O$ ($n = 1$ or 3) (Choudhury, 1941; Alimarin et al., 1958). According to Lokio (1973), H_5IO_6 forms $CeHIO_6 \cdot nH_2O$ compounds when it reacts with Ce(III) or Ce(IV) compounds in the molar ratio 1:1 at a pH of 1.5–3.

When periodic acid reacts with rare earth carbonate in the molar ratio 3:1 at a pH of 0.4–1.1, the compound $R(H_4IO_6)_3 \cdot nH_2O$ ($n = 1$–3) is formed. For the reaction in the case of Ce(IV) the molar ratio must be 4:1 and the product is $Ce(H_4IO_6)_4 \cdot nH_2O$.

Still other known periodates are of type $R_5(IO_6)_3$ (R = Yb, Lu), which are formed upon heating of the corresponding iodate hydrates at 400–600°C (Harmelin, 1966). Preparation of the pure compound is difficult, because before all the iodate has been oxidized to periodate part of the periodate has already decomposed to oxide (Hajek and Hradilova, 1971b). A few ternary periodates are known as well. $La_2Co_2H_3(IO_6)_3 \cdot 12H_2O$ has been synthesized by allowing diperiodatecobalt(III) acid to react with $La(NO_3)_3$ solution (Lister and Yoshino, 1960). In alkaline solution the stability of lanthanide periodate complexes increases in the order $La^{3+} < Pr^{3+} < Er^{3+} < Ce^{4+}$. In alkaline solution a solid cerium periodate, $Na_6Ce(IO_6)_2$, is formed (Alimarin et al., 1962).

6.6.1. *Thermal decomposition*

The dehydration reaction of $RH_2IO_6 \cdot 3H_2O$ to RH_2IO_6 is a two-stage process. RH_2IO_6 is stable in a narrow temperature range between 150 and 200°C (Lokio and Kyrki, 1971) and then begins to decompose to binary periodate, RIO_5, releasing water. Above 300°C the decomposition is complete and RIO_5 compounds remain stable up to 500°C (fig. 109). All the anhydrous RIO_5 compounds are nonhygroscopic and sparingly soluble in water (Varfolomeev et al., 1972). In the decomposition of RIO_5 to oxide, iodine and oxygen are released. According to Varfolomeev et al. (1972) the reaction proceeds in stages, but no clear plateau is seen in the TG curve. The kinetics of the dehydration and decomposition reaction have been studied by Lokio (1974b).

The periodate hydrate of tetravalent cerium, $CeHIO_6 \cdot 3H_2O$, dehydrates in a

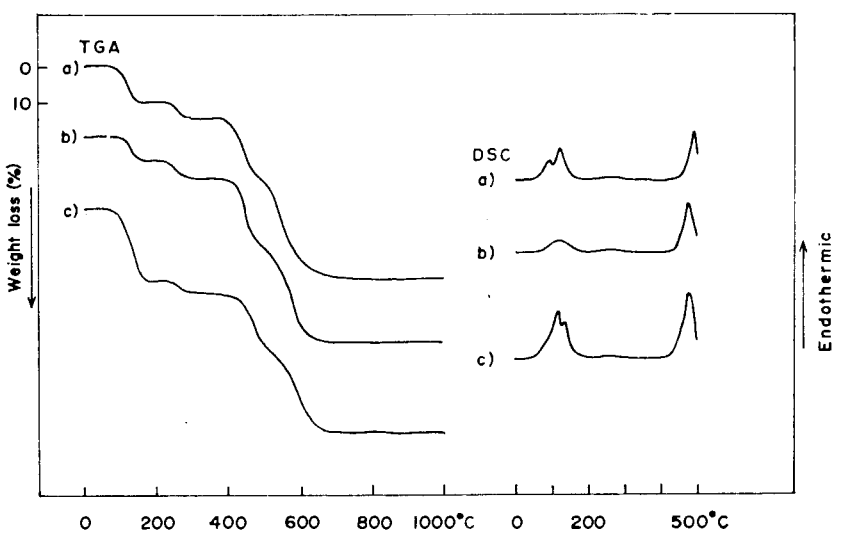

Fig. 109. The TG and DSC curves for (a) $PrH_2IO_6 \cdot 3H_2O$, (b) $PrH_2IO_6 \cdot 1\frac{1}{2}H_2O$, and (c) $PrH_2IO_6 \cdot 5H_2O$ (Lokio and Kyrki, 1971).

similar way to the trivalent compound, but the intermediate phase, $Ce_2I_2O_{11}$, behaves differently in the further decomposition. $Ce_2I_2O_{11}$ is stable in a very narrow temperature range about 350°C, before it decomposes to $Ce_2I_2O_9$. This phase is also unstable and further decomposes to CeO_2 (Lokio, 1973). After several attempts, $Ce_2I_2O_{11}$ and $Ce_2I_2O_9$ have been separated in pure form and their IR absorption spectra have been recorded.

The thermal decomposition of $R(H_4IO_6)_3 \cdot nH_2O$ in air takes place in several stages. The first is the release of crystal water and the formation of water from the hydrogenperiodate ion:

$$R(H_4IO_6)_3 \cdot nH_2O \rightarrow R(H_2IO_5)_3 + (n+3)H_2O\,. \tag{11}$$

The second step also includes the formation of water:

$$R(H_2IO_5)_3 \rightarrow RH_4I_3O_{14} + H_2O\,. \tag{12}$$

Immediately thereafter the reaction becomes endothermic and iodine hexavalent. The composition of the reaction product corresponds to $R_2H_8I_6O_{25}$, which can also be written as $R_2(I_2O_7)_3 \cdot 4H_2O$. The fourth reaction step is the dehydration of $R_2(I_2O_7)_3 \cdot 4H_2O$, and after that $R_2(I_2O_7)_3$ begins to decompose to oxide. The reaction is complete above 600°C (Lokio, 1974a). The decomposition scheme of $Ce(H_4IO_6)_4 \cdot nH_2O$ is similar to that just described, but the composition of the intermediate phase is $Ce(I_2O_7)_2$.

In isothermal heating at 125°C $La(H_4IO_6)_3 \cdot H_2O$ and $Ce(H_4IO_6)_3 \cdot 2H_2O$ decompose to $La(IO_4)_3$ and $Ce(IO_4)_4$. The existence of the IO_4^- ion can be confirmed by IR spectrometry (Lokio, 1974a). Venugopalan and George (1956) report the same product.

6.6.2. *Structure and properties*

The periodates are distinguished by a great variety of structures, owing to the tendency of the oxygen-containing derivatives of iodine(VII) to form condensed anions. A general feature of all the compounds is that the coordination polyhedron of the iodine atom is almost always a distorted octahedron. Only one crystal structure has been determined: that of $RH_2IO_6 \cdot 3H_2O$ (or $RIO_5 \cdot 4H_2O$) (R = Pr · · · Lu) by single-crystal methods (Shamrai et al., 1975). The structure is monoclinic ($P2_1/b$) and contains sheets of $IO_4(OH)_2$ octahedra linked to one another by RO_8 polyhedra. Bonding between the sheets is by hydrogen bonds (fig. 110) (Shamrai et al., 1977a).

All rare earth periodates are sparingly soluble in water. For this reason they have even been used as precipitation agents for the rare earths (Puzdrenkova et al., 1958). The solubility of $RH_2IO_6 \cdot 3H_2O$ varies between 2.6 and 0.2 mg/100 g H_2O, while the solubility of $CeHIO_6 \cdot 3H_2O$ is more than tenfold greater (Lokio, 1974b).

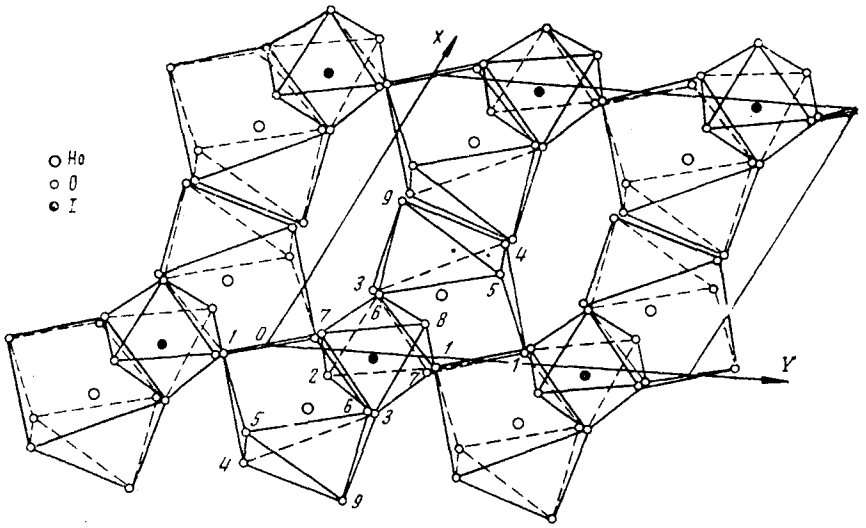

Fig. 110. A projection of the $HoIO_5 \cdot 4H_2O$ structure on the *xy*-plane (Shamrai et al., 1975).

TABLE 21

Infrared absorption frequenies of seleted rare earth periodates and iodates (Lokio, 1973; Lokio and Kyrki, 1973; Petrov et al., 1974).*

$NdH_2IO_6 \cdot 3H_2O$	$CeHIO_6 \cdot 3H_2O$	$Ce_2I_2O_{11}$	$Ce_2I_2O_9$	$La(H_4IO_6)_3 \cdot H_2O$	Assignment
3200 m	3600–3400 s			3300–3100 s	$\nu(H_2O)$
2280 w				2380 w	$\nu(OH)$
1654 sh				1658 sh	
1620 m	1642 m			1625 m	$\delta(H_2O)$
				1285 m	
				1210 m	
1157 w	1156 w			1168 m	$\delta(IOH)$
				1125 sh	
				1108 m	
				845 sh	$\nu(IO_4^-)$
760 m	724 s	781 s	780 s	770 s	$\nu(IO)$
710 m					
675 w				660 s	
640 sh				625 sh	
580 m	587 sh				$\nu(IO–H)$
527 m				540 m	
		494 sh	494 s		
458 m	464 s	450 s	430 s	456 m	$\delta(OIO)$
420 m				430 m	
377 w				365 w	
355 sh					

* m = medium; s = strong; sh = shoulder; w = weak.

TABLE 22
Summary of structural data on rare earth complexes containing halogen oxoanions.[a]

Compound	R	Example	a (Å)	b (Å)	c (Å)	Angle (deg)	Z	Space group	Reference
$R(ClO_2)_3 \cdot 3H_2O$	La	La	8.07		8.30		2	$P\bar{6}2c$	Coda et al., 1965
$R(ClO_4)_3 \cdot 6H_2O$	La · · · Er	Tb	11.93				4	Fm3m	Glaser and Johansson, 1981
$R(BrO_3)_3 \cdot 9H_2O$	La · · · Lu, Y	Tb	11.76		6.71		2	$P6_3/mmc$	Gallucci et al., 1982
$R(IO_3)_3$	Ce · · · Lu, Y	Gd	13.44	8.52	7.14	$\beta = 99.7$	4	$P2_1/a$	Liminga et al., 1977
	Yb, Lu	Yb	8.69	6.07	16.69	$\beta = 115.0$	4	$P2_1/c$	Abrahams et al., 1976a
$R(IO_3)_3 \cdot 0.5H_2O$	La, Ce	La	18.61	7.39	6.74		4	$P2_12_12_1$	Abrahams et al., 1977
$R(IO_3)_3 \cdot H_2O$	Ce · · · Sm	Nd	10.20	6.71	7.35	$\beta = 113.1$	2	$P2_1$	Liminga et al., 1975
	Ce	Ce	19.20	7.24	6.72		4	$C222_1$	Abrahams et al., 1977
$R(IO_3)_3 \cdot 2H_2O$	Tm · · · Lu	Tm	8.23	10.13	7.02	$\alpha = 100.5$	2	$P\bar{1}$	Abrahams et al., 1976a
						$\beta = 94.9$			
						$\gamma = 66.6$			
	Nd · · · Er, Y	Eu	7.47	10.66	7.33	$\alpha = 105.1$	2	$P\bar{1}$	Abrahams et al., 1976a
						$\beta = 110.9$			
						$\gamma = 97.6$			
$R(IO_3)_3 \cdot 5H_2O$	La, Pr	La	6.72	23.14	7.11	$\beta = 112.3$	4	$P2_1/m$	Abrahams et al., 1976a
$R(IO_3)_4 \cdot H_2O$	Ce	Ce	9.90		5.32		2	$P4_2/n$	Staritzky and Cromer, 1956
$R(IO_3)_4 \cdot H_2O$	Ce	Ce	9.57	14.92	8.00	$\beta = 97.6$	4	$P2_1/n$	Ibers and Cromer, 1958
$R(IO_3)_3 \cdot HIO_3$	La · · · Sm	Pr	14.24	7.58	10.62	$\beta = 110.8$	4	$P2_1/a$	Abrahams et al., 1976b
$R(IO_3)_3 \cdot HIO_3 \cdot 7H_2O$	La	La	13.18	21.72	12.16		4	Aba2	Abrahams and Bernstein, 1978
$RIO_5 \cdot 4H_2O$	Pr · · · Lu, Y	Yb	7.46	10.35	10.21	$\beta = 118.7$	4	$P2_1/b$	Shamrai et al., 1977b
$R(IO_3)_3 \cdot OH \cdot H_2O$	Tb	Tb	8.54	10.54	7.52	$\alpha = 84.1$	2	PI	Barnes, 1978
						$\beta = 127.9$			
						$\gamma = 107.8$			

[a] See also tables 34 and 35.

The infrared spectra of the rare earth periodates have been recorded by many authors. The frequencies at 1150–1200 cm^{-1} (νIOH) and 3450–3500 cm^{-1} (νOH) are particularly important because they are informative of the composition of the material (table 21): they do not appear for phases not containing the $H_2IO_6^{3-}$ ion.

To conclude this section, table 22 presents a summary of the structural data of oxohalogen rare earth compounds.

7. Rare earth vanadates

7.1. *Introduction*

Among the rare earth vanadates the orthovanadates, RVO_4, containing pentavalent vanadium, are the best known compounds (Gambino and Guare, 1963). Besides these simple compounds more complex binary vanadates(V) are known, where the anion is a polyvanadate(V) ion, viz. di-, hexa- and decavanadate. The solid rare earth polyvanadates often crystallize with a high content of water. Recently, the structures of several rather complex rare earth polyvanadate hydrates have been solved, e.g., $La_2V_{10}O_{28} \cdot 20H_2O$ (Safyanov et al., 1978b).

Vanadium forms at tetravalent state an oxoanion $V_2O_7^{6-}$ which can combine with rare earth, forming the $R_2V_2O_7$ vanadites (Shin-ike et al., 1977). Trivalent vanadium forms rare earth compounds having the formula RVO_3. These compounds, however, cannot be considered as complex compounds but are binary oxides with perovskite structure (Wold and Ward, 1954; Reuter and Wollnik, 1963; Palanisamy et al., 1975).

Ternary rare earth vanadates are formed with alkali and ammonium ions. At least the following compositions are definitely known: $M_3R(VO_4)_2$ and MRV_2O_7. In both compounds, vanadium is at the pentavalent state.

The physical properties of the rare earth vanadates have been widely investigated. They show interesting magnetic as well as optical properties. Their most important technical significance is in the use of $Eu^{3+}:YVO_4$ as red phosphor in high pressure mercury lamps (Palilla et al., 1965; Luscher and Datta, 1970).

7.2. *Rare earth orthovanadates*

The preparation of anhydrous rare earth orthovanadates, RVO_4, is best accomplished by heating a mixture of vanadium pentoxide and rare earth oxide in air. The reaction temperatures may vary between 650 and 1300°C and the heating times between 1 and 10 h (Schwarz, 1963g; Bagdasarov et al., 1969; General Electric Co., 1968). An excess of V_2O_5 can be used and after the reaction the excess is washed off with water or an ammonium carbonate solution (Saji et al., 1970). The starting vanadium materials can also be sodium vanadate, which is needed in excess, ammonium metavanadate, or alkali orthovanadate (Milligan

and Vernon, 1952; Faria and Palumbo, 1971; Glazyrin and Borisenko, 1972; Isupova et al., 1973). And instead of oxide the rare earth component can be hydroxide, nitrate, oxalate, etc.

Various flux materials have been used for the preparation of europium-activated yttrium vanadate phosphor from vanadium and rare earth oxides. These include sodium nitrate and carbonate, and sodium and ammonium vanadates (Martin and Trond, 1967; Kauders, 1967; Yokota et al., 1970). A precipitation method in which the rare earths are precipitated in nitric acidic solution with NH_4VO_3 is also used in the preparation of phosphors (Martin and Trond, 1967). The precipitate is afterwards calcined to the final composition.

Single crystals of the rare earth orthovanadates can be grown in $2PbO \cdot V_2O_5$ and $4Bi_2O_3 \cdot V_2O_5$ fluxes (Garton et al., 1972). Large single crystals of RVO_4 in the form of both rods and sheets have been obtained in lead, lead fluoride, and molybdenum oxide fluxes by Smith and Wanklyn (1974) and Wanklyn (1978). Zone-melting growth from a polycrystalline rod has been achieved by Udalov and Appen (1982).

The rare earths from cerium to lutetium form isomorphic tetragonal orthovanadates with the well-known zircon structure, also called xenotime structure (Milligan and Vernon, 1952; Schwarz, 1963g; Popov et al., 1969; Brusset et al., 1971a; Fuess and Kallel, 1972). Structural studies of rare earth orthovanadates have also been carried out at low temperatures and by neutron diffraction (Patscheke et al., 1968; Baglio and Gashurov, 1968). $ScVO_4$ has the zircon structure, too, with space group $I4_1/amd$. The coordination number of the rare earth ion is eight and the point symmetry of the RO_8 group is D_{2d} (Gubanov et al., 1977; Escobar and Baran, 1980). The VO_4^{3-} tetrahedron is nearly regular and the bond distance determinations show that although the rare earth size varies over a wide range, the characteristic V–O distance remains the same (Faber and Aldred, 1982).

Of the rare earth orthovanadates only $LaVO_4$ crystallizes with monazite structure type, isomorphic with monoclinic $LaPO_4$. The structure contains approximately tetrahedral VO_4 units and a very irregular coordination polyhedron around lanthanum (fig. 111). In a preliminary structure determination of $LaVO_4$

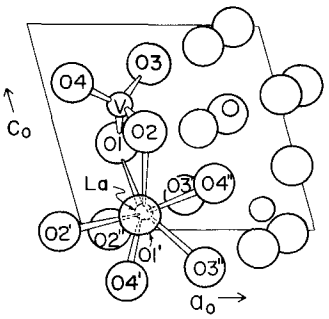

Fig. 111. A projection of the $LaVO_4$ structure showing the oxygen atoms nearest to the La and V atoms in a half of the unit cell (Rice and Robinson, 1976).

Brusset et al. (1971b) reported the coordination number to be eight, but Rice and Robinson (1976) later showed that it should be nine. The coordination polyhedron of La can be visualized as an irregular pentagon with two additional oxygen atoms above and below the plane of the pentagon.

In studies on $LaVO_4$, Ropp and Carroll (1973, 1977) found the product in the precipitation of rare earth vanadates from aqueous solution to be strongly dependent on the pH of the solution (fig. 112). According to them, tetragonal $LaVO_4$ is obtained in the pH range 4.5–8, with unit cell dimensions of 7.44 and 6.50 Å. Firing of the precipitate invariably produces the monoclinic structure type, however. Escobar and Baran (1977) have also described an $LaVO_4$ of zircon type. A report on the polymorphism of $CeVO_4$ has been presented by Yoshimura and Sata (1969). The cerium compound may also have the monoclinic form.

Thermoanalytical studies on RVO_3 have shown that the oxidation to orthovanadate occurs at temperatures below 400°C and the product is monoclinic RVO_4. Oxidation of vanadites at temperatures above 400°C produces a tetragonal form (Bazuev et al., 1975). Stubican and Roy (1963) achieved a reconstructive transformation from xenotime to scheelite structure in most of the rare earth vanadates (Pr · · · Lu) at high pressure and temperatures up to 600°C.

Many of the rare earth orthovanadates have a phase transition at low temperatures. $DyVO_4$ transforms to an orthorhombic Imma structure at 14 K, $TbVO_4$ transforms to a monoclinic structure, which can also be described as orthorhombic

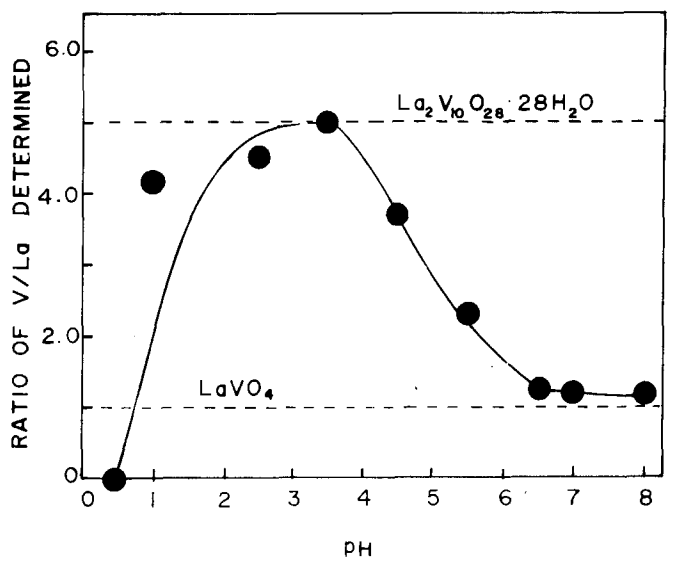

Fig. 112. The effect of pH on the V/La ratios produced. The precipitated compound at pH = 3.5 has a V/La ratio of 5 (= decavanadate). At higher pH values the ratio becomes 1 (= orthovanadate). (Ropp and Carroll, 1977.)

Fddd (Forsyth and Sampson, 1971; Sayetat, 1972; Göbel and Will, 1972b) at 32 K, and $TmVO_4$ has a phase transition at 2.1 K (Smith and Wanklyn, 1974).

The precipitation of rare earth orthovanadates from alkaline solutions where a $R(NO_3)_3$ solution is added to a KOH solution containing NH_4VO_3, produces orthovanadate hydrates. The number of water molecules varies between 1.5 and 3 depending on the rare earth and experimental conditions (Arbit and Serebrennikov, 1968a; Mokhosoeva et al., 1972; Golub and Nedilko, 1973; Nakhodnova and Sirchenko, 1976; Nakhodnova and Zaslavskaya, 1976; Ustalova et al., 1978). Most recently, Nakhodnova and Zaslavskaya (1982, 1984) have studied the composition of precipitated phases in the solutions containing 0.2 M of $R(NO_3)_3$ (R = Sc, Y, La) and Na_3VO_4. The results indicate that scandium behaves differently and forms various hydroxide vanadates.

7.3. *Rare earth vanadates having vanadium in lower oxidation states*

In the trivalent state vanadium forms vanadites of composition RVO_3 with the rare earth oxides. These compounds can be prepared directly from the trivalent oxides in vacuum or in a reductive at high temperatures (Wold and Ward, 1954; Reuter and Wollnik, 1963; Sakai et al., 1976). Another method of preparation is to reduce orthovanadates with hydrogen (Palanisamy et al., 1975).

A study of the phase diagrams in the system R_2O_3–V_2O_3 showed that two compounds are formed in the case of lanthanum, viz. $La_2O_3 \cdot V_2O_3$ and $2La_2O_3 \cdot V_2O_3$ (fig. 113). These compounds melt congruently at 2240 and 2190°C, respectively. In all other cases only the 1:1 compound was obtained (Molodkin et al., 1982a).

With the exception of the lanthanum compound, the rare earth vanadites are isomorphic. The orthorhombic structure can be described as distorted perovskite and thus they are not in fact complex compounds but mixed oxides (Wold and Ward, 1954; Geller, 1957). According to Kestigian et al. (1957) and Brusset et al. (1972), lanthanum vanadite is tetragonal in structure, although there is also one report of a cubic structure.

At high pressures rare earth vanadites have other structure types. At 30 kbar the structure is like calcite and at pressures exceeding 50 kbar the polymorph has a vaterite-like structure (Shin-ike et al., 1980).

With europium, vanadium forms mixed valence vanadates of composition Eu_2VO_4 and $Eu_3V_2O_7$. The more informative way to write the formulas is $EuO \cdot EuVO_3$ and $EuO \cdot 2EuVO_3$ (Shin-ike et al., 1976a), since with respect to vanadium these compounds are vanadites. Their structure is tetragonal with space group I4/mmm. The structure of Eu_2VO_4 was investigated by Shin-ike et al. (1976b) and found to be isomorphic with K_2NiF_4 (fig. 114).

Another type of rare earth vanadite is obtained with tetravalent vanadium. The oxoanion $V_2O_7^{6-}$ is formed and the rare earths (Tm $\cdots$ Lu, Y) combine with it to form $R_2V_2O_7$. At high temperatures the compound can be prepared from oxides

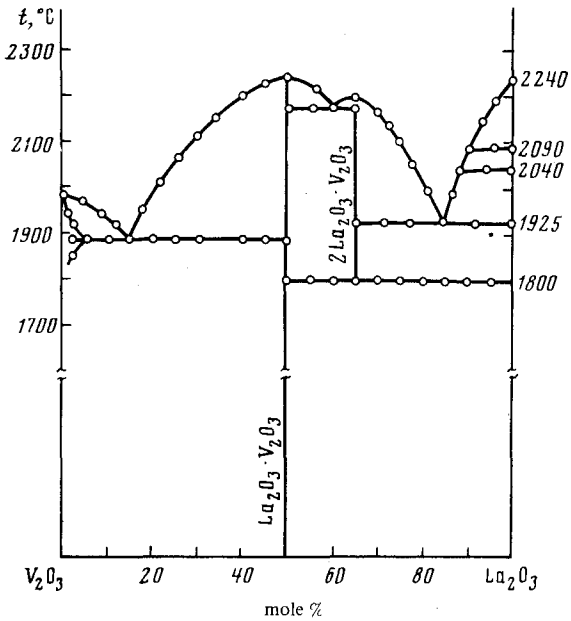

Fig. 113. An equilibrium diagram of the La_2O_3–V_2O_3 system (Molodkin et al., 1982a).

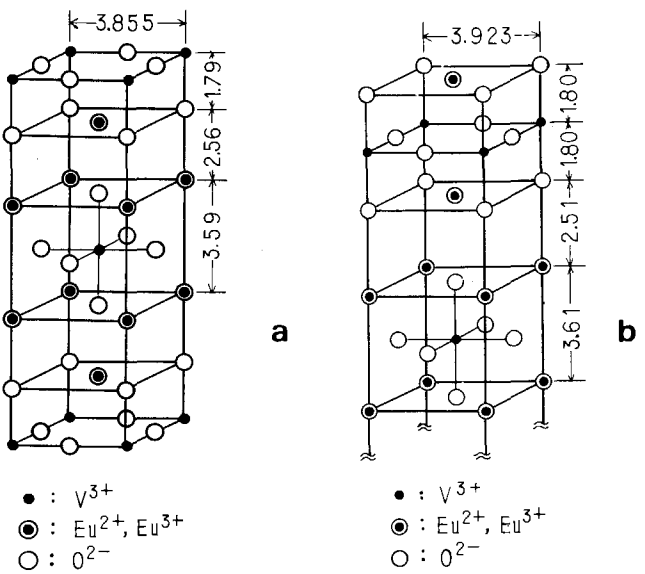

Fig. 114. The structures of Eu_2VO_4 (a) and $Eu_3V_2O_7$ (b) (Shin-ike et al., 1976).

R_2O_3 and V_2O_4 (Shin-ike et al., 1977). The reaction between orthovanadate and trivalent vanadite produces tetravalent vanadite (Greedan, 1971). It should be noted that the simple VO_4^{4-} ion has not been observed either in solution or in the solid state.

The compound $R_2V_2O_7$ has a cubic pyrochlore structure where the rare earth atoms have octahedral coordination. The octahedra form a corner-sharing framework (Shin-ike et al., 1977; Greedan, 1979). The pyrochlore structure is very common in compounds containing tri- and tetravalent ions (Shannon and Sleight, 1968).

7.4. *Polymeric rare earth vanadates*

The precipitation of rare earth vanadates from $R(NO_3)_3$ solution by a Na_3VO_4 solution yields mono-, di-, tri-, hexa-, or decavanadate hydrate, depending on the pH (figs. 112, 115) (Arbit and Serebrennikov, 1965; Nakhodnova and Zaslavskaya, 1976; Ropp and Carroll, 1977). When the pH is high the product is $RVO_4 \cdot xH_2O$, and with increasing acidity $R_4(V_2O_7)_3 \cdot 8H_2O$, $RV_3O_9 \cdot xH_2O$, $R_4(V_6O_{17})_3 \cdot 40H_2O$, and $R_2V_{10}O_{28} \cdot xH_2O$ phases are formed. For formation of the last two compounds the pH is about 4 to 5. The number of water molecules varies with the experimental conditions and the rare earth (Nakhodnova and

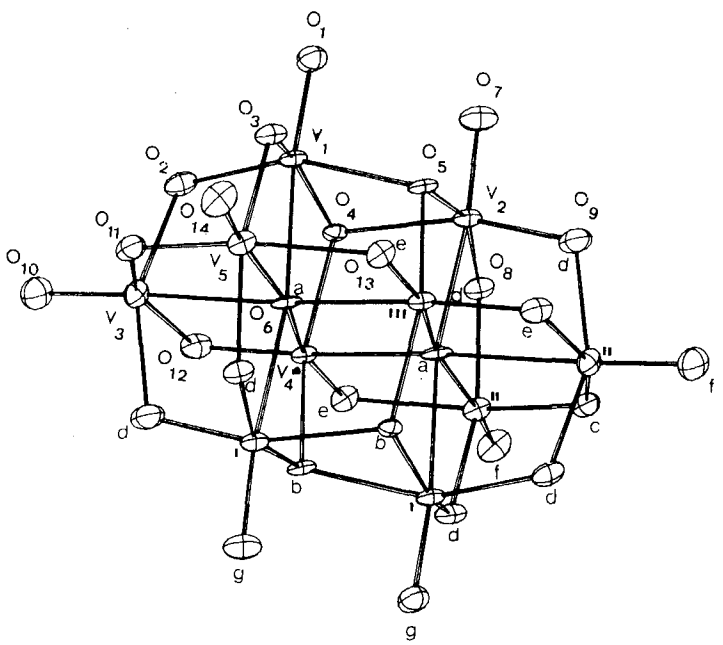

Fig. 115. The arrangement of V and O atoms in the decavanadate polyanion (Rivero et al., 1984).

Zaslavskaya, 1982). The formation of different rare earth polyvanadates follows the general lines observed in the aqueous chemistry of vanadates (Greenwood and Earnshaw, 1984).

The precipitated polymeric rare earth vanadates are amorphous or microcrystalline. Except for the decavanadates the crystal structures are uncertain. The existence of V_2O_7, VO_3, and V_2O_{17} radicals has been proposed and orthorhombic and monoclinic structures have been suggested for the hexavanadates.

Brusset et al. (1971a) have prepared new vanadates in solid-state reactions. All lanthanides form a compound of formula $4R_2O_3 \cdot V_2O_5$ ($R_8V_2O_{17}$). For lanthanides from Sm to Yb the compound $5R_2O_3 \cdot V_2O_5$ was obtained as well, and for Pr and Nd the compound $6R_2O_3 \cdot V_2O_5$; structural studies showed that $R_8V_2O_{17}$ is monoclinic (Brusset et al., 1973). Kiparisov et al. (1973) have found the $3Eu_2O_3 \cdot V_2O_5$ phase for europium. In phase diagram studies of the system Yb_2O_3–V_2O_3–V_2O_5 at 1200°C Kitayama et al. (1983) observed a new mixed valence compound with composition $Yb_7V_3O_{16}$. In the same study they found for europium the nonstoichiometric compound $Eu_{1.62}V_{0.38}O_{3.38}$. The phase diagrams of the systems R_2O_3–V_2O_3–V_2O_5 have systematically been studied by Kitayama et al. (see Kitayama et al., 1983; Kitayama and Katsura, 1983, and references therein).

Four different structure types have been reported for the rare earth decavanadate hydrates (Rigotti et al., 1981). $R_2VO_{10}O_{28} \cdot 22H_2O$ (R = La, Ce) and $R_2V_{10}O_{28} \cdot 26H_2O$ (R = Pr–Sm) are monoclinic ($P2_1/n$ and $P2_1/a$, respectively). Rare earths around gadolinium form triclinic crystals ($P\bar{1}$) with the composition $R_2V_{10}O_{28} \cdot 25H_2O$ (R = Eu–Er) (Rivero et al., 1984). The composition of this structure type was earlier erroneously reported to contain 24 water molecules (Rigotti et al., 1981). The fourth structure type is also triclinic ($P\bar{1}$), having the composition $R_2V_{10}O_{28} \cdot 24H_2O$; it comprises Tm, Yb, Lu, and probably also Y (Safyanov et al., 1978a; Rigotti et al., 1981).

The structures of the Nd, Y, and La compounds have been reported by Safyanov and Belov (1976) and Safyanov et al. (1977, 1978a,b, 1979) while the erbium and ytterbium compounds have been studied by Rivero et al. (1984, 1985). In all structures the decavanadate is formed by ten edge-sharing VO_6 octahedra. The coordination number of R^{3+} is either nine (La and Nd) or eight (Y and Er). The structure of the La compound is unique in that it has two bonds between the R^{3+} central ion and decavanadate oxygens. In all other cases the coordination polyhedra around the rare earth is exclusively formed by water oxygens (fig. 116).

In addition to the coordination aqua ligands, all structures containing a number of water molecules which are kept in the structure of weak to medium strong hydrogen bonds. The existence of these easily removable, interstitial water molecules may explain the discrepancies in the reported formulas of the compounds, e.g., $La_2V_{10}O_{28} \cdot 22H_2O$ (Rigotti et al., 1981) and $La_2V_{10}O_{28} \cdot 20H_2O$ (Safyanov et al., 1978b). Another case where the unit cell constants are similar

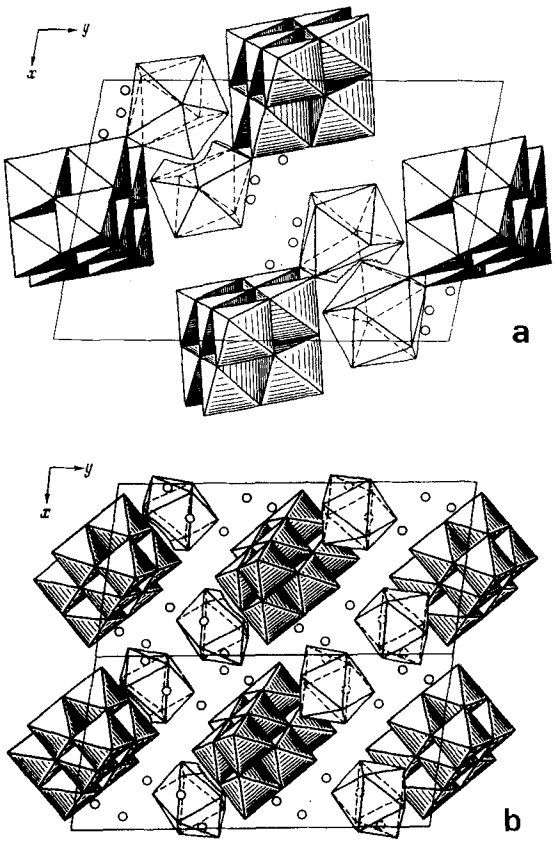

Fig. 116. The projections of the crystal structures of (a) $Y_2V_{10}O_{28} \cdot 24H_2O$, and (b) $La_2V_{10}O_{28} \cdot 20H_2O$ (Safyanov and Belov, 1979).

but the water content is different is the Nd compound, reported to have 26 or 28 moles of H_2O per structure unit (Rigotti et al., 1981 and Safyanov and Belov, 1976, respectively).

7.5. *Ternary rare earth vanadates*

Two types of alkali rare earth vanadates are known in the literature: MRV_2O_7 and $M_3R(VO_4)_2$. Both have pentavalent vanadium. Their preparation is carried out by heating of stoichiometric amounts of alkali carbonate, rare earth oxides, and vanadium pentoxide at temperatures between 500 and 1200°C (Gabe and Chincholkar, 1979; Melnikov et al., 1981c). The sodium compounds have been prepared in powder form from a mixture of Na_3VO_4 and RVO_4 heated for several days at 1050°C. The single crystals have been grown from the powders in a sodium orthovanadate flux (Vlasse et al., 1976).

Structural investigations of compounds $Na_3R(XO_4)_2$, where X = V, P, As, have

revealed three different structure types for the sodium rare earth vanadates (Vlasse et al., 1980a,b). The first type is orthorhombic (La) and the second (Pr···Tb) and third (Dy···Lu) types are monoclinic. All these structures contain isolated VO_4 tetrahedra. The two first structures can be described as analogous to ordered superstructures of β-K_2SO_4, made up of rows of alternating Na and rare earth atoms or alternating Na and VO_4 tetrahedra parallel to the *b*-axis (fig. 117). The rare earths are here eight-coordinated (Parent et al., 1979). The third structure type is similar to that of Na_2CrO_4 with isolated VO_4 tetrahedra and an ordered arrangement of Na and rare earth octahedra (Salmon, 1976) (fig. 118). The sodium rare earth vanadates have also a high temperature form which crystallizes in the glaserite structure, $K_3Na(SO_4)_2$ (Parent et al., 1979; Vlasse et al., 1980a) (fig. 119). The polymorphic transition from the low-temperature form to the glaserite form takes place between 750 and 900°C, depending on the rare earth (fig. 120).

The rubidium rare earth vanadates, $Rb_3R(VO_4)_2$ (R = Gd···Lu), have the same structure as the high-temperature form of $Na_3R(VO_4)_2$, viz., trigonal glaserite (Melnikov et al., 1981c). According to Komissarova et al. (1980) the corresponding potassium compounds are monoclinic and not isomorphic with either the rubidium or sodium compounds. Two isostructural series have been found in $Tl_3R(VO_4)_2$ compounds along the lanthanoid series. The compounds of

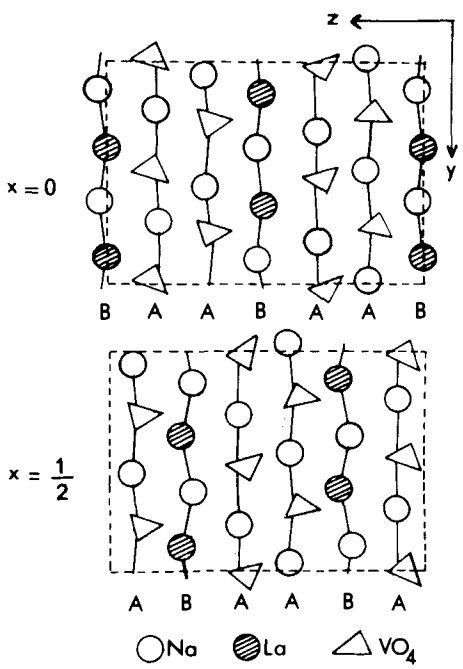

Fig. 117. A projection of the structure of $Na_3La(VO_4)_2$ (low-temperature form) on the (100) plane (Vlasse et al., 1980a).

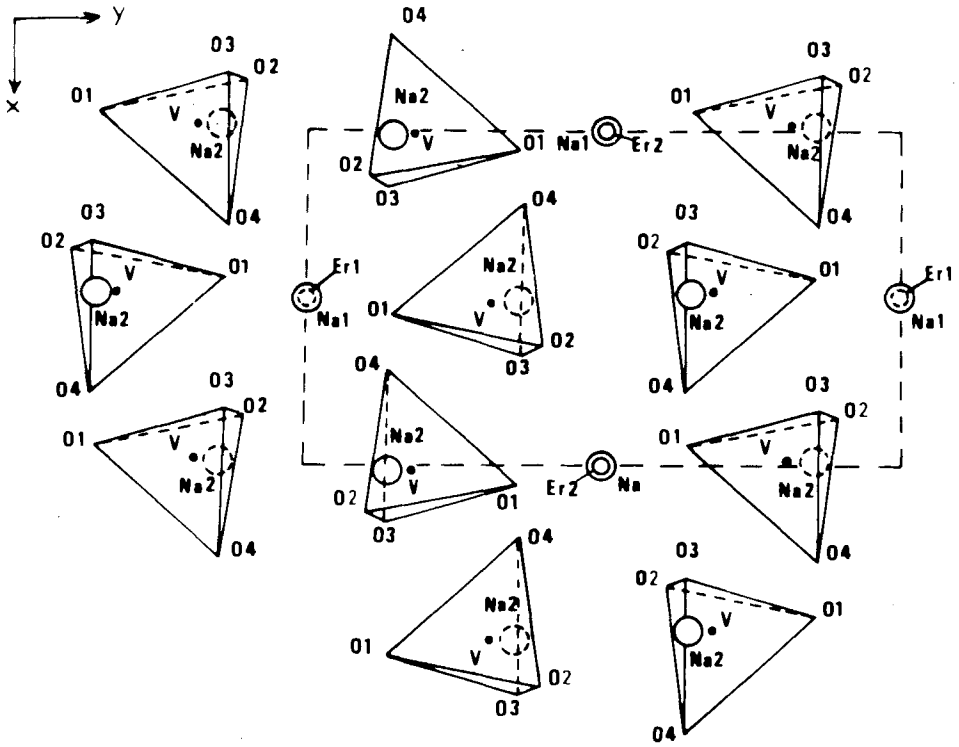

Fig. 118. A projection of the low-temperature structure of $Na_3Er(VO_4)_2$ on the (001) plane (Vlasse et al., 1980a).

the smaller lanthanides have been indexed as orthorhombic (Molodkin et al., 1982e).

The MRV_2O_7 (M = alkali metal) compounds have two structure types: pyrochlore and weberite (Chincholar, 1972). The pyrochlore structure is formed with lithium and for smaller rare earths also with sodium. The potassium compounds and sodium compounds with larger rare earth ions seem to have weberite structure, which is an orthorhombic distortion of cubic pyrochlore (Gabe and Chincolkar, 1979). The corresponding pentavalent niobates and tantalates have similar structural behaviour to the vanadates.

Sodium rare earth vanadates(III) can be prepared in a mixture of the corresponding oxides in a reducing atmosphere at 600–700°C. The solid compounds obtained appear to be isostructural throughout the lanthanide series. Their lattice is orthorhombic and the values $a = 5.34$ Å, $b = 11.02$ Å, and $c = 7.67$ Å have been determined for $Na_3La(VO_3)_2$ (Molodkin et al., 1982d). Scandium forms a vanadate with composition $Na_3Sc_2V_3O_{12}$ having a cubic garnet structure (Belokoneva et al., 1974).

The rare earth compounds with general formula $M_8R_2(XO_4)_6Y_2$, where M is a

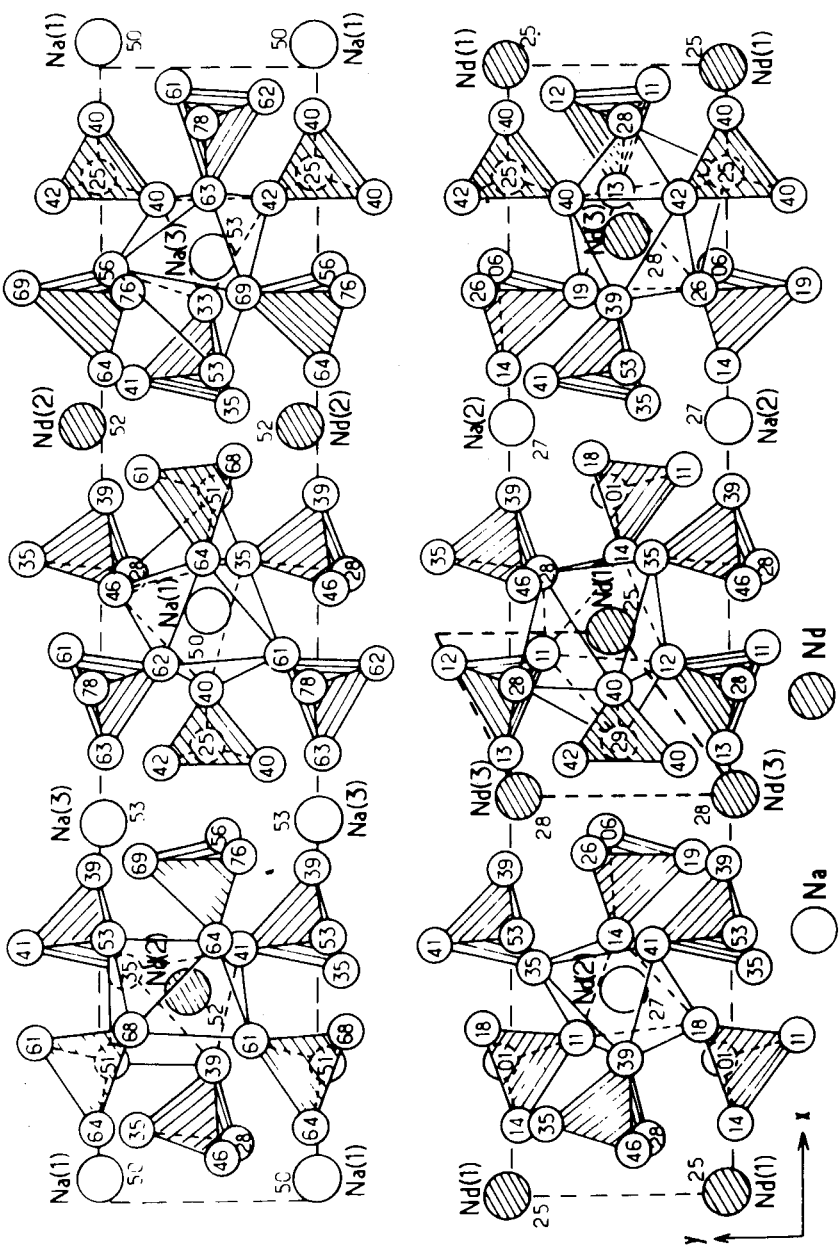

Fig. 119. The projections on the (001) plane of the two $Na_3Nd(VO_4)_2$ structure types: low-temperature (above) and high-temperature (below) (Parent et al., 1979).

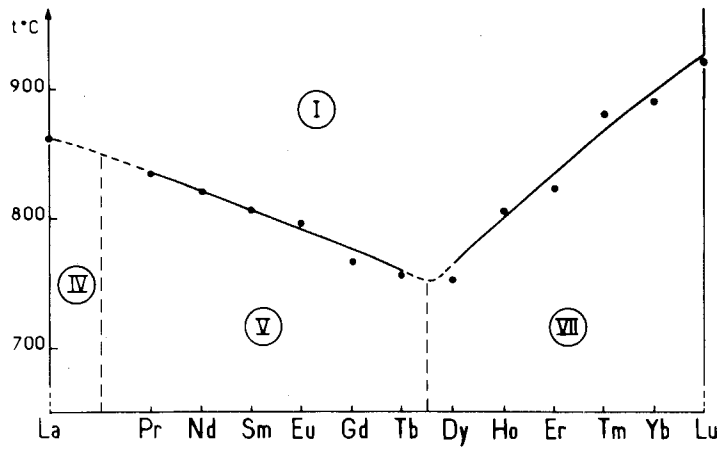

Fig. 120. The thermal behavior of the $Na_3R(VO_4)_2$ phases (Vlasse et al., 1980a). (I): glaserite-type; (IV): orthorhombic $Na_3La(VO_4)_2$-type; (V): monoclinic $Na_3Nd(VO_4)_2$-type; (VII): monoclinic $Na_3Er(VO_4)_2$-type.

divalent cation and Y a halogen or hydroxide ion, have been discussed in connection with silicates, germanates, and phosphates. X can also be pentavalent vanadium (Guillot et al., 1980). All these compounds have the hexagonal apatite structure. The divalent cation can be replaced by alkali metals, to give compounds like $Na_2Pb_6R_2(VO_4)_6Cl_2$ (Escobar and Baran, 1982a).

Triple orthovanadates containing a divalent cation, trivalent rare earth, and tetravalent thorium or cerium, have been studied by Nabar et al. (1981 and 1983). The samples were prepared by mixing soluble compounds of the corresponding elements in water, evaporating the solution and heating at 300°C. The compounds $MRTh(VO_4)_3$, where M = Ca, Cd, crystallize with the tetragonal zircon structure and those where M = Ba with the monoclinic monazite structure. Strontium and lead compounds show dimorphism (Nabar and Mhatre, 1982).

The structural data of rare earth vanadates are summarized in table 23.

7.6. *Physical and chemical properties of rare earth vanadates*

7.6.1. *Solubilities and thermal properties*

The rare earth orthovanadates are insoluble in water and in dilute ammonia and hydrochloric acid solutions (Glazyrin and Borisenko, 1972). The rare earth vanadites are soluble in nitric acid and, upon heating, in sulfuric and hydrochloric acids (Golub and Nedilko, 1973).

The thermal stability of RVO_4 compounds is exceptionally high: they do not decompose even at 1600°C (Gambino and Guare, 1963). The vanadites oxidize in air to orthovanadates in two stages, at temperatures between 350 and 500°C and between 500 and 700°C, depending on the rare earth (Golub and Nedilko, 1973).

TABLE 23
The unit cell parameters of rare earth vanadates.

Compound	R	Example	a (Å)	b (Å)	c (Å)	Angle (deg)	Z	Space group	Reference
RVO_4	La, Ce	La	7.29	7.29	6.73	$\beta = 104.9$	4	$P2_1/n$	Rice and Robinson, 1976
	(La)Ce $\cdots$ Lu, Y, Sc	Ce	7.40		6.50		4	$I4_1/amd$	Brusset et al., 1971a
RVO_3	La	La	5.54		7.85		4		Brusset et al., 1972
	Ce $\cdots$ Lu, Y	Gd	5.35	5.55	7.76		4	Pbnm	Geller, 1957
$R_2V_2O_7$	Tm $\cdots$ Lu, Y	Yb	9.95					Fd3m	Soderholm et al., 1980
$R_8V_2O_7$	La $\cdots$ Lu	Er	10.50	8.40	16.10	$\beta = 98.1$			Brusset et al., 1973
R_2VO_4	Eu	Eu	3.86		12.29		4	I4/mmm	Shin-ike et al., 1976a
$R_2V_{10}O_{28} \cdot 20H_2O$	La, Ce	La	11.13	16.18	12.02	$\beta = 101.7$	2	$P2_1/n$	Safyanov et al., 1978b
$R_2V_{10}O_{28} \cdot 28H_2O$	Pr $\cdots$ Sm	Nd	9.88	19.59	11.99	$\gamma = 98.7$	2	$P2_1/b$	Safyanov and Belov, 1976
$R_2V_{10}O_{28} \cdot 24H_2O$	Y, Tm $\cdots$ Lu	Y	9.43	9.87	23.49	$\alpha = 98.8$	2	$P\bar{1}$	Safyanov et al., 1978a
						$\beta = 90.1$			
						$\gamma = 98.0$			
$R_2V_{10}O_{28} \cdot 25H_2O$	Eu $\cdots$ Er	Er	9.17	10.00	12.70	$\alpha = 68.9$	1	$P\bar{1}$	Rivero et al., 1984
						$\beta = 77.5$			
						$\gamma = 89.3$			
$Na_3R(VO_4)_2$	La	La	5.58	14.24	19.42		8	$Pbc2_1$	Vlasse et al., 1976
	Pr $\cdots$ Tb	Nd	29.14	5.57	14.22	$\beta = 91.4$	12	Cc	Parent et al., 1979
	Dy $\cdots$ Lu	Er	5.49	9.74	7.22	$\beta = 93.1$	2	$P2_1/n$	Salmon et al., 1976
$K_3R(VO_4)_2$	Gd $\cdots$ Lu, Y	Gd	9.84	5.92	7.51	$\beta = 90.6$			Komissarova et al., 1980
	Sc	Sc	5.77		7.48				Komissarova et al., 1980
$Rb_3R(VO_4)_2$	Gd $\cdots$ Lu, Y, Sc	Gd	6.98		7.90		1	$P\bar{3}ml$	Melnikov et al., 1981c
$NaRV_2O_7$	Nd	Nd	7.62	10.82	7.50		4	Imm	Gabe and Chincholkar, 1979
	Y	Y	10.72					Fd3m	Chincholkar, 1972
$Na_3R_2V_3O_{12}$	Sc	Sc	12.60				8	Ia3d	Belonkoneva et al., 1974
$Na_2R_2Pb_6(VO_4)_6Y_2$	Nd	Nd	10.25		7.27		1	$P6_3/m$	Escobar and Baran, 1982a
$MRTh(VO_4)_3$									
(M = Sr, Ba, Pb)	La	La	7.00	7.25	6.73	$\beta = 105.1$	2	$P2_1/n$	Nabar and Mhatre, 1982
(M = Ca, Sr, Cd, Pb)	La	La	7.38		6.52		4	I4/amd	Nabar and Mhatre, 1982

In thermal decomposition the polyvanadates first lose their crystal water, and then at 370–500°C dissociate to orthovanadate and vanadium pentoxide (Mokhosoeva et al., 1972).

The values of thermodynamic functions have been determined for the formation reaction of rare earth vanadates from the oxides. The values of the activation energies lie between 11.3 and 18.4 kJ/mol (Isupova et al., 1973) and values of the reaction enthalpies between −120 and 215 kJ/mol (Rykova et al., 1979). According to Ustalova et al. (1978) the formation enthalpy at 670°C for $HoVO_4$ and $ErVO_4$ is about −170 kJ/mol. The calculated formation enthalpies from elements to RVO_4 vary between −1740 and −1875 kJ/mol (Ustalova et al., 1978; Zielinski and Skupin, 1980). Kitayama and Katsura (1977, 1978) and Kitayama et al. (1979) have determined the Gibbs energies for several reactions involving the formation of orthovanadates and pyrochlores from vanadites and the formation of polyvanadates.

7.6.2. *Magnetic and electrical properties*

Investigations on the magnetic properties of the rare earth orthovanadates have shown them to be paramagnetic and the susceptibilities to follow the Curie–Weiss law at temperatures above 200 K (Saji et al., 1970). At low temperatures some of the rare earth orthovanadates have been shown to exhibit an antiferromagnetic transition. $GdVO_4$ transforms to the antiferromagnetic form at 2.50 K, $DyVO_4$ at 3.1 K, and $ErVO_4$ at 0.4 K (Will et al., 1971c; Smith and Wanklyn, 1974).

The rare earth vanadites are paramagnetic at room temperature and except for $GdVO_3$ become antiferromagnetic at low temperatures (Sakai et al., 1976). The magnetic susceptibilities of rare earth hexavanadates have been reported to be higher than those of orthovanadates (Arbit and Serebrennikov, 1968b).

Measurements of the electrical conductivity have shown the rare earth orthovanadates and hexavanadates to be semiconductors of the p-type, whereas the vanadites and pyrochlores are semiconductors of the n-type (Arbit and Serebrennikov, 1968a; Sakai et al., 1976; Shin-ike et al., 1977). The pyrochlores, $R_2V_2O_7$, are ferromagnetic semiconductors and they show interesting electric properties due to the tetravalent vanadium (Soderholm and Greedan, 1979; Subramarian et al., 1979). They have recently been intensively investigated (Soderholm et al., 1982; Soderholm and Greedan, 1982).

7.6.3. *The luminescence properties of rare earth vanadates*

La, Lu, and Y do not show any UV absorption when used as host cations in rare earth orthovanadate phosphors. Of the usual host cations only gadolinium has absorption and emission bands in the UV region. The rare earth orthovanadates are exceptional phosphor host materials in that the vanadate anion can be excited by both long and short UV radiation (fig. 121). The excitation of YVO_4 in the 320 nm region occurs via the $^1A_1 \rightarrow {}^1T_2$ allowed transition of VO_4^{3-} (Burrus and Paulusz, 1969). The excitation at shorter wavelengths (250 nm) involves

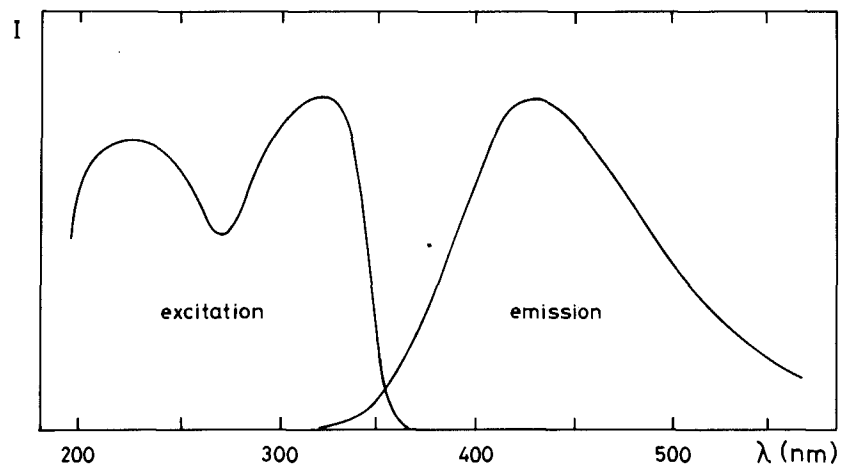

Fig. 121. The excitation and emission spectra of YVO_4 recorded at 77 K (after Wanmaker et al. 1966).

another process, perhaps an interaction between yttrium and oxygen, or it may originate in an exciton process (Datta, 1967a; Ropp, 1968c).

The unactivated YVO_4 has a blue emission which is very strong at low temperatures. The emission has been interpreted as the $^3T_2 \rightarrow {}^1A_1$ transition of the vanadate complex (Walter and Butler, 1968). When a small quantity of the yttrium is replaced by europium, the blue vanadate emission gives way to the bright red emission associated with the electronic transitions of the Eu^{3+} ion (fig. 122). The energy transfer from the excited vanadate ligand to Eu^{3+} must be a highly favorable process. It is interesting that $YVO_4:Eu^{3+}$ has an efficient UV radiation response and excellent performance at high temperatures (Burrus and Paulusz, 1969).

$YVO_4:Eu^{3+}$ is widely used in high-pressure mercury lamps for colour correction and to improve lumen maintenance (Palilla and Levine, 1967; Martin and Trond, 1967; Mathers et al., 1971). Until the 1970's, when it was replaced by $Y_2O_2S:Eu^{3+}$, it was also used in cathode-ray tubes of colour televisions (Levine and Palilla, 1964, 1966). The other trivalent lanthanide ions (except La and Lu) also emit in the orthovanadate matrix, but do not have the practical importance of the activated Eu^{3+} compound (Datta, 1967b).

The partial replacement of vanadate by phosphate in $YVO_4:Eu^{3+}$ has been investigated ever since the discovery of this phosphor in the sixties (Wanmaker et al., 1966; Aia, 1967; Ropp, 1971). Owing to their similar structure a solid solution easily forms between YVO_4 and YPO_4 (Ropp and Carroll, 1975). Though $Y(V,P)O_4:Eu^{3+}$ phosphor has less initial brightness than YVO_4, it has been reported to have better duration in high-pressure lamps and brighter emission at higher temperatures (Wanmaker and Vellijsdonk, 1966; Luscher and Datta, 1970).

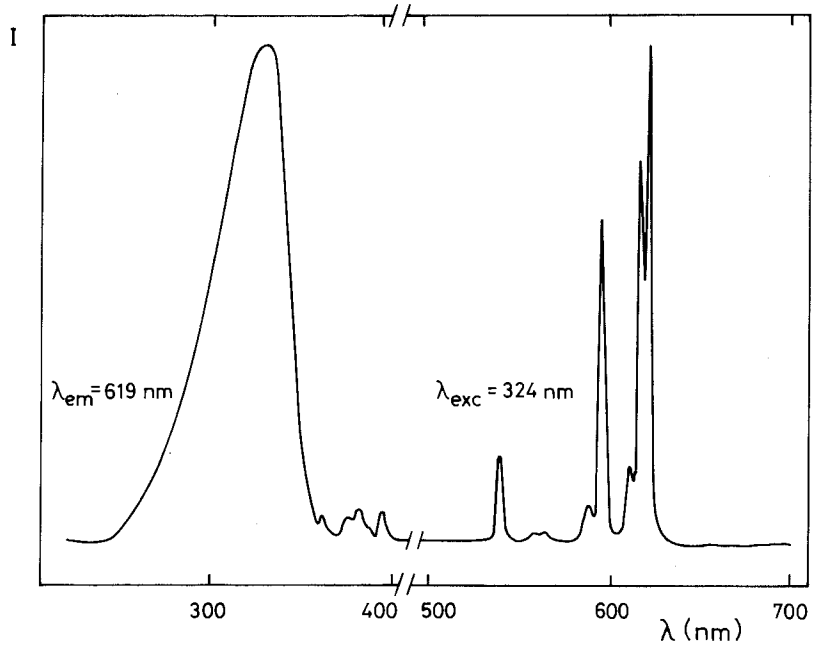

Fig. 122. The excitation and emission spectra of Eu^{3+}-activated YVO_4 recorded at 295 K (Leskelä, 1981).

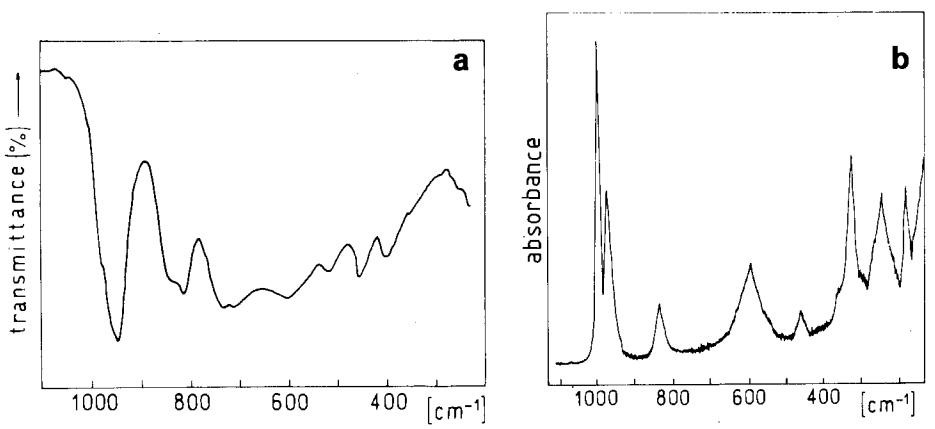

Fig. 123. The IR (a) and Raman spectra (b) of $Dy_2V_{10}O_{28} \cdot 24H_2O$ in the region 1100–200 cm^{-1} (Rigotti et al., 1981).

The optical properties of $Na_3La_{1-x}Nd_x(VO_4)_2$ have been studied in order to estimate its possibility as a coherent light source (Parent et al., 1980a). Nd^{3+} has a high luminescence intensity at low concentrations but strong self-quenching at higher concentrations in this matrix.

7.6.4. *Vibrational spectra*

Vibrational spectra of various solid lanthanide vanadates(III) or vanadates(V) have been studied occasionally in connection with preparative and structural investigations.

Thus, Molodkin et al. (1982a,b) recorded the IR spectra of $Na_3R(VO_3)_2$ and in the case of the $Tl_3R(VO_3)_2$ the assignments are also given. Mokhosoeva et al. (1972) recorded the IR spectra of hydrated yttrium orthovanadate, pyrovanadate, metavanadate, and decavanadate before and after heating.

The most detailed IR study concerns the decavanadates (Rigotti et al., 1981). The study comprised all stable lanthanides (La–Lu) and thus the various structural types were represented. In some cases even the Raman spectra were recorded (fig. 123).

8. Rare earth chromates

8.1. *Introduction*

A large number of the solid rare earth chromates(VI) can be precipitated in the system R_2O_3–Cr_2O_3–H_2O. Different stoichiometries are possible because the Cr(VI) oxoanions exist in a pH- and concentration-dependent equilibrium and because hydroxo compounds may be formed. Since the solubilities are generally low and the solutions often have a viscous consistency, single crystals are difficult to prepare. In fact, only in one case has a complete structural determination based on single-crystal X-ray data been carried out. In all other cases the characterization of solid compounds has been based on X-ray powder diffraction, IR and Raman spectroscopy, or thermoanalytical techniques.

Besides the binary rare earth chromates(VI), a large number of ternary compounds with alkali metals have been prepared. Yet a third group of rare earth chromates that has received considerable attention are the anhydrous chromates(V), $RCrO_4$, which have interesting structural and magnetic properties at low temperatures.

There appear to be no reviews on rare earth chromates in the literature. The two recent reviews on chromium chemistry briefly mention only the $RCrO_4$ compounds (Nag and Bose, 1985; Mitewa and Bontchev, 1985). While attempting to give a comprehensive overall view of the chromate complexes here, we will nevertheless concentrate on the solid-state properties, which have been of interest

in the overwhelming number of studies. The Cr(III) oxidation state, corresponding to perovskite-type $RCrO_3$ compounds, falls outside the scope of this review.

8.2. *Preparation of the binary chromates(VI)*

The most common aqueous ions of Cr(VI) are hydrogenchromate $HCrO_4^-$(aq), chromate CrO_4^{2-}(aq), and dichromate $Cr_2O_7^{2-}$(aq). Decreasing pH and increasing concentration shift the equilibria towards the dichromate ion (Dellien et al., 1976). In strongly acidic, concentrated solutions further polymerization of CrO_4^- tetrahedra may take place and the chain structures of $Cr_3O_{10}^{2-}$ and $Cr_4O_{13}^{2-}$ ions resemble the chain structure of CrO_3 (Löfgren, 1973).

The first lanthanide chromates were prepared in the nineteenth century (Frerichs and Smith, 1874), and the differences in solubility have been explored earlier in the separation of the light and heavier rare earths and also in the precipitation of yttrium (Egan and Balke, 1913; Ryabchikov and Vagina, 1966).

Several preparative routes have been utilized for the rare earth chromates(VI). Schwarz (1963a,b,c) prepared La, Pr, and Nd chromate hydrates by adding $R(NO_3)_3$ to a solution of CrO_3 and NaOH or to Na_2CrO_4. Schwarz (1963a) claimed that by using sodium instead of potassium the formation of ternary dichromates and mixed phases is avoided and binary compounds of type $R_2(CrO_4)_3 \cdot nH_2O$ ($n = 8$ for La, Pr, and 7 for Nd) are precipitated. In a similar way but starting from $PmCl_3$ and $(NH_4)_2CrO_4$, Weigel and Scherer (1967) prepared $Pm_2(CrO_4)_3 \cdot xH_2O$.

If the pH of the solutions is not sufficiently low, basic chromates may precipitate. This is especially apparent in the case of scandium. Anoshina et al. (1970) obtained in the pH range 4–5 the hydroxochromate $Sc(OH)CrO_4 \cdot H_2O$; the starting materials for the synthesis were $Sc(OH)_3$ and CrO_3 and KOH was used for the pH adjustment. Only at pH = 2 did the normal chromate $Sc_2(CrO_4)_3 \cdot nH_2O$ ($n = 6$ at 60°C, 3 at 90°C) precipitate.

Attempts to prepare Ce(III) chromates have not been successful due to the oxidation of cerium by chromate(VI) (Schwartz, 1963a). On the other hand, the Ce(IV) chromate dihydrate $Ce(CrO_4)_2 \cdot 2H_2O$ is easily prepared: by the reaction of $Ce(OH)_4$ and H_2CrO_4, for instance (Lindgren, 1977a).

Bashilova and Tananaev with their coworkers have carried out a series of systematic equilibrium studies in the system R_2O_3–Cr_2O_3–H_2O at 25°C. The composition and solubility of the solid phases were determined and the conditions for their preparation were established. Table 24 summarizes the results of these investigations and fig. 124 gives as an example the equilibrium diagram for the system involving La. The enthalpies of formation for $R_2(CrO_4)_3$ (R = La, Pr, Nd) and their hydrates have been measured by Tsyrenova et al. (1974a,b, 1973).

The solid-state reaction between R_2O_3 and Cr_2O_3 in an oxidative atmosphere leads to the formation of $R_2(CrO_4)_3$ if the temperature is suitable. Doyle and Gibb (1976) prepared $Nd_2(CrO_4)_3$ by this reaction at 350–600°C. At higher

TABLE 24
Composition of solid rare earth chromates crystallized in the system R_2O_3–CrO_3–H_2O.

R	n			Reference
	$[R_2(CrO_2)_3 \cdot nH_2O]$	$[R(OH)CrO_4 \cdot nH_2O]$	$[R_2(Cr_2O_7)_3 \cdot nH_2O]$	
La	7		10, 7	Bashilova et al., 1971
Nd	7		10	Tananaev et al., 1971a
Sm	7		10	Bashilova and Nelyapina, 1976
Gd	7		10, 5	Bashilova and Nelyapina, 1978
Dy	4	2	5	Bashilova and Nelyapina, 1979a
Er	8	1.5	5	Bashilova and Nelyapina, 1979b
Yb	8	2	5	Bashilova and Nelyapina, 1975
Y	8	2	5	Tananaev et al., 1971b

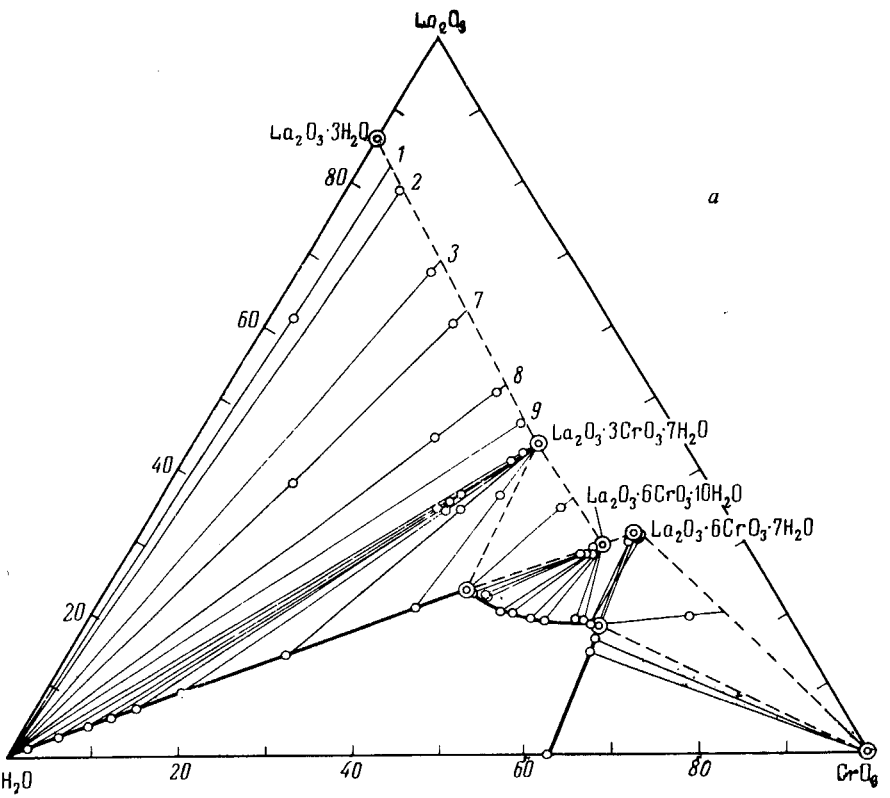

Fig. 124. The equilibrium diagram of the CrO_3–La_2O_3–H_2O system at 25°C (Bashilova et al., 1971).

temperatures a mixture of $Nd_2(CrO_4)_3$ and $NdCrO_3$ is formed, and above 840°C the latter phase is the sole product. The authors note that $Nd_2(CrO_4)_3$ prepared by this process has thermal and spectroscopic properties different from those of the anhydrous $Nd_2(CrO_4)_3$ prepared through the dehydration of $Nd_2(CrO_4)_3 \cdot 7H_2O$. In the absence of quantitative data, it is not clear whether these differences in properties are related to differences in crystallinity or crystal structure. The presence of oxochromate $La_2O_2CrO_4$, which may also be produced by the reaction between R_2O_3 and Cr_2O_3, seems improbable since a high oxygen pressure is required for its synthesis (Berjoan et al., 1975).

8.3. *Properties of the binary chromates(VI)*

As X-ray single-crystal data are lacking in all but one case, the available structural information on the binary chromates and their hydrates is based on powder diffraction studies and interpretation of IR spectra. In addition, a large number of thermoanalytical studies have been made in an attempt to elucidate the complex decomposition mechanism or to prepare rare earth chromates(V) through thermal conversion.

8.3.1. *X-ray diffraction studies*

The X-ray diffraction data available for the R^{3+} chromates seem to be limited to *d*-values and intensity tables for various lanthanum chromates (Bashilova et al., 1971; Tsyrenova et al., 1974a), praseodymium chromates (Tsyrenova et al., 1974b), and neodymium chromates (Tananaev et al., 1971a; Tsyrenova et al., 1973). In addition, there are X-ray powder data for four yttrium chromates, including the hydroxochromate dihydrate (Tananaev et al., 1971b). On the basis of the published data the compounds $R_2(CrO_4)_3 \cdot 7H_2O$ (R = La, Pr, and Nd) seem to be isostructural. A more recent study has shown that the isostructural series extends from La at least to Gd (Aarnio, 1980).

In the case of cerium(IV) chromate dihydrate it has been possible to grow single crystals of sufficient size for a complete structural analysis (Lindgren, 1977a). $Ce(CrO_4)_2 \cdot 2H_2O$ forms monoclinic crystals with the unit cell dimensions $a = 6.5865(12)$ Å, $b = 10.6716(7)$ Å, $c = 5.6699(6)$ Å, and $\beta = 92.59(1)°$. The structural solution confirmed the centrosymmetric space group $P2_1/m$; the unit cell contains two formula units. Cerium is eight-coordinated by oxygens from the two water molecules and from six different chromate groups (cf. fig. 125). The chromate groups are bridging tridentate with the nonbound oxygen significantly closer (1.58 Å) to chromium than the three other oxygens (1.64–1.69 Å). The arrangement of oxygen atoms around Ce is distorted and can be described either as a distorted square antiprism or as a bicapped trigonal prism with the two water oxygens as capping atoms (fig. 126).

8.3.2. *IR spectroscopic studies*

Like other tetrahedral oxoanions, the free chromate ion belongs to the point group T_d. In principle, two of the possible main modes of coordination (mono-

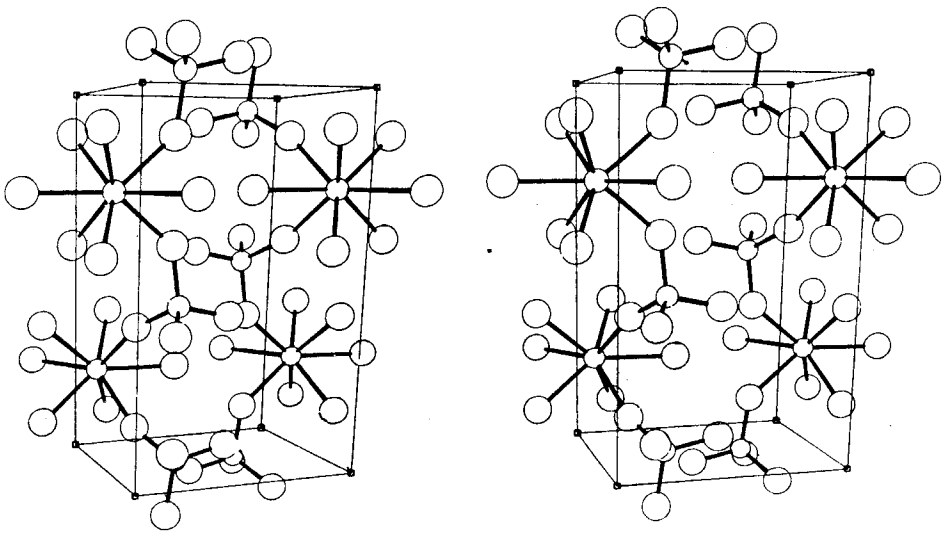

Fig. 125. A perspective view showing the unit cell contents and coordination of the chromate groups in the structure of $Ce(CrO_4)_2 \cdot 2H_2O$ (Lindgren, 1977a).

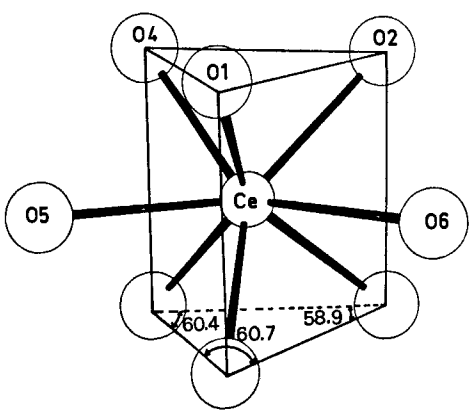

Fig. 126. A view of the coordination polyhedron in the structure of $Ce(CrO_4)_2 \cdot 2H_2O$ (Lindgren, 1977a).

dentate and bidentate) should be distinguishable on the basis of the number of IR-active vibrations, which is different in C_{3v} and C_{2v}. In practice, however, further splitting of the peaks, and in most cases the presence of several absorption bands due to water molecules, do not allow a choice.

In spite of the difficulties, IR spectroscopy, supplemented in some cases by Raman spectroscopy and studies on deuterated compounds, has been widely used to extract structural information from the binary and more complex chromate phases. The work of Stammreich et al. (1958a,b) on the positions of the

fundamental frequencies for the CrO_4^{2-} and $Cr_2O_7^{2-}$ ions has been the starting point for the interpretation of rare earth chromate spectra.

Darrie et al. (1967) used IR spectra to characterize $R_2(CrO_4)_3 \cdot nH_2O$ (R = La, Nd, Sm) and their thermal decomposition intermediates. Later, using deuterated compounds to obtain additional information, Petrov et al. (1975a) assigned the split band around 840 cm^{-1} to the chromate ν_1 symmetric vibration and not to the rocking modes of coordinated water. Table 25 gives the spectral data for the compounds studied by Petrov et al. Interesting is the authors' observation that the compound formulated on the basis of chemical analysis (and in analogy with other light rare earths) as $Nd_2(Cr_2O_7)_3 \cdot 10H_2O$ is according to the IR spectra actually $Nd_2(CrO_4)_2Cr_2O_7 \cdot 8H_2O$.

Petrov et al. (1975a) also conclude that the structure of $Y_2(CrO_4)_3 \cdot 8H_2O$ is different from the corresponding La and Nd compounds as regards the chromate and water coordination. The absence of the $\nu_1(CrO_4)$ symmetric stretching vibration, together with other features of the spectrum, indicate a high symmetry for the chromate group (S_4, D_{2d}, or D_2 at least). The position of a single

TABLE 25

The spectra and their assignments for the $R_2(CrO_4)_3 \cdot nH_2O$ and $R_2(Cr_2O_7)_3 \cdot nH_2O$ (R = La, Nd, Y) compounds (Petrov et al., 1975a). *

$R_2(CrO_4)_3 \cdot nH_2O$:

Assignment	$La_2(CrO_4)_3 \cdot 7H_2O$	$La_2(CrO_4)_3 \cdot 7D_2O$	$Nd_2(CrO_4)_3 \cdot 7H_2O$	$Y_2(CrO_4)_3 \cdot 8H_2O$
$\nu_1(CrO_4^{2-})$	825, 845	825, 845	835 sh, 850	
$\nu_3(CrO_4^{2-})$	867, 900	870, 897	870, 900 sh	860, 900
	925	925, 970 sh	920, 970 sh	960 sh
ν[OH(OD)]	3100–3600	2200–2700	3000–3600	3000–3550
$\delta[H_2O(D_2O)]$	1610 sh, 1650	1180	1615 sh, 1650	1610
		1210		
$\rho[H_2O(D_2O)]$	~640	525	650	
$\nu_4(CrO_4^{2-})$ (?)	435	435	440	

$R_2(Cr_2O_7)_3 \cdot nH_2O$:

Assignment	$La_2(Cr_2O_7)_3 \cdot 7H_2O$	$La_2(Cr_2O_7)_3 \cdot 10H_2O$	$Nd_2(Cr_2O_7)_3 \cdot 10H_2O$	$Y_2(Cr_2O_7)_3 \cdot 5H_2O$
ν_{sym}(CrOCr)	~550 sh		~500 sh, 565	520, 580
ν_{asym}(CrOCr)	720, 800	742, 785	740, 780 sh	730, 760 sh
$\nu_{sym}(CrO_3)$	888, 910	887, 912	890, 915	900
$\nu_{asym}(CrO_3)$	945, 970 sh	930 sh, 945	950, 980 sh	970
	987	960, 985 sh		
ν(OH)	3000–3600	3000–3600	3000–3600	3000–3600
$\delta(H_2O)$	1620	1625	1630	1610
Other	~470			~420

* sh = shoulder.

deformation vibration of water and the absence of libration vibrations suggest that water is not coordinated, in contrast to the La and Nd compounds, which according to the IR spectra contain differently bound water.

The IR spectra of scandium chromates, including the series $Sc_2(CrO_4)_3 \cdot nH_2O$ ($n = 6, 3, 1, 0$) and the basic compounds $ScOHCrO_4$ and $Sc_2O(CrO_4)_2$, have been recorded and interpretated by Komissarova et al. (1969). They note that the spectra of the hexa- and trihydrate are almost identical. In the case of the monohydrate and the anhydrous phase the positions of the absorption bands are shifted by 10–35 cm^{-1} and the spectra are simpler, pointing to a higher symmetry than C_{3v} for the chromate ion (table 26).

Structural details based on the interpretation of IR spectra alone have often been found unreliable. In the case of the rare earth chromates, there is an obvious need for complete crystal-structure analyses to provide a sound basis for spectral studies. As single crystals have proved extremely difficult to grow, the spectral study of $Ce(CrO_4)_2 \cdot 2H_2O$, whose structure is already known, would be worthwhile.

8.3.3. *Thermoanalytical studies*

Thermal degradation of rare earth chromates is a multistep process following the decreases in the oxidation state of Cr. The decomposition of binary chromates(VI) proceeds through both $RCr(V)O_4$ and $RCr(III)O_3$.

8.3.3.1. *Normal chromates(VI)*. The general decomposition scheme for the chromate(VI) hydrates of the light rare earths can be presented as follows (Schwarz, 1963a; Bashilova et al., 1971; Aarnio, 1980; Kelina et al., 1981):

$$R_2(Cr^{VI}O_4)_3 \cdot nH_2O \xrightarrow{-nH_2O} R_2(Cr^{VI}O_4)_3\,, \tag{13}$$

$$R_2(Cr^{VI}O_4)_3 \xrightarrow{-1.25O_2} 2RCr^{V}O_4 + 0.5Cr_2^{III}O_3\,, \tag{14}$$

$$RCr^{V}O_4 \xrightarrow{-0.5O_2} RCr^{III}O_3\,. \tag{15}$$

The dehydration reaction (13) usually proceeds via several intermediate hydrates, as seen from table 27, which gives the DTG peak temperatures for the reaction steps (13–15). In addition to these steps, which involve a weight change, the DTA curve usually reveals a further transition, around 450°C, which is attributed to recrystallization of the anhydrous $La_2(CrO_4)_3$ (cf. fig. 127; Bashilova et al., 1971).

It is clear from table 27 that the temperature variations as a function of the rare earth ionic radius are small. Nevertheless, the thermal stability of the Cr(VI) chromate does tend to decrease and that of Cr(V) to increase as the ionic size diminishes from La to Gd. This trend continues with the heavier rare earths,

TABLE 26
Infrared spectra and their assignment for the scandium chromates(VI) (Komissarova et al., 1969).

$Sc_2(CrO_4)_3$				$ScOHCrO_4$		$Sc_2O\cdot(CrO_4)_2$	$CsSc\cdot(CrO_4)_2$	Assignment *
$6H_2O$	$3H_2O$	$1H_2O$	anhydrous	$1H_2O$	anhydrous			
400 m	400 m	400 m	400 m	417 s	425 m	400 s	415 s	
460 m	465 m	475 m	494 m	493 m	465 w	425 w		a
						500 m		
				545 m		570 w		
		620 w		625 w	635 w	615 w	650 vw	b
658 m	655 w					657 m		
721 m	722 m	714 m	767 m	721 w	720 w	715 s		
800 s	800 s	800 vw	784 vw		803 vs	795 vw	831 vw	c
844 s		833 w		850 m	841 vw	832 vw		
	873 vw		857 m					d
882 m	887 s	883 s	889 s					
		913 w	924 w	922 m	934 s	913 s	900 m	
933 s	935 s	949 m					935 m	e
963 w		970 w	944 w	953 vw	955 s	975 vw	946 m	
984 w	985 vw	983 w	991 w				985 m	
1621 s	1615 m	1591 m		1620 m	1695 vw	–	–	f
1673 w								
		3300 m						g
3400 s, br	3340 s, br	3500 m		3350 m, br	3330 s	3300 vw		

$NH_4Sc(CrO_4)_2$		$NaSc(CrO_4)_2$		$KSc(CrO_4)_2$		$RbSc(CrO_4)_2$		Assignment *
$2H_2O$	anhydrous	$2H_2O$	anhydrous	$2H_2O$	anhydrous	$2H_2O$	anhydrous	
		400 s	400 s				412 s	
425 s	420 s			422 s	430 s	423 s		a
	620 m			635 m		620 m		
634 m		658 m	670 vw				645 w	b
747 vw	715 w			721 w	721 w	720 w	721 w	
		782 s				790 s	787 vw	
800 s	811 s	805 vw	805 vw	802 s				c
835 s	823 vs	843 m	823 vs	843 w	840 s	826 s	838 s	
926 s	921 s	926 s	913 m	926 s	920 s	920 s	903 s	d
953 s	943 s			952 s	942 s	945 m	932 m	
		967 s	960 m				946 m	e
							985 m	
1408 m	1408 m	–	–	–	–	–	–	
1600 m	1603 w	1585 m	–	1592 m	–	1606 m	–	h
		1615 vw		1663 vw				
3140 m				3140 vw				
3255 s	–	3240 vw		3340 m	–	3370 m		g
3480 m								

* Assignment of the frequencies:

(a) $\nu_4(CrO_4)$ (C_{3v}) Sc–O stretching
(b) $\delta_L(H_2O)$ Sc–O–Sc stretching
(c) $\nu_1(CrO_4)$ (C_{3v})
(d) $\nu_{3a}(CrO_4)$ (C_{3v})
(e) $\nu_{3b}(CrO_4)$ (C_{3v})
(f) $\delta(H_2O)$
(g) $\nu(OH, H_2O)$
(h) $\nu(NH_4)$, $\delta(H_2O)$

TABLE 27

Observed DTG peak temperatures for the thermal decomposition of $R_2(CrO_4)_3 \cdot 7H_2O$ (R = La–Gd) in air. Heating rate is 5° min^{-1} and the sample weight is 100 mg. For reactions and other details, see the text. *

R	Reaction		
	13	14	15
La	150	640	695
Pr	140,170	680 **	
Nd	125, 175	635	715
Sm	125, 185	635	715
Eu	125, 185	605	715
Gd	110, 145, 185, 225	605	725

* Aarnio (1980).

** The reaction steps were not resolved.

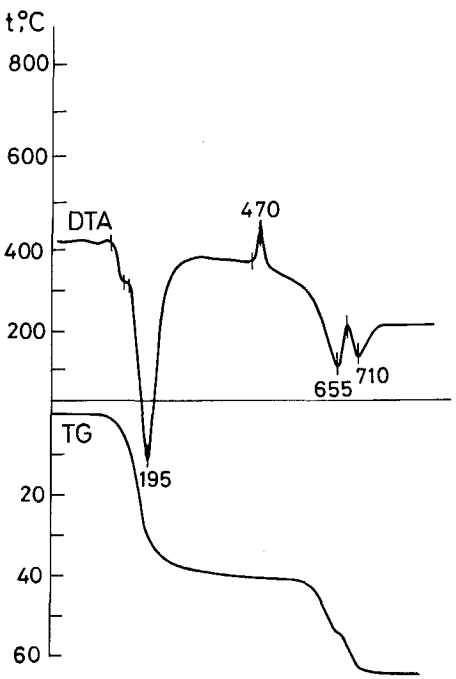

Fig. 127. The TG and DTA curves showing the decomposition of $La_2(CrO_4)_3 \cdot 7H_2O$ in air. The DTA peak temperatures (deg) have been given. (After Bashilova et al., 1971.)

where for the yttrium compound the difference in the peak temperatures of reactions (14) and (15) is around 140°C (Tananaev et al., 1971b).

Scandium behaves differently from the other rare earths: after the multistep dehydration, $Sc_2(CrO_4)_3$ decomposes directly to a mixture of Sc and Cr(III) oxides (Anoshina et al., 1970):

$$Sc_2(CrO_4)_3 \xrightarrow{-2.25O_2} Sc_2O_3 + 1.5Cr_2O_3 . \quad (16)$$

The reaction (16) takes place around 550°C.

8.3.3.2. *Hydroxochromates*. Schwarz (1963d) has noted the increasing tendency of the heavier rare earths and yttrium to form hydroxochromates of type $R(OH)CrO_4 \cdot nH_2O$ and has utilized them for the thermal synthesis of $RCr(V)O_4$ ($R = Sm \cdots Lu$). Of the individual hydroxochromates the Sc (Anoshina et al., 1970), Y (Tananaev et al., 1971b), and Dy (Schwarz, 1963d) compounds have been studied by thermoanalytical methods. The Er and Yb compounds, which have also been isolated (cf. table 24), seem not to have been studied.

The thermal degradation of $Sc(OH)CrO_4 \cdot H_2O$ proceeds both in air and in nitrogen via the anhydrous phase and the oxochromate(VI) $Sc_2O(CrO_4)_2$ to a 1:2 mixture of the Sc and Cr oxides. The stability range of $Sc_2O(CrO_4)_2$ is very narrow and located around 550°C.

The decomposition of $Y(OH)CrO_4 \cdot 2H_2O$ is similar to that of the Sc compound in that the dehydration range extends to a high temperature (380°C), but differs in that the chromate(V) is formed from the oxochromate(VI) at 530–555°C (Tananaev et al., 1971b). Dy hydroxochromate should behave similarly to the Y compound, but owing to the isothermal heating mode the decomposition temperatures and reaction intermediates cannot be compared (Schwarz, 1963d).

8.3.3.3. *Dichromates(VI)*. Of the 10 dichromate phases listed in table 24, only La, Nd, and Y compounds seen to have been characterized by thermoanalytical techniques. After dehydration reactions the anhydrous dichromate is decomposed above 350°C to normal chromate(VI) and Cr(VI) oxide:

$$R_2(Cr_2O_7)_3 \rightarrow R_2(CrO_4)_3 + 3CrO_3 . \quad (17)$$

CrO_3 is not stable at elevated temperatures but is converted to Cr_2O_3 with loss of oxygen. The $R_2(CrO_4)_3$ phase decomposes as described in section 8.3.3.1. The TG curve (fig. 127) is complex in appearance because melting takes place before dehydration and an intermediate product $La_2(CrO_4)_3 \cdot CrO_3$ is formed. The fusion of the hydrate does not seem to occur in the case of Y dichromate pentahydrate (Tananaev et al., 1971b) but is visible in the curves of $Nd_2(Cr_2O_7)_3 \cdot 10H_2O$ (Tananaev et al., 1971a). The latter compound may actually be a chromate–dichromate phase (Petrov et al., 1975a), which would explain the unusual shape of the curve.

8.4. *Preparation of the ternary chromates(VI)*

A large number of anhydrous and hydrated ternary rare earth chromates with monovalent cations have been prepared since the initial work of Cleve one hundred years ago (Cleve, 1885). The preparation may be carried out in aqueous solution, or by a solid-state reaction when anhydrous phases are desired.

8.4.1. *Preparation in aqueous solutions*

The basic preparative procedure involves mixing of solutions containing rare earth nitrate and alkali chromate. The potassium-containing systems have been studied in detail for Pr and Y (Perel'man and Fedoseeva, 1963a,b). In both systems, after 3 days, during which equilibrium was reached, a 1:1 complex between K_2CrO_4 and $R_2(CrO_4)_3$ was precipitated as a hydrate. In addition, 3:1 and 4:1 compounds were found for Y and a 3.5:1 compound for Pr. Later studies based on a similar preparative technique have confirmed only the existence of the hydrated 3:1 phase (Shakhno et al., 1977).

Other soluble starting compounds may be used besides the rare earth nitrates. Thus, Komissarova et al. (1970a) have prepared ternary compounds of Sc starting from $ScCl_3$ and alkali dichromate solutions.

8.4.2. *Preparation by solid-state reaction*

If strict temperature control is employed, pure ternary phases can be prepared by heating a mixture of alkali and rare earth chromates. Schwarz (1963e) used this method to prepare the compounds $MLa(CrO_4)_2$, where M = K, Rb, Tl, from a 1:1 mixture of $La_2(CrO_4)_3$ and M_2CrO_4. The formation of 1:1 compounds during thermal synthesis was monitored by Saveleva et al. (1975a,b, 1978) with the aid of TG and DTA techniques. Besides using anhydrous and hydrated rare earth chromates as starting materials, the authors employed a mixture of R_2O_3, CrO_3, and H_2O when the rare earth chromates proved difficult to prepare. Figure 128 depicts the thermoanalytical curves for the reaction mixtures involving Yb. The peaks in the curve may be explained as follows:

100°C	loss of water,
315°C	fusion of $Na_2Cr_2O_7$,
330°C, 465°C	formation of $NaYb(CrO_4)_2$,
430°C	decomposition of unreacted CrO_3,
625°C	decomposition of $NaYb(CrO_4)_2$,
785°C	fusion of the Na_2CrO_4 formed.

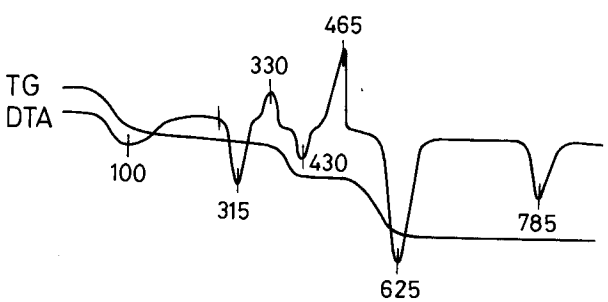

Fig. 128. The TG and DTA curves obtained when a $Yb_2O_3 + Na_2Cr_2O_7 + 2CrO_3$ mixture, dried initially at 65°C, reacts. The DTA peak temperatures (°C) have been given. For interpretations, see the text. (After Saveleva et al., 1978.)

8.5. *Properties of the ternary chromates(VI)*

Similar experimental techniques as used for the study of the binary chromates have been used for the study of the ternary compounds. In the following, the investigations are grouped according to the additional cation, starting with the alkali metals.

8.5.1. *Ternary chromates with sodium*

The ternary chromates of the type $NaR(CrO_4)_2$ prepared by a solid-state reaction have been systematically studied by Saveleva et al. (1975a,b, 1978). They concluded on the basis of X-ray powder diffraction patterns that the compounds Pr–Lu are isostructural and structurally different from the La compound; the unit cell data are not known, however.

TG and DTA data (fig. 128) have been recorded in connection with the preparative study of Saveleva et al. (1975a, 1978). Standard heats of formation for the La, Pr, Nd, and Sm compounds have been determined by Suponitskii et al. (1976). Standard IR data without assignments are available for all compounds. Although the IR spectra show 5 to 6 peaks in the Cr–O stretching region, they are simpler than those of other ternary chromates (Saveleva et al., 1975b, 1978).

There are few reports on the existence of hydrates $NaR(CrO_4)_2 \cdot nH_2O$ other than those of scandium, and those that exist are based on results of chemical analysis. Thus, Martin (1973) found the composition of a solid phase he prepared to correspond to $NaLa(CrO_4)_2 \cdot 3H_2O$. The existence of $NaSc(CrO_4)_2 \cdot 2H_2O$, on the other hand, is well established (Komissarova et al., 1969, 1970a; Anoshina et al., 1969). The anhydrous compound may best be prepared by heating the dihydrate; by 250°C the water of crystallization is lost and the $NaSc(CrO_4)_2$ phase is stable until approximately 500°C (Komissarova et al., 1970a). Attempts to prepare other chromate complexes than those with $M^+:Sc^{3+}$ ratio 1:1 have failed.

The infrared spectra of sodium scandium chromates are similar to those of other Sc ternary compounds. The spectrum for the anhydrous phase is very simple, suggesting high structural symmetry (cf. table 26).

8.5.2. *Ternary chromates with potassium*

There are many more studies in the system involving potassium than in systems involving the other alkali metals. In addition to the early studies by Perel'man and Fedoseeva (1963a,b; see section 8.4.1), reports exist on the preparation and characterization of the $K_3R(CrO_4)_3 \cdot nH_2O$ ($n = 1, 2$) and $KR(CrO_4)_2 \cdot nH_2O$ ($n = 0, 1$) series and on scandium compounds $KSc(CrO_4)_2 \cdot nH_2O$ ($n = 0, 2$).

Kuzina et al. (1980) have studied the extent of their being isostructural in the series $MR(CrO_4)_2$. When M = K, Rb, and R = La, Pr, Nd, or when M = Cs, and R = La, all compounds are isostructural with each other (table 28) and with the mineral huttonite $ThSiO_4$, as suggested by Schwarz (1963e). $ThSiO_4$ has the monazite-type structure. The powder patterns were successfully indexed using the

monoclinic unit cell data of crocoite $PbCrO_4$ and for $KLa(CrO_4)_2$ the following values were obtained: $a = 14.36$ Å, $b = 7.43$ Å, $c = 13.68$ Å, and $\beta = 103.14°$. According to IR and X-ray studies by Petrov et al. (1975b), $KSm(CrO_4)_2$ belongs to this series but Eu and Gd compounds have a different structure.

Another isostructural series exists among the 3:1 compounds: $K_3R(CrO_4)_3 \cdot 2H_2O$ (Pr $\cdots$ Gd) (Shakno et al., 1977). The La compound has a different structure and slightly different composition (monohydrate).

Recently Kuzina et al. (1983) have prepared the monohydrates of the 1:1 compounds $KR(CrO_4)_2 \cdot H_2O$ (R = Ho $\cdots$ Lu, Y) but no data on whether or not they are isostructural are given.

For the interpretation of IR and Raman spectra of $MR(CrO_4)_2$ compounds Petrov et al. (1975b) utilized the structural information available (monazite-type structure). Group theoretical analysis gave a satisfactory result in spite of the large number of spectral components. There are up to nine bands in the Cr–O stretching region (fig. 129) as compared to three in the case of the Sc compound of corresponding stoichiometry (table 26).

Representatives from all rare earth ternary series with potassium have been studied by thermoanalytical methods. Kuzina et al. (1983) have tabulated and interpreted the data for $KR(CrO_4)_2$ (R = La $\cdots$ Dy) and $KR(CrO_4)_2 \cdot H_2O$ (R = Ho $\cdots$ Lu, Y). And Shakhno et al. (1977) have studied $K_3R(CrO_4)_3 \cdot nH_2O$

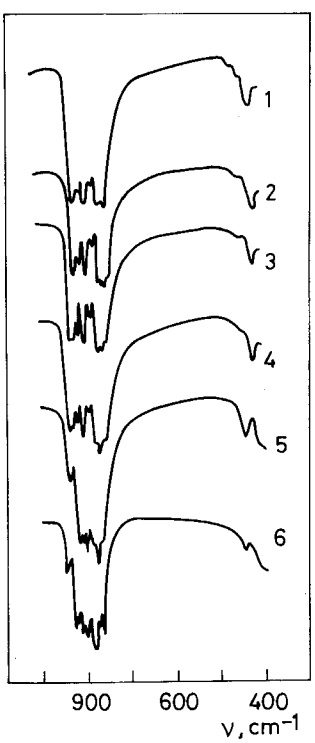

Fig. 129. The IR absorption spectra for $KR(CrO_4)_2$ compounds. The numbers 1–6 refer to R = La, Pr, Nd, Sm, Eu, and Gd, respectively. The scale is in wavenumbers (cm^{-1}). (Petrov et al., 1975b.)

($R = La \cdots Gd$) compounds, where after dehydration the $K_3R(CrO_4)_3$ phase disintegrates to K_2CrO_4 and $KR(CrO_4)_2$. The La compound is most stable and its disintegration starts only at 750°C. The decomposition of $KSc(CrO_4)_2 \cdot 2H_2O$ is analogous to that of $NaSc(CrO_4)_2 \cdot 2H_2O$, except for the solid decomposition products which, in addition to Sc_2O_3 and Cr_2O_3, comprise the dichromate instead of the alkali chromate (Komissarova et al., 1970a).

8.5.3. *Ternary chromates with other alkali metals*

There appears to be only one mention of lithium compounds, viz. $LiLa(CrO_4)_2 \cdot 3H_2O$ (Martin, 1973), and this was not characterized. By contrast, the rubidium and cesium compounds have frequently been studied. Two main series of compounds exist: the anhydrous compounds $MR(CrO_4)_2$ and the corresponding monohydrates. Exceptionally, samarium forms an intermediate hydrate with rubidium containing 0.5 moles of water (Kuzina et al., 1979). Scandium forms the $RbSc(CrO_4)_2 \cdot 2H_2O$ phase in analogy with sodium and potassium but for cesium only the anhydrous phase $CsSc(CrO_4)_2$ has been prepared (Ivanov-Emin et al., 1969; Komissarova et al., 1970a).

As with the other alkali metals the Rb and Cs compounds can be prepared by solid-state or solution techniques. In solution, the heavier rare earths including yttrium tend to form the monohydrate, as can be seen from table 28, which summarizes the structural information available from X-ray powder diffraction studies. As regards the anhydrous Cs compounds, it is not clear how completely they are isostructural; according to Petrov et al. (1975b) $CsR(CrO_4)_2$ ($R = Pr \cdots Gd$) are isostructural, whereas the data of Saveleva et al. (1975) indicate a structural difference in the Pr and Sm compounds. The possibility of polymorphism cannot be excluded; it has been shown that $RbLu(CrO_4)_2$ undergoes a reversible transformation at 540°C (Kuzina et al., 1979).

The IR spectra of the Rb and Cs compounds have been discussed in several

TABLE 28

Ternary chromates $MR(CrO_4)_2 \cdot nH_2O$ (R = Rb or Cs) and their isostructural relationships.

Compound	Isostructural with:	Reference
$RbLa(CrO_4)_2$	Pr, Nd	Kuzina et al., 1980
	$CsLa(CrO_4)_2$	
	$KR(CrO_4)_2$; R = La–Sm	
$RbSm(CrO_4)_2 \cdot 0.5H_2O$	$RbSm(CrO_4)_2$	Plyushchev et al., 1975
		Kuzina et al., 1976a
$RbEu(CrO_4)_2 \cdot H_2O$	Gd–Lu, Y	Kuzina et al., 1976a
$CsPr(CrO_4)_2$	Nd–Gd	Petrov et al., 1975b *
		Saveleva et al., 1975b
$CsTb(CrO_4)_2$	Dy–Yb, Y	Kuzina et al., 1976b, 1979
$CsPr(CrO_4)_2 \cdot H_2O$	Nd–Lu, Y	Kuzina et al., 1973, 1975, 1976b
$RbSc(CrO_4)_2 \cdot 2H_2O$		Komissarova et al., 1970a
$CsSc(CrO_4)_2$		Komissarova et al., 1970a

* See the text.

papers; the most detailed study is that by Petrov et al. (1975b) noted in connection with the potassium compounds. The Raman spectra of the hydrated and anhydrous Cs compounds have been recorded and discussed by Golovin et al. (1972).

When the ternary chromates $MR(CrO_4)_2$ or their monohydrates are heated in air they decompose in a similar way, forming chromate(V) and finally chromite(III). The decomposition temperatures decrease with increasing atomic number, the difference being about 100°C, when $CsLa(CrO_4)_2$ and $CsYb(CrO_4)_2$ decompose to give the chromate(VI) phase (Kuzina et al., 1979). Under thermogravimetric analysis, the Rb and Sc chromates of scandium behave in a way similar to the potassium compound, yielding around 550°C a mixture of Sc_2O_3, Cr_2O_3, and the alkali dichromate (Komissarova et al., 1970a).

The enthalpies of dissolution and formation for $MR(CrO_4)_2$ (M = Rb, Cs; R = La, Pr, Nd, Sm) have been determined (Suponitskii et al., 1978). The ΔH_f^{298} for $RbLa(CrO_4)_2$ is (650.2 ± 1.4) kcal/mol. Corresponding data are available for the sodium compound $NaR(CrO_4)_2$ (Suponitskii et al., 1976).

8.5.4. *Ternary chromates with ammonium*

The ammonium compounds are among the better characterized ternary phases because single-crystal data are available for the isostructural series $NH_4R(CrO_4)_2 \cdot H_2O$ (Aarnio et al., 1981). The anhydrous compounds (Schwarz, 1963e; Aarnio et al., 1981) and the scandium chromate $NH_4Sc(CrO_4)_2 \cdot 2H_2O$ (Komissarova et al., 1970a) are known also, but reports (Martin et al., 1971; Martin, 1973) of the existence of a higher hydrate $NH_4La(CrO_4)_2 \cdot 3H_2O$ remain to be confirmed.

The compounds $NH_4R(CrO_4)_2 \cdot H_2O$ (R = Tb ··· Lu, Y) were obtained at 50–60°C as small, needle-shaped crystals upon slow evaporation of a solution containing $R(NO_3)_3$, CrO_3 and NH_3 at a pH of 5. The compounds are isostructural and the monoclinic unit cell has the dimensions (for the Yb compound) $a = 9.422(3)$ Å, $b = 9.562(4)$ Å, $c = 9.652(3)$ Å, $\beta = 112.84(3)°$. There are four formula units in a cell (Aarnio et al., 1981).

For the lighter rare earths the anhydrous phase $NH_4R(CrO_4)_2$ is obtained as a polycrystalline powder either by the method of Schwarz (1963e) or by using an excess of $(NH_4)_2CrO_4$. The powder patterns indicate that the La compound differs in structure from the other compounds (Pr ··· Eu) (Aarnio et al., 1981). The published powder pattern of $RbLa(CrO_4)_2$ (Kuzina et al., 1980) is so similar to that of $NH_4La(CrO_4)_2$ that the two compounds may well be isostructural and be huttonite-type compounds, as suggested by Schwarz (1963e). The published X-ray line diagrams of $RbR(CrO_4)_2 \cdot H_2O$ compounds are unfortunately incomplete (Kuzina et al., 1976a) and do not allow similar comparisons to be made.

The thermal decomposition of $NH_4R(CrO_4)_2 \cdot H_2O$ is a complicated process due to the presence of the ammonium ions. The following scheme (cf. fig. 130), which corresponds well to the observed weight losses, is based on the evolution of NH_3, O_2, and H_2O as gaseous products, as observed in the mass-spectrometric

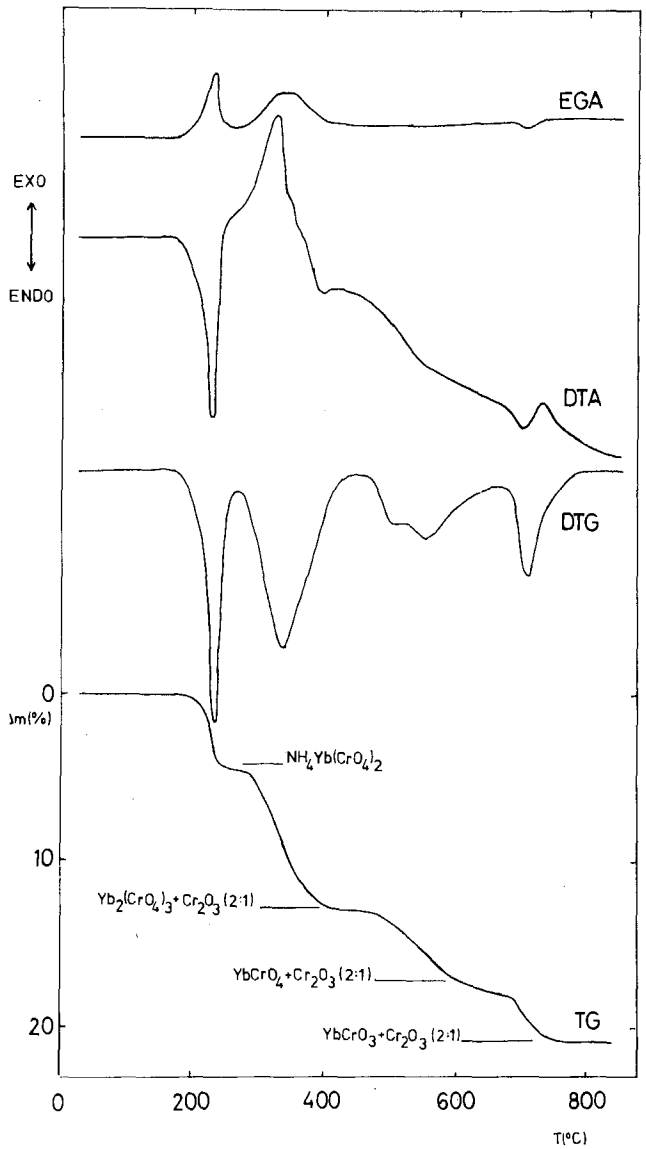

Fig. 130. The thermoanalytical curves for $NH_4Yb(CrO_4)_2 \cdot H_2O$ in air up to 800°C. The horizontal levels correspond to calculated stoichiometries as indicated. (Aarnio et al., 1981.)

study of the decomposition of $(NH_4)_2CrO_4$ (Park, 1972):

$$NH_4R(CrO_4)_2 \cdot H_2O \xrightarrow{-H_2O} NH_4R(CrO_4)_2 \,, \tag{18}$$

$$NH_4R(CrO_4)_2 \xrightarrow{-NH_3,\, 0.5H_2O,\, 0.875O_2} 0.5R_2(CrO_4)_3 + 0.25Cr_2O_3 \,, \tag{19}$$

$$0.5R_2(CrO_4)_3 + 0.25Cr_2O_3 \xrightarrow{-0.625O_2} RCrO_4 + 0.5Cr_2O_3\,, \quad (20)$$

$$RCrO_4 + 0.5Cr_2O_3 \xrightarrow{-0.5O_2} RCrO_3 + 0.5Cr_2O_3\,. \quad (21)$$

8.6. *Binary chromates(V)*

Rare earth chromates (V) belong to the family of oxoanion compounds of the type RXO_4, where X is a pentavalent element. The phosphates, arsenates, and vanadates have long been known but the chromates were discovered only in the 1960's (Schwarz, 1963a), about ten years after the preparation of the corresponding alkali compounds (Scholder and Klemm, 1954). Because of their interesting magnetic behavior, the RXO_4 compounds have been widely investigated.

8.6.1. *Preparation of the chromates(V)*

Thermal decomposition of chromates(VI) produces the chromates(V), as noted above; but in most cases Cr_2O_3 is present simultaneously and separation is difficult. For this reason Schwarz (1963a) started instead with the basic lanthanide chromates, from which he prepared the complete series of compounds including yttrium (Schwarz, 1963a–f). Another possibility is to use trioxalatochromates(III), $RCr(C_2O_4)_3 \cdot nH_2O$, as starting material (Roy and Nag, 1978). Both the basic chromates and the trioxalatochromates have the desired 1:1 ratio between R and Cr atoms, whereas the normal chromates and dichromates have an excess of chromium.

Schwarz (1963a,c,d) also prepared the chromates(V) by heating Cr(III) and lanthanide nitrates in oxygen at 600°C:

$$Cr(NO_3)_3 \cdot 9H_2O + R(NO_3)_3 \cdot 6H_2O \rightarrow RCrO_4 + 6NO_2 + O_2 + 15H_2O\,. \quad (22)$$

$PrCrO_4$ presents some difficulties due to its dimorphism. Moreover, when $Pr(NO_3)_3 \cdot 6H_2O$ is used as a starting material, thermal decomposition produces slowly reacting Pr oxides (Schwarz, 1963b). Nevertheless, both crystal forms have now been prepared: a mixture of the tetragonal and monoclinic forms by the reaction between praseodymium chromates(VI) and nitrate (Schwarz, 1963b), and recently the monoclinic polymorph in pure state by rapid heating of $PrCr(C_2O_4)_3 \cdot 8H_2O$ up to 800°C, where the conversion takes place in 10 min (Manca and Baran, 1981).

8.6.2. *Structure and properties*

Lanthanide chromates(V) are green polycrystalline powders which are soluble in dilute mineral acids; upon dissolution, Cr(V) disproportionates to Cr(III) and Cr(VI).

8.6.2.1. *Structure.* $LaCrO_4$ is isostructural with the mineral huttonite, viz. has the monoclinic monazite structure (Schwarz, 1963a). $PrCrO_4$, as discussed above,

exhibits dimorphism, but from samarium on the heavier lanthanides and yttrium form chromates(V) which have zircon-type structure. Buisson et al. (1964) have determined the space group $I4_1/amd$ and unit cell parameters for Pr–Lu, Y. The cell parameters a, c and the volume decrease more or less linearly with increasing Z (Schwarz, 1963a; Buisson et al., 1964).

Vasilega et al. (1977) have determined the unit cell constants for the monoclinic $LaCrO_4$. Their values and indexing of the powder pattern differ significantly from those presented by Manca and Baran (1982) (cf. table 29). Other values are in good internal agreement.

8.6.2.2. *Spectral and thermal properties.* Spectral and thermal properties of the $RCrO_4$ compounds have been widely studied. The interpretation of the absorption spectra is greatly facilitated by the known crystal symmetry. Darrie and Doyle (1968) have discussed the spectra of $LaCrO_4$, $NdCrO_4$, and $SmCrO_4$ in terms of the different site symmetries and found the main features of the IR spectra to be as expected. They have also recorded the diffuse reflectance spectra for $LaCrO_4$, $SmCrO_4$, and $NdCrO_4$ (Darrie and Doyle, 1968), and for $RCrO_4$ ($R = Pr \cdots Yb$) (Doyle and Pryde, 1976).

The chromates(V) are stable to above 600°C, where decomposition with loss of oxygen takes place and chromites(III) are formed. According to Doyle and coworkers the starting temperature of the decomposition reaction, as measured from the TG and DTA curves, is almost invariant in the series $Sm \cdots Yb$, where the values range from 660 to 692°C. Only praseodymium seems to have lower

TABLE 29
Unit cell parameters for selected rare earth chromates(V).

Compound	a (Å)	b (Å)	c (Å)	β (deg)	Reference
Monazite-type					
$LaCrO_4$	6.793	7.273	6.551	103.35	Vasilega et al., 1977
	7.08	7.27	6.71	104.98	Manca and Baran, 1982
$PrCrO_4$	6.98	7.16	6.63	105.22	Manca and Baran, 1981
Zircon-type					
$PrCrO_4$	7.345		6.422		Schwarz, 1963d
	7.344		6.428		Buisson et al., 1964
$PmCrO_4$	7.28		6.375		Weigel and Scherer, 1967
$TbCrO_4$	7.167		6.293		Schwarz, 1963d
	7.170		6.294		Buisson et al., 1964
	7.166		6.281		Buisson et al., 1976 *
$LuCrO_4$	7.023		6.191		Schwarz et al., 1963d
	7.027		6.200		Buisson et al., 1964
$YCrO_4$	7.109		6.250		Schwarz et al., 1963d
	7.112		6.251		Buisson et al., 1964

* Neutron diffraction data.

stability, as indicated by both the initial and end temperatures of the decomposition (629 and 762°C) (Darrie and Doyle, 1968; Doyle and Pryde, 1976).

The activation energies and reaction order for the decomposition reaction $RCrO_4 \rightarrow RCrO_3 + \frac{1}{2}O_2$ have been determined by Doyle and Pryde (1976) and Roy et al. (1978). As these calculations are strongly dependent on the experimental and calculation methods, the significantly different activation energies obtained by the two groups cannot be directly compared. Nevertheless, it may be noted that both isothermal measurements (Doyle and Pryde, 1976) and nonisothermal measurements combined with another computational procedure (Roy et al., 1978) support a first-order reaction mechanism for $LaCrO_4$.

8.6.2.3. *Magnetic properties.* The magnetic properties of many rare earth chromates(V) have been studied either in a routine way in connection with preparative and other work or in more detail. Routine studies include the determination of the magnetic susceptibility of $LaCrO_4$ by Schwarz (1963a) and Darrie and Doyle (1968) and the determination of the magnetic moment and the recording of the EPR spectrum of $LaCrO_4$ by Roy and Nag (1978).

As examples of the more detailed investigations into the crystallographic and

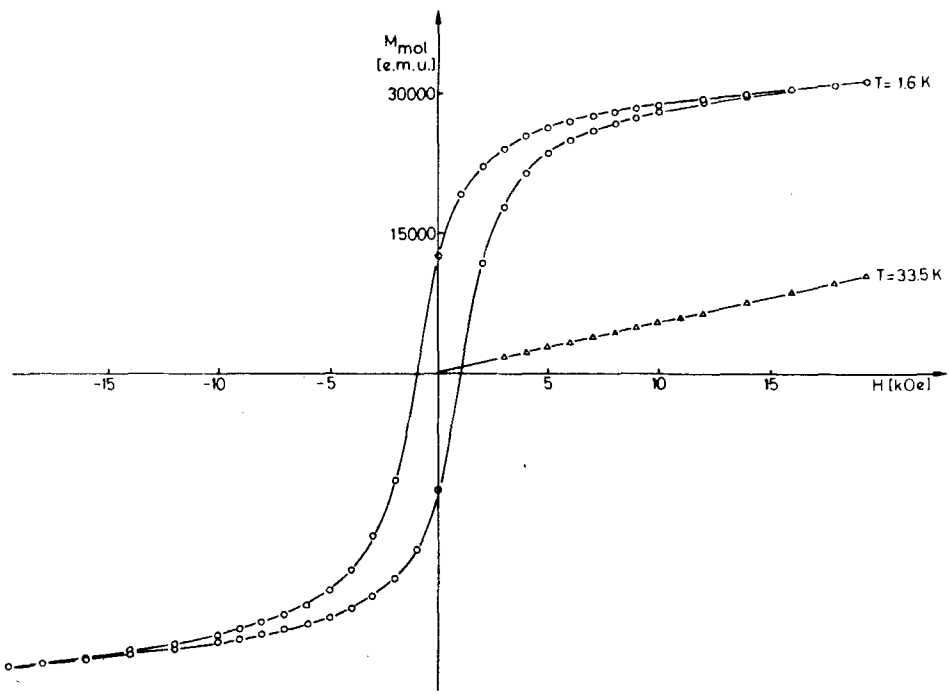

Fig. 131. The magnetization per mole of $DyCrO_4$ as a function of the external field for $T = 1.6$ K and 33.5 K (Walter et al., 1973).

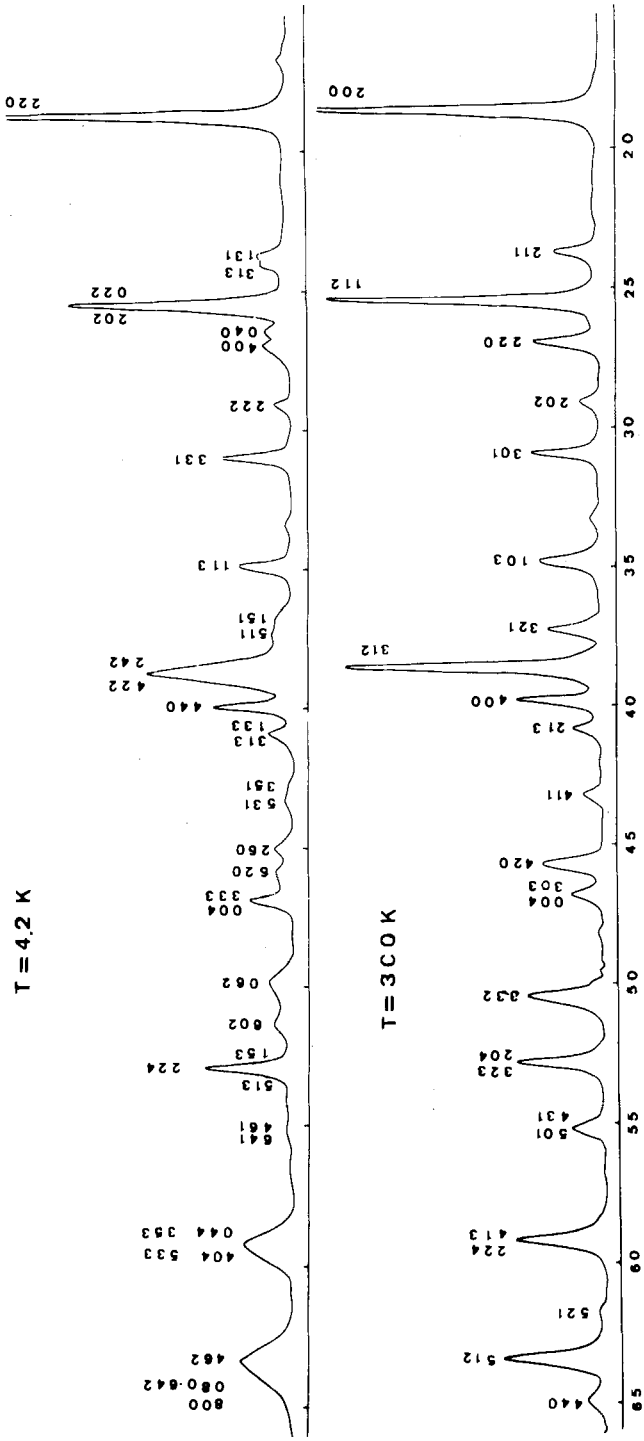

Fig. 132. The X-ray powder patterns of $TbCrO_4$ at 300 and 4.2 K. The indexing is based on tetragonal ($I4_1/4amd$) and orthorhombic (F222) symmetries, respectively. (Buisson et al., 1976.)

magnetic phase transitions the studies of Walter et al. (1973) and Buisson et al. (1976) deserve mention. In the first study, which deals with magnetic and specific heat measurements between 1.2 and 30 K, the magnetic transition temperatures T_c for the zircon-type compounds were found to range from 9.1 K for $PrCrO_4$ to 23.4 K for $YbCrO_4$, and a low transition temperature (9.2 K) was also found for the yttrium compound. While the magnetic behavior of $YCrO_4$ may be explained in terms of a simple molecular field theory, $DyCrO_4$ exhibits a distinct hysteresis loop (fig. 131 (Walter et al., 1973).

Walter et al. (1973) also noted from neutron diffraction experiments at low temperatures a possible crystallographic phase transition to a symmetry lower than tetragonal. This was established (Buisson et al., 1976) by careful X-ray and neutron diffraction experiments to occur for $TbCrO_4$ at 48 K, resulting in an orthorhombic F222 space group (fig. 132). The local symmetry of the Tb^{3+} site is lowered from D_{2d} to D_2. Study of the magnetic transition at 21.8 K from paramagnetic to collinear ferromagnetic showed the spin arrangement to be in good agreement with the F222 space group.

9. Rare earth cyanides and hexacyanometallates

9.1. *Introduction*

As a consequence of the strength of the R–O bond and the usual aqueous environment, nearly all complexes of the rare earths are derived from oxygen-donor ligands (see chapter 56, section 1, of Volume 8 of this Handbook). However, a number of nitrogen-donor complexes can be prepared but often only in strictly anhydrous conditions. They include also inorganic ligands such as NH_3 and SCN^- (Moeller et al., 1973). Complexes where other bonds are present are less common, with the possible exception of those involving the halides.

The cyanides and hexacyanometallates of the rare earths are interesting because of the presence of R–N bonds in hexacyanometallates and possibly R–C bonds in the cyanides. There is a striking difference in the stabilities and other properties between these two groups of compounds, suggesting a different type of bonding.

The binary rare earth cyanides have in general been little studied and their structures have been poorly characterized. A short review on lanthanide and actinide cyanides has been presented by Bagnall (1973). In the reducing conditions employed in most preparations, Sm, Eu, and Yb yield the bicyanides as predominant products. A similarity to the rare earth halide stoichiometries is demonstrated by the existence of monocyanide radicals in the gas phase.

In contrast, the rare earth hexacyanometallates have been studied in detail by a number of techniques, including single-crystal X-ray diffractometry. These compounds have also found applications in the separation and purification of the rare earths by fractional crystallization.

9.2. *Preparation of rare earth cyanides*

In the presence of iron catalysts at temperatures above 300°C, the rare earth chlorides react with alkali cyanides to give $R(CN)_3$. The product is unstable, however, and disproportionates to cyanamide (Perret and Banderet, 1937). Solid $R(CN)_3$ can be prepared by the reaction between LiCN and RBr_3 in tetrahydrofuran solution. Chemical analysis of the product has shown, however, that the solvent participates in the reaction and that the correct composition is $R(CN)_3 \cdot 2THF$ (Rossmanith, 1966).

Other methods for the preparation of rare earth cyanides are the reaction of metallic R with $Hg(CN)_2$ in liquid ammonia and the precipitation with HCN in an ammonia solution of metallic Eu and Yb (McColm and Thompson, 1972). The problem with the first of these methods is the difficulty of removing metallic Hg and the possible excess of $Hg(CN)_2$. The precipitation method has been extended to rare earths insoluble in ammonia, in which case the reaction is effected by electrolysis at −63°C in a concentrated NH_4CN–NH_3 solution, using rare earth and platinum electrodes. In all cases the crystallinity is poor and the particle size of the product is small. The colors of some rare earth cyanides already synthesized are presented in table 30.

McColm and Thompson (1972) have characterized the rare earth cyanides by means of chemical analysis, IR spectrometry, and X-ray diffractometry and have measured their magnetic properties. The results indicate mixed products for Sm, Eu, and Yb (table 30), and the initial precipitate in the case of Eu and Yb contains a high percentage of bicyanide. Although the samarium product has been analyzed as $Sm(CN)_2$, all physical measurements indicate that it is $Sm(CN)_3$, which suggests that $Sm(CN)_2$ is very unstable to disproportionation. They suggested that the X-ray lines of $Ce(CN)_3$ and $Sm(CN)_3$ could be explained in terms of

TABLE 30
Colors of rare earth cyanides and the results of chemical analyses (reaction $R + NH_4CN$). *

Cyanide	Color of precipitate in liquid NH_3	Color after removal of NH_3	Analysis					
			found			theoretical		
			C (%)	N (%)	R (%)	C (%)	N (%)	R (%)
Ce	green	red-brown	16.3	21.2	62.3	16.5	19.3	64.2
Pr	green	yellow-brown	16.3	19.1	66.7	16.4	19.2	64.4
Sm	deep brown	light brown	12.1	15.1	72.0	11.9	13.8	74.3 **
Eu	green	yellow, turning to orange	11.5	13.8	72.7	11.8	13.7	74.5 **
Ho	deep brown	grey	14.3	17.5	68.8	14.8	17.3	67.9
Yb	yellow	purple	12.1	11.5	78.3	10.7	12.4	76.9 **

* McColm and Thompson (1972).
** Calculated as $R(CN)_2$.

TABLE 31
Infrared spectra of solid rare earth cyanides. *

Compound	C≡N stretch (cm^{-1})	M–N or M–C stretch (cm^{-1})
$Ce(CN)_3$	2125, 2095 w, sh	505
$Pr(CN)_3$	2130, 2100	500
$Sm(CN)_3$	2130, 2115 w, sh	500
$Eu(CN)_3$	2180, 2115	
$Ho(CN)_3$	2130, 2100 sh	510
$Yb(CN)_3$	2185, 2100	
$Eu(CN)_2$	2080	460
$Yb(CN)_2$	2100	450

* McColm and Thompson (1972).
sh = shoulder; w = weak.

a large cubic cell with $a = 11.27$ and 11.32 Å, respectively. The purple Yb compound differs from Ce and Sm cyanides, and its diffraction pattern can be indexed as an orthorhombic cell with $a = 3.51$ Å, $b = 4.32$ Å and $c = 4.82$ Å. The diffraction pattern of $Eu(CN)_2$ suggests that the unit cell may have tetragonal symmetry. From the IR spectrum it is impossible to determine whether the rare earth is bonded to the carbon or nitrogen atom (table 31).

The Mössbauer spectrum of the europium compound has a chemical shift of −13.00 mm/s relative to EuF_3 with a half width of 5.50 mm/s. The shift value falls within the range found for ionic divalent europium compounds (−15.0 to −12.8 mm/s). The chemical shift in $Eu(CN)_3$ is 0.75 mm/s with the half width 2.74 mm/s. The explanation of the broad band in the spectrum of the divalent europium compound may be the participation of the d-orbital in the bonding (Colquhoun et al., 1972).

The rare earth cyanides are stable in vacuum below 360°C, but at 600°C the material becomes black. The product is a mixture of free metal, nitride, carbon, and paracyanogen (McColm and Thompson), and not a mixture of carbide and nitride as suggested by Seifer (1963a).

Organolanthanide cyanides are known for cerium(IV). Cyclopentadienyl and indenyl cerium(III) bicyanides have been prepared by refluxing KCN and $CeCl_4$ in THF solution. The products have been characterized by IR spectrometry (Kalsotra et al., 1972).

9.3. *Gaseous rare earth mono- and dicyanides*

Rare earths, like many other elements, form monocyanides at high temperatures in the presence of free carbon and nitrogen (Lvov and Pelieva, 1980). The formation and the thermodynamic functions of gaseous RCN have been determined by electrothermic atomic absorption spectrometry (Lvov and Pelieva, 1973, 1979). The method is based on the use of a graphite furnace heated up to 2500–2700 K. During insertion of the samples, N_2 and Ar were blown, in turn,

TABLE 32
Some physicochemical properties of rare earth monocyanides. *

Element	T (K)	Bond distance (Å)	Bond strength (N/cm)	ΔH^0 (kJ/mol)	Dissociation energy (kJ/mol)	Free energy $\Delta\phi^0$ (J/mol K)	Gibbs energy $\Delta G^0(T)$ (kJ/mol)
La	2600	2.52	1.15	1367	611	240.1	694
Ce	3000	2.42	1.38	–	–	248.4	604
Pr	2600	2.42	1.38	1352	596	232.3	681
Nd	2600	2.43	1.36	1350	594	231.9	679
Sm	2500	2.43	1.36	1310	554	225.9	670
Eu	2600	2.43	1.36	1302	546	220.1	636
Gd	2600	2.38	1.49	1339	583	233.1	669
Tb	2600	2.33	1.65	1323	567	246.3	655
Dy	2600	2.33	1.65	1282	526	235.3	618
Ho	2600	2.33	1.65	1290	534	236.8	626
Er	2600	2.33	1.65	1291	535	238.7	626
Tm	2600	2.34	1.62	1266	510	239.9	604
Yb	2700	2.34	1.62	1259	503	217.0	572
Lu	2700	2.34	1.62	1329	573	238.0	634

* Lvov and Pelieva (1979).

into the furnace, and the absorption signals were compared with those due to the N_2 and Ar streams. The results show that in the series from lanthanum to ytterbium, the dissociation energy of the R–CN bond decreases in a nonlinear fashion from 611 to 503 kJ/mol, with a local maximum at gadolinium (table 32). The values are in good agreement with the known dissociation energies of rare earth monofluorides.

The atomization energies of gaseous Ce, Pr, and Eu monocyanides have also been determined by mass spectrometry. As in the atomic absorption method, first the equilibrium constants were determined and then the other thermodynamic values were derived from them (Cooke et al., 1973; Guido and Gigli, 1975a,b). The results are in good agreement with those reported by Lvov and Pelieva. $Y(CN)_2$ and $Sc(CN)_2$ radicals have been generated from the metals and $(CN)_2$ at low temperatures. Their magnetic properties were recorded by ESR and compared with those of the corresponding dihalide radicals (Knight and Wise, 1980; Knight et al., 1981).

9.4. *Hexacyanometallates of the rare earths*

9.4.1. *Solution studies*

Thermodynamic data for the complexation of trivalent lanthanides by hexacyanoferrate(III) have been interpreted as supporting a model of outer-sphere ion-pairing of $RFe(CN)_6$ (Stampfli and Choppin, 1972). The stability constants for the interaction of $Fe(CN)_6^{3-}$ and $Co(CN)_6^{3-}$ ligands with selected R^{3+} ions have been determined and for La^{3+} at zero ionic strength the $\log K_1$ values

obtained are the same regardless of the metallate ion (3.74 and 3.75) (Dunsmore et al., 1963).

More recently, Bellomo et al. (1973) have studied the reaction between $K_4Fe(CN)_6$ and R^{3+} (R = La, Ce). They determined the K_{sp}, $\Delta G°$, $\Delta H°$, and $\Delta S°$ values for the $KRFe(CN)_6$ compounds by potentiometric titrations in H_2O/EtOH mixtures of varying proportions.

9.4.2. *Preparation and properties of the solid compounds*

The rare earth elements form hexacyanoferrates with both divalent and trivalent iron. The alkali-containing hexacyanoferrate(II) was prepared as early as 1909 by Robinson. A detailed study on the crystallization of rare earth hexacyanoferrates was reported in 1938 by Prandtl and Mohr, who used these compounds in an attempt to purify rare earth oxides. The work was completed by Marsh (1947).

The binary hexacyanoferrates(III) can be prepared by mixing rare earth chloride and $K_3Fe(CN)_6$ solutions. The crystals are grown by very slow diffusion of a dilute solution (Bailey et al., 1973). Single crystals can also be grown by a double infusion technique where two reactants are simultaneously infused into a solvent at constant temperature by means of a double infusion pump (Hulliger et al., 1976a; Huber et al., 1980) (fig. 133). The product is $RFe(CN)_6 \cdot 5H_2O$. The older literature on La hexacyanoferrate(III) and La hexacyanocoboltate(III) reports the water content to be 5.6 water molecules per formula unit (James and Willard, 1916; Prandtl and Mohr, 1938), but Davies and James (1948) later

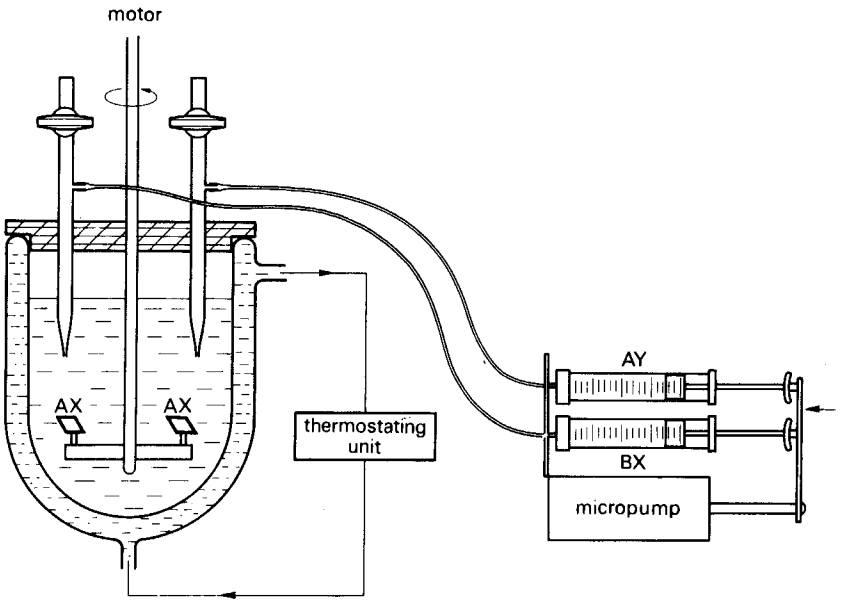

Fig. 133. The schematic representation of the double infusion device used in the preparation of $RFe(CN)_6 \cdot nH_2O$ (Huber et al., 1980).

confirmed the presence of five water molecules. The structure of the lanthanum compound is hexagonal with space group $P6_3/m$ and consists of hexacyanoferrate octahedra linked to nine-coordinated rare earth atoms. The coordination sphere of the rare earth contains, in addition to six nitrogen atoms, three water molecules. The two uncoordinated water molecules occupy the holes in the structure along the threefold axis (Bailey et al., 1973; Kietaibl and Petter, 1974) (fig. 134). $LaFe(CN)_6 \cdot 5H_2O$ can be dehydrated in a controlled environment at 296 K to $LaFe(CN)_6 \cdot 4H_2O$ (Morgan et al., 1978). The monodehydration does not bring about a change in crystal system or space group but does significantly shorten the *c* parameter (table 33). N–O and La–O distances are longer in tetrahydrate than in pentahydrate because the N atoms move closer to each other in the *z*-direction during monohydration. In addition, the nine-coordinated lanthanum grouping can change to the eight-coordinated $LaN_6(OH_2)_2$ group (Mullica et al., 1980).

According to Hulliger et al. (1976a), the rare earth hexacyanoferrate(III) pentahydrates decompose to the tetrahydrate at room temperature within a few days. The heavier rare earths (Sm–Lu, Y) form only tetrahydrates. The structure

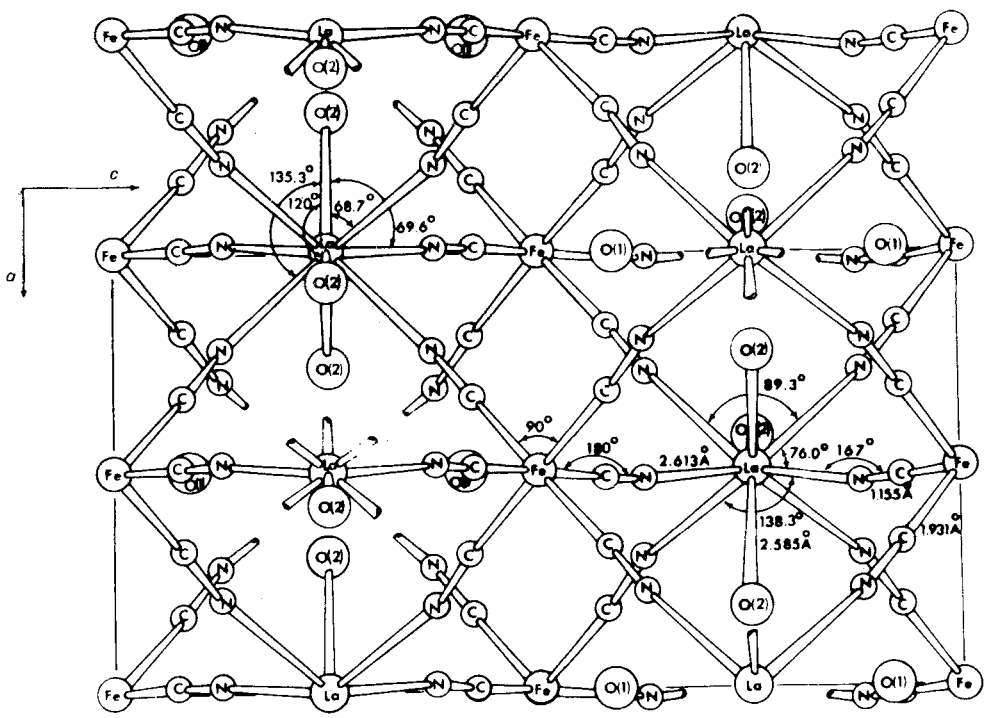

Fig. 134. A view of the structure of $LaFe(CN)_6 \cdot 5H_2O$ perpendicular to the *ac*-plane. Bond lengths and angles are indicated (Bailey et al., 1973).

TABLE 33
Summary on the structural data of rare earth cyanides.

Compound	R	Example	*a* (Å)	*b* (Å)	*c* (Å)	*Z*	Space group	Ref.
$RFe(CN)_6 \cdot 5H_2O$	La–Nd	La	7.55		14.45	2	$P6_3/m$	a
$RFe(CN)_6 \cdot 4H_2O$	La	La	7.54		13.96	2	$P6_3/m$	b
	Ce–Lu, Y	Dy	7.36	12.80	13.61			c
$RCr(CN)_6 \cdot 5H_2O$	La–Nd	La	7.71		14.82	2	$P6_3/m$	c
$RCr(CN)_6 \cdot 4H_2O$	Sm–Lu, Y	Dy	7.49	13.08	13.98			c
$RCo(CN)_6 \cdot 5H_2O$	La–Nd	La	7.51		14.34	2	$P6_3/m$	d
$RCo(CN)_6 \cdot 4H_2O$	Ce–Lu, Y	Ho	7.29	12.66	13.52			e
$RKFe(CN)_6 \cdot 4H_2O$	La, Ce, Nd	Nd	7.36		13.78	2	$P6_3/m$	f

(a) Bailey et al. (1973).
(b) Mullica et al. (1980).
(c) Hulliger et al. (1976a).
(d) Mullica et al. (1979b).
(e) Hulliger et al. (1976b).
(f) Milligan et al. (1982).

of the tetrahydrate is pseudohexagonal and it can better be described as orthorhombic. At higher temperatures all rare earths except lanthanum form tetrahydrates.

In a solution of rare earth chloride and potassium hexacyanoferrate(II), the potassium-containing compound $RKFe(CN)_6 \cdot 4H_2O$ is formed. The structure is isomorphous with $RFe(CN)_6 \cdot 5H_2O$, having the nine-coordinated rare earth group $RN_6(OH_2)_3$. The additional water molecule and the potassium atom occupy the holes in the structure (Beall et al., 1978; Mullica et al., 1979a) (fig. 135). The X-ray diffraction powder data for alkali rare earth hexacyanoferrates(II) have been published by Kuznetsov et al. (1970, 1973a,b) and Kuznetsov

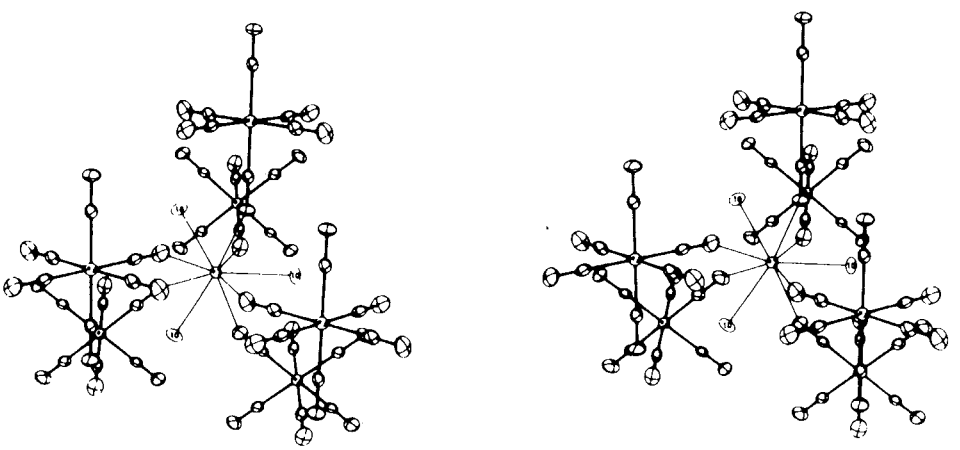

Fig. 135. A stereoscopic view of $CeKFe(CN)_6 \cdot 4H_2O$ (Mullica et al., 1979).

and Yakovleva (1973). The zeolite-like behavior of hexacyanoferrates was first observed by Seifer (1963a,b) for $Ce_4(Fe(CN)_6)_3 \cdot 14.5H_2O$. Structural investigations have confirmed that the structure does not change, even though in $RFe(CN)_6 \cdot 5H_2O$ the number of water molecules changes or one water molecule is replaced by potassium.

The original studies of rare earth hexacyanocoboltates were initiated by James and Willand (1916), who reported that $RCo(CN)_6 \cdot xH_2O$, where R = La, Ce, Nd, Gd, Yb, contains 4.5 water molecules per unit formula. Using X-ray diffraction methods and IR spectroscopy, Bonnet and Paris (1975b) later characterized all $RCo(CN)_6 \cdot 4H_2O$ compounds as having the same hexagonal structure as $LaFe(CN)_6 \cdot 5H_2O$. Shortly thereafter, Hulliger et al. (1976b) showed, however, that only the lighter lanthanides (La–Nd) form hexagonal hexacyanocoboltates and contain five water molecules. The other rare earths form orthorhombic compounds containing only four water molecules. A single crystal study of $LaCo(CN)_6 \cdot 5H_2O$ has confirmed its being isomorphous with $LaFe(CN)_6 \cdot 5H_2O$ (Mullica et al., 1979b).

The hexacyanochromate(III) hydrates display similar behavior to the ferrates and coboltates: the lighter rare earths form hexagonal pentahydrate and the heavier rare earths pseudohexagonal or orthorhombic tetrahydrates (Hulliger et al., 1976a).

Magnetic measurements of the rare earth hexacyanoferrate(III) and chromate(III) hydrates have shown that the complexes with nonmagnetic rare earth ions are all antiferromagnetic at low temperatures, whereas those with magnetic rare earth ions are antiferromagnetic or ferromagnetic. The highest ordering temperatures were found in the terbium compounds: 5.7 and 11.7 K for the ferrate and chromate, respectively (Hulliger et al., 1976a). In the cobaltates no magnetic ordering was detected down to 1 K. The Stark splitting of the J ground state due to the crystalline field has been analyzed for $CeCo(CN)_6 \cdot 4H_2O$ and $SmCo(CN)_6 \cdot 4H_2O$ (Hulliger et al., 1976b).

The thermal stability studies of the rare earth hexacyanometallates show that dehydration occurs below 200°C. The second decomposition stage is the oxidation of cyanide, when RMO_3 mixed oxides are formed. In oxygen the reaction takes place at about 350°C and in air at about 400–450°C (Gallagher, 1968; Bonnet and Paris, 1975a). The decomposition products of rare earth hexacyanoferrates(III) and ammonium rare earth hexacyanoferrates(II) have been shown to be useful precursors for the production of rare earth ferrites (Gallagher, 1968). The decomposition in vacuum or nitrogen is very complex, especially that of the europium compound (Gallagher and Schrey, 1969). Evolved gas analysis and Mössbauer spectroscopical studies have shown that the chain of intermediates for iron is $Fe(CN)_2$–Fe_3C–Fe (fig. 136). In a similar way the decomposition of the europium compound has been shown to proceed via a hydrolytic process to EuOOH, and finally to EuO, after interaction with the free carbon at elevated temperature (Gallagher and Prescott, 1970).

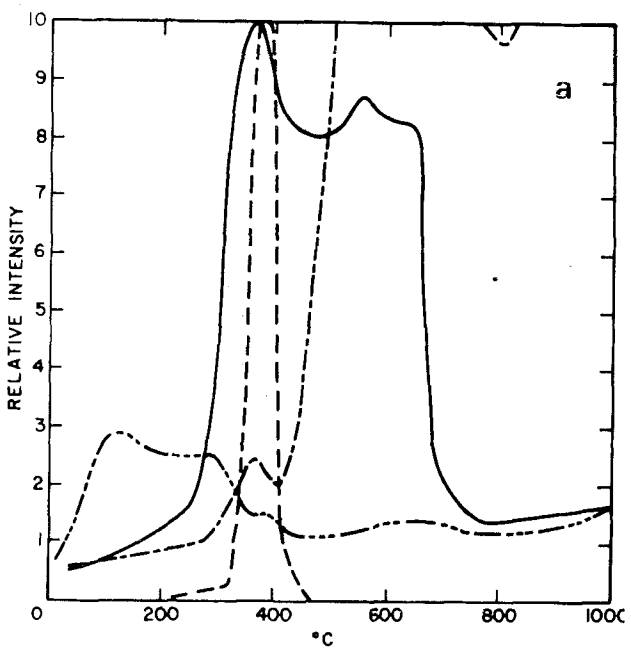

Fig. 136. (a) The evolved gas analysis of $EuFe(CN)_6 \cdot 5H_2O$; ——— : mass 18 (H_2O); ——: mass 27 (HCN); – – – – –: mass 52 [$(CN)_2$]; — — —: mass 28 (CO and N_2).

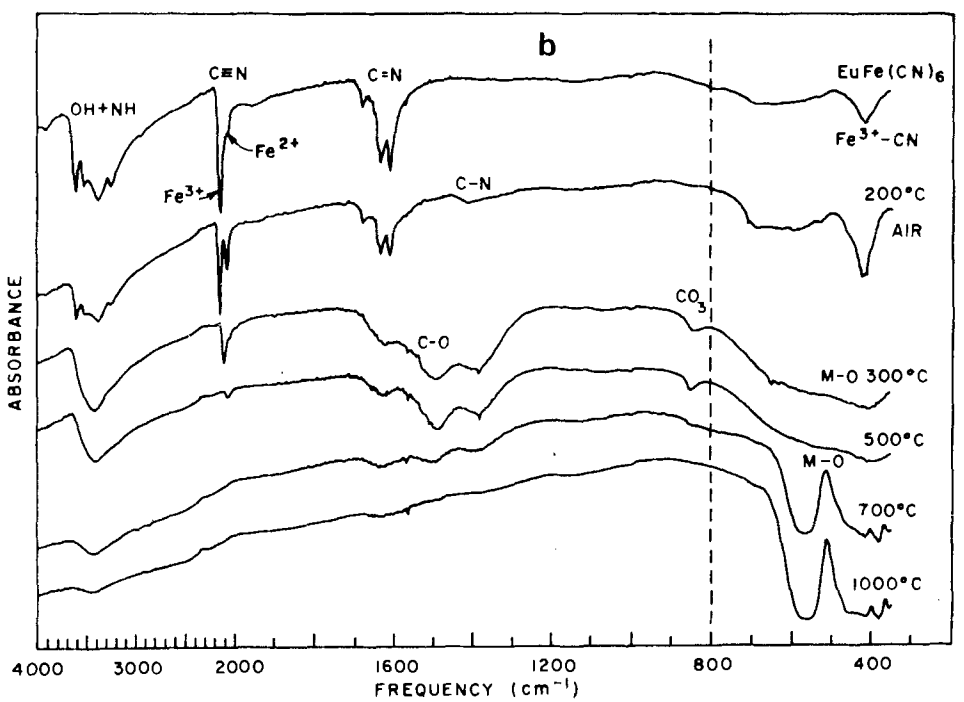

Fig. 136. (b) Selected IR spectra of $EuFe(CN)_6 \cdot 5H_2O$ heated in air. (Gallagher and Prescott, 1970.)

10. Aqua complexes of the rare earths

10.1. *Introduction*

At a sufficiently low pH the R^{3+} ions form unhydrolyzed aqua complexes if stronger complexing ligands are not present. Hydrolyzed species begin to form first around a pH of 4 to 6, depending on the basicity of the lanthanide ion and on the other ions present (Burkov et al., 1982). For instance, solutions of $EuCl_3$ and $Eu_2(SO_4)_3$, when titrated with NaOH, gave initial precipitation at pH = 6 and $Eu(NO_3)_3$ at pH = 6.5 (Mironov and Polyashov, 1970). Due to its smaller ionic radius the hydrated Sc^{3+}, however, readily undergoes acid dissociation above pH = 3.0 (Komissarova, 1980).

Crystallization of rare earth compounds from aqueous solutions yields, in several cases, solid hydrates where the aqua complex structure has been preserved, as determined by X-ray diffrection. Well-known examples include the nona-aqua complexes $[R(OH_2)_9]X_3$, where X is bromate, for instance. Crystal structure determinations of the aqua complexes in the solid state have provided valuable data for comparison with results and structural models obtained by solution studies using various techniques.

The discussion of rare earth aqua complex formation in solution has been focused mainly on (a) coordination number and geometry, (b) possible changes in coordination number along the lanthanide series, and (c) strength of bonding as reflected in the thermodynamic and kinetic data. Especially the first two topics have been frequently debated. It appears that different experimental techniques and approaches tend to give different values for the coordination number and to its changes.

There are several recent reviews on the topic as well as a vast number of original research reports. Marcus (1981) in the *Gmelin Handbook* gives an authoritative overview on solution studies related to aqua complex formation; the literature is covered up to 1978. Carnall (1979) in this Handbook covers approximately the same period, emphasizing spectroscopic studies. Since the late 1970's a few additional reviews have appeared. Grenthe (1978) discusses briefly the thermodynamics and kinetics of R^{3+} complex formation in aqueous solutions, while Williams (1982) focuses his review on the NMR methods and biological systems. The most comprehensive of the recent reviews is that of Lincoln (1987), which discusses the ligand substitution processes and includes data from nonaqueous solutions.

The different behavior of scandium in aqueous solutions is discussed in an authorative way by Komissarova (1980). The recent overview on the chemistry and thermodynamics of europium and its simple inorganic compounds also includes some relevant solution data (Rard, 1985). A general discussion on aqua complexes of metal ions has been presented by Burgess (1978) and by Hunt and Friedman (1983). In the following we will emphasize the results obtained by diffraction methods.

10.2. *Aqua complexes in the solid state*

The high degree of hydration of several solid R^{3+} compounds is an indication that aqua complexes present in solution are also stable in the solid state. The first conclusive proof of the existence of the solid nona-aqua complex was provided by Ketelaar (1937), who investigated the structures of some lanthanide ethyl sulfates. Later, several other hydrated R^{3+} compounds were found to contain the nona-aqualanthanide(III) complex and more recently a few examples of aqua complexes having a lower coordination number, viz. 8 or 6, have been investigated by X-ray diffraction methods.

10.2.1. *The nona-aqua complexes*

Following the work of Ketelaar (1937), Helmholz (1939) determined the structure of $Nd(BrO_3)_3 \cdot 9H_2O$ from two-dimensional X-ray data and found that it too contained the characteristic $[R(OH_2)_9]^{3+}$ complex ion. The structures of Pr and Er ethyl sulfates were refined by Fitzwater and Rundle (1959), and with the increasing availability of X-ray methods the number of single-crystal determinations has grown steadily. Table 34 lists recent structural studies by X-ray and neutron diffraction methods.

It is expected that the list of known aqua complexes will be expanded considerably in the future as there are in the literature a number of compounds of type $RX_3 \cdot 9H_2O$ which may well contain the nona-aqua complex ion. For instance, the iodide nonahydrates have this stoichiometry (Heiniö et al., 1980) and furthermore the iodide ion tends to form only weak complexes with the rare earths.

In all nona-aqualanthanide(III) structures the coordination polyhedron around the R^{3+} is a tricapped trigonal prism in accordance with the stability predictions (Favas and Kepert, 1981; Harrowfield et al., 1983) (fig. 137). Albertsson and Elding (1977) have analyzed the coordination geometry around Pr and Yb in ethylsulfates and bromates and noted the C_{3v} symmetry in the first case and D_{3h} in the latter. The decrease in the prismatic R–O bond lengths is what is expected from the lanthanide contraction (0.16 Å) but van der Waals repulsions between prismatic and equatorial oxygen atoms make the decrease in the equatorial R–O bonds about half this value. This leads to an increase in the ratio between the R–O (capping) and R–O (prismatic) distances when R changes from La to Lu (table 34).

Albertsson and Elding (1977) also studied the variation of the unit cell dimensions in the lanthanide series and found no abrupt changes, although the values of the *a*-parameter plotted against ionic radii showed a different slope in the range La–Tb and Tb–Lu. The variation in the cell dimensions was related to the repulsions between prismatic and equitorial oxygen atoms and to the hydrogen bond system (fig. 138). The strict isostructural nature of the ethylsulfates was confirmed by Gerkin and Reppart (1984), who investigated the lanthanide series by single-crystal neutron diffractometry.

TABLE 34

Summary of recent structural data on solid nona-aqualanthanide(III) complexes.

Compound	R	Example	Crystal data							R–O distance			
			a (Å)	*b* (Å)	*c* (Å)	γ (deg)	Space group	*Z*	*R*-value (%)	I: $R–O_{capping}$ (Å)	II: $R–O_{prismatic}$ (Å)	Ratio I/II	Ref.
$[R(OH_2)_9](BrO_3)_3$	Sm		11.86		6.76		$P6_3/mmc$	2	9.8	2.55	2.46	1.04	a
	Pr, Yb	Pr	11.8395		6.8012				3.4	2.52	2.49	1.01	b
	Tb		11.755		6.712				2.7	2.47	2.40	1.03	c
$[R(OH_2)_9](C_2H_5SO_3)_3$	Ho *		13.92		7.03		$P6_3/m$	2	11.1	2.47	2.37	1.04	d
	Pr, Yb	Pr	14.0454		7.1207				2.5	2.59	2.47	1.05	b
	Y **		13.871		7.007				5.9	2.52	2.37	1.06	e
	La–Lu *	La	14.045		7.0996				2.1	2.62	2.52	1.06	f
		Lu	13.834		6.9612				2.0	2.50	2.32	1.08	
$[R(OH_2)_9](CF_3SO_3)_3$	La, Gd,	La	13.990		7.444		$P6_3/m$	2	4.3	2.62	2.52	1.04	g
	Lu, Y	Lu	13.259		7.751				4.4	2.50	2.29	1.09	g
	Nd, Ho	Ho	13.570		7.577				3.0	2.53	2.37	1.07	h
$[R(OH_2)_9]Br_3 \cdot 2C_4H_8O_2$	Sm		8.010	19.848	7.588		Amm2	2	2.2	2.48	2.47	1.00	i
$R_2V_{10}O_{28} \cdot 28H_2O$	Nd		9.88	19.59	11.99	98.6	$P2_1/b$	2	5.7				j

* Neutron data.

** Neutron data at 110 K.

References:

(a) Sikka (1969).
(b) Albertsson and Elding (1977).
(c) Gallucci et al. (1982).
(d) Hubbard et al. (1974).
(e) Broach et al. (1979).
(f) Gerkin and Reppart (1984).
(g) Harrowfield et al. (1983).
(h) Paiva Santos et al. (1985).
(i) Barnes and Nicoll (1985).
(j) Safyanov and Belov (1976).

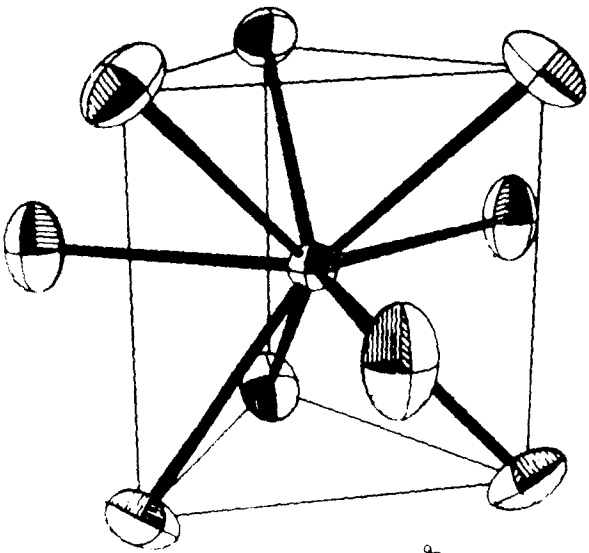

Fig. 137. The regular tricapped prismatic coordination polyhedron of the nona-aqualanthanide(III) ion in solid bromate and ethylsulfate hydrates (Grenthe, 1978).

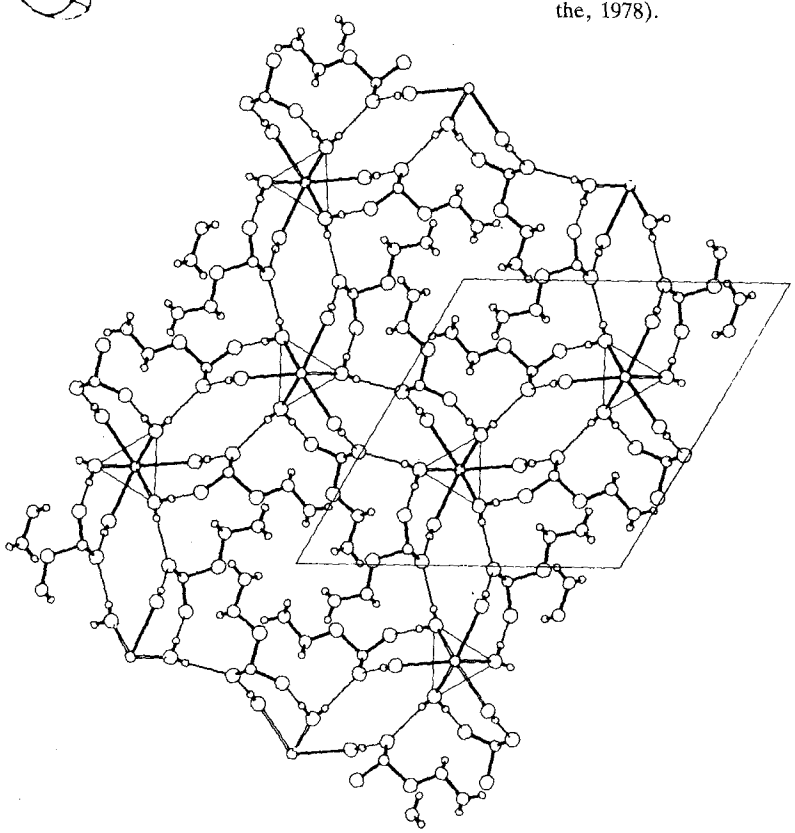

Fig. 138. A projection of the structure of $[Pr(OH_2)_9](C_2H_5SO_3)_3$ on the (001) plane (Albertsson and Elding, 1977).

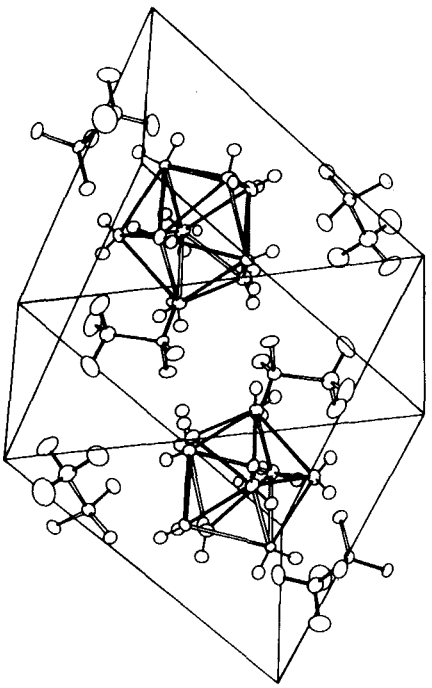

Fig. 139. A perspective view of the unit cell contents of $[Ho(OH_2)_9](CF_3SO_3)_3$ (Paiva Santos et al., 1985).

Besides the ethylsulfates and bromates, the trifluoromethanesulfates have been studied in detail (Harrowfield et al., 1983; Paiva Santos et al., 1985). Data from six three-dimensional X-ray structure analyses are available (table 34); the structures are similar to those of the ethylsulfate nonahydrates (fig. 139). Unit cell data, however, show an interesting and rather unexpected feature. While the cell volume decreases, the *c*-parameter increases significantly with the increasing atomic number, changing the *a*/*c* ratio from 1.88 (La) to 1.71 (Lu) (Harrowfield et al., 1983).

In the case of $[Sm(OH_2)_9]Br_3 \cdot 2C_4H_8O$ (Barnes and Nicoll, 1985), a detailed comparison between the structure and that of the corresponding bromate has been published and it shows that the geometry of the $[Sm(OH_2)_9]^{3+}$ ion is essentially unchanged in spite of the differences in the outer coordination sphere.

10.2.2. *Octa-aqua and hexa-aqua complexes*

Whereas the coordination number of R^{3+} in solid compounds varies between large limits, only a few examples of rare earth aqua complexes are known with a CN other than nine. These include two decavanadate structures and the perchlorate hexahydrates.

During the systematic investigations into the structural chemistry of the highly hydrated R^{3+} decavanadates, Safyanov with coworkers and Rivero et al. (for complete references, see section 7), have discovered a nona-aqua complex

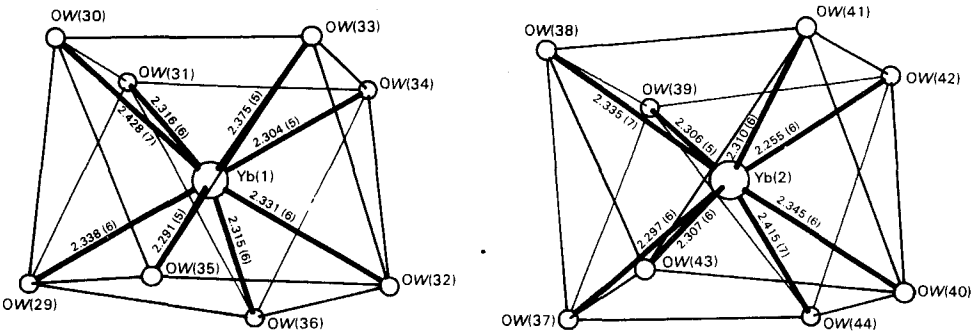

Fig. 140. The Yb–OH_2 distances in the two YbO_8 coordination polyhedra found in the structure of $Yb_2V_{10}O_{28} \cdot 24H_2O$. The polyhedra have been described as distorted antiprisms. (Rivero et al., 1985.)

($R_2V_{10}O_{28} \cdot 28H_2O$, R = La, Ce) and two octa-aqua complexes. It is interesting to note that both decavanadates, which contain the $[R(OH_2)_8]^{3+}$ cation (table 35; fig. 140) are formed by the heavier rare earths. In contrast, the $R_2V_{10}O_{28} \cdot 28H_2O$ structure with CN = 9 is formed only when R = La–Sm. When the water content is lower, e.g., in $R_2V_{10}O_{28} \cdot 20H_2O$, the decavanadate oxygens are involved in the inner-sphere coordination (see section 7).

On the basis of its ionic radius and known structural chemistry with oxygen donor ligands (Valkonen, 1979), scandium would be expected to have the hexahydrated ion in some of its compounds, for instance in the perchlorates and bromates. No structural data appear to be available, however, obviously because of the tendency of scandium compounds to undergo hydrolysis and the difficulty of forming good single crystals in aqueous solutions. Nevertheless, the hexahydrated R^{3+} ion has been discovered recently in the solid hydrates of R^{3+} perchlorates (R = La, Tb, Er) (Glaser and Johansson, 1981). For details of the structure, see table 35 and section 6.

10.3. *Comparison with solution studies by diffraction methods*

The coordination number (or primary hydration number) of an R^{3+} aqua complex has been the subject of continuous debate. Many of the techniques used for its determination provide only indirect evidence, being open for different interpretations. Recent reviews give a good overall picture of the situation, see for instance Marcus (1981), Choppin (1984), and Lincoln (1987).

It appears that X-ray and neutron scattering methods, although limited to fairly concentrated solutions, are able to give valuable information, which can be used to establish with a satisfactory accuracy, not only the type of coordination but in most cases also the coordination number and geometry (Neilson and Enderby, 1980; Caminiti et al., 1979; Ohtaki, 1984). While the choice between the inner- and outer-sphere coordination types is usually unambiguous, establishing the coordination number and geometry from X-ray solution data is not straightforward (Caminiti et al., 1983).

TABLE 35

Summary of structural data on solid octa-aqua and hexa-aqua complexes of the rare earths.

Compound	Crystal data									R–O distance			
	a (Å)	*b* (Å)	*c* (Å)	*α* (deg)	*β* (deg)	*γ* (deg)	Space group	*Z*	*R*-value (%)	Range (Å)		Mean (Å)	Ref.
$Er_2V_{10}O_{28} \cdot 25H_2O$	9.168	10.002	12.703	68.87	77.52	89.34	$P\bar{1}$	1	4.8	2.30–2.40		2.36	a
$Yb_2V_{10}O_{28} \cdot 24H_2O$	9.287	9.821	23.33	99.13	81.51	90.57	$P\bar{1}$	2	4.4	2.29–2.38*[2]		2.34	b
										2.26–2.42		2.32	
$Y_2V_{10}O_{28} \cdot 24H_2O$	9.432	9.874	23.49	98.8	90.1	98.0	$P\bar{1}$	2	8.8	2.26–2.43*[2]		2.36	c
										2.29–2.58		2.41	
$[Gd(OH_2)_8]Cl_3 \cdot 2C_{10}H_8N_2$	8.901		19.319				P4c2	2	6.8	2.35–2.45		2.40	d
$[Y(OH_2)_8]Cl_3 \cdot 2C_{10}H_8N_2$	8.883	8.883	19.231				Pcc2	2	6.8	2.33–2.43		2.38	e
$[Y(OH_2)_8]Cl_3 \cdot 15C5$*[1]	9.202	17.247	15.208		92.39		$P2_1/n$	4	8.1	2.32–2.43		2.37	f
$[La(OH_2)_6] \cdot (ClO_4)_3$	12.173						Fm3m	4	7.0		2.48 (2.30) *[3]		g
$[Tb(OH_2)_6] \cdot (ClO_4)_3$	11.926						Fm3m	4	6.0		2.35 (2.21) *[3]		g
$[Er(OH_2)_6] \cdot (ClO_4)_3$	11.900						Fm3m	4	4.4		2.25 (2.15) *[3]		g

*[1] 1.5C5 = 1,4,7,10,13-pentaoxacyclopentadecane.

*[2] Two crystallographically different $[R(OH_2)_8]^{3+}$ polyhedra.

*[3] Corrected for thermal motion, uncorrected values in parentheses.

References:

(a) Rivero et al. (1984).
(b) Rivero et al. (1985).
(c) Safyanov et al. (1978a).
(d) Bukowska-Strzyzewska and Tosik (1982a).
(e) Bukowska-Strzyzewska and Tosik (1982b).
(f) Rogers and Kurihara (1986).
(g) Glaser and Johansson (1981).

Due to the high solubilities, the R^{3+} halides are suitable systems for XRD and NRD solution studies. Besides the chlorides, $LaBr_3$ and ErI_3 have been investigated (Brady, 1960; Smith and Wertz, 1975, 1977; Steele and Wertz, 1976; Habenschuss and Spedding, 1979a,b, 1980). Neutron data are available for $NdCl_3$ (Narten and Hahn, 1982; fig. 141).

The data of Habenschuss and Spedding (1980) for the chloride solutions show three maxima in the radial distribution functions. For $SmCl_3$ they occur at 2.51 Å (R^{3+}–OH_2), 3.16 Å (H_2O–H_2O) and 4.91 Å (R^{3+}–Cl). The last peak is due to an outer-sphere (solvent-separated) interaction. A correlation was sought between the average atom–atom interactions in the RCl_3 solutions and those in the solid RCl_3 hydrates. Figure 142 shows a summary of the trends, indicating a gradual change in the CN when going from the La–Nd region (CN = 9) towards the heavier rare earths where Tb–Lu have a CN of 8. The variation of R^{3+}–OH_2 and H_2O–H_2O distances seems to be in agreement with this interpretation. Furthermore, a comparison to solid-state structures lends further support to the existence of a change in the coordination number. $RCl_3 \cdot 7H_2O$ (R = La–Pr) has a nine-coordinated structure with $7H_2O$ and $2Cl^-$ around R^{3+} (Peterson et al., 1979) while the heavier lanthanides and yttrium are eight-coordinated by $6H_2O$ and $2Cl^-$ in the structure of solid $RCl_3 \cdot 6H_2O$ (Habenschuss and Spedding, 1978; Kepert et al., 1983). On the other hand, a direct comparison between the solid state and solution structures may not be meaningful at all in this case because it was assumed that in solution the chloride ions do not enter the inner-coordination sphere, as they do in the solid state.

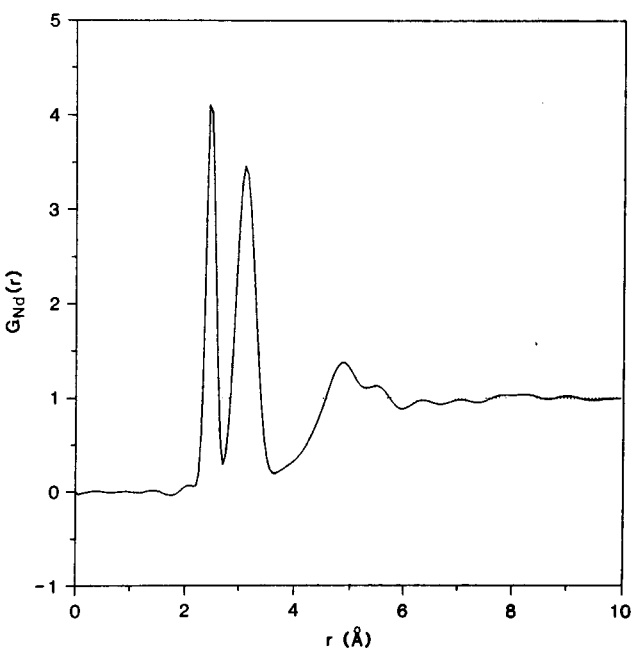

Fig. 141. The radial distribution of water molecules around the Nd^{3+} ion in a 2.85 molar solution of $NdCl_3$ in D_2O (Narten and Hahn, 1982).

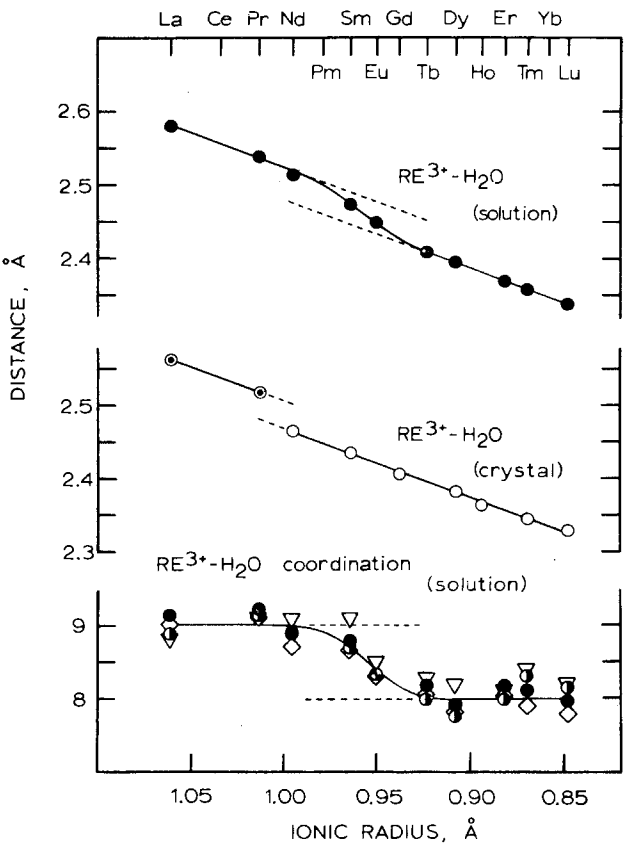

Fig. 142. The average R^{3+}–OH_2 interaction distances and coordination numbers found by X-ray scattering in concentrated RCl_3 solutions, and a comparison to R–OH_2 distances in RCl_3 solid hydrates (Habenschuss and Spedding, 1980).

The recent X-ray solution studies of R^{3+} complexes have involved the first oxoanion systems, viz. the nitrate, selenate and perchlorate systems. Caminiti et al. (1983) studied concentrated $Ce(NO_3)_3$ solutions and found monodentately bound NO_3^-. The coordination number is either 7.5 or 8.0, depending on other assumed interactions. The inner-sphere coordination of nitrate ions to R^{3+} is in agreement with solid-state structures (see Volume 8, chapter 56, section 6, of the Handbook).

Johansson et al. (1985) and Johansson and Wakita (1985) have studied the selenate and perchlorate systems using isomorphous substitution by yttrium to remove the ambiguities involved in the interpretation of the experimental data. The results indicate that selenate ions are monodentate ligands to R^{3+} while the perchlorate ions show no inner-sphere complex formation even at high concentrations. The coordination number was found in all systems to be invariably 8 ± 0.3. This is the same value as Wertz and coworkers have assumed to be valid in concentrated chloride and bromide solutions. On the other hand, the neutron diffraction study by Narten and Hahn (1982) using isotopic substitution gave 8.5 ± 0.2 for 2.85 M $NdCl_3$.

A comparison of the R–OH_2 distances found in the selenate and perchlorate solutions with those calculated on the basis of hydration radii (Marcus, 1983) shows a good agreement. The coordination type, viz. inner-sphere for the selenates and outer-sphere for the perchlorates corresponds also well with the solid-state structural data (see sections 5 and 6), as does the coordination number in the case of selenate complexes. For perchlorates only the structure of hexa-coordinated $[R(OH_2)_6](ClO_4)_3$ is known, as discussed in section 10.2.2, and it contains a 6-coordinated R^{3+}, which is lower than the CN found in solution.

10.4. *Concluding remarks*

Basically two different models have emerged from the X-ray and neutron scattering studies concerning the structure of the R^{3+} aqua complex in solution: (a) an unchanged coordination number (9 or 8) throughout the series La–Lu, Y, or (b) a change in CN (and structure) in the middle of the lanthanide series (from 9 to 8). Solid-state structural data seem to lend support to the first model, involving the nona-aqualanthanide(III) ion with a tricapped trigonal prismatic symmetry, but there is also evidence that can be interpreted in favor of a constant CN of 8 or a change from 9 to 8 as the ionic radius decreases.

Thus, it appears that there is a need for further experimental work before an overall picture is clarified. In the XRD and NRD studies, the use of special techniques (isotopic and isomorphous substitution) appears useful in solving some of the ambiguities which arise when the data are interpreted. However, in spite of the availability of additional data the use of concentrated solutions makes it difficult to compare directly the diffraction results with those obtained by other techniques, most notably by spectroscopic methods. In recent years, for instance, fluorescence (Kanno and Hiraishi, 1982; Tanaka and Yamashita, 1984; Horrocks and Albin, 1984; Marcantonatos et al., 1984; Kaizu et al., 1985) and NMR spectroscopy (Tarasov et al., 1983) have yielded very interesting, although sometimes partially contradictory results on the formation and stability of the aqua complexes in solutions of various concentrations and compositions.

References

Aarnio, P., 1980, M.Sc. Thesis, Helsinki University of Technology, Espoo.

Aarnio, P., M. Leskelä and L. Niinistö, 1981, Finn. Chem. Lett., p. 97.

Abenoza, M., Luu Dang Vinh, F. Rull-Perez and J.M. Pastor, 1977, J. Raman Spectrosc. **6**, 26.

Abrahams, S.C., and J.C. Bernstein, 1978, J. Chem. Phys. **69**, 2505.

Abrahams, S.C., J.L. Bernstein and E.T. Keve, 1971, J. Appl. Crystallogr. **4**, 284.

Abrahams, S.C., R.C. Sherwood, J.L. Bernstein and K. Nassau, 1973, J. Solid State Chem. **7**, 205.

Abrahams, S.C., J.L. Bernstein and K. Nassau, 1976a, J. Solid State Chem. **16**, 173.

Abrahams, S.C., J.L. Bernstein, J.W. Shiever and K. Nassau, 1976b, J. Appl. Crystallogr. **9**, 357.

Abrahams, S.C., J.C. Bernstein and K. Nassau, 1977, J. Solid State Chem. **22**, 243.

Agrawal, P.K., and W.B. White, 1985, Mater. Res. Bull. **20**, 97.

Ahmed Farag, I.J., L.A. Aslanov, V.M. Ionov and M.A. Porai-Koshits, 1973a, Zh. Fiz. Khim. **47**, 1056 [Russ. J. Phys. Chem. **47**, 602].

Ahmed Farag, I.S., L.A. Aslanov, M.A. Porai-Koshits, M.B. Varfolomeev, V.M. Ionov and L.D. Iskhakova, 1973b, Zh. Fiz. Khim. **47**, 1056 [Russ. J. Phys. Chem. **47**, 601].

Ahmed Farag, I.S., M.A. El-Kordy and N.A. Ahmed, 1981, Z. Krist. **155**, 165.
Aia, M.A., 1967, J. Electrochem. Soc. **114**, 367.
Ajgaonkar, V.R., 1981, Thesis, University of Bombay.
Albertsson, J., and I. Elding, 1977, Acta Crystallogr. B **33**, 1460.
Albrand, K.-R., R. Attig, J. Fenner, J.P. Jeser and P. Mootz, 1974, Mater. Res. Bull. **9**, 129.
Aleksandrovich, A.M., and V.V. Serebrennikov, 1962, Tr. Tomsk. Gos. Univ., Ser Khim. **154**, 105 [1964, Chem. Abstr. **60**, 8696e].
Aleksandrovich, A.M., and V.V. Serebrennikov, 1964, Chem. Abstr. **60**, 8696e.
Alimarin, I.P., E. Jen-Yun and I. Puzdrenkova, 1958, Chem. Anaht. **3**, 245.
Alimarin, I.P., I.V. Puzdrenkova and O.A. Shiryaeva, 1962, Vestn. Mosk. Univ. Ser. II Khim. **17**, 61.
Alonso, R., Luu Dang Vinh and J.A. de Saja, 1973, Krist. Techn. **8**, 457.
Angapova, L.E., and U.V. Serebrennikov, 1973a, Russ. J. Inorg. Chem. **18**, 901.
Angapova, L.E., and V.V. Serebrennikov, 1973b, Tr. Tomsk. Gos. Univ. **237**, 198.
Anoshina, N.P., T.S. Buchenkova, L.N. Komissarova and V.M. Shatskii, 1970, Zh. Neorg. Khim. **15**, 1747 [Russ. J. Inorg. Chem. **15**, 897].
Anoshina, W.P., V.M. Schatskii and L.N. Komissarova, 1969, Izv. Sib. Otd. Akad. Nauk SSSR, Ser. Khim. Nauk **5**, 58.
Anthony, J.W., 1957, Am. Mineral. **42**, 904.
Apinitis, S.K., and V.I. Sedmalis, 1978, Izv. Akad. Nauk Latv. SSR **3**, 373.
Arbit, E.A., and V.V. Serebrennikov, 1965, Russ. J. Inorg. Chem. **10**, 410.
Arbit, E.A., and V.V. Serebrennikov, 1968a, Inorg. Mater. **4**, 2137.
Arbit, E.A., and V.V. Serebrennikov, 1968b, Tr. Tomsk. Gos. Univ. **192**, 164.
Armbruster, A., 1976, J. Phys. Chem. Solids **37**, 321.
Ashikhnina, T.Ya., A.S. Karnaukhov and N.N. Runov, 1977, Russ. J. Inorg. Chem. **22**, 735.
Ashurst, K.G., and R.D. Hancock, 1977, J. Chem. Soc., Dalton Trans., p. 1701.
Aslanov, L.A., and I.S.A. Farag, 1974, Zh. Neorg. Khim. **19**, 1968 [Russ. J. Inorg. Chem. **19**, 1078].
Aslanov, L.A., V.B. Rybakov, V.M. Ionov, M.A. Porai-Koshits and V.I. Ivanov, 1972, Dokl. Akad. Nauk SSSR **204**, 1122 [Dokl. Chem. **204**, 508].
Aslanov, L.A., I.S.A. Farag and M.A. Porai-Koshits, 1973a, Zh. Fiz. Khim. **47**, 1057 [Russ. J. Phys. Chem. **47**, 602].
Aslanov, L.A., I.S. Ahmed Farag, V.M. Ionov and M.A. Porai-Koshits, 1973b, Zh. Fiz. Khim. **47**, 2172 [Russ. J. Phys. Chem. **47**, 1233].
Aslanov, L.A., V.M. Ionov, M.A. Porai-Koshits, V.G. Lebedev, B.N. Kulikovskii, O.V. Gilyarov and T.L. Novoderezhkina, 1975, Inorg. Mater. **11**, 117.
Asprey, L.B., F.H. Ellinger and E. Staritzky, 1964, Proc. 3rd Rare Earth Research Conf., p. 11 [see: Gmelin Handbuch der Anorganischen Chemie, 8th Ed., Sc, Y, La–Lu, Vol. 39 C8 (Springer, Berlin, 1981) p. 155].
Awazu, K., and K. Matsunaya, 1974, Jpn Kokai 74 91 084.
Awazu, K., and K. Muto, 1969, J. Electrochem. Soc. **116**, 282.
Azarova, L.A., E.E. Vinogradov, E.M. Mihailova and V.I. Pakhomov, 1972, Dokl. Akad. Nauk SSSR **206**, 613.
Bagdasarov, K.S., E.I. Getman, N.I. Mikhailichenko, I.V. Mokhosoeva, M.V. Mokhosoev and V.I. Popov, 1969, Inorg. Mater. **5**, 1339.
Bagieu, M., I. Tordjman, A. Durif and G. Bassi, 1973, Cryst. Struct. Commun. **2**, 387.
Bagieu-Beucher, M., 1976, J. Appl. Crystallogr. **9**, 368.
Bagieu-Beucher, M., and J.C. Guitel, 1978, Acta Crystallogr. B **34**, 1439.
Bagieu-Beucher, M., and D. Tranqui, 1970, Bull. Soc. Fr. Mineral. & Crystallogr. **93**, 505.
Bagieu-Beucher, M., I. Tordjman and A. Durif, 1971, Rev. Chim. Mineral. **8**, 753.
Baglio, J.H., and G. Gashurov, 1968, Acta Crystallogr. B **24**, 292.
Bagnall, K.W., 1973, Proc. 10th Rare Earth Research Conf. (Springfield, VA) p. 856.
Bahl, R.K., and S. Singh, 1939, J. Indian Chem. Soc. **16**, 376.
Bailey, W.E., R.J. Williams and W.O. Milligan, 1973, Acta Crystallogr. B **29**, 1365.
Ballestracci, R., and J. Mareschal, 1967, Mater. Res. Bull. **2**, 993.
Bamberger, C.E., P.R. Robinson and R.L. Sherman, 1979, Inorg. Chim. Acta **34**, L203.
Bancroft, G.H., and H.D. Gesser, 1965, J. Inorg. Nucl. Chem. **27**, 1545.
Barbieri-Melardi, E., 1954, Ann. Chim. **44**, 20.
Barclay, A., 1980, Cryogenics **20**, 467.
Barnes, J.C., 1978, in: Rare Earths in Modern Science and Technology, eds G.J. McCarthy and J.J. Rhyne (Plenum, New York) p. 291.
Barnes, J.C., and G.Y.R. Nicoll, 1985, Inorg. Chim. Acta **110**, 47.
Bartl, H., 1976, Neues Jahrb. Mineral. Monatsh., p. 437.
Bashilova, N.I., and N.I. Nelyapina, 1975, Zh. Neorg. Khim. **20**, 1440 [Russ. J. Inorg. Chem. **20**, 810].
Bashilova, N.I., and N.I. Nelyapina, 1976, Zh. Neorg. Khim. **21**, 2877 [Russ. J. Inorg. Chem. **21**, 1589].
Bashilova, N.I., and N.I. Nelyapina, 1978, Zh. Neorg. Khim. **23**, 1939 [Russ. J. Inorg. Chem. **23**, 1066].

Bashilova, N.I., and N.I. Nelyapina, 1979a, Zh. Neorg. Khim. **24**, 240 [Russ. J. Inorg. Chem. **24**, 133].
Bashilova, N.I., and N.I. Nelyapina, 1979b, Zh. Neorg. Khim. **24**, 1129 [Russ. J. Inorg. Chem. **24**, 629].
Bashilova, N.I., I.V. Tananaev and E.S. Takhanova, 1971, Zh. Neorg. Khim. **16**, 2566 [J. Inorg. Chem. **16**, 1368].
Bashkov, B.I., L.N. Komissarova, F.M. Spiridonov and V.M. Shatskii, 1972, Vestn. Mosk. Univ. Khim. **13**, 598.
Battison, J.E., M.J.M. Leask, J.B. Lowry and A. Kasten, 1976, J. Phys. C **9**, 2295.
Bazuev, G.V., V.A. Zhilyaev and G.P. Shveikin, 1975, Russ. J. Inorg. Chem. **20**, 1729.
Beall, G.W., D.F. Mullica, W.O. Milligan, J. Korp and I. Bernal, 1978, Acta Crystallogr. B **34**, 1446.
Beall, G.W., L.A. Boatner, D.F. Mullica and W.O. Milligan, 1981, J. Inorg. Nucl. Chem. **43**, 101.
Becher, G., H. Semelson and R. Riley, 1968, J. Chem. Phys. **49**, 3303.
Becher, W., H. Kalbfleisch and G. Mueller-Vogt, 1972, Phys. Status Solidi b **52**, K81.
Begun, G.M., G.W. Beall, L.A. Boatner and W.J. Gregor, 1981, J. Raman Spectrosc. **11**, 273.
Belkova, M.M., and L.A. Alekseenko, 1965, Russ. J. Inorg. Chem. **10**, 1374.
Belkova, M.M., L.A. Alekseenko and V.V. Serebrennikov, 1965, Tr. Tomsk. Gos. Univ. Ser. Khim. **185**, 146.
Bellomo, A., D. de Marco and A. Casale, 1973, Talanta **20**, 355.
Belokoneva, E.L., B.V. Mill, M.A. Simonov and N.V. Belov, 1974, Kristallografiya **19**, 374.
Belokoskov, V.I., G.V. Trofimov and V.P. Skovorodskaya, 1975a, Zh. Neorg. Khim. **20**, 248 [Russ. J. Inorg. Chem. **20**, 1378].
Belokoskov, V.I., V.P. Skovorodskaya, G.V. Trofimov and T.P. Spasibenko, 1975b, Zh. Neorg. Khim. **20**, 2828 [Russ. J. Inorg. Chem. **20**, 1565].
Belokoskov, V.I., O.A. Govurukhina, G.V. Trofimov, R.A. Popova and M.A. Letetskaya, 1979, Zh. Neorg. Khim. **24**, 1334 [Russ. J. Inorg. Chem. **24**, 745].
Belousova, A.P., I.V. Shakno and V.E. Plyushchev, 1968, Zh. Neorg. Khim. **13**, 1948 [Russ. J. Inorg. Chem. **13**, 1037].
Belousova, A.P., I.V. Shakno and V.E. Plyushchev, 1970, Zh. Neorg. Khim. **15**, 226 [Russ. J. Inorg. Chem. **15**, 116].
Ben Amara, M., C. Parent, M. Vlasse, G. Le Flem, E. Antic-Fidancev, B. Piriou and P. Caro, 1983, J. Less-Common Met. **93**, 425.
Benedicks, C., 1900, Z. Anorg. Chem. **22**, 393.
Berjoan, R., G. Benezech, J.-P. Coutures and M. Foex, 1975, C.R. Hebd. Séances Acad. Sci., Ser. C **280**, 601.
Berthier, P., 1843, Ann. Chim. Phys. **7**, 74 [see: J.W. Mellor, A Comprehensive Treatise on Inorganic and Theoretical Chemistry, Vol. 10 (Longmans, Green and Co., London, 1965) ch. 58, p. 820–892].
Berzelius, J.J., 1818, Acad. Handl. Stockholm **39**, 13 [see: J.W. Mellor, A Comprehensive Treatise on Inorganic and Theoretical Chemistry, Vol. 10 (Longmans, Green and Co., London, 1965) ch. 58, p. 820–892].
Beucher, M., 1970, Les Eléments des Terres Rares, Coll. No. 180, Vol. 1 (C.N.R.S., Paris) p. 331.
Biltz, W., 1911, Z. Anorg. Chem. **71**, 430.
Bimberg, H., and D.J. Robbins, 1975, Ger. Offen. 2 607 888.
Birke, P., and G. Kempe, 1973a, Z. Chem. **13**, 65.
Birke, P., and G. Kempe, 1973b, Z. Chem. **13**, 110.
Birke, P., and G. Kempe, 1973c, Z. Chem. **13**, 151.
Birnbaum, E.R., and S. Stratton, 1973, Inorg. Chem. **12**, 379.
Blanzat, B., J.P. Denis, C. Pannel and C. Barthou, 1977, Mater. Res. Bull. **12**, 455.
Blasse, G., and G.J. Dirksen, 1982, Phys. Status Solidi b **110a**, 487.
Bleaney, B., J.F. Gregg, M.J.M. Leask and M.R. Wells, 1983, J. Magn. Magn. Mater. 31–34, 1061.
Bleaney, B., J.F. Gregg, M.J.M. Leask and M.R. Wells, 1984, Proc. R. Soc. London **394**, 69.
Bochu, P., C. Parent, A. Daoudi, G. Le Flem and P. Hagenmueller, 1981, Mater. Res. Bull. **16**, 883.
Bondar, S.A., V.I. Belokoskov and G.V. Trofimov, 1982a, Zh. Neorg. Khim. **27**, 783 [Russ. J. Inorg. Chem. **27**, 439].
Bondar, S.A., G.V. Trofimov, R.A. Popova and L.S. Korobeinikov, 1982b, Izv. Akad. Nauk SSSR Neorg. Mater. **18**, 1209 [Inorg. Mater. **18**, 1019].
Bonnet, M.C., and R.A. Paris, 1975a, Bull. Soc. Chim. Fr., p. 1062.
Bonnet, M.C., and R.A. Paris, 1975b, Bull. Soc. Chim. Fr., p. 1067.
Bosch-Reig, F., F. Burnel-Marti and S. Vicente-Perez, 1970, Inform. Quim. Anal. **24**, 138.
Botto, I.L., and E.J. Baran, 1982, J. Less-Common Met. **83**, 255.
Bourcet, J.C., J. Grafemeyer, J. Janin and F. Gaume-Mahn, 1971, Proc. 9th Rare Earth Research Conf. (Blacksburg, VI) p. 441.
Bourcet, J.C., F.C. Fong, M. Guidon and J. Janin, 1974, Proc. 11th Rare Earth Research Conf. (Traverse City, MI) p. 777.
Brady, G.W., 1960, J. Chem. Phys. **33**, 1079.
Brauer, G., 1980, Handbuch der Präparativen Anorganischen Chemie I–III (F. Enke, Stuttgart).

Brewer, R.M., and M. Nicol, 1981, J. Lumin. **23**, 269.
Bril, A., and W.L. Wanmaker, 1964, J. Electrochem. Soc. **111**, 1363.
Brittain, H.G., 1983, J. Less-Common Met. **93**, 97.
Brixner, L.H., and P.A. Fluoreney, 1965, J. Electrochem. Soc. **112**, 303.
Broach, R.W., J.M. Williams, G.P. Felcher and D.G. Hinks, 1979, Acta Crystallogr. B **35**, 2317.
Brusset, H., F. Madaule-Aubry, B. Blanche, J.P. Glaziou and J.P. Laude, 1971a, Can. J. Chem. **49**, 3700.
Brusset, H., F. Madaule-Aubry, R. Mahe and C. Boursier, 1971b, C.R. Hebd. Séances Acad. Sci., Ser. C **273**, 455.
Brusset, H., R. Mahe and A. Deboichet, 1972, C.R. Hebd. Séances Acad. Sci., Ser. C **274**, 1293.
Brusset, H., R. Mahe and J.P. Laude, 1973, Bull. Soc. Chim. Fr., p. 495.
Buisson, G., F. Bertaut and J. Marschal, 1964, Compt. Rend. **259**, 411.
Buisson, G., F. Tcheou, F. Sayetat and K. Scheunemann, 1976, Solid State Commun. **18**, 871.
Bukovec, N., 1985, Thermochim. Acta **88**, 391.
Bukovec, N., and P. Bukovec, 1985, J. Therm. Anal. **30**, 491.
Bukovec, N., P. Bukovec and J. Šiftar, 1975, Vestn. Slov. Kem. Drus. **22**, 5.
Bukovec, N., P. Bukovec, L. Golič and J. Šiftar, 1977, Monatsh. Chem. **108**, 997.
Bukovec, N., L. Golič, P. Bukovec and J. Šiftar, 1978, Monatsh. Chem. **109**, 1305.
Bukovec, N., P. Bukovec and J. Šiftar, 1979a, Vestn. Slov. Kem. Drus. **26**, 103.
Bukovec, N., L. Golič and J. Šiftar, 1979b, Vestn. Slov. Kem. Drus. **26**, 377.
Bukovec, N., P. Bukovec and J. Šiftar, 1980a, Thermochim. Acta **35**, 85.
Bukovec, N., P. Bukovec and J. Šiftar, 1980b, Thermochim. Acta **36**, 217.
Bukovec, N., V. Kaučič and L. Golič, 1980c, Acta Crystallogr. B **36**, 129.
Bukovec, N., P. Bukovec and J. Šiftar, 1980d, Monatsh. Chem. **111**, 957.
Bukovec, P., and L. Golič, 1975, Vestn. Slov. Kem. Drus. **22**, 19.
Bukowska-Strzyzewska, M., and A. Tosik, 1982a, Acta Crystallogr. B **38**, 265.
Bukowska-Strzyzewska, M., and A. Tosik, 1982b, Acta Crystallogr. B **38**, 950.
Bullock, J.I., M.F.C. Ladd, D.C. Povey and A.E. Storey, 1980, Inorg. Chim. Acta **43**, 101.
Bünzli, J.-C.G., and J.R. Yersin, 1979, Inorg. Chem. **18**, 605.
Bünzli, J.-C.G., and J.R. Yersin, 1982, Inorg. Chem. **21**, 1471.
Bünzli, J.-C.G., D. Wessner and T.T.O. Huynh, 1979, Inorg. Chim. Acta **32**, L33.
Burgess, J., 1978, Metal Ions in Solution (Wiley, New York).
Burkov, K.A., E.A. Busko and I.V. Pichugina, 1982, Zh. Neorg. Khim. **27**, 643 [Russ. J. Inorg. Chem. **27**, 362].
Burns, J.A., and R.D. Baybarz, 1972, Inorg. Chem. **11**, 2233.
Burrus, H.L., and A.G. Paulusz, 1969, GEC J. Sci. Technol. **36**, 105.
Butuzova, T.A., P.P. Melnikov and L.N. Komissarova, 1982, Inorg. Mater. **18**, 592.
Byrappa, K., 1982, J. Mater. Sci. Lett. **1**, 232.
Byrappa, K., and G.I. Dorokhova, 1981, J. Mater. Sci. **16**, 3244.
Callow, R.S., 1967, The Industrial Chemistry of the Lanthanoids, Yttrium, Thorium and Uranium (Pergamon Press, Oxford) p. 63.
Caminiti, R., G. Licheri, G. Piccaluga, G. Pinna and M. Magini, 1979, Rev. Inorg. Chem. **1**, 333.
Caminiti, R., P. Lucca and H. D'Andrea, 1983, Z. Naturforsch. A **38**, 533.
Campbell, D.A., Z.M. Zochowski and P.A.H. Wyatt, 1983, Thermochim. Acta **67**, 73.
Canneri, G., and L. Fernandes, 1925, Gazz. Chim. Ital. **55**, 440.
Carnall, W.T., 1979, in: Handbook on the Chemistry and Physics of Rare Earths, Vol. 3, eds K.A. Gschneidner Jr. and L. Eyring (North-Holland, Amsterdam) ch. 24, pp. 171–208.
Caro, P., 1968, J. Less-Common Met. **16**, 367.
Carron, M.K., M.E. Mrose and K.J. Murata, 1958, Am. Mineral. **43**, 985.
Castellani Bisi, C., and A. Clerici, 1963, Gazz. Chim. Ital. **93**, 1444.
Castellani Bisi, C., and M. Cola, 1962, Gazz. Chim. Ital. **92**, 447.
Catton, G.A., M.E. Harman, F.A. Hart, G.E. Hawkes and G.P. Moss, 1978, J. Chem. Soc., Dalton Trans., p. 181.
Chernova, N.A., L.N. Komissarova, G.Ya. Pushkina and N.P. Khrameeva, 1974, Russ. J. Inorg. Chem. **19**, 1488.
Chincholkar, V.S., 1972, J. Inorg. Nucl. Chem. **34**, 2973.
Chinn, S.R., and H.Y.-P. Hong, 1975, Appl. Phys. Lett. **26**, 649.
Chinn, S.R., and H.Y.-P. Hong, 1976, Opt. Commun. **18**, 87.
Chizhov, S.M., A.N. Pokrovskii and L.M. Kovba, 1980, J. Less-Common Met. **75**, 105.
Chizhov, S.M., A.N. Pokrovskii and L.M. Kovba, 1981, Kristallografiya **26**, 834 [Sov. Phys. Crystallogr. **26**, 471].
Chizhov, S.M., A.N. Pokrovskii and L.M. Kovba, 1982, Kristallografiya **27**, 997 [Sov. Phys. Crystallogr. **27**, 598].
Chloupek, J.B., V.S. Danes and B.H. Danerova, 1932, Coll. Czech. Chem. Commun. **4**, 473.
Choppin, G.R., 1980, Am. Chem. Soc. Symp. Ser. **131**, 173.
Choppin, G.R., 1984, J. Less-Common Met. **100**, 141.

Choppin, G.R., and S.L. Bertha, 1973, J. Inorg. Nucl. Chem. **35**, 1309.
Choudhury, P.C.R., 1941, J. Indian Chem. Soc. **18**, 335.
Chudinova, N.N., 1979, Inorg. Mater. **15**, 654.
Chudinova, N.N., and G.M. Balagina, 1979, Inorg. Mater. **15**, 650.
Chudinova, N.N., and N.V. Vinogradova, 1979, Inorg. Mater **15**, 2171.
Chudinova, N.N., I.U. Tananaev and A.V. Lavrov, 1967, Inorg. Mater. **3**, 1608.
Chudinova, N.N., A.V. Lavrov and I.U. Tananaev, 1972, Inorg. Mater **8**, 1971.
Chudinova, N.N., L.P. Shklover and G.M. Balagina, 1975, Inorg. Mater. **11**, 686.
Chudinova, N.N., G.M. Balagina and L.P. Shklover, 1977a, Inorg. Mater. **13**, 2075.
Chudinova, N.N., M.A. Avaliani and L.S. Guzeeva, 1977b, Inorg. Mater **13**, 2229.
Chudinova, N.N., N.V. Vinogradova, G.M. Balagina and K.K. Palkina, 1977c, Inorg. Mater. **13**, 1494.
Chudinova, N.N., L.P. Shklover, A.E. Balanevskaya, L.M. Shkolnikova, A.E. Obodovskaya and G.M. Balagina, 1978a, Inorg. Mater. **14**, 727.
Chudinova, N.N., L.P. Shklover, L.I. Shkolnikova, A.E. Balanevskaya and G.M. Balagina, 1978b, Inorg. Mater. **14**, 1324.
Chudinova, N.N., L.V. Kubasova and E.V. Oreshnikova, 1978c, Koord. Khim. **4**, 550.
Chudinova, N.N., N.V. Vinogradova and K.K. Palkina, 1978d, Inorg. Mater. **14**, 1595.
Ciampolini, M., P. Dapporto and N. Nardi, 1978, J. Chem. Soc., Chem. Comm., p. 788.
Ciampolini, M., N. Nardi, R. Cini, S. Mangahi and P. Orioli, 1979, J. Chem. Soc., Dalton Trans., p. 1983.
Ciampolini, M., C. Mealli and N. Nardi, 1980, J. Chem. Soc., Dalton Trans., p. 376.
Claringsbull, G.F., and M.H. Hey, 1953, Miner. Mag. **30**, 211.
Cleve, P.T., 1874, Bull. Soc. Chim. Fr. **21**, 196, 246.
Cleve, P.T., 1885, Bull. Soc. Chim. Fr. **43**, 162.
Cocke, D.L., K.A. Gingerich and J. Kordis, 1973, J. Chem. Soc., Chem. Comm., p. 561.
Coda, A., G. Giuseppetti and C. Tadini, 1965, Denodico Mineral **34**, 27.
Colak, S., and W.K. Zwicker, 1983, J. Appl. Phys. **54**, 2156.
Colquhoun, I., N.N. Greenwood, I.J. McColm and G.E. Turner, 1972, J. Chem. Soc., Dalton Trans., p. 1337.
Cooke, A.H., S.J. Swithenby and M.R. Wells, 1973, J. Phys. C **6**, 2209.
Cooley, R.A., and D.M. Yost, 1946, Inorg. Synth. **2**, 69.
Cooley, R.A., D.M. Yost and H.W. Stone, 1946, Inorg. Synth. **2**, 69.
Couchot, P., F. Nguyen Minh Hoang and R. Perret, 1971, Bull. Soc. Chim. Fr., p. 360.
Cromer, D.T., and A.C. Larson, 1956, Acta Crystallogr. **9**, 1015.
Cucinotta, V., S. Gurrieri, S. Musumeci and S. Sammartano, 1976, Thermochim. Acta **17**, 375.
Cuttica, V., 1923, Gazz. Chim. Ital. **53**, 769.
Dago, A.M., D.Yu. Puscharovskii, E.A. Pobedimskaya and N.V. Belov, 1980, Dokl. Akad. Nauk SSSR **251**, 1392.
D'Ambrogio, F., P. Bruesch and H. Kalbfleisch, 1971, Proc. 2nd. Int. Conf. on Light Scattering in Solids, p. 363.
Damen, T.C., H.P. Weber and B.C. Tofield, 1973, Appl. Phys. Lett. **23**, 519.
Danielmeyer, H.G., G. Huber, W.W. Kruhler and J.P. Jeser, 1973, Appl. Phys. **2**, 335.
Darrie, R.G., and W.P. Doyle, 1968, in: Reactivity of Solids, Proc. 6th Int. Symp. on the Reactivity of Solids, eds J.W. Mitchell, R.C. DeVries, R.W. Roberts and P. Cannon (Wiley–Interscience, New York) p. 281.
Darrie, R.G., W.P. Doyle and I. Kirkpatrick, 1967, J. Inorg. Nucl. Chem. **29**, 979.
Datta, R.K., 1967a, Trans. Metall. Soc. AIME **239**, 355.
Datta, R.K., 1967b, J. Electrochem. Soc. **114**, 1057.
Davidenko, N.K., L.N. Lugina and K.B. Yatsimirskii, 1972, Russ. J. Inorg. Chem. **17**, 54.
Davies, C.W., and J.C. James, 1948, Proc. R. Soc. London, Ser. A **195**, 116.
de Camargo, W.G.R., and J.V. Valarelli, 1963, Acta Crystallogr. **16**, 321.
de Carvalho, R.G., and G.R. Choppin, 1967, J. Inorg. Nucl. Chem. **29**, 737.
de Saja, A., J.M. Pastor, F. Rull and J.A. de Saja, 1977, Krist. Techn. **12**, 9.
de Saja, A., J.M. Pastor, F. Rull and J.A. de Saja, 1978, Krist. Techn. **13**, 909.
de Saja, A., J.M. Pastor, E. Hernandez, F. Rull and J.A. de Saja, 1981, Cryst. Res. Techn. **16**, 1389.
Degtyarev, P.A., and A.N. Pokrovskii, 1984, Zh. Neorg. Khim. **29**, 2136 [Russ. J. Inorg. Chem. **29**, 1219].
Degtyarev, P.A., A.N. Pokrovskii, L.M. Kovba and F.M. Korytnaya, 1977a, J. Solid State Chem. **22**, 419.
Degtyarev, P.A., F.M. Korytnaya, A.N. Pokrovskii and L.M. Kovba, 1977b, Vestn. Mosk. Univ. Ser. 2: Khim., p. 705 [Chem. Abstr. **89**, 34513x].
Degtyarev, P.A., A.N. Pokrovskii and L.M. Kovba, 1978a, Kristallografiya **23**, 840 [Sov. Phys. Crystallogr. **23**, 473].
Degtyarev, P.A., F.M. Korytnaya, A.N. Pokrovskii and L.M. Kovba, 1978b, Kristallografiya **23**, 1036 [Sov. Phys. Crystallogr. **23**, 586].
Degtyarev, P.A., A.N. Pokrovskii and L.M. Kovba, 1978c, Ann. Chim. (France) **3**, 187.
Degtyarev, P.A., A.N. Pokrovskii and L.M. Kovba, 1979, J. Less-Common Met. **68**, 107.
Degtyarev, P.A., A.N. Pokrovskii and L.M. Kovba, 1980a, Zh. Neorg. Khim. **25**, 2113 [Russ. J. Inorg. Chem. **25**, 1170].

Degtyarev, P.A., A.N. Pokrovskii and L.M. Kovba, 1980b, J. Inorg. Nucl. Chem. **42**, 1198.
Dellien, I., F.M. Hall and L.G. Hepler, 1976, Chem. Rev. **76**, 283.
Delmas, C., R. Olazcuaga, G. Le Flem, P. Hagenmueller, F. Cherkaoui and R. Brochu, 1981, Mater. Res. Bull. **16**, 285.
Denis, J.P., and J. Loriers, 1970, Ger. Offen. 1948066.
Dereigne, A., and G. Pannetier, 1968, Bull. Soc. Chim Fr., p. 174.
Dereigne, A., J.-M. Manoli, G. Pannetier and P. Herpin, 1972, Bull. Soc. Fr. Mineral. & Cristallogr. **95**, 269.
Domanskii, A.I., Yu.F. Shepelev, Yu.I. Smolin and B.N. Litvin, 1982, Kristallografiya **27**, 229.
Doyle, W.P., and G. Gibb, 1976, J. Inorg. Nucl. Chem. **38**, 487.
Doyle, W.P., and I.J. Pryde, 1976, J. Inorg. Nucl. Chem. **38**, 733.
D'Silva, A.P., and V.A. Fassel, 1974, J. Lumin. **8**, 375.
Duboin, M.A., 1888, C.R. Hebd. Séances Acad. Sci. **107**, 622.
Dunsmore, H.S., T.R. Kelly and G.H. Nancollas, 1963, Trans Faraday Soc. **59**, 2606.
Durif, A., 1956, Acta Crystallogr. **9**, 471.
Durif, A., 1971, Bull. Soc. Fr. Mineral. & Crystallogr. **94**, 314.
Durif, A., and F. Forrat, 1957, C.R. Hebd. Séances Acad. Sci. **245**, 1636.
Duveau, N., 1943, Bull. Soc. Chim. Fr. **10**, 374.
Efremov, V.A., and V.B. Kalinin, 1978, Kristallografiya **23**, 703.
Efremov, V.A., and V.K. Trunov, 1974, Kristallografiya **19**, 989.
Efremov, V.A., P.P. Melnikov and L.N. Komissarova, 1981, Koord. Khim. **7**, 467.
Egan, J.E., and C.W. Balke, 1913, J. Am. Chem. Soc. **35**, 365.
Ehnholm, G.J., T.E. Katila, O.V. Lounasmaa, P. Reivari, G.M. Kalvius and G.K. Shenoy, 1970, Z. Phys. **235**, 289.
Elliott, R.J., R.T. Harvey, W. Haynes and S.R.P. Smith, 1972, Proc. R. Soc. Ser. A **328**, 217.
Engel, G., 1972, Z. Anorg. Allg. Chem. **387**, 22.
Engel, G., and W. Kirchberger, 1975, Z. Anorg. Allg. Chem. **417**, 81.
Ephraim, F., and P. Ray, 1929, Ber. Dtsch. Chem. Ges. **62**, 1509.
Erämetsä, O., and M. Haukka, 1966, Suom. Kemistil. B **39**, 242.
Erämetsä, O., and M. Haukka, 1968, Suom. Kemistil. B **41**, 207.
Erämetsä, O., and L. Niinistö, 1971, Suom. Kemistil. B **44**, 107.
Erämetsä, O., L. Niinistö and T. Korvela, 1972, Suom. Kemistil. B **45**, 394.
Erämetsä, O., T. Pakkanen and L. Niinistö, 1973, Suom. Kemistil. B **46**, 330.
Eriksson, B., L.O. Larsson, L. Niinistö and U. Skoglund, 1974, Inorg. Chem. **13**, 290.
Ermolaev, M.I., and L.T. Kudrina, 1970, Zh. Neorg. Khim. **15**, 1436 [Russ. J. Inorg. Chem. **15**, 737].
Escobar, M.E., and E.J. Baran, 1977, Z. Anorg. Allg. Chem. **441**, 273.
Escobar, M.E., and E.J. Baran, 1978, Z. Chem. **18**, 418.
Escobar, M.E., and E.J. Baran, 1980, Z. Naturforsch. a **35**, 1110.
Escobar, M.E., and E.J. Baran, 1982a, Z. Anorg. Allg. Chem. **489**, 139.
Escobar, M.E., and E.J. Baran, 1982b, Monatsh. Chem. **113**, 43.
Eshchenko, L.S., V.V. Pechovskii and R.N. Dvoskina, 1979, Russ. J. Inorg. Chem. **24**, 1790.
Espil, R.L., 1911, Compt. Rend. **152**, 378.
Et-Tabirou, M., and A. Daoudi, 1980, C.R. Hebd. Séances Acad. Sci., Ser. C **291**, 93.
Evans, D.F., and P.H. Missen, 1982, J. Chem. Soc., Dalton Trans., p. 1929.
Ezhova, Z.A., I.V. Tananaev and E.M. Koval, 1978a, Russ. J. Inorg. Chem. **23**, 1657.
Ezhova, Z.A., I.V. Tananaev, L.N. Zorina, E.M. Koval and N.P. Soshcin, 1978b, Inorg. Mater. **14**, 1610.
Ezhova, Z.A., I.V. Tananaev and E.M. Koval, 1983, Russ. J. Inorg. Chem. **28**, 1594.
Faber, J., and A.T. Aldred, 1982, AIP Conf. Proc. **89**, 72.
Fahey, J.A., 1976, Proc. 12th Rare Earth Research Conf. (Vail, CO), p. 762.
Fahey, J.A., G.J.B. Williams and J.M. Haschke, 1979, Report BNL-26129 Conf.-790641-6 [see: Gmelin Handbuch der Anorganischen Chemie, 8th Ed., Sc, Y, La–Lu, Vol. 39 C8 (Springer, Berlin, 1981) p. 12].
Faria, S., and D. Palumbo, 1971, U.S. Patent 3555337.
Fava, J., G. Le Flem, R. Salmon and C. Parent, 1978, Ger. Offen. 2820889.
Favas, M.C., and D.L. Kepert, 1981, Prog. Inorg. Chem. **28**, 309.
Feigelson, R.S., 1964, J. Am. Ceram. Soc. **47**, 257.
Ferid, M., K.N. Ariguip and M. Trabelsi, 1981, J. Solid State Chem. **38**, 130.
Ferid, M., M. Dogguy, N. Kbir-Ariguip and M. Trabelsi, 1984a, J. Solid State Chem. **53**, 149.
Ferid, M., N. Kbir-Ariguip and M. Trabelsi, 1984b, Thermochim. Acta **81**, 175.
Ferraro, J.R., 1971, Low Frequency Vibrations of Inorganic and Coordination Compounds (Plenum, New York).
Fichter, F., and E. Jenny, 1923, Helv. Chem. Acta **6**, 326.
Finney, J.J., and N.N. Rao, 1967, Am. Mineral. **52**, 13.

Firsching, F.H., and T.R. Paul, 1966, J. Inorg. Nucl. Chem. **28**, 2414.
Fitzwater, D.R., and R.E. Rundle, 1952, U.S.A.E.C. Report ISC-241 [see: R.W.G. Wyckoff, Crystal Structures, Vol. III (Interscience, New York, 1963) p. 850].
Fitzwater, D.R., and R.E. Rundle, 1959, Z. Kristallogr. **112**, 362.
Forsyth, J.B., and C.F. Sampson, 1971, Phys. Lett. A **36**, 223.
Foster, R.J., R.L. Bodner and D.G. Hendricker, 1972, J. Inorg. Nucl. Chem. **34**, 3795.
Frerichs, F., and F. Smith, 1874, Liebigs. Ann. Chem. **191**, 331.
Fuess, H., and A. Kallel, 1972, J. Solid State Chem. **5**, 11.
Fukuzawa, T., T. Suzuki and S. Sato, 1977, U.S. Patent 4 041 319.
Gabe, K., and V.S. Chincholkar, 1979, J. Chem. Soc., Dalton Trans. **12**, 1959.
Gallagher, P.K., 1968, Mater. Res. Bull. **3**, 225.
Gallagher, P.K., and B. Prescott, 1970, Inorg. Chem. **9**, 2510.
Gallagher, P.K., and F. Schrey, 1969, Thermal Analysis, Vol. 2, eds R.F. Shwenker and P.D. Garn (Academic Press, New York) p. 929.
Gallucci, J.C., R.E. Gerkin and W.J. Reppart, 1982, Cryst. Struct. Comm. **11**, 1141.
Gambino, J.R., and C.J. Guare, 1963, Nature **198**, 1084.
Garton, G., S.H. Smith and B.M. Wanklyn, 1972, J. Cryst. Growth **13–14**, 588.
Gatehouse, B.M., and A. Pring, 1981, J. Solid State Chem. **38**, 116.
Gauthier, M., and C.W. Bale, 1983, Metall. Trans. B **14**, 117.
Gebert Sherry, E., 1976, J. Solid State Chem. **19**, 271.
Geller, S., 1957, Acta Crystallogr. **10**, 243.
General Electric Co., 1968, British patent 1 137 576.
Gerkin, R.E., and W.J. Repport, 1984, Acta Crystallogr. C **40**, 781.
Ghouse, K.M., 1968, Ind. J. Pure Appl. Phys. **6**, 265.
Gibbs, G.V., G. Chiari, S.J. Louisnathan and D.W.S. Cruickshank, 1976, Z. Kristallogr. **143**, 166.
Giesbrecht, E., 1960, J. Inorg. Nucl. Chem. **15**, 265.
Giesbrecht, E., and L.F. Audrieth, 1958, J. Inorg. Nucl. Chem. **6**, 308.
Giesbrecht, E., and I. Giolito, 1967, An. Acad. Bras. Cienc. **39**, 233.
Giesbrecht, E., and E.B. Melardi, 1963, An. Acad. Bras. Cienc. **34**, 527.
Giesbrecht, E., and M. Perrier, 1960, An. Asoc. Bras. Quim. **19**, 121.
Giesbrecht, E., M. Perrier and W.W. Wendtlandt, 1962, An. Acad. Bras. Cienc. **34**, 37.
Giesbrecht, E., G. Vicentini and L. Barbieri, 1968, An. Acad. Bras. Cienc. **40**, 453.
Giolito, I., and E. Giesbrecht, 1969, An. Acad. Bras. Cienc. **41**, 517.
Giolito, I., and M. Ionashiro, 1981a, Thermochim. Acta **46**, 77.
Giolito, I., and M. Ionashiro, 1981b, Thermochim. Acta **46**, 83.
Glaser, J., and G. Johansson, 1981, Acta Chem. Scand. A **35**, 639.
Glazyrin, M.P., and N.I. Borisenko, 1972, Inorg. Mater. **8**, 1651.
Gmelin Handbook of Inorganic Chemistry, 1983, 8th Ed., Sc, Y, La–Lu, Vol. 39 C7 (Springer, Berlin).
Gmelin Handbook of Inorganic Chemistry, 1984, 8th Ed., Sc, Y, La–Lu, Vol. 39 A7 (Springer, Berlin).
Gmelin Handbuch der Anorganischen Chemie, 1976, 8th Ed., Sc, Y, La–Lu, Vol. 39 C3 (Springer, Berlin).
Gmelin Handbuch der Anorganischen Chemie, 1977, 8th Ed., Sc, Y, La–Lu, Vol. 39 C6 (Springer, Berlin).
Gmelin Handbuch der Anorganischen Chemie, 1978, 8th Ed., Sc, Y, La–Lu, Vol. 39 C7 (Springer, Berlin).
Gmelin Handbuch der Anorganischen Chemie, 1981a, 8th Ed., Sc, Y, La–Lu, Vol. 39 C8 (Springer, Berlin) p. 14–33.
Gmelin Handbuch der Anorganischen Chemie, 1981b, 8th Ed., Sc, Y, La–Lu, Vol. 39 C8 (Springer, Berlin) pp. 33–348.
Gmelin–Kraut's Handbuch der Anorganischen Chemie, 1928–1932, Band VI, Abt. 1–2 (Carl Winters Universitätsbuchhandlung, Heidelberg).
Göbel, H., and G. Will, 1971, J. Phys. C **4**, 811.
Göbel, H., and G. Will, 1972a, Phys. Lett. A **39**, 79.
Göbel, H., and G. Will, 1972b, Int. J. Magn. **3**, 123.
Göbel, H., and G. Will, 1972c, Phys. Status Solidi b **50**, 147.
Golovin, Yu.M., V.V. Kravchenko, K.I. Petrov and T.I. Kuzina, 1972, Zh. Neorg. Khim. **17**, 3219 [Russ. J. Inorg. Chem. **17**, 1693].
Golub, A.M., and S.A. Nedilko, 1973, Russ. J. Inorg. Chem. **18**, 749.
Goyorukhina, O.A., R.A. Popova, S.D. Nikitina, M.A. Letetskaya and V.I. Belokoskov, 1984, Zh. Neorg. Khim. **29**, 1430 [Russ. J. Inorg. Chem. **29**, 822].
Greedan, J.E., 1971, Phys. Lett. A **36**, 223.
Greedan, J.E., 1979, Mater. Res. Bull. **14**, 13.
Greenwood, N.N., and A. Earnshaw, 1984, Chemistry of the Elements (Pergamon Press, Oxford) pp. 1–1146.
Greenwood, N.N., and T.C. Gibb, 1971, Mössbauer Spectroscopy (Chapman and Hall, London) p. 536.

Grenthe, I., 1978, Kem.-Kemi **5**, 234.
Grisafe, D.A., and F.A. Hummel, 1970, Am. Mineral. **55**, 1131.
Grizik, A.A., and N. Abdullina, 1971, Zh. Neorg. Khim. **16**, 1817 [Russ. J. Inorg. Chem. **16**, 965].
Gubanov, V.A., D.E. Ellis and A.A. Fotiev, 1977, J. Solid State Chem. **21**, 303.
Guido, M., and G. Gigli, 1975a, High Temp. Sci. **7**, 122.
Guido, M., and G. Gigli, 1975b, High Temp. Sci. **7**, 301.
Guillot, M., M. Fadley, H. Le Gall and H. Makram, 1980, Rare Earth Mod. Sci. Technol. **2**, 613.
Gupta, M.K., L. Surendra, S.M. Kaushik and G.V. Jere, 1983, J. Solid State Chem. **43**, 359.
Gushikem, Y., C. Airoldi and O.L. Alves, 1973, J. Inorg. Nucl. Chem. **35**, 1159.
Haapala, I., P. Ervamaa, A. Löfgren and P. Ojanperä, 1969, Bull. Geol. Soc. Finl. **41**, 117.
Habash, F., 1985, J. Chem. Techn. Biotechnol. A **35**, 5.
Habenschuss, A., and F.H. Spedding, 1978, Cryst. Struct. Commun. **7**, 535; also other parts of the series.
Habenschuss, A., and F.H. Spedding, 1979a, J. Chem. Phys. **70**, 2797.
Habenschuss, A., and F.H. Spedding, 1979b, J. Chem. Phys. **70**, 3758.
Habenschuss, A., and F.H. Spedding, 1980, J. Chem. Phys. **73**, 442.
Hagman, L.O., and P. Kierkegaard, 1968, Acta Chem. Scand. **22**, 1822.
Hajek, B., and J. Hradilova, 1971a, Coll. Czech. Chem. Comm. **36**, 3765.
Hajek, B., and J. Hradilova, 1971b, J. Less-Common Met. **23**, 217.
Hajek, B., N. Novotna and J. Hradilova, 1979, J. Less-Common Met. **66**, 121.
Hale, C.F., and F.H. Spedding, 1972, J. Phys. Chem. **76**, 1887.
Harley, R.T., W. Haynes and S.R.P. Smith, 1971, Proc. 2nd Int. Conf. on Light Scattering in Solids, p. 357.
Harley, R.T., W. Haynes and S.R.P. Smith, 1972, J. Phys. C **5**, 1501.
Harmelin, M., 1966, C.R. Hebd. Séances Acad. Sci., Ser. B **262**, 620.
Harris, J.A., 1931, J. Am. Chem. Soc. **53**, 2475.
Harrowfield, J.McB., D.L. Kepert, J.M. Patrick and A.H. White, 1983, Aust. J. Chem. **36**, 483.
Hassen, D.B., N. Kbir-Ariguip and M. Trabelsi, 1984, Thermochim. Acta **79**, 251.
Haynes, J.W., and J.J. Brown Jr, 1968, J. Electrochem. Soc. **115**, 1060.
Hedrick, J.B., 1985, Rare Earth Elements and Yttrium, Preprint from Bulletin 675 (Bureau of Mines, Washington) pp. 1–18.
Heiniö, O., M. Leskelä and L. Niinistö, 1980, Acta Chem. Scand. A **34**, 207.
Hellwege, K.H., 1953, Angew. Chem. **65**, 113.
Hellwege, K.H., and U. Johnsen, 1954, Z. Phys. **139**, 484.
Helmholz, L., 1939, J. Am. Chem. Soc. **61**, 1544.
Hezel, A., and S.D. Ross, 1966, Spectrochim. Acta **22**, 1949.
Hezel, A., and S.D. Ross, 1967, J. Inorg. Nucl. Chem. **29**, 2085.
Hikichi, Y., K. Hukuo and J. Shiokawa, 1978, Bull. Chem. Soc. Jpn **51**, 3645.
Hikichi, Y., K. Hukuo and J. Shiokawa, 1980a, Bull. Chem. Soc. Jpn **53**, 1455.
Hikichi, Y., K. Hukuo and J. Shiokawa, 1980b, Bull. Chem. Soc. Jpn **53**, 1457.
Hillmer, W., 1973, Phys. Status Solidi b **55**, 305.
Hillmer, W., J. Plamper and D. Wappler, 1972, Phys. Status Solidi b **50**, 507.
Hiltunen, L., and L. Niinistö, 1976a, Cryst. Struct. Commun. **5**, 561.
Hiltunen, L., and L. Niinistö, 1976b, Cryst. Struct. Commun. **5**, 567.
Hodges, J.A., P. Imbert and G. Jehanno, 1982, J. Phys. **43**, 1249.
Höfer, H.H., W. Eysel and U. von Alpen, 1978, Mater. Res. Bull. **13**, 265.
Holleck, L., and W. Noddack, 1937, Angew. Chem. **50**, 819.
Hölsä, J., and M. Leskelä, 1985, J. Less-Common Met. **112**, 127.
Hölsä, J., M. Leskelä and L. Niinistö, 1980, Thermochim. Acta **35**, 79.
Hong, H.Y.-P., 1974a, Acta Crystallogr. B **30**, 468.
Hong, H.Y.-P., 1974b, Acta Crystallogr. B **30**, 1857.
Hong, H.Y.-P., 1974c, Mater. Res. Bull. **9**, 129.
Hong, H.Y.-P., 1975a, Mater. Res. Bull. **10**, 635.
Hong, H.Y.-P., 1975b, Mater. Res. Bull. **10**, 1105.
Hong, H.Y.-P., 1979, in: Fast Ion Transport in Solids, Proc. Int. Conf., eds P. Vashista, J.N. Mundy and G.K. Shenoy (North-Holland, Amsterdam) p. 431.
Hong, H.Y.-P., and S.R. Chinn, 1976, Mater. Res. Bull. **11**, 421.
Hong, H.Y.-P., and K. Dwight, 1974, Mater. Res. Bull. **9**, 775.
Hong, H.Y.-P., and J.W. Pierce, 1974, Mater. Res. Bull. **9**, 179.
Horrocks Jr, W. DeW., and M. Albin, 1984, Prog. Inorg. Chem. **31**, 1.
Horvath, I., L.P. Mezentseva and V. Figusch, 1981, Chem. Zvesti **35**, 333.
Hubbard, C.R., C.O. Quicksall and R.A. Jacobson, 1974, Acta Crystallogr. B **30**, 2613.
Huber, W., F. Hulliger and H. Vetsch, 1980, in: Inorganic Synthesis, Vol. 20, ed. D.H. Busch (Wiley, New York) p. 12.
Hudson, R.P., and B.W. Magnum, 1971, Phys. Lett. A **36**, 157.
Hulliger, F., M. Landolt and H. Vetsch, 1976a, J. Solid State Chem. **18**, 283.
Hulliger, F., M. Landolt and H. Vetsch, 1976b, J. Solid State Chem. **18**, 307.

Hunt Jr, E.B., R.E. Rundle and A.J. Stosick, 1954, Acta Crystallogr. **7**, 106.
Hunt, J.P., and H.L. Friedman, 1983, Prog. Inorg. Chem. **30**, 359.
Husain, S.W., M. Ghannadi-Marageh and S. Rastreedzad, 1984, J. Radioanal. Nucl. Chem. **84**, 239.
Ibers, J.A., 1956, Acta Crystallogr. **9**, 225.
Ibers, J.A., and D.T. Cromer, 1958, Acta Crystallogr. **11**, 794.
Ilyashenko, V.S., A.I. Barabash, V.I. Volk, L.L. Zaitseva, M.I. Kovarev, A.A. Kruglov and L.V. Lipis, 1969, Zh. Neorg. Khim. **14**, 1197 [Russ. J. Inorg. Chem. **14**, 627].
Ilyashenko, V.S., L.L. Zaitseva, A.I. Barabash and L.S. Sudakova, 1973, Zh. Neorg. Khim. **18**, 2981 [Russ. J. Inorg. Chem. **18**, 1585].
Imanaka, N., Y. Yamaguchi, G. Adachi and J. Shiokawa, 1985, J. Electrochem. Soc. **132**, 2519.
Immonen, E., M. Koskenlinna, L. Niinistö and T. Pakkanen, 1976, Finn. Chem. Lett., p. 67.
Ionashiro, M., and I. Giolito, 1980, Thermochim. Acta **38**, 285.
Ionashiro, M., and I. Giolito, 1982a, Thermochim. Acta **59**, 231.
Ionashiro, M., and I. Giolito, 1982b, Thermochim. Acta **56**, 375.
Ionkina, E.A., N.N. Morozov, E.N. Muravev, V.P. Orlovskii and V.P. Repko, 1973, Inorg. Mater. **9**, 1130.
Ionov, V.M., L.A. Aslanov, V.B. Rybakov and M.A. Porai-Koshits, 1973a, Kristallografiya **18**, 403.
Ionov, V.M., L.A. Aslanov, V.B. Rybakov and M.A. Porai-Koshits, 1973b, Kristallografiya **18**, 405.
Iskhakova, L.D., and V.E. Plyuschchev, 1973, Zh. Neorg. Khim. **18**, 1500 [Russ. J. Inorg. Chem. **18**, 790].
Iskhakova, L.D., and V.K. Trunov, 1985, Kristallografiya **30**, 279.
Iskhakova, L.D., V.E. Plyuschchev and L.A. Perezhogina, 1971, Zh. Neorg. Khim. **16**, 1836 [Russ. J. Inorg. Chem. **16**, 976].
Iskhakova, L.D., V.E. Plyushchev and N.B. Berlin, 1973, Zh. Neorg. Khim. **18**, 694 [Russ. J. Inorg. Chem. **18**, 363].
Iskhakova, L.D., I.E. Sukhova, D.P. Chernova, I.V. Shakhno and V.E. Plyushchev, 1975, Zh. Neorg. Khim. **30**, 348 [Russ. J. Inorg. Chem. **20**, 193].
Iskhakova, L.D., Z.A. Starikova, E.P. Morochenets and V.K. Trunov, 1979, Zh. Neorg. Khim. **24**, 1539 [Russ. J. Inorg. Chem. **24**, 854].
Iskhakova, L.D., Z.A. Starikova and V.K. Trunov, 1981a, Koord. Khim. **7**, 1713 [J. Coord. Chem. **7**, 856].
Iskhakova, L.D., V.A. Efremov and V.K. Trunov, 1981b, Koord. Khim. **7**, 1417 [J. Coord. Chem. **7**, 714].
Iskhakova, L.D., N.L. Sarukhanyan and V.K. Trunov, 1985, Zh. Neorg. Khim. **30**, 1722.
Ismailzade, I.H., A.I. Alekberov, R.M. Ismailov, R.K. Asadova, T.D. Gabisoniya and Ye.M. Nanobashvili, 1980, Ferroelectrics **23**, 35.
Isupova, E.N., N.A. Godina and E.K. Keler, 1973, Inorg. Mater. **9**, 1076.
Ito, J., 1968, Am. Mineral. **53**, 890.
Ivanov-Emin, B.N., L.G. Korotaeva, V.G. Remizov and A.I. Ezhov, 1966, Zh. Neorg. Khim. **11**, 511 [Russ. J. Inorg. Chem. **11**, 278].
Ivanov-Emin, B.N., L.A. Filatenko, B.E. Zaitsev and A.I. Ezhov, 1969, Zh. Neorg. Khim. **14**, 1168 [Russ. J. Inorg. Chem. **14**, 612].
Ivanov-Emin, B.N., L.G. Korotaeva, V.I. Moskalenko and A.I. Ezhov, 1971, Russ. J. Inorg. Chem. **16**, 1554.
James, C., 1908, J. Am. Chem. Soc. **30**, 182.
James, C., and W.F. Langelier, 1909, J. Am. Chem. Soc. **31**, 913.
James, C., and P.S. Willand, 1916, J. Am. Chem. Soc. **38**, 1497.
Jantsch, G., and A. Ohl, 1911, Ber. Dtsch. Chem. Ges. **44**, 1274.
Jaulmes, S., 1969, C.R. Hebd. Séances Acad. Sci., Ser. C **268**, 935.
Jaulmes, S., 1972, Bull. Soc. Fr. Mineral. & Crystallogr. **95**, 42.
Jezowska-Trzebiatowska, B., and Z. Mazurak, 1980, Acta Crystallogr. B **36**, 1639.
Jezowska-Trzebiatowska, B., S. Ernst and J. Legendziewicz, 1978, Chem. Phys. Lett. **60**, 19.
Johanssen, H., 1974, Theor. Chim. Acta **32**, 273.
Johansson, G., and H. Wakita, 1985, Inorg. Chem. **24**, 3047.
Johansson, G., L. Niinistö and H. Wakita, 1985, Acta Chem. Scand. A **39**, 359.
Jolin, S., 1874, Bull. Soc. Chim. Fr. **21**, 533.
Joukoff, B., M. Fadly, J. Ostorero and H. Makram, 1978, J. Cryst. Growth **43**, 81.
Kahle, H.G., 1959, Z. Phys. **155**, 293.
Kaizu, Y., K. Miyakawa, K. Okada, H. Kobayashi, M. Sumitani and K. Yashihara, 1985, J. Am. Chem. Soc. **107**, 2622.
Kalbfleisch, H., H. Kumberg and G. Mueller-Vogt, 1972, Phys. Status Solidi b **52**, 499.
Kalinin, V.B., G.Ya. Pushkina, V.A. Efremov, P.P. Melnikov and L.N. Komissarova, 1978, Russ. J. Inorg. Chem. **23**, 521.
Kalsotra, B.L., R.K. Multani and B.D. Jain, 1972, J. Inorg. Nucl. Chem. **34**, 2265.
Kanno, H., and H. Hiraishi, 1982, J. Phys. Chem. **86**, 1488.
Karnaukhov, A.S., N.N. Runov and T.A. Osipova, 1977, Russ. J. Inorg. Chem. **22**, 608.
Karvinen, S., and L. Niinistö, 1986, Lanthanide Actinide Research **1**, 169.
Karvinen, S., K. Lumme and L. Niinistö, 1987, J. Therm. Anal., in press.
Kaučič, V., N. Bukovec and L. Golič, 1985, Acta Crystallogr. C **41**, 636.
Kauders, H.J., 1967, South African Patent 67 05 439.

Kelina, I.Yu., M.V. Provotorov, M.R. Mirnaya, E. Baeva and A.A. Maier, 1981, Tr.-Mosk. Khim. Tekhnol. Inst. im. D.I. Mendeleeva **120**, 110 [Chem. Abstr. **97**, 155349x].
Kepert, D.L., J.M. Patrick and A.H. White, 1983, Aust. J. Chem. **36**, 477.
Kestigian, M., J.R. Dickinson and R. Ward, 1957, J. Am. Chem. Soc. **79**, 5598.
Ketelaar, J.A.A., 1937, Physica, p. 619.
Khrameeva, N.P., L.N. Komissarova and G.Ya. Pushkina, 1971, Russ. J. Inorg. Chem. **16**, 1418.
Khrameeva, N.P., G.Ya. Pushkina, L.M. Komissarova and E.G. Teterin, 1973, Russ. J. Inorg. Chem. **18**, 455.
Kierkegaard, P., L.O. Larsson and B. Nyberg, 1972, Acta Chem. Scand. **26**, 218.
Kietaibl, H., and W. Petter, 1975, Helv. Phys. Acta **47**, 425.
Kilpatrick, M., and P. Pokras, 1953, J. Electrochem. Soc. **100**, 85.
Kiparisov, S.S., R.A. Belyaev, V.V. Bondarenko and V.P. Vyskubov, 1973, Inorg. Mater. **9**, 68.
Kitayama, K., and T. Katsura, 1977, Bull. Chem. Soc. Jpn **50**, 889.
Kitayama, K., and T. Katsura, 1978, Bull. Chem. Soc. Jpn **51**, 1358.
Kitayama, K., and T. Katsura, 1983, Bull. Chem. Soc. Jpn **56**, 1084.
Kitayama, K., T. Sugihara and T. Katsura, 1979, Bull. Chem. Soc. Jpn **52**, 458.
Kitayama, K., H. Sou and T. Katsura, 1983, Bull. Chem. Soc. Jpn **56**, 3415.
Kizilyalli, M., and A.J.E. Welch, 1977, Rare Earths Mod. Sci. Technol. **1**, 209.
Kizilyalli, M., and A.J.E. Welch, 1980, Rare Earths Mod. Sci. Technol. **2**, 59.
Klein, L., 1973, Int. J. Magn. **5**, 231.
Klein, L., W. Wuechner, H.G. Kahle and H.C. Schopper, 1971, Phys. Status Solidi b **48**, K139.
Knight, C.B., and M.B. Wise, 1980, J. Chem. Phys. **73**, 4946.
Knight, L.B., M.B. Wise and T.A. Asher, 1981, Inorg. Chem. **20**, 2633.
Kobayashi, Y., H. Akutsu and K. Iwama, 1977, U.S. 4 032 818.
Koizumi, H., 1976a, Acta Crystallogr. B **32**, 266.
Koizumi, H., 1976b, Acta Crystallogr. B **32**, 2254.
Koizumi, H., and J. Nakano, 1977, Acta Crystallogr. B **33**, 2680.
Koizumi, H., and J. Nakano, 1978, Acta Crystallogr. B **34**, 3320.
Komissarova, L.N., 1980, Zh. Neorg. Khim. **25**, 143 [Russ. J. Inorg. Chem. **25**, 75].
Komissarova, L.N., and P.P. Melnikov, 1966, Russ. J. Inorg. Chem. **11**, 674.
Komissarova, L.N., and A.S. Znamenskaya, 1974, Zh. Neorg. Khim. **19**, 295 [Russ. J. Inorg. Chem. **19**, 159].
Komissarova, L.N., P.P. Melnikov, R.N. Kravtsova and V.I. Spitsyn, 1965a, Z. Chem. **11**, 429.
Komissarova, L.N., V.M. Shatskii and G.I. Moiseichenko, 1965b, Zh. Neorg. Khim. **10**, 755 [Russ. J. Inorg. Chem. **10**, 407].
Komissarova, L.N., P.P. Melnikov and N.A. Chernova, 1967, J. Less-Common Met. **13**, 253.
Komissarova, L.N., E.G. Teterin, N.P. Anoshina and V.I. Spitsyn, 1969, Dokl. Akad. Nauk SSSR **188**, 362 [Dokl. Chem. **188**, 746].
Komissarova, L.N., V.M. Shatskii and N.P. Anoshina, 1970a, Zh. Neorg. Khim. **15**, 3218 [Russ. J. Inorg. Chem. **15**, 1678].
Komissarova, L.N., B.I. Bashkov and V.M. Shatskii, 1970b, Zh. Neorg. Khim. **15**, 1507 [Russ. J. Inorg. Chem. **15**, 773].
Komissarova, L.N., B.I. Bashkov and V.M. Shatskii, 1970c, Zh. Neorg. Khim. **15**, 2945 [Russ. J. Inorg. Chem. **15**, 1533].
Komissarova, L.N., P.P. Melnikov, E.G. Teterin and V.F. Chuvaev, 1971a, Russ. J. Inorg. Chem. **16**, 1414.
Komissarova, L.N., V.F. Chuvaev, V.M. Shatskii, B.I. Bashkov and T.A. Zhdanova, 1971b, Zh. Neorg. Khim. **16**, 1258 [Russ. J. Inorg. Chem. **16**, 669].
Komissarova, L.N., G.Ya. Pushkina and N.P. Khrameeva, 1971c, Russ. J. Inorg. Chem. **16**, 813.
Komissarova, L.N., V.F. Chuvaev, V.M. Shatskii, B.I. Bashkov, A.M. Grevtsev and E.G. Teterin, 1974, Zh. Neorg. Khim. **19**, 2606 [Russ. J. Inorg. Chem. **19**, 1423].
Komissarova, L.N., V.B. Kalinin, V.A. Efremov, G.Ya. Pushkina and P.P. Melnikov, 1980, Russ. J. Inorg. Chem. **25**, 1472.
König, K.H., and L. Psotta, 1978a, Z. Anorg. Allg. Chem. **443**, 212.
König, K.H., and L. Psotta, 1978b, Z. Anorg. Allg. Chem. **444**, 243.
Koppel, J., 1904, Z. Anorg. Chem. **41**, 377.
Kornyei, J., L. Szirtes and L. Zsinka, 1977, Radiochim. Radioanal. Lett. **31**, 181.
Kornyei, J., L. Szirtes and L. Zsinka, 1978a, Radiochim. Radioanal. Lett. **35**, 169.
Kornyei, J., L. Szirtes and L. Zsinka, 1978b, Radiochim. Radioanal. Lett. **35**, 193.
Korshunov, B.G., Z.N. Shevtsova, L.A. Mochalova and N.M. Igumova, 1971, Russ. J. Inorg. Chem. **16**, 3152.
Korytnaya, F.M., A.N. Pokrovskii and P.A. Degtyarev, 1980, Thermochim. Acta **41**, 141.
Korytnaya, F.M., S.N. Putilin and A.N. Pokrovskii, 1983, Zh. Neorg. Khim. **28**, 1716 [J. Inorg. Chem. **28**, 968].
Koskenlinna, M., and L. Niinistö, 1973, Suom. Kemistil. B **46**, 326.
Koskenlinna, M., and L. Niinistö, 1975, Finn. Chem. Lett., p. 83.

Koskenlinna, M., and J. Valkonen, 1977, Acta Chem. Scand. A **31**, 457.
Koskenlinna, M., M. Leskelä and L. Niinistö, 1976a, J. Electrochem. Soc. **123**, 75.
Koskenlinna, M., M. Leskelä and L. Niinistö, 1976b, J. Electrochem. Soc. **123**, 1920.
Koskenlinna, M., M. Leskelä, J.E.X. de Matos and L. Niinistö, 1985, Thermochim. Acta **95**, 401.
Kremers, H.E., and T. Moeller, 1944, J. Am. Chem. Soc. **66**, 1795.
Krishnamurthy, V.N., and S. Soundararajan, 1967, Z. Anorg. Allg. Chem. **349**, 220.
Kroger, F.A., and J. Baker, 1941, Physica **8**, 628.
Krstanovic, I., 1965, Z. Krist. **121**, 315.
Krutik, V.M., D.Yu. Pushcharovskii and E.A. Pobedimskaya, 1980, Dokl. Akad. Nauk SSSR **252**, 607.
Kryukova, A.I., I.A. Korshunov, V.A. Mitrofanova, N.V. Voroheva, C.N. Kazantsev and O.V. Skiba, 1977, Russ. J. Inorg. Chem. **22**, 2301.
Kuzina, T.I., I.V. Shakhno, A.N. Krachak and V.E. Plyushchev, 1973, Zh. Neorg. Khim. **18**, 2727 [Russ. J. Inorg. Chem. **18**, 1448].
Kuzina, T.I., I.V. Shakhno, V.E. Plyushchev and A.N. Krachak, 1975, Izv. Vyssh. Uchebn. Zaved. Khim. Khim. Tekhnol. **18**, 171.
Kuzina, T.I., I.V. Shakhno, V.E. Plyushchev, T.F. Sapova, K.I. Petrov and E.V. Zharavova, 1976a, Zh. Neorg. Khim. **21**, 401 [Russ. J. Inorg. Chem. **21**, 215].
Kuzina, T.I., I.V. Shakhno and V.E. Plyushchev, 1976b, Zh. Neorg. Khim. **21**, 1517 [Russ. J. Inorg. Chem. **21**, 828].
Kuzina, T.I., I.V. Shakhno, M.V. Savel'eva and T.I. Bel'skaya, 1979, Zh. Neorg. Khim. **24**, 2101 [Russ. J. Inorg. Chem. **24**, 1164].
Kuzina, T.I., G.A. Sidorenko, I.V. Shakhno and T.I. Bel'skaya, 1980, Zh. Neorg. Khim. **25**, 368 [Russ. J. Inorg. Chem. **25**, 200].
Kuzina, T.I., I.V. Shakhno, M.V. Savel'eva and T.I. Bel'skaya, 1983, Zh. Neorg. Khim. **28**, 91 [Russ. J. Inorg. Chem. **28**, 50].
Kuznetsov, V.G., and V.P. Vasileva, 1967, Inorg. Mater. **3**, 316.
Kuznetsov, V.G., and R.T. Yakovleva, 1973, Russ. J. Inorg. Chem. **18**, 1790.
Kuznetsov, V.G., S.M. Petushkova and I.V. Tananaev, 1969, Russ. J. Inorg. Chem. **14**, 2753.
Kuznetsov, V.G., I.V. Tananaev and R.T. Yakovleva, 1970, Russ. J. Inorg. Chem. **15**, 1252.
Kuznetsov, V.G., I.V. Tananaev and R.T. Yakovleva, 1973a, Russ. J. Inorg. Chem. **18**, 947.
Kuznetsov, V.G., I.V. Tananaev and R.T. Yakovleva, 1973b, Russ. J. Inorg. Chem. **18**, 1465.
Kyrki, J., and A. Lokio, 1971, Suom. Kemistil. B **44**, 105.
Lange, H., 1938, Ann. Phys. **32**, 361.
Larsson, L.O., S. Linderbrandt, L. Niinistö and U. Skoglund, 1973, Suom. Kemistil. B **46**, 314.
Laurie, S.H., and C.B. Monk, 1963, J. Chem. Soc., p. 3343.
Lazarev, A.N., N.Z. Mazhenov and A.P. Mirgordskii, 1978, Inorg. Mater. **14**, 1641.
Lazarevski, E.V., L.V. Kubasova, N.N. Chudinova and I.V. Tananaev, 1982, Inorg. Mater. **18**, 1327.
Lazoryak, B.I., V.B. Kalinin, S.Yu. Stefanovich and V.A. Efremov, 1980, Dokl. Akad. Nauk SSSR **250**, 861.
Le Flem, G., C. Parent and C. Fouassier, 1983, J. Less-Common Met. **93**, 383.
Lebedev, I.A., and Yu.A. Kulyako, 1978, Russ. J. Inorg. Chem. **23**, 3215.
Leskelä, M., 1980a, Helsinki Univ. Techn., Res. Pap. **64**, 1–39.
Leskelä, M., 1980b, Finn. Chem. Lett., p. 205.
Leskelä, M., 1981, unpublished results.
Leskelä, M., 1985, Thermochim. Acta **92**, 759.
Leskelä, M., and J. Hölsä, 1985, Thermochim. Acta **92**, 489.
Leskelä, M., and L. Niinistö, 1980a, Thermochim. Acta **35**, 125.
Leskelä, M., and L. Niinistö, 1980b, J. Therm. Anal. **18**, 307.
Leskelä, M., J.E.X. de Matos and L. Niinistö, 1985, Thermochim. Acta **95**, 407.
Leskelä, M., J.E.X. de Matos and L. Niinistö, 1987, Thermochim. Acta, in press.
Levine, A.K., and F.C. Palilla, 1964, Appl. Phys. Lett. **5**, 118.
Levine, A.K., and F.C. Palilla, 1966, Electrochem. Technol. **4**, 16.
Liminga, R., and S.C. Abrahams, 1976, J. Appl. Crystallogr. **9**, 42.
Liminga, R., S.C. Abrahams and J.L. Bernstein, 1975, J. Chem. Phys. **62**, 755.
Liminga, R., S.C. Abrahams and J.L. Bernstein, 1977, J. Chem. Phys. **67**, 1015.
Lincoln, S.F., 1971, Coord. Chem. Rev. **6**, 309.
Lincoln, S.F., 1986, Adv. Inorg. Bioinorg. Mechanisms **4**, 217.
Linde, S.A., Yu.E. Gorbunova and A.V. Lavrov, 1983, Russ. J. Inorg. Chem. **28**, 804.
Lindgren, O., 1976, Acta Crystallogr. B **32**, 3347.
Lindgren, O., 1977a, Acta Chem. Scand. A **31**, 167.
Lindgren, O., 1977b, Acta Chem. Scand. A **31**, 453.
Lindgren, O., 1977c, Acta Chem. Scand. A **31**, 163.
Lindgren, O., 1977d, Acta Chem. Scand. A **31**, 591.
Lindgren, O., 1977e, On the Oxygen Coordination of Cerium in some Sulfates and Chromates, Thesis (Chalmers University of Technology, and University of Göteborg, Gothenburg, Sweden).

Lipis, L.V., V.S. Ilyashenko, V.N. Egorov, G.V. Yuknevich, V.I. Volk and Yu.E. Shanurin, 1970, Zh. Prikl. Spektrosk. **13**, 866 [J. Appl. Spectrosc. **13**, 1491].

Lipis, L.V., V.S. Ilyashenko, V.N. Egorov, G.V. Yuknevich and V.I. Volk, 1971, Zh. Prikl. Spektrosk. **14**, 1044 [J. Appl. Spectrosc. **14**, 763].

Lister, M.W., and Y. Yoshino, 1960, Can. J. Chem. **38**, 45.

Litvin, B.N., and K. Byrappa, 1981, J. Cryst. Growth **51**, 470.

Litvin, B.N., K. Byrappa, V.A. Masloboev, N.N. Chudinova and N.V. Vinogradova, 1981a, Inorg. Mater. **17**, 1073.

Litvin, B.N., G.I. Dorokhova and O.S. Filipenko, 1981b, Dokl. Akad. Nauk SSSR **259**, 1102.

Litvin, B.N., G.S. Tarasankova, V.A. Masloboev, N.V. Vinogradova and N.N. Chudinova, 1982, Inorg. Mater. **18**, 240.

Löfgren, P., 1973, Chem. Commun., Univ. Stockholm **5**, 1–27.

Lohmueller, G., G. Schmidt, B. Deppisch, V. Gramlich and C. Schuringer, 1973, Acta Crystallogr. B **29**, 141.

Lokio, A., 1971, Suom. Kemistil. B **44**, 337.

Lokio, A., 1973, Acta Chem. Scand. **27**, 146.

Lokio, A., 1974a, Preparation and Properties of Lanthanoid Hexaoxoiodates (VII), Thesis (University of Oulu) pp. 1–44.

Lokio, A., 1974b, Finn. Chem. Lett., p. 5.

Lokio, A., and J. Kyrki, 1971, Suom. Kemistil. B **44**, 334.

Lokio, A., and J. Kyrki, 1973, Suom. Kemistil. B **46**, 206.

Long, F.G., and C.V. Stager, 1977, Can. J. Phys. **55**, 1633.

Luckey, G.W., 1972, U.S. Patent 3 705 858.

Lundgren, G., 1953, Ark. Kem. **5**, 59.

Lundgren, G., 1956, Rec. Trav. Chim. Pays-Bas **75**, 585.

Lundgren, G., 1957, Ark. Kem. **10**, 183.

Luscher, T.W., and R.K. Datta, 1970, J. Illum. Eng. Soc. **65**, 49.

L'vov, B.V., and L.A. Pelieva, 1973, Zh. Anal. Khim. **30**, 1653.

L'vov, B.V., and L.A. Pelieva, 1979, Zh. Prikl. Spektrosk. **31**, 205.

L'vov, B.V., and L.A. Pelieva, 1980, Prog. Anal. At. Spectrosc. **3**, 65.

Lyalina, R.B., and L.V. Soboleva, 1975, Russ. J. Inorg. Chem. **20**, 1424.

Lyutin, V.I., Yu.N. Safyanov, L.D. Iskhakova, V.E. Plyushchev, E.A. Kuzmin, V.V. Ilyukhin and N.V. Belov, 1974, Dokl. Akad. Nauk SSSR **214**, 1315 [Sov. Phys. Dokl. **19**, 59].

Madii, V.A., Yu.I. Krasilov, V.A. Kizel, Yu.V. Denisov, N.N. Chudinova and N.V. Vinogradova, 1978, Inorg. Mater. **14**, 1605.

Magnum, B.W., J.N. Lee and H.W. Moos, 1971, Phys. Rev. Lett. **27**, 1517.

Maier, A.I., T.A. Soldatova and M.K. Karapetyants, 1969, Izv. Akad. Nauk SSSR, Neorg. Mater. **5**, 1712 [Inorg. Mater. **5**, 1451].

Maksimova, S.I., K.K. Palkina, V.B. Loshchenov and V.A. Kuznetsov, 1978, Russ. J. Inorg. Chem. **23**, 2959.

Maksimova, S.I., K.K. Palkina, V.B. Loshchenov and V.G. Kuznetsov, 1979, Inorg. Mater. **15**, 969.

Maksimova, S.I., K.K. Palkina and V.B. Loshchenov, 1981, Inorg. Mater. **17**, 116.

Maksimova, S.I., K.K. Palkina and N.T. Chibiskova, 1982, Inorg. Mater. **18**, 553.

Malhotra, V.M., H.D. Bist and G.C. Upreti, 1974, Chem. Phys. Lett. **28**, 390.

Malhotra, V.M., H.D. Bist and G.C. Upreti, 1978, J. Chem. Phys. **69**, 1919.

Manca, S.G., and E.J. Baran, 1981, J. Phys. Chem. Solids **42**, 923.

Manca, S.G., and E.J. Baran, 1982, J. Appl. Cryst. **15**, 102.

Manoli, J.-M., P. Herpin and G. Pannetier, 1970, Bull. Soc. Chim. Fr., p. 98.

Marcantonatos, M.D., M. Deschaux and J.-J. Vuilleumier, 1984, J. Chem. Soc., Faraday Trans. **2**, 1569.

Marcus, Y., 1981, in: Gmelin Handbook of Inorganic Chemistry, 8th Ed., Sc, Y, La–Lu, Vol 39 D3 (Springer, Berlin) pp. 1–14.

Marcus, Y., 1983, J. Sol. Chem. **12**, 271.

Markovskii, L.Ya., and R.A. Safina, 1968, Zh. Prikl. Khim. **41**, 2537 [Appl. Chem. **41**, 2390].

Marsh, J.K., 1947, J. Chem. Soc., p. 118.

Martin, F., A. Gonzales, J. Jimenez, J. Largo and J.A. de Saja, 1984, J. Therm. Anal. **29**, 257.

Martin, I.J., 1973, Ion (Madrid) **33**, 134.

Martin, I.J., J.G. Vicente, P.A. Pascual and I.E. Roldan, 1971, Ion (Madrid) **31**, 562.

Martin, J.S., and S.S. Trond, 1967, French Patent 1 473 463.

Mascarenhas, Y., and S. Folgueras, 1975, Acta Crystallogr. A **31**, Suppl., 78. (Abstract only).

Masse, R., J.-C. Guittel and A. Durif, 1977, Acta Crystallogr. B **33**, 630.

Mathers, J.E., F.F. Mikus and E.J. Mechalchick, 1971, U.S. Patent 3 629 131.

Mathew, M., I. Mayer, B. Dickens and L.W. Schroeder, 1979, J. Solid State Chem. **28**, 79.

Mayer, I., and Y. Glasner, 1967, J. Inorg. Nucl. Chem. **29**, 1605.

Mayer, I., E. Levy and A. Glasner, 1964, Acta Crystallogr. **17**, 1071.

Mayer, I., R.S. Roth and W.E. Brown, 1974, J. Solid State Chem. **11**, 33.

Mayer, I., A. Semadja and V. Weiss, 1980, J. Solid State Chem. **34**, 223.

Mayer, S.W., and D.S. Schwartz, 1950, J. Am. Chem. Soc. **72**, 5106.

Mazelsky, R., R.C. Ohlman and K. Steinbrügge, 1968, J. Electrochem. Soc. **115**, 68.
McCarthy, G.J., and D.E. Pfoertsch, 1981, J. Solid State Chem. **38**, 128.
McColm, I.J., and S. Thompson, 1972, J. Inorg. Nucl. Chem. **34**, 3801.
McCoy, H.N., 1936, J. Am. Chem. Soc. **58**, 1577.
Meeck, A., and F. Petrů, 1971, Z. Chem. **11**, 154.
Mehran, F., K.W.H. Stevens and T.S. Plaskett, 1979, Phys. Rev. B **20**, 1817.
Meister, J.J., D.R. Patil and H. Channell, 1984, J. Appl. Polym. Sci. **29B**, 3457.
Mellor, J.W., 1965a, A Comprehensive Treatise on Inorganic and Theoretical Chemistry, Vol. 5, New Impression (Longmans, Green and Co, London) ch. 37, pp. 494–709.
Mellor, J.W., 1965b, A Comprehensive Treatise on Inorganic and Theoretical Chemistry, Vol. 10, New Impression (Longmans, Green and Co, London) ch. 58, pp. 820–892.
Melnikov, P.P., and L.N. Komissarova, 1969, Inorg. Mater. **5**, 511.
Melnikov, P.P., and L.N. Komissarova, 1981, Dokl. Akad. Nauk SSSR **256**, 878.
Melnikov, P.P., V.B. Kalinin, A.K. Shevchenko, V.A. Efremov and L.N. Komissarova, 1974, Inorg. Mater. **10**, 2103.
Melnikov, P.P., V.B. Kalinin, V.A. Efremov and L.N. Komissarova, 1976, Rev. CENIC Cienc. Fis. **7**, 175.
Melnikov, P.P., V.B. Kalinin, V.A. Efremov and L.N. Komissarova, 1981a, Inorg. Mater. **17**, 1085.
Melnikov, P.P., L.N. Komissarova and T.A. Butuzova, 1981b, Russ. J. Inorg. Chem. **17**, 1577.
Melnikov, P.P., G.Ya. Pushkina, V.A. Efremov, V.B. Kalinin and L.N. Komissarova, 1981c, Russ. J. Inorg. Chem. **26**, 142.
Melnikov, P.P., T.A. Butuzova, G.Ya. Pushkina and L.N. Komissarova, 1982, Inorg. Mater. **18**, 1333.
Melnikov, P.P., V.A. Efremov, H. Quiroga and L.N. Komissarova, 1983, J. Less-Common Met. **91**, L21.
Melnikov, P.P., J.D. Carillo Hesedero and L.N. Komissarova, 1984, J. Less-Common Met. **99**, L25.
Mezentseva, L.D., A.A. Domanskii and I.A. Bondar, 1977, Russ. J. Inorg. Chem. **22**, 84.
Michel, J.C., D. Morin and F. Auzel, 1975, C.R. Hebd. Séances Acad. Sci., Ser. B **281**, 445.
Millhouse, A.H., J.K. Kjems, M. Steiner and H. Dachs, 1980, J. Magn. & Magn. Mater. **15–18**, 1513.
Milligan, W.O., and L.W. Vernon, 1952, J. Phys. Chem. **56**, 145.
Milligan, W.O., D.F. Mullica and H.O. Perking, 1982, Inorg. Chim. Acta **60**, 35.
Milligan, W.O., D.F. Mullica and G.W. Beall, 1983, Acta Crystallogr. C **39**, 23.
Mioduski, T., and S. Siekierski, 1976, J. Inorg. Nucl. Chem. **38**, 1989.
Mironov, N.N., and I.M. Polyashov, 1970, Zh. Neorg. Khim. **15**, 1 [Russ. J. Inorg. Chem. **15**, 1].
Mironova, V.S., and I.V. Tananaev, 1982, Russ. J. Inorg. Chem. **27**, 81.
Misra, S.K., and P. Mikolajczak, 1979, J. Phys. Chem. Solids **40**, 477.
Mitewa, M., and P.R. Bontchev, 1985, Coord. Chem. Rev. **61**, 241.
Miyamoto, H., H. Shimura and K. Sasaki, 1985, J. Sol. Chem. **14**, 485.
Moeller, T., R.L. Dieck and J.E. McDonald, 1973, Rev. Chim. Miner. **10**, 177.
Mokhosoeva, U.V., V.G. Penkova and A.P. Nakhodnova, 1972, Inorg. Mater. **8**, 1577.
Molodkin, A.K., V.N. Belan, Yu.E. Bogatov and V.N. Moskalenko, 1982a, Russ. J. Inorg. Chem. **27**, 581.
Molodkin, A.K., Yu.E. Bogatov, V.I. Moskalenko, V.G. Remizov, V.M. Skorikov, V.N. Belan, V.V. Kurilkin and G.D. Golik, 1982b, Russ. J. Inorg. Chem. **24**, 509.
Molodkin, A.K., Yu.E. Bogatov, V.I. Moskalenko, T.N. Susanina, I.G. Zhuravleva, V.V. Kurilkin and Z.M. Melo, 1982c, Russ. J. Inorg. Chem. **27**, 797.
Molodkin, A.K., Yu.E. Bogatov, V.I. Moskalenko, V.G. Remizov, V.M. Skorikov, V.M. Belan, V.V. Kurilkin and G.D. Golik, 1982d, Russ. J. Inorg. Chem. **27**, 509.
Molodkin, A.K., Yu.E. Bogatov, V.I. Moskalenko, T.N. Susanina, I.G. Zhuravleva, V.V. Kurilkin and Z.M. Melo, 1982e, Russ. J. Inorg. Chem. **27**, 797.
Monk, C.B., 1951a, Trans. Faraday Soc. **47**, 1233.
Monk, C.B., 1951b, J. Chem. Soc., p. 2723.
Mooney, R.C.L., 1948, J. Chem. Phys. **16**, 1003.
Mooney, R.C.L., 1950, Acta Crystallogr. **3**, 337.
Mooney, R.W., and S.Z. Toma, 1967, J. Chem. Phys. **46**, 3364.
Mooney-Slater, R.C.L., 1962, Z. Krist. **111**, 371.
Morgan, J.A., M. Whitmore and R.L. Garnes, 1978, J. Chem. Eng. Data **23**, 187.
Moskalenko, V.I., M.B. Varfolomeev, K.I. Petrov and A.K. Molodkin, 1975a, Zh. Neorg. Khim. **20**, 85 [Russ. J. Inorg. Chem. **20**, 46].
Moskalenko, V.I., M.B. Varfolomeev and A.K. Molodkin, 1975b, Zh. Neorg. Khim. **20**, 2368 [Russ. J. Inorg. Chem. **20**, 1312].
Moskalenko, V.I., M.B. Varfolomeev, A.K. Molodkin and K.I. Petrov, 1976a, Zh. Neorg. Khim. **21**, 1508 [Russ. J. Inorg. Chem. **21**, 823].
Moskalenko, V.I., L.G. Korotaeva, A.K.

Molodkin and N. Pen'ya, 1976b, Zh. Neorg. Khim. **21**, 1513 [Russ. J. Inorg. Chem. **21**, 826].
Moskalenko, V.I., L.G. Korotaeva, A.K. Molodkin and N. Pen'ya, 1976c, Zh. Neorg. Khim. **21**, 1747 [Russ. J. Inorg. Chem. **21**, 957].
Moskalenko, V.I., M.B. Varfolomeev, K.I. Petrov and A.K. Molodkin, 1977a, Zh. Neorg. Khim. **22**, 2107 [Russ. J. Inorg. Chem. **22**, 1141].
Moskalenko, V.I., M.B. Varfolomeev, A.K. Molodkin and K.I. Petrov, 1977b, Zh. Neorg. Khim. **22**, 3017 [Russ. J. Inorg. Chem. **22**, 1641].
Moskalenko, V.I., M.B. Varfolomeev, A.K. Molodkin and K.I. Petrov, 1977c, Zh. Neorg. Khim. **22**, 3249 [Russ. J. Inorg. Chem. **22**, 1770].
Moskalenko, V.I., L.G. Korotaeva and A.K. Molodkin, 1978, Zh. Neorg. Khim. **23**, 2072 [Russ. J. Inorg. Chem. **23**, 1138].
Moskalenko, V.I., A.K. Molodkin, V.G. Remizov, Yu.E. Bogatov and M.B. Varfolomeev, 1980, Zh. Neorg. Khim. **25**, 1698 [Russ. J. Inorg. Chem. **25**, 944].
Muck, A., and F. Petrů, 1971, J. Less-Common Met. **24**, 473.
Mueller, P.H., A. Kasten and M. Schienle, 1983, Phys. Status Solidi b **119**, 239.
Mullica, D.F., W.O. Milligan and J.D. Oliver, 1979a, J. Inorg. Nucl. Chem. Lett. **15**, 1.
Mullica, D.F., W.O. Milligan and W.T. Kouba, 1979b, J. Inorg. Nucl. Chem. **41**, 967.
Mullica, D.F., W.O. Milligan and R.L. Garner, 1980, Acta Crystallogr. B **36**, 2561.
Murakami, K., M. Otani and H. Ito, 1979, Jpn Kokai Tokkyo Koho 7956086.
Muravev, E.N., V.P. Orlovskii, A.V. Potemkin, L.N. Kargaretelli, N.S. Dzhabishvili and V.D. Vorobev, 1981, Inorg. Mater. **17**, 91.
Nabar, M.A., and V.R. Ajgaonkar, 1981a, Thermochim. Acta **47**, 309.
Nabar, M.A., and V.R. Ajgaonkar, 1981b, Thermochim. Acta **51**, 381.
Nabar, M.A., and V.R. Ajgaonkar, 1982a, Thermochim. Acta **52**, 351.
Nabar, M.A., and V.R. Ajgaonkar, 1982b, J. Appl. Cryst. **15**, 573.
Nabar, M.A., and V.R. Ajgaonkar, 1985, J. Less-Common Met. **106**, 211.
Nabar, M.A., and V.V. Khandekar, 1984, J. Therm. Anal. **29**, 1343.
Nabar, M.A., and B.G. Mhatre, 1982, J. Solid State Chem. **45**, 135.
Nabar, M.A., and S.V. Paralkar, 1976a, Thermochim. Acta **15**, 390.
Nabar, M.A., and S.V. Paralkar, 1976b, Thermochim. Acta **17**, 239.
Nabar, M.A., and S.V. Paralkar, 1980a, Thermochim. Acta **35**, 287.
Nabar, M.A., and S.V. Paralkar, 1980b, Proc. ICTA 1980 (Birkhäuser, Basel) p. 175.
Nabar, M.A., and R.R. Sakhardande, 1985a, J. Less-Common Met. **110**, 415.
Nabar, M.A., and R.R. Sakhardande, 1985b, J. Crystallogr. Spectrosc. Res. **15**, 263.
Nabar, M.A., B.G. Mhatre and A.P. Vasaikar, 1981, J. Appl. Crystallogr. **14**, 469.
Nabar, M.A., B.G. Mhatre and A.P. Vasaikar, 1983, J. Chem. Soc., Dalton Trans., p. 1007.
Nag, K., and S.N. Bose, 1985, Struct. Bonding (Berlin) **63**, 153.
Nakano, J., and T. Yamada, 1976, J. Am. Ceram. Soc. **59**, 172.
Nakano, J., S. Miyazawa and T. Yamada, 1979, Mater. Res. Bull. **14**, 21.
Nakazawa, E., and S. Shionoya, 1970, Phys. Rev. Lett. **25**, 1710.
Nakhodnova, A.P., and T.D. Sirchenko, 1976, Russ. J. Inorg. Chem. **21**, 967.
Nakhodnova, A.P., and L.V. Zaslavskaya, 1976, Russ. J. Inorg. Chem. **21**, 1288.
Nakhodnova, A.P., and L.V. Zaslavskaya, 1982, Russ. J. Inorg. Chem. **27**, 674.
Nakhodnova, A.P., and L.V. Zaslavskaya, 1984, Russ. J. Inorg. Chem. **29**, 835.
Narten, A.H., and R.L. Hahn, 1982, Science **217**, 1249.
Nassau, K., 1976, Proc. 12th Rare Earth Research Conf. (Vail, CO), p. 772.
Nassau, K., and J.W. Shiever, 1975, J. Solid State Chem. **13**, 368.
Nassau, K., J.W. Shiever, B.E. Prescott and A.S. Cooper, 1974, J. Solid State Chem. **11**, 314.
Nassau, K., J.W. Shiever and B.E. Prescott, 1975, J. Solid State Chem. **14**, 122.
Nathans, M.W., and W.W. Wendlandt, 1962, J. Inorg. Nucl. Chem. **24**, 869.
Nazarenko, N.A., and N.S. Poluektov, 1979, Russ. J. Inorg. Chem. **24**, 3234.
Neilson, G.W., and J.E. Enderby, 1980, J. Chem. Soc. Ann. Repts **76C**, 185.
Neogy, D., and J. Nandi, 1982, J. Chem. Phys. **76**, 2591.
Neogy, D., and J. Nandi, 1983, J. Phys. Chem. Solids **44**, 943.
Newton, T.W., and G.M. Arcand, 1953, J. Am. Chem. Soc. **75**, 2449.
Nichia Denshi Kagaku, 1982, Jpn Kokai Tokkyo Koho 8223674.
Niinistö, L., 1973, Chem. Commun. Univ. Stockholm **13**, 1–34.
Niinistö, L., 1983, in: Systematics and the Properties of the Lanthanides, ed. S.P. Sinha (Reidel, Dordrecht) pp. 125–152.
Niinistö, L., 1984a, in: An. VII Simp. Anual da ACIESP, Vol. I: Quimica des Terras Raras, Publicacao ACIESP No. 44-1, eds G. Vicentini and L.B. Zinner (ACIESP, Sao Paulo) pp. 1–23.
Niinistö, L., 1984b, in: An. VII Simp. Anual da ACIESP, Vol. I: Quimica des Terras Raras, Publicacao ACIESP No. 44-1, eds G. Vicen-

tini and L.B. Zinner (ACIESP, Sao Paulo) pp. 44–56.
Niinistö, L., and M. Koskenlinna, 1973, Suom. Kemistil. B **46**, 245.
Niinistö, L., and M. Koskenlinna, 1987, to be published.
Niinistö, L., and L.O. Larsson, 1973, Acta Chem. Scand. **27**, 2250.
Niinistö, L., L.O. Larsson and J. Valkonen, 1975, Finn. Chem. Lett., p. 45.
Niinistö, L., J. Toivonen and J. Valkonen, 1980a, Finn. Chem. Lett., p. 87.
Niinistö, L., J. Valkonen and P. Ylinen, 1980b, Inorg. Nucl. Chem. Lett. **16**, 13.
Niinistö, L., P. Saikkonen and R. Sonninen, 1982, Rare Earths Mod. Sci. Techn. **3**, 257.
Niinistö, L., P. Saikkonen and R. Sonninen, 1984, Proc. Acad. Sci. Est. SSR Chem. **33**, 209.
Nikitina, S.D., and S.A. Bondar, 1983, Zh. Neorg. Khim. **28**, 2251 [Russ. J. Inorg. Chem. **28**, 1275].
Nilson, L.F., 1875, Nova Acta Upsal. **9**, 4; Bull. Soc. Chim. Fr. **23**, 494.
Norten, H.A., and R.L. Halin, 1982, Science **217**, 1249.
Nosova, T.A., 1966, Radiokhimiya **8**, 477.
Nyberg, B., and R. Larsson, 1973, Acta Chem. Scand. **27**, 63.
Nyquist, R.A., and R.O. Kagel, 1971, Infrared Spectra of Inorganic Compounds (Academic Press, New York).
Odehnal, M., 1972, Monatsh. Chem. **103**, 1615.
Ohtaki, H., 1982, Rev. Inorg. Chem. **4**, 103.
Orlovskii, V.P., T.V. Belyaevskaya and V.I. Bugakov, 1977, Russ. J. Inorg. Chem. **23**, 2354.
Orlovskii, V.P., A. Tsivadze, Yu.Ya. Kharitonov, E.G. Tselebrovskaya, A.N. Smirnov, Z.A. Ezhova and V.I. Bugakov, 1979, Inorg. Mater. **15**, 765.
Osipova, T.A., and N.N. Runov, 1981, Russ. J. Inorg. Chem. **26**, 749.
Otsuka, K., and T. Yamada, 1975, Appl. Phys. Lett. **26**, 311.
Paiva Santos, C.O., E.E. Castellano, L.C. Machado and G. Vicentini, 1985, Inorg. Chim. Acta **110**, 83.
Palanisamy, T., J. Gopalakrishnan and M.V.C. Sastri, 1975, Z. Anorg. Allg. Chem. **415**, 275.
Palilla, F.C., and A.K. Levine, 1967, Appl. Opt. **5**, 1467.
Palilla, F.C., and M.R. Tomkus, 1969, U.S. Patent 3 481 884.
Palilla, F.C., A.K. Levine and M. Rinkevics, 1965, J. Electrochem. Soc. **112**, 776.
Palkina, K.K., 1978, Inorg. Mater. **14**, 619.
Palkina, K.K., 1982, Inorg. Mater. **18**, 1199.
Palkina, K.K., V.G. Kuznetsov, N.N. Chudinova and N.T. Chibiskova, 1976a, Dokl. Akad. Nauk SSSR **226**, 357.
Palkina, K.K., U.G. Kuznetsov, N.N. Chudinova and N.T. Chibiskova, 1976b, Inorg. Mater. **12**, 730.
Palkina, K.K., V.Z. Saifutdinov, V.G. Kuznetsov and N.N. Chudinova, 1977, Dokl. Akad. Nauk SSSR **237**, 837.
Palkina, K.K., S.I. Maksimova and V.G. Kuznetsov, 1978a, Inorg. Mater. **14**, 284.
Palkina, K.K., S.I. Maksimova, V.G. Kuznetsov and N.T. Chibiskova, 1978b, Koord. Khim. **4**, 1092.
Palkina, K.K., S.I. Maksimova and V.G. Kuznetsov, 1979, Inorg. Mater. **15**, 2168.
Palkina, K.K., S.I. Maksimova, N.N. Chudinova and N.V. Vinogradova, 1981a, Inorg. Mater. **17**, 110.
Palkina, K.K., N.N. Chudinova, B.N. Litvin and N.V. Vinogradova, 1981b, Inorg. Mater. **17**, 1126.
Palkina, K.K., S.I. Maksimova and N.T. Chibiskova, 1981c, Inorg. Mater. **17**, 924.
Palkina, K.K., S.I. Maksimova and N.T. Chibikova, 1981d, Dokl. Akad. Nauk SSSR **257**, 357.
Palkina, K.K., V.V. Krasnikov and Z.A. Konstant, 1981e, Inorg. Mater. **17**, 1243.
Palkina, K.K., N.N. Chudinova, A.M. Balagina, S.I. Maksimova and N.T. Chibiskova, 1982, Inorg. Mater. **18**, 1337.
Palkina, K.K., S.I. Maksimova, V.S. Mironova, N.T. Chibiskova and I.V. Tananaev, 1983a, Russ. J. Inorg. Chem. **28**, 315.
Palkina, K.K., S.I. Maksimova and N.T. Chibiskova, 1983b, Russ. J. Inorg. Chem. **28**, 995.
Palkina, K.K., S.I. Maksimova, N.T. Chibiskova and V.S. Mironova, 1984a, Inorg. Mater. **20**, 1636.
Palkina, K.K., S.I. Maksimova, N.T. Chibiskova, B.F. Dzhurinskii and L.Z. Gorkhman, 1984b, Inorg. Mater. **20**, 919.
Paralkar, S.V., 1978, Thesis (University of Bombay).
Parent, C., J. Fava, R. Salon, M. Vlasse, G. Le Flem, P. Hagenmueller, F. Antic-Fidancev, M. Lemaitre-Blaise and P. Caro, 1979, Nuov. J. Chim. **3**, 523.
Parent, C., C. Fouassier and G. Le Flem, 1980a, J. Electrochem. Soc. **127**, 2049.
Parent, C., R. Salmon, G. Demgeau and G. Le Flem, 1980b, J. Solid State Chem. **35**, 83.
Parent, C., G. Le Flem, M. Et-Tabirou and A. Daoudi, 1981, Solid State Commun. **37**, 857.
Parent, C., P. Bochu, A. Daoudi and G. Le Flem, 1982, J. Solid State Chem. **43**, 190.
Parent, C., M. Ben Amara, P. Bochu, G. Le Flem and P. Hagenmueller, 1984, J. Solid State Chem. **53**, 168.
Park, H.D., and E.R. Kreider, 1984, J. Am. Ceram. Soc. **67**, 23.
Park, I.-H., 1972, Bull. Chem. Soc. Jpn **45**, 2753.
Parrish, W., 1939, Am. Mineral. **24**, 651.

Pascal, P., 1959, Nouveau Traité de Chimie Minérale (Masson & Cie, Paris) Tome VII.
Patscheke, E., H. Fuess and G. Will, 1968, Chem. Phys. Lett. **2**, 47.
Paulik, J., and F. Paulik, 1981, in: Wilson and Wilson's Comprehensive Analytical Chemistry, ed. G. Svenla (Elsevier, Amsterdam) Vol. 12.
Pavlov-Verevkin, B.S., 1970, Zh. Neorg. Khim. **15**, 892 [Russ. J. Inorg. Chem. **15**, 455].
Pearce, J.N., and W.C. Oelke, 1938, J. Phys. Chem. **42**, 95.
Pearce, P.W., R.G. Russell and J.C. Butler, 1946a, in: Inorganic Synthesis, Vol. 2, ed. W.C. Fernelius (McGraw-Hill, New York) p. 44.
Pearce, P.W., R.G. Russell, L.L. Quill and S. Riccard, 1946b, in: Inorganic Synthesis, Vol. 2, ed. W.C. Fernelius (McGraw-Hill, New York) p. 62.
Perel'man, F.M., and E.I. Fedoseeva, 1963a, Zh. Neorg. Khim. **8**, 2603.
Perel'man, F.M., and E.I. Fedoseeva, 1963b, Zh. Neorg. Khim. **8**, 1255.
Perret, A., and A. Banderet, 1937, C.R. Hebd. Séances Acad. Sci. **204**, 586.
Perret, R., 1970, Bull. Soc. Fr. Mineral. Crystallogr. **93**, 493.
Peterson, E.J., E.I. Onstott and R.B. von Dreele, 1979, Acta Crystallogr. B **35**, 805.
Peterson, E.J., E.M. Foltyn and E.I. Onstott, 1980, Rare Earths Mod. Sci. Techn. **2**, 65.
Peterson, E.J., E.M. Foltyn and E.I. Onstott, 1983, J. Am. Chem. Soc. **105**, 7572.
Petit, R.H., J. Ferre and J. Duran, 1981, Phys. Rev. B **23**, 1216.
Petrov, K.I., V.I. Ivanov and V.G. Pervykh, 1967, Zh. Strukt. Khim. **8**, 356 [J. Struct. Chem. **8**, 310].
Petrov, K.I., G.N. Voronskaya and V.I. Ivanov, 1970, Zh. Neorg. Khim. **15**, 615 [Russ. J. Inorg. Chem. **15**, 317].
Petrov, K.I., G.N. Voronskaya, L.D. Iskhakova and V.E. Plyushchev, 1971, Zh. Neorg. Khim. **16**, 1275 [Russ. J. Inorg. Chem. **16**, 675].
Petrov, K.I., Yu.M. Golovin, M.B. Varfolomeev and E.M. Remennik, 1973, Zh. Neorg. Khim. **18**, 385 [Russ. J. Inorg. Chem. **18**, 201].
Petrov, K.I., V.V. Kravchenko, M.B. Varfolomeev, N.B. Shamrai and V.E. Plyushchev, 1974, Russ. J. Inorg. Chem. **19**, 491.
Petrov, K.I., G.N. Voronskaya, N.I. Bashilova and E.S. Takhanova, 1975a, Zh. Neorg. Khim. **20**, 72 [Russ. J. Inorg. Chem. **20**, 39].
Petrov, K.I., E.V. Zharavova, I.V. Shakhno, T.I. Kuzina and M.V. Savel'eva, 1975b, Zh. Neorg. Khim. **20**, 647 [Russ. J. Inorg. Chem. **20**, 360].
Petrov, K.I., A.E. Kharakoz, I.A. Popova, T.B. Durnyakova and E. Romashov, 1977, Russ. J. Inorg. Chem. **22**, 2149.
Petrů, F., and B. Dusek, 1965, Z. Chem. **5**, 236.
Petrů, F., and B. Dusek, 1968, Coll. Czech. Chem. Comm. **33**, 2397.
Petrů, F., and F. Kutek, 1963, Z. Chem. **3**, 473.
Petrů, F., and F. Kutek, 1964, Z. Chem. **4**, 33.
Petrů, F., and A. Muck, 1967, Z. Anorg. Allg. Chem. **352**, 330.
Petrů, F., and A. Muck, 1971, Coll. Czech. Chem. Commun. **36**, 3774.
Petrů, F., J. Hradilova and B. Hajek, 1970, J. Inorg. Nucl. Chem. **32**, 1485.
Petushkova, S.M., and I.V. Tananaev, 1963, Russ. J. Inorg. Chem. **8**, 552.
Petushkova, S.M., I.V. Tananaev and S.O. Samoilova, 1969a, Russ. J. Inorg. Chem. **14**, 470.
Petushkova, S.M., I.V. Tananaev and S.O. Samoilova, 1969b, Russ. J. Inorg. Chem. **14**, 605.
Petushkova, S.M., I.V. Tananaev and S.O. Samoilova, 1971, Russ. J. Inorg. Chem. **16**, 61.
Pilipchuk, V.I., L.S. Gaigerova and A.N. Pokrovskii, 1980, Zh. Neorg. Khim. **25**, 1805 [Russ. J. Inorg. Chem. **25**, 1001].
Pincott, M., and J.C. Barnes, 1968, J. Less-Common Met. **16**, 393.
Plyushchev, V.E., I.V. Shakhno and T.I. Kuzina, 1975, Izv. Vyssh. Uchebn. Zaved., Khim. Khim. Tekhnol. **18**, 1682.
Podberezskaya, N.V., and S.V. Borisov, 1976, Zh. Strukt. Khim. **17**, 186 [J. Struct. Chem. **17**, 164].
Pokrovskii, A.N., and L.M. Kovba, 1976, Zh. Neorg. Khim. **21**, 567 [Russ. J. Inorg. Chem. **21**, 305].
Poluektov, N.S., R.S. Lauer and S.F. Ognichenko, 1970, Russ. J. Inorg. Chem. **15**, 1233.
Ponomarenko, P.I., M.A. Porai-Koshits, E.N. Kurkutova and K. Sulaimankulov, 1978, Zh. Strukt. Kim. **19**, 856.
Popov, V.I., V.N. Sheptunov and K.S. Bagdasarov, 1969, Inorg. Mater. **5**, 456.
Porcher, P., D.R. Svoronos, M. Leskelä and J. Hölsä, 1983, J. Solid State Chem. **46**, 101.
Pospelova, L.A., V.N. Kokunova and L.M. Zaitsev, 1970, Zh. Neorg. Khim. **15**, 2349 [Russ. J. Inorg. Chem. **15**, 1217].
Postmus, C., and J.R. Ferraro, 1968, J. Chem. Phys. **48**, 3605.
Poulet, H., J.P. Mathieu, D. Vergnat, B. Vergnat, A. Hadni and X. Gerbaux, 1975, Phys. Status Solidi a **32**, 509.
Prandtl, N., and S. Mohr, 1938, Z. Anorg. Allg. Chem. **236**, 243.
Pratt Jr, W.P., S.S. Rosenblum, W.A. Steyert and J.A. Barclay, 1977, Cryogenics **17**, 689.

Prokofev, M.V., 1980, Thesis; see: Kristallografiya **29**, 435 [Sov. Phys. Crystallogr. **29**, 261].
Prokofev, M.V., 1981, Kristallografiya **26**, 598 [Sov. Phys. Crystallogr. **26**, 337].
Prokofev, M.V., A.N. Pokrovskii and L.M. Kovba, 1979, Zh. Neorg. Khim. **24**, 2114 [Russ. J. Inorg. Chem. **24**, 1171].
Pruitt, M.E., R.R. Rickhard and E.I. Wyatt, 1962, Anal. Chem. **34**, 283.
Purkaystha, B.C., and K.N. Dutta, 1963, J. Ind. Chem. Soc. **40**, 869.
Puzdrenkova, I.V., I.P. Alimarin and V.A. Frolkina, 1958, Vestnik. Moskov. Univ., Ser. Mat., Mekh., Astron., Fiz., Khim. **13**, 183 [Ref. CA 1959 53, 6892h].
Rao, B.M., T.B. Sastry and T.S. Parek, 1983, Z. Phys. Chem. (Leipzig) **264**, 906.
Rard, J.A., 1985, Chem. Rev. **85**, 555.
Rawat, J.P., M.A. Khan and P.S. Thind, 1984, Bull. Chem. Soc. Jpn **57**, 1701.
Reed, E.O., and H.W. Moos, 1973a, Phys. Rev. B **8**, 980.
Reed, E.O., and H.W. Moos, 1973b, Phys. Rev. B **8**, 988.
Remizov, V.G., B.N. Ivanov-Emin and L.G. Korotaeva, 1969, Zh. Neorg. Khim. **14**, 2362 [Russ. J. Inorg. Chem. **14**, 1242].
Reuter, B., and M. Wollnik, 1963, Naturwissenschaften **50**, 569.
Rice, C.E., and W.R. Robinson, 1976, Acta Crystallogr. B **32**, 2232.
Richman, I., 1966, J. Opt. Soc. Am. **56**, 1589.
Rigotti, G., G. Punte, B.E. Rivero, M.E. Escobar and E.J. Baran, 1981, J. Inorg. Nucl. Chem. **43**, 2811.
Rimbach, E., and A. Schubert, 1909, Z. Phys. Chem. **67**, 183.
Rinaldi, P.L., S.A. Khan, G.R. Choppin and G.C. Levy, 1979, J. Am. Chem. Soc. **101**, 1350.
Rivero, B.E., G. Rigotti and G. Punte, 1984, Acta Crystallogr. C **40**, 715.
Rivero, B.E., G. Punte, G. Rigotti and A. Navaza, 1985, Acta Crystallogr. C **41**, 817.
Robinson, F.W., 1909, J. Chem. Soc. **95**, 1353.
Rocchiccioli, C., 1960, Ann. Chim. (Paris) **5**, 999.
Rodicheva, G.V., I.V. Tananaev and N.M. Romanova, 1981, Inorg. Mater. **17**, 95.
Rogachev, D.L., M.A. Porai-Koshits, V.Ya. Kuznetsov and L.M. Dikareva, 1974, Zh. Strukt. Khim. **15**, 465 [J. Struct. Chem. **15**, 397].
Rogachev, D.L., S.A. Bondar, M.P. Shulgina and M.P. Ryskina, 1979, Zh. Neorg. Khim. **24**, 2406 [Russ. J. Inorg. Chem. **24**, 1334].
Rogachev, D.L., S.A. Bondar, M.A. Letetskaya and M.P. Ryskina, 1983, Zh. Neorg. Khim. **28**, 345 [Russ. J. Inorg. Chem. **28**, 189].
Rogers, R.D., and L.K. Kurihara, 1986, Inorg. Chim. Acta **116**, 171.
Ropp, R.C., 1968a, J. Electrochem. Soc. **115**, 841.
Ropp, R.C., 1968b, J. Electrochem. Soc. **115**, 531.
Ropp, R.C., 1968c, J. Electrochem. Soc. **115**, 940.
Ropp, R.C., 1969, J. Electrochem. Soc. **116**, 623.
Ropp, R.C., 1970, U.S. Patent 3 507 804.
Ropp, R.C., 1971, Ger. Offen. 2 101 564.
Ropp, R.C., and B. Carroll, 1973, J. Inorg. Nucl. Chem. **35**, 1153.
Ropp, R.C., and B. Carroll, 1975, Inorg. Chem. **14**, 2199.
Ropp, R.C., and B. Carroll, 1976, J. Electrochem. Soc. **123**, 944.
Ropp, R.C., and B. Carroll, 1977, J. Inorg. Nucl. Chem. **39**, 1303.
Rossmanith, K., 1966, Monatsh. Chem. **97**, 1698.
Rosso, B., and R. Perret, 1970, C.R. Hebd. Séances Acad. Sci., Ser. C **270**, 997.
Rouanet, A., J.J. Serra, K. Allaf, J. Coutures and H. Dexpert, 1980, Rev. Int. Hautes Temp. Refract. **16**, 437.
Rouanet, A., J.J. Serra, K. Allaf and V.P. Orlovskii, 1981, Inorg. Mater. **17**, 76.
Roulet, R., and R. Chenaux, 1972, Helv. Chim. Acta **55**, 1959.
Roy, A., and K. Nag, 1978, J. Inorg. Nucl. Chem. **40**, 1501.
Roy, A., M. Chaudhury and K. Nag, 1978, Bull. Chem. Soc. Jpn **51**, 1243.
Rubinchik, Ya.S., T.P. Veremei, M.M. Pavlyuchenko and I.A. Mochal'nik, 1973, Dokl. Akad. Nauk Beloruss. SSR **17**, 380.
Ryabchikov, D.I., and N.S. Vagina, 1966, Zh. Neorg. Khim. **11**, 1038 [Russ. J. Inorg. Chem. **11**, 560].
Rykova, T.A., O.N. Ustalova, V.M. Skorikov and I.V. Tananaev, 1979, Russ. J. Inorg. Chem. **24**, 102.
Rzaigui, M., and N.K. Ariguip, 1985, J. Solid State Chem. **56**, 122.
Rzaigui, M., and N. Kbir-Ariguip, 1981, J. Solid State Chem. **39**, 309.
Rzaigui, M., and N. Kbir-Ariguip, 1983, J. Solid State Chem. **50**, 391.
Rzaigui, M., M. Trabelsi and N. Kbir-Ariguip, 1983a, J. Solid State Chem. **50**, 86.
Rzaigui, M., N. Kbir-Ariguip, M.T. Averbuch-Pouchot and A. Durif, 1983b, J. Solid State Chem. **50**, 240.
Rzaigui, M., N. Kbir-Ariguip, M.T. Averbuch-Pouchot and A. Durif, 1984, J. Solid State Chem. **52**, 61.
Safyanov, Yu.N., and N.V. Belov, 1976, Dokl. Akad. Nauk SSSR **227**, 1112.
Safyanov, Yu.N., E.A. Kuzmin, L.D. Iskhakova, V.V. Ilyukhin and N.V. Belov, 1975, Dokl. Akad. Nauk SSR **220**, 346 [Sov. Phys. Dokl. **20**, 12].

Safyanov, Yu.N., E.A. Kuzmin and N.V. Belov, 1977, Dokl. Akad. Nauk SSSR **235**, 578.
Safyanov, Yu.N., E.A. Kuzmin and N.V. Belov, 1978a, Kristallografiya **23**, 697.
Safyanov, Yu.N., E.A. Kuzmin and N.V. Belov, 1978b, Dokl. Akad. Nauk SSSR **242**, 603.
Safyanov, Yu.N., E.A. Kuzmin and N.V. Belov, 1979, Kristallografiya **24**, 438.
Sahney, R.C., S.L. Aggarwal and M. Singh, 1946, J. Indian Chem. Soc. **23**, 177.
Sahney, R.C., S.L. Aggarwal and S. Singh, 1947, J. Indian Chem. Soc. **24**, 193.
Saji, H., T. Yamadaya and M. Asanuma, 1970, J. Phys. Soc. Jpn **28**, 913.
Sakai, T., G. Adachi, J. Shiokawa and T. Shin-ike, 1976, Mater. Res. Bull. **11**, 1295.
Sakamoto, M., 1984, Polyhedron **3**, 451.
Sakanov, I.E., T.B. Durnyakova and A.E. Kharakoz, 1977, Izv. Akad. Nauk Kirg. SSR, p. 64.
Salmon, R., C. Parent, A. Berrada, R. Brochu, A. Daoudi, M. Vlasse and G. Le Flem, 1975, C.R. Hebd. Séances Acad. Sci., Ser. C **280**, 805.
Salmon, R., C. Parent, G. Le Flem amd M. Vlasse, 1976, Acta Crystallogr. B **32**, 2799.
Salmon, R., C. Parent, M. Vlasse and G. Le Flem, 1978, Mater. Res. Bull. **13**, 439.
Salmon, R., C. Parent, M. Vlasse and G. Le Flem, 1979, Mater. Res. Bull. **14**, 85.
Samartsev, B.G., and A.N. Pokrovskii, 1982, Zh. Neorg. Khim. **27**, 2140 [Russ. J. Inorg. Chem. **27**, 1209].
Samartsev, B.G., A.N. Pokrovskii and L.M. Kovba, 1977, Zh. Neorg. Khim. **22**, 2721 [Russ. J. Inorg. Chem. **22**, 1476].
Samartsev, B.G., M.V. Prokofev, A.N. Pokrovskii and L.M. Kovba, 1978, Zh. Neorg. Khim. **23**, 540 [Russ. J. Inorg. Chem. **23**, 300].
Samartsev, B.G., A.N. Pokrovskii, L.M. Kovba and V.A. Novichkov, 1979, Zh. Neorg. Khim. **24**, 2112 [Russ. J. Inorg. Chem. **24**, 1170].
Samartsev, B.G., A.N. Pokrovskii and L.M. Kovba, 1980a, Kristallografiya **25**, 394 [Sov. Phys. Crystallogr. **25**, 226].
Samartsev, B.G., A.N. Pokrovskii and L.M. Kovba, 1980b, Zh. Neorg. Khim. **25**, 852 [Russ. J. Inorg. Chem. **25**, 475].
Samartsev, B.G., A.N. Pokrovskii and L.M. Kovba, 1980c, Vestn. Mosk. Univ. Ser. 2: Khim. **21**, 190 [Ref. CA 93:17257g].
Sarkar, P.B., 1926, Bull. Soc. Chim. Fr. **39**, 1390.
Sarukhanyan, N.L., L.D. Iskhakova, E.P. Morochenets and V.K. Trunov, 1982, Zh. Neorg. Khim. **27**, 1963 [Russ. J. Inorg. Chem. **27**, 1109].
Sarukhanyan, N.L., L.D. Iskhakova and V.K. Trunov, 1983, Kristallografiya **28**, 452 [Sov. Phys. Crystallogr. **28**, 266].
Sarukhanyan, N.L., L.D. Iskhakova, V.K. Trunov and V.V. Ilyukhin, 1984a, Koord. Khim. **10**, 981 [J. Coord. Chem. **10**, 540].
Sarukhanyan, N.L., L.D. Iskhakova and V.K. Trunov, 1984b, Kristallografiya **29**, 687 [Sov. Phys. Crystallogr. **29**, 407].
Sarukhanyan, N.L., L.D. Iskhakova and V.K. Trunov, 1984c, Kristallografiya **29**, 435 [Sov. Phys. Crystallogr. **29**, 261].
Sarukhanyan, N.L., L.D. Iskhakova, V.K. Trunov and G. Ganeev, 1984d, Kristallografiya **29**, 440 [Sov. Phys. Crystallogr. **29**, 264].
Sarukhanyan, N.L., L.D. Iskhakova and V.K. Trunov, 1985a, Kristallografiya **30**, 274 [Sov. Phys. Crystallogr. **30**, 158].
Sarukhanyan, N.L., L.D. Iskhakova, I.G. Drobinskaya and V.K. Trunov, 1985b, Kristallografiya **30**, 880.
Savchenko, G.S., I.V. Tananaev and A.N. Volodina, 1968, Izv. Akad. Nauk SSSR, Neorg. Mater. **4**, 1097 [Inorg. Mater. **4**, 965].
Saveleva, M.V., I.V. Shakhno, V.E. Plyushchev and E.D. Bakhareva, 1975a, Izv. Vyssh. Uchebn. Zaved., Khim. Khim. Tekhnol. **18**, 359.
Saveleva, M.V., I.V. Shakhno, V.E. Plyushchev, K.I. Petrov and N.I. Zakharova, 1975b, Zh. Neorg. Khim. **20**, 2354 [Russ. J. Inorg. Chem. **20**, 1305].
Saveleva, M.V., I.V. Shakhno, O.V. Mironova and E.M. Avzhieva, 1978, Zh. Neorg. Khim. **23**, 44 [Russ. J. Inorg. Chem. **23**, 24].
Sayetat, F., 1972, Solid State Commun. **10**, 879.
Schaefer, W., and G. Will, 1971, J. Phys. C **4**, 3224.
Scherer, V., 1968, U.S. Atomic Energy Commission Report BMWF-FBK 68-03, p. 27.
Scholder, R., and W. Klemm, 1954, Angew. Chem. **66**, 461.
Scholer, R.P., and A.E. Merbach, 1975, Inorg. Chim. Acta **15**, 15.
Schowalter, R., 1971, Phys. Status Solidi b **48**, 743.
Schröder, W., 1938, Z. Anorg. Chem. **238**, 209, 305.
Schulz, H., K.-H. Thiemann and J. Fenner, 1974, Mater. Res. Bull. **9**, 1525.
Schumann, H., 1952, Z. Anorg. Allg. Chem. **271**, 29.
Schumm, R.H., D.D. Wagman, S. Bailey, W.H. Evans and V.B. Parker, 1973, Natl. Bur. Std. Tech. Note 270-7.
Schwab, A., 1975, Phys. Status Solidi b **68**, 359.
Schwab, G., and W. Hillmer, 1975, Phys. Status Solidi b **70**, 237.
Schwarz, H., 1963a, Z. Anorg. Allg. Chem. **322**, 1.
Schwarz, H., 1963b, Z. Anorg. Allg. Chem. **322**, 15.
Schwarz, H., 1963c, Z. Anorg. Allg. Chem. **322**, 129.

Schwarz, H., 1963d, Z. Anorg. Allg. Chem. **323**, 275.
Schwarz, H., 1963e, Z. Anorg. Allg. Chem. **324**, 60.
Schwarz, H., 1963f, Z. Anorg. Allg. Chem. **322**, 137.
Schwarz, H., 1963g, Z. Anorg. Allg. Chem. **323**, 44.
Seifer, G.B., 1963a, Russ. J. Inorg. Chem. **8**, 792.
Seifer, G.B., 1963b, Russ. J. Inorg. Chem. **8**, 1525.
Serebrennikov, V.V., T.N. Tsybukova and A.A. Velikov, 1984, Zh. Neorg. Khim. **29**, 2392 [Russ. J. Inorg. Chem. **29**, 1368].
Serra, J.J., J. Coutures and A. Rouanet, 1976a, High Temp.–high Press. **8**, 337.
Serra, J.J., J. Coutures and A. Rouanet, 1976b, 12th Rare Earth Research Conf. (Vail, CO) p. 652.
Serra, J.J., J. Coutures, A. Rouanet, H. Dexpert and G. Garon, 1978, Rev. Int. Hautes. Temp. Refract. Fr. **15**, 287.
Serra, O.A., and E. Giesbrecht, 1968, J. Inorg. Nucl. Chem. **30**, 793.
Shakhno, I.V., T.I. Kuzina, T.N. Skorobogat'ko and T.I. Bel'skaya, 1977, Zh. Neorg. Khim. **22**, 1505 [Russ. J. Inorg. Chem. **22**, 819].
Shakhtakhtinskaya, N.G., and M.G. Iskenderov, 1973, Azerb. Khim. Zh., p. 105.
Shakhtakhtinskaya, N.G., and M.G. Iskenderov, 1975, Azerb. Khim. Zh., p. 138.
Shakhtakhtinskii, G.B., B.S. Valiev and A.K. Babaev, 1977, Azerb. Khim. Zh., p. 120.
Shamrai, N.B., M.B. Varfolomeev, Yu.N. Safyanov, E.A. Kuzmin and V.V. Ilyukhin, 1975, Russ. J. Inorg. Chem. **22**, 31.
Shamrai, N.B., M.B. Varfolomeev, Yu.N. Safyanov, E.A. Kuzmin and V.V. Ilyukhin, 1977a, Russ. J. Inorg. Chem. **22**, 461.
Shamrai, N.B., V.M. Ionov, Yu.N. Safyanov, E.A. Keatman, V.V. Ilyukhin and M.B. Varfolomeev, 1977b, Russ. J. Inorg. Chem. **22**, 1243.
Shannon, R.D., and A.W. Sleight, 1968, Inorg. Chem. **7**, 1649.
Shatskii, V.M., B.I. Bashkov, L.N. Komissarova and A.M. Grevtsev, 1974a, Zh. Neorg. Khim. **19**, 2013 [Russ. J. Inorg. Chem. **19**, 1103].
Shatskii, V.M., V.F. Churaev, B.I. Baskov, A.M. Grentsev and L.N. Komissarova, 1974b, Zh. Neorg. Khim. **19**, 2327 [Russ. J. Inorg. Chem. **19**, 1271].
Shatskii, V.M., F.M. Spiridonov, E.G. Teterin, B.I. Bashkov and L.N. Komissarova, 1977, Koord. Khim. **3**, 460.
Shchenev, A.V., and N.N. Runov, 1981a, Russ. J. Inorg. Chem. **26**, 1291.
Shchenev, A.V., and N.N. Runov, 1981b, Russ. J. Inorg. Chem. **26**, 1384.
Sheka, Z.A., and E.I. Sinyavskaya, 1969, Russ. J. Inorg. Chem. **14**, 73.
Shevchuk, V.G., D.A. Storozhenko and N.M. Lazorenko, 1981, Zh. Neorg. Khim. **26**, 1924 [Russ. J. Inorg. Chem. **26**, 1037].
Shevchuk, V.G., A.K. Molodkin, D.A. Storozhenko, V.M. Akimov and Y.A. Grigorev, 1983, Zh. Neorg. Khim. **18**, 2421 [Russ. J. Inorg. Chem. **28**, 1375].
Shin-ike, T., H. Hata, T. Sakai, G. Adachi and J. Shiokawa, 1976a, Mater. Res. Bull. **11**, 1361.
Shin-ike, T., H. Hata, T. Sakai, G. Adachi and J. Shiokawa, 1976b, Mater. Res. Bull. **11**, 801.
Shin-ike, T., G. Adachi and J. Shiokawa, 1977, Mater. Res. Bull. **12**, 1149.
Shin-ike, T., G. Adachi, J. Shiokawa, M. Shimada and M. Koizumi, 1980, Bull. Chem. Soc. Jpn **53**, 3563.
Shklovskaya, S.M., B.I. Arkhipov, B.I. Kidyarov and L.P. Zherdienko, 1977, Russ. J. Inorg. Chem. **22**, 624.
Shvedov, V.P., and S.A. Musaev, 1959, Radiokhimiya **1**, 465.
Sikka, S.K., 1969, Acta Crystallogr. A **25**, 621.
Sillén, L.G., and A.E. Martell, eds, 1964, Stability Constants of Metal-Ion Complexes (Chemical Society, London).
Sillén, L.G., and A.E. Martell, eds, 1971, Stability Constants of Metal-Ion Complexes, Supplement No. 1 (Chemical Society, London).
Simonova, T.N., I.A. Shevchuk, I.N. Malakha and L.I. Konovalenko, 1973, Zh. Anal. Khim. **28**, 1825.
Singer, J., and D.T. Cromer, 1959, Acta Crystallogr. **12**, 718.
Singhal, O.P., 1973, Z. Naturforsch. b **28**, 158.
Sirotinkin, S.P., and A.N. Pokrovskii, 1982a, Zh. Neorg. Khim. **27**, 2142 [Russ. J. Inorg. Chem. **27**, 1211].
Sirotinkin, S.P., and A.N. Pokrovskii, 1982b, Zh. Neorg. Khim. **27**, 2776 [Russ. J. Inorg. Chem. **27**, 1572].
Sirotinkin, S.P., A. Pokrovskii and L.M. Kovba, 1976a, J. Solid State Chem. **17**, 327.
Sirotinkin, S.P., A.N. Pokrovskii and L.M. Kovba, 1976b, Zh. Neorg. Khim. **21**, 789 [Russ. J. Inorg. Chem. **21**, 425].
Sirotinkin, S.P., V.A. Efremov, L.M. Kovba and A.N. Pokrovskii, 1977a, Kristallografiya **22**, 1272 [Sov. Phys. Crystallogr. **22**, 725].
Sirotinkin, S.P., V.A. Efremov, L.M. Kovba and A.N. Pokrovskii, 1977b, Kristallografiya **22**, 966 [Sov. Phys. Crystallogr. **22**, 551].
Sirotinkin, S.P., V.A. Efremov, L.M. Kovba and A.N. Pokrovskii, 1978a, Kristallografiya **23**, 406 [Sov. Phys. Crystallogr. **23**, 227].
Sirotinkin, S.P., S.M. Chizhov, A.N. Pokrovskii and L.M. Kovba, 1978b, J. Less-Common Met. **58**, 101.
Sirotinkin, S.P., A.N. Pokrovskii and L.M. Kovba, 1981, Kristallografiya **26**, 385 [Sov. Phys. Crystallogr. **26**, 219].
Sizova, R.G., A.A. Voronkov and N.V. Belov,

1974, Dokl. Akad. Nauk SSSR **217**, 1073 [Sov. Phys. Dokl. **19**, 472].
Sklyarenko, Yu.S., N.S. Stroganova and V.I. Ivanov, 1965, Zh. Neorg. Khim. **10**, 2209 [Russ. J. Inorg. Chem. **10**, 1203].
Slavkina, R.I., D. Usubaliev and V.V. Serebrennikov, 1963, Tr. Tomsk. Gos. Univ. Ser. Khim. **157**, 304.
Smirnov, N.I., and A.F. Volkov, 1974, Dokl. Akad. Nauk SSSR **217**, 639.
Smith, A.L., 1967, U.S. Patent 3322681.
Smith Jr, L.S., and D.L. Wertz, 1975, J. Am. Chem. Soc. **97**, 2365.
Smith Jr, L.S., and D.L. Wertz, 1977, J. Inorg. Nucl. Chem. **39**, 95.
Smith, S.H., and B.M. Wanklyn, 1974, J. Cryst. Growth **21**, 23.
Smith, S.H., G. Garton, B.K. Tanner and D. Midgley, 1978, J. Mater. Sci. **13**, 620.
Smolin, Yu.I., Yu.F. Shepelev, A.I. Domanskii and N.V. Belov, 1978, Kristallografiya **23**, 187.
Smolin, Yu.I., Yu.F. Shepelev and A.I. Domanskii, 1982, Kristallografiya **27**, 239.
Smolyakova, K.E., A.A. Efremov and V.V. Serebrennikov, 1973, Zh. Fiz. Khim. **47**, 2452 [Russ. J. Phys. Chem. **47**, 1389].
Soderholm, L., and J.E. Greedan, 1979, Mater. Res. Bull. **14**, 1449.
Soderholm, L., and J.E. Greedan, 1982, Mater. Res. Bull. **17**, 707.
Soderholm, L., J.E. Greedan and M.F. Collins, 1980, J. Solid State Chem. **35**, 367.
Soderholm, L., C.V. Stager and J.E. Greedan, 1982, J. Solid State Chem. **43**, 175.
Solomosi, F., 1977, Structure and Stability of Salts of Halogen Oxyacids in the Solid Phase (Wiley, New York) p. 467.
Sommerdijk, J.L., W.L. Wanmaker and J.G. Verriet, 1971, J. Lumin. **4**, 404.
Sonninen, R., 1981, Thesis (Helsinki University of Technology, Espoo).
Spasibenko, T.P., 1974, Zh. Neorg. Khim. **19**, 899 [Russ. J. Inorg. Chem. **19**, 489].
Spasibenko, T.P., and R.A. Popova, 1981, Zh. Neorg. Khim. **26**, 916 [Russ. J. Inorg. Chem. **26**, 493].
Spedding, F.H., and R.S. Bear, 1933, Phys. Rev. **44**, 287.
Spedding, F.H., and S. Jaffe, 1954, J. Am. Chem. Soc. **76**, 882.
Spedding, F.H., and J.A. Rard, 1974, J. Phys. Chem. **78**, 1435.
Spedding, F.H., P.F. Culler and A. Habenschuss, 1974, J. Phys. Chem. **78**, 1106.
Spedding, F.H., L.E. Shiers and J.A. Rard, 1975a, J. Chem. Eng. Data **20**, 66.
Spedding, F.H., L.E. Shiers, M.A. Brown and J.L. Derer, 1975b, J. Chem. Eng. Data **20**, 81.
Spedding, F.H., J.L. Baker and J.P. Walters, 1975c, J. Chem. Eng. Data **20**, 189.
Spedding, F.H., M.A. Mohs, J.L. Derer and A. Habenschuss, 1977a, J. Chem. Eng. Data **22**, 142.
Spedding, F.H., J.A. Rard and H.O. Weber, 1977b, J. Chem. Eng. Data **22**, 187.
Stammreich, H., D. Bassi and O. Sala, 1958a, Spectrochim. Acta **12**, 403.
Stammreich, H., D. Bassi, O. Sala and H. Siebert, 1958b, Spectrochim. Acta **13**, 192.
Stampfli, R., and G.R. Choppin, 1972, J. Inorg. Nucl. Chem. **34**, 205.
Staritzky, E., and D.T. Cromer, 1956, Anal. Chem. **28**, 913.
Starostin, A.D., and S.V. Leontov, 1972, Radiokhimiya **14**, 768.
Staveley, L.A.K., D.R. Markham and M.R. Jones, 1968, J. Inorg. Nucl. Chem. **30**, 231.
Steele, M.L., and D.L. Wertz, 1976, J. Am. Chem. Soc. **98**, 4424.
Steinberg, M., and I. Shidlovsky, 1962, Bull. Res. Council Israel A **11**, 234.
Steinberg, M., and I. Shidlovsky, 1964, J. Inorg. Nucl. Chem. **26**, 887.
Steyert, W.A., 1978, J. Appl. Phys. **49**, 1227.
Stöhr, J., and J.B. Gruber, 1975, Chem. Phys. **7**, 336.
Storozhenko, D.A., 1983a, Zh. Neorg. Khim. **28**, 1158 [Russ. J. Inorg. Chem. **28**, 654].
Storozhenko, D.A., 1983b, Zh. Neorg. Khim. **28**, 1162 [Russ. J. Inorg. Chem. **28**, 656].
Storozhenko, D.A., and V.G. Shevchuk, 1981, Zh. Neorg. Khim. **26**, 1932 [Russ. J. Inorg. Chem. **26**, 1042].
Storozhenko, D.A., N.M. Lazorenko, N.N. Kisel and V.G. Shevchuk, 1981, Zh. Neorg. Khim. **26**, 1928 [Russ. J. Inorg. Chem. **26**, 1040].
Storozhenko, D.A., N.M. Lazorenko and V.G. Shevchuk, 1982, Zh. Neorg. Khim. **27**, 2683 [Russ. J. Inorg. Chem. **27**, 1520].
Storozhenko, D.A., A.K. Molodkin, V.G. Shevchuk, V.M. Akimov and Yu.A. Grigorev, 1983, Zh. Neorg. Khim. **28**, 894 [Russ. J. Inorg. Chem. **28**, 506].
Strada, M., and W. Schwendimann, 1934, Gazz. Chim. Ital. **64**, 662.
Strunz, H., 1942, Naturwissenschaften **30**, 14.
Stubican, V.S., and P. Roy, 1962, Angew. Chem. **74**, 82.
Stubican, V.S., and R. Roy, 1963, Z. Krist. **119**, 90.
Subramarian, M.A., G. Aravamundan and G.V. Subba Rao, 1979, Mater. Res. Bull. **14**, 1457.
Sungur, A., M. Kizilyalli and D.S. Jones, 1983, J. Less-Common Met. **93**, 441.
Suponitskii, Yu.L., I.V. Shakhno, S.B. Tsyrenova, M.V. Saveleva, V.E. Plyushchev and M.Kh. Karapetyants, 1976, Zh. Fiz. Khim. **50**, 1440 [Russ. J. Phys. Chem. **50**, 870].
Suponitskii, Yu.L., S.B. Tsyrenova and M.Kh. Karapetyants, 1978, Zh. Fiz. Khim. **52**, 2691 [Russ. J. Phys. Chem. **52**, 1550].
Surgutskii, V.P., and V.V. Serebrennikov, 1964, Zh. Neorg. Khim. **9**, 786 [Russ. J. Inorg. Chem. **9**, 435].

Szirtes, L., and L. Zsinka, 1974, Izotoptechnika **17**, 545.
Szirtes, L., J. Korney and Z. Poko, 1984, J. Radioanal. Nucl. Chem. **81**, 291.
Tagawa, H., 1984, Thermochim. Acta **80**, 23.
Takezako, Y., Y. Fukuda and M. Fukai, 1977, Japan Kokai 77 75674.
Tanaka, F., and S. Yamashita, 1984, Inorg. Chem. **23**, 2044.
Tananaev, I.V., and V.P. Vasileva, 1963, Russ. J. Inorg. Chem. **8**, 556.
Tananaev, I.V., V.G. Kuznetsov and U.P. Vasileva, 1967, Inorg. Mater. **3**, 87.
Tananaev, I.V., N.I. Bashilova and E.S. Takhanova, 1971a, Zh. Neorg. Khim. **16**, 2821 [Russ. J. Inorg. Chem. **16**, 1502].
Tananaev, I.V., N.I. Bashilova, E.S. Takhanova and N.M. Berdinova, 1971b, Zh. Neorg. Khim. **16**, 2827 [Russ. J. Inorg. Chem. **16**, 1505].
Tananaev, I.V., E.V. Maksimchuk, Yu.T. Bushrev and S.A. Shertor, 1978, Inorg. Mater. **14**, 719.
Tarasov, V.P., G.A. Kirakosyan, S.V. Trots, Yu.A. Buslaev and V.T. Panyushkin, 1983, Koord. Khim. **9**, 205 [Coord. Chem. **9**, 127].
Tarasova, G.N., E.E. Vinogradov and I.B. Kurinov, 1985, Russ. J. Inorg. Chem. **30**, 315.
Tetsu, Hayashi, L.G. Korotaeva and B.N. Ivanov-Emin, 1971, Zh. Neorg. Khim. **16**, 2921 [Russ. J. Inorg. Chem. **16**, 1552].
Tofield, B.C., P.M. Bridenbaugh and H.P. Weber, 1975, Mater. Res. Bull. **10**, 1091.
Tranqui, D., M. Bagieu-Beucher and A. Durif, 1972, Bull. Soc. Fr. Mineral. & Crystallogr. **95**, 437.
Tranqui, D., M. Bagieu and A. Durif, 1974, Acta Crystallogr. B **30**, 1751.
Trofimov, G.V., 1968, Zh. Neorg. Khim. **13**, 2831 [Russ. J. Inorg. Chem. **13**, 1457].
Trofimov, G.V., and V.I. Belokoskov, 1968, Zh. Neorg. Khim. **13**, 260 [Russ. J. Inorg. Chem. **13**, 135].
Trömel, G., 1932, Z. Physik. Chem. **158**, 422.
Trunov, V.K., L.D. Iskhakova and N.N. Soloveva, 1977, Zh. Neorg. Khim. **22**, 2005 [Russ. J. Inorg. Chem. **22**, 1088].
Tsagareishvili, D.S., G.G. Gvelesiani, V.P. Orlovskii, T.V. Belyaevskaya and V.P. Repko, 1972, Inorg. Mater. **8**, 1574.
Tsuhako, M., C. Ikeuchi, T. Matsuo, I. Motooka and M. Kobayashi, 1979, Bull. Chem. Soc. Jpn **52**, 1034.
Tsujimoto, Y., Y. Fukuda and M. Fukai, 1977, J. Electrochem. Soc. **124**, 553.
Tsyrenova, S.B., Yu.L. Suponitskii and M.Kh. Karapetyants, 1973, Zh. Fiz. Khim. **47**, 2132.
Tsyrenova, S.B., Yu.L. Suponitskii and M.Kh. Karapetyants, 1974a, Zh. Fiz. Khim. **48**, 2705.
Tsyrenova, S.B., Yu.L. Suponitskii and M.Kh. Karapetyants, 1974b, Zh. Fiz. Khim. **48**, 1560 [Russ. J. Phys. Chem. **48**, 919].
Udalov, Yu.P., and Z.S. Appen, 1982, Inorg. Mater. **18**, 1349.
Ueda, T., 1967, J. Jpn. Assoc. Min. Petr. Eco. Geol. **58**, 170.
Ukrainskaya, O.M., L.F. Yastrebova, I.U. Tananaev and T.A. Balyuk, 1971, Inorg. Mater **7**, 545.
Ustalova, O.N., G.A. Rykova and V.M. Skorikov, 1978, Russ. J. Inorg. Chem. **23**, 953.
Vaivada, M.A., and Z.A. Konstant, 1979, Inorg. Mater. **15**, 647.
Valkonen, J., 1978a, Acta Crystallogr. B **34**, 1957.
Valkonen, J., 1978b, Acta Crystallogr. B **34**, 3064.
Valkonen, J., 1979, Ann. Acad. Sci. Fenn. Ser. AII **188**, 1–36.
Valkonen, J., and M. Leskelä, 1978, Acta Crystallogr. B **34**, 1323.
Valkonen, J., and L. Niinistö, 1978, Acta Crystallogr. B **34**, 266.
Valkonen, J., and P. Ylinen, 1979, Acta Crystallogr. B **35**, 2378.
Valkonen, J., L. Niinistö, B. Eriksson, L.O. Larsson and U. Skoglund, 1975, Acta Chem. Scand. A **29**, 866.
van den Boom, P.F.J., and A.M.J.H. Seufer, 1979, Ger. Offen. 2841545.
Varfolomeev, M.B., 1985, Zh. Neorg. Khim. **30**, 2467.
Varfolomeev, M.B., N.B. Shamrai, I.F. Sgadova and V.E. Plyushchev, 1971, Russ. J. Inorg. Chem. **16**, 973.
Varfolomeev, M.B., N.B. Shamrai, A.S. Mironova, Yu.B. Ramus and V.E. Plyushchev, 1972, Russ. J. Inorg. Chem. **17**, 609.
Varfolomeev, M.B., N.B. Shamrai, B.G. Berenshtein and V.E. Plyushchev, 1973, Kristallografiya **18**, 175.
Vasilega, M.D., I.E. Kiryakova, V.M. Pavlikov and S.G. Tresvyatskii, 1977, Dopov. Akad. Nauk. Ukr. RSR, Ser. B: Geol. Khim. Biol. Nauk. **5**, 410.
Vasilenko, N.A., and M.L. Chepelevetskii, 1957, Russ. J. Inorg. Chem. **2**, 2486.
Vazhnov, A.K., P.A. Degtyarev, A.N. Pokrovskii and V.V. Fomichev, 1980, Zh. Neorg. Khim. **25**, 468 [Russ. J. Inorg. Chem. **25**, 255].
Vazhnov, A.K., P.A. Degtyarev, A.N. Pokrovskii and V.V. Fomichev, 1983, Zh. Neorg. Khim. **28**, 3016 [Russ. J. Inorg. Chem. **28**, 1710].
Vegard, L., 1927, Philos. Mag. **4**, 511.
Venugopalan, M., and K.F. George, 1956, Naturwissenschaften **43**, 348.
Verma, V.P., 1985, Thermochim. Acta **89**, 363.
Vicentini, G., M. Perrier and E. Giesbrecht, 1961, Chem. Ber. **94**, 1153.
Vickery, R.C., 1955, J. Chem. Soc., p. 2360.
Vinogradova, N.V., and N.N. Chudinova, 1981, Inorg. Mater. **17**, 331.

Vishwamittar, P.P., 1974a, Proc. 11th Rare Earth Research Conf., eds. J.M. Haschke and H.A. Eick (NTIS, Springfield, VA) p. 578.
Vishwamittar, P.S.P., 1974b, Phys. Rev. B **9**, 4673.
Vlasse, M., R. Salmon and C. Parent, 1976, Inorg. Chem. **15**, 1440.
Vlasse, M., C. Parent, R. Salmon, G. Le Flem and P. Hagenmueller, 1980a, J. Solid State Chem. **35**, 318.
Vlasse, M., C. Parent, R. Salmon and G. Le Flem, 1980b, Rare Earths Mod. Sci. Technol. **2**, 195.
Vlasse, M., P. Bochu, C. Parent, J.P. Chaminade, A. Daoudi, G. Le Flem and P. Hagenmueller, 1982, Acta Crystallogr. B **38**, 2328.
von Scheele, C., 1898, Z. Anorg. Chem. **18**, 352.
Voronkov, A.A., N.V. Kadoshnikova, N.V. Mukhtarova, R.K. Rastsvetaev, N.A. Shumyatskaya and V.V. Ilyukhin, 1982, Probl. Teor. Kristallokhim. Slozhnykh. Oksidov., ed. A.N. Lazarev (Izv. Nauka, Leningrad) pp. 5–43.
Wagif, H.S., M. Ghannadi-Maregh and S. Rasheedzad, 1984, J. Radioanal. Nucl. Chem. **84**, 239.
Walter, H., H.G. Kahle, K. Mulder, H.C. Schopper and H. Schwarz, 1973, Int. J. Magn. **5**, 129.
Walter, W., and K.H. Butler, 1968, Abstr. Electrochem. Soc. Spring Meeting, Boston, p. 29.
Wanklyn, B.M., 1978, J. Cryst. Growth **43**, 336.
Wanklyn, B.M., B.E. Watts and B.J. Garrard, 1984, Mater. Res. Bull. **19**, 825.
Wanmaker, W.L., and J.G. Verlijsdonk, 1966, Ger. Offen. 1572221.
Wanmaker, W.L., A. Bril, J.W. ter Vrugt and J. Broos, 1966, Philips Res. Rept. **21**, 270.
Wanmaker, W.L., J.W. ter Vrugt and J.G. Verlijsdonk, 1971, J. Solid State Chem. **3**, 452.
Wappler, D., 1974, Phys. Condens. Mat. **17**, 113.
Weber, H.P., and B.C. Tofield, 1975, IEEE Quantum Electron. **11**, 368.
Weigel, F., 1969, Fortschr. Chem. Forsch. **12**, 539.
Weigel, F., and V. Scherer, 1967, Radiochim. Acta **7**, 46.
Wendtlandt, W.W., 1958, J. Inorg. Nucl. Chem. **7**, 51.
Wendtlandt, W.W., and T.D. George, 1961, J. Inorg. Nucl. Chem. **19**, 245.
Will, G., W. Schaefer and H. Goebel, 1971a, Conf. Dig.-Inst. Phys. (London) **3**, 226.
Will, G., W. Schaefer, W. Scharenberg and H. Goebel, 1971b, Z. Angew. Phys. **32**, 122.
Will, G., W. Lugscheider, W. Zinn and E. Patscheke, 1971c, Phys. Status Solidi b **46**, 597.
Williams, R.J.P., 1982, Struct. Bond. (Berlin) **50**, 79.
Winfree, A.T., 1984, J. Chem. Ed. **61**, 66.
Wold, A., and R. Ward, 1954, J. Am. Chem. Soc. **76**, 1029.
Wortman, D.E., N. Karayianis and C.A. Morrison, 1976, U.S. NTIS, AD Rep. AD-A 030658, pp. 1–103.
Yakunina, G.M., and V.V. Serebrennikov, 1970, Russ. J. Inorg. Chem. **15**, 447.
Yakunina, G.M., and V.V. Serebrennikov, 1974, Russ. J. Phys. Chem. **48**, 1619.
Yakunina, G.M., L.A. Alekseenko and V.V. Serebrennikov, 1969a, Russ. J. Inorg. Chem. **14**, 1414.
Yakunina, G.M., S.E. Kharzeeva and V.V. Serebrennikov, 1969b, Russ. J. Inorg. Chem. **14**, 1541.
Yakunina, G.M., L.A. Alekseenko and V.V. Serebrennikov, 1970, Zh. Fiz. Khim. **44**, 60.
Yokota, K., Y. Kimura and T. Shoji, 1970, Japan. patent 7021369.
Yoshimura, M., and T. Sata, 1969, Bull. Chem. Soc. Jpn **42**, 3195.
Yurchenko, E.N., E.B. Burgina, V.I. Bugakov, E.N. Muravev, V.P. Orlovskii and T.V. Belyaevskaya, 1978, Inorg. Mater. **14**, 1586.
Zaitseva, L.L., M.I. Konarev, A.A. Kruglov and N.T. Chebotarev, 1964, Zh. Neorg. Khim. **9**, 2554 [Russ. J. Inorg. Chem. **9**, 1380].
Zaitseva, L.L., V.S. Ilyashenko and V.S. Romanov, 1972, Zh. Neorg. Khim. **17**, 2358 [Russ. J. Inorg. Chem. **17**, 1231].
Zambonini, F.Z., and S.R. Restaino, 1931, Att. Acad. Lincei **13**, 650.
Zeuter, B., and M. Wollnik, 1963, Naturwissenschaften **50**, 569.
Zhiran, H., and G. Blasse, 1984, J. Solid State Chem. **52**, 130.
Zielinski, S., and W. Skupin, 1980, J. Therm. Anal. **19**, 61.
Zinovev, A.A., and N.A. Shchirova, 1960, Russ. J. Inorg. Chem. **5**, 259.
Znamenskaya, A.S., and L.N. Komissarova, 1973, Zh. Neorg. Khim. **18**, 873 [Russ. J. Inorg. Chem. **18**, 458].
Znamenskaya, A.S., L.N. Komissarova and V.I. Spitsyn, 1972, Zh. Neorg. Khim. **17**, 1828 [Russ. J. Inorg. Chem. **17**, 947].
Znamenskaya, A.S., L.N. Komissarova and V.M. Shatskii, 1977, Zh. Neorg. Khim. **22**, 2124 [Russ. J. Inorg. Chem. **22**, 1150].
Znamenskaya, A.S., L.N. Komissarova and V.M. Shatskii, 1978, Zh. Neorg. Khim. **23**, 2980 [Russ. J. Inorg. Chem. **23**, 1654].
Znamenskaya, A.S., L.N. Komissarova and K.I. Petrov, 1979, Koord. Khim. **5**, 1180 [Coord. Chem. **5**, 930].
Zsinka, L., and L. Szirtes, 1974, Radiochim. Radioanal. Lett. **16**, 271.
Zsinka, L., L. Szirtes, J. Mink and A. Kalman, 1974, J. Chromatogr. **102**, 109.
Zsinka, L., L. Szirtes, Le Van So and Z. Poko, 1978, J. Therm. Anal. **14**, 245.
Zverev, G.M., A.M. Onishchenko, V.P. Orlovskii, V.P. Repko and A.A. Semenov, 1973, Inorg. Mater. **9**, 370.

Handbook on the Physics and Chemistry of Rare Earths, edited by K.A. Gschneidner, Jr. and L. Eyring

Chapter 60

COMPLEXES WITH SYNTHETIC IONOPHORES

Jean-Claude G. BÜNZLI
Université de Lausanne, Institut de chimie minérale et analytique
Place du Château 3, CH-1005 Lausanne, Switzerland

Contents

Abbreviations

Ac = acetate
Aet = aminoethyl
Az = azoxy
Bicy = bicyclic
But = butyl
CN = coordination number
CPL = circularly polarized luminescence
Cy = cyclohexyl
DMF = dimethylformamide
DMSO = dimethylsulfoxide
DOTA = 1,4,7,10-tetraazacyclododecane-N,N′,N″,N‴-tetraacetic acid
DOTMA = [1R-(1R*,4R*,7R*,10R*)]-α,α′,α″,α‴-tetramethyl-1,4,7,10-tetraazacyclododecane-1,4,7,10-tetraacetic acid
dpm = dipivaloylmethane
DSC = differential scanning calorimetry
DTA = differential thermal analysis
DTG = differential thermogravimetry
E_a^* = activation energy
EDTA = ethylenediamine-N,N,N′,N′-tetra-acetic acid
EPR = electron paramagnetic resonance
Et = ethyl
EtOH = ethanol
fod = heptafluorodimethyloctanedionate
Fu = furanyl
Hept = heptyl
HTTA = thenoyltrifluoroacetone
INDO = intermediate neglect of differential overlap
Ket = ketone
Lar = Lariat
LSR = lanthanide shift reagent
Me = methyl
MeCN = acetonitrile
MeOH = methanol
MO = molecular orbital
Napht = naphtyl
NMR = nuclear magnetic resonance
NOTA = 1,4,7-triazacyclononane-N,N′,N″-triacetic acid
Oct = octyl
PC = propylene carbonate
PEG = polyethyleneglycol
Ph = phenyl
Pod1 = 4,5-dimethyl-N,N,N′,N′-tetrapropyl-3,6-dioxaoctanediamide
Polyols = polyalcohols
Py = pyridyl
TDA = tris(dioxa-3,6-heptyl)amine
TETA = 1,4,8,11-tetraazacyclotetradecane-N,N′,N″,N‴-tetraacetic acid
TFA = trifluoroacetate
TFE = trifluoroethanol
TG = thermogravimetry
THF = tetrahydrofurane
TL = total luminescence
TOPO = trioctylphosphine oxide
TRIF = trifluoromethanesulfonate
XPES = X-ray photoelectron spectroscopy

1. Historical backgrounds and motivations

Ionophores are receptor molecules able to form stable, lipophilic complexes with charged hydrophilic species, such as metal cations. They can therefore promote the transfer of the latter from an aqueous medium into a hydrophobic phase. The first examples of naturally occurring ionophores, nigericin and lasalocid, were isolated by Berger et al. (1951), whereas the function of valinomycin as complexing and transporting agent for alkali metal cations was recognized by Moore and Pressman (1964). The processes of complexation and transport are usually quite specific. This is illustrated by the affinity of valinomycin for potassium ions, which is 10^4 times larger than for sodium ions (Wipf et al., 1970).

The complexes between metal ions and ionophores are of the host–guest type.

The guest moiety is spherical and encapsulated in a cavity-like structure formed by the cyclic or open-chain host molecule. The cavity either exists as such in the ligand or the latter adopts its final shape upon complexation, a process associated with structural and conformational rearrangements. In any case, a mutual topological fit between the two reacting entities is essential for the stabilization of the complex. A good ionophore must therefore meet the following requirements:

(a) It should contain several coordinating sites, ideally between six and twelve.

(b) If high selectivity is desired, the coordinating sites must be locked in a rather rigid conformation. Such a rigidity may be enhanced by the presence of bridging structures and hydrogen bonds.

(c) A complete rigidity is, however, not required since it would lead to a very slow kinetics of complexation. The ionophore must retain a certain degree of fluxionality to allow a sufficiently fast ion exchange; this is only possible if the solvation molecules of the cation are substituted in a stepwise mechanism.

The ionophores are divided into two classes: natural and synthetic ionophores. The natural ionophores may be further divided into three subclasses.

(1) Two groups of antibiotics, depsipeptides and macrotetrolides. An example of the first group is valinomycin, a molecule containing a threefold repetition of the sequence D-valine, L-lactic acid, L-valine, and D-γ-hydroxyisovaleric acid. A typical macrotetrolide is nonactin, a 32-membered cyclic dodecaether.

(2) Carboxy ionophores, produced by various streptomyces cultures and sometimes called ionophores of the nigericin subclass. They are open-chain polyethers containing tetrahydrofurane and/or tetrahydropyrane rings; one end of the chain is terminated by a carboxy group and the other by one or two hydroxy groups.

(3) Proteins with N-containing macrocycles, such as porphyrin or corrin ring systems. Myoglobin and hemoglobin are well-known examples of these systems.

Three subclasses of synthetic ionophores are usually considered (Vögtle and Weber, 1979):

(1) Coronands, which are monocyclic molecules containing several coordination sites. The most widely studied coronands are cyclic polyethers known under a special shorthand nomenclature as "crown ethers" (Pedersen, 1967a,b), and cyclic polyamines.

(2) Cryptands, which are polycyclic polyethers with two amine bridgeheads. These compounds have three-dimensional cavities that may be tailored to the size required by different cations (Lehn, 1978). Some of these molecules contain two binding subunits and form dinuclear complexes by inclusion of two metal cations.

(3) Podands, which are acyclic coronand and cryptand analogs.

Until the later 1960's there has been considerable interest in the transition metal complexes of natural and synthetic ionophores (Lindoy, 1975). Reports on alkali and alkaline-earth complexes began to appear in the mid-60's and research in this area was stimulated by the synthesis of macrocyclic polyethers and cryptands. An introductory overview is presented by Weber and Vögtle (1981) while analytical applications are described by Kolthoff (1979), Blasius and Janzen

(1981), and Yoshio and Noguchi (1982). Trivalent lanthanide ions have a $4f^n5s^25p^6$ electronic configuration, resulting in weak crystal field and directional effects. Their chemical properties resemble those of the I_a and II_a cations, so that the investigation of their interaction with macrocyclic ligands is a logical extension of the work with alkali and alkaline-earth metals (Birnbaum, 1980; Bünzli and Wessner, 1984b). Moreover, such a study has additional specific motivations which include: (a) the systematic investigation of the coordination properties of the lanthanide ions; (b) the design of efficient separation and analytical processes; (c) the stabilization of unusual oxidation states, in particular R(II), and (d) the use of lanthanide complexes with ionophores as spectroscopic probes for the analysis of biological material.

In this review, we discuss the properties and applications of the complexes between rare earth ions and the following ligand classes: coronands (especially crown ethers and cyclic polyamines), cryptands, and podands. The properties of some complexes with proteins are also presented, in order to illustrate the use of lanthanide ions as spectroscopic probes, but not those pertaining to porphyrin chemistry (with one exception). The papers referred to in this chapter have been found by means of a computer search of Chemical Abstracts up to the end of March 1986.

2. Nomenclature

According to IUPAC rules, the following nomenclature should be used for the metal ions: lanthanides for Ce to Lu, lanthanoids for La to Lu, and rare earths for Y, Sc, and La to Lu. In this contribution, however, we shall loosely use these terms as synonymous and represent them by the symbol R. Moreover, when the notation La–Lu will be used, "La–Lu, except Pm" will usually be meant. (Promethium is indeed radioactive and very few chemists work with this element.)

The ionophores' nomenclature represents a more difficult problem, since IUPAC rules make the names of macrocyclic and macropolycyclic molecules quite involved. Therefore, simplified systems have been proposed by the discoverers of new ligand classes. Each system is, however, limited and cannot usually cope with the rapid expansion of this research area. A new proposal for a systematic nomenclature of synthetic ionophores was put forward by Weber and Vögtle (1980); this system allows an easier recognition of the ligand type and of other properties, e.g., its topology and the nature of its donor centers. Table 1 illustrates the different nomenclature systems. To keep our text as comprehensible as possible, we shall adopt the simplified nomenclature and notation depicted in fig. 1, in which most of the ligands cited in this contribution are reported. Coronands are designed by the capital letter C and podands by P. The total number of atoms in the ring is given before this letter and the number of heteroatoms after it; for example, 18C6 refers to an 18-membered macrocycle

CROWN ETHERS

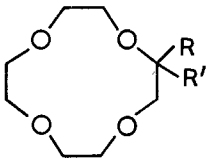

R = R' = H; **12C4**
R = R' = CH_3; **$Me_2$12C4**
R = CH_3, R' = $BrCH_2$;
BrMe,Me12C4

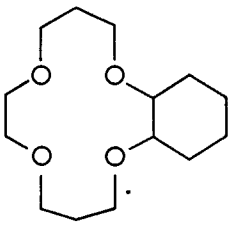

Cy14C4

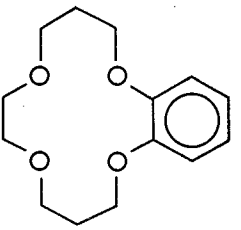

B14C4

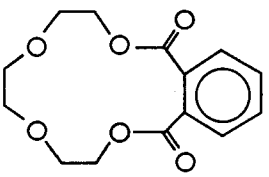

Ket$_2$B14C4

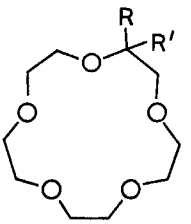

R = H
R' = H; **15C5**
R' = C_8H_{17}; **Oct15C5**
R' = $CH_2O(C_6H_4)OCH_3$
Lar15C5
R = CH_3
R' = $BrCH_2$; **BrMe,Me15C5**
R' = C_2H_5; **Et,Me15C5**
R' = C_3H_7; **Me,Prop15C5**

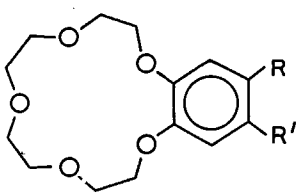

R = H, R' = H; **B15C5**
R' = $(CH_3)_3C$; **ButB15C5**
R' = Br ; **BrB15C5**
R' = NO_2; **NitrB15C5**
R' = CH_3COO; **AcB15C5**
R = CH_3; R' = Br; **Me,BrB15C5**

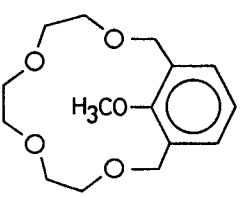

MeOB15C4

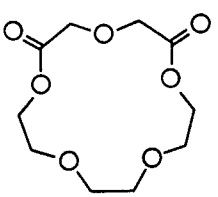

Ket$_2$15C5

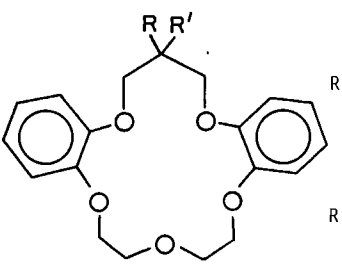

R = H
R' = OCH_2COOH
GlyB$_2$16C5
R' = $OCH(C_8H_{17})COOH$
2-OctGlyB$_2$16C5
R = C_8H_{17}; R' = OCH_2COOH
Oct,GlyB$_2$16C5

Fig. 1. Formulae, names, and abbreviations of most of the ionophores referred to in this review.

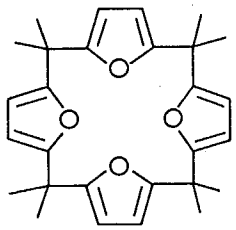

Fu16C4

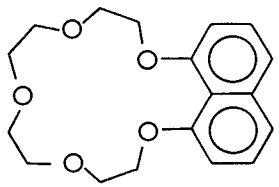

Napht16C5

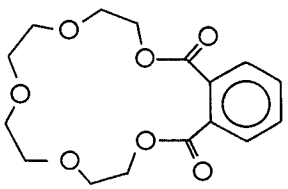

Ket$_2$B17C5

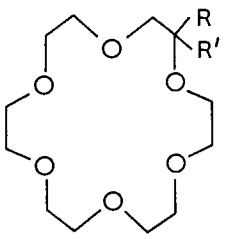

R = H
R' = H; **18C6**
R' = C_8H_{17}; **Oct18C6**
R = CH_3
R' = CH_3; **Me$_2$18C6**
R' = $BrCH_2$; **BrMe,Me18C6**
R' = C_2H_5; **Et,Me18C6**
R' = C_3H_7; **Me,Prop18C6**

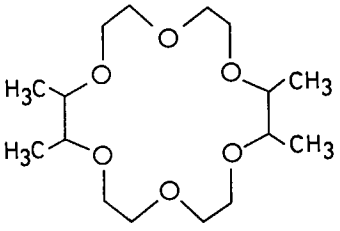

Me$_4$18C6

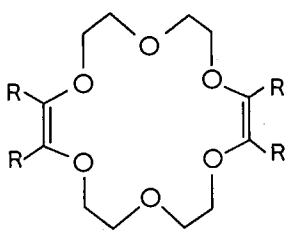

R = C_6H_5; **Ph$_4$18C6**

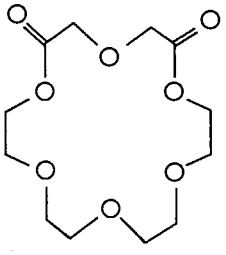

Ket$_2$18C6

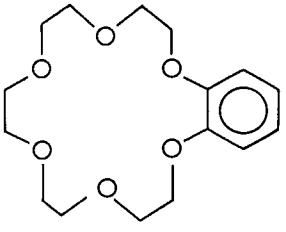

B18C6

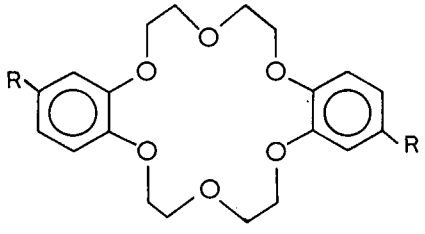

R = H; **B$_2$18C6**
R = $(CH_3)_3C$; **But$_2$B$_2$18C6**

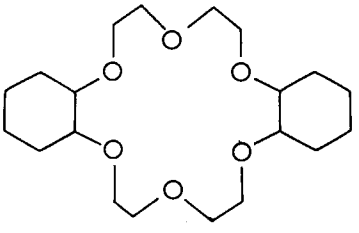

Cy$_2$18C6

Fig. 1 (*continued*).

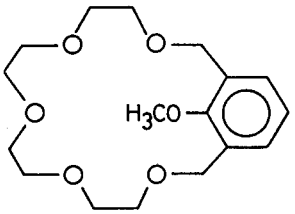

MeOB18C5

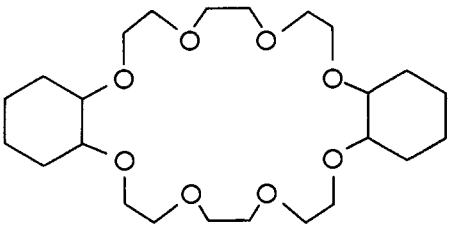

$Cy_2$24C8

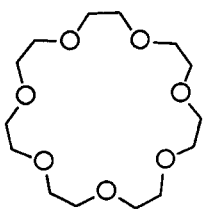

21C7

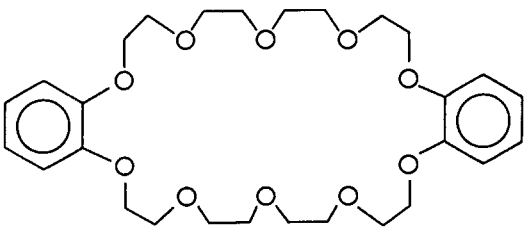

$B_2$30C10

POLYCROWNS

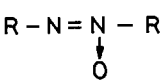

R = B15C5
Az(B15C5)$_2$

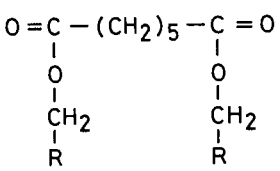

R = B15C5 Hept(B15C5)$_2$
R = B18C6 Hept(B18C6)$_2$

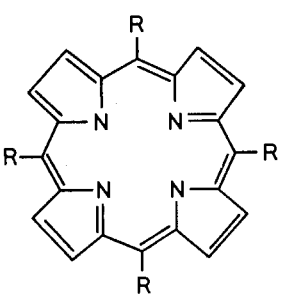

R = B15C5; (B15C5)$_4$Por
R = $B_2$18C6; ($B_2$18C6)$_4$Por

Fig. 1 (*continued*).

BICYCLIC CROWN ETHERS

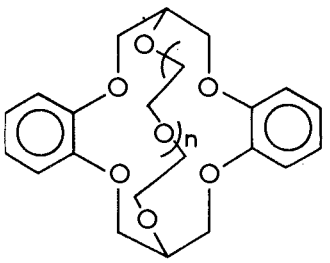

n = 1
Bicy(3,2B,2B)
n = 2
Bicy(4,2B,2B)
n = 3
Bicy(5,2B,2B)

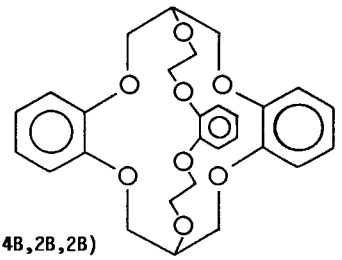

Bicy(4B,2B,2B)

CYCLIC POLYAMINES

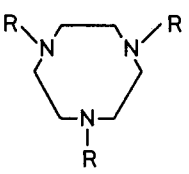

R = H; $N_3$9C3
R = CH_3; Me_3-$N_3$9C3

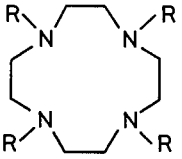

R = H; $N_4$12C4
R = CH_3; Me_4-$N_4$12C4

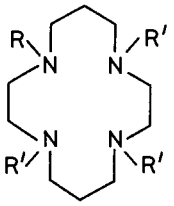

R = R' = H;
cyclam, $N_4$14C4
R = H, R' = CH_3;
Me_3cyclam, Me_3-$N_4$14C4
R = R' = CH_3
Me_4cyclam, Me_4-$N_4$14C4

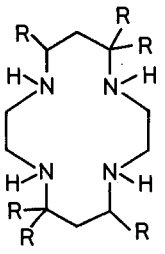

Me_6cyclam
$Me_6N_4$14C4

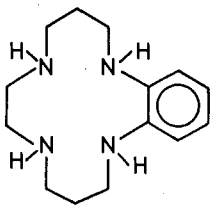

Bcyclam
$BN_4$14C4

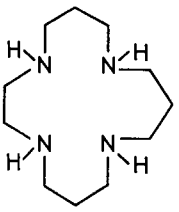

$N_4$15C4

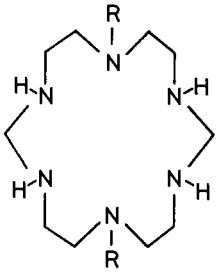

R = H; $N_6$16C6
R = $C_2H_4NH_2$; $(aet)_2N_6$16C6

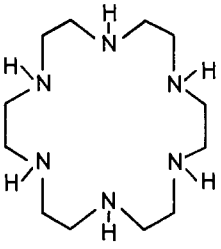

$N_6$18C6

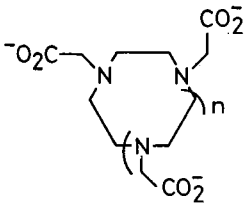

n = 1; NOTA n = 3; TETA

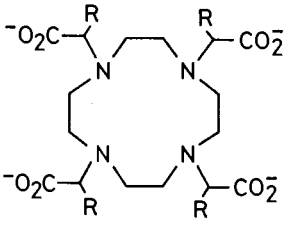

R = H; DOTA R = CH_3; DOTMA

Fig. 1 (*continued*).

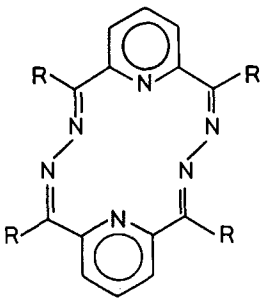

R = CH_3; **$Py_2Me_4N_6$14C6ene$_4$**

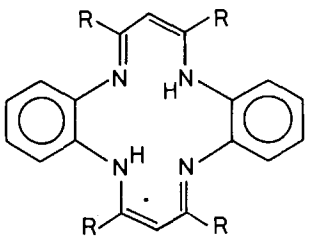

R = CH_3; **$B_2Me_4N_4$14C4ene$_4$**

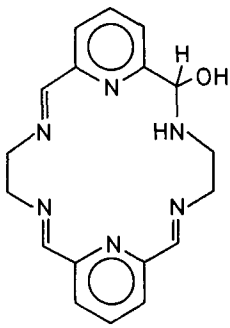

OHP$y_2N_6$18C6ene$_3$

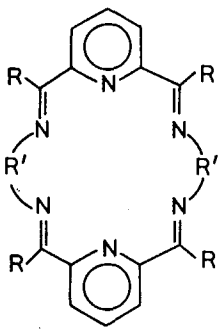

R = H,
R' = CH_2CH_2; **$Py_2N_6$18C6ene$_4$**
R' = $CH_2CH(CH_3)$; **$Py_2Me_2N_6$18C6ene$_4$**
R' = $CH_2CH_2CH_2$; **$Py_2N_6$20C6ene$_4$**
R = CH_3,
R' = CH_2CH_2; **$Py_2Me_4N_6$18C6ene$_4$**
R' = C_6H_4; **$Py_2B_2Me_4N_6$18C6ene$_4$**

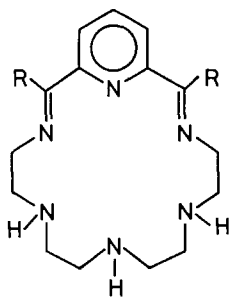

R = CH_3; **$PyMe_2N_6$18C6ene$_2$**

N,O,P, AND S-CONTAINING CORONANDS

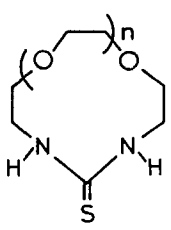

n = 1; **ThioN$_2$O$_2$11C4**
n = 2; **ThioN$_2$O$_3$14C5**
n = 3; **ThioN$_2$O$_4$17C6**

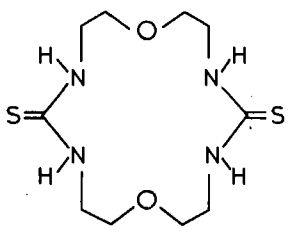

Thio$_2$N$_4$O$_2$16C6

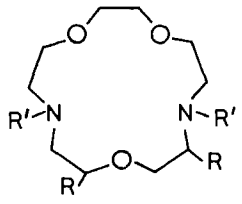

R = R' = H; **$N_2O_3$15C5, (2,1)**
R = CO, R' = H; **Ket$_2$(2,1)**
R = H, R' = CH_2CO_2H; **(2,1)DA**

Fig. 1 (*continued*).

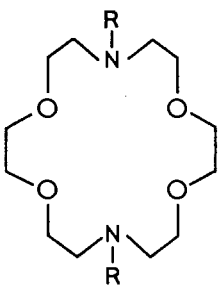

R = H; **$N_2O_4$18C6, (2,2)**
R = CH_2CO_2H; **(2,2)DA**

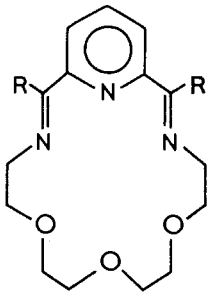

R = CH_3; **$PyMe_2N_3O_3$18C6ene$_2$**

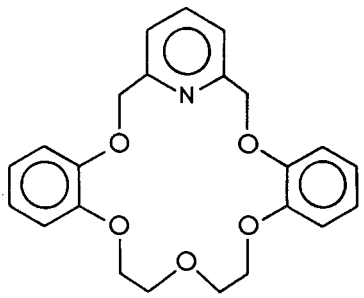

$PyB_2NO_5$18C6

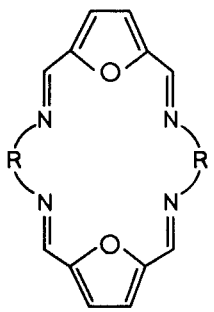

R = CH_2CH_2; **$Fur_2N_4O_2$18C6ene$_4$**
R = $CH_2CH(CH_3)$; **$Fur_2Me_2N_4O_2$18C6ene$_4$**
R = $CH_2CH_2CH_2$; **$Fur_2N_4O_2$20C6ene$_4$**

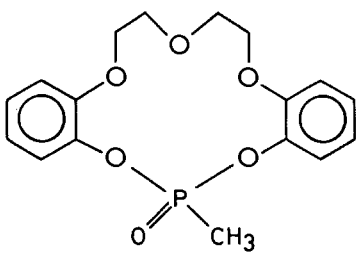

$B_2PO_5$14C6

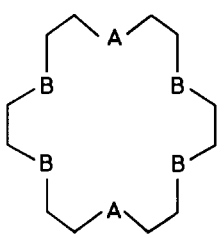

A = O, B = S; **$O_2S_4$18C6**
A = S, B = O; **$O_4S_2$18C6**
A = S, B = S; **$S_6$18C6**

CRYPTANDS

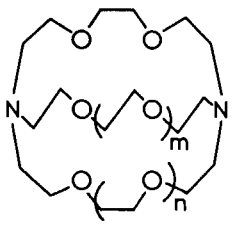

m = 0, n = 0; **(2,1,1)**
m = 0, n = 1; **(2,2,1)**
m = 1, n = 1; **(2,2,2)**

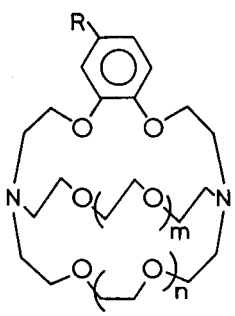

m = 0, n = 1
R = H; **(2B,2,1)**
R = NH_2; **(2aB,2,1)**
R = NO_2; **(2nB,2,1)**
m = 1, n = 1
R = H; **(2B,2,2)**

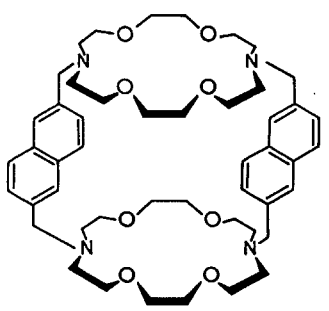

$Naph_2(2,2)_2$

Fig. 1 (*continued*).

PODANDS

$HO(CH_2CH_2O)_nH$

n = 1; **E02**
.....
n = 7; **E08**

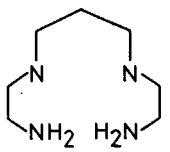

$N_4$11P4, 2,3,2Tet

$R-O(CH_2CH_2O)_n-R$

R = CH_3,	n = 1; **6P2**
	.....
	n = 5; **18P6**
R = C_4H_9,	n = 1; **But7P1**
R = C_9H_6N,	n = 4; **$Q_2$13P5**
R = Ph_2NCOCH_2,	n = 2; **A9P3**

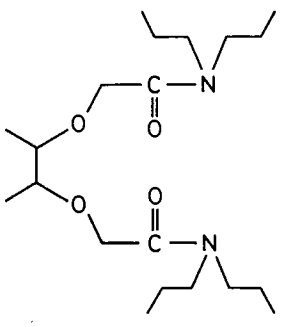

Pod1

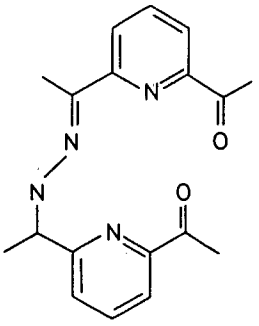

Pod2

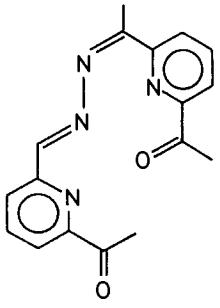

Pod3

NATURAL IONOPHORES

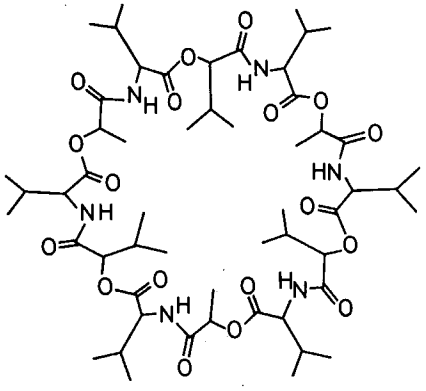

Valinomycin, **Val**

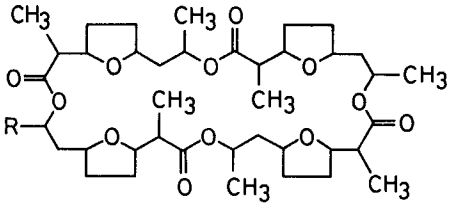

R = CH_3; nonactin, **Non**
R = CH_3CH_2; monactin, **Mon**

Lasalocid (X537A); **Las**

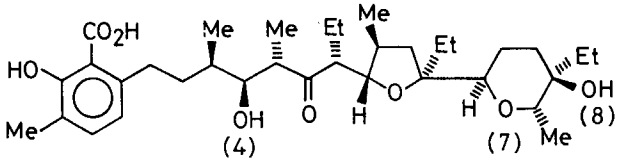

Fig. 1 (*continued*).

TABLE 1
Nomenclature systems for podands, coronands, and cryptands.

	podands	coronands	cryptands
IUPAC name	2,5,8,11,14,17-hexaoxaoctadecane	1,4,7,10,13,16-hexaoxacyclooctadecane	4,7,13,16,21,24-hexaoxa-1,10-diazabicyclo[9.9.9]hexacosane
Weber and Vögtle (1980)	1,16-dimethyl-$\langle O_6$podand-6$\rangle$	18$\langle O_6$coronand-6$\rangle$	$\langle N[O_2]_3N$-cryptand-8$\rangle$
Short or trivial name	pentaglyme	18-crown-6	(2,2,2)cryptand
Notation used in the present chapter	18P6	18C6 [a]	(2,2,2) [b]

[a] Other commonly used notations: [18]C-6, 18-6.
[b] Other commonly used notations: [2,2,2], [2.2.2].

with 6 heteroatoms; in absence of any indication, the latter are supposed to be oxygen atoms. Other heteroatoms are specifically written before the number of atoms in the ring; for example, $S_6$18C6 represents the above-mentioned coronand in which the O atoms have been substituted by S atoms. The abbreviations used for substituents can be easily understood and they are identical with those proposed by Izatt et al. (1985) in a recent review on the thermodynamics and kinetics of the metal-cation/macrocycle interaction. The cryptands are designated according to the numbers of $-CH_2-CH_2-O-$ units in each aliphatic chain fixed onto the N bridgeheads; these numbers are simply written in parentheses, e.g. (2,2,1).

In order to differentiate the metal complexes from the ligands, the suffix "ate" is substituted for "and": coronate, cryptate, podate.

3. Complexes with trivalent rare earth ions

Rare earth ions form quite stable solvates with polar solvents, so that their complexes with ionophores must usually be isolated from nonaqueous solutions in solvents with low to moderate donor strengths, e.g., acetone, acetonitrile or benzene (Wessner and Bünzli, 1985). The metal to ligand ratio depends upon the nature of the R(III) ion, of the counteranion X, and of the ligand L; sometimes, different experimental conditions lead to the isolation of complexes with different stoichiometries. There is usually a relationship between the stability of the complex and the degree of fit between ligand and cation, i.e., the ionic diameter to cavity diameter ratio. The R(III) ion may either be located inside the ligand cavity, i.e., encapsulated, or it can lie outside this cavity, being coordinated by a

more or less folded ligand. In most cases, the metal cation remains exposed to further bonding by the counteranions or by solvent molecules, even in cryptates, which explains why some of these complexes are isolated as solvates.

3.1. *Stoichiometry of the complexes*

The reported metal:ligand ratios range from 2:1 to 3:2, 4:3, 1:1, 1:2, and, possibly 1:3 (in solution). In this section, the different stoichiometries obtained in the solid state are discussed according to the various ligand classes.

A list of the crown ether complexes for which either an elemental analysis or a structure is available, is given in table 2; the solvation of these complexes has been omitted for the sake of clarity. To rationalize the metal:ligand ratios observed, four main factors should be considered:

(1) the ionic diameter to cavity diameter ratio D_{ic};

(2) the nature of the counteranion, in particular its ability to coordinate the metal ion and its steric hindrance;

(3) the macrocycle flexibility, which determines its ability to adapt itself to the size of the metal ion;

(4) the number of donor atoms of the ligand or, more correctly, the need for the R(III) ion to achieve a high coordination number, usually between 8 and 12.

The first criterion is not easy to quantify, since both diameters are difficult to estimate. The effective ionic diameters of the R(III) ions strongly depend on both the atomic number and the coordination number CN: a difference of about 0.4 Å is found between La(III) and Lu(III) and, for a given R(III) ion, between CN = 8 and CN = 12. The cavity diameter depends upon the conformation adopted by the ligand and may be estimated either from molecular models or from crystal structure determinations (table 3).

In absence of appreciable anion interaction, i.e., with ClO_4^- or PF_6^-, the approximate rule holds: if D_{ic} is larger than one, sandwich 1:2 complexes are isolated, while 1:1 compounds form if $D_{ic} < 1$. On the other hand, with the strongly coordinating and bidentate nitrate ion, one observes the easy formation of 1:1 complexes when $D_{ic} > 1$; if $D_{ic} < 1$, the strong anion/cation interaction plays a decisive role; with unsubstituted crown ethers, complexes are formed that contain polynitrato anionic species $[Ln(NO_3)_5]^{2-}$, or $[Ln(NO_3)_6]^{3-}$, corresponding to 3:2 or 4:3 metal:ligand ratios. The 4:3 complexes can either be crystallized out of solutions (18C6, 21C7), or be obtained by thermal decomposition of the corresponding 1:1 complexes (15C5, 18C6; Ammann and Bünzli, 1979). Less data are available for halides and isothiocyanates; nevertheless, it appears that these anions have a similar influence as nitrate. In particular, 4:3 complexes also form; this may be understood considering the large stability of hexakis(halogeno) or hexakis(isothiocyanato) species. The trifluoromethanesulfonate ion (triflate, TRIF) is often proposed as a substitute for the potentially dangerous perchlorate. In fact, it behaves quite differently from the other weakly coordinating anions:

TABLE 2
Stoichiometry of the complexes isolated with crown ethers. [a]

Complex	M:L ratio	Counteranion [R(III) ions]	References
12-crown-4 ether, 12C4	1:2	ClO_4^- (La–Lu) [b]	Desreux and Duyckaerts (1979), Bünzli et al. (1981b)
	1:1	Cl^- (Pr, Eu), Br^- (Eu), $CF_3SO_3^-$ (Pr)	Bünzli and Wessner (1984a)
		NO_3^- (La–Lu)	Bünzli and Wessner (1980)
		CF_3COO^- (La, Ce, Pr)	Bünzli and Giorgetti (1985b)
	3:2	CF_3COO^- (Pr, Eu, Er)	Bünzli and Giorgetti (1985b)
	2:1	CF_3COO^- (Pr, Nd, Sm)	Bünzli and Giorgetti (1985b)
substituted 14-crown-4 ether, Ket_2B14C4	1:1	NO_3^- (Sc)	Tan Minyu et al. (1983)
substituted 15-crown-4 ether, MeOB15C4	1:1	NO_3^- (Dy)	Tomat et al. (1985)
15-crown-5 ether, 15C5	1:2	ClO_4^- (La–Eu) [b]	Bünzli et al. (1979a, 1981b)
		PF_6^- (La–Sm, Gd)	Bünzli and Giorgetti (1985a)
	1:1	NO_3^- (La–Lu)	Bünzli and Wessner (1978, 1981)
		Cl^- (Pr, Eu), Br^- (Eu), NCS^- (Pr), $CF_3SO_3^-$ (Pr)	Bünzli et al. (1979a, 1982c), Bünzli and Wessner (1984a)
	4:3	NO_3^- (Gd–Lu)	Bünzli and Wessner (1981)
	2:1	CF_3COO^- (La–Eu) [c]	Bünzli and Giorgetti (1985b)
benzo-15-crown-5 ether, B15C5	1:1	NO_3^- (Y, La–Lu)	Heckley and King (1973), King and Heckley (1974), Wan Jie et al. (1983), Ren Dehou et al. (1983), Jiang Haiying et al. (1983a,c)
		Cl^- (Nd, Eu)	Seminara and Musumeci (1980)
		NCS^- (Sc, La–Lu)	Cassol et al. (1973), Olszanski and Melson (1978)
	3:2	NCS^- (Sc)	Cassol et al. (1973), Olszanski (1975)
substituted benzo-15-crown-5 ether, NitrB15C5	1:1	NO_3^- (Y, La–Sm, Dy, Er, Lu)	Xiao Wenjin et al. (1985)
substituted benzo-15-crown-5 ether, ClB15C5, BrB15C5, AcB15C5	1:1	NO_3^- (La–Nd)	Wan Zhuli et al. (1982), Wang Genglin et al. (1982)
		NCS^- (Y)	Wang Genglin and Yan Shiping (1981)
substituted 17-crown-5 ether, Ket_2B17C5	1:1	NO_3^- (Sc)	Tan Minyu et al. (1983)
substituted 18-crown-5 ether, MeOB18C5	1:1	NO_3^- (Sm)	Tomat et al. (1983)
18-crown-6 ether, 18C6	1:2	PF_6^- (Ce, Nd)	Bünzli and Giorgetti (1985a)
	1:1	ClO_4^- (Pr, Eu)	Bünzli et al. (1979a)
	1:1	NO_3^- (La–Lu)	Bünzli and Wessner (1978, 1981), Backer-Dirks et al. (1980)
		NO_3^- (Y, Sc)	Jiang Haiying et al. (1983b), Xue Hongfu et al. (1983)
		Cl^- (Pr, Eu)	Bünzli et al. (1979), Bünzli and Wessner (1984a)
		Cl^- (Gd)	Forsellini et al. (1985)
		Br^- (Eu)	Bünzli and Wessner (1984a)

TABLE 2 (continued)

Complex	M:L ratio	Counteranion [R(III) ions]	References
		NCS^-(Pr)	Bünzli et al. (1979a)
		$CF_3SO_3^-$(Pr)	Bünzli et al. (1982c)
		CF_3COO^-(La–Eu)	Bünzli and Giorgetti (1985b)
	4:3	NO_3^-(La–Lu)	Bünzli and Wessner (1978, 1981) Backer-Dirks et al. (1980)
		Cl^-, Br^-(Pr)	Bünzli et al. (1982c), Bünzli and Wessner (1984a)
		Cl^-(Sm, Yb)	Wang Xin and Tan Minyu (1984)
	2:1	CF_3COO^-(Y, Eu–Er, Yb)	Bünzli and Giorgetti (1985b)
dicyclohexyl-18-crown-6 ether, $Cy_2$18C6	1:1	NO_3^-(La–Eu, Ho), Cl^-(La–Eu), NCS^-(La–Eu)	Seminara and Musumeci (1980)
	3:2	NO_3^-(La–Nd)	Gao Yuan et al. (1985)
dibenzo-18-crown-6 ether, $B_2$18C6	1:2	NCS^-(Y)	Olszanski and Melson (1978)
	1:1	ClO_4^-(La–Eu, Dy–Er, Yb)	Ciampolini et al. (1979b), Xiao Wenjin et al. (1981)
		NO_3^-(La–Nd)	Heckley and King (1973), King and Heckley (1974)
		NO_3^-(La, Pr, Nd, Er)	Kalishevich et al. (1984), Gren et al. (1984)
		Cl^-(Sc), (La, Nd–Eu, Dy, Er)	Olszanski and Melson (1978), Kohata et al. (1985)
		NCS^-(Y)	Wang Genglin et al. (1980)
	3:2	Cl^-(Eu)	Bünzli and Wessner (1984a)
substituted-18-crown-6 ether, $Ph_4$18C6ene$_2$	1:1	NO_3^-(Y, La–Nd, Sm)	Wang Jingqiu et al. (1983, 1985)
21-crown-7 ether, 21C7	1:1	NO_3^-(Er, Yb)	Wessner et al. (1982)
	4:3	NO_3^-(La–Nd, Eu, Tb, Lu)	Wessner et al. (1982)
dicyclohexyl-24-crown-8 ether, $Cy_2$24C8	2:1	Cl^-(Sm, Yb)	Wang Xin and Tan Minyu (1984)
dibenzo-30-crown-10 ether, $B_2$30C10	1:1	ClO_4^-(La–Eu, Dy–Yb)	Ciampolini and Nardi (1979)

[a] The solvation of the complexes is not taken into account.
[b] 1:1:1 mixed complexes containing 12-crown-4 and 15-crown-5 ethers have also been isolated (R = Pr–Gd; Bünzli et al., 1979a, 1981b).
[c] These complexes undergo hydrolysis.

sandwich 1:2 complexes are not isolated with this anion but, instead, 1:1 complexes form. This might be related to some degree of association between triflate and R(III) ions, since it has been shown that triflate association with the metal ion induces only slight structural changes in the anion and will therefore often be undetected, for instance by vibrational spectroscopy (Humphrey et al., 1983). Smith and Raymond (1985) have published two crystal structures of coronates in which TRIF anions are found to be coordinated to La(III) and Yb(III). The trifluoroacetate anion (TFA) is potentially bidentate and/or bridging, its donor strength is moderate, and it has a large steric hindrance due to the

TABLE 3
Selected ionic diameters D_i of R(III) ions [a] and cavity diameters D_c of unsubstituted crown ethers.

R	D_i (Å)				Crown ether	D_c (Å)		
	CN = 8	CN = 9	CN = 10	CN = 12		uncomplexed [b]	uncomplexed [c]	complexed [c]
La	2.32	2.43	2.54	2.72	12C4	1.2–1.5	1.5 [d]	1.3 [e]–1.4 [f]
Nd	2.22	2.33	2.45	2.59	15C5	1.7–2.2	not available	1.9 [g]
Eu	2.13	2.24	2.36	2.50	18C6	2.6–3.2	2.7	2.5 [h]
Er	2.01	2.12	2.23	2.38	21C7	3.4–4.3	not available	not available
Lu	1.95	2.06	2.18	2.32				

[a] Inter- or extrapolated from ionic radii versus CN plots (Shannon, 1976).
[b] From molecular models (Dobler, 1981; Dalley, 1978).
[c] From crystal structure determinations.
[d] Groth (1978).
[e] Boer et al. (1974).
[f] Bünzli et al. (1982b).
[g] Bünzli et al. (1982a).
[h] Dalley (1978), Bünzli et al. (1980a).

bulky CF_3 group. These features explain the formation of complexes with various metal:ligand ratios (2:1, 3:2, 1:1). The 2:1 complexes are thermally more stable; they contain polymeric species, reflecting the tendency of the TFA anions to form bridges between metal ions in order to minimize the steric hindrance of the CF_3 groups.

The influence of the ligand flexibility is seen when the R(III) ion is encapsulated in the macrocycle. For instance, 1:1 coronates may be isolated between lanthanide nitrates and 18C6 for La–Lu, while with the more rigid $B_2$18C6, these complexes only form with the larger R(III) ions (La–Nd). Replacing two O atoms of the 18C6 by –NH groups results in a better flexibility of the ring and the 1:1 complexes are more stable than the corresponding 18C6 coronates.

The achievement of a high CN for the R(III) ion is also an important requirement. For instance, mixed perchlorato complexes with 12C4 and 15C5 (CN = 9) do not form for La and Ce, because the 1:2 15C5 coronates (CN = 10) are much more stable and steric hindrance prevents any ClO_4^- association.

Complexes isolated with coronands other than crown ethers are reported in table 4. They all have a 1:1 metal:ligand ratio. Lanthanide ions bind quite strongly to amine groups, which insures an easy formation of the coronates with cyclic amines: the La complex with ligand $Py_2Me_4N_6$18C6ene$_4$ may even be isolated from aqueous solutions. Many complexes with cyclic amines are synthesized via template reactions. The substitution of ether groups by thioether functions has, on the other hand, a destabilizing effect, since these functional groups have a low affinity for hard cations; the complexes with $O_2S_2$18C6, $O_2S_4$18C6, and $S_6$18C6 are therefore difficult to synthesize. The complexes between R(III) and the anionic polyamino polyacetate macrocycles have essen-

TABLE 4
List of isolated 1:1 coronates with ligands other than crown ethers. [a]

	Ligand	Counterion [R(III)]	References
N-containing coronands:	$ThioN_2O_211C4$	$acac^{2-}$ (La, Pr–Sm) [b]	Timofeev et al. (1983)
	$ThioN_2O_314C5$	$acac^{2-}$ (Pr–Sm, Yb) [b]	Timofeev et al. (1983)
	$ThioN_4O_216C6$	$acac^{2-}$ (Nd) [b]	Timofeev et al. (1983)
	$ThioN_2O_417C6$	$acac^{2-}$ (Nd) [b]	Timofeev et al. (1983)
	(2,1)	Cl^- (La–Yb, except Ce)	Almasio et al. (1983)
	(2,2)	NO_3^- (La–Lu)	Desreux et al. (1977), Desreux (1978)
		Cl^- (Sm, Eu)	Almasio (1983)
		$CF_3SO_3^-$ (Sm)	Loufouilou (1986)
	$B_2Me_4N_414C4ene_4$	NCS^- (Sc)	Olszanski and Melson (1977)
	$Py_2Me_4N_414C6ene_4$	ClO_4^- (Sc, Tb–Lu)	Radecka-Paryzek (1979, 1981a)
	$(aet)_2N_616C6$	$CF_3SO_3^-$ (La, Yb)	Smith and Raymond (1985)
	PyB_2NO_518C6	NO_3^- (La, Ce, Pr)	Weber and Vögtle (1976)
	$PyMe_2N_3O_318C6ene_2$	NO_3^- (La, Ce, Nd, Sm)	Arif et al. (1985)
	$Fur_2N_4O_218C6ene_4$	NO_3^- (La–Eu)	Abid and Fenton (1984b)
	$Fur_2Me_2N_4O_218C6ene_4$	NO_3^- (La–Pr)	Abid and Fenton (1984b)
	$PyMe_2N_618C6ene_2$	ClO_4^- (Eu)	Wang Genglin and Miao Lan (1984)
	$Py_2N_618C6ene_4$	NO_3^- (La–Lu)	Abid and Fenton (1984a)
	$Py_2Me_2N_618C6ene_4$	NO_3^- (La–Lu)	Abid and Fenton (1984a)
	$Py_2Me_4N_618C6ene_4$	NO_3^- (La–Lu)	Backer-Dirks et al. (1979), Wang Genglin and Miao Lan (1984), Abid et al. (1984)
		ClO_4^- (La–Tb)	Radecka-Paryzek (1980), Wang Genglin and Miao Lan (1984)
	$Py_2B_2Me_4N_618C6ene_4$	NO_3^- (La–Nd)	Radecka-Paryzek (1981b, 1985)
	$Py_2N_620C6ene_4$	NO_3^- (La–Lu)	Abid and Fenton (1984a)
	$Fur_2N_4O_220C6ene_4$	NO_3^- (La–Pr)	Abid and Fenton (1984b)
S-containing coronands:	S_2O_418C6	ClO_4^- (La–Eu, Ho, Yb)	Ciampolini et al. (1980)
	S_4O_218C6	ClO_4^- (Eu)	Ciampolini et al. (1980)
	S_618C6	ClO_4^- (Sm, Eu, Yb)	Ciampolini et al. (1980)
Aminocarboxylic acid derivatives: (anionic ligands)	DOTA	Na^+ (Eu)	Spirlet et al. (1984a)
	DOTMA	(Eu, Tb)	Brittain and Desreux (1984)
	TETA	Na^+ (Tb)	Spirlet et al. (1984b)

[a] The solvation of the complexes is not indicated.
[b] In the gaseous phase only.

tially been studied in solution (as potential shift reagents, vide infra) and few elemental analyses are reported. These ligands are excellent sequestering agents for rare earth ions and the resulting complexes are among the most stable known.

Rare earth cryptates (table 5) are more stable than coronates and are highly kinetically inert towards dissociation in aqueous solutions. They can therefore be studied in water, but hydrolysis hinders their synthesis in this solvent. On the contrary, the preparation of unsolvated 1:1 complexes requires anhydrous conditions (Gansow and Triplett, 1981). The hydrated lanthanide salt solutions in

TABLE 5
Stoichiometry of the complexes isolated with bicyclic crown ethers and with cryptands. [a]

Ligand	M:L	Counterion [R(III)]	References
Bicy(X,2B,2B), X = 3, 4, 5, or 4B	1:1	Cl^- (La, Nd, Sm, Gd) [b]	Benetollo et al. (1984, 1985a), Truter et al. (1985)
(2,2,1)	1:1	ClO_4^- (La–Lu)	Pruett (1978), Seminara and Musumeci (1980), Gansow and Triplett (1981)
		NO_3^- (La–Lu)	Pruett (1978), Kausar (1978), Gansow and Triplett (1981)
		Cl^- (La–Lu)	Gansow et al. (1977), Pruett (1978), Gansow and Triplett (1981), Almasio et al. (1983)
		$CF_3SO_3^-$ (Sm)	Loufouilou (1986)
	4:3	NO_3^- (La, Tb, Dy)	Pruett (1978), Seminara and Musumeci (1980), Strawczynski (1981)
	3:2	NO_3^- (Ho, Yb), Cl^- (Dy)	Pruett (1978)
	2:1	NO_3^- (Nd, Sm, Eu)	Seminara and Musumeci (1980), Pruett (1978)
(2B,2,1)	1:1	ClO_4^-, NO_3^-, Cl^- (La–Lu)	Kausar (1978), Gansow and Triplett (1981), Gansow and Kausar (1985)
(2aB,2,1)	1:1	NO_3^- (La, Pr, Eu)	Kausar (1978), Gansow and Kausar (1983)
(2nB,2,1)	1:1	NO_3^- (La, Ce, Eu)	Kausar (1978)
(2,2,2)	1:1	ClO_4^- (La–Lu)	Ciampolini et al. (1979a), Gansow and Triplett (1981)
		NO_3^- (La–Lu)	Gansow et al. (1977), Pruett (1978), Kausar (1978), Gansow and Triplett (1981)
		Cl^- (La–Lu)	Pruett (1978), Gansow and Triplett (1981), Almasio et al. (1983)
		$CF_3SO_3^-$ (Sm)	Loufouilou (1986)
		Cl^-, CPh_3^- (La)	Campari and Hart (1982)
	4:3	NO_3^- (La)	Hart et al. (1978)
	3:2	NO_3^- (Sm–Gd)	Pruett (1978)
		Cl^- (Eu)	Strawczynski (1981)
	2:1	NO_3^- (Pr–Eu, Er, Yb, Lu)	Pruett (1978), Burns (1979), Seminara and Musumeci (1980)
$Naph_2(2,2)_2$	1:1, 2:1	NO_3^- (Eu)	Plancherel et al. (1985)

[a] The solvation of the complexes is not indicated.
[b] These complexes hydrolyse to give hydroxo compounds.

weakly coordinating organic solvents (e.g., acetonitrile) are treated by triethylorthoformate prior to complexation with equimolar quantities of cryptand. The crystallization of the complexes is then induced by concentration of the solution and by addition of a nonpolar solvent. This synthetic procedure is claimed to produce unsolvated 1:1 cryptates with all the lanthanide perchlorates, nitrates, and chlorides. When the experimental conditions are less well controlled, various adducts may be isolated, including solvated 1:1, 4:3, 3:2, and 2:1 cryptates. In particular, metal:ligand ratios larger than one tend to be obtained when a polar solvent is used, e.g., methanol. It is noteworthy that only (2,2,1) and (2,2,2)

TABLE 6
Complexes isolated with podands and with naturally occurring ionophores.

Ligand	M:L	Counterion [R(III)]	References
EO3	1:1	NO_3^- (Pr–Eu)	Hirashima et al. (1983b)
EO4, EO5, EO6	1:1	NO_3^- (Y, La–Lu)	Hirashima et al. (1983b), Hirashima and Shiokawa (1979)
		Cl^- (Y, La–Lu)	Hirashima et al. (1983a)
EO8	2:1	NO_3^- (La, Ce)	Hirashima et al. (1983b)
15P5	1:1	NO_3^- (La–Sm)	Hirashima and Shiokawa (1979)
		Cl^- (La–Ho)	Hirashima et al. (1983a,b)
18P6	1:1	NO_3^- (La)	Bünzli et al. (1984)
		Cl^- (La, Pr)	Hirashima et al. (1983a)
	4:3	NO_3^- (La–Eu)	Hirashima et al. (1983b), Bünzli et al. (1984)
21P7	4:3	NO_3^- (La–Nd)	Hirashima et al. (1983b)
Pod1	1:2	BF_4^- (Eu)	Albin et al. (1983)
Pod2	3:2	NO_3^- (Pr, Nd)	Tümmler et al. (1977), Vögtle (1979)
Pod3	1:2	ClO_4^- (La, Pr–Sm)	Radecka-Paryzek (1981a)
	1:1	ClO_4^- (Eu–Lu)	Radecka-Paryzek (1981a)
[a]	1:2	ClO_4^- (Ce)	Thomas and Palenik (1980)
Las	1:2	La, Gd [b]	Hanna et al. (1983)

[a] 2,6-diacetylpyridine bis(semicarbazone).
[b] Isolated as $Ln(Las)_3 \cdot xCH_3CN$ (x between 1 and 2).

cryptands form crystalline complexes with R(III) ions. Their cavities indeed provide a good fit for the lanthanide ions: $D_c = 2.3$ and 2.8 Å, respectively.

Metal complexes with podands are usually less stable and more labile than the corresponding coronates and cryptates. This is also true for rare earth ions, although the macrocyclic and macrobicyclic effects tend to be smaller than those observed for M(I) and M(II) ions, which have a smaller cationic charge. Some rare earth podates and complexes with naturally occurring ionophores are listed in table 6.

3.2. *Structural data*

3.2.1. *Crystal structure determinations*

Several rare earth complexes with ionophores have been studied by single-crystal X-ray diffraction methods and structures have been solved for 32 coronates, 6 bicyclic coronates and cryptates, and 7 podates (table 7). The trivalent ions most studied are lanthanum (16 structures), praseodymium (3), neodymium (7), samarium (5), and europium (5). Nitrate was often chosen as counteranion, since its strong coordinative properties make the complexes less sensitive to

TABLE 7

Structural data for rare earth complexes with synthetic ionophores.

Ligand L	R	Anion	R:L	Space group	Complex species (with symmetry)	CN	Mean R–X distances (Å)		References
							R–ligand	R–anion and/or R–OH	
12C4	Y	NO_3^-	1:1	$P2_1/c$	$[Y(NO_3)_3L]$	10	2.46(4)	2.44(5)	Rogers and Kurihara (1986)
	Eu	NO_3^-	1:1	$P2_1/c$	$[Eu(NO_3)_3L]$	10	2.52(4)	2.47(4)	Bünzli et al. (1982b)
DOTA	Eu	–	1:1	$P\bar{1}$	$[Eu(DOTA)(H_2O)]^-$	9	N: 2.68(16) O: 2.39(11)	2.48	Spirlet et al. (1984a)
$Py_2Me_4N_6$-14C6ene$_4$	Sm	NO_3^-	1:1	$P\bar{1}$	$[Sm(NO_3)(OH)L(H_2O)]^+$	10	2.63(1)	2.51(1) 2.49(4) *	Abid et al. (1984), Fenton et al. (1984)
MeOB15C4	Dy	NO_3^-	1:1	$P\bar{1}$	$[Dy(NO_3)_3(H_2O)_3]$ [a]	9	2.35(2) *	2.45(3)	Tomat et al. (1985)
15C5	La	ClO_4^-	1:2	$P2_1/c$	$[LaL(H_2O)_4]^{3+}$ [b]	9	2.53(3)	2.43(2)	Lee et al. (1985)
	Sm	ClO_4^-	1:2	$P2_1/c$	$[SmL(H_2O)_4]^{3+}$ [b]	9	2.51(2)	2.43(3)	Lee et al. (1983)
	La	NO_3^-	1:1	$P2_1/c$	$[La(NO_3)_3L]$	11	2.69(4)	2.62(4)	Lu Pinzhe et al. (1983)
	Ce	NO_3^-	1:1	$P2_1/a$	$[Ce(NO_3)_3L]$	11	2.57(6)	2.72(9)	Lin Yonghua and Xingyan (1983)
	Pr	NO_3^-	1:1	$P2_1/a$	$[Pr(NO_3)_3L]$	11	2.55(7)	2.69(8)	Lin Yonghua et al. (1982)
	Nd	NO_3^-	1:1	$P2_1/c$	$[Nd(NO_3)_3L]$	11	2.65(4)	2.55(4)	Lu Pinzhe et al. (1983)
	Eu [c]	NO_3^-	1:1	$P3_2$	$[Eu(NO_3)_3L]$	11	2.63(6)	2.53(8)	Bünzli et al. (1982a)
	Pr	TFA	2:1	$P2_1/m$	$[Pr_2(TFA)_2(OH)L_2]^{2+}$	9	2.59(2)	2.45(2) 2.31 *	Harrison et al. (1985)
					$[Pr_2(TFA)_8]_n^{2n-}$	8		2.46(2)	
TETA	Tb	–	1:1	P2/c	$[Tb(TETA)]^-$	8	N: 2.60(2) O: 2.31(1)		Spirlet et al. (1984b)
Napht16C5	La	NO_3^-	1:1	$P2_1/n$	$[La(NO_3)_3L]$	11	2.67(7)	2.60(2)	Wan Zhuli et al. (1982)
$(aet)_2N_6$16C6	La	TRIF	1:1	$P\bar{1}$	$[La(TRIF)_2L]^+$, C_2	10	2.73(6)	2.61(3)	Smith and Raymond (1985)
	Yb	TRIF	1:1	$P\bar{1}$	$[Yb(TRIF)L]^{2+}$	9	2.52(7)	2.39	Smith and Raymond (1985)
MeOB18C5	Sm	NO_3^-	1:1	$P2_1P2_1P2_1$	$[Sm(NO_3)_3L(H_2O)]$	10	2.61(10)	2.51(4)	Tomat et al. (1983)
18C6	La	NO_3^-	1:1	Pbca	$[La(NO_3)_3L]$	12	2.72(6)	2.66(1)	Backer-Dirks et al. (1980)
	Nd	NO_3^-	1:1	Pbca	$[Nd(NO_3)_3L]$	12	2.70(10)	2.60(2)	Bünzli et al. (1980), Bombieri et al. (1980)
	Gd	NO_3^-	1:1	$Pn2_1/a$	$[Gd(NO_3)_3(H_2O)_3]$ [a]	9	2.39(8)	2.45(4)	Backer-Dirks et al. (1980)
	Gd	Cl^-	1:1	$P\bar{1}$	$[GdCl_2L(EtOH)]^+$	9	2.54(4)	2.71(3) 2.41 *	Forsellini et al. (1985)

	Nd	NO_3^-	4:3	C2/m	$[Nd(NO_3)_2L]^+$, C_{2h}, C_s	10	2.60(5)	2.48(7)	Bünzli et al. (1981a)
					$[Nd(NO_3)_6]^{3-}$, C_{2h}	12		2.59(4)	
$B_2$18C6	Sm	ClO_4^-	1:1	Fdd2	$[Sm(ClO_4)_3L]$, C_2	10	2.52(8)	2.50(16)	Ciampolini et al. (1979b)
	Y	NCS^-	1:1	Pnma	$[Y(NCS)_3L]$	9	not available	not available	Xu Zhangbao et al. (1982)
$Cy_2$18C6	La	NO_3^-	1:1 [d]	$P2_1/c$	$[La(NO_3)_3L]$	12	2.61–2.91	2.63–2.71	Harman et al. (1976)
	La	NO_3^-	3:2 [e]	$P\bar{1}$	$[La(NO_3)_2L]^+$	10	2.61(7)	2.58(4)	Fan Yuguo et al. (1984)
					$[La(NO_3)_5ONO_2La(NO_3)L]^-$	10, 11	2.61(6)	2.61(4)	
	Pr	NO_3^-	3:2 [e]	$P\bar{1}$	$[Pr(NO_3)_2L]^+$	10	2.59(5)	2.52(3)	Fan Yuguo et al. (1984)
					$[Pr(NO_3)_5ONO_2Pr(NO_3)L]^-$	10, 11	2.56(2)	2.56(4)	
(2,2)	Eu	NO_3^-	1:1	$P2_1/n$	$[Eu(NO_3)_2L]^+$	10	2.61(2)	2.47(3)	Bünzli et al. (1986)
$PyMe_2N_3O_3$-18C6ene$_2$	La	NO_3^-	1:1	Pbca	$[La(NO_3)_3L]$	12	2.72(5)	2.69(4)	Arif et al. (1985)
$Py_2Me_4N_6$-18C6ene$_4$	La	NO_3^-	1:1	$P2_1/c$	$[La(NO_3)_3L]$	12	2.67–2.73	2.69–2.77	Backer-Dirks et al. (1979)
$S_2$18C6	La	ClO_4^-	1:1	$P2_1/a$	$[La(ClO_4)_2L(H_2O)]^+$	10	O: 2.61(2)	2.64(13)	Ciampolini et al. (1980)
							S: 3.04(1)	2.54 *	
Bicy(4,2B,2B)	La	Cl^-	1:1	$P\bar{1}$	$[LaCl(Cl, OH)L]_2^{2+}$ [f], C_i	10	2.65(6)	2.76(1)	Benetollo et al. (1984, 1985a)
Bicy(4B,2B,2B)	La	NO_3^-	1:1	$P\bar{1}$	$[La(NO_3)_2L]^+$	11 [g]	2.68(11)	2.67(6)	Trüter et al. (1985)
						12 [g]	2.67(9)	2.56(10)	
					$[La(NO_3)_5MeOH]^{2-}$	11	2.54 *	2.63(3)	
(2,2,2)	Eu	ClO_4^-	1:1	$P2_1P2_1P2_1$	$[Eu(ClO_4)L]^{2+}$	10	O: 2.49(3)	2.69(3)	Ciampolini et al. (1978, 1979a)
							N: 2.67(3)		
	La	NO_3^-	4:3	C2/c	$[La(NO_3)_2L]^+$, C_2, C_1	12	O: 2.64–2.74	2.63–2.69	Hart et al. (1978)
							N: 2.81–2.85		
					$[La(NO_3)_6]^{3-}$, C_i	12		2.62–2.71	
	Nd	NO_3^-	2:1	$P\bar{1}$	$[Nd(NO_3)L]^{2+}$	10	O: 2.54(5)	2.52(1)	Benetollo et al. (1985b)
							N: 2.78(1)		
					$[Nd(NO_3)_5(H_2O)]^{2-}$	11	2.54 *	2.58(5)	
	Sm	NO_3^-	2:1	$P\bar{1}$	$[Sm(NO_3)L]^{2+}$	10	O: 2.50(5)	2.49(1)	Burns (1979)
							N: 2.76(2)		
					$[Sm(NO_3)_5(H_2O)]^{2-}$	11		2.55(6)	
EO4	Nd	NO_3^-	1:1	$P2_1/n$	$[Nd(NO_3)_3L]$	10	2.52(3)	2.56(2)	Hirashima et al. (1982)
EO5	La	NO_3^-	1:1	$P2_1/n$	$[La(NO_3)_3L]$	11	2.70(4)	2.64(8)	Casellato et al. (1982)
	Nd	NO_3^-	1:1	$P2_1/n$	$[Nd(NO_3)_3L]$	10 [h]	2.65(4)	2.55(2)	Hirashima et al. (1981b)
EO6	Nd	NO_3^-	1:1	$P2_1/n$	$[Nd(NO_3)_3L]$	10	2.59(3)	2.52(3)	Hirashima et al. (1981a)

TABLE 7 (continued)

Ligand L	R	Anion	R:L	Space group	Complex species (with symmetry)	CN	Mean R–X distances (Å)		References
							R–ligand	R–anion and/or R–OH	
18P6	La	NO_3^-	4:3	I2	$[La(NO_3)_2L]^+$, C_s, C_1 $[La(NO_3)_6]^{3-}$, C_2	10 12	2.64(12)	2.54(4) 2.64(4)	Bünzli et al. (1984)
[i]	Ce	ClO_4^-	1:2	$P2_1/c$	$[CeL_2]^{2+}$	10	O: 2.52(3) N: 2.68(3)	–	Thomas and Palenik (1980)
$C_6H_9N_3$ [j]	La	ClO_4^-	1:4	$P2_1$	$[LaL_4]^{3+}$	12 [k]	2.77	–	Schwesinger et al. (1985)

* R–OH distance.

[a] The ligand is linked to the complex moiety through H bonding.

[b] The second ligand is H bonded.

[c] In the reference, the indices 1 and 2 have inadvertently been permuted, the correct space group is $P3_2$.

[d] Isomer A (cis-syn-cis).

[e] Isomer B (cis-anti-cis).

[f] One site is occupied by Cl^- in one half and by OH^- in the other half. The two parts of the dimer are held together by a $OH\cdots Cl$ hydrogen bond across the pseudo-center of symmetry.

[g] One cation is 11-coordinate with one bidentate and one monodentate nitrates, the other cation is 12-coordinate.

[h] One nitrate is monodentate.

[i] 2,6-diacetylpyridine bis(semicarbazone).

[j] cis-triaza-tris(σ-homobenzene).

[k] The LaN_{12} coordination polyhedron is a slightly distorted icosahedron.

moisture and easier to crystallize. Partial disorders of the ligand and/or the anions (e.g., perchlorate) sometimes prevented an accurate solution of the structure.

The 12C4 and 15C5 complexes with rare earth nitrates have similar arrangements around the metal ion: the ligand is coordinated on one side while the three nitrate groups are bidentate and associated on the opposite side. The R(III) ion is not encapsulated into the polyether cavity, which is too small. Similar structures are obtained with Napht16C5 and, partially, with (2-methoxy-1,3-xylyl)18C5 (MeOB18C5). In the latter complex, however, unfavourable steric and/or conformational situations result in the coordination of only three of the six ether functions of the ligand, including the prominent methoxyarylic O atom. With MeOB15C4, there is no direct interaction with the metal ion: the ligand has a folded structure in which there is a 94° angle between the plane of the aryl group and the best plane of the etheral O atoms. It is linked to the $[Dy(NO_3)_3(H_2O)_3]$ moiety by four rather strong hydrogen bonds with the coordinated water molecules. Similar hydrogen bonds are found in the isostructural La and Sm 1:2 coronates with 15C5. In reality, these pentahydrated perchlorate complexes are 1:1 coronates in which one crown ether is held in the lattice through three H bonds with coordinated water molecules; the fourth coordinated water molecule forms H bonds with one perchlorate ion and with the fifth water molecule. In both structures, the R(III) ion lies ca. 1 Å above the mean plane of the etheral O atoms.

A better encapsulation of the metal ion occurs either when the ligand is substituted with carboxylic or amino functional groups, or when the ligand cavity is larger. In the DOTA and TETA complexes, the N atoms of the ring and the O atoms of the carboxylic groups form two parallel planes. The metal ion lies between these planes, slightly displaced towards the inside of the ligand cavity. The TETA cycle is more flexible and wraps itself around the R(III) ion in a more effective way than the DOTA cycle, resulting in a less symmetrical coordination polyhedron (distorted C_2 dodecahedron versus capped square antiprism). In the complexes of the 16-membered amino-substituted polyamine $(aet)_2N_6$16C6, the eight donor atoms form a cavity that encapsulates the R(III) ions. The ligand adapts itself to the smaller Yb(III) ion by modifying the conformation it has in the La coronate. The change of the coordination number from 10 (La) to 9 (Yb) is then compensated, resulting in smaller R(III)–N distances, 2.52 versus 2.73 Å. A noteworthy feature of these two structures is the coordination of one (Yb) and two (La) TRIF anions, to give di- and monocationic species, respectively. Such a complex cation is also found with the 14-membered pyrido-fused polyamine $Py_2Me_4N_6$14C6ene$_4$. This rigid ligand forms an inclusion cationic complex in which the Sm(III) ion is held into the ligand cavity by one bidentate nitrate ion on one side and by one hydroxy group and one water molecule on the other side. Hydrolysis also occurs for TFA complexes and the 2:1 coronate with 15C5 may be formulated as $[Pr_2(TFA)_3(OH)(15C5)_2]^{2+}[Pr_2(TFA)_8]^{2-}$. There are two Pr sites. One Pr(III) ion is 9-coordinate and is bonded to the polyether, one bridging

hydroxide, and three bridging TFA ions; this gives rise to mirror-related dimeric cations whose coordination polyhedron may be considered as arising from distortion of a square antiprism by addition of a ninth ligand. The second Pr(III) ion is embedded in infinite polymeric zigzag chains; it is 8-coordinate and bonded to one bidentate and three bridging TFA anions.

Several structures of complexes with 18-membered coronands containing six donor atoms have been determined. In 1:1 complexes, the 18C6 ether adopts a folded conformation in order to equalize the Ln–O distances. The two complexes $[R(NO_3)_3L]$, R = La, Nd, are isostructural despite the difference in the ionic radii of the metal ions, 1.36 Å for La(III) and CN = 12, compared with 1.29 Å for Nd(III). The effects of the steric crowding of the Nd complex are in fact absorbed by two O atoms in trans position. The flexibility of the ligand is illustrated by the coordination of a smaller ion, Gd(III). In this case, the guest ion is $[GdCl_2(EtOH)]^+$, so that the metal ion is 9-coordinate; Gd–O distances are, however, 0.1 Å longer than expected for this coordination number. A 1:1 nitrato complex does not form with Gd(III), probably because of unfavourable energetics. Indeed, $Gd(NO_3)_3(18C6)\cdot 3H_2O$ contains the 9-coordinate species $[Gd(NO_3)_3(H_2O)_3]$ while the polyether is held in the lattice by weak hydrogen bonds from coordinated water molecules. In the Nd 4:3 complex with 18C6, the ligand is found to have a strained configuration. This coronate contains three dinitrato complex cations $[Nd(NO_3)_2L]^+$ with two different symmetries, C_{2h} and C_s. * In the cation with C_{2h} symmetry, the 10-coordinate metal ion lies in the center of the polyether and is held into the cavity by one bidentate nitrate group on each side. The crown ether is considerably flattened and the mean plane through its six O atoms contains the Nd(III) ion. The complex cation with C_s symmetry contains a disordered ligand oscillating between two positions. The compound also has hexanitrato anions $[Nd(NO_3)_6]^{3-}$ with C_{2h} symmetry. Dicyclohexyl 18-crown-6 ether forms both 1:1 and 3:2 complexes with lanthanum nitrate. In the former coronate, the configuration of the ligand corresponds to the cis-syn-cis isomer (A) while the cis-anti-cis isomer (B) is found in the 3:2 complexes. The latter are comprised of dinitrato complex cations $[La(NO_3)_2L]^+$ and of complex anionic dimers $[La(NO_3)_2L\cdot La'(NO_3)_5]^-$ in which one bridging nitrate ion is bidentate to La and monodentate to La'. The Pr(III) 3:2 complex is isostructural with the La(III) coronate. No structures with the other isomers of Cy_218C6 have been reported. The 1:1 coronate between dibenzo-substituted 18-crown-6 ether and samarium perchlorate contains neutral tris(perchlorato) complex species with C_2 symmetry. Its overall structure is similar to that of $[R(NO_3)_3(18C6)]$ complexes: the ligand displays a folded conformation and the planes through the benzene rings form an angle close to 120°, two monodentate perchlorate ions are on the less hindered side and one bidentate perchlorate ion on the other side. The anion coordination allows the Sm(III) ion to reach a coordination number of 10.

* Crystallographic symmetries. Local symmetries are D_{2h} and C_1, respectively.

The substitution of two ether functions in 18C6 by either two thioether or two amine groups results in 1:1 coronates in which the complex species is cationic, e.g., $[La(ClO_4)_2(O_4S_2 18C6)(H_2O)]^+$ and $[Eu(NO_3)_2(2,2)]^+$. The substituting groups are displaced out of the plane of the remaining four O atoms by about 1.5 Å for S and 1.1 Å for N, while the R(III) ions are displaced out of this plane in the same direction, by 0.5 Å (La) and 0.37 Å (Eu). The substitution of O atoms by imino-N atoms yields more rigid ligands. However, the structure of the 1:1 complexes with lanthanum nitrate resembles that of the 18C6 coronates, with two bidentate nitrate ions on one side and the third one on the other side. The conformation of the N_3O_3 macrocycle is more folded away from the pair of bidentate nitrate ions than the N_6 macrocycle.

The bicyclic polyethers give rise to complex structures. With lanthanum chloride and Bicy(4,2B,2B), the adduct corresponds approximately to a 1:1 stoichiometry, but a crystalline product is obtained only in the presence of water. The crystal structure analysis shows that partial hydrolysis takes place. In this, the behaviour is reminiscent of the 2:1 TFA complexes with 15C5. Indeed, the unit cell contains a pseudo-centrosymmetric dimer $[LaCl(Cl,OH)L]_2^{2+}$ with an $OH\cdots Cl$ hydrogen bond across the centre of symmetry; one site is occupied by Cl^- in one half and by OH^- in the other half. The ligand in this structure has an approximate twofold axis of symmetry. The O atoms form an end-capped trigonal prism around La(III) and the metal ion lies in the mean plane formed by the O atoms of the aliphatic unsubstituted chain. The other bicyclic polyether, Bicy(4B,2B,2B), forms 3:2 complexes with lanthanum nitrate. The asymmetric unit contains two dinitrato cations $[La(NO_3)_2L]^+$ and one pentanitrato anion $[La(NO_3)_5(MeOH)]^{2-}$. The La(III) ion is 11-coordinate in the anion and one of the cations, in which there is one bidentate and one monodentate nitrate ion. It is 12-coordinate in the other cation.

The (2,2,2) cryptand is flexible enough to include all the hetero-atoms in the coordination polyhedron and to allow the additional bonding of one bidentate anion, either perchlorate or nitrate. Thus all the 1:1, 4:3, and 2:1 cryptates for which a crystal structure has been reported contain a $[RX_n(2,2,2)]^{(3-n)+}$ cation, $X = ClO_4^-$ or NO_3^-, and $n = 1$ or 2. The coordination number is 12 for La(III) and 10 for Nd(III), Sm(III), and Eu(III). The latter ions have a distorted capped-square antiprismatic geometry, two N atoms capping the two "square" faces. The 2:1 Nd and Sm cryptates are isostructural and their asymmetric unit contains 11-coordinate $[R(NO_3)_5(H_2O)]^{2-}$ anions. The water molecule makes weak hydrogen bonds to different anions.

It is of interest to compare the structures of the podates with those of the coronates, even if the polyethyleneglycols are not exact analogues of the crown ethers. The podands adopt a ring-like conformation with all the O atoms pointing towards the metal ion. The R(III) ion and these O atoms are more or less coplanar; two bidentate nitrates are coordinated axially above and below this plane while the third nitrate is either bonded to the metal ion through the open side of the ligand chain or not bonded (podand EO6). In this latter complex, the

coordination number of Nd(III) is lower by two units, compared with the 18C6 complex. A difference exists between the La and Nd podates with tetraethyleneglycol, EO5: the nitrate ion bonded through the open side of the ligand is bidentate with La(III) and monodentate with Nd(III), henceforth the CN change from 11 to 10. The 4:3 La podate with 18P6 retains the essential features of the corresponding Nd coronate with 18C6, but the symmetries are lower: C_2 and C_1 for the cations, and C_2 for the hexanitrato anion. The cation with no symmetry element has a disordered ligand. The podand wraps around the metal ion similarly to EO6, but the presence of the two methyl endgroups prevent nitrate coordination through the open side of the ligand chain.

These structures, some of which are illustrated in fig. 2, demonstrate that the coordination number of the trivalent rare earth ions may be tuned between 8 and 12 by modifying the nature of the ionophore and/or the anion. It is noteworthy that 11-coordination appears to be as common as 10- or 12-coordination. Moreover, the data of table 7 reveal that mean Ln–O or Ln–N distances are not much affected by the nature of the ligand. The ionic radii calculated from these data are in good agreement with values inter- or extrapolated from ionic versus coordination number plots (Shannon, 1976). Finally, one notes the presence of several complex cationic species with +1 or +2 charges, and having the general formula $[RX_nL]^{(3-n)+}$. These species are found in 3:2, 4:3, and 1:1 coronates, cryptates, and podates. They also occur in solution (Bünzli et al., 1986) and their relative stability compared with the neutral $[RX_3L]$ molecules in thermogravimetric analyses was noted (Ammann and Bünzli, 1979; Backer-Dirks et al., 1980; Bünzli and Wessner, 1984b).

3.2.2. *Other structural information*

The crystal structure determination of sandwich 1:2 coronates with 15C5 has been attempted (Bünzli et al., 1985) but all the investigated complexes turned out to be completely disordered. The two coronates $R(ClO_4)_3 \cdot (15C5)_2$, R = Nd, Eu, were found to be isomorphous. They crystallize in an I-centered lattice (Laue group 4/m for R = Eu). The luminescence spectrum of the Eu complex reveals the presence of three different metal sites, one of which having an inversion center. The hexafluorophosphate complex $La(PF_6)_3 \cdot (15C5)_2$ crystallizes in an F-centered lattice.

The structure of many other complexes may be related to the results presented above by comparing both their X-ray powder diagrams and their vibrational spectra (table 8). Lanthanide nitrate complexes with 12C4 are isostructural for R = Nd–Lu and, probably, La–Pr, since the Eu-doped lanthanum complex presents a luminescence spectrum identical to that of the pure Eu complex (Bünzli et al., 1982b). Two isomorphous series were found for $[R(NO_3)_3(15C5)]$, R = La–Nd and R = Sm, Eu, a result which has been confirmed by single-crystal structure determinations (table 7). A practical test of the structure of 18C6 coronates is the ring-breathing vibrational mode which occurs at 880 cm^{-1}; this mode is IR-forbidden and Raman-allowed if the ligand has an inversion center,

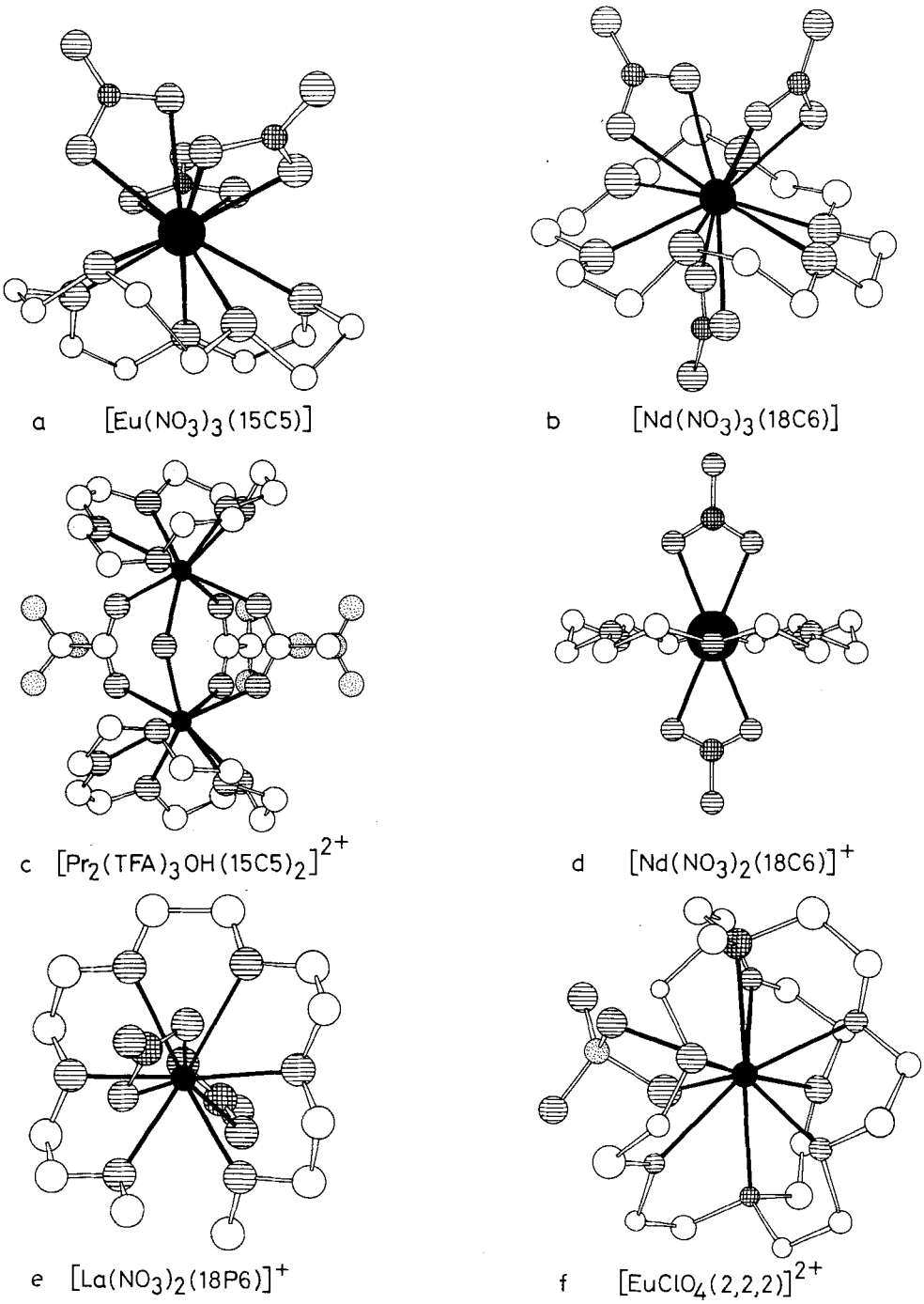

Fig. 2. Molecular structures of some coronates, one podate, and one cryptate. Open circles represent C atoms, black circles R atoms, striped circles O atoms, hatched circles N atoms, and dotted circles either F or Cl atoms. Redrawn from (a) Bünzli et al. (1982a), (b) Bünzli et al. (1980), (c) Harrison et al. (1985), (d) Bünzli et al. (1981a), (e) Bünzli et al. (1984), and (f) Ciampolini et al. (1979a).

TABLE 8
Isomorphous series in nitrato complexes with crown ethers and podands, as determined from X-ray powder patterns.

Ligand	R:L	Isomorphous series	References
12C4	1:1	Nd–Lu	Bünzli and Wessner (1980)
15C5	1:1	La–Nd; Sm, Eu	Bünzli and Wessner (1981)
18C6	1:1	La–Nd	Bünzli and Wessner (1981)
	4:3	Ce–Eu, Ho; Nd–Tb; Dy–Lu	Bünzli and Wessner (1981) Backer-Dirks et al. (1980)
21C7	1:1	Er, Yb	Wessner et al. (1982)
	4:3	La–Eu; Gd, Tb, Ho [a]; Tm–Lu	Wessner et al. (1982)
EO4	1:1	La, Ce; Pr–Lu	Hirashima et al. (1983b)
EO5	1:1	La–Eu; Tb–Lu	Hirashima et al. (1983b)
EO6	1:1	La, Ce; Pr–Lu	Hirashima et al. (1983b)
18P6	4:3	Ce–Nd; Sm, Eu	Bünzli et al. (1984)

[a] From examination of IR spectra.

which is the case in the 4:3 nitrato complexes. The complexes with polyethyleneglycols containing from four to six O atoms usually form two isomorphous series. These are characterized by very similar IR spectra.

3.3. *Solid-state properties*

3.3.1. *Thermoanalytical data*

Thermogravimetric and thermal analyses have been performed for several coronates by use of TG, DTG, DTA, and DSC techniques. The most studied complexes are nitrato coronates with crown ethers, for which the following reactions are observed:

$$R(NO_3)_3 \cdot L \cdot nH_2O \xrightarrow{I} R(NO_3)_3 \cdot L + nH_2O\,,$$

$$4R(NO_3)_3 \cdot L \xrightarrow{II} [R(NO_3)_2 \cdot L]_3[R(NO_3)_6] + L\,,$$

$$[R(NO_3)_2 \cdot L]_3[R(NO_3)_6] \xrightarrow{III} \text{decomposition } (RONO_3, R_2O_3, L)\,,$$

$$R(NO_3)_3 \cdot L \xrightarrow{IV} \text{decomposition } (RONO_3, R_2O_3, L)\,.$$

The temperatures at which these various reaction steps occur are reported in table 9; they depend upon the exact experimental conditions. The 12C4 complexes are stable up to about 300°C and then decompose according to reaction IV in a seemingly one-step exothermic reaction. The 15C5 coronates of the lighter lanthanides (R = La–Eu) decompose at lower temperature. From Gd on, the thermolysis occurs according to reactions I, II, and III, that is, intermediate 4:3 compounds form with a thermal stability interval ranging between 55 and

100°C. The 1:1 to 4:3 transformation is quantitative and the ligand can be recovered unchanged. The decomposition temperature of all the complexes $R(NO_3)_3 \cdot B15C5$ is above 200°C, starting with 275°C for the La complex and decreasing irregularly along the series. Complexes with Napht16C5 (R = La–Nd) do not transform into 4:3 complexes; their decomposition starts at a relatively low temperature and extends over a large temperature range. All the 18C6 1:1 coronates undergo the transformation into the thermally more stable 4:3 complexes; again, this reaction is quantitative and the ligand may be recovered unchanged. Generally speaking, DTA curves recorded simultaneously with TG curves display a small ΔH_r for reaction II, except in the case of $R(NO_3)_3 \cdot 18C6$. For these latter coronates, ΔH_r(II) measured by DSC (Bünzli et al., 1979b) ranges from $+57\ kJ\ mol^{-1}$ (R = La; temperature range 207–233°C), to $47.2\ kJ\ mol^{-1}$ (Ce; 168–187°C), $43.4\ kJ\ mol^{-1}$ (Pr; 128–150°C), and $37.6\ kJ\ mol^{-1}$ (Nd, 101–129°C); no enthalpic effect could be measured for Eu. Other $1:1 \rightarrow 4:3$ transformations are observed for $PrCl_3 \cdot 18C6$ at 210°C ($\Delta H_r = +39.7\ kJ\ mol^{-1}$), and for $EuBr_3 \cdot 18C6$; but not for $PrCl_3 \cdot L$, L = 12C4 and 15C4, and $Pr(NCS)_3 \cdot 18C6$ (Bünzli and Wessner, 1984a).

Isothiocyanato coronates undergo the following thermal changes (Seminara et al., 1975):

$$R(NCS)_3 \cdot L \cdot H_2O \xrightarrow{I} R(NCS)_3 \cdot L + H_2O \xrightarrow{II} Ln(NCS)_3 + L \xrightarrow{III} \text{decomposition}.$$

Step I occurs between 110 and 150°C and step II between 218 and 232°C under N_2 atmosphere or between 170 and 224°C under reduced pressure. The ligand can be collected during step II and identified by its melting point and its IR spectrum. Appropriate treatment of the thermoanalytical curves allows the determination of the enthalpy change ΔH_{diss} of the ligand dissociation and of the "activation energy" E_a^*. The former ranges between 63 and $268\ kJ\ mol^{-1}$ under N_2 atmosphere ($71–184\ kJ\ mol^{-1}$ under reduced pressure) while the latter varies from 142 to $406\ kJ\ mol^{-1}$, or $54–410\ kJ\ mol^{-1}$ under reduced pressure. Step III is exothermic, contrary to steps I and II, and is not well defined; it sometimes starts before ligand dissociation is completed. The $R(NCS)_3 \cdot B_2 18C6$ complexes (R = La–Lu) undergo a one-step ligand dissociation between 224 and 270°C (N_2 atmosphere; 174–250°C under reduced pressure; Gurrieri et al., 1975). The corresponding Y compound dissociates at 285°C (Wang Genglin et al., 1980). The ΔH_{diss} ranges are $142–761\ kJ\ mol^{-1}$ (N_2 atmosphere) and $96–343\ kJ\ mol^{-1}$ (reduced pressure). For both B15C5 and $B_2 18C6$ coronates, the ΔH_{diss} and E_a^* plots versus the reciprocal of the ionic radius display some periodicity between the lighter and the heavier cations. Under the same experimental conditions nitrato complexes with B15C5 and $B_2 18C6$ undergo violent and rapid decomposition, while $EuCl_3 \cdot B_2 18C6 \cdot H_2O$ decomposes in two steps at 220 and 450°C, after loss of the water molecule (Zou Jinping and Tan Minyu, 1983).

TABLE 9

Temperatures (°C) at which various thermal reactions start for the complexes $R(NO_3)_3 \cdot L \cdot nH_2O$ (see the text, §3.3.1, for the reaction schemes I–IV).

Ligand	R	T(I)	T(II)	T(III)	T(IV)	References
12C4	Nd				340	a
	Lu				280	a
15C5	La				260	a, b
	Pr				240	a, b
	Eu				170	a, b
	Gd	100	160	250		a, b
	Tb	100	110	260		a, b
	Dy	90	90	260		a, b
	Ho	90	90	270		a, b
	Er	105	110	275		a, b
	Yb	105	105	270		a, b
B15C5	Y	85			210	c
	La				280	d, e
	Ce				235	d
	Pr				275	d
	Nd				270	d
	Sm				232	d
	Eu–Lu				230–200	f
Napht16C5	La				235	g
	Ce				170	g
	Pr				220	g
	Nd				204	g
	La		210	230	305	a, b
			185	250	310	h
	Ce		180	230	250	h
	Pr		130	220	290	a, b
			155	250	305	h
	Nd		110	180	270	a, b
			160	250	310	h
	Sm				305	h
	Eu				300	h
		50	110	280		a, b
	Gd	95	160	295		h
	Tb	100	160	395		h
		100	110	290		a, b
	Dy	95	160	280		h
	Ho	100	150	270		h
	Er	105	155	260		h
		100	135	270		a, b
	Tm	105	160	245		h
	Yb	110	170	240		h
		105	120	235		a, b
	Lu	120	160	240		h
$B_2$18C6	La				280	d

TABLE 9 (continued)

Ligand	R	T(I)	T(II)	T(III)	T(IV)	References
	Ce				220	d
	Pr				270	d
	Nd				247	d
21C7	Er				150	i

[a] Bünzli et al. (1979b).
[b] Bünzli and Wessner (1981).
[c] Jiang Haiying et al. (1983c).
[d] King and Heckley (1974).
[e] Jiang Haiying et al. (1983a).
[f] Seminara et al. (1975).
[g] Wang Genglin et al. (1982).
[h] Backer-Dirks et al. (1980).
[i] Wessner et al. (1982).

The enthalpies of complexation ΔH_c have been measured in the solid state for $RCl_3 \cdot B_2 18C6$ (Kohata et al., 1985). The thermal reactions of mixtures with a 1:1 molar ratio of hydrated lanthanoid chloride and $B_2 18C6$ are, under reduced pressure, stepwise dehydration, melting, complexation (around 160°C), and decomposition; ΔH_c ranges from -31.0 (R = La), to -24.9 (Nd), -20.3 (Sm), -15.5 (Eu), -14.9 (Dy), and -15.7 kJ mol^{-1} (Er). The stability of the complexes increases with increasing ionic radius, and one water molecule remains coordinated to the metal ion in the heavier lanthanide coronates. The thermal behaviour of another chloride complex, $EuCl_3 \cdot Cy_2 24C8$, has also been reported (Wang Xin and Tan Minyu, 1984).

A study of TFA coronates with 12C4, 15C5, and 18C6 polyethers has been published (Bünzli and Giorgetti, 1985b). The 1:1 and 3:2 complexes with 12C4 undergo a transformation into 2:1 complexes around 120 to 150°C and these latter are stable up to 250°C (La, Pr, Nd, Eu, Er). The 2:1 coronates with 15C5 lose their hydration water between 50 and 100°C and start to decompose between 160 (Eu) and 200°C (La). The 18C6 1:1 complexes with R = La–Pr undergo a one-step decomposition between 180 and 200°C without going through an intermediate 2:1 compound; but such a complex is observed for Sm and Eu between 230 and 250°C. All the 2:1 complexes decompose above 250°C to yield lanthanide trifluorides.

3.3.2. *Magnetic moments*

Magnetic susceptibilities have been measured at room temperature for several crown ether complexes. The calculated paramagnetic moments do not depend much upon the nature of the ligand. They are consistently lower than free ion moments by 6–9% for Ce–Nd, 2–3% for Sm, and Eu, and less than 1% for Gd. The reported data (Bünzli and Wessner, 1984b; Bünzli and Giorgetti, 1985b) point to a weak to moderately strong chemical bonding between the ligand and the R(III) ions.

3.3.3. *Vibrational spectra*

IR and Raman spectra help the routine identification of the complexes. Although quite informative, these spectra will not be reviewed in detail, since their interpretation is not always straightforward. Nevertheless, the following information may be gained:

(a) Within an isomorphous series of complexes, the spectra are similar, except for small systematic shifts, usually towards higher wavenumbers, with increasing atomic number. Henceforth, vibrational spectra may help to recognize such isomorphous series.

(b) Vibrational spectra also afford evidence for the coordination mode of the anions. Perchlorate ions are either uncoordinated (u), monodentate (m) or bidentate (b) and these three forms have been found in crystal structures (Ciampolini et al., 1979a,b, 1980). Since the spectral range around 1100 cm^{-1} is often obscured by ligand vibrations the distinction may be achieved by inspection of the IR 600–660 cm^{-1} range: ClO_4^-(u) absorbs at 625 cm^{-1}, ClO_4^-(m) at 615–625 cm^{-1} and 640–660 cm^{-1}, and ClO_4^-(b) at 610–620 cm^{-1}, 625–635 cm^{-1}, and 640–660 cm^{-1} (Hathaway and Underhill, 1961; Bünzli and Mabillard, 1986). The assignment of nitrate vibrations is more difficult. Unassociated nitrate absorbs at 720, 830, and 1390 cm^{-1} (IR), and 1030 cm^{-1} (Raman). Upon coordination, the symmetry is lowered and six vibrational modes become IR-active (710, 740, 820, 1030, 1300, and 1500 cm^{-1}). The distinction between monodentate, bidentate and bridging (bi- or tridentate) nitrate is difficult, and several criteria have been proposed, e.g., the polarization of Raman emission bands, the magnitude of the splitting of the 1300 and 1500 cm^{-1} bands, as well as the number of components and the splitting of the combination bands in the 1700–1800 cm^{-1} range (Lever et al., 1971). Most of the nitrato complexes with ionophores contain bidentate nitrate groups which are often nonequivalent. Isothiocyanate ions are either uncoordinated or bonded through the N atom, with IR absorptions at 475–490, 780–820, and 1990–2070 cm^{-1} (Olszanski, 1975; Wessner, 1980).

(c) The ligand vibrations are affected by the complexation, especially those involving the donor atoms X. Coronands, for instance, have two ν(CCX) modes, symmetrical and antisymmetrical. The latter is shifted towards lower wave numbers upon complexation while the former, which is often masked by other vibrations, is blue-shifted. Splittings of these vibrations often occur, so that an exact interpretation of the shifts is difficult. In general, $\Delta\nu(CCO)_{as}$ ranges between -20 and -50 cm^{-1}; this shift is larger for cryptates (-40 to -60 cm^{-1}), but approximately the same for N-containing coronates. Vibrational spectra also provide information about the ligand conformational changes induced by complexation (Erk, 1979; Wessner, 1980).

(d) Coordinated solvent molecules may be evidenced, e.g. water (Liang Yingqiu et al., 1983).

A normal coordinate analysis of $La(NO_3)_3 \cdot L$, L = 15C5 and 18C6, has been performed by Zhao Wenyun et al. (1985). More than 50 vibrational modes were fitted to the experimental IR and Raman spectra, which are correctly reproduced,

and force constants are calculated. The force constants for La–O(NO_3^-) and La–O(ether) stretching modes are found to be almost equal: 0.8 and 0.74 mdyn/Å, respectively.

3.3.4. *Electronic absorption spectra*

The weak f–f transitions are difficult to measure by reflectance methods. Moreover, they seem to be relatively little affected by the complexation by ionophores (Heckley, 1974; Backer-Dirks et al., 1980). Benzo-substituted crown ethers exhibit benzenoid absorptions at 227–228 and 275–276 nm, which are slightly shifted and modified upon complexation (Seminara and Musumeci, 1980). Similar effects are reported for N-containing coronates (Radecka-Paryzek, 1979, 1980, 1981a,b, 1985). Ciampolini and Nardi (1979) and Ciampolini et al. (1979a,b, 1980) have studied the ligand-to-metal charge transfer bands for various Sm, Eu, and Yb coronates and cryptates, and have calculated the optical electronegativity (Reisfeld and Jørgensen, 1977) of the ligands (table 10).

TABLE 10

Energies of the ligand-to-metal charge-transfer transitions E_{CT} (from reflectance spectra) for various 1:1 complexes between coronands or cryptands and lanthanide perchlorates, and optical electronegativities χ_{opt} of the ligands.

Ligand	E_{CT} (Sm) (cm^{-1})	E_{CT} (Eu) (cm^{-1})	E_{CT} (Yb) (cm^{-1})	χ_{opt}	References
18C6		39600		3.2	Ciampolini et al. (1980)
$B_2$18C6	32100	22500	27400	2.7	Ciampolini et al. (1979b)
$S_2$18C6	37200	28300	30700	2.8	Ciampolini et al. (1980)
$B_2$30C10	32800	24100	27000	2.7	Ciampolini and Nardi (1979)
(2,2,2)	41300 [a]	32100	38100 [a]	3.0	Ciampolini et al. (1979a)

[a] In acetonitrile solution.

3.3.5. *Luminescence spectra*

Luminescence data (spectra, quantum yields, lifetimes) are very sensitive to changes around the metal ion, and many studies of europium and terbium complexes are reported. The latter are especially well suited to study the energy transfer between aromatic residues and the R(III) ion. For instance, the photophysical properties of B15C5 complexes with various terbium salts have been investigated by De B. Costa et al. (1980). Upon complexation, the fluorescence of the coronand at 302 nm is quenched and the emission from the Tb(III) $^5D_4$ excited level is observed. The phosphorescence of the crown ether occurs at 415 and 440 nm and is not quenched by the metal ion, indicating that the ligand-to-metal energy transfer originates in the singlet state. A similar situation is observed for europium complexes but the fluorescence quenching is less effective. Efficient energy transfer between the phtalimide chromophore of N,N′-bis(N-phtalimido)-methyldiaza-18C6 and R(III) ions, R = Sm, Eu, Tb, Dy, has also been noted (Poluektov et al., 1984b).

The Eu(III) ion is an interesting luminescent probe. Both its fundamental $^7F_0$ and most luminescent $^5D_0$ levels have $J = 0$. They are not split by crystal field effects and the analysis of the $^5D_0 \rightarrow {}^7F_J$ transitions is straightforward. The following information may be extracted from luminescence data:

(a) High resolution excitation spectra in the region of the $^5D_0 \rightarrow {}^7F_J$ transition yield the number of chemically different metal sites in a compound. This transition is forbidden by all the selection rules for f–f transitions, so that it is particularly weak. In addition, it is also forbidden by the symmetry selection rule if an inversion center is present; in this case, the 0–0 transition may be observed as a weak vibronic transition.

(b) The group-theoretical analysis of the $^5D_0 \rightarrow {}^7F_J$ transitions allows the determination of the symmetry of the metal ion site, provided it is selectively excited.

(c) The number of water molecules bound to the metal ion may be estimated by determination of the rate constants k's for nonradiative deactivation via coupling with O–H and, respectively, O–D oscillators: $q = 1.05[k(H_2O) - k(D_2O)]$ (Horrocks and Sudnik, 1979).

(d) The energy transfer efficiency provides a measure of the distance between two metal ion sites:

$$\eta = \frac{1}{1 + (r/R_0)^6} = 1 - \frac{\tau}{\tau_0},$$

where τ is the lifetime in presence of the acceptor, τ_0 is the lifetime in absence of the acceptor, r is the donor–acceptor distance, and R_0 is the critical distance for 50% energy transfer. The R_0 values depend upon an orientation factor, the quantum yield of the donor, the overlap integral between the emission spectrum of the donor, and the absorption spectrum of the acceptor, and upon the refractive index of the medium in which the transfer takes place.

However, care must be exercised in performing luminescence analyses:

(a) The intensity of the (forbidden) f–f transitions may vary considerably upon small perturbations of the R(III) environment, and the determination of the number of components of a given transition is sometimes difficult.

(b) In addition to vibronic transitions, spectra may contain additional bands due either to luminescent traps (Bünzli et al., 1982a) or to resonance effects. The latter occur between the electronic sublevels and the phonon density of states when resolved into sharp peaks (Caro et al., 1985), which is often the case for complexes with ionophores (Bünzli et al., 1982b, 1986).

(c) If energy transfers occur between the various metal ion sites, time-resolved experiments are needed to study a given metal-ion environment.

To be conclusive, luminescent studies should be performed at low temperature (77 K), using laser excitation, and under high resolution (< 0.1 Å). Medium to low resolution often results in the observation of too few transitions and a wrong, too high site symmetry may be deduced. Finally, if powdered samples instead of

monocrystals are suitable for luminescence analysis, it is advisable to perform measurements on doped samples (e.g., 1–2% Eu). Various studies on Eu coronates, cryptates and podates are summarized in table 11.

Resonance phenomena between the electronic $^7F_2$ sublevels and the phonon density of states are described for two coronates. In the 12C4 nitrato complex, the Eu(III) ion lies on a unique crystallographic site without symmetry. One and three sharp components are indeed observed for the $^5D_0 \rightarrow {}^7F_0$ and $^5D_0 \rightarrow {}^7F_1$ transitions, respectively. However, the $^5D_0 \rightarrow {}^7F_2$ transition consists of 23 lines, 14 of which may be assigned to vibronic transitions. The spectrum of the isostructural Lu complex doped with 1.5% Eu displays the same number of components, some of which are separated by 2–5 cm^{-1} only. In the emission spectrum of the (2,2) nitrato coronate, interaction between one $^7F_2$ sub-level and the nitrate

TABLE 11
Luminescence studies of europium-containing coronates, cryptates, and podates.

Ligand	Anion	R:L	Experimental conditions *1	Energy *2	Results, conclusions	References
12C4	NO_3^-	1:1	H, 77 K, doped Lu	E	1 site with low symmetry; phonon/electronic level interaction	a
DOTMA	–	1:1	H, 295 K	–	1 site with C_2 symmetry	b
15C5	ClO_4^-	1:2	H, 77 K	E	4 sites, one with an inversion center	c
	NO_3^-	1:1	H, 77 K, doped La	E	1 site with low symmetry; pseudo pentagonal symmetry; luminescent traps	d, e
	TFA	2:1	H, 77 K, doped La	E	2 sites with low symmetry; polymeric species	f
B15C5	Cl^-	1:1	L, 77 K	E	1 site, C_{2v} symmetry	g
	NCS^-	1:1	L, 77 K	E	9-coordinate species	h
18C6	NO_3^-	1:1	H, 77 K		1 site with low symmetry; decomposes under laser exposure	i
		4:3	H, 77 K, 4 K, doped Gd crystals	E	$[Eu(NO_3)_6]^{3-}$, D_{2h}, C_{2h} or C_i; $[Eu(NO_3)_2L]^+$; 3 sites with D_2 symmetry distorted towards C_{2v}	j
	TFA	2:1	H, 77 K	E	2 sites (anionic, cationic)	f
Cy_218C6	NCS^-	1:1	L, 77 K	E	1 site, C_{4v} symmetry	g
	NO_3^-	1:1	L, 77 K	E	1 site, D_{2d} symmetry	g
		3:2	H, 77 K, doped La, Gd	–	several sites with both A and B isomers	k
21C7	NO_3^-	4:3	H, 77 K	E	$[Eu(NO_3)_6]^{3-}$, D_{2h}, C_{2h} or C_i; $[Eu(NO_3)_2L]^+$, 3 sites with low symmetry	j
(2,2)	NO_3^-	1:1	H, 77 K	E	1 site with low symmetry; phonon/electronic level interaction	m
$Me_2(2,2)$	NO_3^-	4:3	H, 77 K	–	$[Eu(NO_3)_6]^{3-}$, C_i; $[Eu(NO_3)_2L]^+$ with low symmetry	k
Subst.(2,2) *3	Cl^-, NO_3^-	?	L, 295 K	–	not available	n

TABLE 11 (continued)

Ligand	Anion	R:L	Experimental conditions *1	Energy *2	Results, conclusions	References
(2,2,1)	Cl^-	1:1	lifetimes, 77 K	–	1.7 H_2O molecule bound per Eu (2.2 in frozen solution)	o
		1:1	H, 77 K	E	1 site with low symmetry (+1 impurity site)	p
		1:1	lifetimes, L, 4 K	E	nonradiative processes and charge-transfer state	q
(2,2,2)	ClO_4^-	1:1	L, 77 K	E	1 site, distorted bicapped square antiprism	g
	NO_3^-	2:1	L, 77 K	E	Eu(III) lies in the cavity	g
$(Napht)_2(2,2)_2$	NO_3^-	1:1, 2:1	H, 77 K, doped Gd	– –	$^5D_0 \leftarrow {}^7F_0$ excitation spectra	r
18P6	NO_3^-	4:3	H, 77 K	E	$[Eu(NO_3)_6]^{3-}$, low symmetry; $[Eu(NO_3)_2L]^+$, low symmetry	l
Pod1	BF_4^-	1:2	H, 77 K, single crystal	E	1 site with D_2 symmetry; 8-coordinate Eu(III)	s

*1 H = high-, L = low-resolution study; doped La means that the La complex doped with 1–2% Eu has been studied.
*2 E means that the energy levels of the Eu(III) ion are given.
*3 N,N′-bis(N-phtalimido)-methyldiaza-18-crown-6.
[a] Bünzli et al. (1982b).
[b] Brittain and Desreux (1984).
[c] Bünzli et al. (1985).
[d] Bünzli et al. (1982a).
[e] Bünzli and Klein (1982).
[f] Bünzli and Giorgetti (1985b).
[g] Seminara and Musumeci (1980).
[h] Calogero et al. (1979).
[i] Klein (1980).
[j] Bünzli and Pradervand (1986).
[k] Plancherel and Bünzli (1986).
[l] Pradervand (1985).
[m] Bünzli et al. (1986).
[n] Poluektov et al. (1984b).
[o] Sabbatini et al. (1984c).
[p] Moune et al. (1984).
[q] Blasse et al. (1986).
[r] Plancherel et al. (1985).
[s] Albin et al. (1983).

vibration at 1036 cm^{-1} gives rise to a doublet at 616.63 and 616.81 nm (1032 and 1037 cm^{-1} with respect to the energy of the $^7F_0$ level).

The emission spectrum of the 15C5 nitrato coronate has two noteworthy features. The crystal field splittings reflect a pseudo pentagonal symmetry, which may be understood since the coordination polyhedron of the 11-coordinate Eu(III) ion is a distorted monocapped pentagonal antiprism. Moreover, two extraneous bands in the $^5D_0 \rightarrow {}^7F_2$ transition are interpreted as arising from luminescent traps, a consequence of crystal defects. These bands are no more present in the doped Lu complex.

Pradervand (1985) has undertaken a detailed study of 4:3 nitratocomplexes with 18C6, 18P6, and 21C7. For the 18-membered cyclic polyether, high resolution spectra of the $^5D_0 \rightarrow {}^7F_1$ transition at 4.2 K, recorded both on polycrystalline samples and on the doped Gd-complex, reveal that each of the three cationic species generates a series of very similar spectra. These arise from Eu(III) ions experiencing slightly different crystal field effects, that is, by being surrounded by ligands with slightly different conformations. The Eu(III) ion is therefore a sensitive luminescent probe that could be used to perform conformational analysis in the solid state. The replacement of 18C6 by its open-chain analogue 18P6 results in a symmetry lowering reflected in the emission spectra. For the coronate,

the contribution of the centrosymmetrical $[Eu(NO_3)_6]^{3-}$ anion with C_{2h} symmetry to the total luminescence is about 8%, while the hexanitrate with C_2 symmetry contributes 60% to the total luminescence of the podate.

Nd luminescence, in conjunction with absorption spectra, is sometimes used to probe the metal sites. Such a study has been reported by Benetollo et al. (1985b) for the 2:1 cryptate with (2,2,2). The low-temperature luminescence spectrum of the $^4F_{3/2} \rightarrow {}^4I_{9/2}$, $^4I_{11/2}$ transition is consistent with the presence of two Nd sites.

3.3.6. *Mössbauer and XPES investigations*

A Mössbauer study of $Eu(NCS)_3 \cdot (B15C5) \cdot H_2O$ and $Eu(NCS)_3 \cdot (B_218C6)$ reports small positive isomeric shifts, with respect to EuF_3, for both coronates (Calogero et al., 1979). The s-electron density at the europium nucleus is therefore larger in the complexes than in the fluoride.

X-ray photoelectron spectra have been recorded for $R(NO_3)_3 \cdot L$, L = B15C5 and B_218C6, R = La–Nd (Jin Linpei et al., 1985). The binding energies of the R $3d_{5/2}$ levels are smaller in the coronates than in the corresponding nitrates, reflecting an increase in the electron density of the R(III) ion. The intensity of the 3d satellites is correlated with the extent of covalency in the complexes.

3.4. *Solution studies*

3.4.1. *Electronic absorption spectra*

Evidence for an interaction in solution between R(III) ions and various ionophores has been reported by several authors. For instance, the benzene ring absorption at 275 nm is modified upon complexation: for B15C5, two bands assigned to complexed and uncomplexed ligands are observed, indicating incomplete coronate formation. Pedersen (1967b) also mentions the appearance of a second absorption, at slightly longer wavelength, for lanthanum acetate solutions in methanol containing B_218C6. No modification of the absorption spectrum is, however, observed for solutions containing the B_224C8 polyether. Similar hypsochromic shifts (about 5 nm) are reported for $R(NCS)_3$ solutions in acetonitrile (R = Sc, Ce, Nd, Sm, Gd, Tb; Cassol et al., 1973; Olszanski, 1975), and for $R(NO_3)_3$ solutions in acetone containing B15C5 and B_218C6 (Heckley, 1974). Benzene and pyridine absorptions of N-containing coronates have been reported (Weber and Vögtle, 1976; Olszanski and Melson, 1977; Radecka-Paryzek, 1979, 1980, 1981a, 1985), as well as electronic spectra of cryptates (Pruett, 1978; Kausar, 1978; Ciampolini et al., 1979a).

The weak f–f transitions are also affected by complexation. Their energies change only a little, but their oscillator strength may vary up to 30% [for instance for $RX_3 \cdot L$ in CH_3CN/EtOH mixtures with R = Nd, Ho, $X = ClO_4^-, NO_3^-, NCS^-, Cl^-$, and L = B15C5, B_218C6, Cy_218C6, (2,2,1), and (2,2,2) (Seminara and Musumeci, 1980)]. The $^1D_2 \leftarrow {}^3H_4$ transition of the Pr(III) ion has been used to demonstrate the formation of $Pr(NO_3)_3 \cdot 18C6$ in anhydrous acetonitrile (Bünzli and Wessner, 1981). Simon et al. (1985) have studied the complex formation

between Eu(III) and Yb(III) and the crown ethers 15C5, B15C5, and Napht15C5 in acetonitrile. These ligands produce crystal field splittings of the order of $100\,cm^{-1}$ for several Eu(III) f–f transitions. The crystal field splitting patterns seem consistent with a 5-fold symmetry (C_{5v}) for the complex. Broad absorption bands are observed for Eu(III) and Yb(III) and all three ligands, which are assigned as ligand-to-metal charge transfer bands. These bands appear at 38460 (Eu) and $43370\,cm^{-1}$ (Yb) when unsubstituted 15C5 is added to $R(ClO_4)_3$ solutions and at 27000 (Eu) and $31720\,cm^{-1}$ (Yb) when either one of the substituted ligand is added. Using the relationship given by Reisfeld and Jørgensen (1977), the optical electronegativity of the ligands may be calculated, assuming $\chi_{opt}(Eu) = 1.9$ and $\chi_{opt}(Yb) = 1.8$; they amount to 3.2 for 15C5 and 2.8 for B15C5 and Napht15C5, which corresponds to the values found for 18C6 and other benzo-substituted crown ethers (table 10), respectively. The shift between the bands observed with Yb(III) and Eu(III) is consistent with the difference in the reduction potentials of these ions, supporting the assignment to a charge-transfer process from the crown ring to the R(III) ion.

3.4.2. *Luminescence spectra*

Luminescence data are summarized in table 12. They may be used to monitor the complex formation, to determine the symmetry of the complex species, the number of bonded water molecules, and the photophysical parameters of the energy transfer from the ligand.

In ethanolic solutions of $TbX_3 \cdot B15C5$, the quantum yield of the ligand luminescence is quenched; it decreases by 23%, 30%, and 15% for $X = NO_3^-$, NCS^-, and ClO_4^-, respectively. Simultaneously, a metal-ion sensitized emission occurs, with a quantum yield equal to 4×10^{-4}, 3×10^{-4}, and 22×10^{-4} for $X = NO_3^-$, NCS^-, and ClO_4^-, respectively. This emission arises from an energy transfer from the singlet state of the ligand; it occurs only weakly in the corresponding Eu(III) solutions (De B. Costa et al., 1980). Under different experimental conditions, Simon et al. (1985) observed that addition of B15C5 to $Eu(ClO_4)_3$ solutions in MeCN caused the metal fluorescence to decrease until complete quenching for R:L ratios smaller than 1. It is likely that the broad charge-transfer band at 370 nm (cf. §3.4.1) plays an important role in the observed quenching.

In solution, nitrato 4:3 complexes may give rise to several species, e.g.,

$$3[R(NO_3)_2L]^+ + [R(NO_3)_6]^{3-} \rightleftarrows 2[R(NO_3)_2L]^+ + [R(NO_3)_3L] + [R(NO_3)_5]^{2-} \rightleftarrows 3[R(NO_3)_3L] + R(NO_3)_3 .$$

Indeed, hexanitrato anions are known to dissociate completely in solution. High-resolution excitation spectra of Eu solutions in acetonitrile containing various amounts of 21C7 reveal the presence of at least three Eu-containing species. Their $^5D_0 \leftarrow {}^7F_0$ transitions occur at 17259, 17277, and $17289\,cm^{-1}$, and the intensity of the latter decreases upon addition of ligand (Wessner et al.,

TABLE 12
Luminescence data for solutions of coronates, cryptates, and podates.

Ligand	R(III)	Anion	Solvent	Type of study, *1 results	References
15C5	Eu	ClO_4^-	MeCN	little luminescence enhancement; ion pairing with ClO_4^-	a
		NO_3^-	MeCN	lifetime = 500 μs ($[H_2O]/[Eu] = 1$)	b
B15C5	Eu	ClO_4^-	MeCN	complete Eu quenching for R:L = 1; ion pairing with ClO_4^-	a
	Eu, Tb	ClO_4^-, NO_3^-, NCS^-	EtOH	efficient L→Tb energy transfer; small L→Eu energy transfer	c
18C6	Eu	NO_3^-	MeCN	lifetime = 600 μs ($[H_2O]/[Eu] = 1$)	b
$Me_4$18C6	Eu, Tb	ClO_4^-	CF_3CH_2OH	CPL, titration with NO_3^-; formation of $[R(NO_3)_2 \cdot L]^+$;	d
$B_2$18C6	Eu	X^-	EtOH, C_6H_6	investigation of anion influence (Cl^-, NO_3^-, $CH_3CO_2^-$)	e
21C7	Eu	NO_3^-	MeCN	excitation spectrum $^5D_0 \leftarrow {}^7F_0$; presence of 3 different species	f
*2	Eu	Cl^-, NO_3^-	EtOH	binding mode of the Eu(III) ion	g
NOTA	Eu	–	H_2O/D_2O	presence of 2 forms of complex; $n(H_2O) = 3.3$	h
DOTA	Eu	–	H_2O/D_2O	one major form in solution; $n(H_2O) = 1.3$	h
	Eu	–	H_2O/D_2O	axial symmetry; $n(H_2O) = 1.2$	i
DOTMA	Eu, Tb	–	H_2O/D_2O	photophysical parameters, CPL; $n(H_2O) = 1$	j
TETA	Eu	–	H_2O/D_2O	large crystal field splitting; 2 complex species; $n(H_2O) = 0.6$	h
(2,2,1)	Eu	Cl^-	H_2O/D_2O	one Eu-containing species with C_{2v} symmetry; $n(H_2O) = 3.2$	k
				quenching by $[M(CN)_6]^{4-}$; ion pair formation	l, m
Subst. (2,2) *3	Sm, Eu, Tb, Dy	Cl^-, NO_3^-	Alcohols, MeCN, DMF	energy transfer from the phtalimide chromophore	n
Polyols	Eu	Cl^-	H_2O/D_2O	lifetime measurements versus solvent composition	o
*4	Eu	Cl^-, NO_3^-, $CH_3CO_2^-$	EtOH	luminescence enhancement versus ligand type	p

*1 CPL = circularly polarized luminescence; $n(H_2O)$ = number of bound H_2O molecules as determined by lifetime data.
*2 22 carbonyl-substituted crown ethers containing 4 to 12 ether functions and 2 to 8 carbonyl groups.
*3 N,N′-bis-(N-phtalimido)-methyldiaza-18-crown-6 ether.
*4 Several oligo-oxa-alkanes.

[a] Simon et al. (1985).
[b] Bünzli and Wessner (1978).
[c] De B. Costa et al. (1980).
[d] Metcalf et al. (1985).
[e] Koreneva et al. (1978).
[f] Wessner et al. (1982).
[g] Bogatskii et al. (1984).
[h] Bryden and Reilly (1982).
[i] Albin et al. (1982).
[j] Brittain and Desreux (1984).
[k] Sabbatini et al. (1984c).
[l] Sabbatini et al. (1984a).
[m] Sabbatini and Balzani (1985).
[n] Poluektov et al. (1984b).
[o] Vesala and Käppi (1985).
[p] Zolin et al. (1981).

1982). The emission spectrum of $[Eu(NO_3)_2(2,2)]^+NO_3^-$ in MeCN closely resembles the spectrum of the polycrystalline sample and the authors conclude to the presence of the undissociated bis(nitrato) complex cation in this solution (Bünzli et al., 1986). The presence of a similar cation in trifluoroethanol (TFE) has been proved by Metcalf et al. (1985), who have measured the circularly polarized (CPL) and total (TL) luminescence spectra of solutions containing the chiral $Me_4$18C6 and either Eu(III) or Tb(III) perchlorate during the course of a titration with Et_4NNO_3. The TL spectra indicate a 2:1 interaction between NO_3^- and R(III) and the CPL spectra confirm that the NO_3^- has replaced the ClO_4^- and/or TFE in the first coordination sphere, leaving the chiral crown macrocycle still complexed. In these coronates, the chirality induced in the f-electron structure is thought to arise from a conformational twist of the polyether ring.

A detailed photophysical study of EuDOTMA and TbDOTMA has been made by Brittain and Desreux (1984). High-resolution luminescence spectra of aqueous EuDOTMA solutions demonstrate that two nonequivalent species exist in solution; the CPL spectra show a small degree of observable optical activity in the species thought to be axially symmetric and a large amount of chirality in the species not possessing such symmetry. Comparison of the ground- and excited-state optical activities of TbDOTMA reveals that essentially no geometrical changes accompany the promotion of the Tb(III) ion into an excited f-state. The emission lifetimes are 1.45 ms (H_2O) and 2.025 ms (D_2O) for TbDOTMA and 0.405 ms (H_2O) and 0.690 ms (D_2O) for EuDOTMA. Addition of EuDOTMA to a solution of TbDOTMA results in a decrease both in the Tb(III) emission intensity and lifetime; the rate constant for this dynamic bimolecular quenching is $7.25 \times 10^4\ s^{-1}$.

The photophysical properties of Eu cryptates have been investigated in water (Sabbatini et al., 1984a,c). In $EuCl_3 \cdot (2,2,1)$, the metal ion is encapsulated into the ligand cavity and lies on a site with C_{2v} symmetry. The cryptand only partly shields the lanthanide ion against solvent interaction; from lifetime measurements, it is estimated that 3.2 water molecules are bound to Eu(III) through the holes between the aliphatic chains. The $[Eu(2,2,1)]^{3+}$ cryptate has a lifetime of 215 μs and its lowest excited state lies at 2.1 eV. The cryptate may be used as an excited state reactant in bimolecular processes since the emitting state lives long enough to encounter quenchers even at low quencher concentrations. For instance, the luminescence emission of $[Eu(2,2,1)]^{3+}$ is quenched by $[M(CN)_6]^{4-}$, M = Fe, Os, Ru, via a dynamic electron transfer mechanism:

$$[Eu^*(2,2,1)]^{3+} + [M(CN)_6]^{4-} \rightarrow [Eu(2,2,1)]^{2+} + [M(CN)_6]^{3-}$$

The bimolecular quenching constants in aqueous solutions containing 1 M KCl are 7.5×10^8, 2.2×10^8, and $7.8 \times 10^8\ l\,mol^{-1}\,s^{-1}$ for the Fe, Ru, and Os cyanides, respectively. In more concentrated solutions, there is formation of ion pairs and new absorption bands appear between 430 and 530 nm.

Further luminescence studies are presented below in §3.6.1 (Spectroscopic

probes and bio-inorganic chemistry) and in §4.1 [Electrochemical reduction of R(III) ions and stabilization of R(II) ions in the presence of ionophores].

3.4.3. *Stability constants*

An understanding of the leading effects in the R(III)-macrocycle interaction is provided by the stability constants of the complexes and their associated thermodynamic parameters. The log β_n have been measured for many complexes by several different techniques; potentiometry, calorimetry, electronic and NMR spectroscopies. Pertinent data are summarized in tables 13 through 18.

Systematic values in propylene carbonate have been gathered by two research groups for 12-, 15-, 18-membered coronates, for (2,1,1), (2,2,1), and (2,2,2) cryptates, and for one podate (tables 13 and 14). With the small unsubstituted polyethers, 12C4 and 15C5, both 1:1 and 1:2 complexes are observed by Desreux. The log β_1 for 12C4 and 15C5 complexes are more or less constant over the lanthanide series. When Z increases, the cation charge density increases, bringing about stronger electrostatic interactions with both ligand and solvent. Henceforth, it appears that the favourable larger interaction with the ligand is compensated by a more difficult desolvation, leading to almost no variation in log β_1. The stability of the 1:2 complexes is larger than that of the 1:1 adducts by a factor 10^2 to 10^4 and it decreases with increasing Z, an effect that can be accounted for by structural considerations: the two polyethers are brought closer together when the ionic radius decreases and steric interactions are becoming

TABLE 13

Stability constants (log β_n) at 25°C and $\mu = 0.1$ for complexes between $Ln(CF_3SO_3)_3$ and various crown ethers in anhydrous propylene carbonate, as determined by a competitive potentiometric method.

R	12C4 [a]		15C5 [a]		ButB15C5 [a]	18C6 [b]	But_2B_218C6 [c]	B_230C10 [a]
	1:1	1:2	1:1	1:2	1:1	1:1	1:1	1:1
La	5.00 ± 0.12	6.98 ± 0.15	6.49 ± 0.14	10.18 ± 0.11	3.26 ± 0.04 [d]	8.75	5.14 ± 0.05	4.29 ± 0.04
Ce	–	–	–	–	3.62 ± 0.04		4.95 ± 0.03	4.10 ± 0.03
Pr	5.27 ± 0.08	7.09 ± 0.10	6.22 [b]	–	3.60 ± 0.08	8.60	4.79 ± 0.05	4.12 ± 0.04
Nd	5.19 ± 0.09	6.74 ± 0.12	6.55 ± 0.13	8.65 ± 0.04	3.75 ± 0.04		4.58 ± 0.06	4.10 ± 0.05
Sm	5.17 ± 0.10	6.76 ± 0.14	6.11 [b]	–	3.45 ± 0.04	8.10	4.00 ± 0.04	3.75 ± 0.03
Eu			5.6 ± 0.1 [e]			8.50 ± 0.10 [e]		
Tb	5.15 ± 0.13	6.09 ± 0.20	5.96 ± 0.14	7.66 ± 0.19	3.02 ± 0.05		3.62 ± 0.13	3.53 ± 0.04
Gd	–	–	–	–	2.85 ± 0.05		3.50 ± 0.08	4.07 ± 0.06
Dy	–	–	5.66 [b]	–	2.90 ± 0.12	7.90	3.40 ± 0.07	–
Ho	–	–	–	–	2.80 ± 0.08		3.29 ± 0.15	–
Er	–	–	5.53 [b]	–	2.82 ± 0.07	7.67	3.16 ± 0.05	4.48 ± 0.05
Tm	–	–	–	–	2.81 ± 0.05		2.94 ± 0.09	–
Yb	4.94 ± 0.09	[f]	5.53 [b]	–	2.80 ± 0.10	7.50	2.57 ± 0.09	4.76 ± 0.04
Lu	5.00 ± 0.11	[f]	5.83 ± 0.16	7.89 ± 0.22	2.80 ± 0.06		2.51 ± 0.06	4.80 ± 0.05

[a] Desreux and Massaux (1982), Massaux and Desreux (1982), Massaux et al. (1982).
[b] Almasio et al. (1983); ±0.05 to ±0.10.
[c] Massaux et al. (1980, 1982).
[d] Log $\beta_2 = 5.91 \pm 0.08$.
[e] Loufouilou (1986).
[f] No significant concentrations of 1:2 complexes.

TABLE 14

Stability constants ($\log \beta_n$) at 25°C and $\mu = 0.1$ for complexes between $Ln(CF_3SO_3)_3$ and various coronands, podand, and cryptands, in propylene carbonate.

R	(2,1) [a]	(2,2) [b]	TDA [c]		(2,1,1) [b]	(2,2,1) [a]	(2,2,2)	
	1:1	1:1	1:1	1:2	1:1	1:1	1:1 [b]	1:1 [d]
La	14.4	16.5	9.0	16.3	15.1	18.6	16.1	12.91 [e]
Ce	–	–	–	–	–	–	–	14.20 [e]
Pr	14.5	16.1	8.8	16.3	15.5 [e]	18.7	15.9 [e]	15.88 ± 0.15
Sm	14.9	16.5	9.5	17.6	15.3	19.0	17.3	15.99 ± 0.15
Eu	14.65	16.5	7.6	14.0	15.2	19.0	17.2	–
Gd	–	16.5	9.1	16.7	15.4	–	16.8	–
Tb	–	–	–	–	–	–	–	16.58 ± 0.10
Dy	14.15	16.9	9.5	17.5	15.4	19.0	17.1	–
Er	14.8	16.9	9.7	17.7	15.5	19.2	16.8 [e]	–
Yb	15.4	16.9	10.1	18.3	15.6	19.1	18.0	17.56 ± 0.22

[a] Almasio et al. (1983); ±0.05 to ±0.10.
[b] Arnaud-Neu et al. (1986); ±0.1 to ±0.2.
[c] Tripode ligand tris(dioxa-3,6-heptyl)amine; Arnaud-Neu et al. (1986); ±0.1.
[d] Gillain et al. (1984).
[e] Extrapolated from higher temperature.

important at the end of the R(III) series. It is noteworthy that both polyethers show a complexation trend opposite to the one exhibited by noncyclic ligands. Both 1:1 and 1:2 coronates with 15C5 are 10 to 10^3 times more stable than 12C4 complexes, a difference that we attribute to the greater number of donor atoms and to the better flexibility of the macrocycle. The reported $\log \beta_n$ values are consistent with the findings that (a) a 1:1 complex cannot be isolated with 15C5 in MeCN, even in the presence of a large excess of $R(ClO_4)_3$ (Bünzli et al., 1979a), and (b) mixed complexes $R(ClO_4)_3 \cdot (15C5) \cdot (12C4)$ do not crystallize for R = La, Ce (Bünzli et al., 1981b).

The presence of the t-butyl-phenyl substituent on the 15-membered cycle causes a large decrease of the stability constants, by approximately three orders of magnitude and 1:2 complexes are no longer observed, except for La. The lower stability is associated with the electron-withdrawing effect of the substituent, resulting in a lower basicity of the O atoms, as well as with a larger rigidity of the ligand. The $\log \beta_1$ values go through a maximum for Nd(III), and from Tb(III) on they remain constant. This reflects the delicate balance prevailing between the favourable and unfavourable factors influencing the complexation process.

The stability of 18-crown-6 complexes decreases with increasing Z, both for the unsubstituted and benzosubstituted ligands. For this latter coronand, the La(III)/Lu(III) selectivity, $\Delta \log \beta_1 = 2.63$, is much larger than the La(III)/Yb(III) selectivity provided by 18C6, $\Delta \log \beta_1 = 1.25$, a consequence of its larger rigidity. Moreover, the destabilization provided by the t-butyl-phenyl substituent is larger for the 18-membered systems than for the 15-membered polyether: four versus three orders of magnitude.

The $B_2$30C10 ether is a highly flexible ligand which wraps easily around the metal ions. Complexes with 1:1 metal:ligand ratio can be isolated with $R(ClO_4)_3$ for R = La–Eu and Dy–Yb (Ciampolini and Nardi, 1979). This may be partly rationalized considering the log β_1 values, which have an unusual trend: the log β_1 versus $1/r_i$ plot is V-shaped with a sharp minimum at R = Gd. Desreux explains this feature by a structural change occurring after Gd, as indicated by calorimetric data. The ΔS_f^0 values are nearly constant for R = La–Gd, while the ΔH_f^0 values become less exothermic, reflecting a weaker metal/ligand interaction. From Gd to Yb, both ΔS_f^0 and ΔH_f^0 values become more negative. In the "wrap around" structure that may be assumed, the ligand conformation is strained and the decrease in the R(III) ionic radius causes intraligand repulsion to become progressively stronger. Further contraction is no longer possible to accommodate ions smaller than Gd(III), hence the structural change.

The replacement of two ether functions of 15C5 and 18C6 by amine groups has a large stabilizing effect: $\Delta \log \beta_1 = 8$ to 10 for the 15-membered ligands and 7.5 to 9 for the 18-membered coronand.

The stability of the cryptates follows the sequence $[R(2,2,1)]^{3+} > [R(2,2,2)]^{3+} > [R(2,1,1)]^{3+}$, with $\Delta \log \beta_1 = 1.5$ between both (2,2,1) and (2,2,2), and (2,2,2) and (2,1,1) cryptates. This effect may be related to the cavity size of the ligands: $D_c = 2.3$, 2.8, and 1.6 Å, for (2,2,1), (2,2,2), and (2,1,1), respectively. However, one notes the relative insensitivity of the formation constants to ionic radius change within the R(III) series. The stability difference between the cryptates and the corresponding coronates is known as the "macrocyclic effect" (Lehn and Sauvage, 1975). It amounts to $\Delta \log \beta_1 = 4$ for ligands (2,1) and (2,2,1) but is almost inexistent for ligands (2,2) and (2,2,2).

Podates with TDA, a ligand that may be thought of as being the open-chain analogue of cryptand (2,2,2), are less stable than both $[R(2,2)]^{3+}$ and $[R(2,2,2)]^{3+}$ complexes, probably because of the presence of only one amine group. However, this ligand provides an interesting selectivity for the R(III) ions with respect to Eu(III). The Eu podate is indeed 200 times less stable than the Gd complex and 450 times less stable than the Sm podate.

The effects of cavity size and ligand hardness have been discussed by Poluektov et al. (1984a) on the basis of the stability constants in PC. An equation has been proposed to calculate log β(R) from log β(La), the number of f electrons N_f, and the quantum numbers S and L of the R(III) ions:

$$\log \beta(R) = \log \beta(La) + \alpha N_f + \beta S + \gamma' L_{1-6} \text{ (or: } + \gamma'' L_{8-13}) ,$$

where α, β and γ' (or γ'') are adjustable empiric parameters. This equation reproduces the experimental log β within less than 5%.

Several determinations of stability constants have been performed in methanol (table 15) and water (table 16). The lanthanide cryptates have a slow kinetics of formation so that measurements are difficult to perform precisely. For the La(III) ion, Anderegg (1981) has found that one month is necessary to reach equilibrium

TABLE 15
Stability constants ($\log \beta_1$) at 25°C and $\mu = 0.1$ for rare earth coronates and cryptates in methanol.

R	B15C5 [a]	NitrB-15C5 [b]	(2,1) [b]	18C6 [c]	18C6 [d]	$Cy_2$18C6 [d]	(2,2,1) [b]	(2,2,2) [e]
La	2.13	2.34	7.08	3.29 ± 0.03	3.25 [f]	2.49	8.28	9.4
Ce	2.30			3.57 ± 0.20	2.81	2.05		8.4
Pr	2.18	2.45	7.94	2.63 ± 0.28	2.47	1.62	9.31	
Nd	2.27	2.70	7.86	2.44 ± 0.16	2.16	< 1.3	9.86	
Sm	2.37	2.81	7.00	2.03 ± 0.07	< 1.6		9.70	
Eu			8.59	1.84 ± 0.14			10.57	
Gd	2.35	2.98	7.67	1.32 ± 0.12			10.14	
Tb			8.29	[g]			10.26	
Dy	2.60	3.36	8.96				10.45	
Ho			8.81				10.86	
Er	2.40	3.40	8.70				10.78	
Tm			9.46				11.61	
Yb							12.00	
Lu	2.41	3.60						
Y	2.38	3.36	8.66				10.34	

[a] Potentiometry, ClO_4^-, MeOH/Et_4NI; Xiao Wenjin et al. (1985).
[b] Potentiometry, $CF_3SO_3^-$, MeOH/Et_4NClO_4, ±0.1 to ±0.2; Almasio et al. (1983).
[c] Titration calorimetry, Cl^-, MeOH [+9H_2O per R(III) ion], $\mu = 0.005$; Izatt et al. (1977).
[d] Potentiometry, Cl^-, MeOH/Me_4NCl, at 26°C, ±0.01 to ±0.07; Zhou Jinzhong and Wang Dexi (1982), Zhou Jinzhong et al. (1983), Zhou Jinzhong and Wu Xi (1984).
[e] Potentiometry, Cl^-, $\mu = 0.1$, Me_4NCl, MeOH/H_2O 95/5; Anderegg (1981); the value for the (2,2) coronate is 6.18.
[f] 4.08 ± 0.12 by a fluorimetric method, in MeOH, without Me_4NCl added; Wang Genglin and Jiang Zonghui (1980).
[g] No complexation detected.

in MeOH/water. Furthermore, solvolysis competes with the complex formation and this author was unable to determine $\log \beta_1$ for heavier R(III) ions (see also Peterson, 1979). Almasio et al. (1983) report that in methanol the cryptand (2,2,1) provides some specificity towards the ionic radius of the metal ion: $\Delta \log \beta_1(\text{Yb/La}) = 3.72$, the Yb cryptate being more stable. This is consistent with the metal ion specificity observed between (2,2,1) and (2,2,2) cryptates by electrochemical measurements (Yee et al., 1980), the former complexes being more stable by more than two orders of magnitude. At variance with these results are the pH-titration data of Burns and Baes (1981), obtained in water after allowing 4–6 weeks for equilibrium to be reached: almost no difference is observed, neither between (2,2,1) and (2,2,2) cryptates, nor along the lanthanide series. Since this question of specificity is of considerable significance, Pizer and Selzer (1983) carried out the determination of $\log \beta_1$ by a visible spectrophotometric method in DMSO, using murexide as a metal-ion indicator. Their data (cf. table 17) also show a lack of metal-ion specificity which may be caused by larger interactions with the solvent. Indeed, the structural and spectroscopic data discussed previously reveal that small solvent molecules and anions may

TABLE 16
Stability constants (log β_1) at 25°C of rare earth coronates and cryptates in water.

R	$N_6$18C6 [a]	DOTA [b]	(2,1)DA [c]	(2,2)DA [d]	(2,1,1) [e]	(2,2,1) [e]	(2,2,2) [c]
La	5.7 ± 0.3		10.11 ± 0.06	12.21 ± 0.13		6.59 ± 0.09	6.45 ± 0.03
Ce			10.89 ± 0.08	12.23 ± 0.04		6.58 ± 0.04	6.37 ± 0.08
Pr			11.31 ± 0.05	12.22 ± 0.06			
Nd			11.60 ± 0.07	12.21 ± 0.06			
Sm			11.72 ± 0.09	12.12 ± 0.04	6.8 ± 0.2	6.76 ± 0.02	5.94 ± 0.06
Eu		28.2 ± 0.2	11.85 ± 0.11	12.02 ± 0.10		6.8 ± 0.2	5.90 ± 0.09
Gd		28.0 ± 0.2[f]	11.66 ± 0.10	11.93 ± 0.09		6.7 ± 0.1	
Tb		28.6 ± 0.1	11.52 ± 0.10	11.70 ± 0.06		6.6 ± 0.1	
Dy			11.55 ± 0.07	11.57 ± 0.04			
Ho			11.34 ± 0.08	11.18 ± 0.10	6.21 ± 0.08		6.2 ± 0.2
Er			11.15 ± 0.06	11.30 ± 0.08		6.60 ± 0.08	
Tm			10.79 ± 0.09	11.10 ± 0.02	6.8 ± 0.4	6.88 ± 0.05	
Yb			10.76 ± 0.03	10.90 ± 0.04	6.51 ± 0.09		
Lu		29.2 ± 0.2	10.33 ± 0.09	10.84 ± 0.02	6.55 ± 0.09		
Y			10.85 ± 0.02				

[a] Potentiometry, NO_3^-, $\mu = 0.2$, $H_2O/NaClO_4$; Kodama et al. (1980).
[b] Potentiometry, 20°C, $\mu = 1$; Loncin et al. (1986).
[c] Potentiometry, NO_3^-, $\mu = 0.1$, H_2O/Me_4NCl; Chang et al. (1985), Chang and Ochaya (1986).
[d] Potentiometry, NO_3^-, H_2O/Me_4NCl; Chang and Rowland (1983).
[e] Potentiometry, Cl^-, $\mu = 0.25$, H_2O/Me_4NCl; Burns and Baes (1981).
[f] Extrapolated for $\mu = 0$; Desreux (1978).

interact with the R(III) ion through the holes between the aliphatic chains of the cryptands. When chloride is added to the Yb(III) solution containing the (2,2,2) cryptand, log β_1 is reduced by more than one unit. Moreover, stability constants for the formation of $[Eu(2,2,1)X_n]^{(3-n)+}$ and $[Eu(2,2,2)X_n]^{(3-n)+}$, with $X = F^-$ or OH^-, are known; log β_n ranges between 4.3 and 5.5 ($n = 1$) and 6.5 and 6.8 ($n = 2$). The hydroxy anion interaction is stronger than the fluoride association, and, with respect to the aquo ion, the F^- interaction is 10 times larger in the cryptate while the OH^- interaction is the same (Pruett, 1978; Yee et al., 1980).

In the polar solvents H_2O and MeOH, the stability difference between the crown ethers and their diaza-substituted homologue, as well as the macrobicyclic effect, are much smaller than in PC. For instance, $\Delta \log \beta_1 \simeq 2$ for (2,1) and (2,2,1) in methanol, and $\Delta \log \beta_1 \simeq 3$ for (2,2) and 18C6. On the other hand, one notes the relatively large stability of $[La(N_6 18C6)]^{3+}$ in water (log $\beta_1 = 5.7$). Complete sets of data are reported for two diamino-dicarboxy-substituted coronates in water, (2,1)DA and (2,2)DA. Complexes with the latter follow the same stability trend as 18C6 coronates in PC, with a regular decrease from log $\beta_1 = 12.2$ for La, to 10.8 for Lu. With the smaller macrocycle (2,1)DA, the trend is different and the Eu(III) complex is the more stable one. This selectivity is small [$\Delta \log \beta_1 = 0.13$ and 0.19 with respect to Sm(III) and Gd(III), respectively] and is attributed to a variation in the match between the properties of the ligand and the metal ion (Chang and Ochaya, 1986). DOTA, which contains 4 aminocarboxylic

TABLE 17
Stability constants (log β_n) at 25°C of lanthanide coronates and cryptates in various organic solvents.

Ligand	Anion	R	R:L	Log β_n	Method[a]	μ	Medium	Ref.
12C4	TFA	La	1:1	>7	NMR	0.3	CD_3CN	b
15C5	PF_6^-	La	1:2	7.4 ± 0.2	NMR	0.29	CD_3CN	c
		Pr	1:2	4.4 ± 0.2	NMR	0.20	CD_3CN	c
		Nd	1:2	3.8 ± 0.2	NMR	0.18	CD_3CN	c
		Sm	1:2	3.2 ± 0.2	NMR	0.16	CD_3CN	c
18C6	NO_3^-	La	1:1	<1.23	NMR	0.07	DMF	d
		La	1:1	4.4 ± 0.2	NMR	0.052	CD_3CN	e
		Ce	1:1	4.5 ± 0.2	NMR	0.056	CD_3CN	e
		Pr	1:1	3.7 ± 0.2	NMR	0.080	CD_3CN	e
		Nd	1:1	3.5 ± 0.2	NMR	0.102	CD_3CN	e
		Eu	1:1	2.6 ± 0.2	NMR	0.087	CD_3CN	e
		Yb	1:1	2.3 ± 0.2	NMR	0.047	CD_3CN	e
	TFA	La	1:1	>6	NMR	0.2	CD_3CN	b
		Sm	1:1	4.4 ± 0.2	NMR	0.2	CD_3CN	b
(2,1,1)	Cl^-	Pr	1:1	3.86 ± 0.05	Spectr.		DMSO	f
		Nd	1:1	3.97 ± 0.14	Spectr.		DMSO	f
		Gd	1:1	3.87 ± 0.14	Spectr.		DMSO	f
		Ho	1:1	3.80 ± 0.05	Spectr.		DMSO	f
		Yb	1:1	4.43 ± 0.11	Spectr.		DMSO	f
(2,2,1)	Cl^-	Pr	1:1	3.47 ± 0.07	Spectr.		DMSO	f
		Nd	1:1	3.01 ± 0.31	Spectr.		DMSO	f
		Gd	1:1	3.26 ± 0.09	Spectr.		DMSO	f
		Ho	1:1	3.11 ± 0.23	Spectr.		DMSO	f
		Yb	1:1	4.00 ± 0.23	Spectr.		DMSO	f
(2,2,2)	Cl^-	Pr	1:1	3.22 ± 0.07	Spectr.		DMSO	f
		Nd	1:1	3.26 ± 0.14	Spectr.		DMSO	f
		Gd	1:1	3.45 ± 0.11	Spectr.		DMSO	f
		Ho	1:1	3.47 ± 0.15	Spectr.		DMSO	f
		Yb	1:1	4.11 ± 0.11[g]	Spectr.		DMSO	f

[a] Method: Nuclear magnetic resonance (NMR) or visible absorption spectrometry with murexide as indicator (Spectr.).
[b] Bünzli and Giorgetti (1985b).
[c] Bünzli and Giorgetti (1985a).
[d] Boss and Popov (1985).
[e] Bünzli and Wessner (1981).
[f] Pizer and Selzer (1983).
[g] 3.00 in presence of 0.02 M Et_4NCl.

substituents, gives the most stable complex ever reported for a R(III) ion: log $\beta_1 = 28$–29.

The other stability constants measured in inorganic solvents (table 17) provide some insight into the anion influence on log β_1. Moreover, stability constants of $R(NO_3)_3$ complexes with polyethyleneglycols EO3, EO4, and EO5 have also been measured (Hirashima et al., 1986). The EO3 ligand shows a good specificity for the Eu(III) ion in acetone, which is not the case for EO4 and EO5 in ethyl acetate.

Thermodynamic parameters are still relatively scarce and are often given with

TABLE 18

Thermodynamic parameters ΔH_f^0 (kJ mol^{-1}) and ΔS_f^0 (J mol^{-1} K^{-1}) at 25°C for the formation of some coronates, cryptates, and one podate. Uncertainties in the last digit(s) are given in parentheses.

R		18C6 [a]	18C6 [b]	18C6 [c]	18C6 [d]	(2,1) [d]	(2,2) [d]	TDA [d]	(2,1,1) [d]	(2,2,1) [d]	(2,2,2) [d]	(2,2,2) [e]
La	ΔH:	11.8(2)	9.6	−36.2								−55(9)
	ΔS:	102.5	94.0	−37.5								64(26)
Ce	ΔH:	10.6(5)	16.1	−43.0								−77(9)
	ΔS:	104.0	108.1	−55.6								15(9)
Pr	ΔH:	18.7(1.7)	18.6	−44.0	−29(8)	−28.0(8)	−130(4)	−50(13)	−28.9(4)	−138(21)	−105(8)	−94.5(1.5)
	ΔS:	113.0	109.5	−76.9	79(21)	166(1)	−130(17)	−8(42)	201(4)	−100(63)	−42(25)	−28(10)
Nd	ΔH:	20.0(1.1)	25.7	−36.2								
	ΔS:	113.7	127.7	−54.3								
Sm	ΔH:	15.4(2)										−96(3)
	ΔS:	90.4										−17(8)
Eu	ΔH:	12.8(6)		−12.8				−92(8)				
	ΔS:	78.2		8.7				−17(25)				
Gd	ΔH:	15.6(6)										
	ΔS:	77.6										
Tb	ΔH:											−104(5)
	ΔS:											−31(14)
Er	ΔH:					−21(4)	−155(18)	−2.9(8)	−38	−146(8)	−113(4)	
	ΔS:					197(28)	−193(34)	176(4)	163(4)	−117(25)	−50(17)	
Yb	ΔH:	no values available										
	ΔS:											

[a] Izatt et al. (1977); cf. table 15.

[b] Zhou Jinzhong et al. (1983); cf. table 15.

[c] Ammann and Bünzli (1979, 1982); calorimetry in MeCN.

[d] Loufouilou (1986), Arnaud-Neu et al. (1986); cf. tables 13 and 14.

[e] Gillain et al. (1984); cf. table 14.

large uncertainties (table 18). Their interpretation is therefore not clearcut, since the stabilization of the macrocyclic complexes depends upon several, often compensating, factors. Kauffmann et al. (1976) have proposed a simple classification of macrocyclic ligands in terms of the signs of ΔH_f^0 and ΔS_f^0:

Type I: $\Delta H_f^0 < 0$, $\Delta S_f^0 > 0$,

Type II: $\Delta H_f^0 < 0$, $\Delta S_f^0 < 0$,

Type III: $\Delta S_f^0 > 0$, $\Delta H_f^0 < 0$,

Type IV: $\Delta S_f^0 > 0$, $\Delta H_f^0 > 0$.

The first two types of ligands give rise to enthalpy-stabilized complexes with a minor positive or negative entropic contribution, and the latter two give rise to entropy-stabilized complexes with a minor favourable or unfavourable enthalpic contribution. In view of the few data reported for R(III) ions, we shall stay with this classification, although a better discussion would consider the linearity of the $\Delta G_f^0/\Delta H_f^0$ plots (Inoue and Hakushi, 1985). In nonaqueous solvents, PC and MeCN, all the lanthanide complexes are enthalpy-stabilized. Ligands 18C6, (2,1), and (2,1,1) belong to type I, whereas TDA, (2,2), (2,2,1), and (2,2,2) are of type II. The complexes with these latter have larger ΔH_f^0, reflecting stronger R(III)/ligand interactions. In methanol, 18C6 behaves as a type-III ligand, with both positive ΔH_f^0 and ΔS_f^0.

3.4.4. *Kinetic data*

Ligand dissociation processes are usually slow, especially for cryptates which are highly inert complexes. They have been investigated for a few macrocyclic complexes either by NMR spectroscopy or by electrochemical methods. The Ln(III)/Ln(II) reduction kinetics is not discussed here, but will be reviewed in §4.1.

For the $La(ClO_4)_3/12C4/CD_3CN$ system, band-shape analysis of the ^{1}H-NMR spectra as a function of both M:L ratios and temperature (243 to 313 K) indicates a dissociative mechanism with a first-order rate constant of $4\ s^{-1}$ at 298 K (Bünzli et al., 1981b). In CD_3CN solutions of 1:1 and 4:3 nitrato complexes with 18C6, both inter- and intramolecular exchange reactions occur, as demonstrated by low-temperature ^{1}H-NMR spectra (R = La–Nd, Eu, Yb). For Nd, the intermolecular exchange rate at 343 K is $12\ s^{-1}$ (Bünzli and Wessner, 1981). The NMR spectrum of $Yb(NO_3)_3 \cdot (18C6) \cdot 3H_2O$ was analyzed by Backer-Dirks et al. (1980); between 292 and 343 K, the ligand dissociation is approximately constant so that ΔH_{diss} is close to zero. A slow ligand exchange kinetics is also reported for $Pr(NO_3)_3 \cdot (2,2)$ in CD_3NO_2 (Desreux et al., 1977) and for $R(NO_3)_3 \cdot (Py_2Me_4N_6 18C6ene_4)$ in water, R = La, Ce (Backer-Dirks et al., 1979); the kinetic inertness of the latter coronates is ascertained by the fact that no precipitate falls out upon addition of KF or KOH to their aqueous solutions.

On the contrary, rapid ligand exchange takes place in $CDCl_3$ for the complex between 18C6 and the shift reagent $Eu(fod)_3$. At 295 K, $\log k = 4.8$ for 0.05 M solutions and the activation energy, determined between 213 and 313 K, amounts to $E_a = 37.7\ kJ\ mol^{-1}$. A slightly positive entropy of activation is found and Bidzilya (1978) concludes that a dissociative mechanism is operative. Similar values are found for $Pr(fod)_3 \cdot (18C6)$: $\log k = 5.4$ at 393 K and $E_a = 39.8 \pm 0.8\ kJ\ mol^{-1}$ (Bidzilya and Golovkova, 1980b).

Polyaza polyacetic ligands give rise to nonlabile complexes. However, conformational processes take place within the macrocyclic ring, so that two different species are usually observed in water. The relevant data are given in table 19. The free energies of activation are the highest ever reported for a conformational process taking place in lanthanide complexes. The dissociation rate constants for $[R(2,1)DA]^+$ have been determined by Chang et al. (1985) in an acetic acid acetate buffer of pH 4.6 and at ionic strength $\mu = 0.1$, by stopped-flow measurements. They decrease from ca. $0.1\ s^{-1}$ for La to about $3 \times 10^{-3}\ s^{-1}$ for Eu and increase again to about 4×10^{-2} for Lu. A detailed study suggests that for lighter lanthanide complexes the kinetics obeys the rate law:

$$k_{obs} = k_d + k_H[H^+],$$

where k_{obs} is the observed pseudo-first-order rate constant; k_d and k_H are the rate constants for direct dissociation and acid catalyzed pathways, respectively. For the heavier lanthanide complexes, a saturation-type kinetics is observed with rate constants increasing with increasing acid concentration and reaching a limiting value.

The kinetics of dissociation of Eu and Yb cryptates has been followed by voltammetric measurements (Yee et al., 1980). Table 20 summarizes the rate constants and activation parameters. The dissociation is also acid-catalyzed and follows the same rate law as $[R(2,1)DA]^+$ complexes; k_d is equal to $3 \times 10^{-7}\ s^{-1}$

TABLE 19
Kinetic data for the intramolecular rearrangement in polyaza polyacetic complexes, obtained from NMR spectra.

Ligand	R	T (K)	ΔG^* ($kJ\ mol^{-1}$)	ΔH^* ($kJ\ mol^{-1}$)	ΔS^* ($kJ\ mol^{-1}$)	$k(278)$ (s^{-1})	$k(343)$ (s^{-1})
NOTA [a]	Lu	318	64 ± 2				
DOTA [b]	La [c]	298	60.7 ± 1.2	59.4 ± 0.8	-4.6 ± 3.3	23	6.8×10^3
	Pr	334	60.7				
	Eu	330	61.9				
DOTMA [d]	La	373	77.5				
TETA [e]	Eu	315	60.1				
	Lu [f]	298	63.7 ± 7.5	71.7 ± 5.3	27 ± 8	7	2.3×10^3

[a] Geraldès et al. (1985).
[b] Desreux (1980).
[c] 0.1 M solution in D_2O at pH = 11.
[d] Brittain and Desreux (1984).
[e] Desreux and Loncin (1986).
[f] 0.1 M solution in D_2O at pH = 8.

TABLE 20
Rate constants and activation parameters for the dissociation of Eu and Yb cryptates at 298 K. [a]

Ligand	R	Medium	k_{obs} [b] (s^{-1})	ΔH^* ($kJ\,mol^{-1}$)	ΔS^* ($J\,K^{-1}\,mol^{-1}$)
(2,2,1)	Eu	0.5 M $NaClO_4$, pH = 7	4.1×10^{-7}		
		0.5 M $NaClO_4$, pH = 2.5	3.0×10^{-7}	79.1	−106.7
	Yb	0.5 M $NaClO_4$	1.3×10^{-6}	93.3	−43.9
(2,2,2)	Eu	0.1 M Et_4NClO_4, pH = 7	1.1×10^{-3}	57.8	−108.8

[a] Yee et al. (1980).
[b] First-order rate constant obtained at pH values where the acid-independent pathway dominates.

and $1 \times 10^{-3}\ s^{-1}$ and k_H is equal to 10^{-7} and $0.2\,l\,mol^{-1}\,s^{-1}$ for (2,2,1) and (2,2,2) Eu cryptates, respectively. The presence of significant concentrations of OH^- or F^- has an accelerating effect upon the dissociation rates: the half-life for the aquation of $[Eu(2,2,1)]^{3+}$ at 298 K is reduced from 27 days to 2.8 days and to 22 min upon addition of 0.05 M F^- or OH^-, respectively. Approximate half-lives for the aquation of $[Sm(2,2,2)]^{3+}$ and $[Nd(2,2,2)]^{3+}$ at 298 K are equal to 45 and 65 min, respectively (Pruett, 1978).

3.4.5. *NMR investigations: complexation, solution structure, and shift reagents*

NMR investigations are performed to obtain the following informations: (a) evidence for complex formation; (b) structural data on the complexes in solution; (c) study of the interaction with shift reagents; (d) determination of stability constants; and (e) investigation of kinetic processes.

Data pertaining to the last two topics have been presented in the previous sections; the other studies are summarized in table 21.

Solution structures may be determined on the basis of lanthanide-induced shifts. This is, however, a difficult task: the exact origin of the induced NMR shifts is unknown, a great number of lanthanide complexes have a low symmetry and they often present a high lability, e.g., between conformers. The separation of the various contributions to the NMR shifts may be achieved by several procedures under favourable conditions, or can be avoided by selecting the Yb(III) ion as paramagnetic center, since this ion induces shifts that are essentially dipolar in origin. The dipolar shift is expressed by:

$$\Delta\nu = D_1[(3\cos^2\theta - 1)/r^3] + D_2[(\sin^2\theta\cos 2\phi)/r^3]\,,$$

where r, θ, and ϕ are the polar coordinates of the nucleus studied relative to the magnetic susceptibility axes.

Using a simplified equation, taking into account the first term only, Desreux and Duyckaerts (1979) have deduced the average distance between R(III) and the O atoms of 12C4, under the assumption that the investigated $R(ClO_4)_3 \cdot (12C4)_2$ coronates are axially symmetric. This distance increases from Pr to Yb,

in agreement with the concept of ionic radii contraction. Catton et al. (1978) have fitted ^{1}H and ^{13}C spectra of $R(ClO_4)_3 \cdot (Cy_2 18C6)$ complexes, assuming the molecular species present in solution have the same structure as solid $La(NO_3)_3 \cdot (Cy_2 18C6)$, with C_2 symmetry. The nonaxially symmetric susceptibility tensor produces a good fit for both the spectra of the initial solution and those of solutions containing added water and tributylphosphate. It is suggested that the observed anisotropy is caused by unequal ligand fields from the six O atoms and from asymmetric coordination of the ligands situated above the polyether ring. The (2,2,1) cryptates have also been studied in great detail by Gansow et al. (1979). The plots of the paramagnetic shift versus the Bleaney constant D for Ce–Eu and Tb–Er are straight lines going through the origin, meaning the contact interactions are negligible and that the geometry of the complexes is the same for the entire series. Moreover, the analysis of the coupling constants for $La(NO_3)_3 \cdot (2,2,1)$ in acetonitrile indicates that a single conformation of the ligand is favoured. In solutions of (2,2,2) cryptates, the paramagnetic shifts are smaller than for (2,2,1) cryptates and only three $-N-CH_2$ resonances are observed, pointing to highly symmetrical inclusion compounds (Kausar, 1982).

When the investigated complexes are sufficiently rigid and stable in solution, the above-mentioned problems disappear, and a thorough structural study is feasible. In view of their potential applications as water-soluble axially symmetric shift reagents, Desreux and coworkers have determined the solution structures of complexes with NOTA, DOTA, DOTMA, and TETA. At low temperature, rigid DOTA complexes possess a C_4 axis perpendicular to the main plane of the molecule, so that a simplified treatment may be applied. It was found that the R(III)–N distances are similar to those in the EDTA complexes, and an approximate map of the dipolar field could be estimated (Desreux, 1980). Separation of the contact and dipolar ^{17}O shifts was achieved for the light and heavy lanthanide complexes (Bryden et al., 1981). There is a perfect agreement between the solution structure of $YbDOTA^-$ and the X-ray crystal structure of $EuDOTA^-$ (Spirlet et al., 1984a) as demonstrated by the match between experimental and calculated NMR shifts. The latter are evaluated using geometrical factors extracted from the X-ray crystal structure. The $EuDOTA^-$ complex is a good potential shift reagent, contrary to both EuNOTA, which is conformationally less rigid (Geraldès et al., 1985), and $EuTETA^-$, which is nonaxially symmetric.

The shift reagent $Eu(fod)_3$ is a strong Lewis acid and is quite soluble in nonpolar solvents. The complexing constants $\log \beta_n$ for the binding of this reagent to organic molecules can be calculated unambiguously from the determination of the induced paramagnetic shift as a function of the substrate concentration at constant shift reagent concentration. Adducts with various stoichiometries usually form (2:1, 1:1, 1:2) and coexist in equilibrium in solution, so that it is essential to determine these constants from several different resonances. The values for 1:1 adducts with various coronands and podands lie within the range $\log \beta_1 = 0.5$ to 2.5.

TABLE 21

NMR studies of rare earth coronates, cryptates, and podates (complexation, solution structure, shift reagents).

Ligand	R	Anion	Solvent	Nucleus	Type of study [a]	References
12C4	Pr–Yb	ClO_4^-	CD_3NO_2	^1H	S; Ln–O distances	Desreux and Duyckaerts (1979)
	Pr, Eu, Yb	fod	$CDCl_3$	^1H	SR; log β_n	Shen Lianfang et al. (1983)
	Eu	fod	$CDCl_3$, C_6D_6	^{13}C	SR; log β_n	Erk (1983)
B_2PO_514C6	Pr, Eu	fod	$CDCl_3$	^1H	SR; log β_n	Yatsimirskii et al. (1979)
$Py_2Me_4N_6$-18C6ene$_4$	La, Ce	NO_3^-	H_2O	^1H	S; susceptibility tensor	Backer-Dirks et al. (1979)
15C5	La–Sm	PF_6^-	CD_3CN	^1H	C; shifts	Bünzli and Giorgetti (1985a)
	Pr, Eu, Yb	fod	$CDCl_3$	^1H	SR; log β_n	Shen Liangfang et al. (1983)
	Eu	fod	$CDCl_3$, C_6D_6	^{13}C	SR; log β_n	Erk (1983)
Lar15C5	Yb	fod	$CDCl_3$	^{13}C	SR; distances	Kaifer et al. (1984)
$Ket_2$15C5	Eu	fod	$CDCl_3$, C_6D_6	^{13}C	SR; log β_n	Erk (1983)
B15C5	Sc	Cl^-, NCS^-	$(CD_3)_2CO$	^1H, ^{45}Sc	C	Olszanski (1975), Melson et al. (1977), Olszanski and Melson (1978)
	Nd, Eu, Yb	ClO_4^-	CD_3CN	^1H	C; shifts	Simon et al. (1985)
	Sm, Eu, Tm, Yb, Lu	NO_3^-	$(CD_3)_2CO$	^1H	C; coordinated solvent	Heckley (1974); King and Heckley (1974)
	Eu	fod	CCl_4	^1H	SR; O-atom basicity	Lockhart et al. (1979)
	Tb	not available	$(CD_3)_2CO$	^1H	C	De B. Costa et al. (1980)
Me,BrB15C5	La	NO_3^-	$(CD_3)_2CO$	^1H	C; shifts	Jin Linpei (1985)
Napht15C5	Nd, Eu, Yb	ClO_4^-	CD_3CN	^1H	C; shifts	Simon et al. (1985)
$BNO_4$15C5	Eu	fod	CCl_4	^1H	SR; O-atom donor strength	Lockhart et al. (1973)
$BN_2O_3$15C5	Eu	fod	CCl_4	^1H	SR; O-atom donor strength	Lockhart et al. (1973)
18C6	La–Nd, Eu, Yb	NO_3^-	CD_3CN	^1H	C; shifts	Bünzli and Wessner (1981)
	Pr	ClO_4^-	$CDCl_3$/MeCN	^1H, ^{13}C	C; shifts	Shen Lianfang et al. (1982)
		fod	$CDCl_3$	^1H	SR; log β_n	Bidzilya and Golovkova (1980b)
	Eu	fod	$CDCl_3$	^1H	SR; log β_n	Yatsimirskii et al. (1977), Davidenko et al. (1980), Erk (1983)
	Eu	fod	$CDCl_3$, C_6D_6	^{13}C	SR; log β_n	Erk (1983)
$Ket_2$18C6	Eu	fod	$CDCl_3$, C_6D_6	^{13}C	SR; log β_n	Erk (1983)
$Cy_2$18C6	Sc	Cl^-, NCS^-	$(CD_3)_2CO$	^1H, ^{45}Sc	C	Olszanski (1975), Melson et al. (1977), Olszanski and Melson (1978)
	La, Sm, Pr	ClO_4^-	$CDCl_3/CD_3CN$	^1H, ^{13}C	S; C_2 symmetry	Catton et al. (1978)
$B_2$18C6	Sc	Cl^-, NCS^-	$(CD_3)_2CO$	^1H, ^{45}Sc	C; coordinated solvent	Olszanski (1975), Melson et al. (1977), Olszanski and Melson (1978)
	Pr	fod	$CDCl_3$, CD_2Cl_2	^1H	SR; log β_n	Yatsimirskii et al. (1977), Davidenko et al. (1977)

	Eu	fod	$CDCl_3$, CD_2Cl_2	^1H	SR; log β_n	Yatsimirskii et al. (1977), Davidenko et al. (1977, 1980)
$Ph_4$18C6	La–Nd	ClO_4^-, NO_3^-	$CDCl_3$, CD_3CN	^1H	C	Wang Jingqiu et al. (1983, 1985)
$Fur_2N_4O_2$-18C6ene$_4$	La	NO_3^-	DMSO-d_6	^1H	C	Abid and Fenton (1984b)
$O_4S_2$18C6	Eu	fod	$CDCl_3$	^1H	SR; log β_n	Bidzilya and Golovkova (1980a)
(2,2)	Pr	NO_3^-	CD_3NO_2	^1H	S; conformation	Desreux et al. (1977)
$B_4P_2O_{10}$28C12	Pr, Eu	fod	$CDCl_3$	^1H	SR; log β_n	Yatsimirskii et al. (1979)
[b]	Eu	fod	$CDCl_3$	^1H	SR	Elguero et al. (1984, 1985)
[c]	Eu	dpm	CCl_4	^1H	SR; optical isomers	Perrett and Stenhouse (1972)
(2,2,1)	Sc	Cl^-, NCS^-	$(CD_3)_2CO$	^1H, ^{45}Sc	C	Olszanski (1975), Olszanski and Melson (1978)
	La–Nd, Eu, Tb–Er	ClO_4^-, Cl^-, NO_3^-	D_2O, CD_3CN	^1H	C; shifts	Pruett (1978), Gansow et al. (1979)
	Gd	Cl^-	D_2O	^{15}N, ^{89}Y, ^{111}Cd, ^{183}W	relaxation agent	Gansow et al. (1980a, 1980b)
(2B,2,1)	Pr, Eu	NO_3^-	CD_3CN	^1H	C; shifts	Gansow and Kausar (1985)
(2,2,2)	La–Sm	NO_3^-	D_2O, CD_3CN	^1H	C; shifts	Pruett (1978), Kausar (1982)
	Sc	Cl^-, NCS^-	$(CD_3)_2CO$	^1H, ^{45}Sc	C	Olszanski (1975), Olszanski and Melson (1978)
[d]	La	NO_3^-	H_2O, MeOH	^1H	C	Cheney et al. (1972)
NOTA	La–Nd, Eu–Lu	–	D_2O	[e]	S; SR; axial symmetry	Bryden et al. (1981, 1982)
	La, Lu	–	D_2O	^1H, ^{13}C	S	Geraldès et al. (1985)
DOTA	Pr, Nd,	–	D_2O	[e]	S; SR; axial symmetry	Bryden et al. (1981, 1982)
	La, Pr, Eu, Yb	–	D_2O	^1H, ^{13}C	S	Desreux (1980), Brittain and Desreux (1984)
DOTMA	La, Eu, Yb	–	D_2O	^1H, ^{13}C	S	Brittain and Desreux (1984)
TETA	Pr, Eu, Yb, Lu	–	D_2O	^1H, ^{13}C	S	Desreux and Loncin (1986)

[a] C = evidence for complex formation; S = determination of the structure in solution; SR = study by shift-reagent complexation; log β_n = determination of stability constants.

[b] Macrocyclic polyether di- or tetraester ligands containing pyrazole units.

[c] Polyalkene glycols.

[d] {3} cryptate.

[e] ^2H, ^{13}C, ^{17}O, ^{23}Na, and ^{35}Cl.

3.5. *Theoretical studies*

Ultraviolet photoelectron spectroscopy has been used to measure the valence-shell ionization potentials of several crown ethers, cryptands, and N-containing coronands (Baker et al., 1983). Selected values are reported in table 22. The interpretation of these spectra is based, in addition to MO calculations, on the photoelectron spectra of model compounds. In general, evidence is found for appreciable through-bond or through-space interactions among the heteroatom "lone-pair" orbitals in the macrocycles, making these molecules softer ligands than would otherwise be anticipated. This relative softness may be the reason why R(II) ions are stabilized by these ligands (cf. section 4).

Li Zhenxiang et al. (1985) have calculated the electronic structure of $LaX_3 \cdot L$ ($X = NO_3^-, Cl^-$; L = 12C4, 15C5) and $Pr(NO_3)_3 \cdot (12C4)$ by an INDO method. Upon coordination, the ligand-to-metal charge transfer shifts the electronic levels and weakens the R–X bonds. The 4f orbitals participate slightly to the occupied MOs, contrary to 5d, 6s, and 6p orbitals. The same authors (Li Zhenxiang et al., 1984) have found that upon complexation with Lu(III), the annulene-like electronic structure of phtalocyanine remains uncharged, and that similar conclusions as above may be drawn regarding the metal-ion orbitals.

TABLE 22
Band maxima (eV) in the photoelectron spectra of coronands, cryptands, and podands (Baker et al. 1983).

Ligands	Band maxima	Ligands	Band maxima
12C4	9.3, 10.0, 11.4 [a]	$N_4$14C4	8.5, 11.2 [a]
Cy14C4	9.2 [a]	$BN_4$14C4	8.1, 9.0, 9.6, 9.9 [a]
B14C4	8.1, 9.8 [a]	(2,1)	8.4, 9.7, 11.3
15C5	9.6, 11.3 [a]	(2,2)	8.4, 9.7, 11.3
B15C5	8.0, 9.6, 10.7	(2,2,1)	7.7, 9.3, 11.0, 12.3 [a]
18C6	9.7, 10.4 [a]	(2,2,2)	7.8, 9.5, 11.3
$B_2$18C6	7.8, 8.7, 9.5 [a]	12P4	9.8

[a] Merging of bands at higher energy.

3.6. *Applications*

3.6.1. *Spectroscopic probes and bio-inorganic chemistry*

The Gd cryptate with (2,2,1) was proposed as a relaxation agent for ^{15}N, ^{89}Y, ^{111}Cd, and ^{183}W NMR measurements in water (Gansow et al., 1980a,b). This reagent shortens the T_1 relaxation time without inducing contact shifts, since the Gd encapsulation prevents the metal ion from close interaction with solute molecules. The complex $[GdDOTA]^-$ is used in NMR imaging experiments.

Several lanthanide ions display an intense luminescence from long-lived excited states and are therefore useful as spectroscopic probes. Since powerful excitation sources, e.g., lasers, are available and since the photons emitted by a luminescent

sample may be detected with high sensitivity using photon-counting techniques, these luminescent probes are useful to solve a variety of chemical and biochemical problems. Tundo and Fendler (1980) have investigated the chiral recognition in tryptophan derivatives of 18C6. The addition of $TbCl_3$ to methanolic solutions of the polyether produces a quenching of the excited states of the ligand. The formation constants of the Tb(III)/crown ether complexes estimated from a treatment of the luminescence data are the same for both D-crown-L-tryptophan and L-crown-L-tryptophan: $\log \beta_1 = 4.44\,\mathrm{l\,mol^{-1}}$ in MeOH. Henceforth, the Tb complexation is unaffected by the chirality of the host. However, substantial differences are observed in the energy-transfer efficiency from the tryptophan side arms, providing a measure for the host-conformational changes. The Eu(III) ion has been used by Klein (1980), Giorgetti (1985), and Pradervand (1985) to probe the structure of several 12C4, 15C5, 18C6, 21C7, and 18P6 complexes; these studies are discussed in §3.4.2.

An extension of the spectroscopic use of macrocyclic complexes with R(III) ions is to attach them to a more complex support. For instance, the introduction of long alkyl chains to make the macrocyclic ligand insoluble in water and soluble in nonpolar organic solvents; these polymer-linked systems are efficient phase-transfer catalysts which are easily recycled. In this sense, hydroxymethyl derivatives of 18C6 and (2,2,2) bonded onto a polymer have been used to extract shift reagents from dilute aqueous solutions in order to retrieve a normal NMR spectrum after a LSR study (Montanari and Tundo, 1982). Kausar (1978) has proposed a diazo coupling of lanthanide benzocryptates to proteins, which would then become amenable to spectroscopic and radiochemical analyses. The diazotation of $[La(2aB,2,1)]^{3+}$ is carried out in water and followed by a coupling to bovine serum albumine. The modified protein displays a different absorption spectrum. The coupling of the radioactive $[^{143}Pr(2aB,2,1)]^{3+}$ cryptate to ribonuclease-A has also been done to demonstrate that the metal ion remains encapsulated after the cryptate is attached to the biological molecule (Gansow and Kausar, 1984).

The use of R(III) ions to solve problems of biological significance has been recently reviewed (Horrocks, 1982; Horrocks and Albin, 1984), so that we shall only give some examples here which have a close connection with ionophore chemistry.

Hirschy et al. (1984) have characterized the binding of Eu(III) to tetracycline by luminescence and have shown that the formation constant of the 1:1 adduct is pH dependent. Blondeel et al. (1984) have prepared a metalloporphyrin with B15C5 groups attached at each of the meso positions. Cations may be inserted into the crown ether void, in particular Eu(III). Upon irradiation with light $< 500\,\mathrm{nm}$, intramolecular electron transfer occurs from the triplet state of the metalloporphyrine (M = Zn, fig. 3), reducing Eu(III). The larger Eu(II) ion produced is then expelled out of the crown ether void. This also happens when an 18C6 substituent is attached to the metalloporphyrin. In the presence of an electron donor, irradiation of the metalloporphyrin forms the π-radical anion

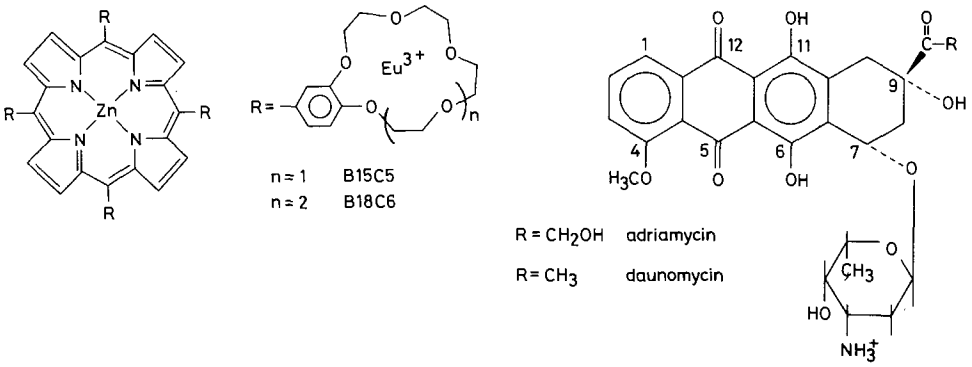

Fig. 3. Formulae of metalloporphyrins (left) and of adriamycin and daunomycin (right).

which transfers its extra electron to the Eu(III) ion housed in the crown ether. Again, Eu(II) ions are displaced out of the coronand.

Antibiotics, the study of which has created the need for model ligands such as crown ethers and cryptands, are a privileged field of investigation. For instance, Alykov (1981) has developed an analytical method to determine antibiotics in milk and other biological systems. The method is based on the quenching of the luminescence of $R(NO_3)_3$ complexes with fluorexone by monomycin, streptomycin, canamycin, hentamycin, or other antibiotics, and its sensitivity is as high as 0.1 μg of antibiotics in 1 ml of biological solution.

Adriamycin and daunomycin (fig. 3) are two antibiotics currently highly investigated because of their effectiveness against malignant cells. The interaction of daunomycin with lanthanide chlorides (Eu, Gd, Tb, Yb) yields complexes that have been analyzed by Mariam and Wells (1984) and Mariam et al. (1984) by spectrophotometry and NMR spectroscopy. Molar ratio and continuous-variation methods indicate the presence of predominantly a ML_2 species at metal-to-ligand ratios less than one; M_2L and ML species are also present. Proton spin-lattice relaxation time and linewidth measurements utilizing the relaxation probe Gd(III) indicate that the primary coordination site is in the 11,12-positions.

Gd(III) and Mn(II) binding sites for the carboxylic polyether lasalocid A (cf. fig. 1) were determined in DMF and $CDCl_3$ by ^{13}C-NMR spin-lattice relaxation methods (Hanna et al., 1983). The binding sites used by the ionophore depend upon both the cation charge and the solvent polarity. In DMF, Gd(III) ions bind only at the anionic carboxylate moiety, whereas Mn(II) ions bind not only at this group but also at the alcohol function of the aliphatic chain (O4) and at the ether function of the six-membered ring (O7). In $CDCl_3$, both cations bind lasalocid via the carboxylate group, O4, O7, and O8. These authors have also prepared $R(Las)_3 \cdot n CHCl_3$ ($R = La$, $n = 1$–2; $R = Gd$, $n = 1.5$). Richardson and Das Gupta (1981) have studied the interactions between the anionic form of lasalocid and several R(III) ions (Pr, Nd, Eu, Gd, Tb) by absorption, luminescence, and circularly polarized luminescence spectroscopies. The R(III) ions bind more strongly than Ca(II). Albin et al. (1984) have monitored the $^5D_0 \leftarrow {}^7F_0$ transition

of Eu(III) in methanolic solutions containing Las^-; they conclude to the formation of both mono- and bis(ionophore) chelates, in agreement with the findings of Richardson and Das Gupta (1981).

The metal complexes of lasalocid are soluble in nonpolar solvents and are permeable through biological membranes. Grandjean and Laszlo (1982, 1983) and Bartsch et al. (1983) have used paramagnetic ions to label the outer and inner compartments of phospho-lipid vesicles. Upon interaction with Pr(III) or Eu(III) ions, the NMR signals (^1H, ^{13}C, ^{31}P) are shifted, with modest line broadening, allowing to monitor the ionophore-mediated cation transport by various carrier molecules, e.g., lasalocid. In particular, these authors have discovered a 5-fold synergistic effect of 2-OctGly$B_2$16C5 on the transport of Pr(III) by lasalocid.

3.6.2. *Separation, extraction, and analysis*

The similarities in ionic radii and chemical propertis of the various rare earth ions make their separation difficult. It was therefore logical to try to take advantage of the size-selective cation-coordinating ability of some ionophores.

3.6.2.1. *Chromatography*. King and Heckley (1974) have chromatographed a mixture of hydrated $R(NO_3)_3$ (R = Pr, Er) on a column made up of solid $B_2$18C6. Visible-spectroscopic analysis of the eluate shows that Pr(III) is obtained free from Er(III), the latter experiencing a weaker retention (King, 1975). Paper chromatography and static adsorption experiments have also been used. For instance, La–Tb mixtures may be separated with ethylene-glycol monoethers mixed with oxine as developing agent (Nagai et al., 1972), and the complexation between B15C5, $B_2$18C6 and their HCHO copolymers has been investigated by Yang Yansheng and Zhu Jiaqin (1982). Finally, Zhai Yingli et al. (1984) have treated a polyether-type polyamide plastic foam material to use it as the stationary phase in the reversed-phase chromatographic separation of Sm(III) and Gd(III).

3.6.2.2. *Solvent extraction*. Solvent extraction and separation of lanthanide ions based on either crown ether- or podand-containing systems has generated several studies (table 23). A review on the general subject of the solvent extraction by crown compounds has been written by Takeda (1984). For several investigators, 15C5 or its derivatives seem to be the best extraction agents. Substituents on the polyethers have a large effect on their extractability, as well as the polarity of the organic phase. For instance, addition of isopropyl or butyl alcohols improves the extraction. On the contrary, the presence of organic acids in the aqueous phase, e.g., acetic, citric, oxalic acids, has a negative influence on the distribution coefficient D (Tsay Linmei et al., 1983). Transition-metal ions usually do not interfere (Fe, Co, Ni, Cu, Zn, Ag, Cd, UO_2^{2+}), except Hg and Pb.

Liquid membranes and polymers may also be used for R(III) ion extraction. For instance, a water–oil emulsion containing sorbitan trioleate, $B_2$18C6, and $CHCl_3$ separates $Pr(NO_3)_3$ from $Eu(NO_3)_3$, this latter remaining in the aqueous

TABLE 23
Solvent-extraction of lanthanide ions by crown ethers and podands.

Organic phase	Aqueous phase [R(III)]	R:L [a] ratio	Separation factors S, comments [b]	Ref.
12C4/$PhNO_2$	$R(NO_3)_3$/picric acid,	1:2	best coronand: 15C5; best	g
15C5/$PhNO_2$	La–Lu	1:1	extracted R(III)'s: Tb, Yb	g
$B_2$18C6/$PhNO_2$		1:1		g
15C5/$CHCl_3$	$Eu(NO_3)_3$/picric acid	1:2	log K_e = 8.2	h
B15C5/$CHCl_3$		1:2	= 11.1	h
18C6/$CHCl_3$		1:2	= 8.5	h
$B_2$18C6/$CHCl_3$		1:2	= 13.3	h
ButB15C5/$PhNO_2$	picrates, ^{144}Ce, ^{147}Nd, ^{152}Eu, ^{154}Eu	1:2	S(Ce/Sm) = 1.14	i
BrB15C5/$PhNO_2$	^{169}Yb, ^{170}Tm, ^{177}Lu	1:2	S(Sm/Lu) = 0.76	i
B15C5/CH_2Cl_2	picrates, La–Lu	1:2	S(Pr/Nd) = 3.66	j
$B_2$18C6/CH_2Cl_2		1:2		j
$Cy_2$18C6/CH_2Cl_2	(Nd–Lu)	3:4		j
	(La–Pr)	1:1		j
MeB15C5/$CHCL_3$	picric acid, ^{144}Ce, ^{147}Nd, ^{152}Eu, ^{154}Eu, ^{169}Yb, ^{170}Tm	1:2	K_e: Nd > Eu > Ce > Tm > Yb	k
Cy15C5/TOPO [c]	$Eu(NO_3)_3/HNO_3$ 1 M	not available	no synergistic effect	l
15C5, 18C6, $Cy_2$18C6, $Cy_2$24C8, $ButO(CH_2CH_2O)_nBut$, (n = 1,2,3) in C_6H_6	$Ln(NO_3)_3/NH_4NO_3$ 8 M, pH = 3–3.5; Y, La–Lu, except Pr, Tb, Ho, Yb	not available	extraction capacities increase with n	m
$Az(B15C5)_2$	not available	not available		n
EO4/$MeCO_2Et$ (EO2, EO3, EO5, EO7)	$R(NO_3)_3/H_2O/MeCO_2Et$, La–Gd	1:1	S(La/Ce) = 1.7, S(Ce/Pr) = 1.4, S(Pr/Nd) = 2.0, S(Nd/Sm) = 5.5, S(Sm/Eu) = 2.9, S(Eu/Gd) = 2.0	o, p
Polyethyleneglycol (PEG), $B_2$18C6	$R(NO_3)_3/HNO_3$, Ce, Eu	not available	sorbtion experiments; synergistic effect for Ce	q
Polyethyleneglycol (PEG-400)/$PhNO_2$	$Eu(NO_3)_3/HClO_4$, ^{152}Eu, ^{154}Eu	1:1, 1:2 1:3	distribution ratio function of PEG concentration	r
Oligooxaalkanes/CCl_4 or C_2H_6	$R(NO_3)_3$/EtOH/H_2O, La, Nd, Eu, Er, Lu	1:1, 1:2	extraction into nonpolar phase is possible	s
K-5/HTTA/$CHCl_3$ [e], $CHCl_3$	$Eu(CH_3CO_2)_3$/pH = 4.8/ $NaNO_3$ 0.5 M; ^{152}Eu	1:1	synergistic effect of K-5	t
TPOD, TPTUD/$PhNO_2$ [f]	$R(picrate)_3$	not available	high extractability	u

[a] Metal:ligand ratio of extracted complex.
[b] $K_e = [LnX_3 \cdot L_2]/([Ln] \cdot [X]^3 \cdot [L]^2)$ in l^5 mol^{-5}.
[c] TOPO = trioctylphosphine oxide.
[d] Nitrobenzene solutions of Co(III)-dicarbolide.
[e] K-5 is the linear polyether 1,13-bis(8-quinolyl)-1,4,7,10,13-pentaoxatridecane; HTTA = thenoyltrifluoroacetone.
[f] TPOD = N,N,N′,N′-tetraphenyl-3,6-dioxaoctane diamide; TPTUD = N,N,N′,N′-tetraphenyl-3,6,9-trioxaundecanediamide.
[g] Tsay Linmei et al. (1983).
[h] Hasegawa and Haruna (1984).
[i] Yang Yusheng et al. (1982).
[j] Kao Yuan and Ni Jiazan (1983).
[k] Wang Wenji et al. (1981).
[l] Kinard et al. (1980).
[m] Yakshin et al. (1984).
[n] Ni Yushan et al. (1984).
[o] Hirashima et al. (1980).
[p] Arakawa et al. (1980).
[q] Rais et al. (1977).
[r] Vanura et al. (1984).
[s] Zolin et al. (1981).
[t] Ensor and Shah (1983, 1984).
[u] Yang Yusheng et al. (1984).

phase (Kudo and Oba, 1978). As seen above, polymer-bonded crown ethers are suitable for extracting R(III) cations from dilute aqueous solutions (Montanari and Tundo, 1982). Zhu Jiaqin and Yang Yansheng (1984) have determined the selectivity ratio of transport for La(III), Sm(III), and Er(III) ions across liquid membranes by B15C5 and $B_2$18C6: $S(\mathrm{Sm/Er}) = 3.28$, $S(\mathrm{Sm/La}) = 1.91$, and $S(\mathrm{La/Er}) = 1.72$ in picrate solutions.

Crown ethers and their derivatives are expensive ligands and attempts have been made to replace them by their much cheaper open-chain analogues; some of them present synergistic effects. For instance, the introduction of PEG in ammonium phosphotungstate sorbents results in a synergistic factor of about 100 for Ce(III) (Rais et al., 1977). Hirashima et al. (1980) and Arakawa et al. (1980) have attempted to separate $R(NO_3)_3 \cdot nH_2O$ by fractional crystallization in the presence of EO_n ligands ($n = 2$–5, 7). The crystallization time in ethylacetate/water mixtures varies from a few seconds (EO4; La, Pr) to several days (EO5; Sm, Eu) or weeks (EO2; Dy, Er). The best ligand is EO4. The TDA podand (cf. §3.4.3) is used in the industrial separation of Eu(III).

3.6.2.3. *Ion-selective electrodes.* Podands have proved useful in the preparation of cation-selective electrodes (Morf et al., 1979), and a system working for 5f cations has been designed (Bertrand et al., 1983). There is, however, only one report mentioning an eventual application to 4f elements (Shono and Kimura, 1977).

3.6.3. *Miscellaneous*

Polymeric thermoplastic materials with interesting electrical properties have been produced; they contain a metal salt, including R(III) salts, and a polymeric backbone incorporating ether or thioether linkages (Wetton and James, 1980).

4. Complexes with divalent lanthanide ions

4.1. *Electrochemical reduction of R(III) ions and stabilization of R(II) ions in the presence of ionophores*

Gansow and coworkers have pointed out that the encryptation of R(III) ions, especially Eu and Yb, has a marked effect on the electrochemical properties of the R(III)/R(II) redox couples. The cyclic voltammograms of the aquo ions are irreversible, while the encapsulated ions display a reversible reduction–oxidation process. The reduction potential of the cryptates is shifted towards less negative values, which means a stabilization of the R(II) oxidation state by the macrocyclic ligand. The difference in formal potential ΔE_f between the complex and uncomplexed one-electron redox couples is directly related to the difference in free energy for these processes:

$$\Delta E_f = \frac{2.303\,RT}{F} \log \frac{\beta_{II}}{\beta_{III}} = \frac{\Delta G^0_{III} - \Delta G^0_{II}}{F}.$$

Crown ethers also stabilize R(II) ions, and results of quantitative determinations are reported in table 24. In propylene carbonate, crown ethers stabilize R(II) over R(III) ions by 1 to 4 orders of magnitude. Because Yb(II) and Ca(II) on the one hand, and Sm(II) and Sr(II) on the other hand, have similar ionic radii, it is expected that they will form complexes with comparable stability. This is indeed the case for the latter pair of metal ions, while the log β_n of the Yb(II) coronands are always intermediate between those of Ca(II) and Sr(II) (Massaux et al., 1982). The determination of the Eu(II/III) stabilization in PC is impossible

TABLE 24
Stabilization of R(II) ions by coronands and cryptands at 295–298 K and $\mu = 1$ (Et_4NClO_4).

R	Ligand	R:L	Solvent	Log β_{II}	Log β_{II}/β_{III}	Ref.
Sm	12C4	1:2	PC	8.4 ± 0.2	1.6 ± 0.3	e
	ButB15C5	1:2	PC	10.8 ± 0.1	[a]	e
	18C6	1:1	PC	8.9 ± 0.1	0.8 ± 0.2	f
	$But_2B_2$18C6	1:1	PC	7.60 ± 0.05	3.63 ± 0.03	g
	$B_2$30C10	1:1	PC	8.3 ± 0.1	4.55 ± 0.13	e
	(2,2)	1:1	PC	11.2 ± 0.1	−5.3 ± 0.2	h
	(2,2,1)	1:1	PC	15.6 ± 0.1	−3.4 ± 0.2	h
			MeOH	11.9 ± 0.1	2.2 ± 0.2	i
			H_2O	about 9.2 [b]	about 2.4	i
	(2,2,2)	1:1	PC	17.6	0.3	h
			H_2O	about 12.2 [c]	about 6.3	i
Eu	18C6	1:1	H_2O	2.7	[a]	j
	(2,2,1)	1:1	H_2O	10.2 ± 0.2 [b]	3.4	k
	(2B,2,1) [d]	1:1	H_2O		4.3	k
	(2aB,2,1) [d]	1:1	H_2O		4.4	l
	(2,2,2)	1:1	H_2O	13.0 ± 0.1 [c]	7.1	k, m
Yb	12C4	1:2	PC	8.3 ± 0.2	[a]	e
	ButB15C5	1:2	PC	8.4 ± 0.1	[a]	e
	18C6	1:1	H_2O	2.4	[a]	j
	$But_2B_2$18C6	1:1	PC	7.32 ± 0.10	4.63 ± 0.05	g
	$B_2$30C10	1:1	PC	7.5 ± 0.1	2.74 ± 0.14	e
	$(aet)_2N_6$16C6	1:1	MeCN		14.2	n
	(2,2,1)	1:1	H_2O		5.4–5.5	k, m
	(2B,2,1)	1:1	H_2O		5.4	o, p

[a] Value for R(III) ion is not available.
[b] R(III) value from Burns and Baes (1981).
[c] R(III) value from Chang and Ochaya (1986).
[d] Electrolyte: 0.5 M $NaClO_4$.
[e] Massaux and Desreux (1982).
[f] Almasio (1983).
[g] Massaux et al. (1980).
[h] Loufouilou (1986).
[i] Almasio et al. (1983).
[j] Shiokawa and Suzuki (1984).
[k] Yee et al. (1980).
[l] Kausar (1978).
[m] Koizumi and Aoyagui (1981).
[n] Raymond (1986).
[o] Gansow et al. (1977).
[p] Gansow and Triplett (1981).

by electrochemical methods either because of the reduction by the amalgam used or because the III→II polarographic wave of the complexed metal ion is displaced beyond the oxidation wave of mercury. A slight stabilization of Sm(II) and Yb(II) by 18C6 was observed in PC, but $\log(\beta_{II}/\beta_{III})$ remains smaller than one. For R = Sm, no stabilization occurs with the diaza-substituted ligand (2,1) (Almasio et al., 1983) while a large *destabilization* is observed with the coronand (2,2). In water, polarographic experiments tend to demonstrate a stabilization of Sm(II), Eu(II), and Yb(II) in presence of 18C6 (Yamana et al., 1982; Shiokawa and Suzuki, 1984).

Table 24 also contains the quantitative results gathered for cryptates. During the R(III→II) reduction, the formal potentials do not vary upon addition of an excess ligand or upon a change in electrolyte. Moreover, the logarithmic analysis of the reduction waves yields linear relationships with a slope close to 59 mV. Yee et al. (1980) have therefore concluded that the reduction process goes through a one-electron exchange mechanism. In water, the stabilization by the (2,2,1) cryptand increases with decreasing ionic radius of the R(III) ion; it ranges between $\log(\beta_{II}/\beta_{III}) = 2.4$ (Sm) and 5.5 (Yb). The stabilization by the (2,2,2) cryptand is even larger, ranging between 6.3 (Sm) and 7.1 (Eu). The $\Delta G^0_{III\to II}$ is positive because of large enthalpic contributions, $\Delta S^0_{III\to II}$ being positive (Yee et al., 1983). However, the stabilization of the R(II) cryptates is reduced when a less polar solvent is used; it is even negative in PC (Almasio et al., 1983; Loufouilou, 1986).

Both R(II) and R(III) cryptates are substitutionally inert on the cyclic voltametric time scale and the rate constant for electrochemical exchange is between 0.8 and 1.1 $cm\,s^{-1}$ (Koizumi and Aoyagui, 1981). Yee et al. (1983) have measured the reduction kinetics of the Eu(III) cryptates with (2,2,1) and (2,2,2) by the aquo ions V(II) and Eu(II), as well as the oxidation kinetics of $[Eu(2,2,1)]^{2+}$ by $[Co(NH_3)_6]^{3+}$. For reactions involving V(II), the rate constants for the Eu(III/II) self-exchange are 2×10^{-6}, 13, and 4×10^{-2} $l\,mol^{-1}\,s^{-1}$ for Eu_{aq}, $[Eu(2,2,1)]^{3+}$, and $[Eu(2,2,2)]^{3+}$, respectively. The authors suggest that nonadiabaticity is not primarily responsible for the low reactivity of the aquo ion.

4.2. *Photochemical reduction of R(III) complexes*

Donohue (1980, 1982) has found that the quantum yield for the photoreduction of $EuCl_3$ solutions in methanol is dramatically increased in the presence of 18C6. Upon photolysis by an Ar laser (351–363 nm), the 320 nm band of the divalent species increases by a factor of 10. A similar enhancement is also observed when $SmCl_3$ solutions are irradiated by an excimer KrF laser (248 nm); the lifetime of the resulting transient blue colour of Sm(II) increases from a few seconds to 3 h and 4 h, respectively, when 18C6 and (2,2,2) are added. Attempts to photoreduce R(III) ions using a mercury lamp have been unsuccessful, which points to a multiphoton process.

Sabbatini and Balzani (1985) have reported a study of the photo-induced electron-transfer processes involving (2,2,1) Eu cryptates. Both Eu(II) and Eu(III) cryptates are suitable as redox quenchers of excited-state molecules, e.g., ruthenium complexes:

$$[^*RuL_3]^{2+} + [Eu(2,2,1)]^{3+/2+} \rightarrow [RuL_3]^{3+/+} + [Eu(2,2,1)]^{2+/3+} .$$

With L = bipyridyl, the rate constants are equal to 4.9×10^7 and 1.3×10^9 l mol^{-1} s^{-1} for the Eu(III) and Eu(II) cryptates, respectively. Moreover, owing to its long lifetime (0.215 ms), $[Eu(2,2,1)]^{3+}$ can be dynamically quenched via an electron-transfer mechanism within ion pairs (cf. §3.4.2). Poon and Tang (1984) have successfully applied Marcus's theory to predict the rate constants of outer-sphere reduction of trans-dihalogenotetraaminеruthenium(III) cations by Eu(II), where the tetraamine is $N_4$11P_4, $N_4$14C4, or $Me_6N_4$14C4. For the $Eu(III/II)_{aq}$ couple, the self-exchange rate constants fall within the range of 2.3×10^{-3} to 1.7×10^{-3} l mol^{-1} s^{-1}, at 298 K and $\mu = 0.5$. Photoredox processes in metalloporphyrin-crown ether systems have been mentioned in §3.6.1.

4.3. *Isolation and properties of R(II) complexes*

The isolation of Ln(II) complexes with macrocyclic ligands is difficult, since the compounds are often sensitive to oxidation. Good starting solutions for crystallizing complexes are either $EuCl_2 \cdot 2H_2O$ in methanol (Bünzli and Wessner, 1984a) or SmI_2 in THF. This latter solution is prepared by reacting metallic Sm (Yb may also be used) with 1,2-diiodoethane (Kagan and Namy, 1984). It is essential to check the purity of the complexes by measuring their magnetic susceptibility. Indeed, some of the complexes may contain only 30–60% R(II), the remainder being already oxidized. Isolated complexes are given in table 25.

The emission spectrum of $SmI_2 \cdot$(18C6) at 77 K displays a broad and structured band at 720 nm assigned to a $4f^5 5d^1 \rightarrow 4f^6$ transition; f–f transitions appear on top of this band and the $^5D_0 \rightarrow {}^7F_1$ transition displays only two components, indicating that the Sm(II) ion may lie on a site with relatively high symmetry (Bünzli and Wessner, 1984a). The same authors have shown by EPR measurements that the dissolution of $EuCl_2 \cdot$(18C6) in degassed absolute methanol results in rapid oxidation of the Eu(II) ion. They explain this finding by the fact that the dissociation of the trivalent complex in MeOH may be more rapid than the one-electron exchange process. Kamenskaya and Mikheev (1985) have studied the Sm(II) oxidation in water, MeCN and THF. In water, the reaction is a first-order process with half-time of 0.32 and 1.05 h in absence and in presence of 18C6, respectively. On the contrary, in MeCN the oxidation rate is increased 1.5 times in presence of 18C6 (1.1×10^{-6} versus 0.7×10^{-6} s^{-1}).

Of special interest is the crystal structure determination of $SmI_2 \cdot (9P3)_2$. The complex crystallizes in the monoclinic $P2_1/n$ space group. The 8-coordinate Sm(II) lies on an inversion centre and its coordination polyhedron is a distorted

TABLE 25
Divalent lanthanide complexes with coronands and one podand. [a]

Ligand	Anion	R:L	R(II)	Starting material or properties	Ref.
B15C5	Cl^-	4:3	Eu	reduction of $EuCl_3$ by Li/napht.	b
18C6	I^-	1:1	Nd, Sm, Dy, Tm	violet (Nd), blue (Sm), green (Dy), blue-green (Tm); contain about 20% Nd(II) and 40% Dy(II)	c, d
			Sm	blue; $\mu = 3.36$ B.M. at 294 K	e
	Cl^-	1:1	Sm, Tm	violet (Sm)	c
			Eu	easy oxidation in MeOH	e
$B_2$18C6	ClO_4^-	1:1	Eu	colourless; turns pale-blue on irradiation with light	f
	Cl^-	4:3	Eu	reduction of $EuCl_3$ by Li/napht.	b
	I^-	1:1	Sm, Dy, Tm	blue (Sm), green (Dy), blue-green (Tm)	c
$Cy_2$18C6	Cl^-	4:3	Eu, Yb	reduction of $EuCl_3$ by Li/napht.	b
$PyMe_2N_6$18C6ene$_2$	ClO_4^-	1:1	Eu		g
9P3	I^-	1:2	Sm	dark brown; 8-coordinate Sm(II), crystal structure	h

[a] The solvation is not taken into account.
[b] Zou Jinping and Tan Minyu (1983).
[c] Kamenskaya and Mikheev (1985).
[d] Kamenskaya et al. (1985).
[e] Bünzli and Wessner (1984a).
[f] Wang Genglin et al. (1983a).
[g] Wang Genglin and Miao Lan (1984).
[h] Chebolu et al. (1985).

hexagonal bipyramid. The Sm–I bond distance is 3.265(1) Å and the average Sm–O bond distance is 2.689(4) Å (Chebolu et al., 1985).

The luminescence and photochemical properties of R(II) complexes have been investigated by several authors. Sabbatini et al. (1982) have studied $[Eu(2,2,2)]^{2+}$ in water. Whereas no emission spectrum is observed for $Eu(II)_{aq}$ at room temperature, the cryptate displays a measurable luminescence with a lifetime of 3 ns (550 ns at 77 K). The corresponding values for $[Eu(2,2,1)]^{2+}$ are 1.5 (293 K) and 610 ns (77 K). The addition of methanol to the solutions results in (a) a lengthening of the lifetimes by about 50% and (b) a considerable increase of the emission quantum yield from about 10^{-3} in water at 293 K to 1.0 in MeOH/water 6/4 (v/v) at 77 K (Sabbatini et al., 1984b). The minimum of the lowest $4f^6 5d$ excited state lies below the lowest $4f^7$ excited level, explaining why the broad $d \rightarrow f$ emission band, which is parity-allowed, dominates the emission spectrum.

A systematic study of the luminescent properties of freshly prepared methanolic solutions of Eu(II) complexes with various crown ethers, cryptands, and podands has been undertaken by Adachi et al. (1980, 1983, 1985a,b). The stoichiometry of the complexes formed in solution is determined by Job's plots in which the emission intensity is plotted versus the L:M molar ratio. Such plots have to be interpreted with care in the case where different complexes form which have similar emission spectra but different quantum yields. Some of these stoichiometries have been confirmed by NMR measurements. The luminescence quantum yields (table 26) are markedly enhanced by complex formation, especially with

TABLE 26
Stoichiometry, quantum yields Q, and lifetimes τ of $EuCl_2$ complexes in anhydrous MeOH, at room temperature and $[Eu(II)] = 4 \times 10^{-3}$ M. (From Adachi et al., 1983, 1985a, 1985b.)

Ligand	Eu:L	Q (%)	τ (ns)
MeOH	not available	0.04	20
12C4	not available	3.6	300
15C5	1:3 [a]	24	830
Oct15C5	not available	21	761
B15C5	not available	1.5	143
18C6	1:1 [a]	6.7	200
Oct18C6	1:1	6.7	143
B18C6	1:1	0.2	28
$Cy_2$18C6	1:1	3.8	89
Hept(B18C6)$_2$	2:1	0.05	not available
$Cy_2$24C8	1:1	2.9	290
(2,1)	not available	7.1	42 [b]
(2,2)	3:2	4.6	16
(2,1,1)	not available	0.05	not available
(2,2,1)	3:1	1.4	24
(2,2,2)	1:1 [a]	9.3	200
EO4	not available	0.06	not available
EO5	not available	0.14	not available
EO6	1:1	0.10	not available
EO7	2:1	0.12	43 [b]
EO8	2:1	0.18	59 [b]

[a] Confirmed by NMR measurements.
[b] Unreliable value.

15C5. This latter seems to form a 1:3 adduct shielding the metal ion from solvent interaction and preventing radiationless deexcitation. A low-temperature NMR study of the solution with 15C5 ether reveals the presence of two differently coordinated ligands in the ratio 1:2. When a bromoalkyl chain is attached to crown ethers, e.g., to give BrMe,Me15C5 or BrMe,Me18C6, the complex formation is induced by UV irradiation and the blue Eu(II) luminescence is enhanced (Adachi et al., 1984).

Ishida et al. (1986) have found that the luminescence quenching rate constant of $EuCl_2 \cdot L$ (L = 15C5, 18C6) by 5-substituted-1,3-dimethyluracils increases with increasing the electron-withdrawing properties of the substituents.

4.4. *Applications*

The production of luminescent blue phosphors from methanolic solutions of Eu(II) coronates has been suggested in a Japanese patent (1981). Moreover, Brown et al. (1983) propose to reduce $Eu(NO_3)_3 \cdot$ (18C6) before transporting the europium through $H_2O/CHCl_3/H_2O$ liquid membranes. They show that the $Eu(NO_3)_2$ flux through the membrane is indeed comparable to that of $Sr(NO_3)_2$ and 600 times larger than the $Eu(NO_3)_3$ flux.

5. Complexes with cerium(IV)

Only five Ce(IV) coronates have been characterized. Reacting $Ce(NO_3)_4$ with $B_2$18C6 in MeCN leads to the isolation of a dark-brown crystalline complex $Ce(NO_3)_4 \cdot (B_2$18C6$) \cdot$ MeCN. This complex is almost insoluble in most organic solvents, except DMF and DMSO, and is decomposed by water. Its thermal decomposition starts at 471 K and involves four different steps (Tan Minyu and Gao Yici, 1978, 1980a,b). Similarly, $Ce(NO_3)_4 \cdot (Ph_4$18C6ene$_2)$ may be isolated either from MeCN or C_6H_6 solutions (Wang Jingqiu et al., 1983). The crystal and molecular structure of a $Ce(NO_3)_4 \cdot 5H_2O$ complex with the A isomer of $Cy_2$18C6 has been solved by Dvorkin et al. (1984). The yellowish rhombic crystals belong to space group $P\bar{1}$ and their formula is $[(H_3O^+, H_2O)_4(Cy_2$18C6$)_4] \cdot [Ce(NO_3)_6] \cdot H_2O$. The Ce(IV) ion is therefore not encapsulated by the coronand; H_3O^+ and H_2O molecules are distributed statistically and are linked to the crown ether by hydrogen bonds. Bünzli and Wessner (1984a) have isolated a yellow-orange diamagnetic adduct $(NH_4)_2Ce(NO_3)_6 \cdot (12C4)_4$ that yields $(NH_4)_2 \cdot (12C4)$ upon sublimation. Wang Genglin et al. (1983b) have obtained, via a template reaction, a 1:1 complex between $Ce(NO_3)_4$ and $Py_2Me_2N_6$18-C6ene$_4$, the correct formulation of which is $[Ce(NO_3)_2 \cdot L](NO_3)_2 \cdot H_2O$.

The template reaction leading to the formation of a 1:2 fluorinated Schiff base complex, bis[1,1,1,2,2,2-hexafluoro-2,11-bis(trifluoromethyl)-4,9-dimethyl-2,11-diolato-5,8-diazadodeca-4,8-diene(2-)]-cerium(IV), was investigated by Timmons et al. (1980). The pale yellow adduct crystallizes in space group $P2_1/c$; the Ce(IV) is 8-coordinate with mean Ce–O and Ce–N bond lengths equal to 2.21(2) and 2.62(1) Å, respectively. This is the first crystallographic evidence for Ce–N bonding.

Two other studies have shown that Ce(IV) complexes are involved in the catalyzed graft polymerization of acrylamide onto polyether urethane (Qiu Kunyuan et al., 1981) as well as in the emulsion polymerization of styrene (Ohtsuka and Kawaguchi, 1974).

6. Conclusions

Macrocyclic ligands and their open-chain analogues have added a new dimension to the coordination chemistry of lanthanide ions. In particular, they allowed the study of high and unusual coordination numbers, e.g. 11-coordination. Basic thermodynamic data are still needed to get a better understanding of the complexation process and of both macrocyclic and macrobicyclic effects. Moreover, kinetic data on ligand exchange remain scarce and studies in this field are certainly desirable.

In the future, we foresee developments in the following area: (a) study of Ln–Ln energy transfer and magnetic interaction on model di- or polynuclear

compounds containing ionophoric cavities, (b) investigation of photophysical properties, (c) further attempts to stabilize R(II) and R(IV) ions using softer macrocyclic ligands, (d) use of macrocyclic complexes as spectroscopic probes, and (e) development of efficient separation and analytical procedures (e.g., ion-selective electrodes).

7. Recent developments

7.1. *Complexes with trivalent rare earth ions*

Jin Linpei et al. (1986) have isolated and characterized 1:1 complexes between lanthanum and praseodymium nitrates and 4-methyl-5-bromo-benzo-15-crown-5 (Me,BrB15C5). Complexes with the hexaaza macrocycle $Py_2Me_4N_6$18C6ene$_4$ have been studied in detail by De Cola et al. (1986): $R(NO_3)_3 \cdot L$, $R(ClO_4)_2(OH) \cdot L \cdot nH_2O$, and $R(CH_3CO_2)_2Cl \cdot L \cdot nH_2O$. The crystal and molecular structure of the lutetium acetate complex has been solved by Bombieri et al. (1986); it contains 9-coordinate Lu(III) complex cations $[Lu(CH_3CO_3)(MeOH, H_2O) \cdot L]^{2+}$. Barthelémy (1987) has synthesized and studied dinuclear complexes containing (2,2) units; he has also determined the first crystal structures of lanthanide (2,2,1) cryptates: $[R(2,2,1)(MeCN)_2](ClO_4)_3$, with R = Pr and Er, and $[Pr_2(2,2,1)_2(OH)_2](ClO_4)_4 \cdot 2MeCN$.

The stability constants of several series of complexes have been measured. In propylene carbonate, Barthelémy et al. (1986) have found that the stability sequence of the 15P5 podates is very similar to sequences previously reported for complexes with 15-membered crown ethers (cf. table 13); this open-chain ligand also stabilizes Sm(II) and Yb(II), which is not the case with the smaller glymes. Loncin et al. (1986) have shown that DOTA forms the most stable lanthanide chelates in water (cf. table 16) whereas the stability of TETA complexes at 80°C is comparable to that of the EDTA complexes, with log β ranging between 14.5 and 16.5. The solution structure of $LnDOTA^-$ complexes (Ln = Ce, Pr, Eu, Yb) has been determined by NMR spectroscopy: the complexes have an approximate square-antiprism geometry (Ascenso et al., 1986). In an acetate–acetic acid buffer medium, Sekhar and Chang (1985) have shown that the (2,1)DA complexes exhibit an acid-independent and an acid-dependent dissociation pathway (Sekhar and Chang, 1986). Chang et al. (1986a) have reported the stability constants and the dissociation kinetics of the ternary complexes $[R \cdot L(acac)_n]^{(n-1)-}$, L = (2,1)DA and (2,2)DA and $n = 1$ and 2. The interaction between Nd(EDTA), Eu(EDTA) and the coronand (2,2) has been studied in water and water–methanol solutions by spectrophotometric and luminescence techniques (Nazarenko et al., 1986). The photophysical properties of Sm and Tb cryptates with (2,2,1) have been investigated by Sabbatini et al. (1986a); the same research group has also studied the photoinduced electron transfer between poly-

(pyridine)Ru(II) complexes and Eu-cryptates with (2,2,1) (Sabbatini et al., 1986b).

MO calculations have been performed on B12C4, 15C5, and 18C6 coronates with lanthanum and praseodymium chlorides and nitrates (Li Zhen-xiang et al., 1986a,b).

Applications have been developed in the field of rare earth extraction, adsorption, and ion transport through membranes. The general use of macrocyclic ligands in the extraction of lanthanides is described in an European patent (Rollet et al., 1986). It has been found that the addition of substituted 15C5 ethers creates a synergistic effect in the extraction of Ce, Pm, Eu, and Tm (Ensor et al., 1986). The amino-carboxylic ligand (2,1)DA kinetically separates La and Yb (Chang et al., 1986b), whereas both (2,1)DA and (2,2)DA are useful in the extraction of La and Nd (Manchanda and Chang, 1986). Polyethyleneglycols increase the separation factor of both Eu and Ce (Makrlik and Vanura, 1986). Adsorption studies have been performed by Shih Jengshang et al. (1985) with polyacrylamide resins modified with 15C5. The effect of B15C5 and DB18C6 on liquid membrane extraction of R(III) has been investigated by Yang Yansheng and Zhu Jiaqin (1985), while Izatt et al. (1986) have worked on the macrocycle-facilitated transport of Eu(II) and Eu(III) in liquid membrane and vesicle systems.

7.2. *Complexes with divalent lanthanide ions*

The redox potentials of R(II/III) cryptates with (2,2,1) and (2,2,2) have been measured in various solvents for R = Sm, Eu, Yb (Tabib et al., 1986). The luminescence properties of Eu(II) complexes with 15C5 derivatives have been measured in methanol (Adachi et al., 1986). New complexes between $YbCl_2$ and 12C4, 15C5 and 18C6 have been observed in methanol by absorption and emission spectroscopies (Lin Wenlian et al., 1986).

7.3. *Complexes with cerium(IV)*

One new complex has been isolated: $Ce(NO_3)_4 \cdot (2,2) \cdot 2.5Me_2CO$. It has been characterized by chemical analysis, vibrational and absorption spectroscopies (Zhu Wenxiang et al., 1986).

Acknowledgments

The work performed in the authors' laboratories is supported by the Swiss National Science Foundation and by the Fondation Herbette (Lausanne). We thank Mrs. R. Imhoff for the outstanding help in the preparation of this manuscript and Mr. G. Beyeler for drawing the formulae.

References

Abid, K.K., and D.E. Fenton, 1984a, Inorg. Chim. Acta **95**, 119.

Abid, K.K., and D.E. Fenton, 1984b, Inorg. Chim. Acta **82**, 223.

Abid, K.K., D.E. Fenton, U. Casellato, P.A. Vigato and R. Graziani, 1984, J. Chem. Soc., Dalton Trans., p. 351.

Adachi, G.-Y., K. Tomokiyo, K. Sorita and J. Shiokawa, 1980, J. Chem. Soc., Chem. Commun., p. 914.

Adachi, G.-Y., K. Sorita, K. Kawata, K. Tomokiyo and J. Shiokawa, 1983, J. Less-Common Met. **93**, 81.

Adachi, G.-Y., K. Sakai, K. Kawata and J. Shiokawa, 1984, Inorg. Chem. **23**, 3044.

Adachi, G.-Y., H. Fujikawa and J. Shiokawa, 1985a, in: New Frontiers in Rare Earth Science and Applications, Vol. I, eds. Xu Guangxian and Xiao Jimei (Science Press, Beijing) p. 300.

Adachi, G.-Y., K. Sorita, K. Kawata, K. Tomokiyo and J. Shiokawa, 1985b, Inorg. Chim. Acta **109**, 117.

Adachi, G.-Y., H. Fujikawa, K. Tomokiyo, K. Sorita, K. Kawata and J. Shiokawa, 1986, Inorg. Chim. Acta **113**, 87.

Albin, M., W. deW. Horrocks Jr and F.J. Liotta, 1982, Chem. Phys. Lett. **85**, 61.

Albin, M., A.C. Goldstone, A. Somerville Withers and W. deW. Horrocks Jr, 1983, Inorg. Chem. **22**, 3182.

Albin, M., B.M. Cader and W. deW. Horrocks Jr, 1984, Inorg. Chem. **23**, 3045.

Almasio, M.C., 1983, Ph.D. Thesis, Ecole Nationale Supérieure de Chimie, Strasbourg (France).

Almasio, M.C., F. Arnaud-Neu and M.J. Schwing-Weill, 1983, Helv. Chim. Acta **66**, 1296.

Alykov, N.M., 1981, Russ. J. Anal. Chem. **35**, 1489.

Ammann, B., and J.-C.G. Bünzli, 1979, Angewandte Chemische Thermodynamik und Thermoanalytik, Experientia Supplementum **37**, 50.

Ammann, B., and J.-C.G. Bünzli, 1982, Calorimétrie et Analyse Thermique, Journées de Genève, Vol. XIII, p. III-6.36.

Anderegg, G., 1981, Helv. Chim. Acta **64**, 1790.

Arakawa, T., Y. Hirashima and J. Shiokawa, 1980, Kenkyu Hokoku – Asahi Garasu Kogyo Gijutsu Shoreikai **36**, 277.

Arif, A.M., C.J. Gray, F.A. Hart and M.B. Hursthouse, 1985, Inorg. Chim. Acta **109**, 179.

Arnaud-Neu, F., E.L. Loufouilou and M.-J. Schwing-Weill, 1986, J. Chem. Soc., Dalton Trans., p. 2629.

Ascenso, J.R., R. Delgado and J.J.R.F. Da Silva, 1986, J. Chem. Soc., Dalton Trans., p. 2395.

Backer-Dirks, J.D.J., C.J. Gray, F.A. Hart, M.B. Hursthouse and B.C. Schoop, 1979, J. Chem. Soc., Chem. Commun. p. 774.

Backer-Dirks, J.D.J., J.E. Cooke, A.M.R. Galas, J.S. Ghotra, C.J. Gray, F.A. Hart and M.B. Hursthouse, 1980, J. Chem. Soc., Dalton Trans., p. 2191.

Baker, A.D., G.H. Armen and S. Funaro, 1983, J. Chem. Soc., Dalton Trans., p. 2519.

Barthelémy, P.P., 1987, Ph.D. Thesis (Université de Liège, Belgium).

Barthelémy, P.P., J.F. Desreux and J. Massaux, 1986, J. Chem. Soc., Dalton Trans., p. 2497.

Bartsch, R.A., J. Grandjean and P. Laszlo, 1983, Biochem. Biophys. Res. Commun. **117**, 340.

Benetollo, F., G. Bombieri, G. de Paoli, D.L. Hughes, D.G. Parsons and M.R. Truter, 1984, J. Chem. Soc., Chem. Commun., p. 425.

Benetollo, F., G. Bombieri, G. de Paoli, D.L. Hughes, D.G. Parsons and M.R. Truter, 1985a, Acta Cryst. C **41**, 34.

Benetollo, F., G. Bombieri, A. Cassol, G. de Paoli and J. Legendziewicz, 1985b, Inorg. Chim. Acta **110**, 7.

Berger, J., A.I. Rachlin, W.E. Scott, L.H. Sternbach and M.W. Goldberg, 1951, J. Am. Chem. Soc. **73**, 5295.

Bertrand, P.A., G.R. Choppin, Lin Geng Rao and J.-C.G. Bünzli, 1983, Anal. Chem. **55**, 364.

Bidzilya, V.A., 1978, Teor. & Eksp. Khim. **14**, 708 [Theor. & Exp. Chem. **14**, 553].

Bidzilya, V.A., and L.P. Golovkova, 1980a, Teor. & Eksp. Khim. **16**, 258 [Theor. & Exp. Chem. **16**, 214].

Bidzilya, V.A., and L.P. Golovkova, 1980b, Teor. & Eksp. Khim. **16**, 261 [Theor. & Exp. Chem. **16**, 218].

Birnbaum, E.R., 1980, in: Gmelin's Handbuch der Anorganischen Chemie, Sc, Y, Seltenernerden (Springer, Berlin) Band D3, ch. 7.

Blasius, E., and K.-P. Janzen, 1981, Top. Curr. Chem. **98**, 165.

Blasse, G., M. Buys and N. Sabbatini, 1986, Chem. Phys. Lett. **124**, 538.

Blondeel, G., A. Harriman, G. Porter and A. Wilowska, 1984, J. Chem. Soc. Faraday Trans. II **80**, 867.

Boer, F.P., M.A. Neuman, F.P. van Remoortere and E.C. Steiner, 1974, Inorg. Chem. **13**, 2826.

Bogatskii, A.V., V.F. Zolin, L.G. Koreneva, N.G. Lukyanenko, Yu.A. Popkov and V.A. Spapkin, 1984, Koord. Khim. **10**, 1048.

Bombieri, C., F. Benetollo, A. Polo, L. De Cola, D.L. Smailes and L.M. Vallarino, 1986, Inorg. Chem. **25**, 1127.

Bombieri, G., G. de Paoli, F. Benetollo and A. Cassol, 1980, J. Inorg. Nucl. Chem. **42**, 1417.

Boss, R.D., and A.I. Popov, 1985, Inorg. Chem. **24**, 3660.

Brittain, H.G., and J.F. Desreux, 1984, Inorg. Chem. **23**, 4459.

Brown, P.R., R.M. Izatt, J.J. Christensen and J.D. Lamb, 1983, J. Membrane Sci. **13**, 85.
Bryden, C.C., and C.N. Reilley, 1982, Anal. Chem. **54**, 610.
Bryden, C.C., C.N. Reilley and J.F. Desreux, 1981, Anal. Chem. **53**, 1418.
Bryden, C.C., C.N. Reilley and J.F. Desreux, 1982, in: The Rare Earths in Modern Science and Technology, eds G.J. McCarthy, H.B. Silber and J.J. Rhyne (Plenum Press, New York) Vol. 3, p. 53.
Bünzli, J.-C.G., and A. Giorgetti, 1985a, J. Less-Common Met. **112**, 355.
Bünzli, J.-C.G., and A. Giorgetti, 1985b, Inorg. Chim. Acta **110**, 225.
Bünzli, J.-C.G., and B. Klein, 1982, in: The Rare Earths in Modern Science and Technology, eds G.J. McCarthy, H.B. Silber and J.J. Rhyne (Plenum Press, New york) Vol. 3, p. 97.
Bünzli, J.-C.G., and C. Mabillard, 1986, Inorg. Chem. **25**, 2750.
Bünzli, J.-C.G., and G.-O. Pradervand, 1986, J. Chem. Phys. **85**, 2489.
Bünzli, J.-C.G., and D. Wessner, 1978, Helv. Chim. Acta **61**, 1454.
Bünzli, J.-C.G., and D. Wessner, 1980, Inorg. Chim. Acta **44**, L55.
Bünzli, J.-C.G., and D. Wessner, 1981, Helv. Chim. Acta **64**, 582.
Bünzli, J.-C.G., and D. Wessner, 1984a, Isr. J. Chem. **24**, 313.
Bünzli, J.-C.G., and D. Wessner, 1984b, Coord. Chem. Rev. **60**, 191.
Bünzli, J.-C.G., D. Wessner and H.T.T. Oahn, 1979a, Inorg. Chim. Acta **32**, L33.
Bünzli, J.-C.G., D. Wessner and P. Tissot, 1979b, Angewandte Chemische Thermodynamik und Thermoanalytik, Experientia Supplementun **37**, 44.
Bünzli, J.-C.G., B. Klein and D. Wessner, 1980, Inorg. Chim. Acta **44**, L147.
Bünzli, J.-C.G., B. Klein, D. Wessner, K.J. Schenk, G. Chapuis, G. Bombieri and G. de Paoli, 1981a, Inorg. Chim. Acta **54**, L43.
Bünzli, J.-C.G., H.T.T. Oanh and B. Gillet, 1981b, Inorg. Chim. Acta **53**, L219.
Bünzli, J.-C.G., B. Klein, G. Chapuis and K.J. Schenk, 1982a, Inorg. Chem. **21**, 808.
Bünzli, J.-C.G., B. Klein, D. Wessner, N.W. Alcock, 1982b, Chim. Acta **59**, 269.
Bünzli, J.-C.G., D. Wessner, A. Giorgetti and Y. Frésard, 1982c, in: The Rare Earths in Modern Science and Technology, eds G.J. McCarthy, H.B. Silber and J.J. Rhyne (Plenum Press, New York) Vol. 3, p. 85.
Bünzli, J.-C.G., J.-M. Pfefferlé, B. Ammann, G. Chapuis and F.-J. Zuniga, 1984, Helv. Chim. Acta **67**, 1121.
Bünzli, J.-C.G., W.D. Harrison, G.-O. Pradervand and N.W. Alcock, 1985, Inorg. Chim. Acta **109**, 59.
Bünzli, J.-C.G., G.A. Leonard, D. Plancherel and G. Chapuis, 1986, Helv. Chim. Acta **69**, 288.
Burns, J.H., 1979, Inorg. Chem. **18**, 3044.
Burns, J.H., and C.F. Baes, 1981, Inorg. Chem. **20**, 616.
Calogero, S., A. Seminara and U. Russo, 1979, Gazz. Chim. Ital. **109**, 45.
Campari, G., and F.A. Hart, 1982, Inorg. Chim. Acta **65**, L217.
Caro, P., O.K. Moune, F. Antic-Fidancev and M. Lemaitre-Blaise, 1985, J. Less-Common Met. **112**, 153.
Casellato, U., G. Tomat, P. di Bernardo and R. Graziani, 1982, Inorg. Chim. Acta **61**, 181.
Cassol, A., A. Seminara and G. de Paoli, 1973, Inorg. Nucl. Chem. Lett. **9**, 1163.
Catton, G.A., M.E. Harman, F.A. Hart, G.E. Hawkes and G.P. Moss, 1978, J. Chem. Soc., Dalton Trans., p. 181.
Chang, C.A., and V.O. Ochaya, 1986, Inorg. Chem. **25**, 355.
Chang, C.A., and M.E. Rowland, 1983, Inorg. Chem. **22**, 3866.
Chang, C.A., V.O. Ochaya and V.C. Sekhar, 1985, J. Chem. Soc. Chem. Commun., p. 1724.
Chang, C.A., B.S. Garg, V.K. Manchanda, V.O. Ochaya and V.C. Sekhar, 1986a, Inorg. Chim. Acta **115**, 101.
Chang, C.A., V.K. Manchanda and J. Peng, 1986b, personal communication.
Chebolu, V., R.R. Whittle and A. Sen, 1985, Inorg. Chem. **24**, 3082.
Cheney, J., J.M. Lehn, J.P. Sauvage and M.E. Stubbs, 1972, J. Chem. Soc. Chem. Commun., p. 1101.
Ciampolini, M., and N. Nardi, 1979, Inorg. Chim. Acta **32**, L9.
Ciampolini, M., P. Dapporto and N. Nardi, 1978, J. Chem. Soc. Chem. Commun., p. 788.
Ciampolini, M., P. Dapporto and N. Nardi, 1979a, J. Chem. Soc., Dalton Trans., p. 974.
Ciampolini, M., N. Nardi, R. Cini, S. Mangani and P. Orioli, 1979b, J. Chem. Soc., Dalton Trans., p. 1983.
Ciampolini, M., C. Mealli and N. Nardi, 1980, J. Chem. Soc., Dalton Trans., p. 376.
Dalley, N.K., 1978, in: Synthetic Multidentate Macrocyclic Compounds, eds R.E. Izatt and J.J. Christensen (Academic Press, New York) ch. 4.
Davidenko, N.K., V.A. Bidzilya, L.P. Golovkova, S.L. Davydova and K.B. Yatsimirskii, 1977, Theor. & Eksp. Khim. **13**, 404.
Davidenko, N.K., V.A. Bidzilya and L.P. Golovkova, 1980, Sov. J. Coord. Chem. **6**, 757.
De B. Costa, S.M., M.M. Queimado and J.J.R.F. Da Silva, 1980, J. Photochem. **12**, 31.
De Cola, L., D.L. Smailes and L.M. Vallarino, 1986, Inorg. Chem. **25**, 1729.
Desreux, J.F., 1978, Bull. Acad. Royale Belgique (Classe des Sciences) **64**, 814.
Desreux, J.F., 1980, Inorg. Chem. **19**, 1319.

Desreux, J.F., and G. Duyckaerts, 1979, Inorg. Chim. Acta **35**, L313.
Desreux, J.F., and M.F. Loncin, 1986, Inorg. Chem. **25**, 69.
Desreux, J.F., and J. Massaux, 1982, in: The Rare Earths in Modern Science and Technology, eds G.J. McCarthy, H.B. Silber and J.J. Rhyne (Plenum Press, New York) Vol. 3, p. 87.
Desreux, J.F., A. Renard and G. Duyckaerts, 1977, J. Inorg. Nucl. Chem. **39**, 1587.
Dobler, M., 1981, in: Ionophores and Their Structures (Wiley Interscience, New York).
Donohue, T., 1980, in: The Rare Earths in Modern Science and Technology, eds G.J. McCarthy, H.B. Silber and J.J. Rhyne (Plenum Press, New York) Vol. 2, p. 105.
Donohue, T., 1982, in: The Rare Earths in Modern Science and Technology, eds G.J. McCarthy, H.B. Silber and J.J. Rhyne (Plenum Press, New York) Vol. 3, p. 223.
Dvorkin, A.A., N.F. Krasnova, Yu.A. Simonov, V.M. Abashkin, V.V. Yakshin and T.I. Malinovskii, 1984, Sov. Phys. Crystallogr. **29**, 282.
Elguero, J., P. Navarro and M.I. Rodrigues-Franco, 1984, Chem. Lett., p. 425.
Elguero, J., P. Navarro, M.I. Rodriguez-Franco, F.H. Cano, C. Foces-Foces and A. Samat, 1985, J. Chem. Research (S), p. 312.
Ensor, D.D., and A.H. Shah, 1983, Solv. Extract. Ion Exch. **1**, 241.
Ensor, D.D., and A.H. Shah, 1984, Solv. Extract. Ion Exch. **2**, 591.
Ensor, D.D., G.R. McDonald and C.G. Pippin, 1986, Anal. Chem. **58**, 1814.
Erk, C., 1979, Chim. Acta Turcica **7**, 255.
Erk, C., 1983, Fresenius Z. Anal. Chem. **316**, 477.
Fan, Yuguo, Shen Cheng, Fengsham Wang, Zhongsheng Jin, Yuan Gao and Jiazan Ni, 1984, Mol. Sci. Chem. Res. (China) **4**, 371.
Fenton, D.E., U. Casellato, A.P. Vigato and M. Vidali, 1984, Inorg. Chim. Acta **95**, 187.
Forsellini, E., F. Benetollo, G. Bombieri, A. Cassol and G. de Paoli, 1985, Inorg. Chim. Acta **109**, 167.
Gansow, O.A., and A.R. Kausar, 1983, Inorg. Chim. Acta **72**, 39.
Gansow, O.A., and A.R. Kausar, 1984, Inorg. Chim. Acta **91**, 213.
Gansow, O.A., and A.R. Kausar, 1985, Inorg. Chim. Acta **109**, 1.
Gansow, O.A., and K.B. Triplett, 1981, US Patent 4257955.
Gansow, O.A., A.R. Kauser, K.M. Triplett, M.J. Weaver and E.L. Yee, 1977, J. Am. Chem. Soc. **99**, 7087.
Gansow, O.A., D.J. Pruett and K.B. Triplett, 1979, J. Am. Chem. Soc. **101**, 4408.
Gansow, O.A., K.M. Triplett, T.T. Peterson, R.E. Botto and J.D. Roberts, 1980a, Org. Magn. Resonance **13**, 77.
Gansow, O.A., R.K.C. Ho and W. Klemperer, 1980b, J. Organomet. Chem. **187**, C27.
Gao, Yuan, Ni Jiazan, Chen Chuanzheng and Yue Jin, 1985, in: New Frontiers in Rare Earth Science and Applications, Vol. I, eds Xu Guangxian and Xiao Jimei (Science Press, Beijing) p. 166.
Geraldès, C.F.G.C., M.C. Alpoim, M.P.M. Marques, A.D. Sherry and M. Singh, 1985, Inorg. Chem. **24**, 3876.
Gillain, G., P. Barthelemy, J. Massaux and J.F. Desreux, 1984, J. Chem. Soc., Dalton Trans., p. 2847.
Giorgetti, A., 1985, Ph.D. Thesis, University of Lausanne.
Grandjean, J., and P. Laszlo, 1982, Biochem. Biophys. Res. Commun. **104**, 1293.
Grandjean, J., and P. Laszlo, 1983, in: Physical Chemistry of Transmembrane Ion Motions, ed. G. Spach (Elsevier, Amsterdam) p. 289.
Gren, A.I., N.F. Zakhariya, N.V. Vityuk and V.S. Kalishevich, 1984, Ukr. Khim. Zhur. **50**, 517.
Groth, P., 1978, Acta Chem. Scand. A **32**, 279.
Gurrieri, S., A. Seminara, G. Siracusa and A. Cassol, 1975, Thermochim. Acta **11**, 433.
Hanna, D.A., Chiisun Yeh, Jiajiu Shaw and G.W. Everett Jr, 1983, Biochem. **22**, 5619.
Harman, M.E., F.A. Hart, M.B. Hursthouse, G.P. Moss and P.R. Raithby, 1976, J. Chem. Soc. Chem. Commun., p. 396.
Harrison, D.W., A. Giorgetti and J.-C.G. Bünzli, 1985, J. Chem. Soc., Dalton Trans., p. 885.
Hart, F.A., M.B. Hursthouse, K.M.A. Malik and S. Moorhouse, 1978, J. Chem. Soc. Chem. Commun., p. 549.
Hasegawa, Y., and S. Haruna, 1984, Solv. Extr. Ion. Exch. **2**, 451.
Hathaway, B.J., and A.E. Underhill, 1961, J. Chem. Soc., p. 3091.
Heckley, P.R., 1974, Dissertation, Univ. Microfilms, Order No 75-8152.
Heckley, P.R., and R.B. King, 1973, Proc. 10th Rare Earth Res. Conf., p. 311.
Hirashima, Y., and J. Shiokawa, 1979, Chem. Lett., p. 463.
Hirashima, Y., Y. Moriwaki and J. Shiokawa, 1980, Chem. Lett., p. 1181.
Hirashima, Y., K. Kanetsuki, J. Shiokawa and N. Tanaka, 1981a, Bull. Chem. Soc. Jpn **54**, 1567.
Hirashima, Y., R. Tsutsui and J. Shiokawa, 1981b, Chem. Lett., p. 1501.
Hirashima, Y., T. Tsutsui and J. Shiokawa, 1982, Chem. Lett., p. 1405.
Hirashima, Y., K. Ito and J. Shiokawa, 1983a, Chem. Lett., p. 9.
Hirashima, Y., K. Kanetsuki, I. Yonezu, K. Kamakura and J. Shiokawa, 1983b, Bull. Chem. Soc. Jpn **56**, 738.
Hirashima, Y., K. Kanetsuki, I. Yonezu, N. Isobe and J. Shiokawa, 1986, Bull. Chem. Soc. Jpn **59**, 25.
Hirschy, L.M., T.F. Van Geel, J.D. Winefordner, R.N. Kelly and S.G. Schulman, 1984, Anal. Chim. Acta **166**, 207.

Horrocks Jr, W. deW., 1982, Adv. Inorg. Biochem. **4**, 201.
Horrocks Jr, W. deW., and M. Albin, 1984, Progr. Inorg. Chem. **31**, 1.
Horrocks Jr, W. deW., and D.R. Sudnik, 1979, J. Am. Chem. Soc. **101**, 334.
Humphrey, M.B., W.M. Lamanna, M. Brookhart and G.R. Husk, 1983, Inorg. Chem. **22**, 3355.
Inoue, Y., and T. Hakushi, 1985, J. Chem. Soc. Perkin Trans II., p. 935.
Ishida, A., S. Toki and S. Takamuku, 1986, Chem. Lett., p. 117.
Izatt, R.M., J.D. Lamb, J.J. Christensen and B.L. Haymore, 1977, J. Am. Chem. Soc. **99**, 8344.
Izatt, R.M., J.S. Bradshaw, S.A. Nielsen, J.D. Lamb and J.J. Christensen, 1985, Chem. Rev. **85**, 271.
Izatt, R.M., G.A. Clark, J.S. Bradshaw, J.D. Lamb and J.J. Christensen, 1986, Sep. & Pur. Methods **15**, 21.
Japanese Patent, 1981, Kokai Tokkyo Koho, 81'104'986.
Jiang, Haiying, Ren Dehou, Xue Hongfu, Zhuang Zhiyang and Wang Hongxi, 1983a, Fenzi Kexue Yu Huaxue **3**, 97.
Jiang, Haiying, Ren Dehou, Xue Hongfu, Dai Cangding and Wang Li, 1983b, Chem. J. Chin. Univ. **5**, 29.
Jiang, Haiying, Ren Dehou, Xue Hongfu, Hui Xiqing and Wang Xiurong, 1983c, Huaxue Xuebao (Acta Chim. Sin.) **41**, 610.
Jin, Linpei, 1985, personal communication.
Jin, Linpei, Liu Gui, Ren Liping, Chen Batao and Wang Dianxun, 1985, in: New Frontiers in Rare Earth Science and Applications, eds Xu Guangxian and Xiao Jimei (Science Press, Beijing) Vol. I, p. 296.
Jin, Linpei, Ren Liping, Chen Batao and Wang Liangbao, 1986, Gaodeng Xuaxiao Huaxue Xuebao (Chem. J. Chin. Univ.) **7**, 95.
Kagan, H.B., and J.L. Namy, 1984, in: Handbook on the Physics and Chemistry of Rare Earths, Vol. 6, eds K.A. Gschneidner Jr. and L. Eyring (North-Holland, Amsterdam) ch. 50.
Kaifer, A., L. Echegoyen and G.W. Gokel, 1984, J. Org. Chem. **49**, 3029.
Kalishevich, V.S., D.V. Zagorevskii, A.I. Gren and O.S. Timofeev, 1984, Dopov. Akad. Nauk. Ukr. RSR Ser. B: Geol. Khim. Biol. Nauk., p. 34.
Kamenskaya, A.N., and N.B. Mikheev, 1985, Inorg. Chim. Acta **110**, 27.
Kamenskaya, A.N., N.B. Mikheev, S.A. Kulyukhin and S.V. Kondrashova, 1985, Zh. Neorg. Khim. **30**, 615.
Kao, Yuan, and Ni Jiazan, 1983, He Huaxue Yu Fangshe Huaxue **5**, 146.
Kauffmann, E., J.-M. Lehn and J.-P. Sauvage, 1976, Helv. Chim. Acta **59**, 1099.
Kausar, A.R., 1978, Dissertation, Univ. Microfilms, Order no 80-10778.
Kausar, A.R., 1982, J. Chem. Soc. Pak. **4**, 151.
Kinard, W.F., W.J. McDowell and R.R. Shoun, 1980, Separation Sci. and Techn. **15**, 1013.
King, R.B., 1975, US NTIS Rep., AD-AO13817.
King, R.B., and P.R. Heckley, 1974, J. Am. Chem. Soc. **96**, 3118.
Klein, B., 1980, Ph.D. Thesis, University of Lausanne.
Kodama, M., E. Kimura and S. Yamaguchi, 1980, J. Chem. Soc., Dalton Trans., p. 2356.
Kohata, S., S. Ohta and A. Ohyashi, 1985, Thermochim. Acta **87**, 75.
Koizumi, N., and S. Aoyagui, 1981, J. Electron. Anal. Chem. **124**, 345.
Kolthoff, I.M., 1979, Anal. Chem. **51**, 1R.
Koreneva, L.G., V.A. Barabanova, V.F. Zolin and S.L. Davydova, 1978, Sov. J. Coord. Chem. **4**, 143.
Kudo, T., and Y. Oba, 1978, Jpn patent JP Kokai Tokkyo Koho 78137080 [1979, C.A. **91**, 23424 j].
Lee, T.J., H.R. Sheu, T.I. Chiu and C.T. Chang, 1983, Acta Crystallogr. C **39**, 1357.
Lee, T.J., J.C. Hsieh, T.Y. Lee, C.Y. Chiu and C.T. Chang, 1985, Proc. Nat. Sci. Council (Taiwan) A **9**, 99.
Lehn, J.-M., 1978, Acc. Chem. Res. **11**, 51.
Lehn, J.-M., and J.P. Sauvage, 1975, J. Am. Chem. Soc. **97**, 6700.
Lever, A.B.P., E. Mantovani and B.S. Ramaswamy, 1971, Can. J. Chem. **49**, 1957.
Li, Zhenxiang, Ni Jiazan, Li Lemin and Xu Guangxian, 1984, Mol. Sci. Chem. Res. (China) **3**, 281.
Li, Zhenxiang, Ni Jiazan, Xu Guangxian and Ren Jingqing, 1985, in: New Frontiers in Rare Earth Science and Applications, eds Xu Guangxiang and Xiao Jimei (Science Press, Beijing) Vol. I, p. 293.
Li, Zhenxiang, Ni Jiazan, Xu Guangxian and Ren Jingqing, 1986a, Kexue Tongbao **31**, 956.
Li, Zhenxiang, Ni Jiazan, Xu Guangxian and Ren Jingqing, 1986b, J. Inorg. Chem. (China) **2**, 1.
Liang, Yingqiu, Zhad Yongnian, Zhang Shugong, Yu Fenglan and Ni Jiazan, 1983, Huaxue Xuebao (Acta Chim. Sin.) **41**, 198.
Lin, Wenlian, G.-Y. Adachi and J. Shiokawa, 1986, Inorg. Chim. Acta **117**, 87.
Lin, Yonghua, and Xingyan, 1983, Huaxue Xuebao (Acta Chim. Sin.) **41**, 97.
Lin, Yonghua, Xingyan and Jin Songchun, 1982, Wuli Xuebao **31**, 685.
Lindoy, L.F., 1975, Chem. Soc. Rev. **4**, 421.
Lockhart, J.C., A.C. Robson-Lindsell, M.E. Thompson, S.D. Furtado, C.K. Kaura and A.R. Allan, 1973, J. Chem. Soc., Perkin Trans. I, p. 577.
Lockhart, J.C., B. Atkinson, G. Marshall and B. Davies, 1979, J. Chem. Research (S), p. 32.

Loncin, M.F., J.F. Desreux and E. Merciny, 1986, Inorg. Chem. **25**, 2646.
Loufouilou, E.L., 1986, Ph.D. Thesis, Ecole Nationale Supérieure de Chimie, Strasbourg (France).
Lu, Pinzhe, Shen Cheng, Fan Yuguo, Jin Songchun, Zhang Shugong and Yu Fenglan, 1983, Fenzi Kexue Yu Huaxue Yanjiu **3**, 77.
Makrlik, E., and P. Vánura, 1986, Coll. Czech. Chem. Commun. **51**, 498.
Manchanda, V.K., and C.A. Chang, 1986, Anal. Chem. **58**, 2269.
Mariam, Y.H., and W. Wells, 1984, J. Sol. Chem. **13**, 269.
Mariam, Y.H., W. Wells and B. Wright, 1984, J. Sol. Chem. **13**, 259.
Massaux, J., and J.F. Desreux, 1982, J. Am. Chem. Soc. **104**, 2967.
Massaux, J., J.F. Desreux, C. Delchambre and G. Duykaerts, 1980, Inorg. Chem. **19**, 1893.
Massaux, J., G. Roland and J.F. Desreux, 1982, Inorg. Chim. Acta **60**, 129.
Melson, G.A., D.J. Olszanski and A.K. Rahimi, 1977, Spectrochim. Acta A **33**, 301.
Metcalf, D.H., R.G. Ghirardelli and R.A. Palmer, 1985, Inorg. Chem. **24**, 634.
Montanari, F., and P. Tundo, 1982, J. Org. Chem. **47**, 1298.
Moore, C., and B.C. Pressman, 1964, Biochem. Biophys. Res. Commun. **15**, 562.
Morf, W.E., D. Ammann, R. Bissig, E. Pretsch and W. Simon, 1979, in: Progress in Macrocyclic Chemistry, eds R.M. Izatt and J.J. Christensen (Wiley, New York) Vol. 1.
Moune, O.-K., C. Almasio, M.-J. Schwing-Weill and P. Caro, 1984, C.R. Acad. Sci. Paris Ser. II **299**, 679.
Nagai, H., T. Deguchi and K. Nakai, 1972, Bunseki Kagaku (Jpn Analyst) **21**, 788.
Nazarenko, N.A., N.S. Poluektov, E.V. Malinka and S.V. Bel'tyukova, 1986, Dopov. Akad. Nauk. Ukr. RSR Ser. B: Geol. Khim. Biol. Nauk., p. 39.
Ni, Yushan, Shao Yunglin and Xu Jiping, 1984, Youji Huaxue, p. 359.
Ohtsuka, Y., and H. Kawaguchi, 1974, Kobunshi Ronbunshu (Engl. Ed.) **3**, 1553.
Olszanski, D.J., 1975, Dissertation, Univ. Microfilms Order No 76-5618.
Olszanski, D.J., and G.A. Melson, 1977, Inorg. Chim. Acta **23**, L4.
Olszanski, D.J., and G.A. Melson, 1978, Inorg. Chim. Acta **26**, 263.
Pedersen, C.J., 1967a, J. Am. Chem. Soc. **89**, 2495.
Pedersen, C.J., 1967b, J. Am. Chem. Soc. **89**, 7017.
Perrett, B.S., and I.A. Stenhouse, 1972, United Kingdom Atomic Energy Authority, Research Group, Rep. (AERE-R 7042).
Peterson, J.R., 1979, Report ORO-4447-085, Avail. NTIS.
Pizer, R., and R. Selzer, 1983, Inorg. Chem. **22**, 1359.
Plancherel, D., and J.-C.G. Bünzli, 1986, unpublished results.
Plancherel, D., J.-C.G. Bünzli and J.-M. Lehn, 1985, in: New Frontiers in Rare Earth Science and Applications, eds Xu Guangxian and Xiao Jimei (Science Press, Beijing) Vol. I, p. 117.
Poluektov, N.S., E.V. Malinka, S.B. Mieshkova, S.V. Bel'tyukova and M.M. Dalinkovicz, 1984a, Dokl. Akad. Nauk SSSR **278**, 379.
Poluektov, N.S., E.V. Malinka, S.V. Bel'tyukova and V.N. Pastushok, 1984b, Dopov. Akad. Nauk. Ukr. RSR. Ser. B: Geol. Khim. Biol. Nauk., p. 51.
Poon, C.-K., and T.-W. Tang, 1984, Inorg. Chem. **23**, 2130.
Pradervand, G.O., 1985, Ph.D. Thesis, University of Lausanne.
Pruett, D.J., 1978, Dissertation, Univ. Microfilms Order No. 80-10779.
Qiu, Kunyuan, Feng Xiaojun and Feng Xinde (Voong Sing-Tuh), 1981, Kexue Tongbao **26**, 991.
Radecka-Paryzek, W., 1979, Inorg. Chim. Acta **35**, L349.
Radecka-Paryzek, W., 1980, Inorg. Chim. Acta **45**, L147.
Radecka-Paryzek, W., 1981a, Inorg. Chim. Acta **52**, 261.
Radecka-Paryzek, W., 1981b, Inorg. Chim. Acta **54**, L251.
Radecka-Paryzek, W., 1985, Inorg. Chim. Acta **109**, L21.
Rais, J., P. Selucky, V. Jirasek and F. Sebesta, 1977, J. Radioanal. Chem. **35**, 351.
Raymond, K.N., 1986, personal communication.
Reisfeld, R., and C.K. Jørgensen, 1977, in: Lasers and Excited States of Rare Earths (Springer, Berlin).
Ren, Dehou, Jiang Haiying, Xue Hongfu, Dai Cangding and Wang Li, 1983, Chin. J. Appl. Chem. **1**, 66.
Richardson, F.S., and A. Das Gupta, 1981, J. Am. Chem. Soc. **103**, 5716.
Rogers, R.D., and L.K. Kurihara, 1986, Inorg. Chim. Acta **116**, 171.
Rollet, A., J.-L. Sabot, M. Burgard and T. Delloye, 1986, Eur. Patent 86 400 049.2.
Sabbatini, N., and V. Balzani, 1985, J. Less-Common Met. **112**, 381.
Sabbatini, N., M. Ciano, S. Dellonte, A. Bonazzi and V. Balzani, 1982, Chem. Phys. Lett. **90**, 265.
Sabbatini, N., A. Bonazzi, M. Ciano and V. Balzani, 1984a, J. Am. Chem. Soc. **106**, 4055.
Sabbatini, N., M. Ciano, S. Dellonte, A. Bonazzi, F. Bolletta and V. Balzani, 1984b, J. Phys. Chem. **88**, 1534.
Sabbatini, N., S. Dellonte, M. Ciano, A. Bonazzi and V. Balzani, 1984c, Chem. Phys. Lett. **107**, 212.

Sabbatini, N., S. Dellonte and G. Blasse, 1986a, Chem. Phys. Lett. **129**, 541.
Sabbatini, N., S. Dellonte, A. Bonazzi, M. Ciano and V. Balzani, 1986b, Inorg. Chem. **25**, 1738.
Schwesinger, R., K. Piontek, W. Littke and H. Prinzbach, 1985, Angew. Chem. Int. Ed. Engl. **24**, 318.
Sekhar, V.C., and C.A. Chang, 1986, Inorg. Chem. **25**, 2061.
Seminara, A., and A. Musumeci, 1980, Inorg. Chim. Acta **39**, 9.
Seminara, A., S. Gurrieri, G. Siracusa and A. Cassol, 1975, Thermochim. Acta **12**, 173.
Shannon, R.D., 1976, Acta Crystallogr. A **32**, 751.
Shen, Lianfang, Gao Yuan, Xiao Yanwen and Ni Jiazan, 1982, Zhongguo Kexueyuan Changchun Yingyong Huaxue Yanjiuso Jikan **19**, 43.
Shen, Lianfang, Gao Yuan, Xiao Yanwen and Ni Jiazan, 1983, Zhongguo Kexueyuan Changchun Yingyong Huaxue Yanjiuso Jikan **20**, 1.
Shih, Jengshang, Tsay Linmei and Wu Shawchii, 1985, Analyst **110**, 1387.
Shiokawa, Y., and S. Suzuki, 1984, Bull. Chem. Soc. Jpn **57**, 2910.
Shono, T., and K. Kimura, 1977, Kagaku (Kyoto) **32**, 314.
Simon, J.D., W.R. Moomaw and T.M. Ceckler, 1985, J. Phys. Chem. **89**, 5659.
Smith, P.H., and K.N. Raymond, 1985, Inorg. Chem. **24**, 3469.
Spirlet, M.-R., J. Rebizant, J.-F. Desreux and M.-F. Loncin, 1984a, Inorg. Chem. **23**, 359.
Spirlet, M.-R., J. Rebizant, M.-F. Loncin and J.-F. Desreux, 1984b, Inorg. Chem. **23**, 4278.
Strawczynski, A., 1981, Diploma Thesis, University of Lausanne (Switzerland).
Tabib, J., J.T. Hupp and M.J. Weaver, 1986, Inorg. Chem. **25**, 1916.
Takeda, Y., 1984, Topics in Current Chemistry **121**, 1.
Tan, Minyu, and Gao Yici, 1978, Lan Chou Ta Hsueh Hsueh Pao, Tzu Jan K'o Hsueh Pao **3**, 143.
Tan, Minyu, and Gao Yici, 1980a, Kexue Tongbao **25**, 170.
Tan, Minyu, and Gao Yici, 1980b, Kexue Tongbao **25**, 482.
Tan, Minyu, Wang Liufang, Ma Tairu, Shu Cisheng, Yu Lanping and Quian Limin, 1983, Gaodeng Xuexiao Huaxue Xuebao (Chem. J. Chinese Univ.) **4**, 271.
Thomas, J.E., and G.J. Palenik, 1980, Inorg. Chim. Acta **44**, L303.
Timmons, J.H., J.W.L. Martin, A.E. Martell, P. Rudolf, A. Clearfield, J.H. Arner, S.J. Loeb and C.J. Willis, 1980, Inorg. Chem. **19**, 3553.
Timofeev, O.S., N.G. Lukyanenko, T.I. Kirichenko, V.S. Kalishevich, A.V. Bogatsky and A.I. Gren, 1983, Inorg. Chim. Acta **77**, L245.
Tomat, G., G. Valle, A. Cassol and P. Di Bernardo, 1983, Inorg. Chim. Acta **76**, L13.
Tomat, G., G. Valle, Di Bernardo and L. Zanonato, 1985, Inorg. Chim Acta **110**, 113.
Truter, M.R., D.G. Parsons, D.L. Hughes, G. de Paoli, G. Bombieri and F. Benetollo, 1985, Inorg. Chim. Acta **110**, 215.
Tsay, Linmei, Shih Jengshang and Wu Shawchii, 1983, Analyst **108**, 1108.
Tümmler, B., G. Maass, E. Weber, W. Wehner and F. Vögtle, 1977, J. Am. Chem. Soc. **99**, 4683.
Tundo, P., and J.H. Fendler, 1980, J. Am. Chem. Soc. **102**, 1760.
Vanura, P., M. Benesova, E. Makrlik, M. Kyrs and J. Rais, 1984, Coll. Czech. Chem. Commun. **49**, 1367.
Vesala, A., and R. Käppi, 1985, Acta Chem. Scand. A **39**, 287.
Vögtle, F., 1979, Chimia **33**, 239.
Vögtle, F., and E. Weber, 1979, Angew. Chem. Int. Ed. Engl. **18**, 753.
Wan, Jie, Ji Zhengping, Wang Jingqiu, Yang Zbikuan, Ni Xiaoling and Xiao Wenjin, 1983, Wuhan Daxue Xuebao Ziran Kexueban, p. 75.
Wan, Zhuli, Rao Zihe, Liang Dongcai, Yao Xinkan, Yan Shiping and Wang Genglin, 1982, Huaxue Xuebao (Acta Chim. Sin.) **40**, 1087.
Wang, Genglin, and Jiang Zonghui, 1980, Gaodeng Xuexiao Huaxue Xuebao (Chem. J. Chin. Univ.) **1**, 117.
Wang, Genglin, and Miao Lan, 1984, Xuexiao Huaxue Xuebao (Chem. J. Chin. Univ.) **5**, 281.
Wang, Genglin, and Yan Shiping, 1981, Huaxue Shiji (6), 343.
Wang, Genglin, Zhang Yunshi, Yao Xinkan, Yan Shiping and Wang Lianyuan, 1980, Gaodeng Xuexiao Huaxue Xuebao (Chem. J. Chin. univ.) **1**, 23.
Wang, Genglin, Yan Shiping, Li Xueyao, Yao Xinkan, Wan Zhuli, Rao Zihe and Liang Dongcai, 1982, Sci. Sin. (Engl. Ed.) B **25**, 916.
Wang, Genglin, Yan Shiping and Li Xueyao, 1983a, Gaodeng Xuexiao Huaxue Xuebao (Chem. J. Chin Univ.) **4**, 13.
Wang, Genglin, Zhang Ruohua and Jiang Zonghui, 1983b, Gaodeng Xuexiao Huaxue Xuebao (Chem. J. Chin. Univ.) **4**, 535.
Wang, Jingqiu, Yang Zhikuan, Wan Jie, Ji Zhenping and Xiao Wenjin, 1983, Gaodeng Xuexiao Huaxue Xuebao (Chem. J. Chin. Univ.) **4**, 691.
Wang, Jingqiu, Fang Youling, Fu Lijuan and Qin Zinbin, 1985, in: New Frontiers in Rare Earth Science and Applications, eds Xu Guangxian and Xiao Jimei (Science Press, Beijing) Vol. I, p. 170.

Wang, Wenji, Chen Bozhong, Hin Zhonggao and Wang Ailing, 1981, Gaodeng Xuexiao Huaxue Xuebao (Chem. J. Chin. Univ.) **2**, 431.
Wang, Xin, and Tan Minyu, 1984, Huaxue Xuebao (Acta Chim. Sin.) **42**, 434.
Weber, E., and F. Vögtle, 1976, Chem. Ber. **109**, 1803.
Weber, E., and F. Vögtle, 1980, Inorg. Chim. Acta **45**, L65.
Weber, E., and F. Vögtle, 1981, Top. Curr. Chem. **98**, 1.
Wessner, D., 1980, Ph.D. Thesis, University of Lausanne (Switzerland).
Wessner, D., and J.-C.G. Bünzli, 1985, Inorg. Synthesis **23**, 149.
Wessner, D., A. Giorgetti and J.-C.G. Bünzli, 1982, Inorg. Chim. Acta **65**, L25.
Wetton, R.E., and D.B. James, 1980, US Patent 4200701.
Wipf, H.K., A. Olivier and W. Simon, 1970, Helv. Chim. Acta **53**, 1605.
Xiao, Wenjin, Wang Jingqiu, Wan Jie, Yang Zhikuan and Lou Runhou, 1981, Wuhan Ta Hsueh Hsueh Pao, Tzu Jan Kô Hsueh Pan, p. 66.
Xiao, Wenjin, Ji Zhengping, Lou Runhuo, Dong Nianchu, Ren Yi, Liu Xia, Yu Shaojun, Ni Xiaoling and Qin Zibin, 1985, in: New Frontiers in Rare Earth Science and Applications, eds Xu Guangxian and Xiao Jimei (Science Press, Beijing) Vol. I, p. 208.
Xu, Zhangbao, Gu Yuanxin, Zheng Qitai, Shen Fulin, Yao Cingkai, Yan Shiping and Wang Genglin, 1982, Wuli Xuebao **31**, 956.
Xue, Hongfu, Jiang Haiying, Ren Dehou and Ma Shengxiang, 1983, J. Northwest Univ. (China) **3**, 29.
Yakshin, V.V., A.T. Fedorova, A.V. Val'kov and B.N. Laskorin, 1984, Dokl. Akad. Nauk SSSR **277**, 1417.
Yamana, Hajimu, Toshiaki Mitsugashira, Yoshinobu Shiokawa and Shin Suzuki, 1982, Bull. Chem. Soc. Jpn **55**, 2615.
Yang, Yansheng, and Zhu Jiaqin, 1982, Gaodeng Xuexiao Huaxue Xuebao (Chem. J. Chin. Univ.) **31**, 6.
Yang, Yansheng, and Zhu Jiaqin, 1985, in: New Frontiers in Rare Earth Science and Applications, Vol. I, eds Xu Guangxian and Xiao Jimei (Science Press, Beijing) p. 414.
Yang, Yusheng, Ding Yuzhen, Wang Qiuyin, Yao Zhongqi and Pan Guangming, 1982, He Huaxue Yu Fangshe Huaxue **4**, 21.
Yang, Yusheng, Ding Yuzhen, Tan Ganzu, Xu Junzhe, Yao Zhongqi and Zhang Fusheng, 1984, He Huaxue Yu Fangshe Huaxue **6**, 196.
Yatsimirskii, K.B., N.K. Davidenko, V.A. Bidzilya and L.P. Golovkova, 1977, Stroenie, Svoistva i Primen. Beta-Diketonatov Met., [1978, Mater. Uses. Semin.] 3rd, p. 19.
Yatsimirskii, K.B., V.A. Bidzilya, L.P. Golovkova and A.S. Shtepanek, 1979, Dokl. Akad. Nauk SSSR, **244**, 1142 (Engl. Transl. **244**, 78).
Yee, E.L., O.A. Gansow and M.J. Weaver, 1980, J. Am. Chem. Soc. **102**. 2278.
Yee, E.L., J.T. Hupp and M.J. Weaver, 1983, Inorg. Chem. **22**, 3465.
Yoshio, M., and H. Noguchi, 1982, Anal. Lett. A **15**, 1197.
Zhai, Yingli, Chen Xuenian, Su Zhixing and Tan Minyu, 1984, Lanzhou Daxue Xuebao Ziran Kexueban **20**, 126.
Zhao, Wenyun, Zhang Yuanfu, Liang Yingqiu, Zhang Shugong, Yu Fenglan and Ni Jiazan, 1985, Sci. Sin. (Engl. Transl.) B **28**, 569.
Zhou, Jinzhong, and Wang Dexi, 1982, He Huaxue Yu Fangshe Huaxue **4**, 174.
Zhou, Jinzhong, and Wu Xi, 1984, He Huaxue Yu Fangshe Huaxue **6**, 78.
Zhou, Jinzhong, Wu Xi and Wang Dexi, 1983, Abstracts, First ICLA, Venice, Sept. 5-10, p. 41.
Zhu, Jianqin, and Yang Yansheng, 1984, Gaodeng Xuexiao Huaxue Xuebao (Chem. J. Chin. Univ.) **5**, 404.
Zhu, Wenxiang, Li Qin, Zhang Aijun, Chen Botao, Zhao Jizhou and Jin Linpei, 1986, Gaodeng Xuaxiao Huaxue Xuebao (Chem. J. Chin. Univ.) **7**, 397.
Zolin, V.F., L.G. Koreneva, V.M. Dziomko, I.S. Markovich, L.I. Blokhina, N.I. Kruglova and Y.S. Ryabokobylko, 1981, Sov. J. Coord. Chem. (Engl. Transl.) **7**, 114.
Zou, Jinping, and Tan Minyu, 1983, J. Chin. Rare Earth Soc. **1**, 34.

Handbook on the Physics and Chemistry of Rare Earths, edited by K.A. Gschneidner, Jr. and L. Eyring

Chapter 61

RARE EARTH COORDINATION CATALYSTS IN STEREOSPECIFIC POLYMERIZATION

Zhiquan SHEN
Department of Chemistry, Zhejiang University
Hangzhou, People's Republic of China

Jun OUYANG
Changchun Institute of Applied Chemistry, Chinese Academy of Sciences
Changchun, People's Republic of China

Contents

Abbreviations

A	= acetylene	alk	= alkyl
acac	= acetylacetonate	BA	= benzoylacetonate
$Alalk_3$	= aluminum trialkyl	Bd	= butadiene

BTA = benzoyl trifluoroacetonate
BuOH = butanol
C_5H_5 = cyclopentadienyl
DEAC = diethyl aluminum chloride
DMSO = dimethyl sulfoxide
DPY = dipyridine
E = ethylene
EASC = ethyl aluminum sesquichloride
EDA = ethylene diamine
Et = ethyl
Et_3N = triethylamine
Et_2O = ether
EtOH = ethanol
GPC = gel permeation chromatograph
H_{pip} = hexahydropyridine
Hd = hexadiene
HDPE = high-density polyethylene
HMPA = hexamethyl phosphoramide
HMTA = hexamethylene tetramine
I_{sc} = short-circuit current
iBu, ibu = isobutyl
Ip = isoprene
ipr = isopropyl
iprOH = isopropyl alcohol
LDPE = low-density polyethylene
MBd = 2,3-dimethyl butadiene
MW = molecular weight
MWD = molecular weight distribution
N, naph = naphthenate
oct = octanoate
P = propylene

P_{204} = 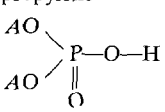

P_{229} = 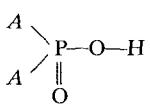

P_{350} = 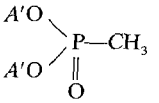

P_{507} = 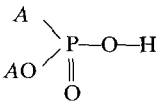

A = alkyl 

A' = alkyl' 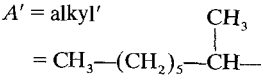

PA = polyacetylene
PBd = polybutadiene
PC = propylene carbonate
Pd = pentadiene
PhA = phenylacetylene
phen = 1, 10-phenanthroline
Pip = piperidine
PIp = polyisoprene
polymn = polymerization
PPA = polyphenylacetylene
PP-gr-PAAC = polyacrylate-grafted polypropylene
py = pyridine
SAAC = copolymer of styrene and acrylic acid
SCE = saturated calomel electrode
SMAC = copolymer of styrene-methacrylic acid
SMC = copolymer of styrene-2-(methyl sulfinyl)-ethyl methacrylate
TBP = triisobutyl phosphate
THF = tetrahydrofuran
TTA = thenoyl trifluoacetonate
V_{oc} = open-circuit voltage

1. Introduction

Thirty years have passed since the discovery of Ziegler–Natta catalysts. Traditional Ziegler–Natta catalysts encompass literally thousands of different combinations of a Group I–III organometallic compound and a transition metal compound of Group IV–VIII. Abundant resources of rare earth ores in China

challenged our interest in the investigation of the possibilities of using compounds of the Group IIIB elements as stereospecific polymerization catalysts. Early in the 1960's, we scouted rare earth compounds as butadiene polymerization catalysts for the first time (Shen et al., 1964, 1965). A new "family" of rare earth coordination catalysts with fairly high activity and high stereospecificity in polymerization of conjugated dienes has been developed since then.

In later work in the Changchun Institute of Applied Chemistry, the correlation between stereospecificity, catalytic activity and catalyst composition, polymerization mechanism and kinetics with rare earth coordination catalysts, as well as the structure and physical properties of the raw and vulcanized rubbers obtained therewith, have been studied. The results of these investigations have been reviewed in several articles (Shen, 1980; Shen et al., 1980; The Fourth Laboratory, Changchun Institute of Applied Chemistry, 1974, 1981; Ouyang et al., 1981; Ouyang, 1981; Ouyang et al., 1983).

Meanwhile, Throckmorton (1969) reported the polymerization of butadiene with rare earth catalysts in 1969. The Russians (Rafikov et al., 1976; Monakov et al., 1977a,b; Berg et al., 1978) and the Italians (Mazzei, 1980; Wang Fosong et al., 1981) are also engaged in diene polymerization with rare earth coordination catalysts.

Rare earth catalysts represent an unprecedented case where either butadiene, isoprene, or mixtures of butadiene and isoprene can be polymerized to elastomers with high cis-1,4 content. Polybutadienes prepared with rare earth catalysts having cis contents as high as 99% are unique in their linearity of chain structure, high molecular weight, broad molecular weight distribution, good processing behavior and mechanical properties, and higher oil extension possibilities (Qian Baogong et al., 1981). Polyisoprene so prepared has a cis-1,4 content of 94–96%, in between that of polyisoprenes prepared with lithium (92%) and titanium (97%) catalysts; it shows properties which can compete satisfactorily with titanium-catalyzed polyisoprene. Monomer moieties of Bd–Ip copolymer have a cis-1,4 content greater than 96%. The copolymers exhibit excellent low-temperature properties. Polymerization of pentadiene (Xie et al., 1979) and hexadiene (Wang Fosong et al., 1981), ethylene (Zhao and Ouyang, 1980) and propylene (Cai et al., 1984) with rare earth catalysts have been studied in recent years.

Since 1981 Shen and coworkers (Shen et al., 1982b, 1983; Shen and Farona, 1983a,b, 1984) have been extending the study of using rare earth coordination catalysts toward polymerization of acetylene, phenylacetylene and some terminal alkynes. Thus, a new area of usage of rare earth coordination catalysts has been opened. Using rare earth catalysts, acetylene can be polymerized at room temperature into polyacetylene film, with a cis content as high as 98%, with metallic sheen.

The discovery of rare earth coordination catalysts in stereospecific polymerization not only contributes to the development of Ziegler–Natta catalysts and stereospecific polymerization from the usual d-orbital transition elements to

elements involving f-orbitals (which poses new problems in coordination polymerization, having theoretical significance) but also shows the potential catalytic activities of rare earths in producing new varieties of polydienes, polyethylene, polyacetylene, and polyphenylacetylene, etc., with characteristic properties.

This chapter presents studies on the effect of the rare earth elements and ligands, as well as the reaction conditions, on polymerization and the structure of the polymers obtained, shedding light on the nature of these catalysts.

Since the ligands which are to be considered are often complicated organic molecules, it has become customary to employ appropriate abbreviations in order to avoid problems with the nomenclature. The number of abbreviations used in this chapter has been kept as small as possible; they are listed at the beginning of the chapter.

2. Types of rare earth coordination catalysts

Initially, the rare earth coordination catalysts we used in butadiene polymerization were a binary system composed of rare earth chloride (RCl_3; R = Y, La, Ce, Pr, Nd, Sm, Gd, Er, Yb) and $Al(alk)_3$(alk = Et, i-Bu) (Shen et al., 1964). It was found that the stereospecificity of these catalysts was high, yet their catalytic activity was rather low. The adoption of rare earth β-diketone chelates such as NdB_3, NdB, NdBTA, NdTTA, PrB_3, PrB, PrTTA, YB_3, YBTA, and LaBTA instead of the chloride made the catalyst system homogeneous with a somewhat higher activity (Shen et al., 1965). Throckmorton (1969) modified the catalyst system from a binary to a ternary one [cerium octanoate-$Al(alk)_3$-halide] which showed a higher polymerization activity. However, a drawback of this system is that the Ce-containing residue must be completely removed from the resulting polymers because the cerium ion can promote rubber oxidation.

In the 1970's, we Chinese chemists developed three-component systems, including lanthanide naphthenate, lanthanide carboxylate or lanthanide phosphonate, together with aluminum-alkyl and halide-containing compounds (section 3, The Fourth Laboratory, Changchun Institute of Applied Chemistry, 1974). These catalysts are used for butadiene polymerization, for isoprene polymerization, and for 2,4-hexadiene and Bd–Ip copolymerization. Subsequently, it was found that the addition of the appropriate amount of alcohol to the original lanthanide-chloride–aluminum-alkyl binary system led to greatly enhanced activity without any decrease in stereospecificity (Yang Jihua et al., 1980). Further investigation revealed that the lanthanide halide first reacts with the alcohol added to form an alcoholate which then reacts with $Al(alk)_3$ to form an active catalyst. Thus, a new efficient binary system of $RCl_3 \cdot 3$alcohol–aluminum alkyl has been established (Yang Jihua et al., 1980). Since 1980 many new binary systems composed of

aluminum alkyl and the following rare earth compounds have been developed: $NdCl_3 \cdot 3P_{350}$ (section 3, The Fourth Laboratory, 1974); $NdCl_3 \cdot 3TBP$ (Wang Fosong et al., 1980); $RCl_3 \cdot 4DMSO$ (Pang et al., 1984); $RCl_3 \cdot n$HMPA (Rafikov et al., 1980); $RCl_3 \cdot 2THF$ (Yang Jihua et al., 1982); Nd $(OPr\text{-}i)_{3-n}Cl_n$ (Shan et al., 1983); $(CF_3COO)_2NdCl \cdot Et_2O$ or $(CF_3COO)_2NdCl \cdot EtOH$ (Jin Yingtai et al., 1979, 1984a,b); $NdCl_3 \cdot 1.5Py$, $NdCl_3 \cdot 1.5DPy$, $NdCl_3 \cdot 2HMTA$, $NdCl_3 \cdot 2Phen$, and $NdCl_3 \cdot 3EDA$, etc. $NdCl_3 \cdot$ N-containing complexes (Yang Jihua et al., 1984a,b,c); $C_5H_5RCl_2 \cdot n$THF (C_5H_5 = cyclopentadienyl, R = Ce, Pr, Nd, Gd, Y; $n = 0, 1, 2, 3$) and $C_5H_5RCl_2 \cdot HCl \cdot 2THF$ (R = Pr, Nd) (Yu Guanqian et al., 1983); $C_9H_7RCl_2 \cdot (C_4H_8O)_x$ (R = Nd, Pr, Gd, Sm; C_9H_7 = indenyl, C_4H_8O = tetra hydrofuran, $x = 0, 1, 2$) (Qian Hanying et al., 1984).

Since the end of the 1960's attachment of transition metal complexes to organic polymers has appeared as a suitable means to approach the formation of stable catalysts with good reproducibility, activity and selectivity as homogeneous systems and which are easily separable from the reaction products as heterogeneous catalysts. Efforts to make polymer-supported rare earth complexes in combination with aluminum alkyl for the polymerization of butadiene and isoprene have been made by Li et al. (1981, 1984). The following polymer-supported rare earth catalysts have been developed: $SAAC \cdot NdCl_3$; $SMAC \cdot NdCl_3$; PP-grPAAC $\cdot NdCl_3$, and $SMC \cdot RCl_3$ (R = La, Pr, Nd, Eu, Ho, Er, Tm, Yb). Bergbreiter et al. (1985) recently reported that attachment of Ce or Nd to insoluble divinylbenzene styrene copolymers or to polyethylene via carboxylate groups gave recyclable Bd polymerization catalysts that possessed the same stereospecificity for formation of high MW polymer.

Recently, Cai et al. (1984) declared that propylene can be polymerized with supported neodymium catalysts: $NdCl_3 \cdot L/MgCl_2$ and $NdCl_3 \cdot L/MgCl_2/AlCl_3$. *

In 1981, one of us succeeded in carrying out the first study on rare earth coordination catalysis for the stereospecific polymerization of acetylene. It was revealed that high-cis or all-cis polyacetylene films with a silvery metallic appearance were obtained at ambient temperatures in the presence of rare earth coordination catalysts composed of two or three components: naphthenates [$R(naph)_3$], or phosphonates [$R(P_{204})_3$, $R(P_{507})_3$, . . .], or isoproxide $(i\text{-}prO)_3R$, etc., of all rare earth elements from Sc to Lu, trialkyl aluminum and/or a third component (Shen et al., 1982b, 1983; Shen and Farona 1983a,b, 1984; Yang Mujie et al., 1984a,b,c; Zhang et al., 1986). These catalysts have been used toward the polymerization of phenylacetylene and also of terminal alkynes.

Table 1 summarizes the rare earth coordination catalysts developed.

* L = $CH_3—\underset{\underset{O}{\|}}{P}—(O—\underset{\underset{CH_3}{|}}{CH}—C_6H_{13})_2$

TABLE 1
Rare earth coordination catalysts in stereospecific polymerization.

R compound	Aluminum alkyl	Third component	Monomer
chloride			
RCl_3 (R = Y, La, Pr, Nd, Ce, Sm, Gd, Er, Yb)	$AlEt_3$	–	Bd
RCl_3 (R = Y, La–Lu)	$AlEt_3$, $Al(i\text{-}Bu)_3$, $Al(i\text{-}Bu)_2H$	alcohol (EtOH, prOH, BuOH, etc.)	Bd, Ip, Pd, E
oxygen-containing chloride complex			
$RCl_3 \cdot 3EtOH$	$AlMe_3$, $AlEt_3$, $Al(ibu)_3$, $Alibu_2H$	–	Bd, Ip
$RCl_2C_5H_5 \cdot n$THF (R = Ce, Pr, Nd, Gd, Y; $n = 0, 1, 2, 3$)	$AlEt_3$, $Alibu_3$	–	Bd
$RCl_2C_5H_5 \cdot HCl \cdot 2THF$ (R = Pr, Nd)	$Alibu_2H$	–	Bd
$RCl_2C_9H_7 \cdot (C_4H_8O)_x$ (R = Nd, Pr, Gd, Sm; $x = 0, 1, 2$)	$Al(ibu)_2H$	–	Bd
$NdCl_3 \cdot 4DMSO$	$AlEt_3$, $Alibu_2H$	–	Bd
phosphorus-containing chloride complex			
$NdCl_3 \cdot 3P_{350}$, $NdCl_3 \cdot 3TBP$, $RCl_3 \cdot n$HMPA	$AlEt_3$, $Alibu_3$	–	Bd
nitrogen-containing chloride complex			
$NdCl_3 \cdot 1.5Py$, $NdCl_3 \cdot 1.5DPY$	$AlEt_3$		
$NdCl_3 \cdot 2HMTA$, $NdCl_3 \cdot 2Phen$ $NdCl_3 \cdot 3EDA$	$Alibu_3$, $Alibu_2H$	–	Bd, Ip
Alkoxide $Nd(Oalk)_{3-n}Cl_n$ ($n = 0, 1, 2$)	$AlEt_3$	–	Bd
$Nd(O\text{-}ipr)_3$	$Al(i\text{-}Bu)_3$	–	A
carboxylate			
$R(naph)_3$ (R = Sc, Y, La–Lu)	$AlEt_3$, $Alibu_3$	with or without EtOH	A, PhA, alkyne
$R(naph)_3$ (R = Y, La–Lu)	$AlEt_3$, $Alibu_3$, $Alibu_2H$	$Al_2Et_3Cl_3$, etc. (halogen-containing compounds)	Bd, Ip, MBd, Hd

$Nd(alkCOO)_3$ (alkCOO = stearate, octanoate, isooctanoate, $C_{5-9}COO$)	$AlEt_3$, $Alibu_3$	$Al_2Et_3Cl_3$	Bd, Ip
$(CF_3COO)_2NdCl \cdot Et_2O$ or $(CF_3COO)_2NdCl \cdot EtOH$	$AlEt_3$, $Alibu_3$	–	Bd, Ip
phosphorate or phosphonate			
$R(P_{204})_3$, $R(P_{507})_3$, $R(P_{215})_3$, etc.	$Alibu_3$	$Al_2Et_3Cl_3$	Bd, Ip
$R(P_{204})_3$, $R(P_{507})_3$, etc.	$Alibu_3$	P_{204}, O-donor, N-donor	A, alkyne
chelate			
Rbenzoylacetonate (RB, RB_3, RTTA, etc.) (R = Nd, Pr, La, Y)	$AlEt_3$, $Alibu_3$	–	Bd
Rbenzoylacetonate	$Alibu_3$	$Al_2Et_3Cl_3$	Ip
$R(acac)_3 \cdot 2H_2O$	$AlEt_3$, $Alibu_3$	$Al_3Et_3Cl_3$	Ip
$R(acac)_3 \cdot 2H_2O$	$Alibu_3$	P_{204}, etc.	A
$Nd(8\text{-oxy quinoline})_3$	$Alibu_3$	$Al_2Et_3Cl_3$	Ip
polymer supported			
$SAAC \cdot NdCl_3$	$Alibu_3$	$AlEt_2Cl$, Ph_3CCl, etc.	Bd
$SMAC \cdot NdCl_3$	$Alibu_3$	$AlEt_2Cl$	Bd
$SMC \cdot RCl_3$ (R = La, Pr, Nd, Eu, Ho, Er, Tm, Yb)	$Alibu_3$	–	Bd, Ip
supported			
$NdCl_3 \cdot L/MgCl_2$ or $NdCl_3 \cdot L/MgCl_2/AlCl_3$	–	–	P

3. Features in the polymerization of dienes, olefins, and acetylenes with rare earth coordination catalysts

Ziegler–Natta catalysts first described in the literature did not include rare earth elements in Group IIIB. However, rare earth catalysts are indeed excellent catalysts for stereospecific polymerization of conjugated dienes, acetylene, and its derivatives. Although in the mechanism of stereospecific polymerization, rare earth catalysts hold the general rule of coordination catalysts composed of transition metals involving d-orbitals: such as a living polymer chain of coordinated anionic type, a two-step propagation including monomer complexation and insertion, and chain transfer to aluminum alkyl and monomer, etc., they yet possess characteristics of their own, which are presented briefly in this and the following sections.

3.1. *Polymerization of butadiene and isoprene*

Most of the catalysts mentioned in section 2 have been used in the polymerization of Bd and Ip; yet the effect of polymerization parameters on the yield, the cis-1,4 content (polymer structure), and the molecular weight of polymers with catalyst systems such as $R(naph)_3$–$Alibu_3$–$Al_2Et_3Cl_3$, RCl_3–iprOH–$AlEt_3$ or $RCl_3 \cdot 3$iprOH–$AlEt_3$ and $Nd(Oalk)_{3-n}Cl_n$–$AlEt_3$, were studied in detail.

The role of different rare earth elements in the stereospecific polymerization of dienes can be generalized as follows: the stereoregularity of polydienes obtained with different rare earth elements is nearly the same and reflects the similarity in chemical nature of 4f-orbital electrons in all rare earth elements. On the other hand, the activity of the rare earth catalysts in diene polymerization varies from one another within the series. This indicates the difference in complexing ability due to the electronic structure or the number of 4f-orbital electrons in each kind of element in the series.

Both polybutadiene and polyisoprene with high cis-1,4 content can be obtained by the same rare earth catalyst. This is one of the characteristics of the rare earth catalyst system. As shown in table 2, about 97% cis-1,4 content is achieved for PBd prepared by any active rare earth catalyst system, except in the case of Er and Tm which give a somewhat lower cis-1,4 content. For polyisoprene, about 95% cis-1,4 content is obtained by La, Ce, Pr, and Nd catalyst; catalysts prepared from the remaining elements can yield polyisoprene with a slightly higher cis-1,4 content but these are weaker in activity.

All the compounds of Group IIIB elements in different periods of the Periodic Table can initiate cis polymerization of butadiene and isoprene to different degrees. The cis content of polybutadiene increases with an increase in the period number, or ionic radius of the element; however, that of polyisoprene decreases in the same order, as shown in table 3.

The catalytic activity of various individual rare earth compounds with the same

TABLE 2
Microstructure of polydienes prepared with R catalysts containing different rare earth elements (in %).

Rare earth element	Polybutadiene (RCl_3 catalyst)			Polyisoprene			
				cis-1,4-		3,4-	
	cis-1,4	trans-1,4	1,2-	(a)	(b)	(a)	(b)
La	97.2	2.1	0.7	94.1	94.2	5.9	5.8
Ce	97.2	2.1	0.7	94.8	93.6	5.2	6.7
Pr	97.2	2.2	0.6	94.9	93.9	5.1	6.1
Nd	97.3	2.2	0.5	94.7	95.0	5.1	5.0
Sm	98.0	1.6	0.4	96.7	94.6	3.3	5.4
Gd	97.3	2.2	0.5	96.8	96.0	3.2	4.0
Tb	97.9	1.6	0.5	97.2	95.2	2.8	4.8
Dy	97.5	1.9	0.6	97.2	95.2	2.8	4.8
Ho	96.7	2.8	0.5	97.4	95.5	2.6	4.5
Er	93.0	6.1	0.9	97.4	94.7	2.6	5.3
Tm	90.6	8.7	0.7	97.6	–	2.4	–
Yb	97.1	2.6	0.3	98.0	–	2.0	–

(a) RCl_3 catalyst.
(b) $R(naph)_3$ catalyst.

TABLE 3
The stereospecificity of different elements in Group IIIB for diene polymerization.

Period number	Element	Radii of tri-valent ions (Å)	Cis-1,4 content(%)	
			Polybutadiene	polyisoprene
4	Sc	0.68	88.6	99.2
5	Y	0.88	91.8	97.4
6	Nd	0.99	94.3	94.9
7	U	1.06	96.3	91.7

ligand shows the same trend in relative activities in diene polymerization with the following three different catalyst systems: $R(naph)_3$–$Al(i\text{-}Bu)_3$–$Al_2Et_3El_3$; RCl_3–$AlEt_3$–EtOH; $RCl_3 \cdot (TBP)_3$–$Al(i\text{-}Bu)_3$, as shown in figs. 1 and 2, where the elements are arranged in the order of their atomic numbers. That is, the activity decreases in the following order:

$$Nd > Pr > Ce > Gd > Tb > Dy > La > Ho > Y > Er \sim Sm > Tm > Yb > Lu \sim Sc \sim Eu\,.$$

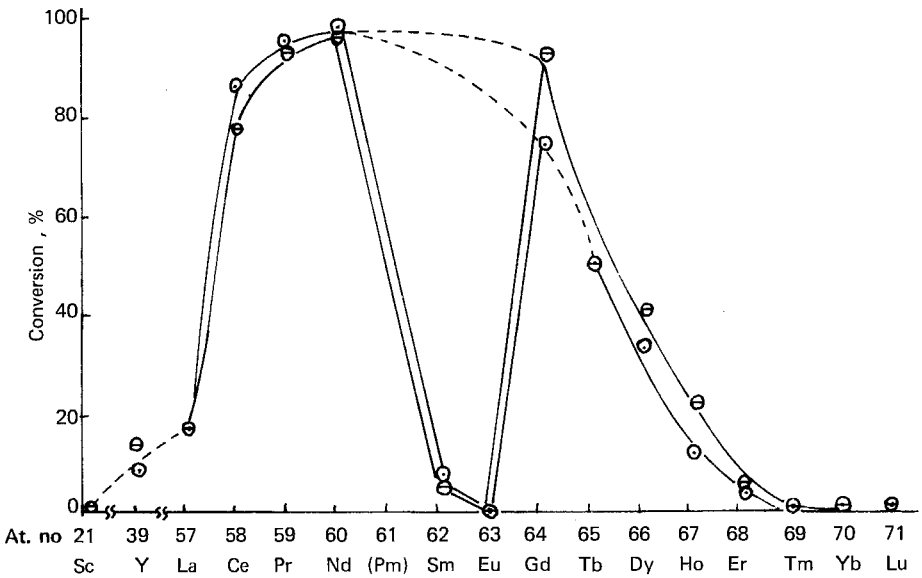

Fig. 1. Diene polymerization activity of various rare earth elements in R catalytic systems [RCl_3 $-C_2H_5OH-Al(C_2H_5)_3$]; ⊖: butadiene; ⊙: isoprene.

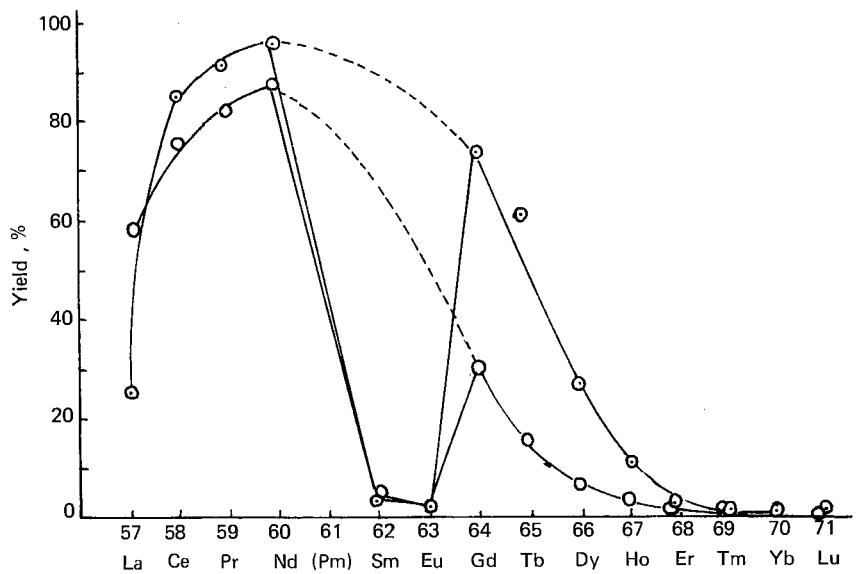

Fig. 2. Activity of various rare earth elements in R catalytic systems for polymerizing isoprene; ○: $RCl_3 \cdot (TBP)_3-Al(i\text{-}C_4H_9)_3$; ⊙: $R(Naph)_3-Al(i\text{-}C_4H_9)_3-Al_2(C_2H_5)_3Cl_3$. TBP = tri-butylphosphate; Naph = naphtenate.

For the active catalysts, the rare earth elements remain in the trivalent state, as evidenced by chemical analysis and spectrophotometric study. On the other hand, elements having vary low or no polymerization activity, such as Sm and Eu, show reduction to bivalency accompanied by a color change. Two explanations were suggested for the different activities of the elements maintaining their trivalent state; one opinion is that the activity difference is the result of the difference in energy change during the formation of a bond between the diene and rare earth ions (Wang Fosong et al., 1980); the other opinion is that the difference of the R–C bond strength affects the inserting activity of the monomer (The Fourth Laboratory, Changchun Institute of Applied Chemistry, 1981).

It is well known that the number of vacant sites on the active metal ions and the distribution of their electron density, i.e., bond polarity and bond strength of the coordination complex, can be changed by varying the ligands coordinated to it and the sorts of aluminum alkyl used, which in turn influences the activity and stereospecificity of the catalyst thus prepared. Table 4 shows the effects of ligand groups and alkyl groups in aluminum alkyl on the polymerization activity, molecular weight and microstructure of polyisoprene.

The order of activity of Nd catalysts with different ligands for isoprene polymerization is as follows:

$$\begin{aligned} &Nd(P_{507})_3 > Nd(P_{229})_3 > Nd(P_{204})_3 > NdCl_3 \cdot 3P_{350} \\ &\quad > Nd(naph)_3 > Nd(oct)_3 > Nd(C_{5-9}COO)_3 > Nd(acac)_3 \cdot 2H_2O \\ &\quad \simeq Nd(BA)_3 \cdot 2H_2O \simeq Nd(BA)_4 \cdot PiP > Nd(XX)_3\,{}^* > NdCl_3(\text{anhydrous}). \end{aligned}$$

Data from table 5, which summarize the effect of a halogen atom in the NdX_3–$AlEt_3$–EtOH system on the polymerization of dienes, shows that the rare earths are capable of producing 96–98% cis PBd with all four halides; whereas, for Ti, Co, and Ni catalysts, in order to prepare high cis PBd, a suitable electronegativity of the halide is required, as shown in table 6. In the $Nd(Oalk)_{3-n}Cl_n$–$AlEt_3$ system (Shan et al., 1983), the variation of n has an obvious effect on the microstructure of polydienes, as shown in table 7.

Yang Jihua et al. (1984a,b,c) reported that the activity sequences of $NdCl_3 \cdot$ N-containing complexes for butadiene polymerization in combination with various alkyl aluminum are different; this can be summarized as follows:

(a) In combination with $AlEt_3$, the activity is decreased in the order

$$\text{EDA} > \text{THF} > \text{i-PrOH} > \text{PY} > \text{HMTA} > \text{DPY} \gg \text{Phen}.$$

* XX = 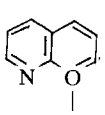

TABLE 4
The effect of components in R catalytic systems on the polymerization of isoprene.

Catalyst component	Yield (%)	[η] (dl/g)	Microstructure of polyisoprene (%)		
			cis-1,4	trans-1,4	3,4-
$NdX_3 + C_2H_5OH + Al(C_2H_5)_3$					
X: F	–	–	95.2	0	4.8
Cl	84	5.7	96.2	0	3.8
Br	42	6.6	93.7	0	6.3
I	5	5.8	90.5	0	9.5
$NdL_3 + Alalk_3 + Alalk_2X$					
L: $Nd(AA)_3 \cdot 2H_2O$	58	5.0	94.1	0	5.9
$Nd(BA)_3 \cdot 2H_2O$	60	6.4	94.5	0	5.5
$Nd(P_{204})_3$	96	3.5	94.7	0	5.3
$Nd(naph)_3$	82	–	95	0	5.0
$Nd(naph)_3 + Al_2(C_2H_5)_3Cl_3 + Alalk_3$					
$Alalk_3$: $Al(CH_3)_3$	20	6.28	94	0	6
$Al(C_2H_5)_3$	41	7.10	95	0	5
$Al(i\text{-}C_4H_9)_3$	66	7.81	94	0	6
$Al(i\text{-}C_4H_9)_2H$	70	4	94	0	6

TABLE 5
The effect of various NdX_3 in NdX_3–C_2H_5OH–$Al(C_2H_5)_3$ catalyst systems on polymerization.

X in NdX_3	Yield (%)	[η] (dl/g)	Microstructure of polybutadiene (%)			Yield (%)	[η] (dl/g)	Microstructure of polybutadiene (%)	
			cis-1,4	trans-1,4	1,2-			cis-1,4	3,4-
F*	2	–	95.7	2.5	1.8	–	–	95.2	4.8
Cl	94	8.3	96.2	3.5	0.3	84	5.7	96.2	3.8
Br	80	11.0	96.8	2.0	1.2	42	6.6	93.7	6.3
I	24	14.8	96.7	2.2	1.1	5	5.8	90.5	9.5

* The amount being 2.5 times greater than that of other halides.

TABLE 6
The effect of the electronegativity of the ligand on the microstructure of polybutadiene.

Ligand		Cis-1,4 content in polybutadiene (%)				
halide	electronegativity	Ti	Co	Ni	Ce	Nd
F	4.0	35	93	98	97	95.7
Cl	3.0	75	98	85	98	96.2
Br	2.8	87	91	80	98	96.8
I	2.5	93	50	10	98	96.7

TABLE 7
The relationship between n and the microstructure of PBd.

n	Microstructure of polybutadiene			Microstructure of polyisoprene	
	cis-1,4	trans-1,4	1,2	cis-1,4	trans-1,4
0	79.1	16.7	4.2	86.7	13.3
1	86.1	12.6	1.2	93.9	6.1
2	94.0	5.1	0.9	94.4	5.1
3	96.6	1.8	1.6	–	–

(b) In the case of $Al(i\text{-}Bu)_3$ the order is

$$EDA \simeq THF > i\text{-}PrOH > HMTA > DPY > PY \gg Phen .$$

(c) In combination with $HAl(i\text{-}Bu)_2$ the order is

$$Phen > THF > i\text{-}PrOH > EDA > HMTA > PY > DPY .$$

That is, $NdCl_3 \cdot 3EDA$ forms very highly active systems with both $AlEt_3$ and $Al(i\text{-}Bu)_3$, while $NdCl_3 \cdot 2Phen$ is active only with $HAl(i\text{-}Bu)_2$ as a cocatalyst. The molecular weight of the polymer is easier to regulate by varying the amount of the catalyst or $HAl(i\text{-}Bu)_2$ in the latter system. The high cis-content microstructure of polydienes remains unchanged.

The third component plays an important role on catalytic activity. In addition to the factors mentioned above, the activity of the catalyst is also affected remarkably by the molar ratio of the components, especially the ratio of alkyl aluminum chloride to lanthanide naphthenate in the $R(naph)_3$–$Al(i\text{-}Bu)_3$–$Al_2Et_3Cl_3$ system and the ratio of alcohol to RCl_3 in the RCl_3–$AlEt_3$–EtOH system. The order of addition of the individual ingredients, and mixing temperature and concentration, i.e., catalyst preparation, and aging conditions, etc., also affect the activity of the catalyst. However, the high cis stereospecificity of PBd and PIp is quite indifferent to the changes in composition and the relative proportion of the catalyst components, as well as other conditions used in the polymerization process. This shows another characteristic of rare earth coordination catalysts.

Linear high-cis PBd with MW from 10^4 to 10^6 and MWD from 3 to 10 could be prepared with rare earth catalysts. These PBds have the following features: excellent compounding behavior; high tensile strength of the vulcanizates; better cold-flow resistance, linear PIp of high MW ($[\eta] = 10$ dl/g, $MW = 2 \times 10^6$) and varying MWD ($M_w/M_n = 2$–10) could be obtained. Properties of the PIp gum, compound, and vulcanizate are comparable to the corresponding properties of the Ti catalyzed polyisoprene.

3.2. *Polymerization of pentadiene, 2,3-dimethyl butadiene and hexadiene*

1,3-pentadiene has two isomers – cis and trans. The trans form is usually more active and could be polymerized to high MW polypentadiene with Co, Ti and V coordination catalysts (Shen, 1981). Xie et al. (1979) claimed that trans isomer of 1,3-Pd could also be polymerized into a high molecular weight polymer with high conversion by rare earth catalysts. The structure of the PPd obtained as examined by IR, NMR and X-ray diffraction contains 70% cis-1,4 unit, 10% trans-1,4, and 20% 1,2 units with an isotactic configuration; it exhibits crystallinity. It was reported that PPd of 80–82% cis content, 18% trans-1,2 content was obtained by neodymium stearate–$Al(i\text{-}Bu)_3$–$AlEt_2Cl$ (Panasenko et al., 1977).

Wang Fosong et al. (1981) studied the polymerization of 2,4-hexadiene with $Nd(naph)_3$–$Al(i\text{-}Bu)_3$–$AlEt_2Cl$ in heptane at 0°C and 17°C, and revealed that only (E,E)-2,4-hexadiene gave high molecular weight crystalline polymers with a conversion of about 70% after 100–150 h at room temperature. IR, NMR, degradative oxidation, and X-ray analysis indicated that the polymer contains stereoregular sequences with trans-1,4-threodiisotactic structure.

2,3-dimethyl butadiene-1,3 could also be polymerized in heptane with the same ternary catalyst: $Nd(naph)_3$–$Al(i\text{-}Bu)_3$–$AlEt_2Cl$ at 50°C to a white powder. The microstructure of the polymer obtained consisted mainly of cis-1,4 units (Wang Fosong and Bolognesi, 1982).

The above-mentioned results have revealed that the structure of the monomer exerts significant influence on the microstructure of polymers. In the presence of rare earth catalysts butadiene forms a polymer with a cis-1,4 content greater than 98%, isoprene with 96% cis content, 2,3-dimethyl butadiene with mainly cis content, and polypentadiene with about 70% cis content; while 2,4-hexadiene forms a trans 1,4-polymer. This may suggest that the steric interaction between the incoming monomer, the catalytic complex, and the last polymerized unit plays some role in determining the stereospecificity of polymerization.

3.3. *The polymerization of ethylene and propylene*

The polymerization of ethylene with rare earth catalysts was claimed by Finch (1960) and several patents. (Merckling, 1960; Anderson and Merckling, 1960; Stuart, 1960). Zhao and Ouyang (1980) first used the ternary diene polymerization catalyst: $NdCl_3$–EtOH–$AlEt_3$ to polymerize ethylene at room temperature, under a gauge pressure of 20 mm Hg, to a fluffy powder with very high MW, and high T_m and density. The catalytic activity sequence of a variety of RCl_3 is in the following order, which is different from that for diene polymerization (Wang Shenlong, 1983):

$$Pr > Nd > Gd > Dy > La > Er$$

TABLE 8
The properties of various polyethylenes.

Polyethylene	$[\eta]$ (dl/g)	Crystallinity (%)	Crystallite size (Å)	Density (g/ml)	Elongation (%)	T_m (°C)	Tensile strength (kg/cm^2)
Rare earth PE	12.2	77	131	0.9369	451	139.5	318
HDPE	3.4	77	134	0.9467	429	133.5	208
LDPE	1.1	54	72	0.9204	795	105.5	194

The morphology of nascent polyethylene powder shows a fibrous structure in a scanning electronic micrograph. The branched content, crystallinity, and crystallite size of rare earth polyethylene are similar to those of high-density polyethylene, whereas its melting point and MW are higher than those of high-density polyethylene, as shown in table 8 (Wang Shenlong et al., 1983). The data indicate that the PE obtained shows characteristics of an extended molecular chain.

Ballard et al. (1978) reported in 1978 that the fully characterized group IIIA and rare earth complexes $[M(\eta\text{-}C_5H_4alk)_2Me]_2$ (M = Y or Er, alk = H, Me, or $SiMe_3$; and M = Yb, alk = H or Me) and $[M(\eta\text{-}C_5H_4alk)_2Me_2AlMe]_2$ (M = Y, Er, Ho or Yb, alk = H or Me; and M = Y, alk = $SiMe_3$) are active homogeneous ethylene polymerization catalysts having activities of 10–200 g m mol^{-1} atm^{-1} h^{-1}. These results give new information about the type of structural intermediates which may be encounted in Ziegler–Natta systems. Watson (1983) discussed three general pathways of organolanthanide complexes $[M(\eta^5\text{-}C_5Me_5)_2alk]$ (M = Lu, Yb, Y; alk = H, CH_3) in the polymerization of ethylene.

Polymerization of propylene has not been successful with rare earth coordination catalysts under mild conditions for quite a long time. Cai et al. (1984) reported that propylene can be polymerized by a supported neodymium catalyst: $NdCl_3 \cdot L/MgCl_2$ * at 60°C and 9 atm with catalytic activity of 1077 g PP/gNd. Cogrinding $NdCl_3 \cdot L/MgCl_2$ with $AlCl_3$ raised the catalytic activity, but the isotacticity of the polymer is only about 30%.

3.4. *The polymerization of acetylene and its derivatives*

3.4.1. *Acetylene*

Because of the metallic conductivity ($10^3\ \Omega^{-1}\ cm^{-1}$) possessed by doped polyacetylene (called synthetic metal) there is considerable interest in this simplest conjugated polymer. Polyacetylene has cis and trans isomers. Both cis and trans polyacetylene can be doped. The cis polymer is more elastic, flexible and easy to

* L = $[(CH_3—\underset{\underset{O}{\|}}{P}—(—O—\underset{\underset{CH_3}{|}}{CH}—C_6H_{13})_2]_4$

process. Furthermore, the doping effect of the cis polymer is even greater than that of the trans one. Therefore, efforts have been made to synthesize high-cis PA recently. The commonly used catalysts for preparing high-cis PA are $Ti(OBu)_4$–$AlEt_3$ (−78°C), $Co(NO_3)_2$–$NaBH_4$ (−80°C) and $C_5H_4(C_5H_5)_3Ti_2$ (−80°C). Shen et al. (1982b, 1983) for the first time have investigated the stereospecific polymerization of acetylene by using rare earth compounds as catalysts. This development is based upon work on diene stereospecific polymerization. Thus a new family of coordination catalysts based upon rare earth compounds for high-cis or rich-cis acetylene polymerization at room temperature has been developed. Thus, a variety of polyacetylene rare earth PA results. Shen et al. (1982b, 1983, 1985a,b) have carried out a systematic and detailed study of a variety of new catalysts as mentioned in section 2. These studies include polymerization processes, kinetics and mechanism, electrochemical properties, structure and the fabrication of rare earth PA cells.

Table 9 lists the cis contents of PA obtained by all rare earth catalysts composed of naphthenate and phosphonate with aluminum alkyl. It can be seen that the cis content of PA obtained by a $R(P_{204})_3$ system is somewhat lower than that of $R(naph)_3$ catalyzed PA. Rare earth naphthenates combined with $Al(i\text{-}Bu)_3$ systems are the best catalysts to synthesize easily and conveniently high-cis PA with metallic appearance at room temperature.

Tables 10 and 11 show that variation of polymerization parameters such as polymerization temperature and molar ratio of aluminum alkyl to the rare earth compound have no significant effect on the PA's microstructure (Shen et al., 1985b).

The catalytic activity on the PA film yielded with the $R(naph)_3$–$Al(i\text{-}Bu)_3$ system at 30°C decreased in following order:

$$Y \sim Ce > Nd \sim Tb > Pr > La > Lu \sim Gd > Tm \sim Er > Ho \sim Yb \sim Eu > Sm > Dy .$$

TABLE 9
The cis content of polyacetylene (%).

Rare earth	$R(naph)_3$	$R(P_{204})_3$	Rare earth	$R(naph)_3$	$R(P_{204})_3$
Sc	96.0	96.0 *	Gd	96.1	84.0
Y	96.2	88.5	Tb	96.0	91.1
La	95.0	92.2	Dy	95.8	90.1
Ce	92.4	83.5	Ho	96.6	83.4
Pr	96.0	94.9	Er	96.7	89.4
Nd	96.9	92.2	Tm	96.0	85.5
Sm	95.3	86.3	Yb	93.6	79.5
Eu	88.0	76.4	Lu	90.9	83.7

* Polymerization temperature O°C.

TABLE 10
The effect of the polymerization temperature on the percentage of cis of polyacetylene.

Temperature (°C)	Catalyst system	
	$Nd(naph)_3$	$Y(naph)_3$
−15	95.5	96.6
0	95.8	97.7
15	95.1	96.4
30	95.4	94.7
45	93.8	92.1
60	83.4	87.3

TABLE 11
The effect of the Al/R molar ratio on the percentage of cis of polyacetylene.

Al/R molar ratio	Catalyst system	
	$Nd(naph)_3$	$Gd(naph)_3$
2	96.8	94.3
3	96.9	96.4
5	96.0	95.4
7	95.1	94.0

Nevertheless in the $R(P_{204})_3$ system the catalytic activity has the following sequence:

$$Nd > Gd > La > Y \sim Er > Lu > Sc .$$

It is postulated that the activity may be related to the radii of the rare earth ions and the hardness of the ionic hard–soft acid (Yu Luping et al., 1985a).

The addition of an appropriate third component not only facilitates the formation of silvery PA film or raises the polymer yield, but it also can raise the cis content of PA. The effectiveness upon the addition of a third component (donor) has the following order in the $R(P_{204})_3$–$Al(i\text{-}Bu)_3$ system (Zhang et al., 1986):

P_{204} > dioxane > pyridine > tributyl phosphate
> n-octanol > triethyl amine > aniline > triphenyl phosphine
> methyl ethyl ketone > butanol > anisole .

The effectiveness of a third component in raising the yield of PA film with the Nd

$(O\text{-ipr})_3$-$Al(i\text{-}Bu)_3$ system has the following order (Yang Mujie et al., 1984a):

$$P_{204} > BuOH > EtOH > P_{507} > Et_3N > (BuO)_3PO\,.$$

Polyacetylenes obtained by rare earth coordination catalysts are silvery grey films with a metallic luster which are not soluble in organic solvents or inorganic acids and bases. It is worth noting that the PA so obtained is comparatively stable and isomerizes only slowly when it is stored in air at room temperature.

The electron spin resonance spectra of PA show that the polymers are paramagnetic and their unpaired electron concentrations (N) and g-values are about 10^{16} spins/g and 2.0042 ± 0.0007, respectively, as shown in table 12. Their floatation densities have also been summarized in table 12.

Differential scanning calorimetry of the PA so obtained reveals the existence of two exothermic peaks at 195–200°C and 375–380°C, and one endothermic peak at 460°C, which are attributed to cis–trans isomerization; hydrogen migration, cross linking, and decomposition of PA. These temperatures are higher than that of $Ti(OBu)_4$ catalyzed PA, thus they also reflect the thermal stability of rare earth PA.

The X-ray diffraction patterns of these PA films reveal that the specimens are crystalline polymers characterized by an intense and sharp reflection at a Bragg angle between $2\theta = 23.1$–$23.3°$. Shen et al. (1985a) have found that Sc catalyzed PA has a crystallinity of 70% and belongs to the orthorhombic system, having the following unit cell parameters: $a = 7.58$ Å, $b = 4.40$ Å, $c = 4.38$ Å. Cao et al. (1982) have studied the crystalline structure of trans-PA isomerized from cis-PA prepared by $Nd(P_{507})_3$–$AlEt_3$–BuOH. They have observed a clear spot diagram, typical of a single crystal, in the electron diffraction pattern.

The scanning and transmission electron micrograph images of rare earth catalyzed PA show clearly discernible fibrillar morphology. They consist of a fleece of randomly oriented fibers with diameters of 200–650 Å and of indefinite

TABLE 12
Values of N, g, and density of polyacetylene.

Rare earth	d (g/cm^3)	g	N (10^{16} spins/g)	Rare earth	d (g/cm^3)	g	N (10^{16} spins/g)
Sc	–	2.0032	3.4	Gd	1.22	2.0038	5.9
Y	1.21	2.0039	4.5	Tb	1.19	2.0041	5.6
La	1.17	2.0044	5.6	Dy	1.20	2.0038	5.3
Ce	1.18	2.0036	6.6	Ho	1.25	2.0040	5.1
Pr	1.20	2.0047	5.6	Er	1.20	2.0040	4.5
Nd	1.22	2.0049	6.5	Tm	1.18	2.0041	4.9
Sm	1.18	2.0036	8.1	Yb	1.17	2.0036	10.9
Eu	1.19	2.0041	7.4	Lu	1.16	2.0042	9.8

length, depending on the catalyst and polymerization conditions used (Yang Mujie et al., 1984b).

In order to have more insight into the characteristics of these catalyst systems, the kinetics and mechanism of polymerization of acetylene in rare earth coordination catalysts were investigated (Yu Luping et al., 1985a). It was shown that the initial rate of the reaction, R_0, is first order with respect to the overall concentration of catalyst and the pressure of acetylene in the system. The kinetic equation can be written as:

$$R_0 = k_p[\mathrm{M}][\mathrm{C}^*] ,$$

where [M] is the concentration of monomer and [C*] is the concentration of active species. The active species was assumed to be deactivated by a bimolecular mechanism. According to the results and arguments, an anionic coordination mechanism for polymerization of acetylene in rare earth coordination catalysts has been proposed (Yu Luping et al., 1985a), as shown in fig. 3.

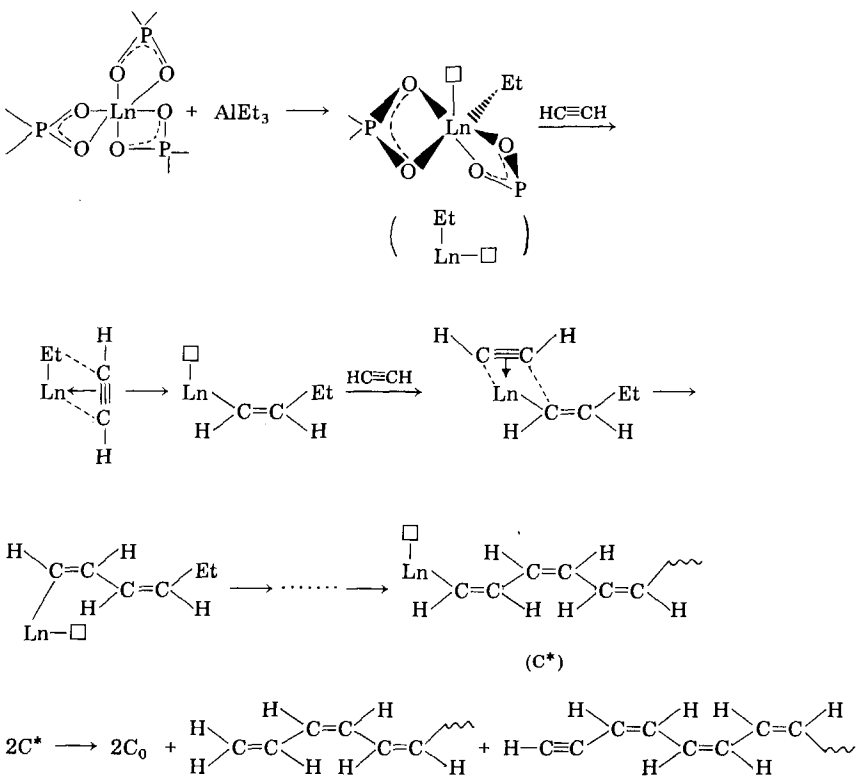

Fig. 3. The mechanism of acetylene polymerization by rare earth coordination catalysts.

The electrical resistivity of rare earth catalyzed PA with high-cis content is 10^8–10^{10} Ω cm. Therefore, pristine PA film is an organic semiconductor or insulator, but it can be doped either chemically or electrochemically. The electrical conductivities of iodine-doped PA raised eleven to twelve orders of magnitude to the metallic conducting regime, as shown in table 13 (Yang Mujie et al., 1983). The iodine complexes of PA have also been characterized by IR, DSC, X-ray and SEM. Very recently, Shen et al. (1986) reported that the conductivities of heavily ferric chloride doped cis and trans PA $[CH(FeCl_4)_y]_x$ were 446 and 38 Ω^{-1} cm^{-1}, respectively, and their fibril morphology remained unchanged after doping. Qiao et al. (1986) and Yu Luping et al. (1985b) have studied both the electrochemical doping of rare earth catalyzed PA employing organic and aqueous electrolytes and the electrochemistry of several PA batteries. The electrical potentials of the PA so obtained have been shown in table 14. The study revealed that the rare earth PA could be utilized as the cathode of a battery either in an aqueous or organic electrolyte solution. The aqueous PA battery can be utilized as a primary battery and gives a large short-circuit current of several hundred mA and an open-circuit voltage of about 1.9 V. The V_{oc} of a Li/0.3 M $LiClO_4$, PC/$(CHI_y)_x$ battery reaches 3.3–3.5 V.

Yang Mujie et al. (1984c) have synthesized polymer composite films of rare earth PA and various elastomers: butadiene styrene rubber, natural rubber, cis-1,4 PBd, and ethylene–propylene–diene terpolymer; these showed higher toughness, tensile strength, and resistance to oxygen attack.

TABLE 13
The electrical conductivity $\sigma(10^2\ \Omega^{-1}\ cm^{-1})$ of iodine-doped rare earth PA at 20°C. *

La	Pr	Nd	Gd	Dy	Tm	Yb	Lu	Y	Sc
7.6	4.0	9.9	7.2	5.2	4.0	7.3	4.3	8.7	3.0

* Composition of PA: cis-$(CHI_y)_x$; $y = 0.13$ for La, Nd, Dy, Tm, Yb, Lu, and Y; $y = 0.12$ for Pr, Gd; $y = 0.09$ for Sc.

TABLE 14
The electrical potentials of rare earth polyacetylene electrodes.

Electrodes	Electrolyte solution	Potentials (versus SCE)
Pristine $(CH)_x$	5.0 M KCl	−0.2702
Pristine $(CH)_x$	6.3 M NaCl	−0.2300
I_2-doped $(CH)_x$	6.3 M NaCl	+0.2375
I_2-doped $(CH)_x$	2.0 M HCl	+0.1949
I_2-doped $(CH)_x$	1.0 M $MgSO_4$	+0.1894
I_2-doped $(CH)_x$	1.0 M $MgCl_2$	+0.2033
I_2-doped $(CH)_x$	1.0 M $LiClO_4$	+0.2166

3.4.2. *Phenylacetylene*

Since the rare earth coordination catalysts produced high-cis PA, these catalysts were also investigated as polymerization catalysts for phenylacetylene by Shen and Farona (1983a,b). The rare earth naphthenates of Y, Sc, La, Ce, Pr, Nd, Sm, Eu, Gd, Tb, Dy, Ho, Er, Tm, Yb, and Lu, in combination with triethyl aluminum, were found for the first time to be active in phenylacetylene polymerization and produced atactic polyphenylacetylene (PPA), as shown in table 15. The polymers are all yellow or dark yellow powders with low ($\bar{M}_n = 1000$) to moderate ($\bar{M}_n = 4000$) molecular weights. IR and NMR spectra of these samples indicated that they are similar to those reported by Simionescu et al. (1978). These polymers exhibit a low degree (28%) of crystallinity. A dark red precipitate formed during the polymerization reaction under the following reaction conditions: $PhA/R(naph)_3 = 25$ (molar ratio); $EtOH/R(naph)_3 = 3$; $Al(i\text{-}Bu)_3/R(naph)_3 = 7.5$; $M = 1.0$ mol/l; 20°C; 24 h; chlorobenzene. The polymer is insoluble in common organic solvents at room temperature, but slowly goes into O-dichlorobenzene at 135°C. These properties are consistent with a cis-cisoidal conformation of polyphenylacetylene, and indeed, the infrared spectrum of this compound is identical with that reported for the polymer. The degree of crystallinity of cis-cisoid ppA is about 45% by X-ray diffraction analysis.

3.4.3. *Terminal alkynes*

The polymerization of alkyl-substituted, terminal acetylenes was carried out at 20°C, using rare earth naphthenates with tri-isobutylaluminum or triethylaluminum as the catalyst in cyclohexane or chlorobenzene by Shen and Farona

TABLE 15
Properties of polyphenylacetylene.

Lanthanide	Yield (%)	Softening temperature (°C)	M_n
La	11.3	120–130	980
Ce	12.8	115–120	820
Pr	13.6	138–145	1150
Nd	25.2	196–202	3250
Sm	8.2	154–158	1575
Eu	0.5	–	–
Gd	12.1	198–202	4120
Tb	12.8	182–188	2196
Dy	11.5	204–210	4396
Ho	25.8	152–156	1361
Er	12.2	190–194	2330
Tm	25.5	122–128	960
Yb	1.2	–	–
Lu	14.6	140–148	1213

(1983b, 1984). The monomers (1-hexyne, 1-pentyne, 3-methyl-1-pentyne, 4-methyl-1-pentyne, and isopropylacetylene) gave light yellow, occasionally elastomeric, polymers in very high yields in some cases. Membrane osmometric measurements revealed that the molecular weights of the polymers obtained are in the 80 000–170 000 range, which is extremely high for polymers of substituted acetylenes. These polymers were studied by ultraviolet, infrared, and NMR spectrometry.

The states, conversion, and molecular weights of the polyalkynes obtained with $Sc(naph)_3$–$Al(i\text{-}Bu)_3$ and $Nd(naph)_3$–$Al(i\text{-}Bu)_3$ systems are shown in tables 16 and 17. It is apparent that the position of the methyl group with respect to the triple bond strongly affects the rate of polymerization of the monomer. The lowest conversions for both catalysts were obtained with 3-methyl-1-butyne, in which steric hindrance would be expected to be the greatest. All the polyalkynes dissolved readily in aliphatic and aromatic hydrocarbons and other organic solvents.

TABLE 16
Polymerization of 1-alkynes by $ScN_3/Al(i\text{-}C_4H_9)_3$.

Monomer	State of Polymer	Cyclohexane		Benzene		Chlorobenzene	
		Conversion (%)	$\bar{M}_n$ ($\times 10^{-4}$)	Conversion (%)	$\bar{M}_n$ ($\times 10^{-4}$)	Conversion (%)	$\bar{M}_n$ ($\times 10^{-4}$)
1-Hexyne	Yellow, rubbery solid	95	2.4	88	2.5	96	3.2
1-Pentyne	Yellow, rubbery solid	96	2.3	78	2.7	96	3.2
3-Methyl-1-pentyne	Light yellow solid	32	1.5	–	–	–	–
4-Methyl-l-pentyne	Yellow solid	56	1.2	31	2.1	45	2.1
3-Methyl-1-butyne	Light yellow solid	27	0.8	8	0.8	14	0.9
Phenylacetylene	Orange-red solid	15	a	20	a	46	a

[a] Insoluble at 20°C.
* n = naph.

TABLE 17
Polymerization of terminal alkynes by $NdN_3/Al(i\text{-}C_4H_9)_3$. *

Monomer	State of Polymer	Cyclohexane		Chlorobenzene	
		Conversion (%)	$\bar{M}_n$ ($\times 10^{-4}$)	Conversion (%)	$\bar{M}_n$ ($\times 10^{-4}$)
1-Hexyne	Yellow rubbery solid	100	3.5	99	2.0
1-Pentyne	Yellow rubbery solid	100	3.7	99	2.4
3-Methyl-1-pentyne	Light yellow solid	38	3.0	–	–
4-Methyl-l-pentyne	Yellow solid	63	2.6	69	2.3
3-Methyl-l-butyne	Light yellow solid	29	0.8	30	0.9

* n = naph.

TABLE 18
Conversion (%) data on the polymerization of terminal alkynes by $RN_3/Al(i\text{-}C_4H_9)_3$ catalysts.

Monomer	Sc	Y	La	Ce	Pr	Nd	Sm	Eu	Gd	Tb	Dy	Ho	Er	Tm	Yb	Lu
1-Hexyne	95	23	12	9	11	100	6	3	6	19	11	32	12	17	10	17
1-Pentyne	96	26	12	8	10	100	5	2	5	18	10	30	11	17	9	15
Phenyl-acetylene	46	2	3	2	2	40	5	1	2	4	3	5	4	7	5	4

* Reaction conditions: monomer/RN_3 = 25 (molar ratio); C_2H_5OH/RN_3 = 3 (molar ratio); $Al(i\text{-}C_4H_9)_3/RN_3$ = 7.5 (molar ratio); [M] = 1.0 mol/l; 20°C; 24 h.

Infrared and UV spectra of these polymers are indicative of the conformation of the chain; for example, fully conjugated, planar polyenes should show a ν(C=C) absorption around 1600 cm^{-1} whereas isolated double bonds absorb near 1680 cm^{-1}. For all these polymers the major ν(C=C) band occurs at 1675 cm^{-1} and a minor band appears in the 1620 cm^{-1} region, which indicates that the double bonds behave more like nonconjugated than conjugated systems and means that the chain must be twisted from planarity to minimize the molecular orbital overlap in the conjugated chain. A further examination of the IR spectra of these polymers revealed that trans double bonds appear to be minimal in these polymers, whereas strong cis absorption is observed in all cases. The UV spectra are in support of the infrared spectral indications. Fully conjugated, planar, polyene should absorb in or near the visible region. Yet, electronic transition absorptions in these polymers are observed in the 200–325 nm region, showing that the effects of polyconjugation are not present. If the conformation of the chains is essentially cis-cisoid the polymers will be helical and twisted out of planarity with respect to the conjugated double bonds. This will result in reduced molecular orbital overlap and the double bonds will be more isolated. The IR- and UV-spectra results agree with this contention. The H-NMR spectra of the alkyl-substituted polyalkynes are similar to one another in that the integrated intensities of the aliphatic- to olefinic protons are in accord with the expected structures.

The yields of the polymerization of three alkynes by all rare earth catalyst systems in chlorobenzene are given in table 18. The scandium and neodymium systems show the highest activities. Clearly, these new Ziegler–Natta catalysts are capable of promoting high-molecular-weight, cis-cisoid polymers in high yields.

4. Copolymerization of olefinic monomer

4.1. *Copolymerization of butadiene and isoprene*

In the field of polymer science, a copolymerization study is essential not only for investigating the nature of the polymerization process but also in obtaining

new polymers with desired properties. The copolymerization of Bd with Ip first was investigated by using lanthanide naphthenate systems; it was found unique in that both Bd or Ip monomer moieties in the copolymers are in a high-cis-1,4 configuration, in contrast to copolymerizations with Co- or Ti-based catalysts, where usually only one of the comonomers polymerizes to a high-cis-1,4 configuration while the other is polymerized to a lower cis-1,4 content than in its homopolymerization (Hu et al., 1974). Monakov et al. (1977a,b) reported the copolymerization of these two monomers, using the Nd stearate system. Shen et al. (1982a) have studied the copolymerization kinetics of Bd and Ip by using highly active RCl_3–EtOH–$Alalk_3$ catalyst systems with a variation of rare earth element, aluminum alkyl, solvent, and alcohol complex. The microstructure of the copolymers so prepared with rare earth catalysts is not affected materially by the composition of the monomer mixtures, while the microstructures of copolymers prepared with Ti- or Co-catalysts change tremendously with the content of the comonomer. The Al/R molar ratio, polymerization temperature, and sort of solvent do not exert much influence on the microstructure of the copolymer either. Both butadiene and isoprene repeat units in copolymers have cis-1,4 contents above 95%.

The reaction of Bd–Ip copolymerization with the $NdCl_3$–EtOH–$AlEt_3$–hexane system at various temperatures indicates that the rate is second order with respect to the total monomer concentration and is first order with respect to the total concentration of catalyst. Thus the copolymerization rate equation is described as follows:

$$R_p = k_p[M^2][Cat],$$

where [M] is the concentration of monomer and [Cat] is the concentration of catalyst. The data in table 19 show that the copolymerization rate with $NdCl_3$ catalyst was the highest, about three times greater than that with Pr catalyst. The

TABLE 19
Apparent activation energy of copolymerization of Bd and Ip with various catalytic systems.

Catalytic system	Copolymerization rate K ($\times 10^3$)				Apparent activation energy [± 0.5 (kJ mol^{-1})]
	50°C	40°C	25°C	10°C	
$NdCl_3$-C_2H_5OH–$Al(C_2H_5)_3$-hexane	56.7	38.4	21.5	10.5	31.0
$PrCl_3$-C_2H_5OH–$Al(C_2H_5)_3$-hexane	18.5	12.3	8.2	2.8	34.3
$CeCl_3$-C_2H_5OH–$Al(C_2H_5)_3$-hexane	13.5	8.9	5.2	2.2	33.9
$GdCl_3$-C_2H_5OH–$Al(C_2H_5)_3$-hexane	10.4	6.4	2.8	1.1	41.9
$TbCl_3$-C_2H_5OH–$Al(C_2H_5)_3$-hexane	4.7	3.4	1.5	0.6	39.8
$NdBr_3$-C_2H_5OH–$Al(C_2H_5)_3$-hexane	6.2	4.4	2.2	1.0	34.8
$NdCl_3$-C_2H_5OH–$Al(i\text{-}C_4H_9)_3$-hexane	19.2	12.4	7.6	3.8	30.6

order of activity of catalysts containing various rare earth elements is not differing from that shown in both monomer homopolymerization, i.e.,

$$Nd > Pr > Ce > Gd > Tb > Dy > La \sim Ho > Y > Sm \sim Er > Tm > Lu \sim Yb \sim Sc \sim Eu .$$

In the present case, no matter what kind of catalytic system was chosen, the butadiene content in the copolymer is always greater than that in the feed. Values of the reactivity ratios (and their product) found with different catalysts are listed in table 20. Generally, if the reactivity ratio of Bd is greater than that of isoprene, the copolymerization process is assumed to be by a coordination anionic mechanism. Thus, rare earth coordination catalysts again exhibit a coordination-anionic mechanism in the polymerization of diene.

Recently, Shan and Ouyang (1983) studied the relationship between the value of n in $Nd(Opr^i)_{3-n}Cl_n$ and the reactivity ratio of Bd and IP with the binary catalyst $Nd(Opr^i)_{3-n}Cl_n$–$AlEt_3$. The results indicate that the r of isoprene, which has higher electron density on its conjugated double bond, is increased with an increase of the value of n.

The monomer sequence distribution of Bd–Ip copolymer was determined by ^{13}C NMR spectrometry (Xie and Xiao, 1982). The dyad distribution and number average sequence length of these copolymers were quantitatively determined. The results show that the sequence distribution of monomer units in copolymers

TABLE 20

Reactivity ratios of Bd and Ip obtained using a different rare earth compound as a catalyst component.

Rare earth element	r_1 (Bd)	r_2 (Ip)	$r_1 r_2$
La [a]	1.76	0.77	1.36
Ce	1.17	1.04	1.22
Pr	1.10	0.88	0.96
Nd	1.24	0.73	0.91
Sm [b]	1.71	1.03	1.76
Gd	1.58	0.90	1.41
Tb	1.16	0.38	0.44
Dy [a]	1.93	0.66	1.27
Ho [a]	1.90	0.44	0.84
Er [a]	1.85	0.49	0.91
Tm [c]	0.80	0.14	0.11
Lu [c]	2.41	0.55	1.33
Y [d]	1.61	0.72	1.15

[a] $LnCl_3$/monomer = 4×10^{-4} mol.
[b] $LnCl_3$/monomer = 10×10^{-4} mol.
[c] $LnCl_3$/monomer = 16×10^{-4} mol.
[d] $LnCl_3$/monomer = 5×10^{-4} mol.

prepared with Nd, Pr, and Ce catalysts follows a Bernoullian statistical model, while copolymers prepared with Y, Sm, Dy, and Gd catalysts show some deviation from it.

The Bd–Ip copolymers have excellent low-temperature properties (Ouyang et al., 1981).

The copolymerization of Bd and pentadiene also can be carried out by a $NdCl_3$–EtOH–$AlEt_3$ catalyst (Xie et al., 1979). The copolymer is a random one.

Marina et al. (1984) reported the effect of solvent nature on the copolymerization of butadiene with trans-piperylene. An aliphatic solvent (heptane) rather than an aromatic solvent (PhMe) ensured a high polymerization rate and favorable reactivity ratios, and gave a copolymer with a high content of cis-1,4 units.

4.2. *Copolymerization of ethylene and butadiene*

Wang Shenlong et al. (1984) prepared a copolymer of ethylene and butadiene with rare earth coordination catalysts. Factors affecting the copolymerization reaction, such as the variation of the monomer ratio, aluminum alkyl, ligand and rare earth element, have been investigated. It was found that the catalytic activity of various ligands and rare earth elements in copolymerization have the following order:

$$Nd(naph)_3 > NdCl_3 > Nd(P_{507})_3 > Nd(P_{204})_3 ,$$

and

$$Pr > Nd > Gd > Dy > La > Er .$$

This order agrees with that of ethylene polymerization, but differs from that in diene polymerization.

The polymers obtained have been confirmed to be copolymers containing long ethylene-ethylene sequences, as evidenced by DSC, X-ray diffraction, and electron micrography. The Bd unit in the copolymer was exclusively in a cis-1,4 structure. Its crystalline form is of the polyethylene type with a slight deviation of the structure parameters. The melting point, crystallinity and crystallite size increased with increasing ethylene unit content. The green strength of the copolymer is 20–30 kg/cm^2, which is higher than that of polybutadiene.

5. Kinetics and mechanism of diene polymerization

Kinetic studies on the rare earth catalyzed polymerization of diene have been carried out by Chinese scientists (Pan et al., 1982; Hu et al., 1982; Gong et al., 1983; Qian Hanying et al., 1984; Zhu et al., 1984), as well as Russian scientists (Monakov et al., 1982). Here only a few points of the results will be mentioned.

Tritiated and C^{14} labelled methanol (CH_3OT and $^{14}CH_3OH$) quenching techniques have been used for determining the number of active centers in Bd polymerization with the neodymium compound $Al(i\text{-}Bu)_2Cl$–$Alalk_3$ systems (Pan et al., 1982). It was found that the specific radioactivity of the polymer quenched by CH_3OT was over 100 times greater than that of the polymer quenched by $C^{14}H_3OH$. The quenching process can be described as follows:

$$cat^+ \cdots CH_2P + CH_3OT \rightarrow cat\text{–}OCH_3 + T\text{–}CH_2P\,,$$

where cat = catalytic species, and P = polymer chain. This result suggests that the polymerization of diene by rare earth coordination catalysts follows an anionic coordination mechanism. The mechanism was further supported by the change of composition of Bd–Ip copolymer with rare earth catalysts. It has been shown in the same manner as that with the Ti catalyst which has been determined to follow an anionic coordination polymerization (Hu et al., 1982; Shen et al., 1982a).

Generally, the equation of the Bd polymerization rate can be described as:

$$V = k[R][Al]^n[M]\,,$$

or

$$R_p = k_p[C^*][M]\,,$$

where [R] = concentration of rare earth catalyst; [Al] = concentration of alkyl aluminum; [M] = concentration of monomer; R_p = rate of propagation; k_p = rate constant of propagation; [C*] = concentration of active species; in the case of $AlEt_3$, $n = 1/2$; for $Al(i\text{-}Bu)_3$, $n = 1$ and in the case of $Al(i\text{-}Bu)_2H$, $n = 1/3$. Tables 21 and 22 summarize the kinetic parameters of Bd polymerization (Pan et al., 1982; Hu and Ouyang, 1983).

For isoprene polymerization the following rate equation has been established:

$$R_p = k_p[M][cat]^{1.75}\,,$$

TABLE 21
Catalytic activity of Nd catalysts.

Catalyst	Conversion after 60 min polymerization (%)	$\frac{[C^*]}{[Nd]}$ ($\times 10^2$)	k_p (l/mol s)
$NdCl_3$–EtOH–$Al(i\text{-}Bu)_3$	16.5	0.7	97
$NdCl_3 \cdot 3P_{350}$–$Al(i\text{-}Bu)_3$	19.6	0.6	89
$NdBr_3 \cdot 3P_{350}$–$Al(i\text{-}Bu)_3$	19.6	0.7	88
$Nd(C_7H_{15}COO)_3$–$Al(i\text{-}Bu)_3$–$Al(i\text{-}Bu)_2Cl$	42.7	2.4	94
$Nd(naph)_3$–$Al(i\text{-}Bu)_2Cl$–$Al(i\text{-}Bu)_3$	65.9	3.9	99

TABLE 22
Kinetic parameters of Bd polymerization with $NdCl_3 \cdot 3$ ipr OH–$AlEt_3$-hexane (30°C).

k_i (l/mol s)	k_p (l/mol s)	k_{trM} ($l^{1/2}/mol^{1/2}$ s)	k_{trA} ($l^{1/2}/mol^{1/2}$ s)	E_a (kcal/mol)	E_p (kcal/mol)	$\frac{[C^*]}{[Nd]}$ ($\times 10^2$)	τ[a] (min)
2.4	7.4	1.5×10^{-3}	0.21	9.6	7.0	6	6–7

[a] Average lifetime of propagating chain (Hu and Ouyang, 1983).

and $E = 7.5$ kcal/mol (Monakov et al., 1977a,b); $E = 9.0$ kcal/mol (Gong et al., 1983). Zhu et al. (1984) studied the kinetics of the polymerization of isoprene in hexane using an $R(naph)_3$–$Al(i\text{-}Bu)_3$–$Al_2Et_3Cl_3$ catalyst and found the reaction is first order with respect to the monomer and 1.75th order with respect to the catalyst. The concentration of the propagating chain has been calculated to be 3×10^{-6} mol/l. The efficiency of the rare earth catalyst is 2.8% and the rate constant of absolute propagation is 411·s/mol (50°C).

The number of active species of the $Nd(naph)_3$ and $NdCl_3$ systems in Bd polymerization, determined by tritiated methanol quenching, kinetic and retarding agent methods, amounts to 0.6–10 mol% of Nd, while the Ti catalyst systems are generally only about 0.5%. Hu et al. (1982), and Hu and Ouyang (1983) proposed that the polymerization of conjugated diene with rare earth catalysts was the same as that of d-orbital transition metal catalysts such as Ti and Co and could be described as follows:

Initiation:

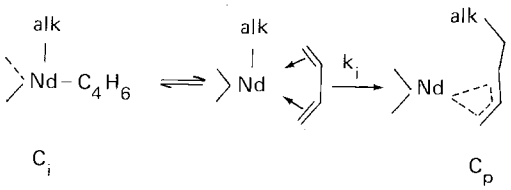

Propagation: including two steps; (a) monomer coordinate onto rare earth ion, (b) coordinated monomer insert into the metal-carbon bond.

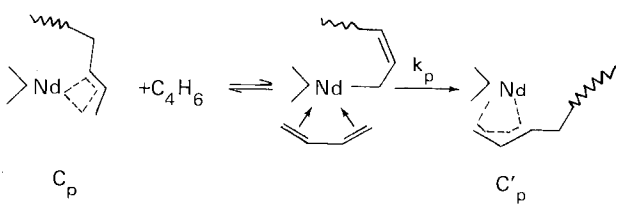

In rare earth catalyzed polymerization, chain transfer with alkyl aluminum and

monomer have been observed and the former predominates:

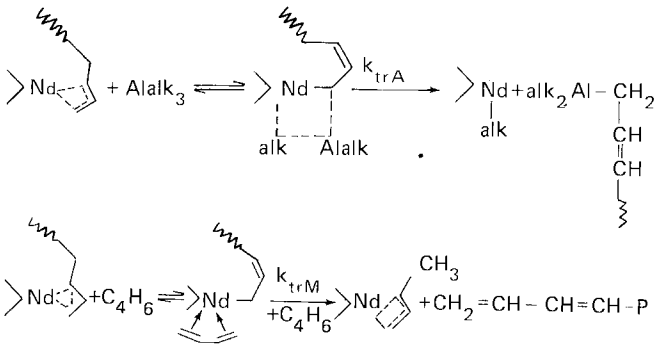

Here k_{trA} and k_{trM} are transfer constants with Alalk and monomer.

It was found that $HAl(i\text{-}Bu)_2$ is mainly the chain transfer agent in Bd polymerization whereas with the $NdCl_3 \cdot 2phen–HAl(i\text{-}Bu)_2$ binary system the Al/Bd ratio is a key parameter controlling the MW of PBd obtained (Yang Jihua et al., 1984a,b,c).

In rare earth catalyzed polymerization there is no chain termination without impurity. But it was found that in Bd polymerization with a $Nd(naph)_3–Al(i\text{-}Bu)_3–HAl(i\text{-}Bu)_2$ catalyst the chain termination is second order with respect to the concentration of active species (Pan et al., 1982).

It has been reported that under certain conditions isoprene polymerization with a $Nd(naph)_3–Al(i\text{-}Bu)_3–Al_2Et_3Cl_3$ catalyst proceeds by a "living" polymerization mechanism. This means that the MW of polymer increases proportionally with increasing conversion. The MWD of a polymer remains unchanged during polymerization. The termination and transfer of the growing polymer chain are almost entirely absent and a block copolymer can be prepared (Shen et al., 1980; Wang Fosong and Shen, 1981). Very recently the above-mentioned phenomenon has been found also in Bd polymerization with $NdCl_3 \cdot iprOH–Al(i\text{-}Bu)_3$ binary catalyst. That is, the MW of PBd increased with polymerization time or conversion while the number of macromolecules per mole of Nd kept constant, indicating the absence of a chain transfer and termination at polymerization temperatures below −30°C. Block copolymers of Bd–Ip were formed under the given conditions (Ji et al., 1985).

Rare earth catalysts have a long lifetime of activity. Experimental data indicate that their catalytic activity is retained unchanged even after aging 40 days. In absence of a solvent, the mixture of rare earth catalyst components after being heated to 150–180°C under reduced pressure for one hour is still active for diene polymerization and keeps its high stereospecificity. This indicates that the thermal stability of the rare earth metal–carbon bond is relatively high (Pang and Ouyang, 1981).

6. Active species of rare earth coordination catalysts

Since the discovery of Ziegler–Natta catalysts, a large effort has been directed toward the understanding of the structure of Z–N catalysts having polymerization activity. The isolation of an active catalytic species from a homogeneous catalyst solution presents an intriguing and succesful method in identifying the structure of the species at work in coordination polymerization and in clarifying the polymerization mechanism. Due to many Z–N catalysts being heterogeneous and because of experimental difficulties in handling the ordinarily unstable intermediates, not many active polymerization species have been isolated. Ballard et al. (1978) have isolated rare earth containing bimetallic complexes active for ethylene polymerization, as mentioned in section 3.3.

Rare earth active species for diene polymerization have been isolated from the following catalyst systems:

(1) $(CF_3COO)_2RCl \cdot EtOH–AlEt_3$ or $(CF_3COO)_2RCl \cdot 2THF–AlEt_3$ catalyst system.

Six R (R = La, Ce, Pr, Nd, Sm, Eu) Al containing bimetallic complexes have been isolated from a titled homogeneous catalyst by Jin et al. (1982, 1984a,b, 1985) since 1980. By quantitative analysis these complexes, except for the Eu–Al complex, are assumed to have the structure $CF_3COOEtRClEtAlEtH$:

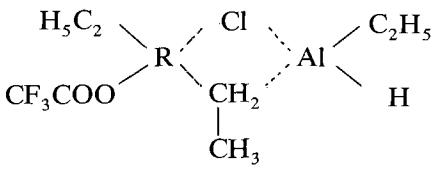

Most of them are brown crystalline solids and decompose above 170°C without melting. They alone can function as active catalysts in the polymerization of

TABLE 23
A comparison of the catalytic activity of a bimetallic complex and a binary catalyst.

R	Catalytic activity (g polymer/g R)			
	Binary system		Bimetallic complex	
	PBd	PIp	PBd	PIp
La	137	96	142	110
Ce	857	809	221	259
Pr	1183	615	126	204
Nd	1759	833	522	523
Sm	22	3	5	5
Eu	0	0	0	0

TABLE 24
A comparison of the microstructure of a polydiene binary catalyst and a bimetallic complex.

R	Binary system					Bimetallic complex				
	PBd			PIp		PBd			PIp	
	cis-	trans-	1,2-	cis-	3,4-	cis-	trans-	1,2-	cis-	3,4-
La	90.9	8.4	0.7	89.5	10.5	96.1	1.4	1.2	89.7	10.3
Ce	82.0	15.6	2.4	88.4	11.6	96.4	2.4	1.2	84.1	10.9
Pr	93.0	6.4	0.6	92.2	7.8	97.8	1.3	0.9	91.4	8.6
Nd	92.4	6.9	0.7	93.3	6.7	97.5	2.0	0.5	91.3	8.7
Sm	90.8	8.5	0.7	94.7	5.3	–	–	–	92.8	7.2
Eu	–	–	–	–	–	–	–	–	–	–

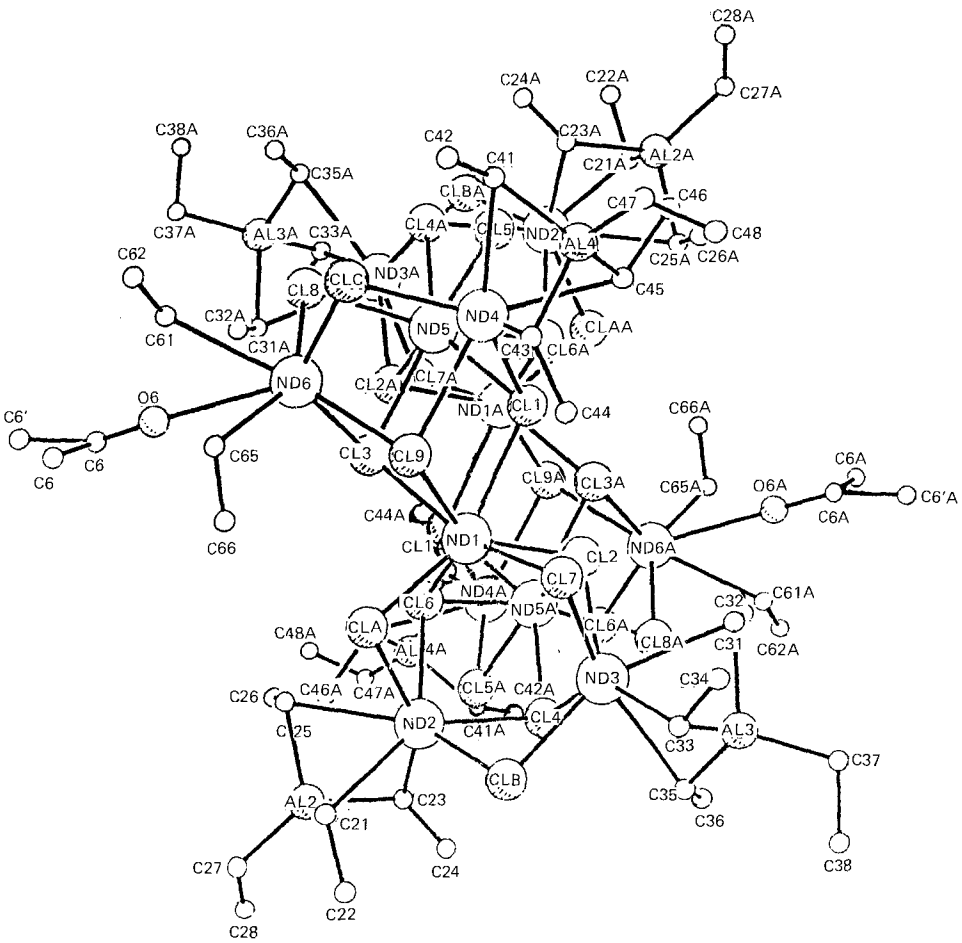

Fig. 4. The single-crystal structure of a rare earth Ziegler–Natta crystal.

butadiene or isoprene, giving the same regularity and stereospecificity of polymerization as the binary system, as shown in tables 23 and 24.

In the presence of tetrahydrofuran a new bi- or mono-rare-earth organometallic complex is formed. It contains a Nd–C bond but shows no activity for isoprene polymerization.

(2) The ternary $(iprO)_3Nd–AlEt_3–AlEt_2Cl$ and the binary $(iprO)_2NdCl–AlEt_3$ system.

In 1983 Shan et al. (1986a,b) obtained a single crystal from the titled ternary system. The crystal was confirmed by a four-circle diffractometer study to have the following parameters of a triclinic unit cell space group PT: $a = 15.195(6)$ Å, $b = 15.263(3)$ Å, $c = 13.749(4)$ Å, $\alpha = 90.01(2)°$, $\beta = 95.123°$, $\gamma = 82.65(3)°$, $V = 3149.5$ Å^3, $Z = 1$. It is a dimer of the polynuclear Nd–Al bimetallic complex with a formula of $[Al_3Nd_6(\mu\text{-}Cl)_6(\mu_3\text{-}Cl)_6(\mu_2\text{-}Et)_9Et_5(Oipr)]_2$. The structure of the single crystal is shown in fig. 4.

The single crystal is a purplish red parallelepipedon which has no distinct melting point, and decomposes above 200°C, changing to black. It reacts with water or ethanol vigorously; hydrogen, ethane, and ethylene are released along with the production of isopropanol. It is insoluble in n-hexane but slightly soluble in toluene.

The single crystal has high activity and stereospecificity for catalyzed polymerization of butadiene. An active bimetallic complex Nd–Al was also isolated from the titled binary catalyst system.

References

Anderson,, A.W., and N.A. Merckling, 1960, U.S. Pat. 2953531: Chem. Abstr. 55(1961)6042.

Ballard, D.G.H., A. Courtis, J. Holton, J. McMeeking and R. Pearce, 1978, J. Chem. Soc. Chem. Commun., p. 994.

Berg, A.A., Yu.B. Monakov, V.P. Budtov and S.R. Rafikov, 1978, Vysokomol. Soedin. B **20**, 295.

Bergbreiter, D.M.E., Li Ban Chen and Rama Chandran, 1985, Macromol. **18**, 1055.

Cai, Shimian, Shijing Xiao and Huanqin Liu, 1984, Chin. J. Catalysis **5**, 287.

Cao, Yong, Renyuan Qian, Fosong Wang and Xiao Zhao, 1982, Macromol. Chem. Rapid Commun. **3**, 687.

Finch, C.A., 1960, Int. Symp. on Macromolecular Chemistry, Moscow, **11**, 364.

Gong, Zhi, Bolin Li, Guajie Yang and Fosong Wang, 1983, Gaofenzi Tongxun (Polymer Communications) p. 116.

Hu, Jingyu, and Jun Ouyang, 1983, Collected Papers of the Changchun Institute of Applied Chemistry **20**, 1.

Hu, Jingyu, Shufen Pang, Demin Xie and Jun Ouyang, 1974, J. Appl. Chem., p. 43.

Hu, Jingyu, Zangyu Zhou and Jun Ouyang, 1982, Collected Papers of the Changchun Institute of Applied Chemistry **19**, 63.

Ji, Xianzhong, Shufen Pang, Yuliang Li and Jun Ouyang, 1985, Sci. Sin. B, p. 120.

Jin, Yingtai, Yufang Sun and Jun Ouyang, 1979, Gaofenzi Tongxun (Polymer Communications) p. 367.

Jin, Yingtai, Xingmin Li, Yufang Sun and Jun Ouyang, 1982, Kexue Tongbao **27**, 1189.

Jin, Yingtai, Xingmin Li, Yufang Sun and Jun Ouyang, 1984a, Polym. Commun., p. 358.

Jin, Yingtai, Xingmin Li, Yufang Sun and Jun Ouyang, 1984b, China–Japan Bilateral Symp. on the Synthesis and Materials Sciences of Polymers, Beijing, Preprints, p. 11.

Jin, Yingtai, Xingmin Li, Yufang Sun and Jun Ouyang, 1985, Kexue Tongbao, p. 435.

Li, Yuliang, Xuehua Li, Shufen Pang and Jun Ouyang, 1981, Symp. on Functional Polymers, Kumming, People's Rep. of China, Preprints, p. 109.

Li, Yuliang, Hefeng Pan and Jun Ouyang, 1984, Symp. on Functional and Specialty Polymers, Guilin, People's Rep. of China, Preprints, p. 266.

Marina, N.G., N.V. Duvakina, Yu.B. Monakov and S.R. Rafikov, 1984, Dokl. Akad. Nauk SSSR **274**, 1414.
Mazzei, A., 1980, IUPAC Macromolecular Symposium, Florence, Preprints, Vol. I, p. 33.
Merckling, N.G., 1960, U.S. Pat. 2907157: Chem. Abstr. 54(1960)12657.
Monakov, Yu.B., N.G. Marina, N.V. Duvakina and S.R. Rafikov, 1977a, Dokl. Akad. Nauk SSSR **236**, 617.
Monakov, Yu.B., Ya.Kh. Bieshev, A.A. Berg and S.R. Rafikov, 1977b, Dokl. Akad. Nauk SSSR **234**, 1125.
Monakov, Yu.B., N.G. Marina and S.R. Rafikov, 1982, Dokl. Akad. Nauk SSSR **265**, 1431.
Ouyang, Jun, 1981, Japan–China Bilateral Symp. on Polymer Science and Technology, Tokyo, Preprints, p. 67.
Ouyang, Jun, Fosong Wang and Zhiquan Shen, 1981, Proc. China–U.S. Bilateral Symp. (Science Press, Beijing) p. 382.
Ouyang, Jun, Fosong Wang and Baotong Huang, 1983, in: Transition-metal-catalyzed Polymerization (Alkenes and Dienes) Part A, eds R.P. Quirk et al. (Harwood, New York) p. 265.
Pan, Enli, Chongqi Zhong, Demin Xie and Jun Ouyang, 1982, Acta Chim. Sin. **40**, 301, 395.
Panasenko, A.A., V.N. Obinokov, Yu.B. Manokov and S.R. Rafikov, 1977, Vysokomol. Soedin. B **19**, 656.
Pang, Shufen, and Jun Ouyang, 1981, Polym. Commun., p. 393.
Pang, Shufen, Yuliang Li, Weiping Ding, Jianwei Xue and Jun Ouyang, 1984, Chin. J. Appl. Chem. **1**, 50.
Qian, Baogong, Fusheng Yu, Rongshi Cheng, Wen Qin and Enle Zhou, 1981, Proc. China–U.S. Bilateral Symposium on Polymer Chemistry and Physics (Science Press, Beijing) p. 155.
Qian, Hanying, Yu Guangquin and Wenqi Chen, 1984, Polym. Commun., p. 226.
Qiao, Yinan, Yifeng Zhang, Luping Yu, Mujie Yang and Zhiquan Shen, 1986, Sci. Sin. B, p. 897.
Rafikov, S.R., Yu.B. Monakov, Ya.Kh. Bieshev, I.F. Valitova, Yu.I. Murinov, G.A. Tolstikov and Yu.E. Nikitin, 1976, Dokl. Akad. Nauk SSSR **229**, 1174.
Rafikov, S.R., Yu.B. Monakov, N.G. Marina and G.A. Tikhomirova, 1980, Chem. Abstr. **93**, 72926, 96152.
Shan, Chengji, and Jun Ouyang, 1983, Polym. Commun., p. 238.
Shan, Chengji, Yuliang Li, Shufen Pang and Jun Ouyang, 1983, Acta Chim. Sin., p. 127, 136.
Shan, Chengji, Yonghua Lin, Mingyi Wang, Endong Shi and Jun Ouyang, 1986a, Kexue Tongbao, to be published.
Shan, Chengji, Yonghua Lin, Songchun Jin, Jun Ouyang, Yuguo Fan, Guangdi Yang and Jinsheng Yu, 1986b, Kexue Tongbao, submitted.
Shen, Zhiquan, 1980, Chin. J. Catalysis **1**, 15.
Shen, Zhiquan, 1981, Synthetic Rubbers by Coordination Polymerization (Science Press, Beijing) ch. 5.
Shen, Zhiquan, and M.F. Farona, 1983a, Polym. Bull. **10**, 8.
Shen, Zhiquan, and M.F. Farona, 1983b, Polym. Bull. **10**, 298.
Shen, Zhiquan, and M.F. Farona, 1984, J. Polym. Sci. Polym. Chem. Ed. **22**, 1009.
Shen, Zhiquan (Sheng Tse-chuan), Chungyuan Gong, Chungchi Chung and Jun Ouyang (Chun Ouyang), 1964, Sci. Sin. **13**, 1339.
Shen, Zhiquan (Sheng Tse-chuan), Chungyuan Gong and Jun Ouyang (Chun Ouyang), 1965, Gaofenzi Tongxun (Polymer Communications) **7**, 193.
Shen, Zhiquan, Jun Ouyang, Fosong Wang, Zhenya Hu, Fusheng Yu and Baogong Qian, 1980, J. Polym. Sci. Polym. Chem. Ed. **18**, 3345.
Shen, Zhiquan, Xiangyu Song, Shuxiu Xiao, Jipo Yang and Xianglan Kan, 1982a, Sci. Sin. B **25**, 124.
Shen, Zhiquan, Mujie Yang, Mingxiao Shi and Yiping Cai, 1982b, J. Polym. Sci. Polym. Lett. **20**, 411; Proc. IUPAC 28th Macromolecular Symp. p. 431.
Shen, Zhiquan, Xiangyu Song, Shuxiu Xiao, Jipo Yang and Xianglan Kan, 1983a, J. Appl. Polym. Sci. **28**, 1585.
Shen, Zhiquan, Mujie Yang, Mingxiao Shi and Yiping Cai, 1983b, Sci. Sin. B **26**, 785.
Shen, Zhiquan, Luping Yu and Mujie Yang, 1985a, Inorg. Chim. Acta **109**, 55.
Shen, Zhiquan, Zhung Wang and Yiping Cai, 1985b, Inorg. Chim. Acta **111**, 55.
Shen, Zhiquan, Zhongxin Chen and Mujie Yang, 1986, Acta Chim. Sin. **44**, 575.
Simionescu, C.I., V. Percec and S.V. Dumitrescu, 1978, J. Polym. Sci. Polym. Symp. **64**, 209.
Stuart, A.P., 1960, U.S. Pat. 2921060; Chem. Abstr. **54**, 2818.
The Fourth Laboratory, Changchun Institute of Applied Chemistry, 1974, Sci. Sin. **17**, 656.
The Fourth Laboratory, Changchun Institute of Applied Chemistry, 1981, Collected Papers on Synthetic Rubbers by Rare Earth Catalysts (Science Press, Beijing).
Throckmorton, M.C., 1969, Kautsch. Gummi Kunst. **22**, 293.
Wang, Fosong, and A. Bolognesi, 1982, Polym. Commun., p. 238.
Wang, Fosong, and Qi Shen, 1981, Collected Papers on Synthetic Rubbers by Rare Earth Catalysts (Science Press, Beijing) p. 258.
Wang, Fosong, Renyu Sha, Yingtai Jin, Yuling Wang and Yulian Zheng, 1980, Sci. Sin. **23**, 172.
Wang, Fosong, A. Bolognesi, A. Immirzi and L. Porri, 1981, Macromol. Chem. **182**, 3617.
Wang, Fosong, Yingtai Jin, Chengji Shan,

Xianzhong Ji and Jun Ouyang, 1984, China–Japan Bilateral Symposium on the Synthesis and Material Science of Polymers, Beijing, Preprints, p. 117.
Wang, Shenglong, 1983, Abstract of M.S. Thesis, Chin. J. Appl. Chem. p. 118.
Wang, Shenglong, Xiaojang Zhao and Fosong Wang, 1983, Polym. Commun. p. 350.
Wang, Shenglong, Zhongzhi Li and Fosong Wang, 1984, Polym. Commun. p. 425.
Watson, P.L., 1983, Inorg. Chim. Acta **94**, 26; ACS Symp. Ser. **212**, 459.
Xie, Demin, and Yenwen Xiao, 1982, Polym. Commun., p. 202.
Xie, Demin, Chongqi Zhong, Ainai Yuan, Yufang Sun, Shuxiu Xiao and Jun Ouyang, 1979, Polym. Commun., p. 233.
Yang, Jihua, Jingyu Hu, Shufen Pang, Enli Pan, Demin Xie, Chongqi Zhong and Jun Ouyang, 1980, Sci. Sin. **23**, 734.
Yang, Jihua, M. Tsutsui, Zonghan Chen and D.E. Bergbreiter, 1982, Macromol. **15**, 230.
Yang, Jihua, Shufen Pang, Tao Sun, Ying Li and Jun Ouyang, 1984a, Chin. J. Appl. Chem., p. 11.
Yang, Jihua, Shufen Pang and Jun Ouyang, 1984b, Polym. Commun., p. 73.
Yang, Jihua, Shufen Pang, Ying Li and Jun Ouyang, 1984c, Chin. J. Catalysis, p. 291.
Yang, Mujie, Yiping Cai, Zheng Wang, Junguan Sun and Zhiquan Shen, 1983, Chin. J. Appl. Chem. **1**, 79.
Yang, Mujie, Yiping Cai and Zhiquan Shen, 1984a, J. Chin. Rare Earth Soc. **2**, 8.
Yang, Mujie, Yifeng Zhang, Zhiquan Shen, Laiyou Zhang, Ziqing Wang, Jijing Cai and Huarong Lu, 1984b, J. Zhejiang Univ. **18**, 54.
Yang, Mujie, Yinan Qiao, Xinzhen Xiang, Zhongxing Chen and Zhiquan Shen, 1984c, Symp. on Functional and Specialty Polymers, Guilin, People's Rep. of China, Preprints, p. 354.
Yu, Guanqian, Wenqi Chen and Yuling Wang, 1983, Kexue Tongbao **28**, 408.
Yu, Luping, Zhiquan Shen and Mujie Yang, 1985a, Synth. Met. **11**, 53.
Yu, Luping, Yinan Qiao and Zhiquan Shen, 1985b, Acta Chim. Sin. **43**, 688.
Zhang, Yifeng, Yiping Cai and Zhiquan Shen, 1986, Polym. Commun., p. 125.
Zhao, Xiaojang, and Jun Ouyang, 1980, Chin. Petrochem. Chem. Eng., p. 6.
Zhu, Xinghao, Yugin Qiao and Dongni Han, 1984, Polym. Commun., p. 207.

ERRATA

Vol. 1, ch. 2, Beaudry and Gschneidner

1. Page 225, line 8 of the text below table 2.15, change "158 kJ/mole" to "164 kJ/mole".
2. Page 226, fig. 2.10: The point for the heat of sublimation of europium (Eu) should be raised slightly to 175 kJ/mole, and the average value listed just above the lower dashed line, "148", should be changed to "164".

Vol. 3, ch. 26, Libowitz and Maeland

1. Page 311, fig. 26.7, line 2 of the figure caption: dihydride instead of "dehydride".

Vol. 3, ch. 28, Bevan and Summerville

1. Page 451, line 4 from the bottom: produce instead of "product".

Vol. 3, ch. 29, Khattak and Wang

1. Page 539 (table 29.2): the entry "$SmScD_3$" should be $SmScO_3$.
2. Page 548 (table 29.2): the entry "Ba_2DyTaO_3" should be Ba_2DyTaO_6.
3. Page 549 (table 29.2): the entry between $BaCePaO_6$ and Ba_2NdPaO_6 should be Ba_2PrPaO_6 instead of "Be_2PrPaO_6".

Vol. 3, ch. 30, Brixner, Barkley and Jeitschko

1. Page 638 (table 30.7): the second-last entry "$Gd_{1.3}Ho_{.7}(MoO_3)_4$" should be $Gd_{1.3}Ho_{.7}(MoO_4)_3$.

Vol. 4, ch. 36, Fong

1. Page 327 (table 36.2) second entry: $YAlO_3:Ho^{3+}$ instead of "$YalO_3:Ho^{3+}$".
2. Page 327 (table 36.2), third entry: $YAlO_3:Eu^{3+}$ instead of "$YalO_3:Eu^{3+}$".
3. Page 327 (table 36.2) fourth entry: $Y_3Al_5O_{12}:Pr^{3+}$ instead of "$Y_3AI_5O_{12}:Pr^{3+}$".

Vol. 4, ch. 40, Haley

1. Page 559, line 3 from bottom: Ce_2O_3 instead of "Ce_3O_3".

Vol. 8, ch. 54, Gschneidner and Calderwood

1. Page 4 (table 2): the atomic volume for α-Ce should be 17.2 cm^3/mol.

SUBJECT INDEX